

DEVELOPMENT AND MECHANISTIC INVESTIGATION OF POTASSIUM
TERT-BUTOXIDE CATALYZED C–H SILYLATION

Thesis by

David Phillip Schuman

In Partial Fulfillment of the Requirements

for the Degree of

Doctor of Philosophy

CALIFORNIA INSTITUTE OF TECHNOLOGY

Pasadena, California

2020

(Defended March 20, 2020)

© 2020

David P. Schuman

All Rights Reserved

To my Mom, Dad, wife,

and

all the people who supported me on my journey

ACKNOWLEDGEMENTS

I would like to begin by thanking all of the people who helped me throughout my graduate career. This process would not have been possible without the support and guidance of the Caltech faculty and staff, coworkers, family, and friends.

Professor Brian Stoltz has been an excellent advisor and I am honored to be part of this research group. Brian is an exceptional scientist and a caring advisor, both of which are apparent in daily interactions and the overall guidance of the Stoltz group.

I would especially like to thank all of my current and former coworkers who have made the Stoltz group an amazing place to learn and work. Having such a supportive, intelligent, hardworking, and fun group of people has made the long hours and challenges infinitely better. The members of the Stoltz group have guided my growth as a scientist and I hope to have done the same for others.

My Ph.D. Thesis Committee comprised of Professors Sarah Resiman, Brian Stoltz, Theo Agapie, and Bob Grubbs deserves thanks for their insightful discussions and advice. I would like to mention in particular both Professor Resiman and her research group, who participate in a number of joint activities with the Stoltz group and provide valuable expertise and camaraderie. I would also like to thank Professor Grubbs for his guidance and support in the joint research project detailed later in this thesis.

I would like to thank Professor Shannon Stahl and Dr. Adam Weinstein for supporting me as an eager undergraduate at UW-Madison. They established the foundation of my laboratory skills and critical thinking, and I would not be here without their early support.

My Ph.D. at Caltech would not have been possible without the support of all of the talented staff and faculty in the CCE. I want to thank Dr. Scott Virgil for all of his work developing and maintaining the Catalysis Center. A large portion of the experiments I have conducted at Caltech were setup, run, and analyzed solely in the Catalysis Center, which would not have been possible without Dr. Virgil. Furthermore, Dr. Virgil is an amazing scientist and has provided crucial assistance with mechanistic experiments, compound separations, and scientific discussions. I would also like to thank Dr. David VanderVelde for both maintaining the excellent NMR facilities at Caltech and hiring me as a GLA.

I would like to thank my excellent project partners including Professor Boger Liu, Dr. Anton Toutov, and Kerry Betz. I am lucky to have such a talented and friendly group of coworkers. I am especially grateful to Boger, who allowed me to join the silylation project when I was a first year student and provided excellent mentorship throughout my time at Caltech. Boger was an excellent mentor and I am excited to see what new developments may come from the Liu Group.

Finally, I would like to thank all of my friends and family for their support. I would not have considered pursuing graduate school if it were not for the advice and encouragement from friends and family. Even when graduate work consumed all of my time, my friends and family were still there to support and encourage me. I would like to especially thank my parents, who have always supported my curiosity and excitement. They have always been there for me, even when distance and time commitments made it challenging. Finally, I would like to thank my wife. She has been the most amazing, supportive, and accommodating person during the most challenging times in graduate school.

ABSTRACT

The synthetic organic community has a long history of concurrent development of new methods, total syntheses, and mechanistic investigations. For example, new methods may allow the synthesis of previously inaccessible synthetic targets or a challenging transformation in a total synthesis may lead to the development of new reaction methods. Understanding the mechanism of a reaction may lead to the development of new methods or application in total synthesis. Historically, the Stoltz group has found great success focusing on the synergistic development of reaction methods, total synthesis, and mechanistic investigation. This thesis focuses on the mechanistic investigation of a novel method developed by our group and a number of new methods inspired by this better understanding of the reaction mechanism.

Initially, an overview of transition-metal-free, catalytic C–H silylation reactions is presented. Next, a detailed mechanistic investigation into the KO*t*-Bu-catalyzed C–H silylation reaction of aromatic heterocycles is presented. This investigation covers a series of experimental, computational, and analytic techniques to probe possible radical or ionic reaction mechanisms. The development of a number of new methods is presented including the catalytic trimethylsilylation of aromatic heterocycles and catalytic silylation of terminal alkynes.

Finally, the current progress of our efforts toward the total synthesis of the natural product illisimonin A are presented.

PUBLISHED CONTENT AND CONTRIBUTIONS

1. Toutov, A. A.;[†] Betz, K. N.;[†] Schuman, D. P.; Liu, W.-B.; Fedorov, A.; Stoltz, B. M.; Grubbs, R. H. “Alkali metal hydroxide–catalyzed C(sp)–H bond silylation” *J. Am. Chem. Soc.* **2017**, *139*, 1668–1674. [†]Equal Contribution. DOI: 10.1021/jacs.6b12114.

D.P.S. participated in experimental work, data acquisition and analysis, and manuscript preparation.

2. Liu, W.-B.;[†] Schuman, D. P.;[†] Yang, Y.-F.;[†] Toutov, A. A.; Liang, Y.; Klare, H. F. T.; Nesnas, N.; Oestreich, M.; Blackmond, D. G.; Virgil, S. C.; Banerjee, S.; Zare, R. N.; Grubbs, R. H.; Houk, K. N.; Stoltz, B. M. “Potassium tert-Butoxide-Catalyzed Dehydrogenative C–H Silylation of Heteroaromatics: A Combined Experimental and Computational Mechanistic Study” *J. Am. Chem. Soc.* **2017**, *139*, 6867–6879. [†]Equal Contribution. DOI: 10.1021/jacs.6b13031.

D.P.S. participated in project design, experimental work, data acquisition and analysis, and manuscript preparation.

3. Banerjee, S.;[†] Yang, Y.-F.;[†] Jenkins, I. D.;[†] Liang, Y.; Toutov, A. A.; Liu, W.-B.; Schuman, D. P.; Grubbs, R. H.; Stoltz, B. M.; Krenske, E. H.; Houk, K. N.; Zare, R. N. “Ionic and Neutral Mechanisms for C–H Bond Silylation of Aromatic Heterocycles Catalyzed by Potassium tert-Butoxide” *J. Am. Chem. Soc.* **2017**, *139*, 6880–6887. [†]Equal Contribution. DOI: 10.1021/jacs.6b13032.

D.P.S. participated in project design, data analysis, and manuscript preparation.

4. Wang, X.; Zhu, M.-H.; Schuman, D. P.; Zhong, D.; Wang, W.-Y.; Wu, L.-Y.; Liu, W.; Stoltz, B. M.; Liu, W.-B. “General and Practical KOMe/Disilane-Mediated Dehalogenative Deuteration of (Hetero)Arylhalides” *J. Am. Chem. Soc.* **2018**, *140*, 10970–10974. DOI: 10.1021/jacs.8b07597.

D.P.S. participated in experimental work, data acquisition and analysis, and manuscript preparation.

5. Schuman, D. P.; Liu, W.-B.; Nesnas, N.; Stoltz, B. M. Transition-Metal-Free Catalytic C—H Bond Silylation. In *Organosilicon Chemistry: Novel Approaches and Reactions*; Hiyama, T., Oestreich, M., Eds.; Wiley-VCH: Weinheim, Germany, 2019; Chapter 7, pp. 213–239. ISBN: 978-3-527-34453-6.

D.P.S. led the writing and editing of the book chapter.

TABLE OF CONTENTS

Dedication	iii
Acknowledgements	iv
Abstract.....	vi
Published Content and Contributions	vii
Table of Contents	ix
List of Figures	xv
List of Schemes.....	xix
List of Tables	xxiii
List of Abbreviations.....	xxv

CHAPTER 1		
<i>Transition-Metal-Free Catalytic C–H Bond Silylation</i>		
1.1	Introduction	1
1.2	Lewis Acid Catalysis	1
1.2.1	BCl ₃ Catalyst	1
1.2.2	B(C ₆ F ₅) ₃ , A "Frustrated" Lewis Acid Catalyst	3
1.2.3	Lewis Acid Conclusions	12
1.3	Brønsted Acid	13
1.4	Brønsted Base	15
1.4.1	Early Example of Catalytic C–H Silylation by Brønsted Base	15
1.4.2	Fluoride/Base Catalysis	16
1.4.3	Brønsted Base Catalyzed C–H Silylation of Alkynes	19
1.5.	Radical Dehydrosilylation.....	23
1.5.1	"Electron" as a C–H Silylation Catalyst.....	23
1.5.2	KOt-Bu-Catalyzed C–H Silylation	26
1.5.2.1	Discovery of Unusual KOt-Bu-Catalyzed C–H Silylation.....	26
1.5.2.2	KOt-Bu Catalyzed C–H Silylation Methodology	26
1.5.2.3	Mechanistic investigations of KOt-Bu Catalyzed C–H Silylation and Related Chemistry	29
1.6	C(sp ³)–H Silylation	34
1.7	Conclusion	35
1.8	References and Notes	36

CHAPTER 2 **40**
A Combined Experimental and Computational Mechanistic Study of the KOt-Bu-Catalyzed Dehydrogenative C–H Silylation of Aromatic Heterocycles

2.1	Introduction and Background	40
2.2	Mechanistic Investigation Overview	42
2.3	Investigation of Silylation Reaction Yield and Kinetics	43
2.3.1	Catalyst Activity	43
2.3.2	Reaction Profile	44
2.3.3	Impact of Catalyst Identity on Reaction Kinetics	45
2.3.4	Silylation Product Distribution and Reversibility	46
2.3.5	Reaction Rate Dependence on Substrate Loading	48
2.3.6	Silylation Reaction Safety	49
2.3.7	Cross-dehydrogenative Formation of H ₂	52
2.4	Investigation of Radical Intermediates	54
2.4.1	Radical Trap Experiments.....	54
2.4.2	Radical Clock Experiments.....	56
2.4.3	Electron Paramagnetic Resonance (EPR) Studies.....	58
2.4.4	Radical Initiation.....	60
2.4.4.1	Background	60
2.4.4.2	Amine Additives	60
2.4.4.3	Radical Initiation via Hydrogen Atom Abstraction.....	61
2.5	Pentacoordinate Silicate Intermediates	63
2.5.1	Background	63
2.5.2	ReactIR Studies of Pentacoordinate Silicate	63
2.5.3	ATR-IR Studies of Pentacoordinate Silicate.....	65
2.5.4	Computational Studies of Pentacoordinate Silicate.....	67
2.5.5	Radical Initiation via Pentacoordinate Silicate.....	69
2.6	Alternative Radical Initiation Pathways	70
2.6.1	Catalyst Speciation.....	70
2.6.2	Radical Initiation via Trace Oxygen	71
2.7	Silylation Reaction Mechanism	73
2.7.1	Kinetic Isotope Effect Studies.....	73
2.7.2	Proposed Reaction Mechanism	75
2.7.3	Stereochemical Course of Silicon	77
2.7.4	Computational Study of Proposed Mechanism	80
2.7.5	Computational Study of Product Selectivity.....	83
2.8	Conclusion	84
2.9	Experimental Section	85

2.9.1	Materials and Methods.....	85
2.9.1.1	Computational Details	86
2.9.1.2	Preparation of Known Compounds	87
2.9.2	Experimental Procedures and Spectroscopic Data	87
2.9.2.1	General Procedure for the Screening of Base Catalysts and Kinetic Profile	87
2.9.2.2	General Procedure for Time-Course Reaction Monitoring by <i>in situ</i> ^1H NMR	87
2.9.2.3	General Procedure for Regioselectivity Studies	88
2.9.2.4	Procedure for Reversibility of Studies	88
2.9.2.5	Procedure for Reversibility Crossover Studies.....	88
2.9.2.6	Procedure of Gas Collection by Eudiometry	89
2.9.2.7	Procedure for Radical Trap Experiments Using TEMPO.....	89
2.9.2.8	General Procedure for Additive Screening	90
2.9.2.9	General Procedure for Studies Using <i>in situ</i> Generated tert-butoxyl Radicals .	91
2.9.2.10	General Procedure for ReactIR Time-Course Experiments	91
2.9.2.11	General Procedure for ATR-IR Studies of Pentacoordinate Silicate	91
2.9.2.12	Procedure for Acquisition of EPR Spectra.	92
2.9.2.13	General Procedure for Calorimetry Studies.....	92
2.9.2.14	General Procedure for KOt-Bu-Catalyzed Silylation Reactions	93
2.9.2.15	Procedure for the Synthesis of Radical Clock Substrates	94
2.9.2.16	Procedure for Silylation of Radical Clock Substrates.....	98
2.9.2.17	Experimental Procedures and Spectroscopic Data for the Silylation of Stereochemical Probe 176	102
2.10	References and Notes	103

APPENDIX 1 **112**
Spectra Relevant to Chapter 2:

APPENDIX 2	147	
<i>Computational Details Relevant to Chapter 2:</i>		
A2.1	General Parameters	148
A2.1.1	Computational Values to Chapter 2	148
A2.2	Cartesian Coordinates of the Structures	150
A2.3	References	207

APPENDIX 3 **209**
Alternative Reaction Mechanisms of KOt-Bu-Catalyzed Dehydrogenative C–H Silylation of Aromatic Heterocycles:

A3.1	Introduction and Background	209
------	-----------------------------------	-----

A3.2	Ionic Reaction Mechanism	210
A3.2.1	Detection of Ionic Intermediates by DESI-MS	210
A3.2.2	Cation- π Interactions	212
A3.2.3	Proposed Ionic Mechanism	213
A3.2.4	Energy Profile of Proposed Ionic Mechanism	214
A3.2.5	Energy Profile of Proposed Neutral Mechanism	216
A3.2.6	Ionic and Neutral Mechanism Conclusion	218
A3.3	Electron Transfer Mechanism	219
A3.4	Conclusion	220
A3.5	Experimental Section	220
A3.5.1	Materials and Methods	220
A3.5.2	Silylation Reaction for Mass Spectrometric Study	220
A3.5.3	Desorption Electrospray Ionization Mass Spectrometry	221
A3.5.4	Electrospray Ionization Mass Spectrometry.	222
A3.5.5	Computational Details	222
A3.6	Relevant Spectra	222
A3.7	References and Notes	223

CHAPTER 3 **225**
Catalytic C–H Trimethylsilylation of Aromatic Heterocycles via Base Catalysis:

3.1	Background	225
3.1.1	Literature Examples of Catalytic C–H Trimethylsilylation	226
3.2	Base-Catalyzed C–H Trimethylsilylation	227
3.2.1	Introduction	227
3.2.2	C–H Silylation Using Trimethylsilane Gas	228
3.2.3	C–H Silylation Using Disilane	229
3.2.3.1	Introduction and Background	229
3.2.3.2	Reaction Optimization	230
3.2.3.3	Substrate Scope	232
3.2.3.4	Mechanistic Details	233
3.3	Conclusion	235
3.4	Experimental Section	236
3.4.1	Materials and Methods	236
3.4.2	Experimental Procedures and Spectroscopic Data	237
3.4.2.1	General Experimental Procedure and Spectroscopic Data for the C–H Silylation Using Trimethylsilane Gas	237
3.4.2.2	General Procedure for Optimization Using Hexamethyldisilane	242

3.4.2.3	General Experimental Procedure and Spectroscopic Data for the C–H Silylation Using Hexamethyldisilane	242
3.4.2.4	Procedure for Time Course Reaction Monitoring by <i>in situ</i> ^1H NMR	247
3.5	References and Notes	247

APPENDIX 4 **250**
Spectra Relevant to Chapter 3:

APPENDIX 5	276	
<i>Observation of Unusual, Double Dehydrogenative C–H Silylation Products:</i>		
A5.1	Introduction and Background	276
A5.2	Indoline	277
A5.2.1	Observation of Partially Hydrogenated Substrate	277
A5.2.2	Unusual Reactivity of Indoline	278
A5.2.3	Mechanistic Insights into Double Dehydrogenative C–H Silylation	279
A5.3	Conclusion	280
A5.4	Experimental Section	281
A5.4.1	Materials and Methods.....	281
A5.4.2	General Procedure for Indoline Dehydrogenation and Silylation.....	282
A5.4.3	General Procedure for Time Course Reaction Monitoring by <i>in situ</i> ^1H NMR.	
	283
A5.5	References and Notes	283

APPENDIX 6 **285**
Hydroxide-Catalyzed Dehydrogenative C–H Silylation of Terminal Alkynes:

A6.1	Introduction and Background	285
A6.1.1	Literature Examples of Alkyneilsilane Synthesis	286
A6.2	Dehydrogenative C–H Silylation of Terminal Alkynes	286
A6.2.1	Initial Hit and Reaction Optimization	286
A6.2.2	Scope of Alkyne C–H Silylation	288
A6.2.3	Applications of Alkyne C–H Silylation	292
A6.2.4	Mechanistic Details of Alkyne C–H Silylation	294
A6.3	Conclusions	295
A6.4	Experimental Section	295
A6.4.1	Materials and Methods	295
A6.4.2	General Procedure for Reaction Optimization	297
A6.4.3	General Procedure for Alkyne C–H Silylation Reactions.....	297
A6.4.4	Spectroscopic Data for Alkyne C–H Silylation Reactions.....	298
A6.5	Relevant Spectra	333

A6.6	References and Notes	333
------	----------------------------	-----

APPENDIX 7 336

Hydroxide-Catalyzed Dehydrogenative C–H Silylation of Terminal Alkynes:

A7.1	Introduction and Background.....	336
A7.2	Retrosynthetic Analysis of Illisimonin A	337
A7.2.1	Literature Examples of Cyclopentadienone Reactivity.	339
A7.3	Forward Synthesis	340
A7.3.1	Cyclopentadienone Route.....	340
A7.4	Revised Retrosynthesis	341
A7.4.1	Biosynthetic Inspiration.....	341
A7.4.2	Benzilic Acid Disconnection.....	342
A7.5	Revised Forward Synthesis	344
A7.6	Future Directions	348
A7.6.1	Oxidative Dearomatization.....	348
A7.7	Rychnovsky Synthesis of Illisimonin A	348
A7.8	Conclusion	349
A7.9	Experimental	350
A7.9.1	Materials and Methods.....	350
A7.9.2	Experimental Methods and Spectroscopic Data.....	351
A7.9.2.1	Synthesis of Model Cyclopentenone Diels–Alder Precursor.....	351
A7.9.2.2	Attempted Oxidation of Model Cyclopentenone Diels–Alder Precursor.	352
A7.9.2.3	Synthesis of Model o-Quinone Precursor.	353
A7.9.2.4	Attempted Oxidation of Model o-Quinone Precursor.....	355
A7.9.2.5	Synthesis of Fully Elaborated o-Quinone Precursor..	356
A7.9.2.6	Attempted Oxidation of Fully Elaborated o-Quinone Precursor.....	358
A7.10	Relevant Spectra	360
A7.11	References and Notes	368

APPENDIX 8 370

Notebook Cross-Reference for New Compounds

Comprehensive Bibliography.....	374
Index	397
About the Author.....	398

LIST OF FIGURES

CHAPTER 1

Transition-Metal-Free Catalytic C–H Bond Silylation

CHAPTER 2

A Combined Experimental and Computational Mechanistic Study of the KOt-Bu-Catalyzed Dehydrogenative C–H Silylation of Aromatic Heterocycles

Figure 2.1 A Representative Time Course of the Formation of 109 , Monitored by <i>in situ</i> ^1H NMR.....	45
Figure 2.2 Time-Course Investigation of Silylation Catalyst	46
Figure 2.3 Time-Course Investigation of Reaction Dependence on Substrate Concentration	49
Figure 2.4 Reaction Heat Flow.....	50
Figure 2.5 Investigation of H_2 Formation	51
Figure 2.6 Hydrogen Gas Labeling Study	53
Figure 2.7 Radical Trap Using TEMPO.....	55
Figure 2.8 TEMPO Induced Reaction Bleaching.....	55
Figure 2.9 EPR Studies	59
Figure 2.10 ReactIR Investigation of Pentacoordinate Silicate	64
Figure 2.11 ATR-IR Spectra of Select Base-Silane Mixtures	66
Figure 2.12 Dissociation of $[\text{KOt-Bu}]_4$	71
Figure 2.13 Computed Pathway for Radical Initiation by Trace Oxygen.....	73
Figure 2.14 Stereochemical Silicon Probe.....	78
Figure 2.15 Free Energy Profile of C ₂ - and C ₃ -Silylation	81
Figure 2.16 Free Energy Profile of Silylation with $[\text{KOt-Bu}]_4$ Participation	82

APPENDIX 1

Spectra Relevant to Chapter 2:

Figure A1.1 ^1H NMR (400 MHz, CDCl_3) of compound 201	113
Figure A1.2 Infrared spectrum (Thin Film, NaCl) of compound 201	114
Figure A1.3 ^{13}C NMR (101 MHz, CDCl_3) of compound 201	114
Figure A1.4 ^1H NMR (400 MHz, CDCl_3) of compound 205	115
Figure A1.5 Infrared spectrum (Thin Film, NaCl) of compound 205	116
Figure A1.6 ^{13}C NMR (101 MHz, CDCl_3) of compound 205	116
Figure A1.7 ^1H NMR (400 MHz, CDCl_3) of compound 208	117
Figure A1.8 Infrared spectrum (Thin Film, NaCl) of compound 208	118
Figure A1.9 ^{13}C NMR (101 MHz, CDCl_3) of compound 208	118

Figure A1.10	^1H NMR (400 MHz, CDCl_3) of compound 122	119
Figure A1.11	Infrared spectrum (Thin Film, NaCl) of compound 122	120
Figure A1.12	^{13}C NMR (101 MHz, CDCl_3) of compound 122	120
Figure A1.13	^1H NMR (400 MHz, CDCl_3) of compound 123	121
Figure A1.14	Infrared spectrum (Thin Film, NaCl) of compound 201	122
Figure A1.15	^{13}C NMR (101 MHz, CDCl_3) of compound 201	122
Figure A1.16	^1H NMR (400 MHz, CDCl_3) of compound 124	123
Figure A1.17	Infrared spectrum (Thin Film, NaCl) of compound 124	124
Figure A1.18	^{13}C NMR (101 MHz, CDCl_3) of compound 124	124
Figure A1.19	^1H NMR (400 MHz, CDCl_3) of compound 120	125
Figure A1.20	Infrared spectrum (Thin Film, NaCl) of compound 120	126
Figure A1.21	^{13}C NMR (101 MHz, CDCl_3) of compound 120	126
Figure A1.22	^1H NMR (400 MHz, CDCl_3) of compound 121, R = H	127
Figure A1.23	Infrared spectrum (Thin Film, NaCl) of compound 121, R = H	128
Figure A1.24	^{13}C NMR (101 MHz, CDCl_3) of compound 121, R = H	128
Figure A1.25	^1H NMR (400 MHz, CDCl_3) of compound 121, R = SiHEt₂	129
Figure A1.26	Infrared spectrum (Thin Film, NaCl) of compound 121, R = SiHEt₂	130
Figure A1.27	^{13}C NMR (101 MHz, CDCl_3) of compound 121, R = SiHEt₂	130
Figure A1.28	^1H NMR (400 MHz, CDCl_3) of compound 55 [0.26–0.028]	131
Figure A1.29	^1H NMR (400 MHz, C_6D_6) of collected H_2 gas.....	132
Figure A1.30	ATR-IR of Et_3SiH	133
Figure A1.31	ATR-IR of $\text{KO}t\text{-Bu}$	134
Figure A1.32	ATR-IR of $\text{KO}t\text{-Bu}$ and Et_3SiH	135
Figure A1.33	ATR-IR of KOEt and Et_3SiH	136
Figure A1.34	ATR-IR of KOMe and Et_3SiH	137
Figure A1.35	ATR-IR of KOTMS and Et_3SiH	138
Figure A1.36	ATR-IR of KOH and Et_3SiH	139
Figure A1.37	ATR-IR of $\text{RbOH} \bullet x\text{H}_2\text{O}$ and Et_3SiH	140
Figure A1.38	ATR-IR of $\text{CsOH} \bullet x\text{H}_2\text{O}$ and Et_3SiH	141
Figure A1.39	ATR-IR of $\text{Na}O t\text{-Bu}$ and Et_3SiH	142
Figure A1.40	ATR-IR of $\text{Li}O t\text{-Bu}$ and Et_3SiH	143
Figure A1.41	ATR-IR of $\text{Mg(O}t\text{-Bu)}_2$ and Et_3SiH	144
Figure A1.42	EPR of $\text{KO}t\text{-Bu}$ and Et_3SiH	145
Figure A1.43	EPR of compound 55 , $\text{KO}t\text{-Bu}$ and Et_3SiH	146

APPENDIX 3

Alternative Reaction Mechanisms of KOt-Bu-Catalyzed Dehydrogenative C–H Silylation of Aromatic Heterocycles:

- Figure A3.1.** Energy Profile of Ionic Mechanism..... 216
Figure A3.2. Energy Profile of Neutral Mechanism..... 217

CHAPTER 3

Catalytic C–H Trimethylsilylation of Aromatic Heterocycles via Base Catalysis:

- Figure 3.1** Substrate Scope of C–H Silylation using Me₃Si–SiMe₃. 234

APPENDIX 4

Spectra Relevant to Chapter 3:

- Figure A4.1.** ¹H NMR (400 MHz, CDCl₃) of compound **184**. 251
Figure A4.2. Infrared spectrum (Thin Film, NaCl) of compound **184**. 252
Figure A4.3. ¹³C NMR (101 MHz, CDCl₃) of compound **184**. 252
Figure A4.4. ¹H NMR (400 MHz, CDCl₃) of compound **235**. 253
Figure A4.5. Infrared spectrum (Thin Film, NaCl) of compound **235**. 254
Figure A4.6. ¹³C NMR (101 MHz, CDCl₃) of compound **235**. 254
Figure A4.7. ¹H NMR (400 MHz, CDCl₃) of compound **236**. 255
Figure A4.8. Infrared spectrum (Thin Film, NaCl) of compound **236**. 256
Figure A4.9. ¹³C NMR (101 MHz, CDCl₃) of compound **236**. 256
Figure A4.10. ¹H NMR (400 MHz, CDCl₃) of compound **237**. 257
Figure A4.11. Infrared spectrum (Thin Film, NaCl) of compound **237**. 258
Figure A4.12. ¹³C NMR (101 MHz, CDCl₃) of compound **237**. 258
Figure A4.13. ¹H NMR (500 MHz, CDCl₃) of compound **238**. 259
Figure A4.14. Infrared spectrum (Thin Film, NaCl) of compound **238**. 260
Figure A4.15. ¹³C NMR (125 MHz, CDCl₃) of compound **238**. 260
Figure A4.16. ¹H NMR (500 MHz, CDCl₃) of compound **71**. 261
Figure A4.17. Infrared spectrum (Thin Film, NaCl) of compound **71**. 262
Figure A4.18. ¹³C NMR (125 MHz, CDCl₃) of compound **71**. 262
Figure A4.19. ¹H NMR (500 MHz, CDCl₃) of compound **239**. 263
Figure A4.20. Infrared spectrum (Thin Film, NaCl) of compound **239**. 264
Figure A4.21. ¹³C NMR (125 MHz, CDCl₃) of compound **239**. 264
Figure A4.22. ¹H NMR (400 MHz, CDCl₃) of compound **240**. 265
Figure A4.23. Infrared spectrum (Thin Film, NaCl) of compound **240**. 266
Figure A4.24. ¹³C NMR (101 MHz, CDCl₃) of compound **240**. 266

Figure A4.25. ^1H NMR (400 MHz, C_6D_6) of compound 241	267
Figure A4.26. Infrared spectrum (Thin Film, NaCl) of compound 241	268
Figure A4.27. ^{13}C NMR (101 MHz, C_6D_6) of compound 241	268
Figure A4.28. ^1H NMR (400 MHz, CDCl_3) of compound 242	269
Figure A4.29. Infrared spectrum (Thin Film, NaCl) of compound 242	270
Figure A4.30. ^{13}C NMR (101 MHz, C_6D_6) of compound 242	270
Figure A4.31. ^1H NMR (400 MHz, CDCl_3) of compound 243	271
Figure A4.32. Infrared spectrum (Thin Film, NaCl) of compound 243	272
Figure A4.33. ^{13}C NMR (101 MHz, C_6D_6) of compound 243	272
Figure A4.34. ^1H NMR (500 MHz, CDCl_3) of compound 244	273
Figure A4.35. Infrared spectrum (Thin Film, NaCl) of compound 244	274
Figure A4.36. ^{13}C NMR (101 MHz, CDCl_3) of compound 244	274
Figure A4.37. ^1H - ^{29}Si HSQC NMR (500 MHz, $\text{THF}-d_8$) corresponding to Figure 4.1.....	275

APPENDIX 5

Observation of Unusual, Double Dehydrogenative C–H Silylation Products:

Figure A5.1 ^1H NMR Time Course of the C–H Silylation of N-methylindoline.	279
---	-----

APPENDIX 6

Hydroxide–Catalyzed Dehydrogenative C–H Silylation of Terminal Alkynes:

Figure A6.1 One-Pot Catalytic Geminal Di-Functionalization of Terminal Alkynes.....	294
--	-----

APPENDIX 7

Progress Toward the Synthesis of Illisimonin A:

Figure A7.1 Illisimonin A and Illicium simonsii.	337
Figure A7.2. ^1H NMR (600 MHz, CDCl_3) of compound 291	360
Figure A7.3. Infrared spectrum (Thin Film, NaCl) of compound 291	361
Figure A7.4. ^{13}C NMR (125 MHz, CDCl_3) of compound 291	361
Figure A7.5 ^1H NMR (400 MHz, CDCl_3) of compound 317	362
Figure A7.6 Infrared spectrum (Thin Film, NaCl) of compound 317	363
Figure A7.7 ^{13}C NMR (100 MHz, CDCl_3) of compound 317	363
Figure A7.8 ^1H NMR (400 MHz, CDCl_3) of compound 318	364
Figure A7.9 Infrared spectrum (Thin Film, NaCl) of compound 318	365
Figure A7.10 ^{13}C NMR (100 MHz, CDCl_3) of compound 318	365
Figure A7.11 ^1H NMR (400 MHz, C_6D_6) of compound 334	366
Figure A7.12 Infrared spectrum (Thin Film, NaCl) of compound 334	367
Figure A7.13 ^{13}C NMR (100 MHz, C_6D_6) of compound 334	368

LIST OF SCHEMES

CHAPTER 1

Transition-Metal-Free Catalytic C–H Bond Silylation

Scheme 1.1	Early Example of C–H Silylation Catalyzed by Lewis Acid.....	2
Scheme 1.2	Possible Reaction Pathways for BCl_3 -Catalyzed C–H Silylation	2
Scheme 1.3	Competitive (De)hydrosilylation and Hydrogenation Using Lewis Acid Catalysis	3
Scheme 1.4	$\text{B}(\text{C}_6\text{F}_5)_3$ -Catalyzed Intra/Intermolecular Silylation	5
Scheme 1.5	Proposed Intramolecular Silylation Mechanism.....	6
Scheme 1.6	Attempts Toward Heterocycle Cyclization	7
Scheme 1.7	Proposed Mechanism of $\text{B}(\text{C}_6\text{F}_5)_3$ -Catalyzed C–H Silylation in Aniline-type ...	10
Scheme 1.8	Overview for the Use of Acid as Dehydrosilylation Catalyst.....	13
Scheme 1.9	Early Example of Gas-Phase Direct Silylation by Catalytic Brønsted Base	16
Scheme 1.10	Inspiration for Base-catalyzed C–H Silylation and Final Reaction Overview...	17
Scheme 1.11	Proposed Mechanism for Brønsted Base-Catalyzed Reaction.....	19
Scheme 1.12	Dehydrosilylation of Terminal Alkynes Using Brønsted Base	19
Scheme 1.13	Proposed Mechanism of Base-Catalyzed Direct C–H Silylation of Alkynes....	20
Scheme 1.14	Proposed Mechanism for Intramolecular C–H Silylation	25
Scheme 1.15	Uncatalyzed Radical C–H Silylation/Annulation	25
Scheme 1.16	Overview of KOt-Bu -Catalyzed C–H Silylation	27
Scheme 1.17	Select Examples of Applications of the KOt-Bu -Catalyzed C–H Silylation	29
Scheme 1.18	Overview of Radical Mechanism for C–H Silylation Reaction	29
Scheme 1.19	Overview of Mechanistic Investigations	30
Scheme 1.20	Overview for Ionic Reaction Mechanism	31
Scheme 1.21	Reaction Intermediate Observed by DESI-MS.....	32
Scheme 1.22	Proposed Ionic Mechanism.....	33
Scheme 1.23	Overview of Electron Transfer and Hydride Transfer in Stoltz-Grubbs Silylation System	34
Scheme 1.24	Examples of $\text{C}(\text{sp}^3)$ –H Silylation	35

CHAPTER 2

A Combined Experimental and Computational Mechanistic Study of the KOt-Bu -Catalyzed Dehydrogenative C–H Silylation of Aromatic Heterocycles

Scheme 2.1	C–H Silylation Catalyst Systems	41
Scheme 2.2	Select Examples of KOt-Bu -Catalyzed Cross-Dehydrogenative C–H Silylation Method	42
Scheme 2.3	Reversibility of Silylation Reaction	48

Scheme 2.4	Detection of TEMPO–Silyl Adduct	56
Scheme 2.5	Radical Clock Studies	57
Scheme 2.6	Computed Results of Pentacoordinate Silicate Formation.....	68
Scheme 2.7	Plausible Formation of Pentacoordinate Silicate and Radical Initiation.....	69
Scheme 2.8	Computational Analysis of Key Steps in Pentacoordinate Silicate Radical Initiation	70
Scheme 2.9	Kinetic Isotope Studies	74
Scheme 2.10	Proposed Reaction Mechanism	76
Scheme 2.11	Stereochemical Path of Silicon During Silylation Reaction	78
Scheme 2.12	Base Scrambling of Silicon Center Stereochemistry	79
Scheme 2.13	Key Calculated Energy Barrier for Representative 5-Membered Heterocycles .	84
Scheme 2.14	Synthesis of C3-Cyclopropyl Radical Trap Substrate.....	94
Scheme 2.15	Synthesis of C3-Cyclopropylmethyl Radical Trap Substrate	95
Scheme 2.16	Synthesis of C4-Cyclopropyl Radical Trap Substrate.....	97
Scheme 2.17	Silylation of C3-Cyclopropyl Radical Trap Substrate	98

APPENDIX 3

Alternative Reaction Mechanisms of KOt-Bu-Catalyzed Dehydrogenative C–H Silylation of Aromatic Heterocycles:

Scheme A3.1.	Negative Mode DESI-MS of Silylation Reaction Mixture	210
Scheme A3.2.	Negative Mode DESI-MS of Silylation Reaction Mixture	211
Scheme A3.3.	Negative Mode DESI-MS of Silylation Reaction Mixture	212
Scheme A3.4.	ESI-MS Investigation of Cation- π Complex Formation.....	212
Scheme A3.5.	Proposed Ionic Mechanism	214
Scheme A3.6.	Electron Transfer and Hydrogen Atom Transfer Mechanisms	219

CHAPTER 3

Catalytic C–H Trimethylsilylation of Aromatic Heterocycles via Base Catalysis:

Scheme 3.1	Silylation via Nucleophile Trapping.	225
Scheme 3.2	Reported Examples of Catalytic, C–H Trimethylsilylation.....	227
Scheme 3.3	Base-Catalyzed C–H Trimethylsilylation.	228
Scheme 3.4	KOt-Bu-Catalyzed Silylation Using Me ₃ Si–H.....	229
Scheme 3.5	KOt-Bu-Catalyzed Silylation Using Me ₃ Si–H.....	230
Scheme 3.6	Substrate Scope of C–H Silylation using Me ₃ Si–SiMe ₃	232
Scheme 3.7	Comparison of C–H Silylation using Hydrosilane and Disilanes.....	233
Scheme 3.8	Proposed Mechanism of C–H Silylation using Me ₃ Si–SiMe ₃	235

APPENDIX 5*Observation of Unusual, Double Dehydrogenative C–H Silylation Products:*

Scheme A5.1 Undesired Hydrogenation and Hydrosilylation in C–H Silylation Reactions.	277
Scheme A5.2 Formation of Indoline in KOT-Bu-Catalyzed C–H Silylation of Indole.	277
Scheme A5.3 Unexpected Reactivity in the C–H Silylation of Indoline.	278
Scheme A5.4 Attempted C–H Silylation of Partially Saturated Heterocycles.	278
Scheme A5.5 Proposed Mechanism for the Formation and Reactivity of Indoline.	280

APPENDIX 6*Hydroxide–Catalyzed Dehydrogenative C–H Silylation of Terminal Alkynes:*

Scheme A6.1 C–H Silylation of Terminal Alkynes	286
Scheme A6.2 Hydrosilane Scope of Alkyne Silylation	289
Scheme A6.3 Substrate Scope of Alkyne Silylation	291
Scheme A6.4 Selective Mono and Bis Silylation of Diynes.	292
Scheme A6.5 One-Pot Catalytic Geminal Di-Functionalization of Terminal Alkynes	293

APPENDIX 7*Progress Toward the Synthesis of Illisimonin A:*

Scheme A7.1 Retrosynthetic Analysis of Illisimonin A.	338
Scheme A7.2 Revised Retrosynthetic Analysis of Illisimonin A.	338
Scheme A7.3 Dehydrogenative Generation of Cyclopentadienone.	339
Scheme A7.4 Generation of Cyclopentadienone via Elimination	340
Scheme A7.5 Forward Synthesis of a Model System via Cyclopentadienone Route	340
Scheme A7.6 Challenges in the Cyclopentadienone Route.....	341
Scheme A7.7 Proposed Biosynthesis of Illisimonin A.....	342
Scheme A7.8 Wagner-Meerwein Retrosynthetic Disconnect	343
Scheme A7.9 Retrosynthesis via Benzilic Acid Rearrangement Disconnect.	343
Scheme A7.10 Reported Benzilic Acid Rearrangement in a [2.2.2.] Bicyclic Scaffold.	344
Scheme A7.11 Synthesis of Diels–Alder and Benzilic Acid Model System.	344
Scheme A7.12 Deprotection/Oxidation of Diels–Alder and Benzilic Acid Model System.	345
Scheme A7.13 Forward Synthesis of Diels–Alder and Benzilic Acid Route.	345
Scheme A7.14 Deprotection and/or Oxidation of Catechol Acetal.	346
Scheme A7.15 Competitive Deprotection of Catechol Acetal and Methyl Ether.	347
Scheme A7.16 Protecting Group Strategy for Arene Fragment.	347
Scheme A7.17 Diels–Alder via Oxidative Dearomatization Disconnect.....	348
Scheme A7.18 Rychnovsky Synthesis of Illisimonin A.....	348
Scheme A7.19 Synthesis of Cyclopentenone Diels–Alder Precursor	351
Scheme A7.20 Attempted Oxidation of Model Cyclopentenone Diels–Alder Precursor	352

Scheme A7.21 Synthesis of Model <i>o</i> -Quinone Precursor	353
Scheme A7.22 Deoxygenation of Model <i>o</i> -Quinone Precursor.....	354
Scheme A7.23 Attempted Deprotection/Oxidation of Catechol Acetal	355
Scheme A7.24 Synthesis of Fully Elaborated <i>o</i> -Quinone Precursor.	356
Scheme A7.25 Attempted Oxidation of Fully Elaborated <i>o</i> -Quinone Precursor.	358

LIST OF TABLES

CHAPTER 1

Transition-Metal-Free Catalytic C–H Bond Silylation

Table 1.1	Selected Examples from Reaction Optimization Experiments	4
Table 1.2	FLP-Catalyzed Electrophilic C–H Silylation of Heteroaromatics.....	5
Table 1.3	Optimization and Substrate Scope of Intramolecular Silole Synthesis	6
Table 1.4	One-Pot Hydrosilylation/Dehydrosilylation.....	8
Table 1.5	Scope of Silanes in $B(C_6F_5)_3$ Catalyzed System.....	8
Table 1.6	Substrate Scope of C–H Silylation	9
Table 1.7	Substrate Scope of Disproportionation C–H Silylation.....	11
Table 1.8	Substrate Scope of Double-Silylation Selective Disproportionation C–H Silylation.....	11
Table 1.9	Substrate Scope of Convergent Disproportionation C–H Silylation	12
Table 1.10	Optimization of Acid-Catalyzed Indole Silylation	13
Table 1.11.	Selected Examples of Silane and Substrate Scope	15
Table 1.12.	Optimization of Fluoride-Catalyzed C–H Silylation.....	17
Table 1.13	Substrate Scope of Fluoride-Catalyzed C–H Silylation.....	18
Table 1.14	Base Screen for Dehydrogenative Cross-Coupling of Alkynes and Hydrosilanes	20
Table 1.15	Reaction Optimization and Silane Scope	21
Table 1.16	Comparison of Alkyne Dehydrosilylation Catalysts and Substrate Scope.	22
Table 1.17.	Optimization of Intramolecular C–H Silylation	23
Table 1.18	Selected Substrate Scope of Intramolecular C–H Silylation.....	24
Table 1.19	Optimization of Reductive Aryl Ether Cleavage.....	26
Table 1.20	Selected Examples from Optimization of C–H Silylation	27
Table 1.21	Representative Substrate Scope of the $KOt\text{-}Bu$ -Catalyzed C–H Silylation Reaction	28

CHAPTER 2

A Combined Experimental and Computational Mechanistic Study of the $KOt\text{-}Bu$ -Catalyzed Dehydrogenative C–H Silylation of Aromatic Heterocycles

Table 2.1	Investigation of Silylation Catalysts	44
Table 2.2	Investigation of Silylation Product Distribution.....	47
Table 2.3	Radical Generation via Amine Additives	61
Table 2.4	Radical Initiation via <i>tert</i> -Butoxy Radicals	62
Table 2.5	Shift of Si–H IR Feature in Select Base Catalyst Mixtures	67

CHAPTER 3*Catalytic C–H Trimethylsilylation of Aromatic Heterocycles via Base Catalysis:***Table 3.1** Optimization of C–H Silylation using Me₃Si–SiMe₃. 231**APPENDIX 6***Hydroxide–Catalyzed Dehydrogenative C–H Silylation of Terminal Alkynes:***Table A6.1** Reaction Optimization..... 287**Table A6.2** Select Mechanistic Investigation Studies of Terminal Alkyne Silylation 295*Notebook Cross-Reference for New Compounds***Table A8.1** Notebook cross-reference for compounds in Chapter 2 371**Table A8.2** Notebook cross-reference for compounds in Chapter 3 372**Table A8.3** Notebook cross-reference for compounds in Appendix 7 373

LIST OF ABBREVIATIONS

°C	degrees Celsius
Å	Ångstrom
Ac	acetyl
AcOH	acetic acid
APCI	atmospheric pressure chemical ionization
app	apparent
aq	aqueous
Ar	aryl
atm	atmosphere
Bn	benzyl
Boc	<i>tert</i> -butyloxycarbonyl
bp	boiling point
br	broad
Bu	butyl
Bz	benzoyl
<i>c</i>	concentration for specific rotation measurements (g/100 mL)
ca.	about (Latin <i>circa</i>)
CAN	ceric ammonium nitrate
calc'd	calculated
cat	catalytic
cm ⁻¹	wavenumber(s)
Cp	cyclopentadienyl
Cy	cyclohexyl
d	doublet
D	deuterium
DCE	1,2-dichloroethane

DDQ	2,3-dichloro-5,6-dicyano- <i>p</i> -benzoquinone
DFT	density functional theory
DME	1,2-dimethoxyethane
DMF	<i>N,N</i> -dimethylformamide
DTBP	Di- <i>tert</i> -butyl peroxide
e.g.,	for example (Latin exempli gratia)
EI+	electron impact
EPR	electron paramagnetic resonance
equiv	equivalent(s)
ESI	electrospray ionization
Et	ethyl
EtOAc	ethyl acetate
EWG	electron withdrawing group
FAB	fast atom bombardment
g	gram(s)
GC	gas chromatography
gCOSY	gradient-selected correlation spectroscopy
h	hour(s)
HMBC	heteronuclear multiple bond correlation
HMPA	hexamethylphosphoramide
HPLC	high-performance liquid chromatography
HRMS	high-resolution mass spectroscopy
HSQC	heteronuclear single quantum correlation
Hz	hertz
<i>i</i> -Pr	isopropyl
i.e.,	that is (Latin id est)
IPA	isopropanol, 2-propanol
IR	infrared (spectroscopy)
<i>J</i>	coupling constant

K	Kelvin(s) (absolute temperature)
KC ₈	potassium intercalated graphite
kcal	kilocalorie
KHMDS	potassium hexamethyldisilazide
KIE	kinetic isotope effect
L	liter; ligand
LDA	lithium diisopropylamide
LG	leaving group
lit.	literature value
m	multiplet; milli
<i>m</i>	meta
M	metal; molar; molecular ion
<i>m/z</i>	mass-to-charge ratio
Me	methyl
mg	milligram(s)
MHz	megahertz
min	minute(s)
MM	mixed method
mol	mole(s)
MOM	methoxymethyl acetal
mp	melting point
Ms	methanesulfonyl (mesyl)
MS	molecular sieves
n	nano
N	normal
<i>n</i> -Bu	butyl
NBS	<i>N</i> -bromosuccinimide
NMR	nuclear magnetic resonance
Nu	nucleophile

<i>o</i>	ortho
<i>p</i>	para
Pd/C	palladium on carbon
Ph	phenyl
pH	hydrogen ion concentration in aqueous solution
Pin	2,3-dimethylbutane-2,3-diol (pinacol)
Piv	trimethylacetyl, pivaloyl
p <i>K_a</i>	p <i>K</i> for association of an acid
ppm	parts per million
PPTS	pyridinium <i>p</i> -toluenesulfonate
Pr	propyl
Py	pyridine
q	quartet
R	generic for any atom or functional group
Ref.	reference
<i>R_f</i>	retention factor
s	singlet or strong or selectivity factor
sat.	saturated
t	triplet
<i>t</i> -Bu	<i>tert</i> -butyl
TBDPS	<i>tert</i> -butyldiphenylsilyl
TBHP	<i>tert</i> -butyl hydroperoxide
TBME	<i>tert</i> -butyl methyl ether
TBS	<i>tert</i> -butyldimethylsilyl
TES	triethylsilyl
TFA	trifluoroacetic acid
THF	tetrahydrofuran
TIPS	triisopropylsilyl
TLC	thin-layer chromatography

TMS	trimethylsilyl
TOF	time-of-flight
Tol	tolyl
t_R	retention time
Ts	<i>p</i> -toluenesulfonyl (tosyl)
UV	ultraviolet
v/v	volume to volume
w	weak
w/v	weight to volume
X	anionic ligand or halide
λ	wavelength
μ	micro

CHAPTER 1

Transition-Metal-Free Catalytic C–H Bond Silylation [†]

1.1 INTRODUCTION

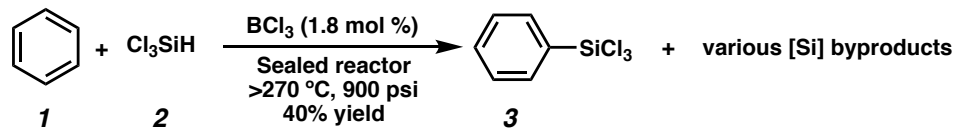
Although transition-metal-free catalytic C–H silylation has been known for some time (Section 1.2.1) it has only recently been heavily investigated. We begin by describing an early example of catalytic, transition-metal-free C–H silylation before discussing to the current state of this field.

1.2 Lewis Acid Catalysis

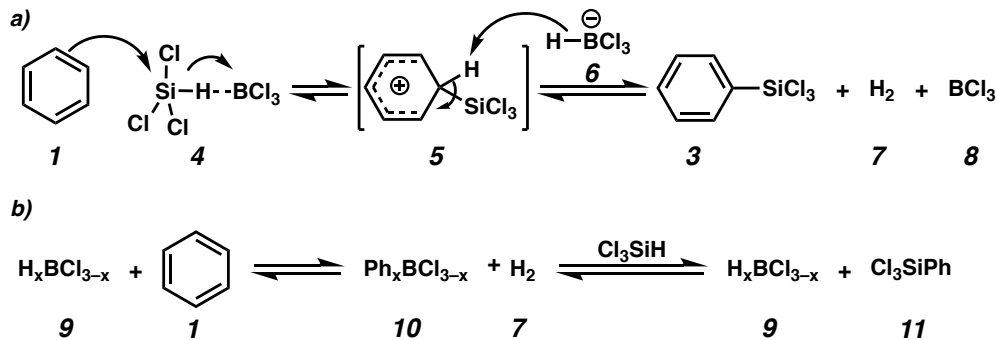
1.2.1 BCl_3 Catalyst

In the late 1950s, one of the earliest relevant examples of such reactivity involving the BCl_3 -catalyzed C–H silylation of benzene was reported by Dow Chemists (Scheme 1.1).^{1,2,3,4}

[†] This work was performed in collaboration with Prof. W.-B. Liu and Prof. N. Nesnas. Portions of this chapter have been reproduced with permission from Schuman, D. P.; Liu, W.-B.; Nesnas, N.; Stoltz, B. M. Transition-Metal-Free Catalytic C–H Bond Silylation. In *Organosilicon Chemistry: Novel Approaches and Reactions*; Hiyama, T., Oestreich, M., Eds.; Wiley-VCH: Weinheim, Germany, 2019; Chapter 7, pp. 213–239. ISBN: 978-3-527-34453-6. © Wiley-VCH Verlag GmbH & Co. KGaA. Reproduced with permission.

Scheme 1.1 Early Example of C–H Silylation Catalyzed by Lewis Acid

While this reaction demonstrates a direct C–H silylation, the very forcing reaction conditions significantly limit the scope of this chemistry. Furthermore, the authors showed that in a matter of hours, the reaction reaches equilibrium of starting material, product, and various silane-containing byproducts. Further investigations indicated that this reaction might proceed through a Friedel–Crafts-type pathway (Scheme 1.2a) or through compound **10** via an initial borylation, followed by a phenyl group transfer (Scheme 1.2b).

Scheme 1.2 Possible Reaction Pathways for BCl_3 -Catalyzed C–H Silylation

Later publications by the same researchers included only limited mechanistic investigations, but these studies indicated neither nucleophilic aromatic substitution nor radical pathways were the operative mechanism in this unusual reactivity.³

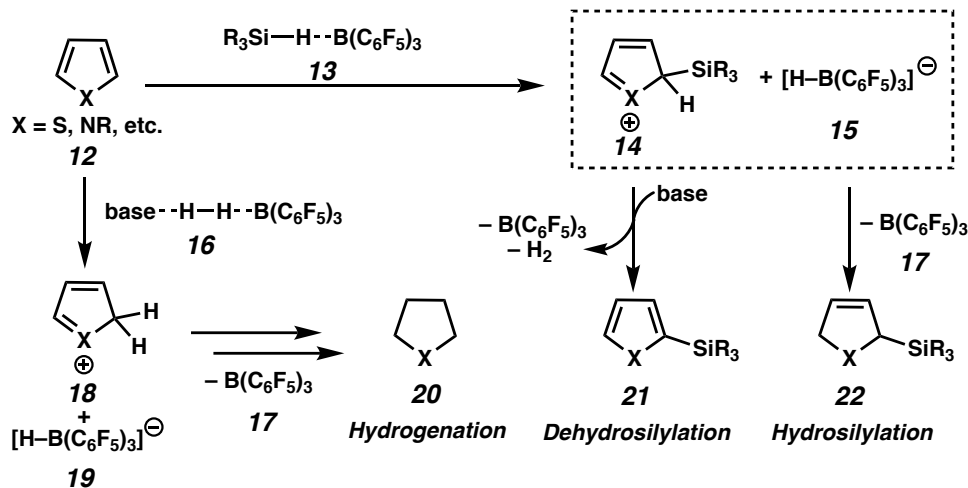
This report of Lewis acid-catalyzed C–H silylation highlights a number of key challenges in the development of such a method. The catalyst can often activate both the [Si]–H bond in the starting material and the [Si]–C bond in the resulting product. Furthermore, the forcing conditions (i.e., high temperature and pressure) exacerbate the

issue of selective bond activation and limit functional group compatibility. Thus, future studies would need to address these issues for higher selectivity and yield.

1.2.2. $\mathbf{B(C_6F_5)_3}$, A “Frustrated” Lewis Acid Catalyst

Bulky Lewis acids have been shown to activate a variety of Si–H and H–H bonds via the formation of frustrated Lewis pairs (FLP).⁵ A recent report from Ingleson detailed the reaction of heterocycles with hydrosilanes activated by $\mathbf{B(C_6F_5)_3}$ (**17**, Scheme 1.3).⁶ The $\mathbf{B(Ar)_3}$ –hydrosilane FLP **13** can go on to react with substrate **12** with the possible products of hydrogenation (**20**), dehydrosilylation (**21**), and hydrosilylation (**22**).

Scheme 1.3 Competitive (De)hydrosilylation and Hydrogenation Using Lewis Acid Catalysis



A significant challenge in this reaction is ensuring a rapid deprotonation of the arenium cation **14** to avoid hydrosilylation (**14** to **22**). Hydrogen gas must be evolved to render the reaction catalytic but the electrophilic reaction intermediates (**14**, **18**) and Lewis acid catalyst (**17**) necessitates the use of a suitably bulky, yet weakly nucleophilic base. The resulting buildup of hydrogen may lead to competitive hydrogen activation via **16** and substrate hydrogenation to afford **20**. Toward this end, the authors found 2,6-dichloropyridine ($\text{Cl}_2\text{-py}$) to be a suitable base for the silylation of 2-methylthiophene.

While the authors rendered the reaction catalytic in both Lewis acid and base, the reaction always proceeds with the formation of hydrogenated and/or hydrosilylated byproducts **25** (Entries 2–5, Table 1.1). The buildup of such byproducts was shown to be detrimental to the reaction as the inclusion of tetrahydrothiophene inhibits product formation (Entry 6), likely due to competitive coordination of tetrahydrothiophene to the Lewis acid catalyst. Efforts to limit the hydrogenation pathway by conducting the reaction under static vacuum results in decreased overall yield (Entry 1 versus Entry 7). The authors further demonstrated the reaction scope using an *N*-protected indole substrate **26** (Table 1.2), though the same issue of competitive reduction (hydrogenation only, in the case of indole substrates) limited overall utility of this method.

Table 1.1 Selected Examples from Reaction Optimization Experiments

23			24	25
	B(C₆F₅)₃	Cl₂-py		R R = H, SiPh ₃
1	100	100	51	33
2	20	20	56	34
3	5	5	42	18
4	5	100	51	27
5 ^a	5	5	46	32
6 ^b	100	100	0	0
7 ^c	100	100	33	unreported

[a] 1.5 equiv silane used. [b] 1 equiv tetrahydrothiophene added.

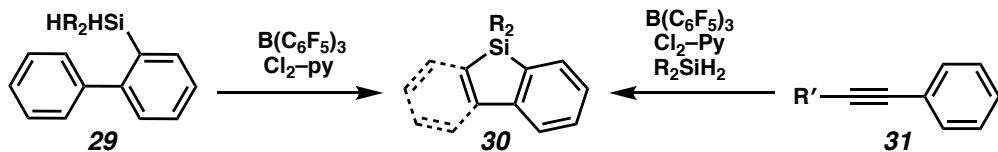
[c] Conducted under vacuum.

Table 1.2 FLP-Catalyzed Electrophilic C–H Silylation of Heteroaromatics

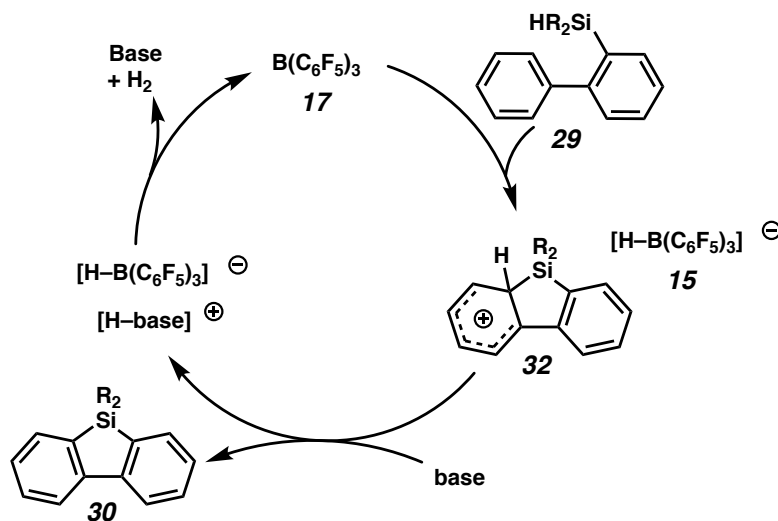
Entry	$B(C_6F_5)_3$ (mol %)	$Cl_2\text{-py}$ (mol %)	27 (% yield)	28 (% yield)
1	100	100	59	19
2	100	0	30	21

The report by Ingleson demonstrated an initial investigation into Lewis acid-catalyzed C–H silylation and documents many of the challenges present in such a reaction manifold.

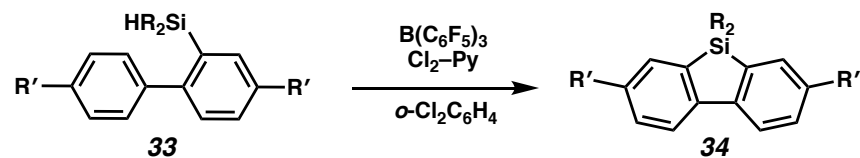
A following report, again from the lab of Ingleson, demonstrated that a biphenyl-silyl scaffold undergoes intramolecular C–H silylation with a Lewis acid/base catalyst system (Scheme 1.4, left).⁷ They were also able to effect a tandem hydrosilylation, dehydrosilylation procedure to form cyclized product **30** from aryl alkyne starting material **31** (Scheme 1.4, right).

Scheme 1.4 $B(C_6F_5)_3$ -Catalyzed Intra/Intermolecular Silylation

The authors proposed a mechanistic cycle that begins with Lewis acid activation of the pendant silane and nucleophilic attack by the aryl ring to afford cationic intermediate **32**. This intermediate is deprotonated by base to regenerate aromaticity in product **30**, while the protonated base can go on to react with Lewis acid complex **15** to generate hydrogen gas and regenerate both base and Lewis acid catalyst **17** (Scheme 1.5).

Scheme 1.5 Proposed Intramolecular Silylation Mechanism

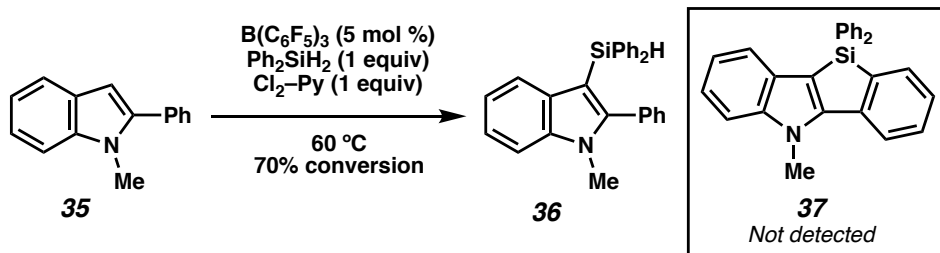
Based on the observations in their previous studies,⁶ the authors hypothesized that the use of biphenyl-silyl scaffold **29** would limit undesired reduction by biasing the system toward rearomatization of the silolane product (**32** to **30**) as shown in their proposed mechanism (Scheme 1.5). The authors were able to realize this strategy, render the reaction catalytic, and apply their optimized conditions toward the synthesis of a variety of substituted siloles (**34**) (Table 1.3).

Table 1.3 Optimization and Substrate Scope of Intramolecular Silole Synthesis

Entry	R	R'	$\text{B}(\text{C}_6\text{F}_5)_3$ (mol %)	$\text{Cl}_2\text{-py}$ (mol %)	t (h)	T (°C)	Yield (%)
1	Ph	H	100	100	18	60	99
2	Ph	H	10	10	24	100	99
3	Ph	H	5	5	96	100	99
4	Ph	H	10	0	168	100	50
5	Ph	t-Bu	5	5	5	100	99
6	i-Bu	H	5	5	96	100	96

Unfortunately this methodology did not translate to the cyclization of heterocyclic substrates **35** (Scheme 1.6). Instead of forming the desired silole product **37**, only the initial C–H silylation product **36** was detected. Through further experimentation, the authors believe the catalyst was entirely consumed in an off cycle hydrogen FLP process and therefore could not affect the ring closing cyclization.

Scheme 1.6 Attempts Toward Heterocycle Cyclization

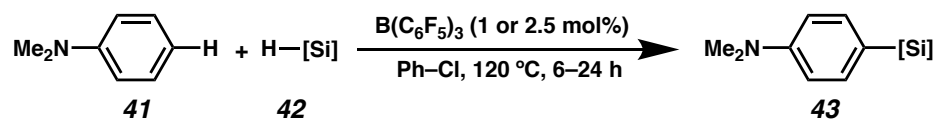


Interestingly, the authors were able to design a tandem one-pot hydrosilylation/dehydrosilylation procedure in order to convert internal alkynes **38** to silaindenes **40** (Table 1.4). This reaction proceeds through an initial alkyne hydrosilylation, which may occur in either a *syn* or *trans* process leading to *trans*- and/or *cis*-**39**. Only *cis*-**39** can proceed to form the silole product **40**. While this chemistry provided an intriguing application of the $\text{B}(\text{C}_6\text{F}_5)_3/\text{Cl}_2\text{-py}$ system, competing reduction pathways and catalyst inhibition remained a major limitation.

Table 1.4 One-Pot Hydrosilylation/Dehydrosilylation

Entry	$B(C_6F_5)_3$ (mol %)	t (h)	cis (%)	trans (%)	$Cl_2\text{-py}$ (mol %)	t (h)	yield (%)
1	100	5	84	16	100	72	84
2	5	5	85	15	5	48	23
3	5	4	84	16	100	72	70
4	5	-	-	-	100	72	50

Given these limitations, it was surprising when the Hou group recently reported an aromatic C–H silylation using $B(C_6F_5)_3$ alone, with no added base and a relatively broad scope (Table 1.5 and 1.6).^{8,9} This reaction tolerates a variety of hydrosilanes **42**, including chlorosilanes (entries 11, 12), furnishing the dehydrosilylated product in moderate to good yields (Table 1.5).

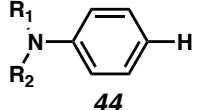
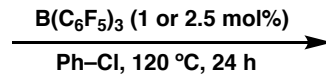
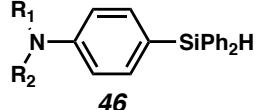
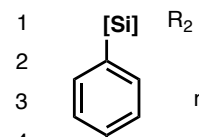
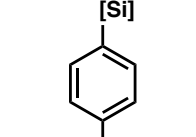
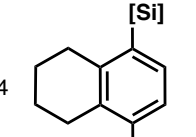
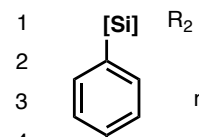
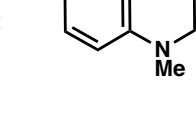
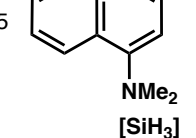
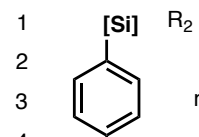
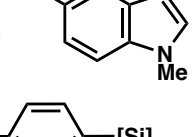
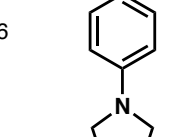
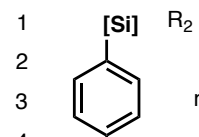
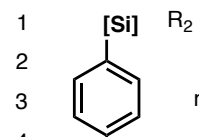
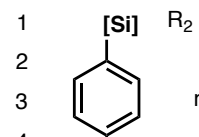
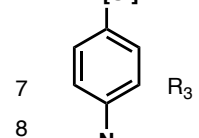
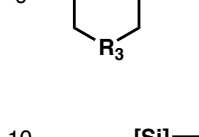
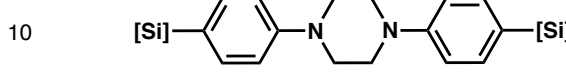
Table 1.5 Scope of Silanes in $B(C_6F_5)_3$ Catalyzed System

Entry	Silane	Yield (%)	Entry	Silane	Yield (%)
1	Ph_2SiH_2	84	7	$n\text{-}Bu_3SiH$	61
2	$PhSiH_3$	80	8	$PhMe_2SiH$	85
3	$PhMeSiH_2$	82	9	Ph_2MeSiH	80
4	Et_2SiH_2	65	10	Ph_3SiH	67
5	$EtMe_2SiH$	68	11	Ph_2SiClH	51 ^a
6	Et_3SiH	60	12	$PhSiClH_2$	70 ^a

[a] Yield over two steps

Turning to the matter of substrate scope, a variety of anilines and *N*-aryl substrates are able to undergo C–H silylation exclusively at the *para*- (relative to nitrogen) position (Table 1.6).

Table 1.6 Substrate Scope of C–H Silylation

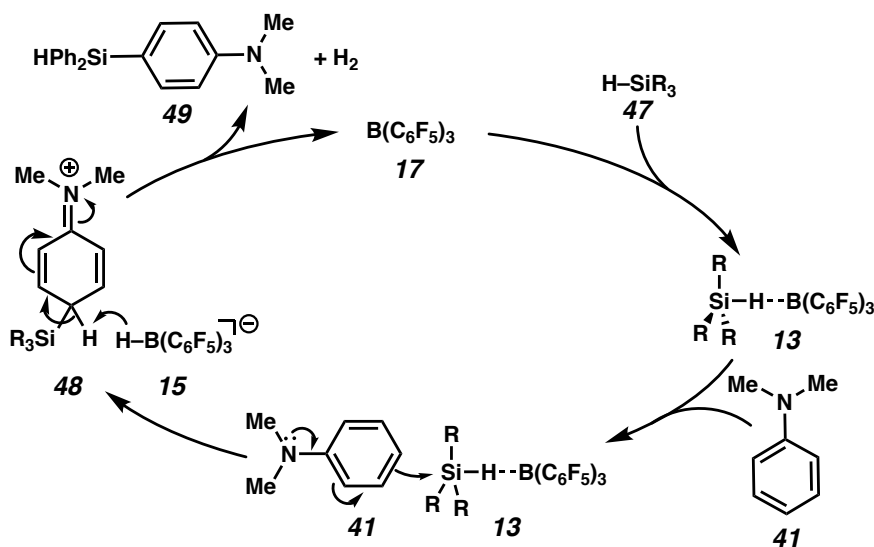
 + 								
Entry	Product	Yield (%)	Entry	Product	Yield (%)	Entry	Product	Yield (%)
1		R ₂ = Et 82%	11		71%	14		90%
2		i-Pr 81%	12		72%	15		45%
3		n-C ₆ H ₁₃ 80%	13		34%	16		86%
4		TMS 78%						
5		allyl 75%						
6		Ph 41%						
7		R ₃ = CH ₂ 90%						
8		O 73%						
9		NMe 73%						
10		81%						

The authors noted the interesting C-5 silylation of *N*-methylindole (Table 1.6, Entry 13), which is difficult to access using other silylation reactions, but did not provide rationale as to why C-5 silylation is favored over C-3 silylation.

While a thorough mechanistic study was not undertaken, the authors proposed a mechanism based on the current literature of B(C₆F₅)₃-catalyzed silylation (Scheme 1.7). The hydrosilane forms the activated FLP **13**, which is attacked by the electron-rich arene **41**. The resulting Wheland intermediate (**48**) is deprotonated by [H–B(C₆F₅)₃][–] (**15**) to

form the silylated product **49**, hydrogen gas, and regenerate the catalyst **17**. This specific reaction does not require exogenous base or result in reduction products (i.e., hydrosilylation and hydrogenation) that plague similar systems discussed here. One can postulate that the electron-rich nature of the substrate may play a role or that the tertiary amine substrate itself may act as a base during the reaction, in a stepwise deprotonation/hydrogen release mechanism.

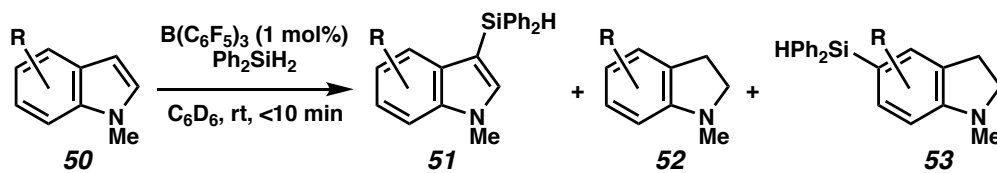
Scheme 1.7 Proposed Mechanism of $B(C_6F_5)_3$ -Catalyzed C–H Silylation in Aniline-type



A following report by Zhang and coworkers describes similar reactivity to that of Ingleson and Hou.¹⁰ Zhang does not initially aim to reduce the hydrogenation byproduct often observed in these types of silylation reactions, but instead uses this to help drive the reaction to completion in a type of disproportionation reaction (**52** and **53**, Table 1.7). While the silylated product yields are limited to 50% of the starting material, a variety of indole substrates (**51**) were shown to undergo silylation in good relative yields. The reactions are complete in short periods of time and, by modifying the reaction conditions, can be used to form double C–H silylation products (**54**, Table 1.8). The authors show

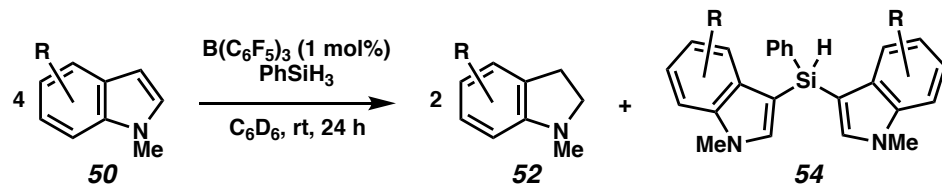
NMR studies and a proposed mechanism that is in line with the previous FLP mechanisms discussed earlier.

Table 1.7 Substrate Scope of Disproportionation C–H Silylation



Entry	R =	Equiv Ph_2SiH_2	Yield 51 (%)	Yield 52 (%)	Yield 53 (%)
1	H	0.5	43	45	2
2	5-Me	0.5	49	48	0
3	6-Br	0.5	48	47	1
4	6-F	0.5	41	42	12
5	5-Ph	0.5	45	47	0
6	H	2	41	41	18
7	5-Me	2	49	49	0
8	6-Br	2	44	46	9
9	6-F	2	20	26	52
10	5-Ph	2	49	49	0

Table 1.8 Substrate Scope of Double-Silylation Selective Disproportionation C–H Silylation



Entry	R =	Yield 52 (%)	Yield 54 (%)
1	H	45	44
2	5-Me	43	45
3	6-Br	46	44
4	6-F	43	37
5	5-Ph	49	43

Zhang was able to render this reaction a convergent disproportionation, where the indoline formed in the reaction (52) is reoxidized to indole (51) and can reenter the catalytic cycle (Table 1.9). While this did require significant heating compared to the

disproportionation reaction, the reaction yields significantly increased. This method is specific to indole substrates but the authors were able to solve many of typical issue associated with using a FLP silylation catalyst.

Table 1.9 Substrate Scope of Convergent Disproportionation C–H Silylation

Entry	R =	Silane ^a	Time (h)	Yield 51 (%)
1	H	Ph ₂ MeSiH	2.5	86
2	H	Ph ₃ SiH	9	94
3	5-Me	Ph ₂ SiH ₂	48	69
4	5-Me	Ph ₃ SiH	2.5	93
5	5-Me	Ph ₂ MeSiH	2.5	95
6	5-F	Ph ₃ SiH	2.5	92
7	5-Cl	Ph ₃ SiH	2.5	91
8	5-Br	Ph ₃ SiH	2.5	83
9	5-Ph	Ph ₃ SiH	2.5	99

[a] 2 equiv silane used

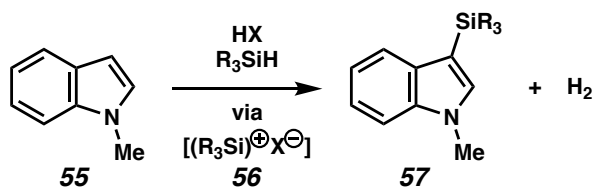
1.2.3 Lewis Acid Conclusions

While Lewis acid catalysis provides a rapid and simple method for the activation of [Si]–H bonds, challenges exist in this mode of reactivity. Reduction via hydrogen activation or hydrosilylation can compete with product formation and potentially lead to catalyst poisoning. Nevertheless, this reaction manifold remains an interesting and evolving area in transition-metal-free C–H silylation chemistry.

1.3 Brønsted Acid

Hydrosilanes may also be activated by protonation and subsequent loss of hydrogen to generate an activated silyl cation intermediate **56** (Scheme 1.8), which can then be trapped by a nucleophilic substrate in a manner similar to Lewis acid catalysis (Section 1.2). Inspired by stoichiometric examples of such reactions, the Oestreich group sought to develop a catalytic C–H silylation variant.¹¹ They were successful in utilizing a Brønsted acid for the catalytic C–H silylation of aromatic heterocycles.

Scheme 1.8 Overview for the Use of Acid as Dehydrosilylation Catalyst



During reaction optimization, they observed degradation of the silane using TfOH and settled on the use of Brookhart's acid, $\{[\text{H(OEt}_2)_2]^\oplus[\text{BAr}^F_4]^\ominus\}$ (**58**), for further optimization studies (Table 1.10).

Table 1.10 Optimization of Acid-Catalyzed Indole Silylation

c1ccc2c(c1)nc3ccccc3N2Me **55** $\xrightarrow[\text{Brookhart's Acid, Me}_2\text{PhSiH, nbe}]{\text{Ph-Me, 80 }^\circ\text{C, 18 h}}$ c1ccc2c(c1)nc3ccccc3N2Me **57**

Entry	58 (mol %)	nbe (equiv)	Yield (%)
1	-	-	NR
2 ^b	1	-	NR
3	1	-	70
4	2	-	77
5	4	-	53
6	2	0.5	85
7	2	1	95
8	1	1	97

[a] 2 equiv substrate, 1 equiv silane [b] NaBArF₄ used as catalyst

The control reaction demonstrates the $[\text{BAr}^{\text{F}}_4]^-$ counter ion displayed no catalytic activity alone (Entry 2, Table 1.10). Interestingly, the inclusion of norbornene (nbe) and lowering the catalyst loading both led to increased yield (Entries 6–8). In this reaction, norbornene may act as a proton scavenger, and together with lower catalyst loadings, help to balance proton removal from the reaction intermediate with hydrogen release. Both of these processes could serve to limit the overall proton concentration in solution, thus inhibiting protodesilylation of the product.

The reaction scope in both silane and substrate was investigated (Table 1.11). Mono- and di-phenylsilanes (Entries 1, 2, and 6) afford good yields of the corresponding silylated products, but tris-phenyl (Entry 3), tris- $\text{C}(\text{sp}^3)$ alkyl (Entry 4) and dialkoxysilanes (Entry 5) all performed poorly. Aryl halides, Nitrogen-containing heterocycles, and anilines undergo silylation smoothly, however, oxygen- and sulfur-containing heterocycles or anisoles did not react under these conditions. Furthermore, the reaction does not tolerate substitution at the site of reactivity (i.e., C-3 of indole or *para* of aniline).

Table 1.11. Selected Examples of Silane and Substrate Scope

Entry	Product	Yield (%)	Entry	Product	Yield (%)
1	[Si] = Me ₂ PhSi	96	12	Me N—C ₆ H ₄ —SiPh ₂ H	67
2	MePh ₂ Si	93	13	C ₆ H ₅ N—C ₆ H ₄ —SiPh ₂ H	66
3	Ph ₃ Si	8	14	SiPh ₂ H C ₆ H ₅ N—Bn	58
4	Et ₃ Si	7	15	C ₆ H ₅ N—C ₆ H ₄ —SiPh ₂ H	75
5	(EtO) ₂ MeSi	0			
6	Ph ₂ SiH	96			
7	R = Me	94			
8	F	98			
9	Cl	96			
10	BrH	96			
11 ^b	Ph Me Si—C ₆ H ₄ —C ₆ H ₄ —Si—Me	73			
Unreactive substrates					
	Me N—C ₆ H ₄ —Me		MeO—C ₆ H ₄		
			X = O, S		

[a] 2 equiv substrate, 1 mol % **58**, 1 equiv [Si]–H, 1 equiv nbe, PhMe, rt to 80 °C, 18 h
[b] 3 equiv N-methylindole (**55**) used

While only a single transition-metal-free catalytic example has been reported, the use of Brønsted acids as a C–H silylation catalyst provides an interesting and orthogonal route compared to other methods. Unfortunately, this class of catalyst faces limited substrate scope and functional group compatibility, but may continue to develop as a C–H silylation methodology.

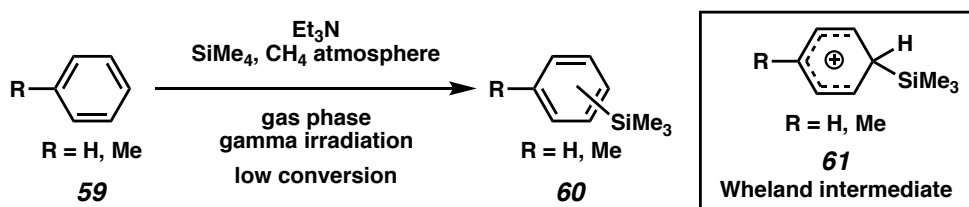
1.4. Brønsted Base

1.4.1 Early Example of Catalytic C–H Silylation by Brønsted Base

Taking the term “catalytic” in a broader sense allows us to present an interesting publication from Fornarini involving gas-phase, mechanistic investigations of silyl

cations and aromatic nucleophiles in the presence of catalytic base (Scheme 1.9).¹² The author proposed Wheland intermediate **61** can be accessed by the reaction of arenes with silyl cations generated by irradiation. Depending on the base identity or concentration used, the base could engage the activated silyl group of the Wheland intermediate **61**, resulting in a formal desilylation event and reforming starting material **59**. Alternatively, the base could deprotonate the Wheland intermediate to form the silylated product **60**. While this report is not of particular synthetic relevance, it provides an interesting mechanistic and initial study for C–H silylation by Brønsted bases.

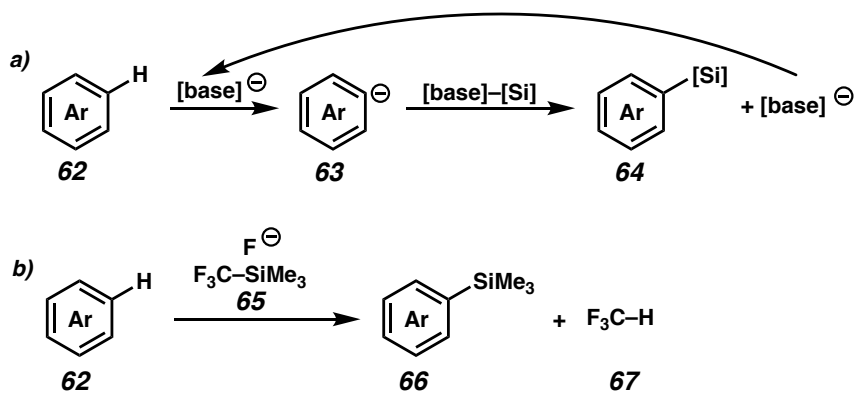
Scheme 1.9 Early Example of Gas-Phase Direct Silylation by Catalytic Brønsted Base



1.4.2 Fluoride/Base Catalysis

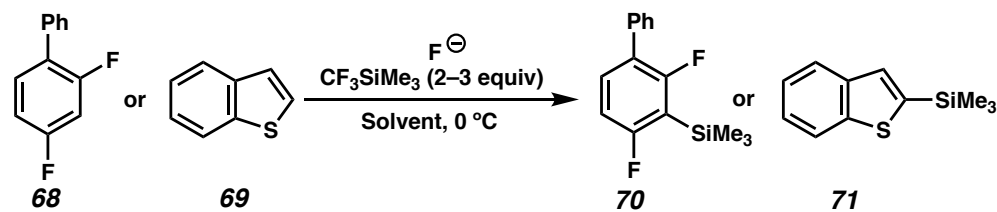
An intriguing base-catalyzed C–H silylation method was proposed by Kondo, whereby suitable choice of an activating reagent and leaving group on silicon could result in the generation of base upon addition of a nucleophile to silicon (Scheme 1.10a).^{13,14} The authors achieved the desired reactivity using a fluoride base as the initiator and the Ruppert–Prakash reagent (**65**) as the tethered base and silylating agent (Scheme 1.10b).

Scheme 1.10 Inspiration for Base-catalyzed C–H Silylation and Final Reaction Overview



A variety of fluoride salts were found to afford the C–H silylation product (Entries 1–4, Table 1.12) and the reaction performs well using 1,3-dimethyl-2-imidazolidinone (DMI) or 1,2-dimethoxyethane (DME) as a solvent (Entries 8 and 11 versus 10). Further investigation showed the reaction is rapid and results in high product yields after only a few hours (Entries 9 versus 8 and 6 versus 3).

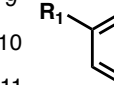
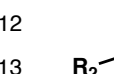
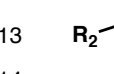
Table 1.12. Optimization of Fluoride-Catalyzed C–H Silylation



Entry	Substrate	Fluoride (mol %)	Solvent	Time (h)	Yield (%)
1	69	KF (50)	DMI	24	51
2	69	RbF (50)	DMI	24	86
3	69	CsF (50)	DMI	24	83
4	69	(Me ₄ N)F (50)	DMI	24	trace
5	69	–	DMI	24	0
6	69	CsF (50)	DMI	2	97
7	68	CsF (50)	DMI	2	100
8	68	CsF (20)	DMI	2	100
9	68	CsF (10)	DMI	2	50
10	68	CsF (20)	DMF or Ph-Me	2	0
11	68	CsF (20)	DME	2	86
12	68	CsF (20)	DME	1	90

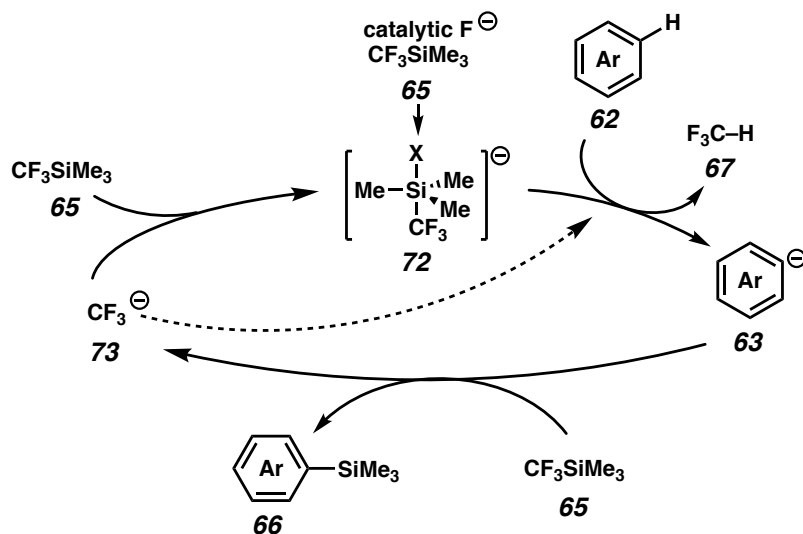
With these optimized conditions in hand, the authors demonstrated that a number of heterocyclic and substituted aromatic compounds could undergo silylation in good to excellent yields (Table 1.13). Aryl halides were well tolerated (Entries 4, 5, 11, and 12) as well as both electron donating (Entry 2) and withdrawing groups (Entries 6–8, 10, and 13).

Table 1.13 Substrate Scope of Fluoride-Catalyzed C–H Silylation

Entry	Product	Yield (%)	Entry	Product	Yield (%)	
1	R = H	85	9	R ₁ –  – S	R ₁ = Me	81
2	OMe	71	10	 – S	CN	60
3	Me	57	11	 – S	Br	91
4	Br	100	12	 – O	R ₂ = I	46
5	I	71	13	 – O	CN	84
6	CN	75	14		CO ₂ Et	0
7	NO ₂	76				
8	C(O)NMe ₂	71				

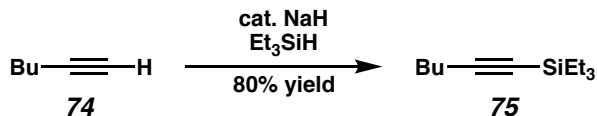
See Refs. 11 and 12 for conditions

The authors proposed a mechanism based on their mechanistic studies of the present system, combined with their previous studies of similar in situ generation of reactive bases (Scheme 1.11).¹⁵ The reaction begins by initial generation of a pentacoordinate silicon **72** (X = F) from the [F⁻] catalyst, which produces a [CF₃⁻]-equivalent **72** to deprotonate the arene **62**. The resulting anion **63** proceeds to react with the Ruppert–Prakash reagent (**65**) resulting in the silylated product **66** and CF₃⁻ (**73**). It is possible that the CF₃⁻ anion (**73**) directly deprotonates the arene **62** (Scheme 1.11, dashed line) thereby completing the catalytic reaction or the CF₃⁻ anion (**73**) may form a pentacoordinate silicate **72** (X = CF₃) and complete the cycle as drawn. Although the authors were able to detect CF₃H during the catalytic reaction, further mechanistic study is required to determine these final steps of the reaction mechanism.

Scheme 1.11 Proposed Mechanism for Brønsted Base-Catalyzed Reaction

1.4.3 Brønsted Base-Catalyzed C–H Silylation of Alkynes

Direct dehydrogenative, C–Si bond formation may be achieved by deprotonation of an alkyne with a Brønsted base, followed by electrophilic trapping of the alkynyl carbanion with a silane. This process may be rendered catalytic if the pentacoordinate silicate intermediate acts as a base to deprotonate another equivalent of the starting alkyne. In 1969, such an example was reported by Calas and Bourgeois, wherein NaH is used as a catalyst for the dehydrogenative C–H silylation of 1-hexyne (**74**) and Et_3SiH , however, this was the only example disclosed (Scheme 1.12).¹⁶

Scheme 1.12 Dehydrosilylation of Terminal Alkynes Using Brønsted Base

Further independent studies by the research groups of Itoh and Ono found that heterogeneous Brønsted bases (i.e., MgO , $\text{KNH}_2/\text{Al}_2\text{O}_3$, and $\text{KF}/\text{Al}_2\text{O}_3$), alkali metal

hydrides, metal alkoxides, alkylmetals, and metal amides could all affect C–H silylation (Table 1.14).^{17,18,19,20,21,22}

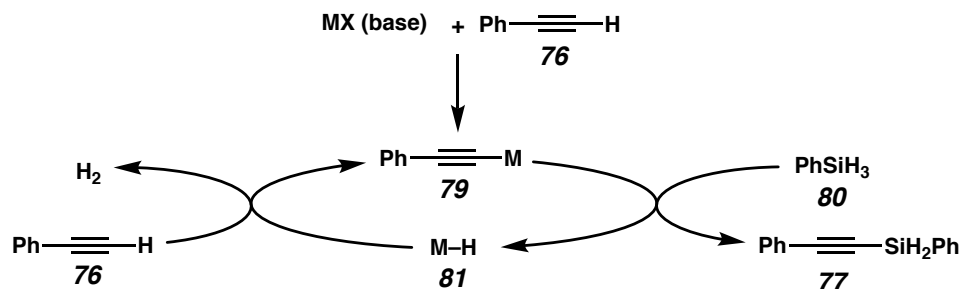
Table 1.14 Base Screen for Dehydrogenative Cross-Coupling of Alkynes and Hydrosilanes

Entry	Catalyst	mol %	Solvent	Yield (%)	
				77	78
1 ^a	MgO	> 400	benzene	43	24
2 ^b	LiAlH ₄	5	diglyme (120 °C)	42	9
3 ^c	LiOEt	0.5	diglyme	34	6
4 ^c	NaOEt	0.6	diglyme/THF (10/1)	46	18
5 ^c	KOEt	0.7	diglyme/Et ₂ O (10/1)	6	<1
6 ^c	Ba(OMe) ₂	0.5	diglyme	49	25
7 ^c	Ba(OC ₈ H ₁₇) ₂	0.6	toluene (40 °C)	73	6
8 ^c	n-BuLi	0.6	diglyme	40	7
9 ^c	PhLi	0.7	diglyme	45	10
10 ^c	Ba(CCPPh) ₂	0.4	diglyme	54	30
11 ^c	LiN(SiMe ₃) ₂	0.6	diglyme	43	13

[a] See Ref. 16 [b] See Ref. 17 [c] See Ref. 18

Preliminary mechanistic investigations conducted by Itoh supported an ionic reaction pathway (Scheme 1.13). Deprotonation of the terminal alkyne by strong base generates a metal acetylide, which can then react with the hydrosilane to form the desired product and a metal hydride, thereby completing the catalytic cycle. (Note that in this reaction the deprotonation may occur from a pentacoordinate silicate similar to that in Scheme 1.11, rather than by regeneration of a metal hydride.)

Scheme 1.13 Proposed Mechanism of Base-Catalyzed Direct C–H Silylation of Alkynes



These methods typically result in low yields of the desired products along with various byproducts. Moreover, the scope of both the alkynes and silanes are very limited. This reaction was recently revisited by Stoltz and Grubbs, who developed a facile and practical dehydrosilylation of terminal alkynes using hydroxide catalysts. (Table 1.15).²³ This work was inspired by their previously established KOt-Bu-catalyzed C–H silylation of aromatic heterocycles [See below for discussion of KOt-Bu-catalyzed C–H silylation].²⁴ A wide variety of hydrosilanes were found to be amenable to C–H silylation including aryl, alkyl, bulky triisobutyl, alkoxy, and pyridyl silanes (Entries 9–13).

Table 1.15 Reaction Optimization and Silane Scope

Entry	Base	Silane	Yield (%)	Entry	Base	Silane	Yield (%)
1	KOt-Bu	Et ₃ SiH	89	8	LiOH	PhMe ₂ SiH	0
2	NaOt-Bu	Et ₃ SiH	46	9	NaOH	t-Bu ₂ SiH ₂	91
3	LiOt-Bu	Et ₃ SiH	<1	10	KOH	i-Bu ₃ SiH	69
4	Pyridine	Et ₃ SiH	0	11	NaOH	(EtO) ₃ SiH	68
5	KOH	Et ₃ SiH	95	12	KOH	i-Pr ₂ (o-py)SiH	78
6	KOH	PhMe ₂ SiH	89	13	NaOH	Me ₂ (o-py)SiH	78
7	NaOH	PhMe ₂ SiH	93				

Interestingly, the authors found varied success for either KOH or NaOH between substrates, but there did not appear to be a direct correlation between choice of substrate or silane and catalyst performance. Therefore, a series of substrates were subjected to catalytic reactions using NaOH, KOH, and KOt-Bu to compare the yield of dehydrosilylation product (Entries 1–18, Table 1.16). Upon exploration of the substrate scope, the reaction was found to be compatible with a variety of synthetically useful functional groups including heterocycles (Entries 1–6, 25), secondary and tertiary amines

(Entries 27 and 22), and a variety of aryl functional groups (Entries 7–12, 19–24, 28). By changing reaction conditions, mono- and bis-silylated diynes (Entries 29, 30) and symmetrical or unsymmetrical sila-diyne (Entries 30, 31) could be synthesized in useful yields. Overall, the reaction has been shown to be compatible with a wide variety of both hydrosilanes and alkyne substrates.

Table 1.16 Comparison of Alkyne Dehydrosilylation Catalysts and Substrate Scope.

$\begin{array}{c} \text{R} \equiv \text{H} \\ 84 \end{array}$				Base (10 mol %) [Si]–H (3 equiv)	$\begin{array}{c} \text{R} \equiv \text{[Si]} \\ 85 \end{array}$	
				DME, 45–85 °C		
Entry	Product	Base	Yield (%)	Entry	Product ^a	Yield (%)
1		NaOH	82	19 ^a		R = H 89
2		KOH	19	20 ^a		F 88
3		KOt-Bu	<5	21 ^a		Br 52
4		NaOH	77	22 ^a		NMe ₂ 99
5		KOH	7	23 ^a		Me 92
6		KOt-Bu	0	24 ^a		MeO 91
7		NaOH	90	25 ^a		93
8		KOH	38	26 ^a		70
9		KOt-Bu	<5	27 ^a		80
10		NaOH	52	28 ^a		95
11		KOH	<5	29 ^b		65
12		KOt-Bu	0	30 ^c		88
13		NaOH	79	31 ^d		58
14		KOH	0			
15		KOt-Bu	0			
16		NaOH	0			
17		KOH	69			
18		KOt-Bu	0			

[a] NaOH used [b] 20 mol % NaOH, 0.33 equiv Me₂PhSiH, yield based on [Si]–H

[c] 20 mol % NaOH, 3 equiv Me₂PhSiH [d] 10 mol % NaOH, 3 equiv Et₂SiH₂ then

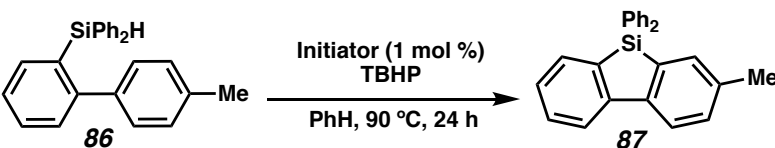
filter/conc. 10 mol % NaOH, 1.5 equiv m-Cl aryl alkyne

1.5 Radical Dehydrosilylation

1.5.1 “Electron” as a C–H Silylation Catalyst

If we again take a liberal interpretation of the term catalyst an interesting report from the lab of Studer details the use of an electron as a catalyst in an intramolecular C–H silylation of biarylsilanes **86** (Table 1.17, top).^{25,26}

Table 1.17. Optimization of Intramolecular C–H Silylation



Entry	TBHP (equiv)	Initiator	Yield (%)	Entry	TBHP (equiv)	Initiator	Yield (%)
1	2.2	FeCP ₂	34	5	3.3	TBAI	65
2	2.2	FeCl ₃	37	6	4.4	TBAI	62
3	2.2	CuI	66	7	5.5	TBAI	58
4	2.2	TBAI	55	8 ^b	3.3	TBAI	46

[a] TBHP = *t*-BuOOH, TBAI = (Bu)₄Ni [b] 0.4 mol % initiator

Their method uses a stoichiometric radical initiator and excess peroxide as an oxidant. They were able to optimize the reaction to use low loadings of the radical initiator (Entry 8), but unfortunately had to use a large excess of the peroxide oxidant (Table 1.17) and observed lower yields than related reactions using B(C₆F₅)₃ catalysts (see Section 1.2.2).

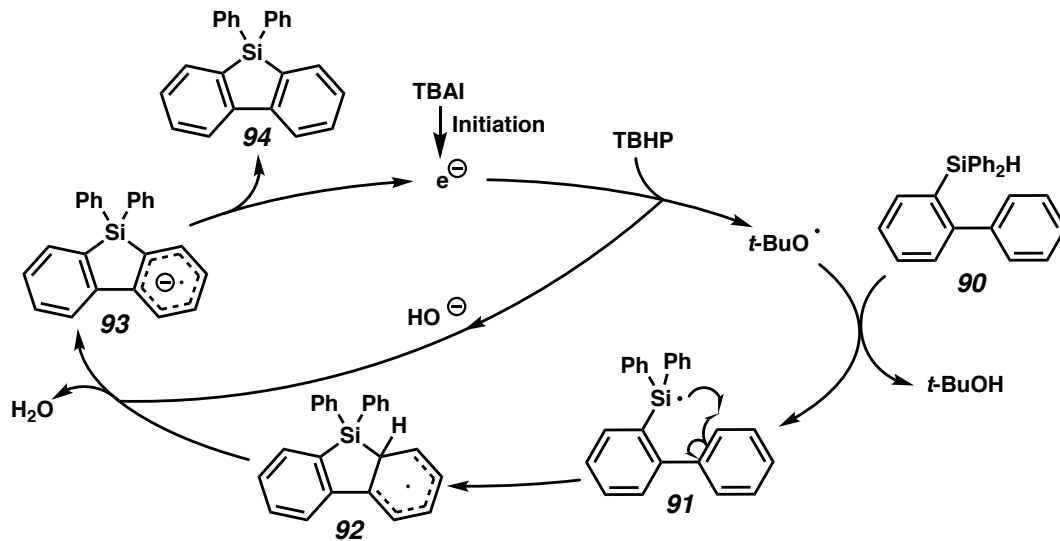
The authors went on to demonstrate the substrate scope of their intramolecular C–H silylation reaction (Table 1.18). The reaction was shown to tolerate some substitution on both aryl rings of the biphenyl, including a variety of halide substitution (Entries 4, 5, 8, 10) and even pyridine (Entry 9). Both electron-rich (Entries 7, 11) and electron-poor substrates (Entries 4, 6) resulted in moderate formation of the cyclized product.

Table 1.18 Selected Substrate Scope of Intramolecular C–H Silylation

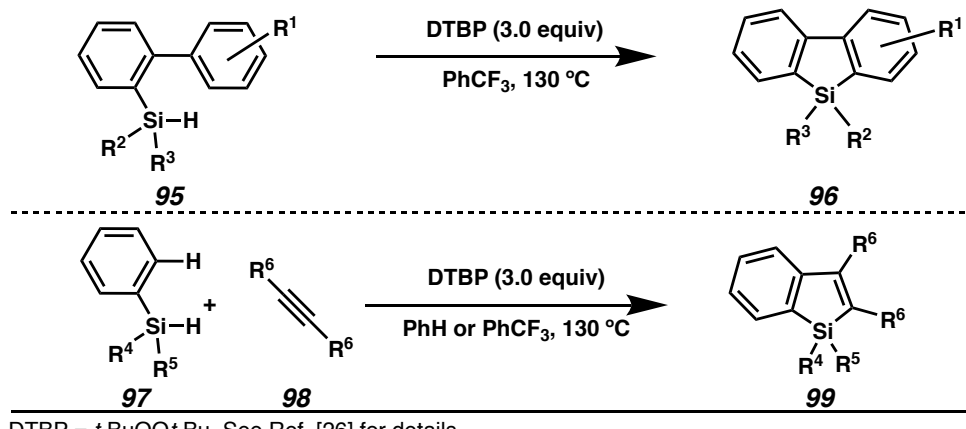
Entry	Product		Yield (%)	Entry	Product		Yield (%)
1		R = Me	55	9			39
2		H	66	10			55
3		t-Bu	71				
4		F	67				
5		Cl	77				
6		CF ₃	75				
7		OMe	68				
8			75				

[a] TBHP = *t*-BuOOH, TBAI = (Bu)₄Ni

Based on their observations and reaction conditions, they propose a single electron transfer (SET) type mechanism, whereby an electron acts as a catalyst in their reaction cycle (Scheme 1.14). While this reaction does require superstoichiometric peroxide oxidant, it is still an interesting reaction to discuss as an introduction to catalytic, radical C–H silylation. It must also be mentioned that this reaction does show significant similarities to the classical Minisci reaction, the addition of alkyl radicals to protonated heterocycles.²⁷

Scheme 1.14 Proposed Mechanism for Intramolecular C–H Silylation

The group of Li reported a similar reaction at higher temperature without the use of catalytic TBAI (Scheme 1.15, top).²⁸ A series of silafluorenes **96** were synthesized by radical, intramolecular cyclization of biphenyl-2-hydrosilane substrates. A cascade process was also established to synthesize silaindenes by first radical addition to alkynes followed by radical cyclization (Scheme 1.15, bottom). While these strategies proved to be quite limited in scope, the reactions serve as an interesting study in radical C–H silylation methods.

Scheme 1.15 Uncatalyzed Radical C–H Silylation/Annulation

1.5.2 KOt-Bu-Catalyzed C–H Silylation

1.5.2.1 Discovery of Unusual KOt-Bu-Catalyzed C–H Silylation

The lab of Grubbs discovered the interesting direct C–H silylation side products **102**–**106** (Table 1.19) while working on a system for the reductive cleavage of aryl ethers **100**.²⁹

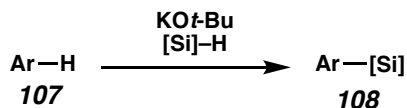
Using substoichiometric base (entry 4), C–H silylated dibenzofurans **102**, **103**, and **104** form in reasonable yield. Inspired by this initial result, they sought to further develop this chemistry.

Table 1.19 Optimization of Reductive Aryl Ether Cleavage

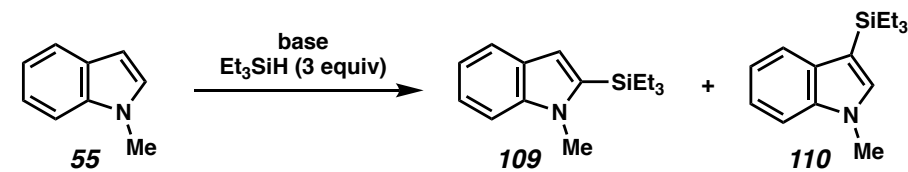
Entry	Et ₃ SiH (equiv)	KOt-Bu (equiv)	Solvent	T (°C)	Yield (%)					
					101	102	103	104	105	106
1	5	2	Ph-Me	100	38	16	10	21	2	7
2	5	5	Ph-Me	100	63	10	2	20	-	2
3	3	3	mesitylene	165	85	3	-	5	2	-
4	5	0.5	Ph-Me	100	12	48	20	9	-	1
5	5	2	mesitylene / 1,4-cyclohexadiene	165	95	-	-	-	-	-

1.5.2.2 KOt-Bu-Catalyzed C–H Silylation Methodology

In a collaborative effort between the Grubbs and Stoltz groups, a detailed reaction optimization was conducted and a wide array of aromatic heterocycles **107** (Scheme 1.16) were found to undergo dehydrogenative C–H silylation to afford the silylated product **108**.²⁴

Scheme 1.16 Overview of KOt-Bu -Catalyzed C–H Silylation

During the reaction optimization, the authors quickly found that catalytic amounts of KOt-Bu are able to furnish high yields of the silylated products (Table 1.20, entries 2 versus 4). Other *t*-butoxy bases with smaller counter ions (i.e., Li^+ or Na^+) are not competent catalysts (entry 1) for this reaction, but other bases with a potassium cation do afford product, albeit with decreased yield (entry 3 versus 2). While the reaction works in a number of ethereal solvents (entries 4–6), they were pleased to find that the reaction also worked well in the absence of solvent (entry 7).

Table 1.20 Selected Examples from Optimization of C–H Silylation

Entry	Base	mol %	T (°C)	t (h)	Solvent	Yield 109 (%)	Ratio 109:110
1	$\text{Li/NaO}\text{t-Bu}$	100	25	16	THF	0	-
2	KOt-Bu	100	25	16	THF	67	>20:1
3	KHMDS	100	25	16	THF	44	>20:1
4	KOt-Bu	20	45	60	THF	98	4:1
5	KOt-Bu	20	45	60	MTBE	89	>20:1
6	KOt-Bu	20	45	60	DME	95	3.4:1
7	KOt-Bu	20	45	48	neat	88	>20:1

With these optimized conditions in hand, a large substrate scope was shown to undergo facile C–H silylation, with only a small subset shown here (Table 1.21). A variety of protected indoles (Entries 1–8, 11–13), azaindoles (Entries 14–17), thiophene and furan (Entries 9 and 10), and other heterocycles undergo silylation in good to excellent yields. Interestingly, 5,6-fused heterocycles undergo silylation preferentially at

the C-2 position (α for thiophene and furan) rather than the typically more nucleophilic C-3 position.

Table 1.21 Representative Substrate Scope of the $KOEt\text{-}Bu$ -Catalyzed C–H Silylation Reaction

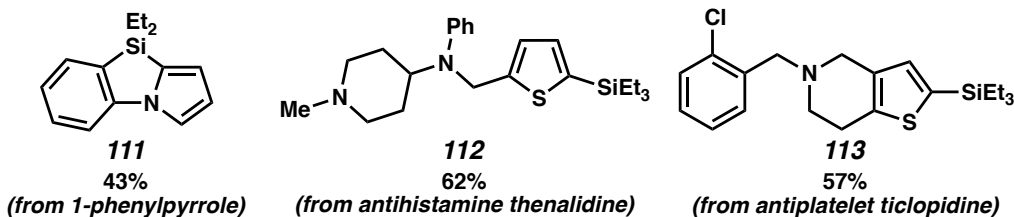
Entry	Product		Yield (%)	Entry	Product		Yield (%)
1		X =	S	93	14 ^d		33
2 ^b		N-SEM	67				
3		N-Me	78				
4		N-Bn	82				
5 ^c		N-MOM	55	15		31	
6		[Si] = SiPhMe ₂	75				
7		SiEt ₂ H	76				
8		SiEtMe ₂	71	16		50	
9		X =	S	92			
10		O	95				
11		R =	OMe	64	17		71
12			OBn	68			
13			CH ₂ OMe	48			

[a] 20 mol % $KOEt\text{-}Bu$, 3 equiv base, THF or neat, 25–60 °C, C2:C3 ratio >20:1

[b] 14:1 C2:C3 [c] 10:1 C2:C3 [d] 6:1 C2:C3

To further demonstrate the synthetic utility of this methodology, the silylation reaction was shown to effect tandem inter/intramolecular silylation to from cyclic silanes **111** (Scheme 1.17) and late-stage silylation of pharmaceutically active compounds **112** and **113**.

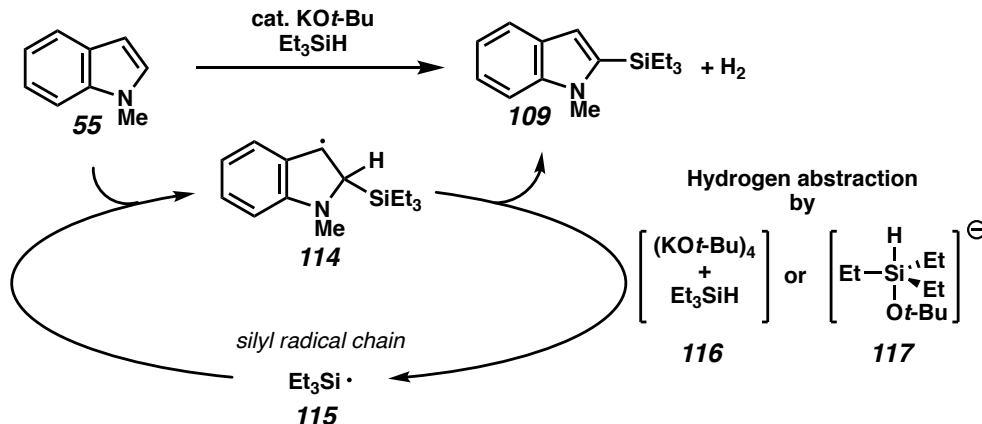
In addition to the synthetic applications previously discussed, this methodology was shown to be applicable for the ultra-deep desulfurization of fuels³⁰ and was further developed to the alkyne C–H methods discussed in Section 1.4.3²³ and a catalytic O–H silylation method.³¹

Scheme 1.17 Select Examples of Applications of the *KOt-Bu*-Catalyzed C–H Silylation

See Ref. 22 for reaction conditions

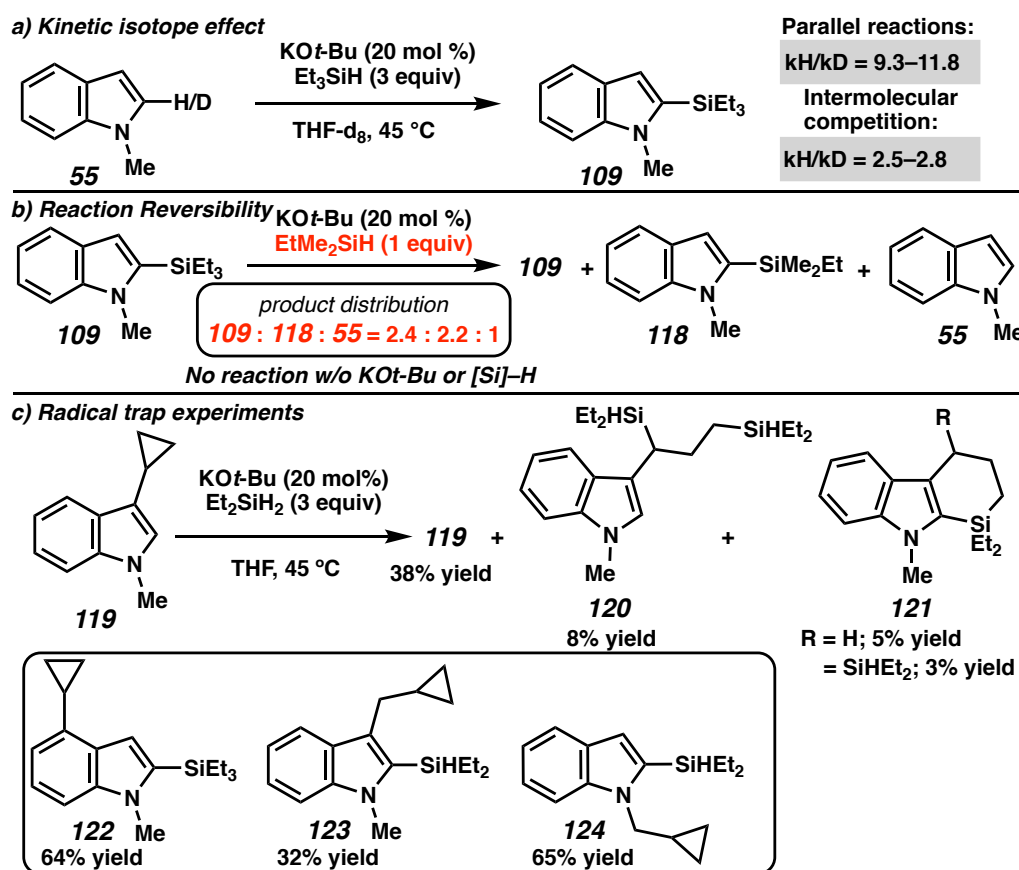
1.5.2.3 Mechanistic Investigations of *KOt-Bu*-Catalyzed C–H Silylation and Related Chemistry

During the course of the initial disclosure for this novel reaction, a brief mechanistic investigation was conducted and the initial results indicated the reaction might occur by a radical mechanism.²⁴ To date, three reports exploring this reaction mechanism have been published. One indicates a radical type reaction mechanism may be operative under these reaction conditions (Scheme 1.18).³² A key aspect of this mechanism is the generation of a silyl radical **115**, which then adds to the heterocycle forming a stabilized radical heterocycle **114**. A hydrogen atom removal event then regenerates aromaticity and generates another silyl radical thereby closing the catalytic cycle.

Scheme 1.18 Overview of Radical Mechanism for C–H Silylation Reaction

A variety of techniques were used to probe the active reaction mechanism and a few of which are highlighted here. The authors demonstrated a very large KIE effect at the C-2 position of indole H/D-**55** (Scheme 1.19), showed the silylation event is reversible by reacting **109** with EtMe₂Si–H to afford a mixture containing **109**, **118**, and **55**, and that cyclopropyl radical traps will open only at the presumed site of radical formation **119** versus **122–124**.

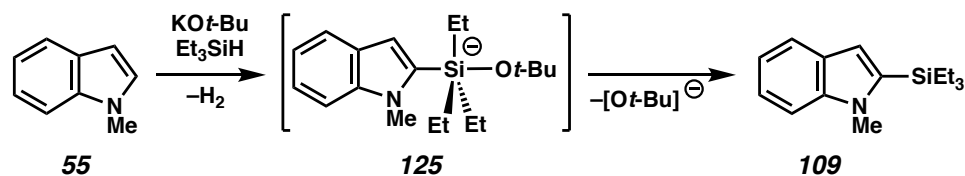
Scheme 1.19 Overview of Mechanistic Investigations



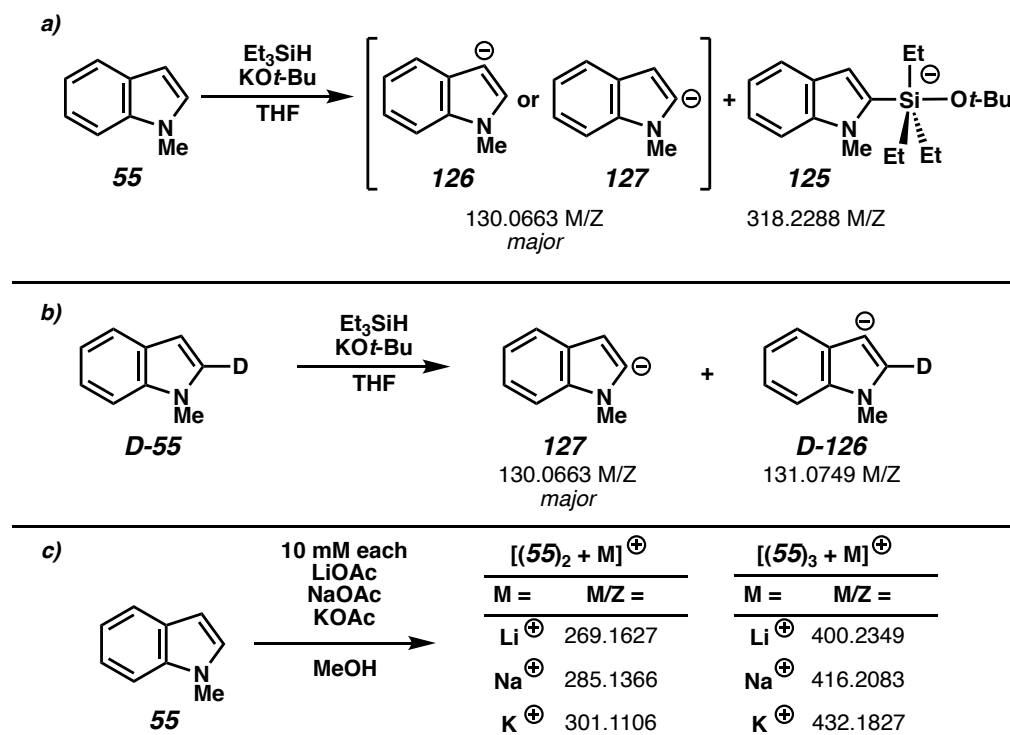
An extensive computational investigation was conducted to determine the energetic feasibility of such a reaction pathway and while many aspects between experimental and computational results are in agreement, the radical initiation event is inconclusive. [see Ref. 32 for full discussion].

During the course of the mechanistic investigation it became apparent that a second reaction pathway might be possible. This second mechanism focused on the same KOt-Bu-catalyzed C–H silylation reaction but proposes an ionic/neutral mechanism (Scheme 1.20).³³

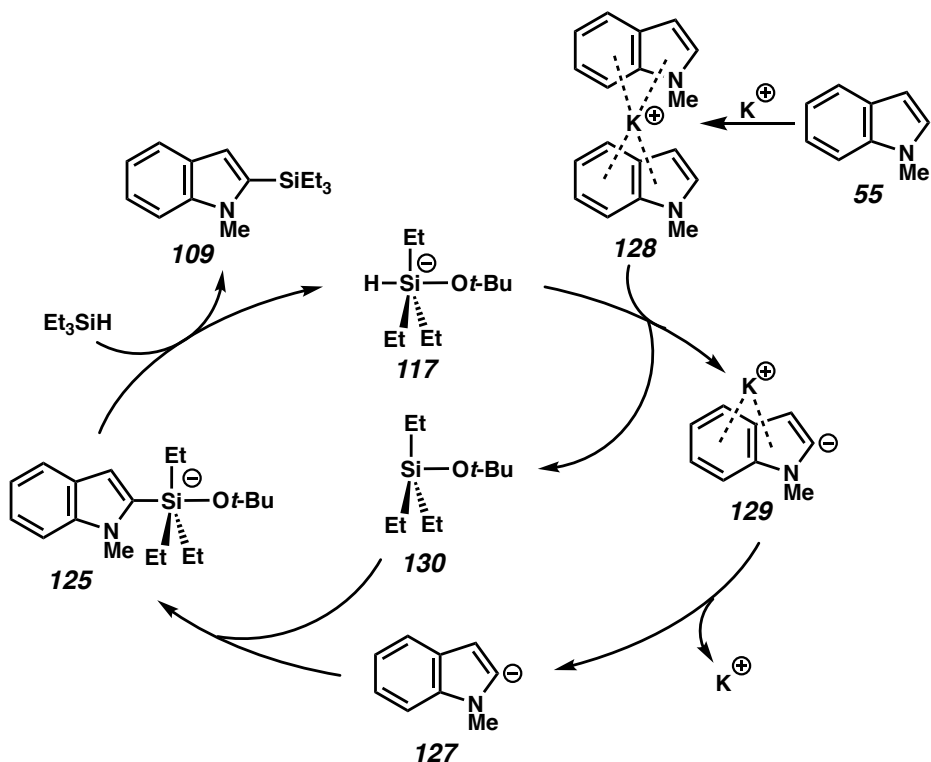
Scheme 1.20 Overview for Ionic Reaction Mechanism



The Zare group was able to use desorption electrospray ionization mass spectrometry (DESI-MS) as a method to identify reaction intermediates. They were able to identify both the deprotonated indole substrate **126**, **127**, and **D-126** (Scheme 1.21) and the silylation intermediate formed by nucleophilic addition of indole to coordinated silane after loss of hydrogen (**125**). Furthermore, subjecting a mixture of Li⁺, Na⁺, and K⁺ solutions to DESI-MS with indole substrate the authors were able to detect the bis- and tris-coordinated π-arene complexes (Scheme 1.21c). These complexes may help to weaken the corresponding C–H bond and facilitate deprotonation.

Scheme 1.21 Reaction Intermediate Observed by DESI-MS

Given these results, and a multitude of computational and other studies that are left out here due to space constraints, the authors propose a mechanism whereby the arene is coordinated by potassium cation **128** (Scheme 1.22), which facilitates deprotonation by pentacoordinate silicate **117** to afford coordinated anion **129** or free anion **127**. The deprotonated arene **127** then attacks the silyl ether **130**, generating the silylated anion **125**, which, after release of *t*-butoxide and subsequent regeneration of the pentacoordinate silicon **117**, forms the silylated product **109**.

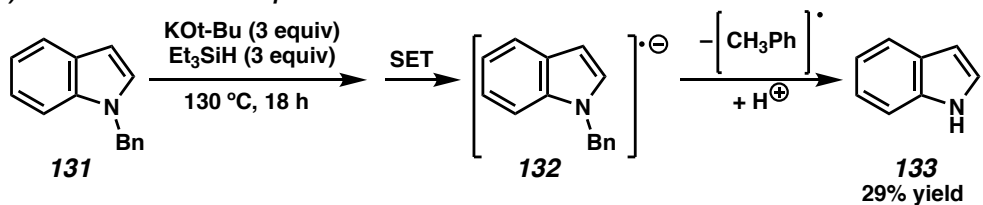
Scheme 1.22 Proposed Ionic Mechanism

The neutral mechanism (not shown here, see Ref. 33) involves a similar transformation but no discrete ions are formed. While neither the radical nor ionic/neutral mechanism can disprove the other, both have shown significant mechanistic evidence and may be operative under different reaction conditions.

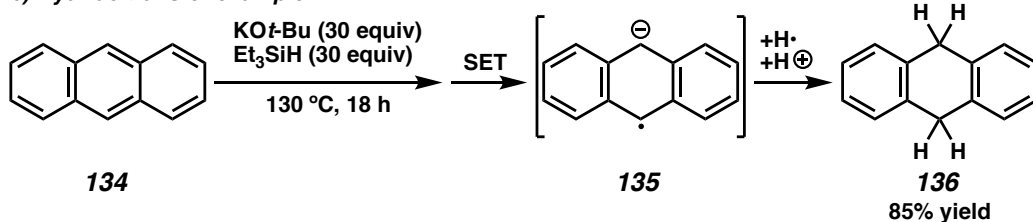
A third mechanistic study has recently been reported by the groups of Murphy and Tuttle which uses modified $KOt\text{-}Bu$ -catalyzed silylation reaction conditions to effect electron transfer and hydride transfer reactions (Scheme 1.23).³⁴

Scheme 1.23 Overview of Electron Transfer and Hydride Transfer in Stoltz-Grubbs Silylation System
Proposed by Murphy and Tuttle et al.

a) **Electron Transfer Example**



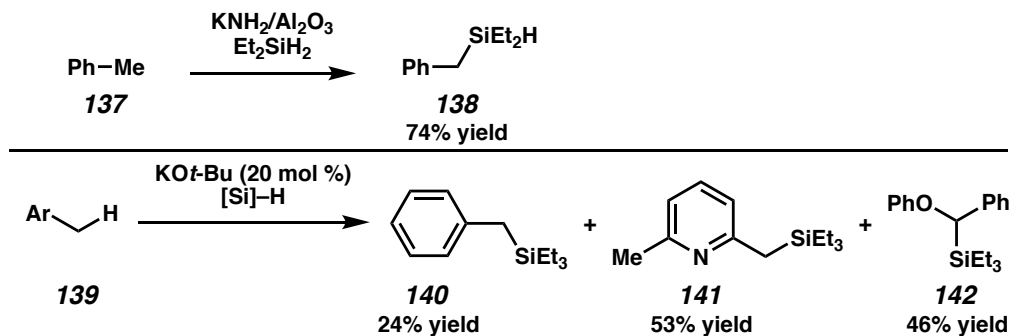
b) **Hydride transfer example**



While this is an interesting report related to the previously mentioned KOt-Bu-catalyzed C–H silylation methodology, it is unclear if either of these mechanisms (i.e. electron transfer or hydride transfer) is active under catalytic conditions or whether this is an opportunity to access new types of reactivity.

1.6 C(sp³)–H Silylation

To our knowledge, only two examples of catalytic, transition-metal-free C(sp³)–H silylation reactions have been reported in the literature. Both catalyst systems were already presented here (See 1.4.3 and 1.5.2.2, respectively) and both systems are limited to the activation of benzylic C–H bonds (Scheme 1.24).^{17, 24}

Scheme 1.24 Examples of $C(sp^3)$ –H Silylation

1.7 Conclusion

This chapter has focused on detailing the major developments in transition-metal-free, C–H silylation reactions. One broad category of such catalysts involves the generation of an electrophilic silicon which is trapped by the nucleophilic substrate. FLPs, especially using $B(C_6F_5)_3$, have seen widespread use in this mode of C–H silylation, as they both activate silicon and may act as a base or hydride transfer reagent. While these catalysts have some common issues, they have proven to be useful in C–H silylation. Development of new Lewis acid catalysts may help to suppress H_2 activation, Lewis pair formation with substrate or byproduct, and expand the scope to less nucleophilic substrates.

The sole report by Oestreich detailing the use of Brønsted acid in analogous reactivity is exciting as this may provide an orthogonal method of silane activation and expand reactivity to less nucleophilic substrates. It goes without saying that many complex molecules are incompatible with strong acid, and selective protonation of the silicon will be key to the further development of such acid catalyst systems.

Brønsted base silylation catalysts allow access to classes of substrates commonly made through a metatation and trapping approach but without the need for pyrophoric or

otherwise undesired reagents. The key to this reactivity is the *in situ* generation of a transient, significantly stronger base than the catalyst itself. Especially if the Si–H bond of hydrosilanes can be used as a hydride base, this mode of catalysis is likely to see significant future use due to the familiar reactivity (i.e., versus an [Si]–X, base system) but with increased safety and decreased waste.

The final mode of catalysis explored is radical type C–H bond silylation. In recent years, this mode of catalysis has been a major focus. This reactivity allows the activation of a wide variety of aromatic and even some aliphatic C–H bonds using simple reaction protocols. Catalytic generation of such a radical intermediate does pose challenges with functional group compatibility (i.e. carbonyl, nitro, cyano, some olefins, etc.), which has limited the reaction scope. Future catalyst development may help to avoid unwanted reactivity by modulating the reduction potential of the radical intermediate or decreasing the radical lifetime and concentration (i.e., by precomplexation of substrate and silane before radical generation).

A particular focus was devoted to discussing the different nature of the reaction catalysts and mechanisms, when known. Understanding the mechanism and inherent limitations will serve to guide the design of future C–H silylation catalysts. Given the interest this field has experienced in the recent years, we are excited to see what future developments bring.

1.8 REFERENCES AND NOTES

- (1) Barry, A. J.; Gilkey, J. W.; Hook, D. E. *Ind. Eng. Chem. Res.* **1959**, *51*, 131–138.

- (2) Barry, A. J.; Gilkey, J. W.; Hook, D. E. in *Metal-Organic Compounds*, Vol. 23, Advances in Chemistry; American Chemical Society, Washington D.C., USA **1959**, pp 246–264.
- (3) Wright, A. *J. Organomet. Chem.* **1978**, *145*, 307–314.
- (4) For a review on related Catalytic Friedel–Crafts reactivity see: Bähr, S.; Oestreich, M. *Angew. Chem. Int. Ed.* **2017**, *56*, 52–59.
- (5) (a) Piers, W. E.; Marwitz, A. J. V.; Mercier, L. G. *Inorg. Chem.* **2011**, *50*, 12252–12262.; (b) Stephan, D. W. *J. Am. Chem. Soc.* **2015**, *137*, 10018–10032.
- (6) Curless, L. D.; Clark, E. R.; Dunsford, J. J.; Ingleson, M. J. *Chem. Commun.* **2014**, *50*, 5270–5272.
- (7) Curless, L. D.; Ingleson, M. J. *Organometallics* **2014**, *33*, 7241–7246.
- (8) Ma, Y.; Wang, B.; Zhang, L.; Hou, Z. *J. Am. Chem. Soc.* **2016**, *138*, 3663–3666.
- (9) Similar reactivity was described by Prof. Oestreich, but their optimized system involved a transition-metal-based catalyst: Yin, Q.; Klare, H. F. T.; Oestreich, M. *Angew. Chem. Int. Ed.* **2016**, *55*, 3204–3207.
- (10) Han, Y.; Zhang, S.; He, J.; Zhang, Y. *J. Am. Chem. Soc.* **2017**, *139*, 7399–7407.
- (11) For stoichiometric examples see: Chen, Q.-A.; Klare, H. F. T.; Oestreich, M. *J. Am. Chem. Soc.* **2016**, *138*, 7868–7871.
- (12) Fornarini, S. *J. Org. Chem.* **1988**, *53*, 1314–1316.
- (13) Sasaki, M.; Kondo, Y. *Org. Lett.* **2015**, *17*, 848–851.
- (14) Nozawa-Kumada, K.; Osawa, S.; Sasaki, M.; Chataigner, I.; Shigeno, M.; Kondo, Y. *J. Org. Chem.* **2017**, *82*, 9487–9496.

- (15) See Ref. 13, 14 and the references cited within
- (16) Calas, R.; Bourgeois, P. *C. R. Acad. Sci., Paris, Ser. C* **1969**, *268*, 72–74
- (17) Baba, T.; Kato, A.; Yuasa, H. Toriyama, F.; Handa, H.; Ono, Y. *Catal. Today* **1998**, *44*, 271–276.
- (18) Note-A single example of C(sp²) silylation using benzene is also reported with the same catalyst system described in Ref 17
- (19) Itoh, M.; Mitsuzuka, M.; Utsumi, T.; Iwata, K.; Inoue, K. *J. Organomet. Chem.* **1994**, *476*, C30–C31.
- (20) Itoh, M.; Kobayashi, M.; Ishikawa, J. *Organometallics* **1997**, *16*, 3068–3070.
- (21) Ishikawa, J.-I.; Inoue, K.; Itoh, M. *J. Organomet. Chem.* **1998**, *552*, 303–311.
- (22) Ishikawa, J.-I.; Itoh, M. *J. Catal.* **1999**, *185*, 454–461.
- (23) Toutov, A. A.; Betz, K. N.; Schuman, D. P.; Liu, W.-B.; Fedorov, A.; Stoltz, B. M.; Grubbs, R. H. *J. Am. Chem. Soc.* **2017**, *139*, 1668–1674.
- (24) Toutov, A. A.; Liu, W.-B.; Betz, K. N.; Fedorov, A.; Stoltz, B. M.; Grubbs, R. H. *Nature* **2015**, *518*, 80–84.
- (25) Leifert, D.; Studer, A. *Org. Lett.* **2015**, *17*, 386–389.
- (26) For a stoichiometric example of related reactivity see: Du, W.; Kaskar, B.; Blumbergs, P.; Subramanian, P. K.; Curran, D. P. *Bioorg. Med. Chem.* **2003**, *11*, 451–458.
- (27) For a review on radical addition to heterocycles, including Minisci Reactions, see the following and references cited within; Tauber, J.; Imbri, D.; Opitz, T. *Molecules* **2014**, *19*, 16190–16222.

- (28) Xu, L.; Zhang, S.; Li, P. *Org. Chem. Front.* **2015**, *2*, 459–463.
- (29) Fedorov, A.; Toutov, A. A.; Swisher, N. A.; Grubbs, R. H. *Chem. Sci.* **2013**, *4*, 1640–1645.
- (30) Toutov, A. A.; Salata, M.; Fedorov, A.; Yang, Y.-F.; Liang, Y.; Cariou, R.; Betz, K. N.; Couzijn, E. P. A.; Shabaker, J. W.; Houk, K. N.; Grubbs, R. H. *Nature Energy* **2017**, *2*, 17008.
- (31) Toutov, A. A.; Betz, K. N.; Haibach, M. C.; Romine, A. M.; Grubbs, R. H. *Org. Lett.* **2016**, *18*, 5776–5779.
- (32) Liu, W.-B.; Schuman, D. P.; Yang, Y.-F.; Toutov, A. A.; Liang, Y.; Klare, H. F. T.; Nesnas, N.; Oestreich, M.; Blackmond, D. G.; Virgil, S. C.; Banerjee, S.; Zare, R. N.; Grubbs, R. H.; Houk, K. N.; Stoltz, B. M. *J. Am. Chem. Soc.* **2017**, *139*, 6867–6879.
- (33) Banerjee, S.; Yang, Y.-F.; Jenkins, I. D.; Liang, Y.; Toutov, A. A.; Liu, W.-B.; Schuman, D. P.; Grubbs, R. H.; Stoltz, B. M.; Krenske, E. H.; Houk, K. N.; Zare, R. N. *J. Am. Chem. Soc.* **2017**, *139*, 6880–6887.
- (34) Smith, A. J.; Young, A.; Rohrbach, S.; O'Connor, E. F.; Allison, M.; Wang, H. S.; Poole, D. L.; Tuttle, T.; Murphy, J. A. *Angew. Chem. Int. Ed.* **2017**, *56*, 13747–13751.

CHAPTER 2

*A Combined Experimental and Computational Mechanistic Study of the
KOt-Bu-Catalyzed Dehydrogenative C–H Silylation of Aromatic
Heterocycles[†]*

2.1 INTRODUCTION AND BACKGROUND

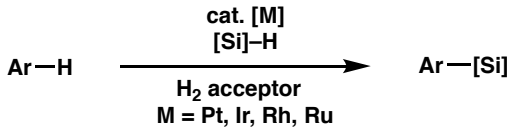
Heteroarenes are important components of natural products and bioactive molecules, and considerable research has focused on their functionalization and derivatization.¹ Direct functionalization of unactivated C–H bonds in heteroarenes is a powerful method to access heteroarylsilanes and heteroarylboranes.² These intermediates provide routes to build complexity in molecules by well-established cross-coupling techniques.³ Heteroarylsilanes are stable and find widespread use in polymer synthesis, medical imaging applications, and drug discovery.⁴ Given the diversity and abundance of both heteroarenes and hydrosilanes, direct C–H silylation between heteroarenes and

[†] This work was performed in collaboration with Dr. Wen-Bo Liu, Dr. Yun-Fang Yang, Dr. Anton Toutov, Dr. Yong Liang, Dr. Hendrik Klare, and Dr. Nasri Nesnas. Portions of this chapter have been reproduced with permission from Liu, W.-B.; Schuman, D. P.; Yang, Y.-F.; Toutov, A. A.; Liang, Y.; Klare, H. F. T.; Nesnas, N.; Oestreich, M.; Blackmond, D. G.; Virgil, S. C.; Banerjee, S.; Zare, R. N.; Grubbs, R. H.; Houk, K. N.; Stoltz, B. M. *J. Am. Chem. Soc.* **2017**, *139*, 6867–6879. © 2017 American Chemical Society.

silanes is a powerful tool for the selective construction of C–Si bonds.^{5,6} In comparison with traditional methods (i.e., metalation/nucleophile trapping), direct cross-dehydrogenative C–H silylation constitutes an appealing alternative without requiring prefunctionalization of the heteroarene, cryogenic conditions, or pyrophoric reagents.⁷ Significant advances in this field include the development of transition-metal catalysts that efficiently enable C–H silylation of heteroarenes in the presence of superstoichiometric sacrificial hydrogen acceptors (Scheme 2.1a). Recently, examples of acceptorless, catalytic C–H silylation have been reported using both transition-metal and transition-metal-free catalysts (Scheme 2.1b, c).^{6,8,9}

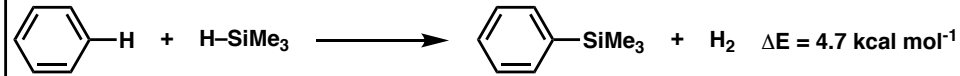
Scheme 2.1 C–H Silylation Catalyst Systems

a) Transition-Metal Catalyst using Hydrogen Acceptor

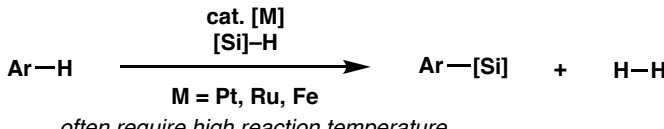


commonly used H_2 acceptors include cyclohexene, norbornene, etc.

Why is a hydrogen acceptor required?



b) Transition-Metal Catalyst without using Hydrogen Acceptor



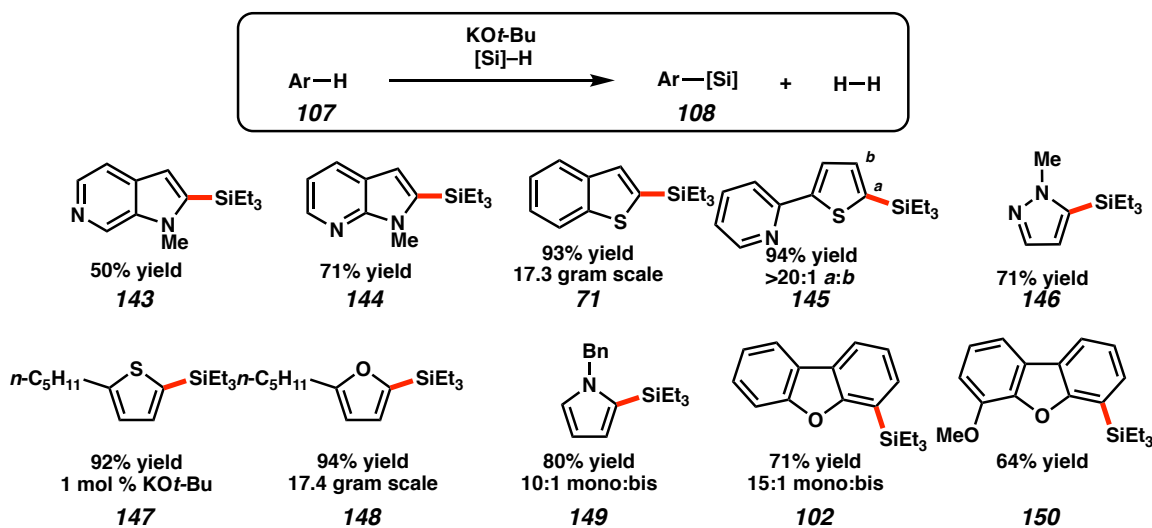
c) Transition-Metal-Free Catalyst without using Hydrogen Acceptor



reported catalysts include strong Lewis acids and Brønsted acids

Given the state of the art in C–H silylation, we sought a practical, sustainable, and scalable silylation method achieving efficient silylation of a broad scope of substrates. In cooperation with the Grubbs group, we have demonstrated that potassium *tert*-butoxide (KOt-Bu) can catalyze the direct cross-dehydrogenative coupling of heteroarenes with hydrosilanes (Scheme 2.2).¹⁰ This method features mild reaction conditions, an operationally simple procedure, good functional group tolerance, and environmentally friendly reagents.

Scheme 2.2 Select Examples of KOt-Bu-Catalyzed Cross-Dehydrogenative C–H Silylation Method



Reaction conditions: heterocycle (0.5 mmol), [Si]–H (1.5 mmol), and KOt-Bu (0.1 mmol,) neat or in THF (0.5 mL). Isolated yields shown.

2.2 MECHANISTIC INVESTIGATION OVERVIEW

However, the mechanism by which this reaction occurs was both unprecedented in the literature and not initially apparent. We began a mechanistic investigation which culminated in a collaborative study described in a series of publications detailing possible radical and ionic/neutral reaction mechanisms.^{11, 12} This chapter is a detailed account of

2.3 INVESTIGATION OF SILYLATION REACTION YIELD AND KINETICS

2.3.1 Catalyst Activity

A detailed study of the catalytic competency of a variety of alkali, alkaline earth, and other metal derived bases as silylation catalyst has been conducted. As shown in Table 2.1, alkoxides and hydroxides of alkali metals with larger radius cations (i.e., radius $\geq K^+$), such as K^+ , Rb^+ , and Cs^+ could provide the silylation product in moderate to good yields (Table 1, entries 1–4, 6, 9 and 10). Among all the catalysts examined, KOt-Bu was proven to be the ideal catalyst, affording the highest overall yield. However, no product was detected when KOAc or KH was employed as the catalyst (entries 5 and 7). Perhaps surprisingly, potassium on graphite (KC_8) afforded the desired product in good yield (entry 8). Alkali metal bases with small cations (e.g., LiOt-Bu and NaOt-Bu) demonstrated a complete lack of reactivity and no product was observed even after extended reaction time (entries 11 and 12). Alkoxides of alkali earth metals or aluminum were also investigated as catalysts and failed to afford any product (entries 13–16).

Table 2.1 Investigation of Silylation Catalysts

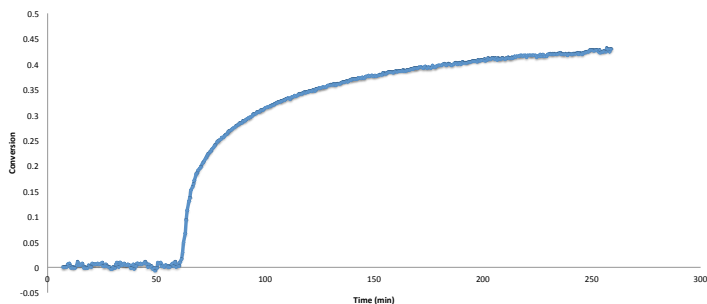
entry	catalyst	time (h)	conv (%) ^b	109 : 110^b
1	$KOt\text{-}Bu$	10	88	11:1
2	$KOEt$	10	55	9:1
3	$KOMe$	20	35	9:1
4	$KOTMS$	20	53	12:1
5	$KOAc$	60	0	–
6	KOH^c	20	52	11:1
7	KH	36	0	–
8	KC_8^d	10	73	8:1
9	$CsOH \cdot H_2O$	10	64	8:1
10	$RbOH \cdot xH_2O$	10	38	10:1
11	$LiOt\text{-}Bu$	36	0	–
12	$NaOt\text{-}Bu$	36	0	–
13	$Mg(Ot\text{-}Bu)_2$	36	0	–
14	$Ca(Oi\text{-}Pr)_2$	36	0	–
15	$Ba(Ot\text{-}Bu)_2$	36	0	–
16	$Al(Ot\text{-}Bu)_3$	36	0	–

[a] Reaction conditions: **55** (0.5 mmol), Et_3SiH (1.5 mmol), and catalyst (0.1 mmol, 20 mol%) in THF (0.5 mL) at 45 °C. [b] Determined by GC analyses. [c] Dried KOH, see APPENDIX XX for details. [d] Potassium graphite.

2.3.2 Reaction Profile

The kinetic behavior of the silylation reaction with $KOt\text{-}Bu$ catalyst was studied using *in situ* 1H NMR spectroscopy. As depicted in Figure 2.1, the silylation reaction was found to take place in three stages: an induction period (Figure 1, 0–3500 s), an active period with rapid formation of product (3500–4500 s), and a final period with significantly reduced reaction rate (>4500 s).

Figure 2.1 A Representative Time Course of the Formation of **109**, Monitored by *in situ* ^1H NMR.

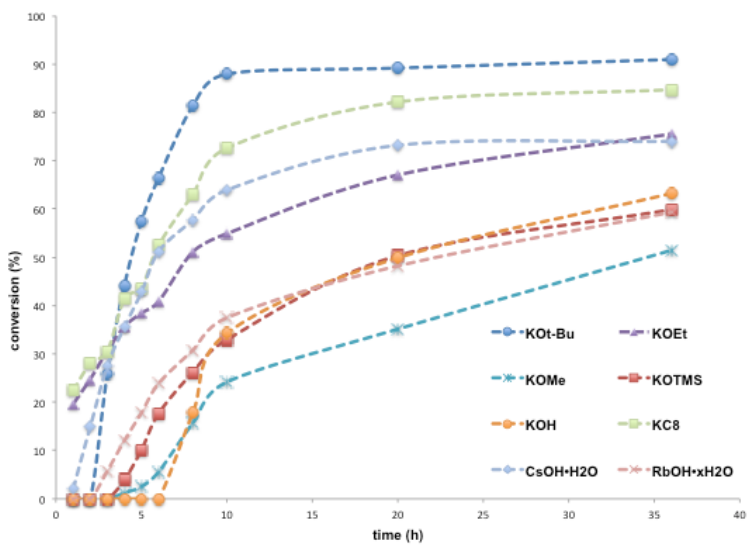


Reaction conditions: **55** (0.25 mmol), Et₂SiH (0.75 mmol), and KOt-Bu (0.05 mmol, 20 mol %) in THF-D₈ (0.25 mL) at 45 °C in a sealed NMR tube.

2.3.3 Impact of Catalyst Identity on Reaction Kinetics

Our investigations were then expanded to include each active catalyst presented in Table 2.1 (Figure 2.2). The length of the induction period was found to depend on the nature of both metal and counter ion. For anions, the induction period increased in the order of KC₈ (shortest) < KOEt < KOt-Bu < KOH (longest). An increase in induction period was observed with decreasing radius of cations, with CsOH (shortest) < RbOH < KOH (longest). It is worth noting that the induction periods vary based on catalyst loading, solvents, and reaction temperature. Additives and moisture could also have a significant impact on the induction period, generally prolonging the duration of such period. Nevertheless, the induction period showed good reproducibility for identical reactions setup at different times. Although the induction period with KOt-Bu is not the shortest of all catalysts tested (Figure 2.2), this catalyst provides the highest post-initiation turnover frequency and product yield. Further discussion related to the cause of this induction period is explored in later spectroscopic and computational experiments.

Figure 2.2 Time-Course Investigation of Silylation Catalyst



Reaction conditions: **55** (0.5 mmol), Et₃SiH (1.5 mmol), and catalyst (0.1 mmol) in THF (0.5 mL) at 45 °C. Conversion determined by GC analysis of crude reaction mixture

2.3.4 Silylation Product Distribution and Reversibility

Although the major product of KOt-Bu-catalyzed silylation is the incorporation of a silyl group at the C2-position of 1-methylindole (i.e., **109**), C3-silylation products (i.e., **110**) are also observed. Increased in reaction time and temperature tend to shift the major product from C2- to C3-silylation. As illustrated in Table 2.2, a silylation reaction conducted in THF at 45 °C affords an 11:1 ratio of C2-:C3-products (**109:110**) after 10 h, but after 15 days under the same conditions only C3-product **110** is observed (i.e., 1:>20 C2-:C3-, entries 1 and 2). Similarly, when a reaction is conducted at 100 °C, C3-silylation predominates with a 1:9 ratio of products **109:110** (entry 3). These results are consistent with C2-silylation as the kinetic product, while C3-silylation is the thermodynamic product. Finally, solvent selection was found to have a dramatic impact on the C2- and C3-selectivity. In the absence of solvent, the C2-product is exclusively

Table 2.2 Investigation of Silylation Product Distribution

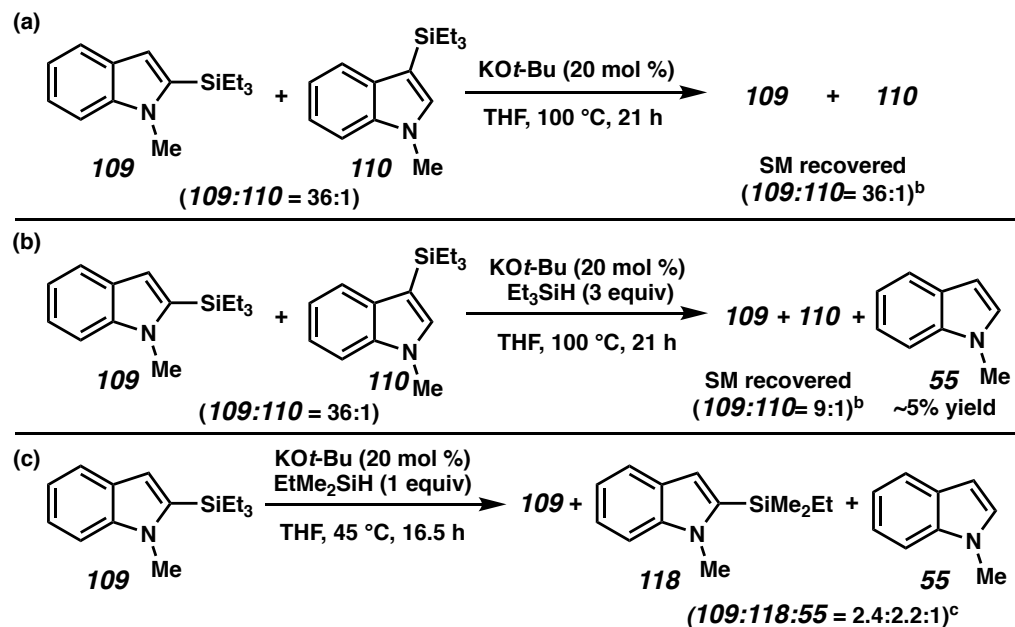
entry	solvent	temp (°C)	time (h)	conv (%) ^b	109 : 110 ^b
1	THF	45	10	88	11:1
2	THF	45	15d ^c	>95	1:>20
3	THF	100	20	94	1:9
4	neat	45	48	88	>20:1
5	neat	100	24	>95	4:1

[a] Reaction conditions: **55** (0.5 mmol), Et₃SiH (1.5 mmol), and KOt-Bu (0.1 mmol,) in THF (0.5 mL, if indicated).

[b] Determined by GC analyses. [c] After 15 days.

Several experiments were conducted to probe the reversibility of the silylation reaction (Scheme 2.3). Treatment of C2-silylated compound **109** with KOt-Bu in THF does not result in conversion to the C3-silylated **110** (Scheme 2.3a), showing that catalyst alone is insufficient for reversibility. However, treatment of **109** with both Et₃SiH and KOt-Bu in THF led to the conversion of C2-silylated product **109** to C3-silylated product **110**, along with approximately 5% of desilylated product **55** (Scheme 2.3b). Moreover, a crossover experiment involving compound **110**, stoichiometric EtMe₂SiH, and catalytic KOt-Bu provided a mixture of starting material **110**, cross-silylation product **118**, and desilylation product **55** (Scheme 2.3c). These results indicate that the conversion of C2-to C3-silylation product likely does not occur through intramolecular silyl migration. In fact, the observation of cross-silylation and desilylation can be better explained by a reversible silylation reaction under these conditions.

Scheme 2.3 Reversibility of Silylation Reaction



[a] Reaction conditions: **55** or **109** + **110** (0.5 mmol), Et_3SiH (1.5 mmol), and $KO\ddot{t}\text{-}Bu$ (0.1 mmol,) in THF (0.5 mL, if indicated).

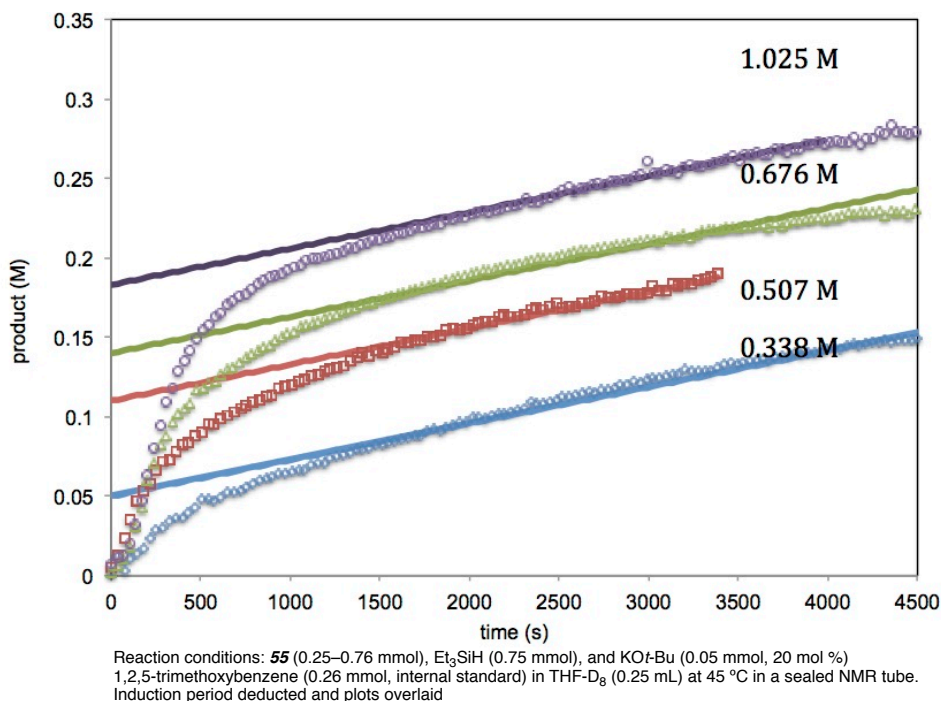
[b] Determined by GC analyses. [c] Determined by NMR analyses.

2.3.5 Reaction Rate Dependence on Substrate Loading

Our efforts to investigate the reaction rate dependence of each reaction component found limited success due to the induction period. Depending on our selection of $T=0$, significant variation occurred in the measured initial rate and the rapid formation of product during the burst period further complicated measurements (i.e., limited number of data points due to time constraint and $>10\%$ consumption of reactant). We did observe an interesting trend in a series of time-course experiments while varying substrate **55** concentration (Figure 2.3). In each case, an initial burst phase of product formation is observed while the rate of product formation appears consistent during the burst phase regardless of the substrate concentration. The length of the burst phase does appear to be correlated to substrate concentration. Interestingly, after the burst phase the reaction rate of all cases appear to be consistent, indicating the steady state reaction may

Chapter 2 – A Combined Experimental and Computational Mechanistic Study of the $\text{KO}t\text{-Bu}$ -Catalyzed Dehydrogenative C–H Silylation of Aromatic Heterocycles 49
not depend on **55**. This work helped us to understand the reaction occurred in the following 3 regimes; induction, burst, and sustained reaction periods.

Figure 2.3 Time-Course Investigation of Reaction Dependence on Substrate Concentration

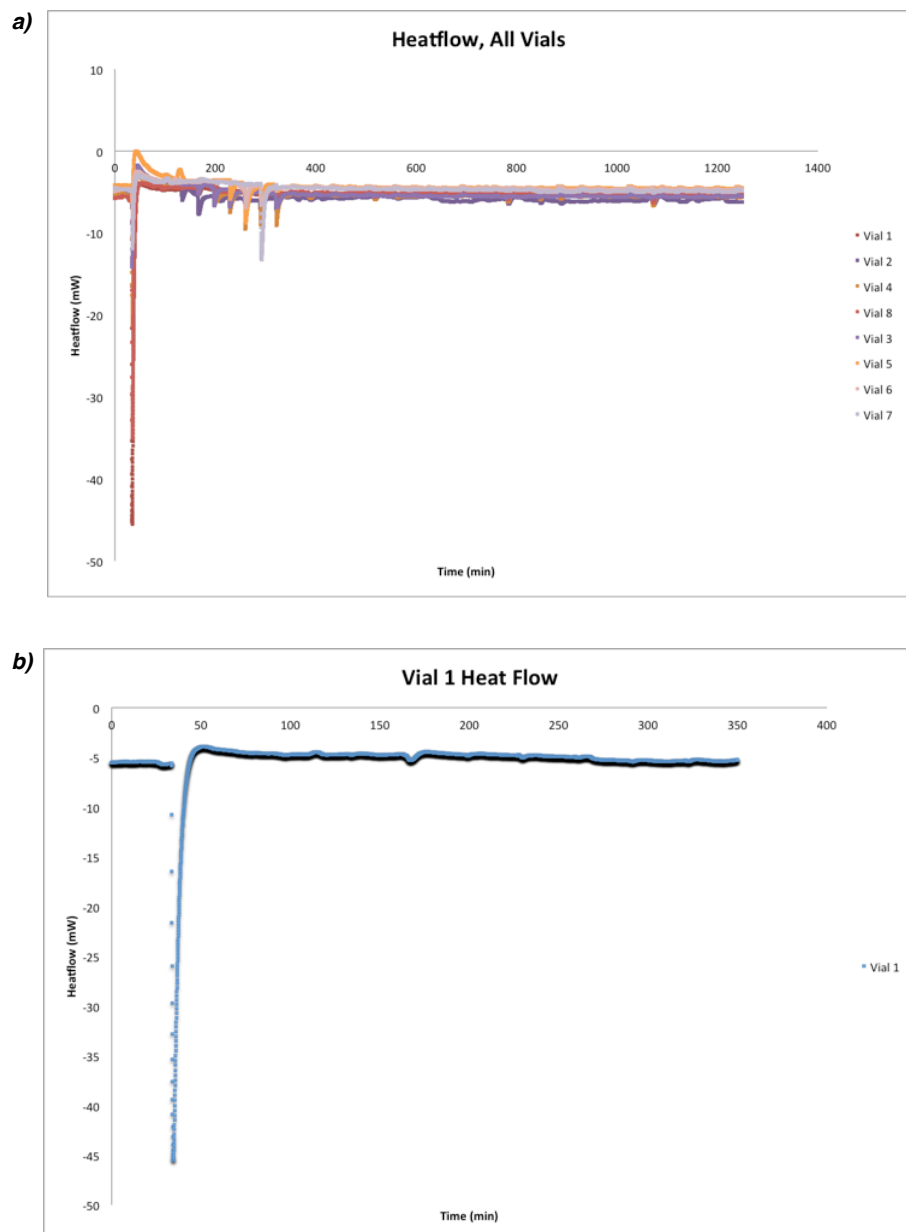


2.3.6 Silylation Reaction Safety

We investigated possible safety concerns related to the rapid formation of product during the burst phase of the silylation reaction (i.e., rapid generation of heat or gas). Eight identical reactions were conducted in parallel in a calorimeter and the heat flow for each vial is shown in Figure 2.4a. A large negative heat of mixing is observed when the $\text{KO}t\text{-Bu}$ solution in THF is added at $T=$ ~50 min. The repeated negative heat flow spikes are caused by minute changes in pressure due to sampling (i.e., using a syringe and needle to remove an aliquot for a GC sample). Therefore, one vial was not sampled until the endpoint (Figure 2.4b), while an additional vial was sampled at each time point (i.e.,

vial 2 at first time point, then vial 2 and 3 at the second time point, etc.). All vials had comparable conversion upon workup as measured by GC-MS (52–60% yield of **109**). Based on the GC-MS yield and variation in the observed heat flow, we estimate the heat of reaction to be ± 1 kcal/mol or less.

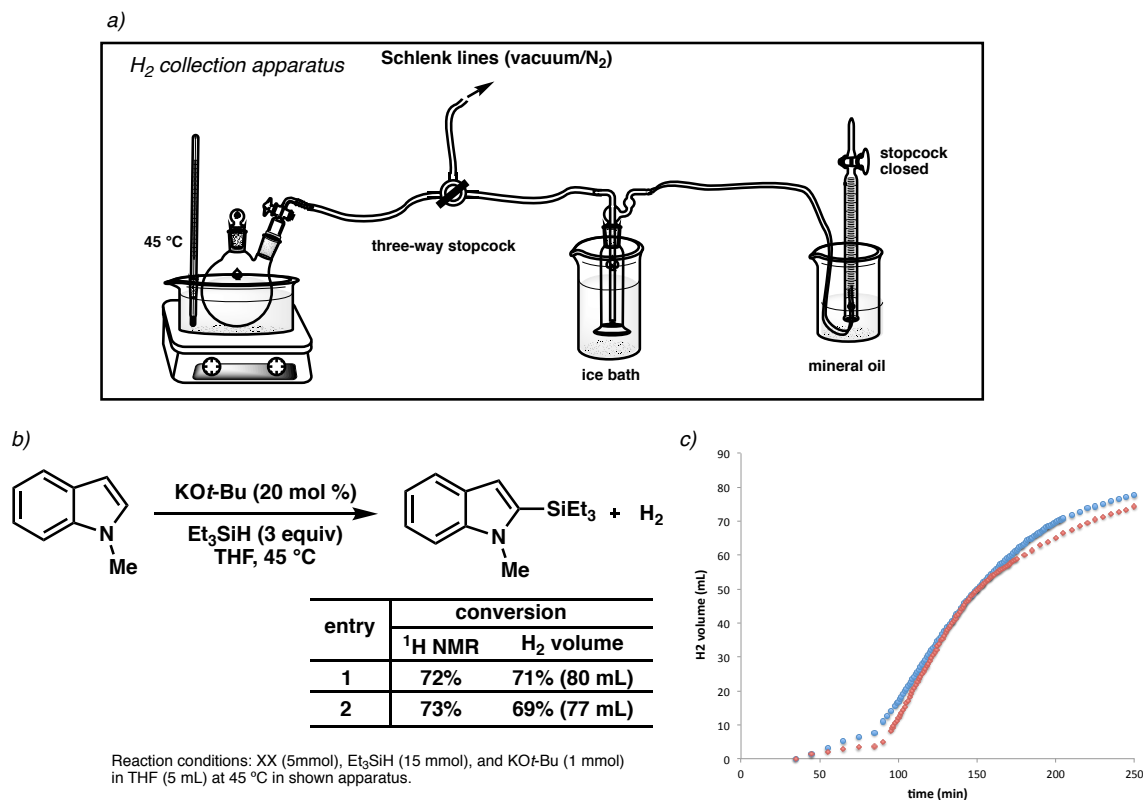
Figure 2.4 Reaction Heat flow



Reaction conditions: **55** (4 mmol), Et₃SiH (12 mmol), and THF (3.2 mL) in a sealed calorimeter vial and initiated using KOt-Bu sol. (1M in THF, 0.8 mL) in a plugged syringe equilibrated to 45 °C separately

The formation of hydrogen gas was investigated utilizing the eudiometry apparatus shown in Figure 2.5a. A relatively large scale silylation reaction was conducted with the generated gas captured and the gas volume measured throughout the reaction progress. The final conversion as estimated by H_2 gas formation was in good agreement with the value found by 1H NMR (Figure 2.5b) and the plot of gas formation over time (Figure 2.5c) demonstrates the same profile as the previously presented plots of product formation over time (ie., Figure 2.1). A sample of the gas was found to have a 1H NMR spectrum identical to H_2 .

Figure 2.5 Investigation of H_2 Formation

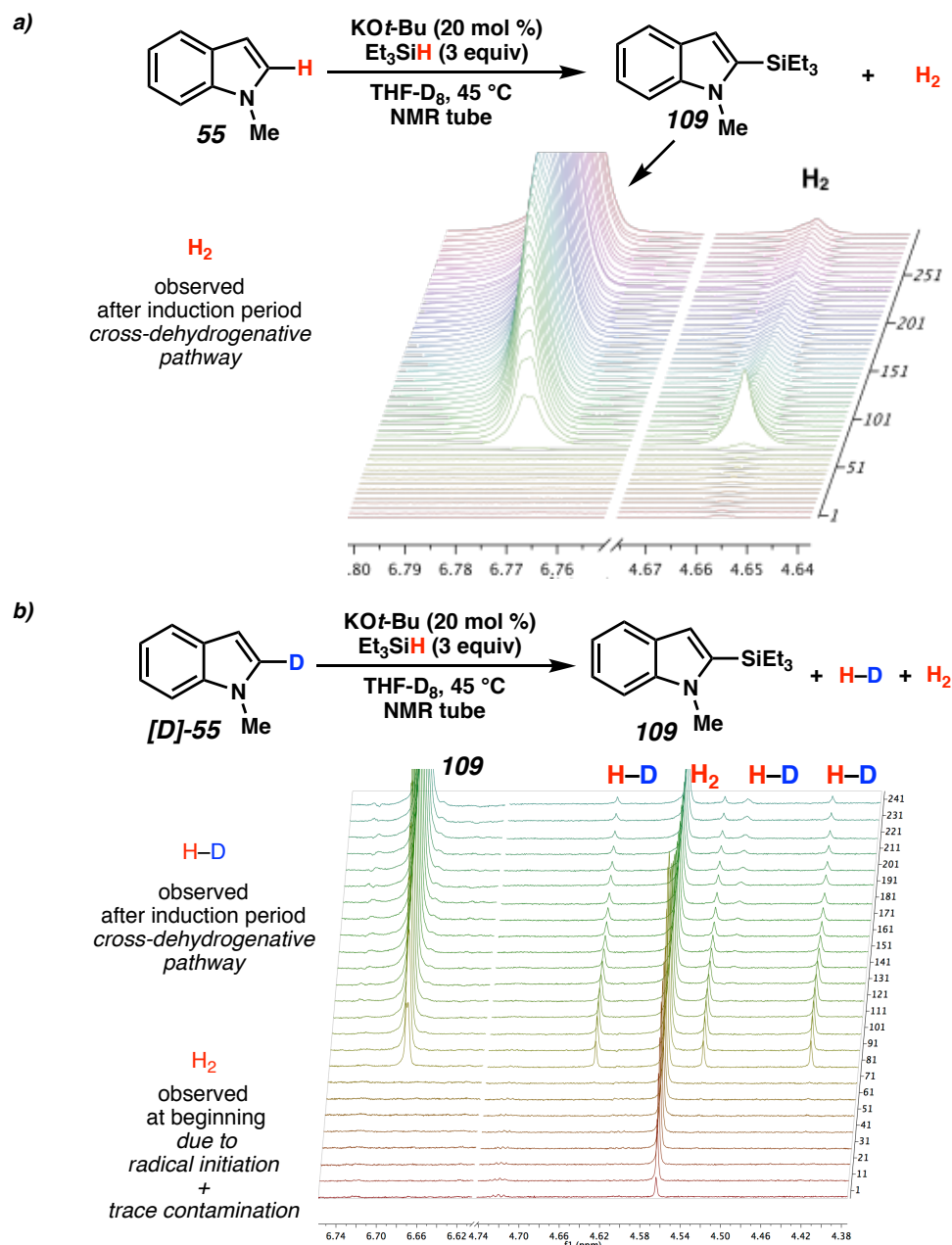


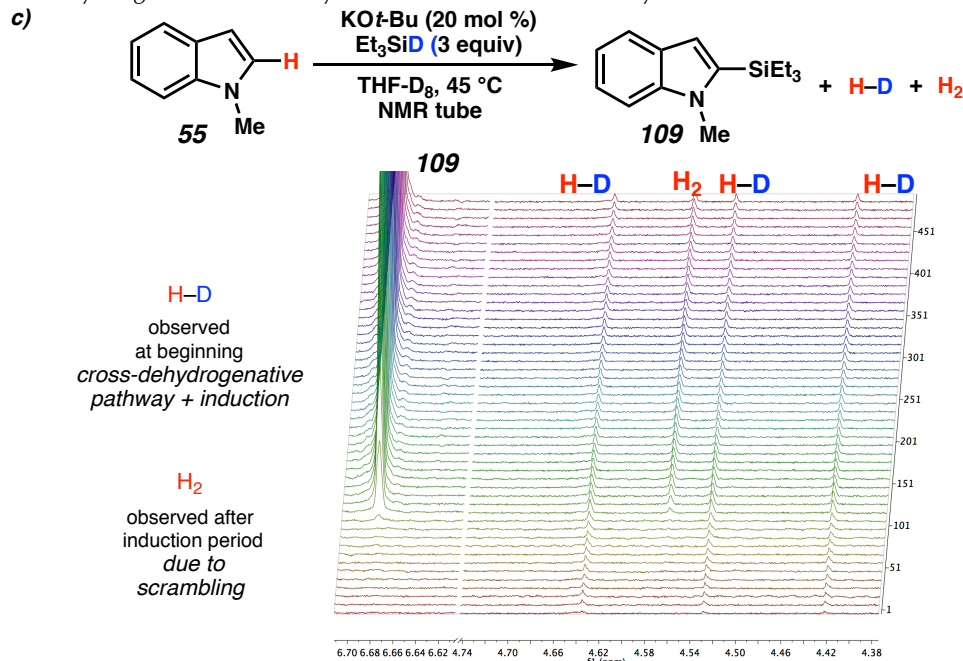
2.3.7 Cross-dehydrogenative Formation of H₂

The process of H₂ formation was probed by in situ NMR using deuterium labeled substrates. As shown in Figure 2.6a, a trace amount of H₂ was detected during the induction period followed by rapid H₂ evolution, along with generation of the silylation product **109**. When C-2 deuterated substrate (**D-55**) is subjected the same reaction conditions, H₂ is initially slowly generated during the induction period, followed by the formation of HD (1:1:1 triplet, J = 43 Hz) (Scheme 2.6b). We attribute the formation of H₂ to the radical initiation process involving Et₃Si–H and possible consumption of trace impurities.¹³ The simultaneous formation of H–D and **109** would be consistent with a cross-dehydrogenative pathway.

Further experimentation with protio-substrate **55** and Et₃Si–D was conducted under the same conditions and the results shown in Figure 2.6c. A minor peak corresponding to H–D was detected at the beginning of the reaction and the H–D signal intensity increased when formation of product **109** occurred. These results would also be consistent with a radical initiation process and consumption of trace impurities (now generating H–D when using Et₃Si–D) followed by the cross-dehydrogenative reaction pathway. The growth of a peak corresponding to H₂ gas under these conditions at later time points (i.e.; well after product **109** is initially observed) indicated a possible scrambling process may be active under these conditions, consistent with the data presented in **2.3.4**.

Figure 2.6 Hydrogen Gas Labeling Study



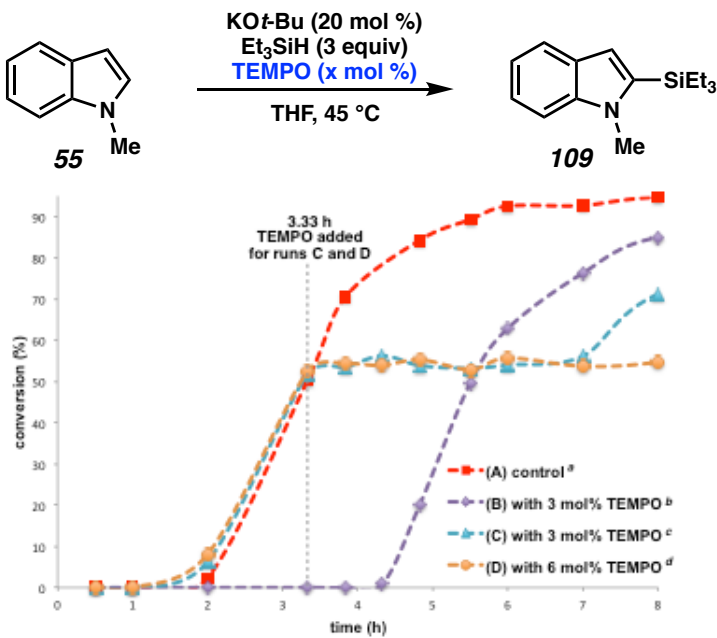


2.4 INVESTIGATION OF RADICAL INTERMEDIATES

2.4.1 Radical Trap Experiments

To probe the nature of the induction period, we performed a series of experiments using (2,2,6,6-tetramethylpiperidin-1-yl)oxyl (**151**, TEMPO) as a radical inhibitor. As shown in Figure 2.7, the addition of 3 mol % of TEMPO at the beginning of the reaction essentially doubles the delay in product formation (i.e., TEMPO inhibition plus induction) compared to the control (plot A). A similar effect was observed when TEMPO was added after the initiation period (i.e., at 3.33 h with 54% conversion, plot c and d); product formation ceased for a period and then continued. A larger TEMPO addition, 6 mol % compared to 3 mol %, prolongs the resultant induction period accordingly.

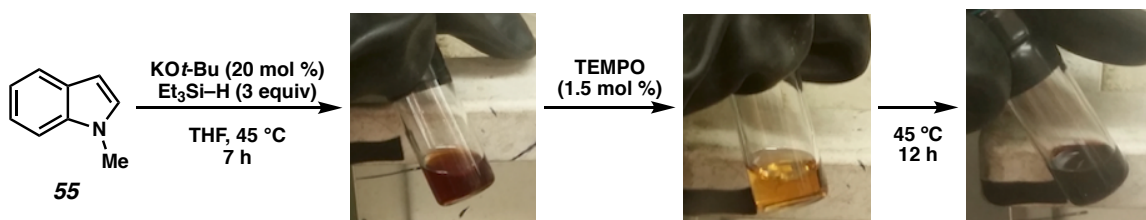
Figure 2.7 Radical Trap Using TEMPO



[a] Reaction conditions: **55** (0.5 mmol), **Et₃SiH** (1.5 mmol), and **KOt-Bu** (0.1 mmol, 20 mol%) in THF (0.5 mL) at 45 °C. Conversion determined via GC. [b] TEMPO (3 mol %) added at the beginning of the reaction. [c] TEMPO (3 mol %) added at $t = 3.33$ h. [d] TEMPO (6 mol %) added at $t = 3.33$ h, product formation resumes at 11 h.

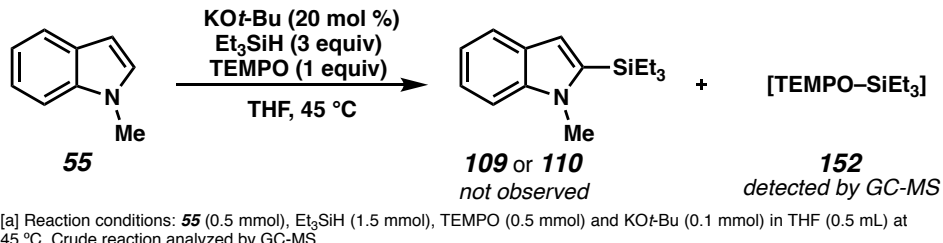
Interestingly, the addition of TEMPO to the initiated reaction mixture leads to immediate bleaching from dark purple to light yellow as shown in Figure 2.8. Allowing the mixture to continue to react results in the dark purple color returning over the period of hours. Attempts to characterize the highly colored species using UV–Vis spectroscopy were unsuccessful as the standard reaction conditions (i.e., 1M in substrate) resulted in insufficient light transmission and the colored species does not appear stable in sufficiently dilute samples.

Figure 2.8 TEMPO Induced Reaction Bleaching



When a stoichiometric amount of TEMPO is included, as shown in Scheme 2.4, the expected products **109** or **110** are not observed. Careful analysis of the crude reaction mixture by GC-MS displayed a signal with m/z that matches a TEMPO– SiEt_3 adduct (**152**) formed from the capture of the triethylsilyl radical by TEMPO.¹⁴

Scheme 2.4 Detection of TEMPO–Silyl Adduct



[a] Reaction conditions: **55** (0.5 mmol), Et_3SiH (1.5 mmol), TEMPO (0.5 mmol) and $KOt\text{-}Bu$ (0.1 mmol) in THF (0.5 mL) at 45 °C. Crude reaction analyzed by GC-MS.

These results would be consistent with TEMPO interception of a silyl radical, terminating the radical chain process. Product formation restarts only after the substoichiometric amount of TEMPO has been fully consumed.¹⁵

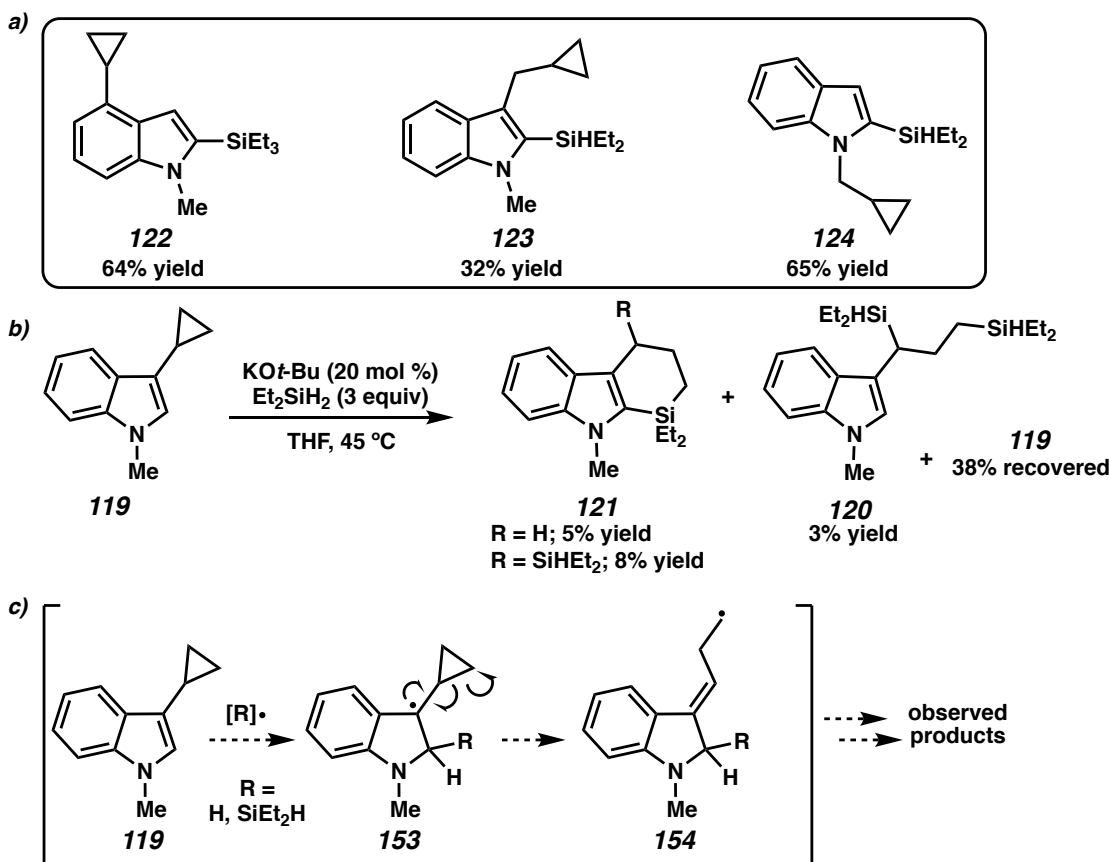
2.4.2 Radical Clock Experiments

To better understand how the triethylsilyl radical reacts with substrate, a series of cyclopropane containing substrates were employed as radical probes to investigate the formation of radical intermediates. Several indole substrates bearing cyclopropyl or cyclopropylmethyl groups were synthesized and subjected to the silylation reaction conditions (Scheme 2.5a). Substrates with 4-cyclopropyl-, 3-cyclopropylmethyl-, and 1-cyclopropylmethyl-substitution delivered the desired silylation products **122**, **123**, and **124**, respectively in moderate yields without the detection of ring-opening reactions.

In comparison, the reaction of 3-cyclopropyl-substituted indole **119** did not result in the expected C–H silylation product as shown in Scheme 2.5b. Instead a mixture of

were observed. These products could arise from a silyl radical, or hydrogen atom, addition to the substrate (**153**) followed by rapid cyclopropane ring opening (**154**) and further silylation or cyclization (Scheme 2.5c). The low yields of trapped products **120**–**121** could be explained by a number of radical termination processes limiting reaction rate. Overall, the results of our radical trap experiments are consistent with the formation of a C3-centered radical (i.e., **153**).

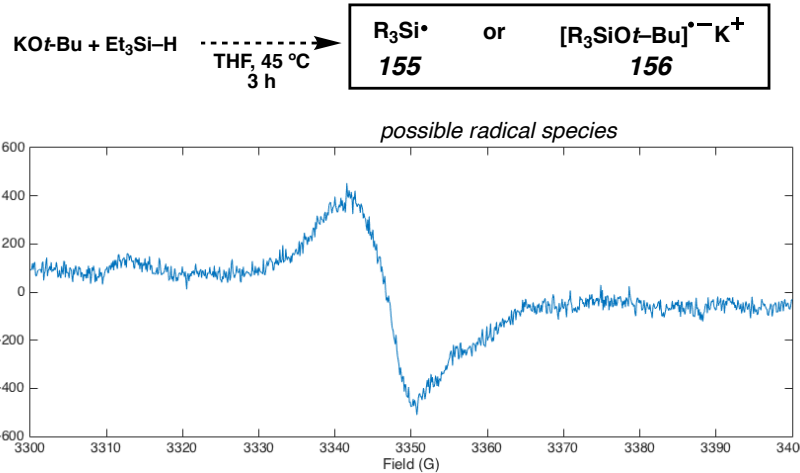
Scheme 2.5 Radical Clock Studies



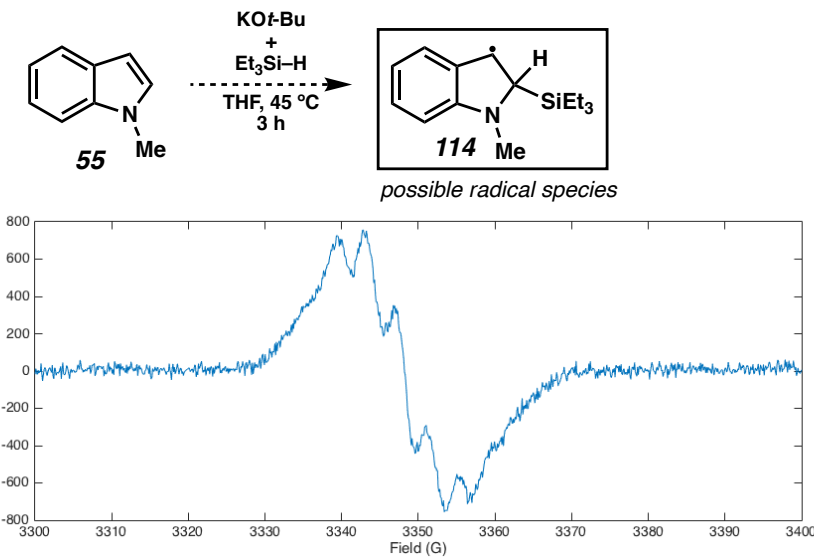
2.4.3 Electron Paramagnetic Resonance (EPR) Studies

EPR spectroscopy was utilized in an effort to directly detect and characterize radical intermediates present in the silylation reaction. KOt-Bu and Et₃SiH (Figure 2.9a) or **55**, KOt-Bu, and Et₃SiH (Figure 2.9b) were found to be EPR active and the resulting spectra are shown. While we were unable to conclusively determine the radical species present, the observed spectra are consistent with a number of catalytically relevant species such as **155** and **156**, in the absence of substrate **55**, or **114**, upon inclusion of substrate.

a)



b)



Reaction conditions: **55** (if used, 0.5 mmol), Et_3SiH (1.5 mmol), and $KOt\text{-}Bu$ (0.1 mmol) in THF (0.5 mL) at 45°C for 3 h, then frozen at 77 K and EPR spectrum acquired.

2.4.4 Radical Initiation

2.4.4.1 Background

Although there are a considerable number of examples of silyl radical reactions known in the literature, the means of generating silyl radicals are rather limited.¹⁶ In our case, the silylation reaction results in comparable yields when kept in the dark as exposed to ambient light, which rules out the possibility of visible light-induced radical formation. Radical generation from trace metal contamination was previously ruled out by a series of inductively coupled plasma mass spectrometry (ICP-MS) studies.¹⁰

2.4.4.2 Amine Additives

Itami, Lei and others reported that KOt-Bu could mediate the cross-coupling of aryl bromide and benzene without the use of transition-metal catalysis. Subsequent mechanistic studies revealed that in the presence of 1,10-phenanthroline a radical species was generated.¹⁷ This process is accelerated dramatically with catalytic amounts of organic electron transfer reagents, such as *N*-methylpyrrolidone, *N*-methlyglycine, and glycine, as demonstrated by Murphy.¹⁸

In the current silylation manifold the addition of any of these compounds resulted in a significant decrease in reactivity (Table 2.3, entries 1–4).

Table 2.3 Radical Generation via Amine Additives

The reaction scheme shows the conversion of indole derivative **55** (a substituted indole with a methyl group at position 3) to two products, **109** and **110**. Product **109** is the 3-silylindole where the methyl group is replaced by a trimethylsilyl group. Product **110** is the 2-silylindole where the hydrogen atom at position 2 is replaced by a trimethylsilyl group.

entry	additive	time (h)	conversion (%) ^b	109 : 110^b
1	1,10-phenanthroline	8 24	52 79	>20:1 >20:1
2	<i>N</i> -methylpyrrolidone	8 24	0 50	— >20:1
3	<i>N</i> -methylglycine	8 24	7 67	>20:1 19:1
4	glycine	8 24	10 54	>20:1 >20:1
5	none	8	93	>20:1

[a] Reaction conditions: **55** (0.5 mmol), Et₃SiH (1.5 mmol), KOt-Bu (0.1 mmol), and additive (0.025 mmol) in THF (0.5 mL) at 45 °C. [b] Determined by GC analysis.

2.4.4.3 Radical Initiation via Hydrogen Atom Abstraction

A reported method for the generation of silane based radicals is the abstraction of a hydrogen atom from hydrosilanes using organic radicals (e.g., *n*-Bu₃Sn•, *t*-BuO•).¹⁹ To test whether this mechanism is active under these conditions, we have undertaken a series of experiments with *in situ* generated *tert*-butoxy radicals. No product was obtained using catalytic quantities of di-*tert*-butyl peroxide (DTBP) at 135 °C (Table 2.4, entry 2). Utilizing stoichiometric DTBP at 135 °C led to only small amounts of desired product along with very complicated mixtures as indicated by the GC-MS traces (entry 3).

Attempts to carry out the silylation reaction under milder conditions with catalytic di-*tert*-butyl hyponitrite (TBHN) or a mixture of TBHN and NaOt-Bu failed to furnish product (entries 5 and 6). Addition of KOt-Bu to reactions containing either DTBP or

Chapter 2 – A Combined Experimental and Computational Mechanistic Study of the $KOt\text{-}Bu$ -Catalyzed Dehydrogenative C–H Silylation of Aromatic Heterocycles 62
 TBHN furnished the desired silylation product, albeit with decreased yields (entries 4 and 7).

Moreover, under our standard reaction conditions (i.e., entry 1), the desired product **109** was always accompanied by $t\text{-BuOSiEt}_3$ (**157**). The reactions with DTBP or TBHN did not produce $t\text{-BuOSiEt}_3$, indicating $t\text{-BuOSiEt}_3$ may not be arise from the reaction of $t\text{-BuO}\bullet$ with silane or silyl radical but different pathway.

Table 2.4 Radical Initiation via *tert*-Butoxy Radicals

entry	conditions (mol %)	temp (°C)	time (h)	conv (%) ^b	detection of 157 ^b		
					109	110	157
1	$KOt\text{-}Bu$ (20)	45	24	80	yes		
2	DTBP (20)	135	14	1	no		
3	DTBP (100)	135	14	10	no		
4	DTBP (20) + $KOt\text{-}Bu$ (20)	45	14	42	yes		
5	TBHN (10)	45	10 24	0 0	no no		
6	TBHN (10) + $NaOt\text{-}Bu$ (20)	45	10 24	0 0	no no		
7	TBHN (10) + $KOt\text{-}Bu$ (20)	45	10 24	0 54	no yes		

[a] Reaction conditions: **55** (0.5 mmol), Et_3SiH (1.5 mmol), $KOt\text{-}Bu$ (0.1 mmol, if used), and radical initiator in THF (0.5 mL) at 45 °C. [b] Determined by GC analysis.

Although the involvement of a *t*-butoxy radical cannot be excluded based on these experiments, there is little evidence to support the initiation of a triethylsilyl radical via hydrogen atom abstraction from Et_3SiH by *t*-butoxy radical.

2.5 PENTACOORDINATE SILICATE INTERMEDIATES

2.5.1 Background

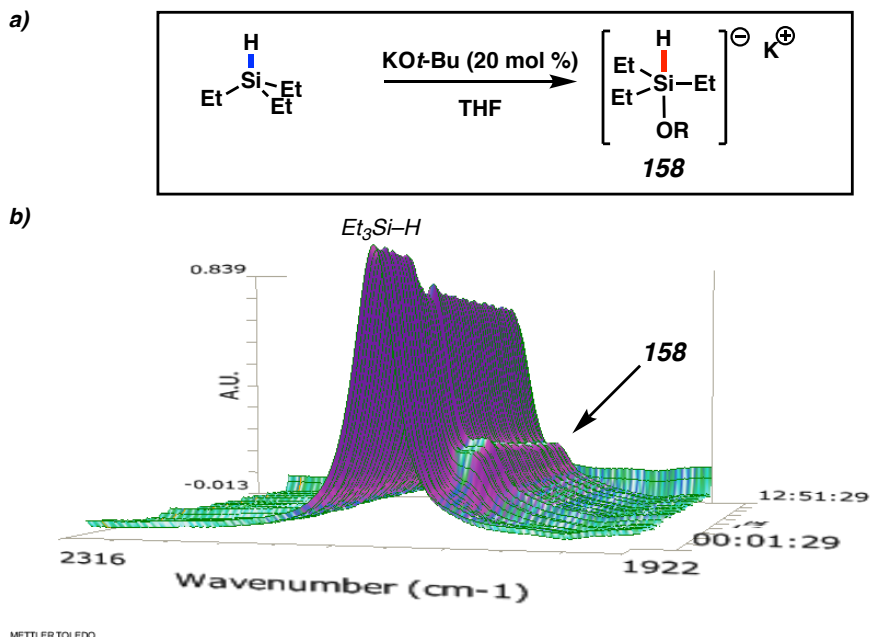
It has been well documented that the addition of strong silicophilic Lewis bases (e.g., fluoride, alkoxide) can increase the reactivity of hydrosilanes in the hydrosilylation of C=O bonds.²⁰ It is believed that strongly reducing hypercoordinate silicate complexes are formed by coordination of nucleophilic anions during such processes, which typically weakens the Si–H bond and increases the hydridic character of this bond.^{21,22} Studies by Corriu et al. revealed that the direct reaction of (RO)₃SiH with the corresponding KOR (R = alkyl or aryl) in THF at room temperature affords the anionic, five-coordinate hydridosilicate [HSi(OR)₄]K in good yield.²³ Such species are found to be very effective in the reduction of carbonyl compounds, can act as an electron donor toward the dehalogenation of organic halides, or can donate one electron to a metal complex. Although the formation of similar pentacoordinate species from trialkylsilanes and potassium alkoxide is unknown, we envisioned that such a complex is a possible intermediate in our reaction and may play a crucial role in radical initiation.

2.5.2 ReactIR Studies of Pentacoordinate Silicate

Unfortunately, attempts to isolate and structurally characterize such species by NMR were unsuccessful. However, by monitoring the silylation reaction using ReactIR, we found evidence for the existence of a new, possibly pentacoordinate silicate species (Figure 2.10). A new peak is visible in situ IR spectrum at 2056 cm⁻¹ adjacent to the Si–H stretching band in Et₃SiH (2100 cm⁻¹). This lower frequency peak would be consistent with an elongated, weakened Si–H axial bond in a five-coordinate silicate, as expected in such pentacoordinate complexes (i.e., in **158**).²⁴ A similar shift was reported previously

[$\text{H}_3\text{Si}(\text{CH}_2)_3\text{NMe}_2$] from 2151 to 2107 cm^{-1} .²⁵ In this case, the authors rationalize the observed redshift occurs by an N–Si interaction to form a hypercoordinate complex as confirmed by X-ray analysis.

Figure 2.10 ReactIR Investigation of Pentacoordinate Silicate

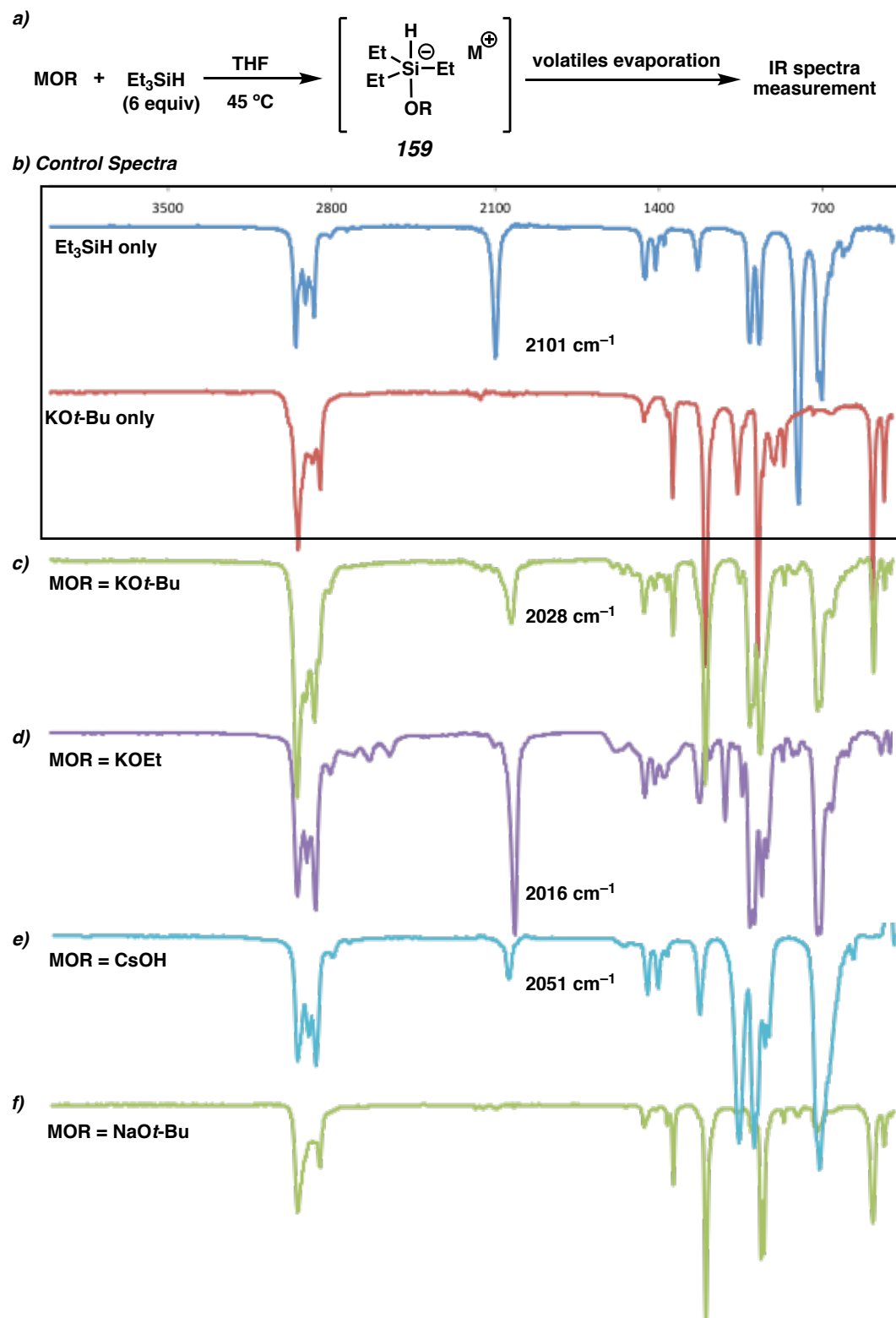


A correlation between the newly formed IR peak (Figure 2.10b) and the onset of product formation (i.e., the induction period ending) was observed. Once the new IR peak reached a steady state, the consumption of substrate **55** and formation of silylation product **109** occurs immediately. Furthermore, the new IR peak was visible throughout the reaction. This is consistent with the observation that premixing Et₃SiH and KOT-Bu in THF for 2 h at 45 °C followed by the addition of substrate **55** eliminates the induction period, suggesting that the formation of pentacoordinate silicate is responsible for the observed induction period.

2.5.3 ATR-IR Studies of Pentacoordinate Silicate

Further investigations were conducted to probe the formation of pentacoordinate silicates using a number of base catalysts listed in Table 2.1. The catalyst of interest was allowed to react with Et₃SiH in THF at elevated temperature, resulting in the possible formation of pentacoordinate silicates. Working inside a nitrogen-filled glove box, the mixture was placed on the window of an attenuated total reflectance infrared (ATR-IR) spectrometer, the volatile components (i.e., THF, Et₃SiH) were allowed to evaporate, and an ATR-IR spectrum was acquired (Figure 2.11a). Any alkoxide base which was a competent silylation catalyst developed a lower energy Si–H feature (from 2016–2051 cm⁻¹) potentially corresponding to the Si–H bond of a pentacoordinate species (Figure 2.11c–e). In sharp contrast, no such species were detected with unreactive catalysts (e.g., NaOt-Bu, Figure 2.11F) demonstrating that this new pentacoordinate complex is likely crucial for the radical initiation. For the pentacoordinate silicates formed from KOt-Bu and KOEt, the decrease in the frequencies of Si–H absorption correlates to a shortening of induction period, which is consistent with a longer bond requiring less energy for the homolytic cleavage (Figure 2.11c and d).

Figure 2.11 ATR-IR Spectra of Select Base-Silane Mixtures



Normalized and stacked ATR-IR spectra of Si–H stretching region of select metal alkoxides with hydrosilane. Reaction conditions: base (0.1 mmol) and Et_3SiH (0.5 mmol) in THF (0.5 mL).

Finally, although there is a large variation in the induction periods with KOH, RbOH and CsOH, no differentiating Si–H frequencies of the pentacoordinate silicates derived from those bases are observed (Table 2.5, entry 6–8). We propose that this indicates the hydroxides are converted to the silanolates, and subsequently silicates, which serve as the active catalysts (entry 5 versus 6–8).²⁶ It is possible that the weak cation-anion interaction of late alkali metal bases could accelerate the formation of pentacoordinate silicates and thus account for the differing rate of radical initiation.²⁷

Table 2.5 Shift of Si–H IR Feature in Select Base Catalyst Mixtures

entry	Base	t (h) ^a	ν [Si–H] (cm ⁻¹) ^b	Δν vs Et ₃ Si–H (cm ⁻¹) ^c
1	–	–	2099	–
2	KOt-Bu	2	2028	71
3	KOEt	2	2016	83
4	KOMe	7	2054	45
5	KOTMS	7	2047	52
6	KOH	20	2045	54
7	RbOH·xH ₂ O	7	2052	47
8	CsOH·H ₂ O	7	2051	48
9	NaOt-Bu	36	–	–
10	Mg(Ot-Bu) ₂	36	–	–
11	LiOt-Bu	36	–	–

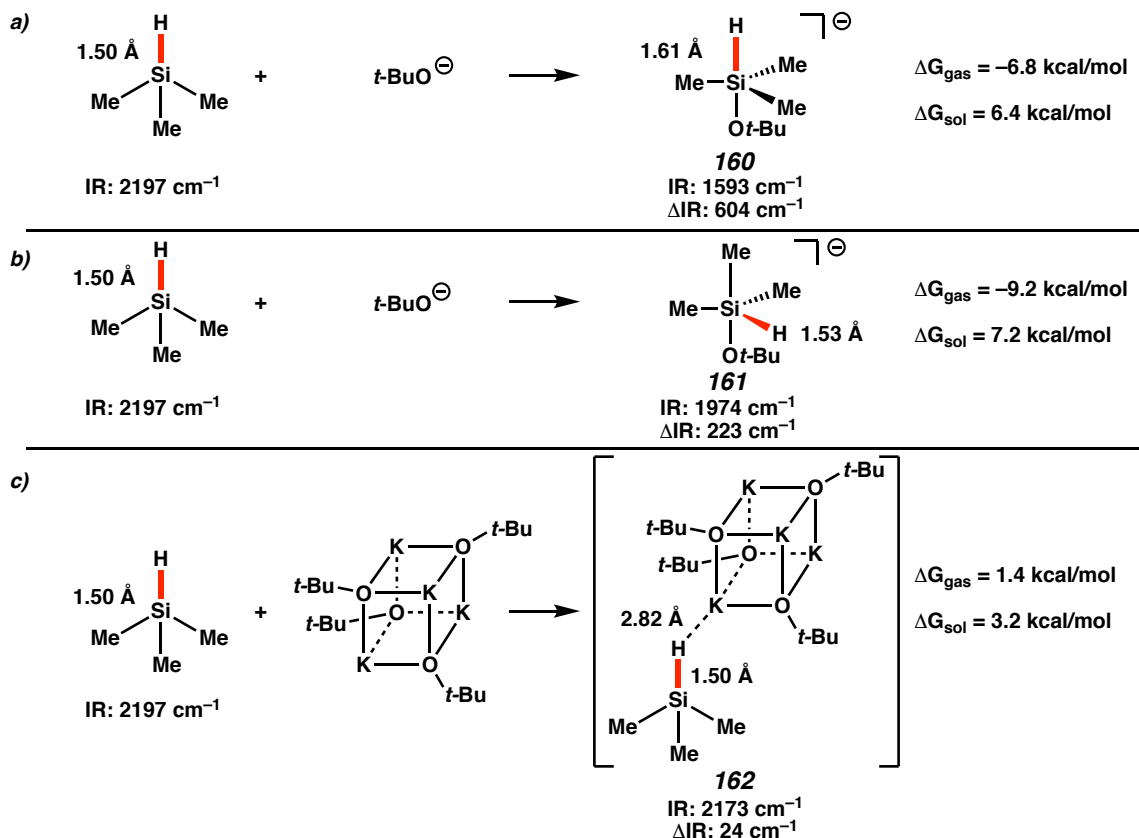
Reaction conditions: base (0.1 mmol) and Et₃SiH (0.5 mmol) in THF (0.5 mL). [a] Reaction time before IR spectrum was measured. [b] Frequency of new Si–H bond feature, if present. ^cFrequency shift of observed feature versus Et₃Si–H.

2.5.4 Computational Studies of Pentacoordinate Silicate

We also performed computational studies to understand the nature of the coordinated species. Scheme 2.6 shows the calculated energetics of complex formation and the predicted Si–H stretching frequencies. Formation of the pentacoordinate silicate with the hydrogen atom in the axial position (**160**) requires 6.4 kcal/mol, and with hydrogen in the equatorial position (**161**) requires 7.2 kcal/mol. In both cases the

for a 1M standard state causes the corresponding free energies to be unfavorable. The predicted IR shifts from trimethylsilane to these two silicate isomers are 604 cm^{-1} and 223 cm^{-1} , respectively. Both of these IR shifts are larger than the experimentally observed IR shift of 73 cm^{-1} . The formation of tetrameric KOt-Bu associated silane complex **162** is 3.2 kcal/mol endergonic, and the IR shift from silane to the corresponding $(\text{KOt-Bu})_4$ associated silane complex is only 24 cm^{-1} . The M062x functional and various basis sets were tested to probe the energetics of formation of these coordinated silicon species, and provided similar results.

Scheme 2.6 Computed Results of Pentacoordinate Silicate Formation

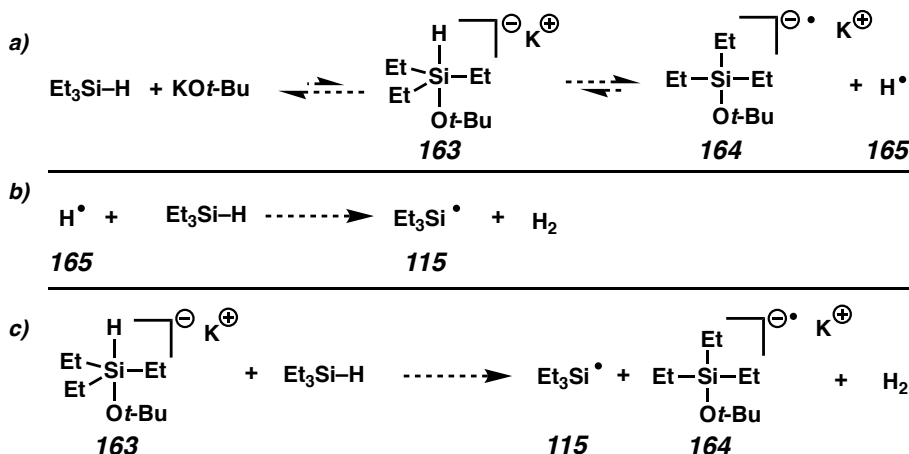


Calculated energetics of formation of pentacoordinate silicates or tetrameric KOt-Bu associated silane complex and the calculated IR stretching frequency of the Si–H bond.

2.5.5 Radical Initiation via Pentacoordinate Silicate

The bond dissociation energy for the Si–H bond of Et₃SiH is 90.1 kcal/mol,²⁸ and the corresponding Si–H bond of silicate **163** would be weakened due to a change in electronics in the pentacoordinate structure (Scheme 2.7a). Thus a possible pathway for the radical initiation from silicate **163** would be the homolytic scission of Si–H to form a hydrogen radical and a coordination anion-radical complex **164** (consistent with the resultant *t*-BuOSiEt₃ detected by GC after workup of the reaction), as shown in Scheme 2.7a. This hydrogen radical **165** could then abstract a hydrogen atom from Et₃SiH to generate hydrogen gas, as detected by in situ ¹H NMR, and a triethylsilyl radical **115** which we believe is the active species (Scheme 2.7b). Alternatively, reaction of pentacoordinate complex **163** and Et₃SiH could result in the formation of both a silicon based radical (**115**) and radical anion (**1664**) as shown in Scheme 2.7c.²⁹

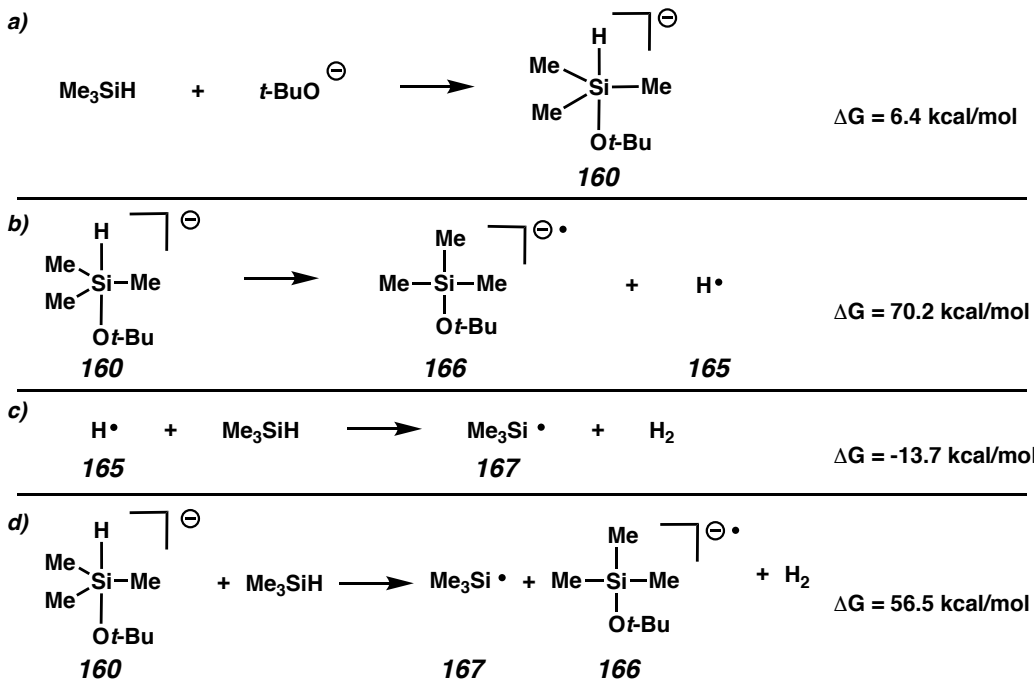
Scheme 2.7 Plausible Formation of Pentacoordinate Silicate and Radical Initiation



Unfortunately, our attempts to calculate such a radical initiation mechanism resulted in large activation energies (Scheme 2.8). While we still believe a Si–H bond homolysis of a pentacoordinate silicate may be relevant given our aforementioned

with more reasonable activation energies.

Scheme 2.8 Computational Analysis of Key Steps in Pentacoordinate Silicate Radical Initiation



DFT calculated energetics of the generation of silyl radical through homolytic Si–H bond fission of hypercoordinate silicate. Gibbs free energies including THF solvation are shown.

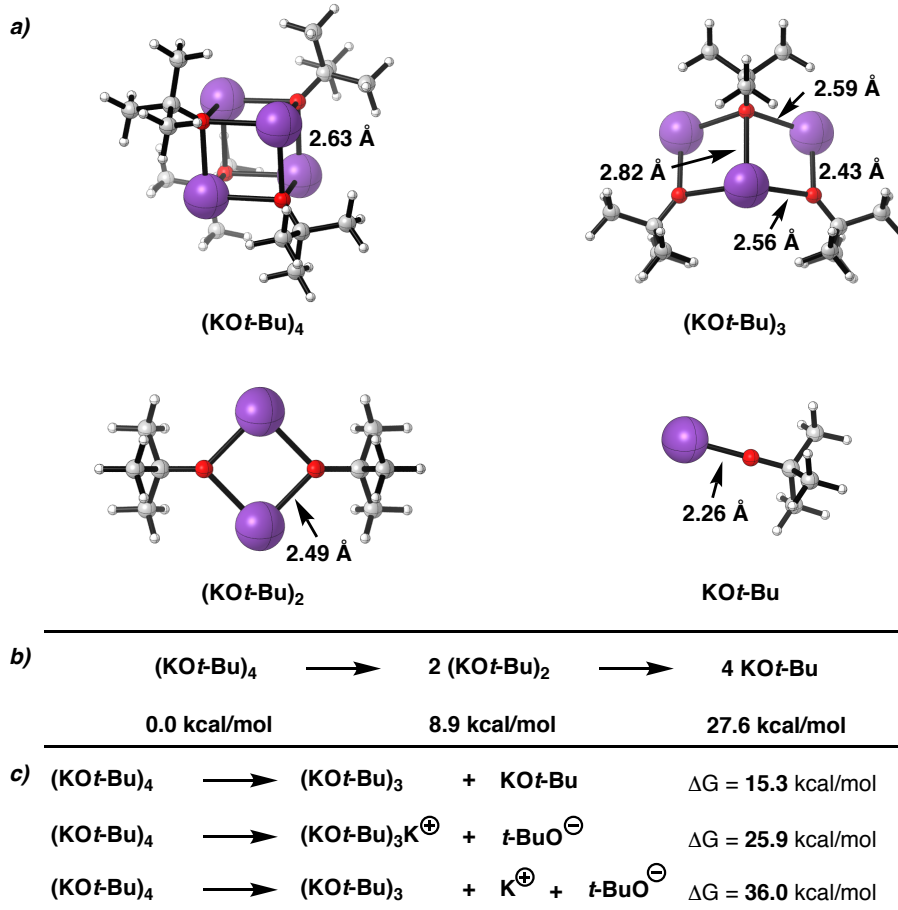
2.6 ALTERNATIVE RADICAL INITIATION PATHWAYS

2.6.1 Catalyst Speciation

The extent of $\text{KO}_t\text{-Bu}$ aggregation in this reaction may be key to determining its catalytic behavior. The X-ray structure of anhydrous $\text{KO}_t\text{-Bu}$ crystallized from THF–*n*-pentane reveals a tetrameric $[\text{KO}_t\text{-Bu}]_4$, with a cubane-like structure (computed structure shown in Figure 2.12a).³⁰ This tetrameric structure is very stable, and persists in the solid and gas phase. Even in solution, mild Lewis basic solvents such as THF and diethyl ether do not break up the tetramer and the calculated energy of dissociation shows that these processes are very unfavorable (Figure 2.12b). As shown in Figure 2.12c, the

anion requires 25.9 kcal/mol. Therefore, the tetramer $[KOt\text{-}Bu]_4$ is used as reference point in further calculations unless otherwise noted.

Figure 2.12 Dissociation of $[KOt\text{-}Bu]_4$

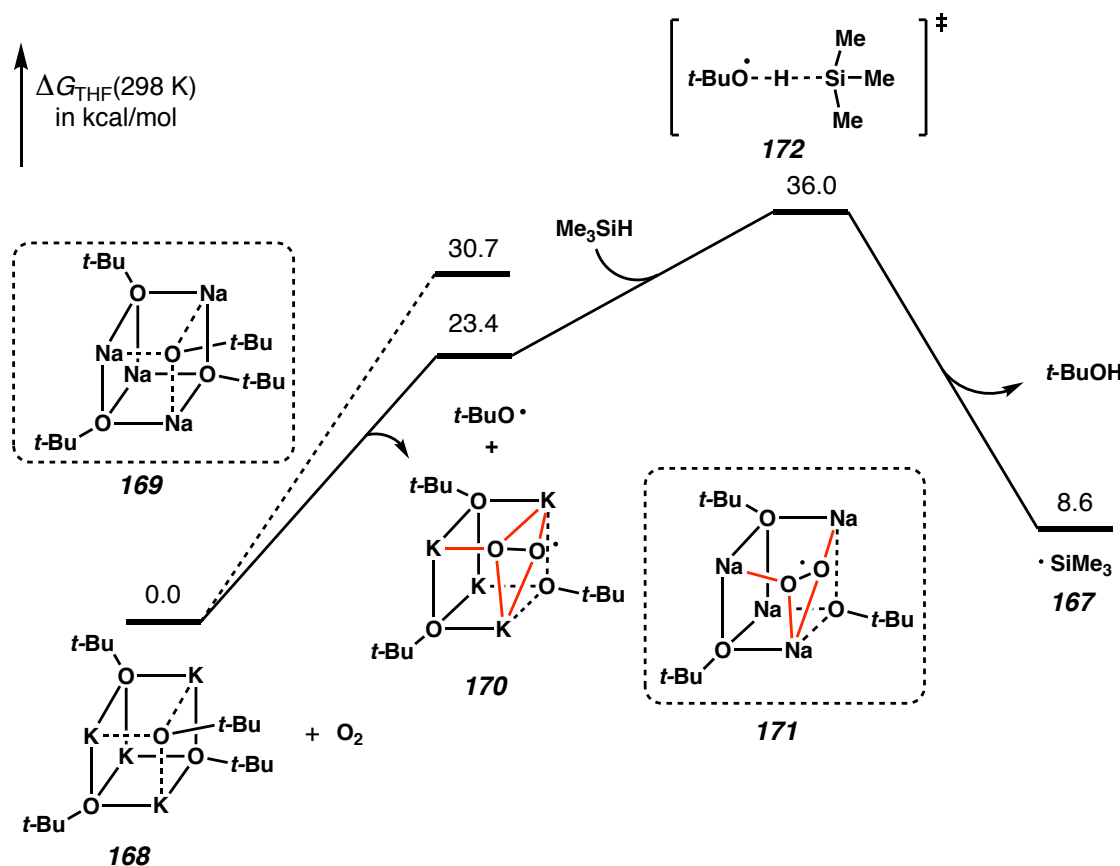


2.6.2 Radical Initiation via Trace Oxygen

Our computational results show that the radical initiation pathway through homolytic Si–H bond fission of hypercoordinate silane is relatively high energy (Scheme 2.8 and Figure 2.12). To address this unrealistic barrier, we have explored many different pathways of generation of the silyl radical, the most reasonable of which is shown in Figure 2.13. Trace molecular oxygen might serve as a temporary electron acceptor to

[KOt-Bu]₄, *tert*-butoxyl radical and potassium peroxide radical **170** are generated. This process requires 23.4 kcal/mol, while the same process with tetramer [NaOt-Bu]₄ requires 30.7 kcal/mol, shown in dashed line. This is consistent with the failure of NaOt-Bu as a catalyst for the silylation reaction. This effect can be understood since the smaller sodium ion size would lead to a larger distortion from the tetramer structure **169** to sodium peroxide radical **171**, as compared to KOt-Bu. Only one Na–O bond is formed from **169** to **171**, while two K–O bonds are formed from **168** to **170**. Once the *tert*-butoxyl radical is formed, it can react with hydrosilane Me₃SiH to generate the silyl radical through transition state **172** (36.0 kcal/mol, Figure 2.13). The entire silyl radical generation process is endergonic by 8.6 kcal/mol, but only a trace amount of radicals are needed to initiate the proposed chain mechanism. The high-energy barrier for initiation would be consistent with the observed induction period.

Figure 2.13 Computed Pathway for Radical Initiation by Trace Oxygen



Free energy profile for generation of silyl radical involving traces of oxygen. Gibbs free energies, including THF solvation, are shown in kcal/mol.

2.7 SILYLATION REACTION MECHANISM

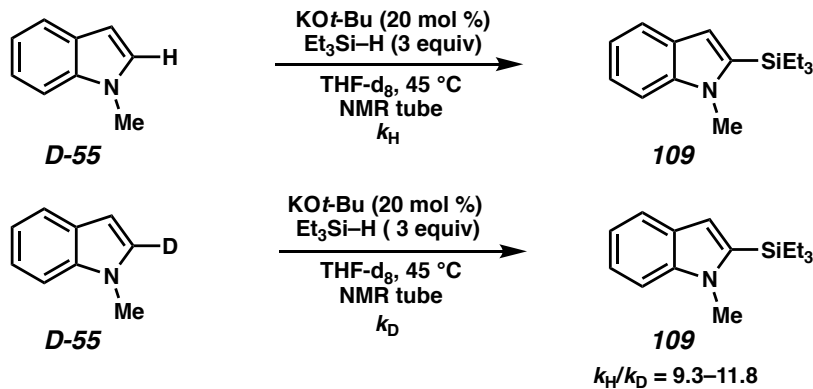
2.7.1 Kinetic Isotope Effect Studies

We envisioned that a β C–H fission from a C3-centered radical species (e.g. **153**, Scheme 2.4c) resulting in the formation of hydrogen gas is most likely the rate determining step of the proposed radical chain process. To gather more information about this hypothesis, C2-deuterium labeled substrate (**D-55**) was used to study the kinetic isotopic effects (KIE) during the reaction. First, two separate, parallel reactions of triethylsilane with **55** and [**D-55**] were performed to determine the KIE value (Scheme 2.9). As monitored by in situ ^1H NMR, a significant KIE was observed using the initial

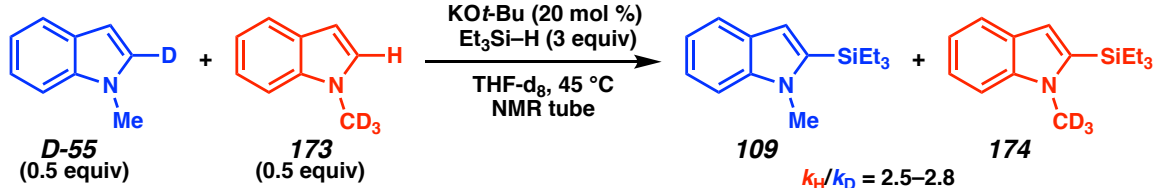
rates method for each reaction at the onset of product formation ($k\text{H}/k\text{D} = 9.3\text{--}11.8$). The intermolecular competition reaction of [D]-55 and 1-CD₃-indole 173 in the same pot also showed a clear isotopic effect ($k\text{H}/k\text{D} = 2.5\text{--}2.8$) calculated from the relative initial rates of formation for 109 and 174. These results provide evidence that the C–H bond breaking of indole is involved in the rate-determining step.

Scheme 2.9 Kinetic Isotope Studies

a) parallel reactions



b) intermolecular competition



Reaction conditions: D-55 or 55 + 173 (0.25 mmol), Et_3SiH (0.75 mmol), and $KO\ddot{t}\text{-}Bu$ (0.05 mmol), and 1,2,5-trimethoxybenzene (if used, 0.024 mmol, internal standard) in THF-D_8 (0.25 mL) at 45 °C in a sealed NMR tube.

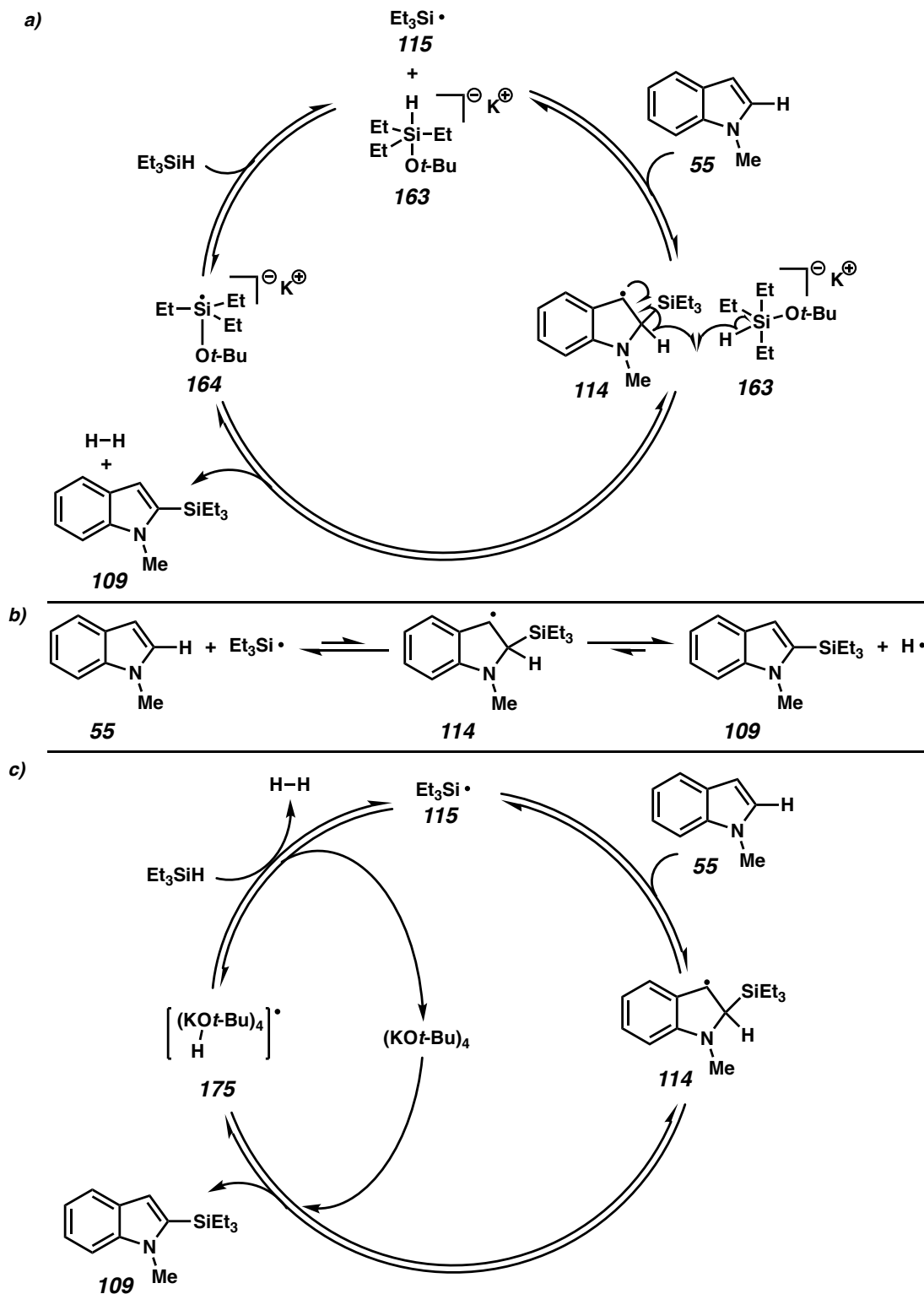
We also investigated the reaction using Et_3SiH and Et_3SiD , finding that the reactions with deuterated silane demonstrated a significantly longer induction period and a decreased reaction rate was observed. The combination of a prolonged induction period and decreased initial rate prevented an exact KIE measurement. The relative rate differences observed may arise from the homolytic cleavage of a Si–D bond in a pentacoordinate species requiring higher energy, therefore prolonging the induction

Chapter 2 – A Combined Experimental and Computational Mechanistic Study of the KOt-Bu-Catalyzed Dehydrogenative C–H Silylation of Aromatic Heterocycles 75
period. Furthermore the slower abstraction of deuterium compared to hydrogen limits the overall reaction rate in the radical chain mechanism.³²

2.7.2 Proposed Reaction Mechanism

The addition of silyl radicals to double bonds has been shown to readily occur, driven by the formation of a stronger σ-bond at the expense of a weaker π-bond.³³ Therefore, we propose that Et₃Si• adds to indole at the C2 position to generate a stabilized benzylic radical **114** (Scheme 2.10), as evidenced by radical clock experiments shown in Scheme 2.5. Fragmentation of the weaker C2–H bond α to the radical center by a β-H scission restores aromaticity in the indole system and generates H₂, providing an entropic driving force for the overall reaction.^{34,35} The resultant silicate radical anion **164** can then react with an equivalent of triethylsilane thereby regenerating the Et₃Si•, continuing the chain process. Tetrameric [KOt-Bu]₄ may also be involved as a hydrogen atom transfer catalyst, by abstracting a hydrogen atom from benzylic radical **114**, producing the silylated product **109** as well as the base–hydrogen radical adduct **175**. This radical adduct then reacts with another equivalent of hydrosilane to produce H₂ and regenerates the silyl radical, thus completing the catalytic cycle.

Scheme 2.10 Proposed Reaction Mechanism



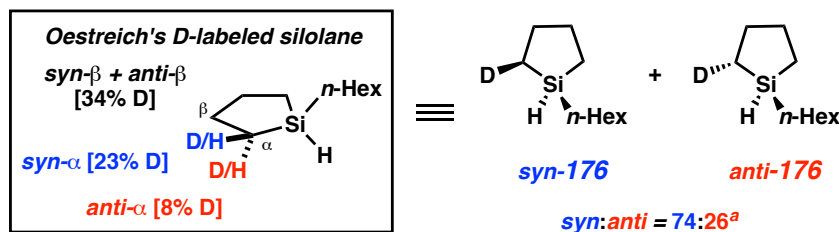
The significant KIE observed at the C2-position suggests that the β -H scission is the rate-determining step after radical initiation (**114** to **109**). The nucleophilic β -silyl radical **114** is slow to abstract a hydrogen atom from Et₃Si–H due to the similar polarities of the two radicals (i.e., **114** vs Et₃Si•) and a hydrosilylation product was never observed.³⁶ The reversibility of the silylation reaction can be explained by the addition of H• to silylation product **55**, providing radical **114**, followed by C–Si bond scission to from an equivalent of Et₃Si• instead of H• resulting in the formation of starting material (Scheme 2.10b).

2.7.3 Stereochemical Course of Silicon

To gain further evidence for the proposed reaction mechanism, we envisioned using a method to study the stereochemical course at silicon during the C–H silylation. Since the synthesis of silicon-stereogenic silanes (chiral silane) and determination of stereochemical outcomes in Si–C bond-forming reactions (i.e., determination of the absolute configuration of the silylated product) is challenging, we decided to utilize a recently reported method by the Oestreich group.³⁷ In this method, a mixture of isomers of deuterium-labeled silolanes **176** are used as a stereochemical probe (Figure 2.13).³⁸ The syn and anti designations are the relative orientation of deuterium to the *n*-hexyl group.

²H NMR allows for tracking the relative ratio of syn-**176** and anti-**176** and therefore determine configurational changes at the silicon atom based on changes in the syn:anti ratio, thus removing the need to know the exact distribution of deuterium in this complex mixture of isomers.

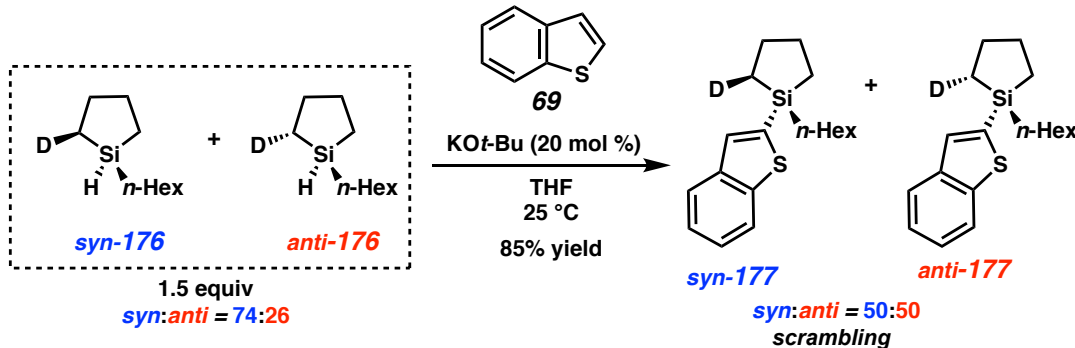
Figure 2.14 Stereochemical Silicon Probe



[a] Syn:anti ratio determined by ^2H NMR [b] Deuteration at the α -position is omitted for clarity.

Oestreich's deuterium labeled silolane was prepared according to the reported procedure, resulting in a mixture of isomers with the syn:anti-**176** ratio of 74:26. $KOt\text{-}Bu$ -catalyzed silylation of **69** under our previously reported conditions proceeds with complete scrambling of the configuration at the silicon atom as indicated by the 1:1 ratio of products syn-**177** and anti-**177** (Scheme 2.11).

Scheme 2.11 Stereochemical Path of Silicon During Silylation Reaction



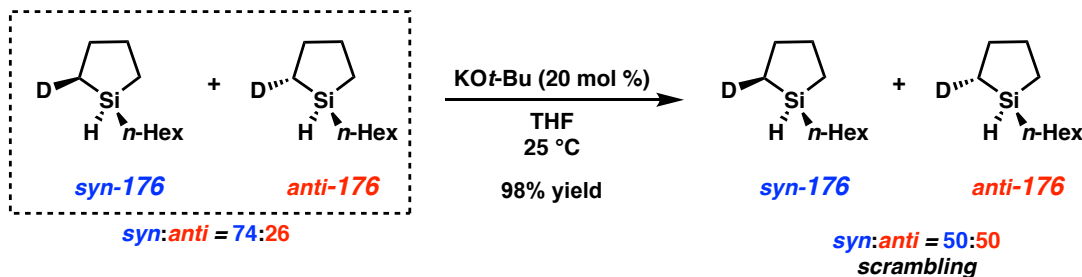
This observed scrambling is in contrast to Falck's protocol using an iridium(I) catalyst, where complete retention of the stereochemistry at the silicon atom is observed due to a traditional oxidative addition/reductive elimination pathway.^{38,39}

Previous studies by Sommer, Oestreich, and others have shown that a nucleophilic substitution at the silicon center can occur with either retention or inversion

Chapter 2 – A Combined Experimental and Computational Mechanistic Study of the KOt-Bu-Catalyzed Dehydrogenative C–H Silylation of Aromatic Heterocycles 79
of stereochemistry, depending on the nature of the nucleophile and the leaving group on silicon.⁴⁰ Yet these reactions are highly stereospecific and do not result in scrambling of the deuterium labeled silolane.³⁸

We theorized that the observed scrambling may occur without participation of the heteroarene. A control experiment treating a mixture of **176** with KOt-Bu alone in THF resulted in complete scrambling of the deuterium labeled silolane (Scheme 2.12).

Scheme 2.12 Base Scrambling of Silicon Center Stereochemistry



While consistent with a number of our proposed intermediates, we cannot distinguish if stereochemical scrambling occurs at the stage of pentacoordinate silicate anion **163**, radical anion **164**, or a tricoordinate silyl radical **115** (cf. Scheme 2.10a). Pentacoordinate silicon intermediates may undergo pseudorotational processes resulting in loss of stereochemical information at the silicon atom.⁴¹ Although silyl radicals are pyramidal and can be configurationally stable under certain conditions,⁴² racemization of a chiral silyl radical could take place due to the fast inversion of the pyramidal radical.⁴³ Nevertheless, all three of these intermediates are on pathway in our proposed mechanism (Scheme 2.10a, c).

Furthermore, a handful of examples of direct nucleophile trapping by a hydrosilane are known in the literature, including KOt-Bu-catalyzed protection of alco-

Chapter 2 – A Combined Experimental and Computational Mechanistic Study of the KOt-Bu-Catalyzed Dehydrogenative C–H Silylation of Aromatic Heterocycles 80
hols. In such cases, an inversion at the silicon center was observed with chiral silanes, which is not in line with our observed scrambling.

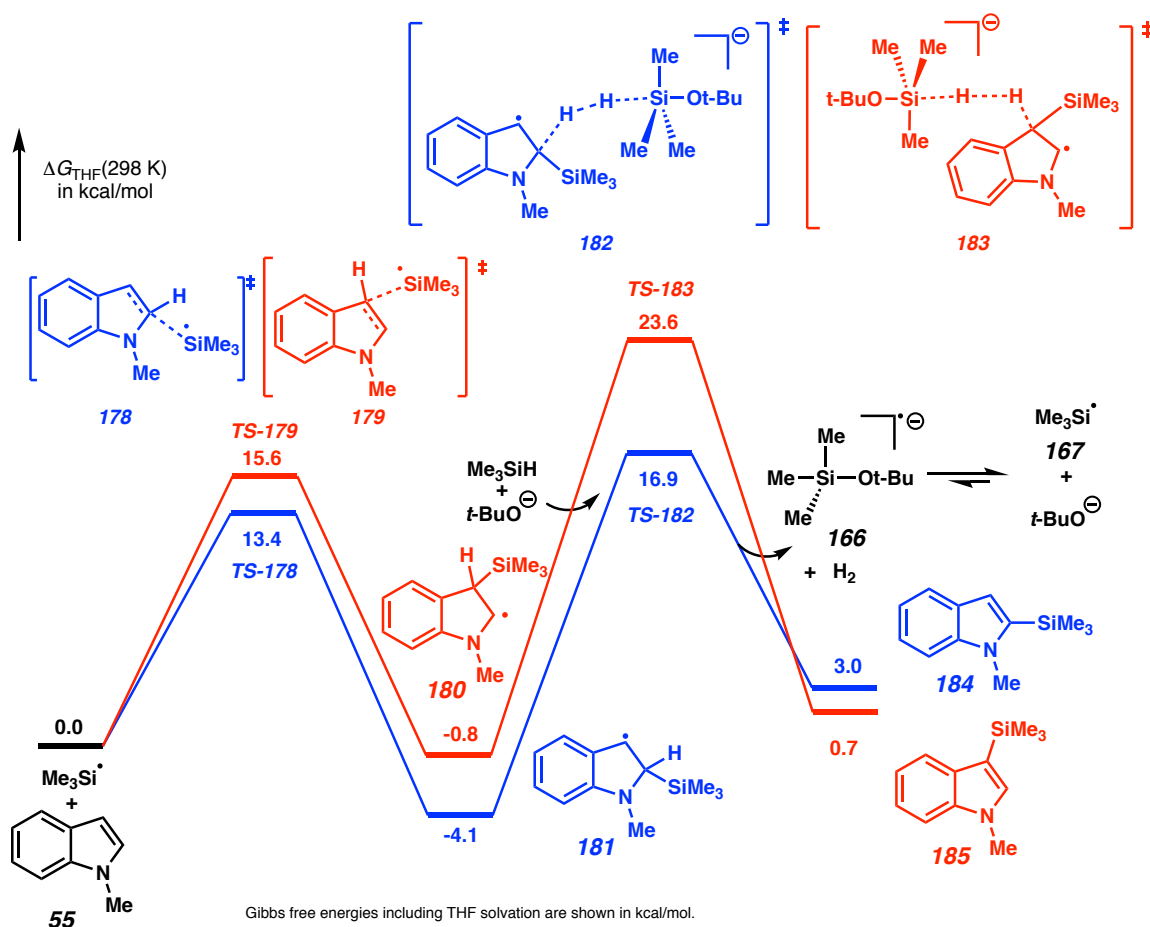
2.7.4 Computational Study of Proposed Mechanism

We have performed a computational study that explores the mechanism and origin of regioselectivity of this C–H silylation reaction. We propose that the reaction can proceed by either of the two radical chain mechanisms, shown in Scheme 2.10. The free energies of both C2- and C3-silylation of 1-methylindole (**55**) are shown in Figure 2.15 and 2.16, for the cycles in Scheme 2.10a and 2.10c, respectively.

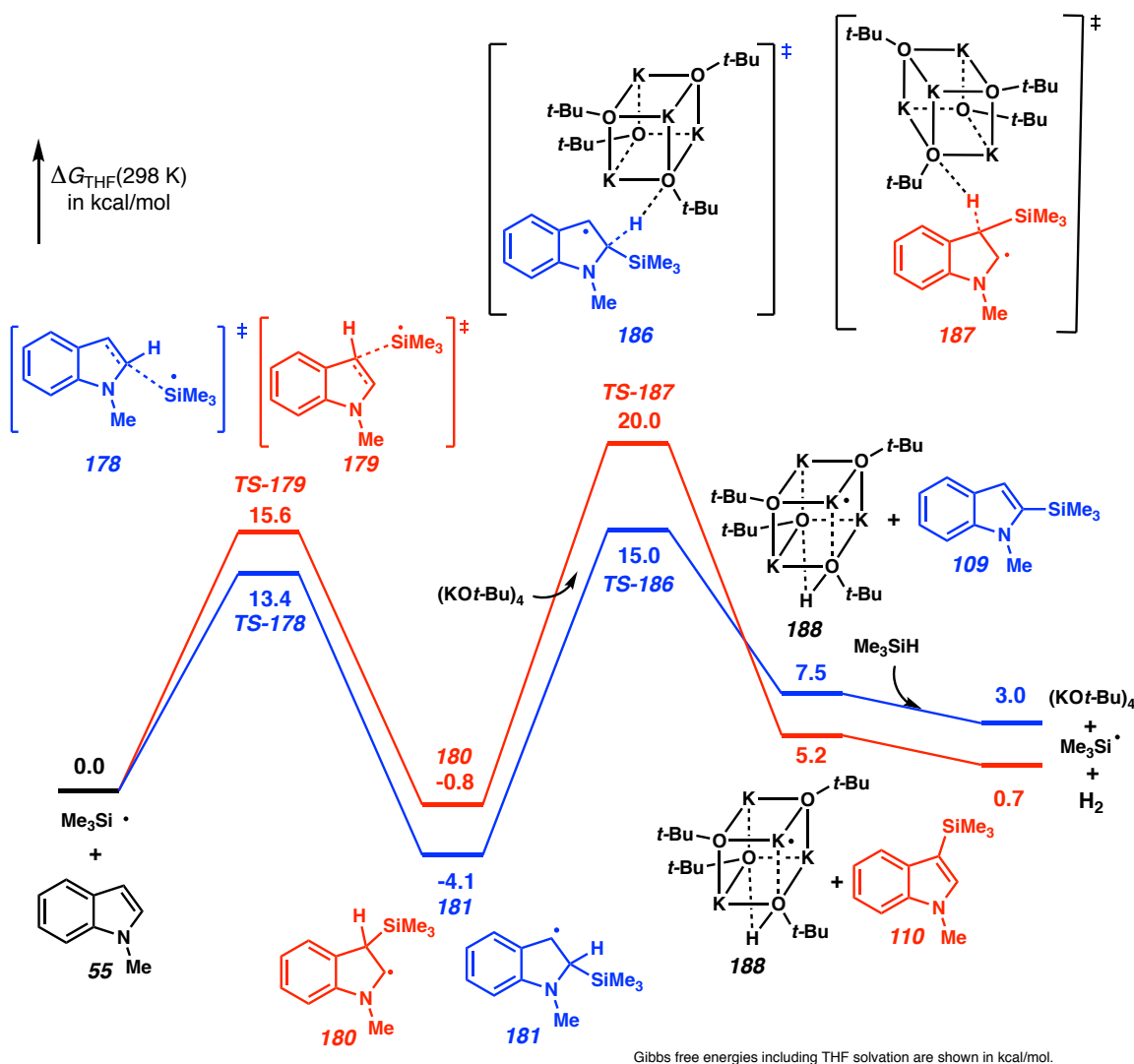
Starting with the trimethylsilyl radical, the radical addition is facile and reversible, generating intermediate **178** or **179**. The pentacoordinate silicate anion can then abstract the ipso hydrogen atom to generate H₂ gas, silylation product, and silicate radical anion **166**. The silicate radical anion then dissociates to form silyl radical **167** and *tert*-butoxide anion. Hydrogen atom abstraction is the rate-determining step, with a calculated barrier of 21.0 kcal/mol for C2-silylation.

Since the radical addition to 1-methylindole is fast and reversible, the subsequent hydrogen abstraction determines the regioselectivity. The hydrogen abstraction at C2 position, via TS-**182**, is lower than the competing hydrogen abstraction at C3 position, via TS- **183**, by 6.7 kcal/mol.

Figure 2.15 Free Energy Profile of C2- and C3-Silylation



Alternatively, the mechanism in which $[KOt\text{-}Bu]_4$ acts as a hydrogen atom transfer catalyst is shown in Figure 2.16. The hydrogen atom abstraction at the C2 position, via TS-186, requires 19.1 kcal/mol. This pathway is lower energy than TS-182, which requires 16.9 kcal/mol relative to $t\text{-}BuO}^-$ or 42.8 kcal/mol relative to tetrameric $[KOt\text{-}Bu]_4$. Therefore, computational models predict the hydrogen atom abstraction by tetrameric $[KOt\text{-}Bu]_4$ is favorable compared to direct hydrogen evolution by pentacoordinate silicate anion.

Figure 2.16 Free Energy Profile of Silylation with $[KOt-Bu]_4$ Participation


TS-182 or TS-186 are lower in energy than the competing hydrogen abstraction at the C3 position via TS-183 or TS-187, respectively, indicating the C2 silylation product is the kinetic product. This result is consistent with the experimentally observed C2 silylation regioselectivity at room temperature (cf. Table 2.2). At higher temperatures or longer reaction times, C3 silylation becomes the major product. The calculations indicate that the C3 silylation product is 2.3 kcal/mol lower energy than the C2 silylation product.

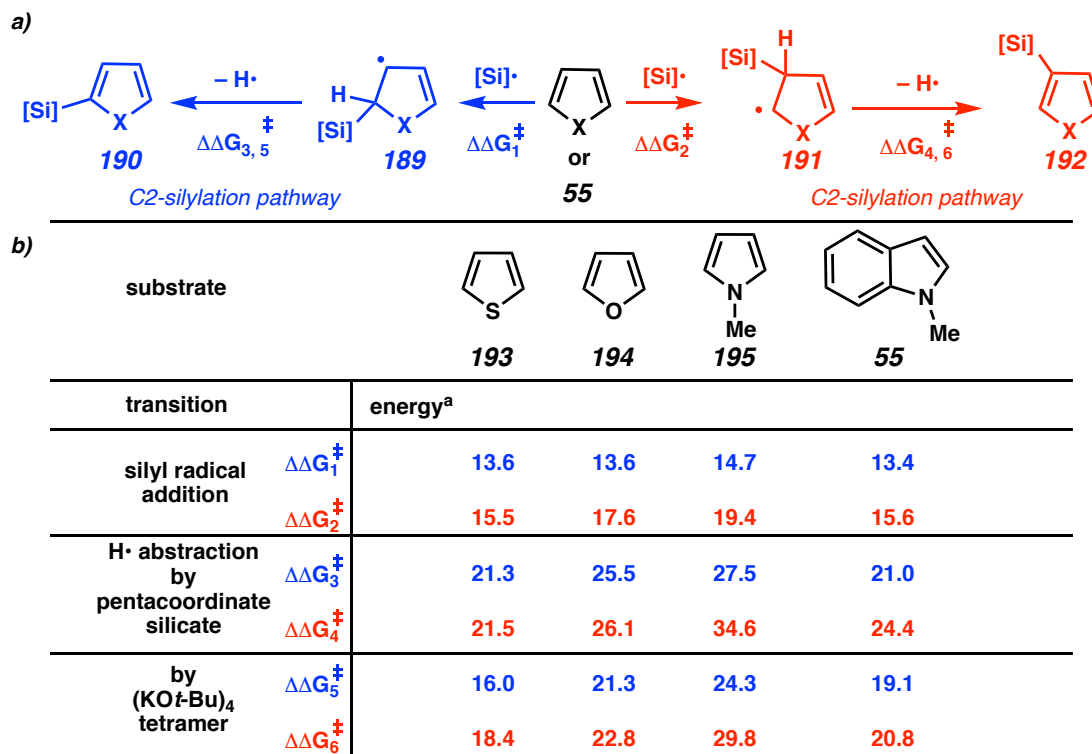
This is consistent with the experimental observation that C3 silylation is the thermodynamic product.

2.7.5 Computational Study of Product Selectivity

We also studied the reactivities of a series of 5-membered heterocycles, 1-methylpyrrole (**195**), furan (**194**), and thiophene (**193**). The experimentally determined relative rates utilizing competition experiments are: thiophene > furan > 1-methylpyrrole.

¹⁰ Our computational results show that 1-methylpyrrole **55** has the highest reaction barrier for C-H silylation at the C2 position in the 5-membered aromatic heterocycles investigated (Scheme 2.13). While electrophilic aromatic substitution reactions favor C3 regioselectivity, silyl radical additions favor C2 regioselectivity. This is due to the nucleophilic character of silyl radicals. The silyl radical is strongly bent out of the plane and highly prefers a pyramidal structure. The singly occupied molecular orbital (SOMO) of silyl radical has a high percentage of 3s character,³³ and is more nucleophilic than electrophilic.

As shown in Scheme 2.13, the product determining step for each of the 5-membered aromatic heterocycles is lower for the C2 pathway (blue, $\Delta\Delta G_3^\ddagger$ or $\Delta\Delta G_5^\ddagger$) as compared to C3-silylation (red, $\Delta\Delta G_4^\ddagger$ or $\Delta\Delta G_6^\ddagger$) which matches with the observed experimental regioselectivity (i.e., C2 > C3).¹⁰ Comparing the highest energy step for each of the 5-membered heterocycles, highlights the expected inverse relationship of energy barrier to relative reaction rate (i.e., thiophene has the lowest energy barrier and demonstrates the highest rate in the competition reaction).

Scheme 2.13 Key Calculated Energy Barrier for Representative 5-Membered Heterocycles


[a] Gibbs free energies including THF solvation are shown in kcal/mol

2.8 CONCLUSION

We have reported a systematic mechanistic investigation of the KOt-Bu-catalyzed silylation of aromatic heterocycles. Specifically, a wide array of experimental tools, including NMR and ReactIR *in situ* studies, radical trap and radical clock experiments, stereochemical analysis, and others were applied to elucidate the pathway for the silylation reaction. These experimental results were further complemented by computational analysis of the reaction. The results of these experiments are consistent with a radical chain mechanism, wherein a triethylsilyl radical is generated by the thermal cleavage of Si–H bond of the coordinated silicon species or by traces of oxygen which facilitate radical formation. The radical clock and KIE experiments support a cycle in

which C–Si bond formation through silyl radical addition and subsequent β–H scission regenerates the silyl radical and continues the chain process. Furthermore, the opening of only the cyclopropane near the C3-position of indole provides direct evidence for an indole radical intermediate. The overall reaction is reversible, with an equilibrium shifted toward product by the cross-dehydrogenative H₂ evolution as an entropic driving force. The use of deuterium labeled silolane as a stereochemical probe supports a number of on-pathway intermediates in our postulated radical mechanism.

2.9 EXPERIMENTAL SECTION

2.9.1 MATERIALS AND METHODS

Unless otherwise stated, reactions were performed in a nitrogen-filled glovebox or in flame-dried glassware under an argon or nitrogen atmosphere using dry, deoxygenated solvents. Solvents were dried by passage through an activated alumina column under argon.⁴⁴ Reaction progress was monitored by thin-layer chromatography (TLC), GC or Agilent 1290 UHPLC-MS. TLC was performed using E. Merck silica gel 60 F254 precoated glass plates (0.25 mm) and visualized by UV fluorescence quenching, *p*-anisaldehyde, or KMnO₄ staining. Silicycle SiliaFlash® P60 Academic Silica gel (particle size 40–63 nm) was used for flash chromatography. ¹H NMR spectra were recorded on Varian Inova 500 MHz or Bruker 400 MHz spectrometers and are reported relative to residual CHCl₃ (δ 7.26 ppm), C₆H₆ (δ 7.16 ppm), or THF (δ 3.58, 1.72 ppm). ¹³C NMR spectra were recorded on a Varian Inova 500 MHz spectrometer (125 MHz) or Bruker 400 MHz spectrometers (100 MHz) and are reported relative to CHCl₃ (δ 77.16 ppm). Data for ¹H NMR are reported as follows: chemical shift (δ ppm) (multiplicity, coupling constant (Hz), integration). Multiplicities are reported as follows: s = singlet, d = doublet, t = triplet, q = quartet, p = pentet, sept = septuplet, m = multiplet, br s = broad singlet, br d = broad doublet, app = apparent. Data for ¹³C NMR are reported in terms of chemical shifts (δ ppm). IR spectra were obtained by use of a Perkin Elmer Spectrum BXII spectrometer or Nicolet 6700 FTIR spectrometer using thin films deposited on

NaCl plates and reported in frequency of absorption (cm^{-1}). GC-FID analyses were obtained on an Agilent 6850N gas chromatograph equipped with a HP-1 100% dimethylpolysiloxane capillary column (Agilent). GC-MS analyses were obtained on an Agilent 6850 gas chromatograph equipped with a HP-5 (5%-phenyl)-methylpolysiloxane capillary column (Agilent). High-resolution mass spectra (HRMS) were obtained from Agilent 6200 Series TOF with an Agilent G1978A Multimode source in electrospray ionization (ESI+), atmospheric pressure chemical ionization (APCI+), or mixed ionization mode (MM: ESI-APCI+), or obtained from Caltech mass spectrometry laboratory. FT-ATR-IR measurements were carried out on a Thermo Scientific Nicolet iS 5 FT-IR spectrometer equipped with an iD5 ATR accessory. ReactIR measurements were carried out on a Mettler-Toledo ReactIR ic10 using a K4 conduit with a Sentinel high-pressure probe and SiComp window. EPR spectra were acquired on a X-band Bruker EMX spectrometer. An Omnical SuperCRC or Insight CPR 220 reaction calorimeter was used to monitor heat flow.

Triethyl silane (99%, Sure/SealTM) and KOt-Bu (sublimed grade, 99.99% trace metals basis) were purchased from Aldrich and used directly. KOH was pulverized and dried in a desiccator over P_2O_5 under vacuum for 24 h prior to use. Other reagents were purchased from Sigma-Aldrich, Acros Organics, Strem, or Alfa Aesar and used as received unless otherwise stated.

2.9.1.1 Computational Details

Calculations were carried out with Gaussian 09.⁴⁵ Geometry optimizations and energy calculations were performed with the B3LYP method.⁴⁶ The 6-31G (d) basis set was used for all atoms.⁴⁷ Frequency analysis verified the stationary points are minima or first-order saddle points. Single point energies were calculated at the M06-2X /6-311+G(d,p) level.⁴⁸ Solvent effect (solvent = THF) was calculated by using CPCM solvation model.⁴⁹ Gibbs free energies in THF at 298.15 K were calculated by adding the thermochemical quantities derived from the B3LYP frequency calculation to the M06-

2.9.1.2 Preparation of Known Compounds

Di-*tert*-butyl hyponitrite⁵⁰ and **176**³⁸ were synthesized according to literature procedure.

2.9.2 EXPERIMENTAL PROCEDURES AND SPECTROSCOPIC DATA

2.9.2.1 General Procedure for the Screening of Base Catalysts and Kinetic Profile:

Based on previously reported screening procedure.¹⁰ In a nitrogen-filled glove box, 1-methylindole **55** (0.5 mmol, 1 equiv), triethylsilane (1.5 mmol, 3 equiv), the indicated base (0.1 mmol, 20 mol %), and THF (5 mL) were added to a 1 dram vial equipped with a magnetic stirring bar. At the indicated time, aliquots were removed using a glass capillary tube, diluted with Et₂O, and analyzed using GC-FID to determine regioselectivity and yield. GC conversion is reported as product (C2- and C3-silylation) divided by product and starting material.

2.9.2.2 General Procedure for Time-Course Reaction Monitoring by *in situ* ¹H NMR

In a nitrogen-filled glove box, a stock solution containing KOt-Bu (60.5 mg, 0.539 mmol) and 1,2,5-trimethoxybenzene (if used, 45.4 mg, 0.267 mmol) is prepared in THF-D₈ (2.7 ml). Continuing in the glove box, a J-Young gas-tight NMR tube is then charged with **55** (32.8 mg, 0.25 mmol, 1 equiv), Et₃SiH (0.75 mmol, 3 equiv), and 0.25 mL of stock solution. The tube is tightly capped with the corresponding Teflon plug, removed from the glove box, placed in the bore of the NMR, and heated to 45 °C. ¹H

NMR spectra were acquired in “array” mode, with a spectrum taken approximately every 3 minutes for the length of experiment. The data was processed using MestReNova and peak integrations were normalized to 1,2,5-trimethoxybenzene (if used). Data is decimated and displayed using the MestReNova “stack” function.

2.9.2.3 General Procedure for Regioselectivity Studies

In a nitrogen-filled glove box, 1 dram vials were charged with KOt-Bu (0.1 mmol, 20 mol), **55** (0.5 mmol, 1 equiv), silane (174.4 mg, 1.5 mmol, 3 equiv) and THF (0.5 mL, if used) then sealed with a PTFE-lined screw-cap and heated to the indicated temperature. After the indicated reaction time, the crude reaction mixture was diluted with Et₂O, or a small aliquot was removed by glass capillary tube, and analyzed by GC-FID.

2.9.2.4 Procedure for Reversibility of Studies

In a nitrogen-filled glove box, 1 dram vials with a magnetic stir bar were charged with a mixture of **109** and **110** (24.2 mg, 0.1 mmol, 1 equiv, ratio of **109**:**110** determined by GC-FID), KOt-Bu (2.4 mg, 0.02 mmol, 20 mol %), Et₃Si–H (49 µL, 3 mmol, 3 equiv), and THF (0.1 mL, 1 M). The reactions were heated to 100 °C and stirred for the indicated time, after which they were quenched with Et₂O and analyzed by GC.

2.9.2.5 Procedure for Reversibility Crossover Studies

In a nitrogen-filled glove box, 1 dram vials with a magnetic stir bar were charged with **109** (122.7 mg, 0.5 mmol, 1 equiv), KOt-Bu (11.2 mg, 0.1 mmol, 20 mol %), EtMe₂Si–H (44 mg, 0.5 mmol, 1 equiv), and THF (0.5 mL, 1 M). The reaction was heated to 45 °C and stirred for the indicated time, then quenched with Et₂O (ca. 1mL), concentrated in vacuo, and analyzed by ¹H NMR. Product ratio assigned by correlation to known products.¹⁰ Note, product ratio of **109**:**110** outside of ¹H NMR detection.

2.9.2.6 Procedure of Gas Collection by Eudiometry

The eudiometer apparatus used for measuring H₂ gas evolution in the KOt-Bu-catalyzed cross-dehydrogenative silylation reactions. Note that a Schlenk round-bottom flask with a Teflon valve was used instead of the two neck round-bottom flask and ground glass stopcock as depicted in Figure 2.5.

In a nitrogen-filled glove box, KOt-Bu (114 mg, 1 mmol, 20 mol %), **55** (656.4 mmol, 1 equiv), and THF (5 mL) were added to a 25 mL Schlenk flask equipped with a magnetic stirring bar, followed by silane (2.4 mL, 15 mmol, 3 equiv). The flask was sealed and removed from the glove box and placed in a preheated oil bath (45 °C). After stirring at 800 rpm for 15 min for equilibration, the side neck of the Schlenk flask was quickly connected to the gas collection set up. The reaction was stirred for another 20 min (at which point the apparatus was set to volume = 0 mL), the gas volume was recorded over 4 h. For experiment 1, 80 mL of H₂ gas was collected, and the conversion by ¹H NMR based on silylation product **55** was 72%. For experiment 2: 77 mL of H₂ gas was collected, and the conversion by ¹H NMR based on silylation product **55** was 73%. The gas was confirmed by ¹H NMR as H₂ by transferring to a J-Young gas-tight NMR tube with 0.6 mL of frozen C₆D₆. A control experiment with Et₃SiH (2.4 mL) in THF (5 mL) heated to 45 °C in the identical reaction setup resulted in no gas formation in 10 h.

2.9.2.7 Procedure for Radical Trap Experiments Using TEMPO

In a nitrogen-filled glove box, 1 dram vials with magnetic stirring bars were charged with the KOt-Bu (0.1 mmol, 20 mol %), **55** (65.6 mg, 0.5 mmol, 1 equiv), triethylsilane (174.4 mg, 1.5 mmol, 3 equiv), 2,2,6,6-tetramethyl-1-piperidinyloxy

(TEMPO **151**, 3 or 6 mol % if used), and THF (0.5 mL, 1M) then sealed with a PTFE-lined screw-cap and heated to 45 °C while stirring. At the indicated time points, an aliquot was removed with a clean, dry glass capillary tube, diluted with Et₂O, and analyzed by GC-FID. Conversion is reported as the percent of both C2- and C3-silylation products divided by products and starting material. Despite our efforts, we were not able to observe the TEMPO–SiEt₃ adduct by GC-MS from above experiments.

Following the procedure above, but using 1 equiv of TEMPO resulted in no product formation. After 52 h TEMPO–SiEt₃ (TEMPO–TES) adduct was observed by GC-MS and after 91 h the ratio of TEMPO:TEMPO–TES was 40:60. A control experiment conducted in the exact same manner but excluding substrate **55** (i.e., TEMPO, KOt-Bu, Et₃SiH, and THF) also resulted in the detection of TEMPO–TES after 52 h. At 91 h, the ratio of TEMPO:TEMPO–TES was 34:66. No TEMPO adduct was observed when NaOt-Bu was in this same control reaction after 9 days.

2.9.2.8 General Procedure for Additive Screening

Based on previously reported screening procedure.¹⁰ In a nitrogen-filled glove box, 1 dram vials with magnetic stirring bars were charged with the KOt-Bu (0.1 mmol, 20 mol%), **55** (65.6 mg, 0.5 mmol, 1 equiv), triethylsilane (174.4 mg, 1.5 mmol, 3 equiv), additive, and THF (0.5 mL, 1M) then sealed with a PTFE-lined screw-cap and heated to 45 °C while stirring. At the indicated time points, an aliquot was removed with a clean, dry glass capillary tube, diluted with Et₂O, and analyzed by GC-FID. Conversion is reported as the percent of both C2- and C3-silylation products divided by products and starting material. All additives increased the length of the induction period and result in lower yields overall.

2.9.2.9 General Procedure for Studies Using *in situ* Generated *tert*-butoxyl Radicals

In a nitrogen-filled glove box, 1 dram vials with magnetic stirring bars were charged with peroxide source [*t*-BuO–Ot-Bu (DTBP) or *t*-BuO–N=N–Ot-Bu (TBHN)], KOt-Bu (if used, 0.1 mmol, 20 mol %), **55** (65.6 mg, 0.5 mmol, 1 equiv), triethylsilane (174.4 mg, 1.5 mmol, 3 equiv), and THF (0.5 mL, 1M) then sealed with a PTFE-lined screw-cap, and heated indicated temperature while stirring. At the indicated time points, an aliquot was removed with a clean, dry glass capillary tube, diluted with Et₂O, and analyzed by GC-MS. A number of unidentified decomposition products were observed.

2.9.2.10 General Procedure for ReactIR Time-Course Experiments

The glass reaction vessel for use with the ReactIR Sentinel high-pressure probe and a magnetic stirring bar were oven dried, fitted with the PTFE adapter, and brought into a nitrogen-filled glove box, or cooled under a flow of argon and standard air-free technique is used for all additions. KOt-Bu (0.8 mmol, 20 mol %), **55** (1.05 g, 8 mmol, 1 equiv, if used), triethylsilane (13.89 mL, 24 mmol, 3 equiv), additive (if used), and THF (8 mL, 1M) were added to reaction vessel, which was fitted to the ReactIR probe and heated to 45 °C while stirring under argon. The spectrum was recorded over the course of the reaction and data was analyzed using the ReactIR software.

2.9.2.11 General Procedure for ATR-IR Studies of Pentacoordinate Silicate

In a nitrogen-filled glove box, base (0.1 mmol), Et₃SiH (80 µL, 0.5 mmol, 5 equiv), and THF (0.5 mL) were added to a 1 dram scintillation vial equipped with a magnetic stirring bar. The vial was sealed and the mixture stirred at 45 °C for the indicated time. The vial was transferred to second nitrogen-filled glove box containing

Chapter 2 – A Combined Experimental and Computational Mechanistic Study of the KOt-Bu-Catalyzed Dehydrogenative C–H Silylation of Aromatic Heterocycles 92
an ATR-FTIR and a few drops of this mixture placed on the ATR crystal. After waiting for 5 minutes to evaporate all the volatiles (i.e., THF and silanes), the IR spectrum of the residue was recorded.

2.9.2.12 Procedure for Acquisition of EPR Spectra.

In a nitrogen-filled glove box, KOt-Bu (11.2 mg, 0.1 mmol), Et₃SiH (81 µL, 0.5 mmol, 5 equiv), **55** (0.5 mmol, if used), and THF (0.5 mL) were added to a 1 dram scintillation vial equipped with a magnetic stirring bar. The vial was sealed and the mixture stirred at 45 °C for 5 h. The reaction mixture was then transferred into an EPR tube, fitted with a plastic cap, taped with parafilm, removed from the glove box, and quickly frozen in liquid nitrogen. The sample was kept at 77 °K and the EPR spectrum was acquired at 77 °K.

2.9.2.13 General Procedure for Calorimetry Studies.

A calorimeter screw-cap vial is flame dried and cooled in a vacuum desiccator with the corresponding cap and septum. KOt-Bu (112.2 mg, 1 mmol, 20 mol %) is quickly weighed into the vial, which is then evacuated and refilled with argon 3 times. Et₃SiH (2.4 mL, 15 mmol, 3 equiv) and **55** (655.8 mg, 5 mmol, 1 equiv) are added using standard air-free technique. The sample was held at 40 °C overnight with no heat flow detected or silylation product **109** detected by GC or TLC. The temperature was then ramped up to 45 °C, a rapid heat flow corresponding to the sample heating was seen but no further heat flow was observed despite the observed product upon workup.

A series of 8 identical reactions were conducted in parallel. The calorimeter can detect the temperature change due to minute changes in pressure (i.e., using a syringe and needle to remove an aliquot for a GC sample). Therefore one vial was not sampled until

the endpoint, while an additional vial was sampled at each time point (i.e., vial 2 at first time point, then vial 2 and 3 at the second time point, etc.). All vials had comparable conversion upon workup (52–60% C2-silylation product **109**).

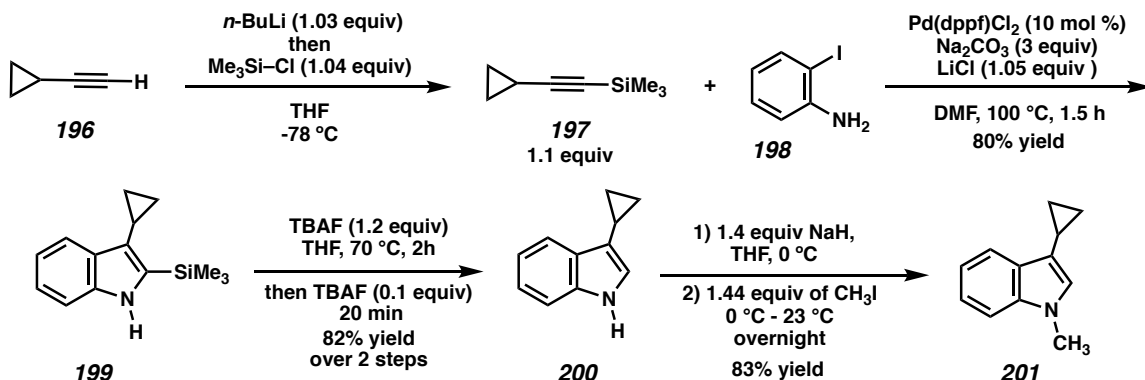
8 calorimeter screw-cap vials with the corresponding cap and septum were flame dried and allowed to cool under vacuum, then refilled with argon. **55** (524.7 mg, 4 mmol, 1 equiv), Et₃SiH (1.92 mL, 12 mmol, 3 equiv) and THF (3.2 mL) are added using standard air-free technique. The reactions are equilibrated at 45 °C using an argon filled balloon and then the reaction is initiated using 1M solution of KOt-Bu (0.8 mL, 0.8 mmol, 20 mol %, equilibrated to 45 °C in plugged syringe). An initial negative heat of mixing is observed.

2.9.2.14 General Procedure for KOt-Bu-Catalyzed Silylation Reactions

Based on previously reported procedures.¹⁰ In a nitrogen-filled glove box, KOt-Bu (11.2 mg, 0.1 mmol, 20 mol %), substrate (0.5 mmol, 1 equiv), and THF (0.5 mL, if used) were added to a 1 dram scintillation vial equipped with a magnetic stirring bar, followed by silane (1.5 mmol, 3 equiv). Then the vial was sealed and the mixture was stirred at 45 °C for the indicated time. The vial was removed from the glove box, diluted with diethyl ether (2 mL) and concentrated under reduced pressure. The regioselectivity (C2 silylation product to C3 silylation product: C2:C3) was determined by ¹H NMR or GC analysis of the crude mixture. The residue was purified by silica gel flash chromatography to give the desired product. Note- reagent order of addition and the use of stirring were found to have no appreciable effect on product yield during reaction screening.

2.9.2.15 Procedure for the Synthesis of Radical Clock Substrates

Scheme 2.14 Synthesis of C3-Cyclopropyl Radical Trap Substrate



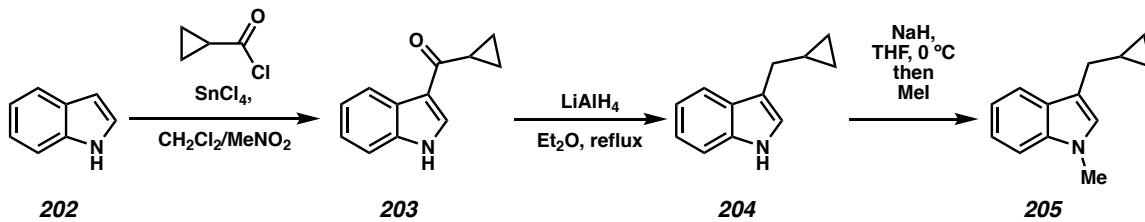
(cyclopropylethynyl)trimethylsilane (197). Based on a modification of a reported procedure.⁵¹ To a stirring solution of cyclopropylacetylene **196** (1.44 g, 21.8 mmol, 1 equiv) in dry THF (7 mL) at -78 °C was added *n*-BuLi (8.95 mL of 2.5 M in THF, 22.4 mmol, 1.03 equiv) dropwise via syringe. The solution was allowed to stir for 30 minutes at -78 °C, after which TMS–Cl (freshly distilled from CaH_2 , 2.90 mL, 22.8 mmol, 1.04 equiv) was added dropwise and the solution was stirred at -78 °C for 1 hour. The reaction was then allowed to warm to room temperature, diluted with diethyl ether, and filtered through a pad of Na_2SO_4 layered on silica gel, eluting 1:4 Et_2O : pentane. The filtrate was concentrated in vacuo and then carried on crude.

3-cyclopropyl-2-(trimethylsilyl)-1*H*-indole (199) and 3-cyclopropyl-1*H*-indole (200) were synthesized following known procedure using **197** and 2-iodoaniline.⁵²

3-cyclopropyl-1-methyl-1*H*-indole (201). To a round-bottom flask equipped with a magnetic stirring bar was added NaH (60 % dispersion in mineral oil, 155 mg, 3.9 mmol, 1.4 equiv) and **200** (440 mg, 2.8 mmol, 1 equiv). The flask was placed in an ice bath and THF was added while stirring. The reaction was stirred at 0 °C for 45 minutes and then at 23 °C for 15 minutes. The reaction was again placed in an ice bath and $\text{Me}-\text{I}$ (250 μL , 4 mmol, 1.4 equiv) was added dropwise. This mixture was stirred overnight,

The solvents were removed under reduced pressure and the crude mixture was purified by silica gel flash chromatography (5→10% CH₂Cl₂ in hexanes) to give 3-cyclopropyl-1-methyl-1*H*-indole **201** (398 mg, 83% yield) R_f = 0.35 (10% CH₂Cl₂ in hexanes) 1H NMR (400 MHz, Chloroform-d) δ 7.74 (dt, J = 7.9, 0.9 Hz, 1H), 7.31 – 7.27 (m, 1H), 7.25 – 7.20 (m, 1H), 7.12 (t, J = 8.0 Hz, 1H), 6.76 (s, 1H), 3.72 (s, 3H), 2.11 – 1.87 (m, 1H), 0.92 – 0.85 (m, 2H), 0.71 – 0.56 (m, 2H). ¹³C NMR (101 MHz, Chloroform-d) δ 137.14, 128.59, 125.43, 121.73, 119.36, 118.74, 117.74, 109.25, 32.69, 6.19.; HRMS (MM: ESI-APCI⁺) calc'd for C₁₂H₁₃N [M⁺H]⁺: 172.1121, found: 172.1119.

Scheme 2.15 Synthesis of C3-Cyclopropylmethyl Radical Trap Substrate

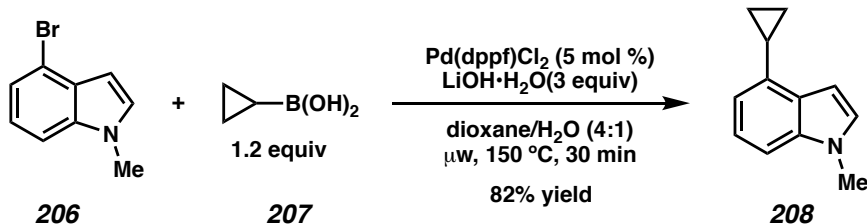


3-3-(cyclopropylmethyl)-1-methyl-1*H*-indole (205). To a stirring solution of indole (1.17 g, 10 mmol) in CH₂Cl₂ (20 mL) was added SnCl₄ (1.44 mL, 12 mmol) in a single portion via syringe at 0 °C. The solution was allowed to warm to room temperature and stirred for 30 min, then cyclopropanecarbonyl chloride (10 mmol) was added in small portions to the suspension by syringe, followed by nitromethane (15 mL). The reaction mixture was stirred at 25 °C for 2 h, after which ice-water (30 mL) was slowly added. The mixture was then filtered, extracted with ethyl acetate (50 mL), dried over Na₂SO₄, and concentrated at reduced pressure to give the product **203** as a yellow solid, which was used directly for next step.

To a solution of crude **203** in Et₂O (50 mL) was added LiAlH₄ (0.69 g, 20 mmol) in small portions, and the mixture refluxed overnight. The reaction was cooled to 0 °C, diluted with Et₂O (40 mL), and quenched with water (0.76 mL)/15% NaOH aqueous (0.76 mL)/water (2.28 mL). The mixture was stirred for 1 h, dried over Na₂SO₄, concentrated at reduced pressure, and purified by silica gel flash chromatography (10% Et₂O in hexanes) to give 3-(cyclopropylmethyl)-1*H*-indole **204** (0.63 g, 3.7 mmol) as a yellow oil.

To a dried flask with NaH (60% dispersion in oil, 178 mg, 4.4 mmol) and THF (15 mL) was added the THF (15 mL) solution of **204** (630 mg, 3.7 mmol) dropwise by syringe at 0 °C. After the mixture was stirred at 0 °C for 30 min, MeI (0.35 mL, 5.6 mmol) was added slowly. This mixture was stirred overnight, quenched with aqueous NH₄Cl, extracted with Et₂O (30 mL x 3), and dried over Na₂SO₄. The solvents were removed under reduced pressure and the crude mixture was purified by silica gel flash chromatography (10% CH₂Cl₂ in hexanes) to give 3-(cyclopropylmethyl)-1-methyl-1*H*-indole **205** (0.59 g, 32% yield over three steps) as a colorless oil. R_f = 0.4 (10% CH₂Cl₂ in hexanes); ¹H NMR (400 MHz, Chloroform-*d*) δ 7.70 (dt, J = 7.9, 1.1 Hz, 1H), 7.37 (dt, J = 8.3, 1.0 Hz, 1H), 7.31 (m, J = 6.9, 1.1 Hz, 1H), 7.19 (ddd, J = 8.0, 6.9, 1.2 Hz, 1H), 7.01 (s, 1H), 3.82 (s, 3H), 2.77 (d, J = 6.7 Hz, 2H), 1.18 (ttt, J = 8.0, 6.7, 4.9 Hz, 1H), 0.66 – 0.59 (m, 2H), 0.39 – 0.26 (m, 2H); ¹³C NMR (101 MHz, Chloroform-*d*) δ 137.12, 128.13, 126.26, 121.52, 119.24, 118.66, 115.12, 109.20, 32.67, 30.03, 11.50, 5.03. IR (Neat Film NaCl) 3073, 3054, 2999, 2905, 2837, 1615, 1552, 1483, 1472, 1423, 1371, 1355, 1327, 1293, 1253, 1235, 1201, 1156, 1129, 1057, 1013, 975, 929, 884, 828,

Scheme 2.16 Synthesis of C4-Cyclopropyl Radical Trap Substrate

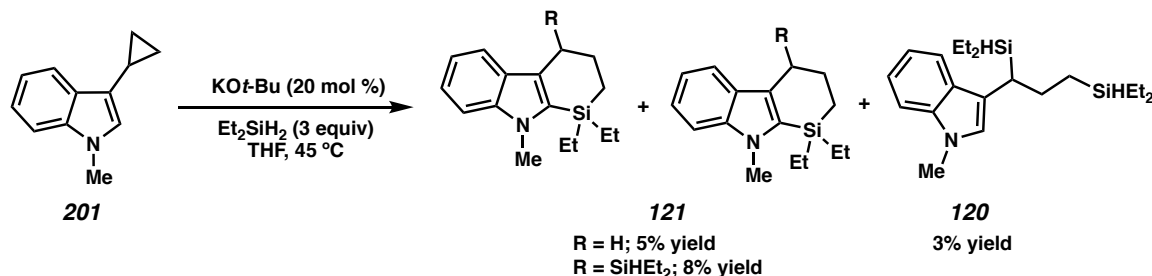


4-cyclopropyl-1-methyl-1*H*-indole (208). To a 20 mL microwave vial was added Pd(dppf)Cl₂ (367 mg, 0.5 mmol, 5 mol %), lithium hydroxide mono-hydrate (1.26 g, 30 mmol, 3 equiv), 4-bromo-1-methyl-1*H*-indole (2.10g, 10 mmol), and cyclopropylboronic acid (1.03 g, 12 mmol, 1.2 equiv), followed by dioxane (10 mL) and degassed H₂O (2.5 mL). The vial is purged with N₂ for 15 min, then heated to 150 °C for 30 minutes in a Biotage Initiator 2.5 microwave reactor under normal absorption mode. The vial was cooled and the solution concentrated under reduced pressure, diluted with ethyl acetate (100 mL), washed with saturated sodium bicarbonate (50 mL) then brine (50 ml), dried over Na₂SO₄, and concentrated under reduced pressure. The crude mixture was purified by silica gel flash chromatography (2→10% CH₂Cl₂ in hexanes) to give 4-cyclopropyl-1-methyl-1*H*-indole **208** (1.39 g, 81% yield) as a white solid. R_f = 0.2 (10% CH₂Cl₂ in hexanes); ¹H NMR (400 MHz, Chloroform-*d*) δ 7.20 – 7.13 (m, 2H), 7.07 (d, J = 3.1 Hz, 1H), 6.79 – 6.70 (m, 1H), 6.67 (d, J = 3.1 Hz, 1H), 3.80 (s, 3H), 2.26 (ttd, J = 8.5, 5.2, 0.7 Hz, 1H), 1.08 – 0.95 (m, 1H), 0.92 – 0.80 (m, 1H). ¹³C NMR (101 MHz, Chloroform-*d*) δ 136.52, 136.17, 128.53, 128.33, 121.84, 114.59, 106.83, 99.40, 33.09, 13.20, 7.76. IR (Neat Film NaCl) 3002, 2943, 1581, 1498, 1458, 1418, 1336, 1291, 1252, 1154, 1088,

[M⁺H]⁺: 172.1121, found: 172.1120.

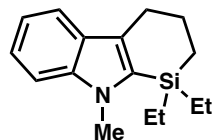
2.9.2.16 Procedure for Silylation of Radical Clock Substrates

Scheme 2.17 Silylation of C3-Cyclopropyl Radical Trap Substrate



The general procedure in **2.8.2.14** was followed. The reaction was performed with KOt-Bu (6.7 mg, 0.06 mmol, 20 mol %), 3-cyclopropyl-1-methyl-1*H*-indole **201** (51.3 mg, 0.3 mmol, 1 equiv), Et₂SiH₂ (79.2 mg, 0.9 mmol, 3 equiv), and 0.3 mL of THF at 45 °C for 10 days. Three products shown above, along with some unidentified impurity, were isolated by silica gel flash chromatography (3% CH₂Cl₂ in hexanes). Unreacted starting material **201** was recovered in 30% yield (15.4 mg). Analytic pure compounds **121**, R=H (3.9 mg, 5% yield), **121**, R=SiHET₂ (8.8 mg, 8% yield), and **120** (1.9 mg, 3% yield) were purified by preparative HPLC (ACE 5 C18, 250 x 21 2mm id column; gradient, 30→80% MeCN in H₂O in 3 min, then 80→100% MeCN in H₂O in 7 min, followed by 100% MeCN; flow rate = 10 mL/min; λ = 230 nm.).

2.9.2.17 Spectroscopic Data for the Silylation of Radical Clock Substrates

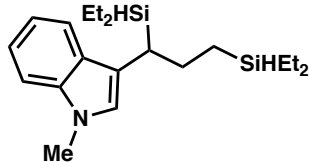


1,1-Diethyl-9-methyl-2,3,4,9-tetrahydro-1*H*-silino[2,3-*b*]indole (121, R=H): R_f = 0.5 (10% CH₂Cl₂ in hexanes); ¹H NMR (400 MHz, CDCl₃) δ 7.55 (dt, J = 7.9, 1.0 Hz, 1H),

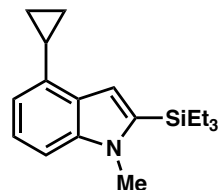
7.29 (dt, $J = 8.3, 0.9$ Hz, 1H), 7.22 (ddd, $J = 8.2, 6.9, 1.2$ Hz, 1H), 7.07 (ddd, $J = 7.9, 6.8,$
 1.1 Hz, 1H), 3.78 (s, 3H), 2.91 – 2.80 (m, 2H), 2.07 – 1.95 (m, 2H), 1.05 – 0.90 (m, 8H),
 0.90 – 0.78 (m, 4H); ^{13}C NMR (100 MHz, CDCl_3) δ 139.4, 133.6, 128.3, 127.4, 122.2,
 118.8, 118.3, 108.9, 33.1, 25.2, 23.0, 8.9, 7.9, 6.0. IR (Neat Film NaCl) 2951, 2909,
 2872, 1504, 1455, 1361, 1336, 1307, 1234, 1165, 1138, 1011, 920, 806, 761 cm^{-1} ;
 HRMS (FAB+) calc'd for $\text{C}_{16}\text{H}_{23}\text{NSi} [\text{M}]^+$: 257.1600, found: 257.1601.



**4-(Diethylsilyl)-1,1-diethyl-9-methyl-2,3,4,9-tetrahydro-1H-silino[2,3-b]indole (121
 R=SiHET₂):** $R_f = 0.5$ (10% CH_2Cl_2 in hexanes); ^1H NMR (400 MHz, CDCl_3) δ 7.48 (dt, $J = 7.9, 1.0$ Hz, 1H), 7.26 (dt, $J = 8.2, 1.0$ Hz, 1H), 7.19 (ddd, $J = 8.2, 6.8, 1.2$ Hz, 1H),
 7.02 (ddd, $J = 7.9, 6.8, 1.1$ Hz, 1H), 3.82 – 3.79 (m, 1H), 3.77 (s, 3H), 2.84 – 2.81 (m,
 1H), 2.36 – 2.30 (m, 1H), 2.07 – 1.98 (m, 1H), 1.06 – 0.91 (m, 11H), 0.91 – 0.76 (m, 7H),
 0.75 – 0.65 (m, 2H), 0.62 – 0.44 (m, 2H); ^{13}C NMR (100 MHz, CDCl_3) δ 139.4, 132.1,
 130.0, 127.9, 122.1, 119.5, 117.9, 108.8, 33.1, 25.8, 22.3, 8.63, 8.61, 8.11, 8.09, 7.2, 6.7,
 6.1, 3.4, 2.8. IR (Neat Film NaCl) 2953, 2910, 2873, 2100, 1495, 1455, 1414, 1361,
 1321, 1262, 1234, 1164, 1135, 1080, 1013, 968, 809, 761 cm^{-1} ; HRMS (FAB+) calc'd
 for $\text{C}_{20}\text{H}_{33}\text{NSi}_2 [\text{M}]^+$: 343.2152, found: 343.2140.



3-(1,3-Bis(diethylsilyl)propyl)-1-methyl-1*H*-indole (120). ^1H NMR (500 MHz, CDCl_3) δ 7.56 (dt, $J = 7.9, 1.0$ Hz, 1H), 7.30 – 7.25 (m, 1H), 7.19 (ddd, $J = 8.2, 6.9, 1.1$ Hz, 1H), 7.06 (ddd, $J = 7.9, 6.9, 1.1$ Hz, 1H), 6.72 (s, 1H), 3.79 – 3.76 (m, 1H), 3.76 (s, 3H), 3.61 (hept, $J = 3.1$ Hz, 1H), 2.46 – 2.34 (m, 1H), 1.97 – 1.77 (m, 2H), 0.98 (t, $J = 7.9$ Hz, 3H), 0.95 – 0.91 (m, 6H), 0.89 (t, $J = 7.9$ Hz, 3H), 0.81 – 0.74 (m, 1H), 0.69 – 0.41 (m, 9H); ^{13}C NMR (125 MHz, CDCl_3) δ 137.0, 128.6, 125.3, 121.3, 119.6, 118.2, 116.4, 109.1, 32.8, 27.0, 25.3, 10.8, 8.6, 8.6, 8.4, 8.4, 2.9, 2.9, 2.4, 2.1. IR (Neat Film NaCl) 2952, 2932, 2910, 2872, 2094, 1469, 1414, 1372, 1325, 2235, 1012, 970, 810, 736 cm^{-1} ; HRMS (FAB+) calc'd for $\text{C}_{20}\text{H}_{35}\text{NSi}_2$ $[\text{M}]^+$: 345.2308, found: 345.2314.



4-cyclopropyl-1-methyl-2-(triethylsilyl)-1*H*-indole (122). The general procedure was followed using KOt-Bu (6.7 mg, 0.06 mmol, 20 mol %), *N*-methyl-4-(cyclopropyl)-indole **208** (51.3 mg, 0.3 mmol, 1 equiv), Et₃SiH (146 μL , 0.9 mmol, 3 equiv), and 0.3 mL of THF at 45 °C for 48 h. **122** was purified by silica gel flash chromatography (5 → 10% CH₂Cl₂ in hexanes, 54.7 mg, 64% yield) as a yellow oil. $R_f = 0.4$ (10% CH₂Cl₂ in hexanes); ^1H NMR (400 MHz, Chloroform-*d*) δ 7.20 – 7.12 (m, 2H), 6.91 (s, 1H), 6.74 – 6.65 (m, 1H), 3.85 (s, 3H), 2.31 (ttd, $J = 8.5, 5.2, 0.6$ Hz, 1H), 1.10 – 1.01 (m, 11H), 1.00 – 0.92 (m, 6H), 0.91 – 0.86 (m, 2H); ^{13}C NMR (101 MHz, Chloroform-*d*) δ 140.05,

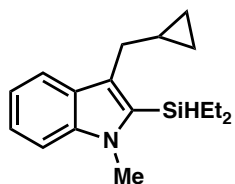
137.59, 136.03, 128.59, 122.24, 113.88, 111.28, 106.59, 33.23, 13.06, 8.14, 7.70, 4.16;

IR (Neat Film NaCl) 3080, 3051, 3002, 2953, 2909, 2874, 1581, 1503, 1454, 1441, 1415,

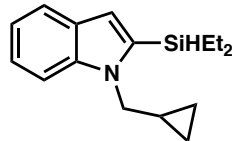
1370, 1351, 1323, 1277, 1237, 1171, 1137, 1070, 1017, 977, 885, 841, 787, 769, 745,

734, 700, 679 cm^{-1} ; HRMS (MM+) calc'd for $\text{C}_{18}\text{H}_{27}\text{NSi}$ $[\text{M}+\text{H}]^+$: 286.1986 found:

286.1997.

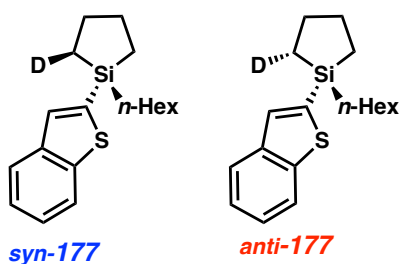


3-(Cyclopropylmethyl)-2-(diethylsilyl)-1-methyl-1H-indole (123). The general procedure was followed using KOt-Bu (4.5 mg, 0.04 mmol, 20 mol %), **205** (37.0 mg, 0.2 mmol, 1 equiv), Et₂SiH₂ (78 μL , 0.6 mmol, 3 equiv), and 0.2 mL of THF at 45 °C for 5 days. **123** was purified by silica gel flash chromatography (2.5% CH₂Cl₂ in hexanes, 17.2 mg, 32% yield) as colorless oil. $R_f = 0.5$ (10% CH₂Cl₂ in hexanes); ¹H NMR (500 MHz, CDCl₃) δ 7.67 (dt, $J = 7.9, 1.0$ Hz, 1H), 7.31 (dt, $J = 8.2, 0.9$ Hz, 1H), 7.26 (ddd, $J = 8.2, 6.8, 1.1$ Hz, 1H), 7.10 (ddd, $J = 7.9, 6.8, 1.0$ Hz, 1H), 4.54 – 4.46 (m, 1H), 3.83 (s, 3H), 2.86 (d, $J = 6.4$ Hz, 2H), 1.10 – 1.02 (m, 7H), 1.03 – 0.87 (m, 4H), 0.53 – 0.43 (m, 2H), 0.33 – 0.22 (m, 2H); ¹³C NMR (125 MHz, CDCl₃) δ 139.9, 132.3, 128.6, 127.0, 122.3, 119.7, 118.6, 109.1, 32.9, 30.3, 13.3, 8.9, 5.2, 4.8. IR (Neat Film NaCl) 3073, 2999, 2931, 2909, 2872, 2131, 1503, 1457, 1424, 1355, 1319, 1292, 1246, 1228, 1167, 1139, 1087, 1013, 975, 836, 809 cm^{-1} ; HRMS (MM+) calc'd for $\text{C}_{17}\text{H}_{26}\text{NSi}$ $[\text{M}+\text{H}]^+$: 272.1829, found: 272.1823.



1-Benzyl-5-methoxy-2-(triethylsilyl)-1*H*-indole (124). The general procedure was followed using *KOt-Bu* (4.6 mg, 0.04 mmol, 20 mol %), 1-(cyclopropylmethyl)-1*H*-indole (34.2 mg, 0.2 mmol, 1 equiv), Et₂SiH₂ (78 μL, 0.9 mmol, 3 equiv), and 0.2 mL of THF at 45 °C for 96 h. **124** was purified by silica gel flash chromatography (gradient, 2-→3.3% CH₂Cl₂ in hexanes, 29.7 mg, 58% yield) as colorless oil. R_f = 0.5 (10% CH₂Cl₂ in hexanes); ¹H NMR (500 MHz, CDCl₃) δ 7.64 (dt, J = 7.9, 1.0 Hz, 1H), 7.42 (dq, J = 8.3, 0.9 Hz, 1H), 7.26 – 7.18 (m, 1H), 7.10 (ddd, J = 7.9, 6.9, 1.0 Hz, 1H), 6.77 (d, J = 0.9 Hz, 1H), 4.47 (p, J = 3.3 Hz, 1H), 4.17 (d, J = 6.4 Hz, 2H), 1.33 – 1.24 (m, 1H), 1.14 – 1.05 (m, 6H), 1.03 – 0.89 (m, 4H), 0.62 – 0.47 (m, 2H), 0.46 – 0.37 (m, 2H); ¹³C NMR (126 MHz, CDCl₃) δ 139.6, 136.1, 128.9, 122.0, 120.8, 119.2, 112.8, 110.1, 50.4, 12.3, 8.4, 4.3, 3.8. IR (Neat Film NaCl) 3006, 2955, 2933, 2912, 2874, 2113, 1493, 1466, 1455, 1435, 1413, 1390, 1377, 1351, 1334, 1322, 1301, 1233, 1214, 1165, 1153, 1091, 1047, 1015, 974, 819 cm⁻¹; HRMS (MM: ESI-APCI+) calc'd for C₁₆H₂₄NSi [M+H]⁺: 258.1673, found: 258.1676.

2.9.2.17 Experimental Procedures and Spectroscopic Data for the Silylation of Stereochemical Probe 176



1-(Benzo[*b*]thiophen-2-yl)-1-hexylsilolane (177, 1:1 syn:anti). In a nitrogen-filled glove box, KOt-Bu (4.5 mg, 0.04 mmol, 20 mol %) and benzo[*b*]thiophene **69** (26.8 mg, 0.20 mmol, 1.0 equiv) were added to an oven-dried scintillation vial equipped with a magnetic stirring bar, followed by deuterium labeled 1-hexylsilolane **176** (51.4 mg, 0.30 mmol, 1.5 equiv, syn:anti = 74:26 by 2H NMR) and THF (0.2 mL). The vial was sealed and the mixture was stirred at 25 °C for 48 h. The vial was removed from the glove box, and the reaction mixture was passed through a short plug of silica gel, eluting with diethyl ether. The residue was purified by flash chromatography on silica gel (100% *n*-pentane) to give the desired product **177** (51.7 mg, 85%, C2:C3 > 20:1) as a colorless oil. R_f = 0.7 (100% *n*-pentane). ^1H NMR (700 MHz, C_6D_6): δ 7.68 – 7.65 (m, 2H), 7.41 (s, 1H), 7.18 (ddd, J = 8.0, 7.0, 1.0 Hz, 1H), 7.08 (ddd, J = 8.0, 7.0, 1.0 Hz, 1H), 1.78 – 1.70 (m, 2H), 1.68 – 1.60 (m, 2H), 1.47 – 1.41 (m, 2H), 1.36 – 1.31 (m, 2H), 1.31 – 1.21 (m, 4H), 1.03 – 0.96 (m, 2H), 0.94 – 0.90 (m, 2H), 0.89 (t, J = 7.3 Hz, 3H), 0.86 – 0.79 (m, 2H). The analytical data are in accordance with those reported.³⁸

2.10 REFERENCES AND NOTES

- (1) (a) Liu, C.; Yuan, J.; Gao, M.; Tang, S.; Li, W.; Shi, R.; Lei, A. *Chem. Rev.* **2015**, *115*, 12138–12204. (b) DiRocco, D. A.; Dykstra, K.; Krska, S.; Vachal, P.; Conway, D. V.; Tudge, M. *Angew. Chem., Int. Ed.* **2014**, *53*, 4802–4806. (c) Bandini, M.; Eichholzer, A. *Angew. Chem., Int. Ed.* **2009**, *48*, 9608–9644. (d) Bergman, R. G. *Nature* **2007**, *446*, 391–393. (e) Godula, K.; Sames, D. *Science* **2006**, *312*, 67–72. (f) Labinger, J. A.; Bercaw J. E. *Nature* **2002**, *417*, 507–514.

- (2) (a) Cernak, T.; Dykstra, K. D.; Tyagarajan, S.; Vachal, P.; Krska, S. W. *Chem. Soc. Rev.* **2016**, *45*, 546–576. (b) Jin, J.; MacMillan, D. W. C. *Nature* **2015**, *525*, 87–90. (c) Légaré, M.-A.; Courtemanche, M.-A.; Rochette, É.; Fontaine, F.-G. *Science* **2015**, *349*, 513–516. (d) Rossi, R.; Bellina, F.; Lessi, M.; Manzini, C. *Adv. Synth. Catal.* **2014**, *356*, 17–117. (e) O'Brien, A. G.; Maruyama, A.; Inokuma, Y.; Fujita, M.; Baran, P. S.; Blackmond, D. G. *Angew. Chem., Int. Ed.* **2014**, *53*, 11868–11871. (f) Fujiwara, Y.; Dixon, J. A.; O'Hara, F.; Funder, E. D.; Dixon, D. D.; Rodriguez, R. A.; Baxter, R. D.; Herlé, B.; Sach, N.; Collins, M. R.; Ishihara, Y.; Baran, P. S. *Nature* **2012**, *492*, 95–99.
- (3) (a) Ball, L. T.; Lloyd-Jones, G. C.; Russell, C. A. *Science* **2012**, *337*, 1644–1648. (b) Sore, H. F.; Galloway, W. R. J. D.; Spring, D. R. *Chem. Soc. Rev.* **2012**, *41*, 1845–1866. (c) Nakao, Y.; Hiyama, T. *Chem. Soc. Rev.* **2011**, *40*, 4893–4901. (d) Denmark, S. E.; Baird, J. D. *Chem. Eur. J.* **2006**, *12*, 4954–4963. (e) Denmark, S. E.; Ober, M. H. *Aldrichimica Acta* **2003**, *36*, 75–85. (f) Langkopf, E.; Schinzer, D. *Chem. Rev.* **1995**, *95*, 1375–1408.
- (4) (a) Franz, A. K.; Wilson, S. O. *J. Med. Chem.* **2013**, *56*, 388–405. (b) Zhang, F.; Wu, D.; Xu, Y.; Feng, X. *J. Mater. Chem.* **2011**, *21*, 17590–17600. (c) Wang, Y.; Watson, M. D. *J. Am. Chem. Soc.* **2006**, *128*, 2536–2537. (d) Showell, G. A.; Mills, J. S. *Drug Discov. Today* **2003**, *8*, 551–556.
- (5) Hartwig, J. F. *Acc. Chem. Res.* **2012**, *45*, 864–873.
- (6) For reviews of catalytic C–H silylation, see: (a) Cheng, C.; Hartwig, J. F. *Chem. Rev.* **2015**, *115*, 8946–8975. (b) Yang, Y.; Wang, C. *Sci. China Chem.* **2015**, *58*,

- 1266–1279. (c) Sharma, R.; Kumar, R.; Kumar, I.; Singh, B.; Sharma, U. *Synthesis* **2015**, *47*, 2347–2366. (d) Xu, Z.; Huang, W.-S.; Zhang, J.; Xu, L.-W. *Synthesis* **2015**, *47*, 3645–3668.
- (7) Whisler, M. C.; MacNeil, S.; Snieckus, V.; Beak, P. *Angew. Chem., Int. Ed.* **2004**, *43*, 2206–2225. See Ref. 3f.
- (8) (a) Cheng, C.; Hartwig, J. F. *J. Am. Chem. Soc.* **2015**, *137*, 592–595. (b) Cheng, C.; Hartwig, J. F. *Science* **2014**, *343*, 853–857. (c) Lu, B.; Falck, J. R. *Angew. Chem., Int. Ed.* **2008**, *47*, 7508–7510.
- (9) Friedel–Crafts silylation of electron-rich arenes were also reported recently: (a) Chen, Q.; Klare, H. F. T.; Oestreich, M. *J. Am. Chem. Soc.* **2016**, *138*, 7868–7871. (b) Ma, Y.; Wang, B.; Zhang, L.; Hou, Z. *J. Am. Chem. Soc.* **2016**, *138*, 3663–3666. (c) Bähr, S.; Oestreich, M. *Angew. Chem., Int. Ed.* DOI: 10.1002/anie.201608470 (d) Yin, Q.; Klare, H. F. T.; Oestreich, M. *Angew. Chem., Int. Ed.* **2016**, *55*, 3204–3207. (e) Klare, H. F. T.; Oestreich, M.; Ito, J.-i.; Nishiyama, H.; Ohki, Y.; Tatsumi, K. *J. Am. Chem. Soc.* **2011**, *133*, 3312–3315.
- (10) (a) Toutov, A. A.; Liu, W.-B.; Stoltz, B. M.; Grubbs, R. H. *Org. Synth.* **2016**, *93*, 263–271. (b) Toutov, A. A.; Liu, W.-B.; Betz, K. N.; Stoltz, B. M.; Grubbs, R. H. *Nature Protocols* **2015**, *10*, 1897–1903. (c) Toutov, A. A.; Liu, W.-B.; Betz, K. N.; Fedorov, A.; Stoltz, B. M.; Grubbs, R. H. *Nature* **2015**, *518*, 80–84. (d) Fedorov, A.; Toutov, A. A.; Swisher, N. A.; Grubbs, R. H. *Chem. Sci.* **2013**, *4*, 1640–1645.

- (11) Liu, W.-B.; Schuman, D. P.; Yang, Y.-F.; Toutov, A. A.; Liang, Y.; Klare, H. F. T.; Nesnas, N.; Oestreich, M.; Blackmond, D. G.; Virgil, S. C.; Banerjee, S.; Zare, R. N.; Grubbs, R. H.; Houk, K. N.; Stoltz, B. M. *J. Am. Chem. Soc.* **2017**, *139*, 6867–6879.
- (12) Banerjee, S.; Yang, Y.-F.; Jenkins, I. D.; Liang, Y.; Toutov, A. A.; Liu, W.-B.; Schuman, D. P.; Grubbs, R. H.; Stoltz, B. M.; Krenske, E. H.; Houk, K. N.; Zare, R. N. *J. Am. Chem. Soc.* **2017**, *139*, 6880–6887.
- (13) Hu, S.-W.; Wang, Y.; Wang, X.-Y.; Chu, T.-W.; Liu, X.-Q. *J. Phys. Chem. A* **2004**, *108*, 1448–1459.
- (14) (a) Bravo-Zhivotovskii, D.; Ruderfer, I.; Yuzefovich, M.; Kosa, M.; Botoshansky, M.; Tumanskii, B.; Apeloig, Y. *Organometallics* **2005**, *24*, 2698–2704. (b) Lucarini, M.; Marchesi, E.; Pedulli, G. F.; Chatgilialoglu, C. *J. Org. Chem.* **1998**, *63*, 1687–1693.
- (15) (a) Schley, N. D.; Fu, G. C. *J. Am. Chem. Soc.* **2014**, *136*, 16588–16593. (b) Newcomb, M. *Tetrahedron* **1993**, *49*, 1151–1176.
- (16) For examples see: (a) Chatgilialoglu, C. *Acc. Chem. Res.* **1992**, *25*, 188–194. (b) Sommer, L. H.; Ulland, L. A. *J. Am. Chem. Soc.* **1972**, *94*, 3803–3806. (c) Bennett, S. W.; Eaborn, C.; Hudson, A.; Jackson, R. A.; Root, K. D. *J. J. Chem. Soc., A* **1970**, 348–351.
- (17) (a) Zhang, L.; Yang, H.; Jiao, L. *J. Am. Chem. Soc.* **2016**, *138*, 7151–7160. (b) Yi, H.; Jutand, A.; Lei, A. *Chem. Commun.* **2015**, *51*, 545–548.

- (18) (a) Barham, J. P.; Coulthard, G.; Emery, K. J.; Doni, E.; Cumine, F.; Nocera, G.; John, M. P.; Berlouis, L. E. A.; McGuire, T.; Tuttle, T.; Murphy, J. A. *J. Am. Chem. Soc.* **2016**, *138*, 7402–7410. (b) Barham, J. P.; Coulthard, G.; Kane, R. G.; Delgado, N.; John, M. P.; Murphy, J. A. *Angew. Chem., Int. Ed.* **2016**, *55*, 4492–4496. (c) Zhou, S.; Doni, E.; Anderson, G. M.; Kane, R. G.; MacDougall, S. W.; Ironmonger, V. M.; Tuttle, T.; Murphy, J. A. *J. Am. Chem. Soc.* **2014**, *136*, 17818–17826.
- (19) (a) Xu, L.; Zhang, S.; Li, P. *Org. Chem. Front.* **2015**, *2*, 459–463. (b) Cai, Y.; Roberts, B. P. *J. Chem. Soc., Perkin Trans. I* **1998**, 467–476. (c) Chatgilialoglu, C.; Scaiano, J. C.; Ingold, K. U. *Organometallics* **1982**, *1*, 466–469.
- (20) (a) Rendler, S.; Oestreich, M. *Synthesis* **2005**, *11*, 1727–1747. (b) Chuit, C.; Corriu, R. J. P.; Reye, C.; Young, J. C. *Chem. Rev.* **1993**, *93*, 1371–1448. (c) Holmes, R. R. *Chem. Rev.* **1996**, *96*, 927–950. (d) Corriu, R. J. P.; Perz, R.; Reye, C. *Tetrahedron* **1983**, *39*, 999–1009. (e) Boyer, J.; Corriu, R. J. P.; Perz, R.; Reye, C. *Tetrahedron* **1981**, *37*, 2165–2171.
- (21) Shekar, S.; Brown, S. N. *J. Org. Chem.* **2014**, *79*, 12047–12055.
- (22) Yang, D.; Tanner, D. D. *J. Org. Chem.* **1986**, *51*, 2267–2270.
- (23) (a) Corriu, R. J. P.; Guerin, C.; Henner, B.; Wang, Q. *Organometallics* **2002**, *10*, 2297–2303. (b) Corriu, R.; Guérin, C.; Henner, B.; Wang, Q. *J. Organomet. Chem.* **1989**, *365*, C7–C10.

- (24) (a) Denmark, S. E.; Beutner, G. L. *Angew. Chem., Int. Ed.* **2008**, *47*, 1560–1638.
(b) Couzijn, E. P. A.; Ehlers, A. W.; Schakel, M.; Lammertsma, K. *J. Am. Chem. Soc.* **2006**, *128*, 13634–13639.
- (25) Mitzel reported a redshift (from 2151 to 2107 cm^{−1}) of the trans Si–H stretching in *N,N*-dimethylaminopropylsilane [H₃Si(CH₂)₃NMe₂] by IR, due to an attractive N–Si interaction to form a hypercoordinate complex as characterized by X-ray analysis, see: Hagemann, M.; Berger, R. J. F.; Hayes, S. A.; Stammler, H-G.; Mitzel, N. W. *Chem. Eur. J.* **2008**, *14*, 11027–11038.
- (26) Ido, E.; Kakiage, K.; Kyomen, T.; Hanaya, M. *Chem. Lett.* **2012**, *41*, 853–854.
- (27) These trends are consistent with the reported pentacoordinate silicate hydrosilylation of ketones, see: Deiters, J. A.; Holmes, R. R. *J. Am. Chem. Soc.* **1990**, *112*, 7197–7202.
- (28) Kanabus-Kaminska, J. M.; Hawari, J. A.; Griller, D.; Chatgilialoglu, C. *J. Am. Chem. Soc.* **1987**, *109*, 5267–5268.
- (29) Alternatively, given the precedent of pentacoordinate silicate serving as a single electron donor, a single electron transfer from a pentacoordinate silicate to Et₃SiH, followed by the evolution of H₂ and generation of triethylsilyl radical is also possible. See 18a.
- (30) Chisholm, M. H.; Drake, S. R.; Naiini, A. A.; Streib, W. E. *Polyhedron* **1991**, *10*, 337–345.
- (31) (a) Postigo, A.; Kopsov, S.; Zlotsky, S. S.; Ferreri, C.; Chatgilialoglu, C. *Organometallics* **2009**, *28*, 3282–3287. (b) Zaborovskiy, A. B.; Lutsyk, D. S.;

- Prystansky, R. E.; Kopylets, V. I.; Timokhin, V. I.; Chatgilialoglu, C. *J. Organomet. Chem.* **2004**, *689*, 2912–2919.
- (32) Sommer, L. H.; Ulland, L. A. *J. Am. Chem. Soc.* **1972**, *94*, 3803–3806.
- (33) (a) Bottoni, A. *J. Phys. Chem. A.* **1997**, *101*, 4402–4408. (b) Chatgilialoglu, C. *Chem. Rev.* **1995**, *95*, 1229–1251. (c) Chatgilialoglu, C.; Ingold, K. U.; Scaiano, J. C. *J. Am. Chem. Soc.* **1983**, *105*, 3292–3296.
- (34) The bond energy of a C–H bond in an ethyl radical is nearly a factor of 3 smaller than that of ethane, see: Blanksby, S. J.; Ellison, G. B. *Acc. Chem. Res.* **2003**, *36*, 255–263.
- (35) (a) Honraedt, A.; Raux, M.-A.; Le Grogne, E.; Jacquemin, D.; Felpin, F.-X. *Chem. Commun.* **2014**, *50*, 5236–5238. (C₂, C₃ selectivity), (b) O’Hara, F.; Blackmond, D. G.; Baran, P. S. *J. Am. Chem. Soc.* **2013**, *135*, 12122–12134 (regioselectivity). (c) Roberts, B. P. *Chem. Soc. Rev.* **1999**, *28*, 25–35. (d) Cole, S. J.; Kirwan, J. N.; Roberts, B. P.; Willis, C. R. *J. Chem. Soc., Perkin Trans. 1* **1991**, 103–112.
- (36) This type of proton abstraction usually requires polarity-reversal catalysis (PRC), see Ref. 46c.
- (37) Murai, M.; Takeuchi, Y.; Yamauchi, K.; Kuninobu, Y.; Takai, K. *Chem. Eur. J.* **2016**, *22*, 6048–6058.
- (38) Fallon, T.; Oestreich, M. *Angew. Chem., Int. Ed.* **2015**, *54*, 12488–12491.
- (39) Lu, B.; Falck, J. R. *Angew. Chem., Int. Ed.* **2008**, *47*, 7508–7510.

- (40) (a) Sommer, L. H.; Korte, W. D.; Rodewald, P. G. *J. Am. Chem. Soc.* **1967**, *89*, 862–868. (b) Sommer, L. H.; Rodewald, P. G.; Parker, G. A. *Tetrahedron Lett.* **1962**, *3*, 821–824.
- (41) Couzijn, E. P. A.; Slootweg, J. C.; Ehlers, A. W.; Lammertsma, K. *J. Am. Chem. Soc.* **2010**, *132*, 18127–18140. See also Ref. 28b.
- (42) Sakurai, H.; Murakami, M.; Kumada, M. *J. Am. Chem. Soc.* **1969**, *91*, 519–520.
- (43) (a) Sommer, L. H.; Ulland, L. A. *J. Org. Chem.* **1972**, *37*, 3878–3881. (b) Sakurai, H.; Murakami, M. *Chem. Lett.* **1972**, *1*, 7–8.
- (44) A. M. Pangborn, M. A. Giardello, R. H. Grubbs, R. K. Rosen and F. J. Timmers, *Organometallics*, **1996**, *15*, 1518.
- (45) Frisch, M. J.; Trucks, G. W.; Schlegel, H. B.; Scuseria, G. E.; Robb, M. A.; Cheeseman, J. R.; Scalmani, G.; Barone, V.; Mennucci, B.; Petersson, G. A.; Nakatsuji, H.; Caricato, M.; Li, X.; Hratchian, H. P.; Izmaylov, A. F.; Bloino, J.; Zheng, G.; Sonnenberg, J. L.; Hada, M.; Ehara, M.; Toyota, K.; Fukuda, R.; Hasegawa, J.; Ishida, M.; Nakajima, T.; Honda, Y.; Kitao, O.; Nakai, H.; Vreven, T.; Montgomery, Jr., J. A.; Peralta, J. E.; Ogliaro, F.; Bearpark, M.; Heyd, J. J.; Brothers, E.; Kudin, K. N.; Staroverov, V. N.; Keith, T.; Kobayashi, R.; Normand, J.; Raghavachari, K.; Rendell, A.; Burant, J. C.; Iyengar, S. S.; Tomasi, J.; Cossi, M.; Rega, N.; Millam, J. M.; Klene, M.; Knox, J. E.; Cross, J. B.; Bakken, V.; Adamo, C.; Jaramillo, J.; Gomperts, R.; Stratmann, R. E.; Yazyev, O.; Austin, A. J.; Cammi, R.; Pomelli, C.; Ochterski, J. W.; Martin, R. L.; Morokuma, K.; Zakrzewski, V. G.; Voth, G. A.; Salvador, P.; Dannenberg, J. J.;

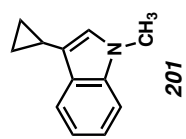
- Dapprich, S.; Daniels, A. D.; Farkas, O.; Foresman, J. B.; Ortiz, J. V.; Cioslowski, J.; Fox, D. J. Gaussian 09, Rev. D.01; Gaussian, Inc., Wallingford, CT, 2010.
- (46) (a) Lee, C.; Yang W.; Parr, R. G. *Phys. Rev. B* **1988**, *37*, 785–789. (b) Stephens, P. J.; Devlin, F. J.; Chabalowski, C. F.; Frisch, M. J. *J. Phys. Chem.* **1994**, *98*, 11623–11627. (c) Becke, A. D. *J. Chem. Phys.* **1993**, *98*, 5648–5652. (d) Becke, A. D. *J. Chem. Phys.* **1993**, *98*, 1372–1377.
- (47) (a) Hariharan, P. C.; Pople, J. A. *Theor. Chim. Acta* **1973**, *28*, 213–222. (b) Hehre, W. J.; Ditchfield, R.; Pople, J. A. *J. Chem. Phys.* **1972**, *56*, 2257–2261. (c) Ditchfield, R.; Hehre, W. J.; Pople, J. A. *J. Chem. Phys.* **1971**, *54*, 724–728.
- (48) Zhao, Y.; Truhlar, D. G. *Theor. Chem. Acc.* **2008**, *120*, 215–241.
- (49) (a) Barone, V.; Cossi, M. *J. Phys. Chem. A* **1998**, *102*, 1995–2001. (b) Cossi, M.; Rega, N.; Scalmani, G.; Barone, V. *J. Comput. Chem.* **2003**, *24*, 669–681. (c) Takano, Y.; Houk, K. N. *J. Chem. Theory Comput.* **2005**, *1*, 70–77.
- (50) (a) Banks, J. T.; Scaiano, J. C.; Adam, W.; Oestrich, R. S. *J. Am. Chem. Soc.* **1993**, *115*, 2473. (b) Mendenhall, G. D. *Tetrahedron Lett.* **1983**, *24*, 451.
- 51 Kozhushkov, S. I.; Wagner-Gillen, K.; Khlebnikov, A. F.; de Meijere, A. *Synthesis* **2010**, *2010*, 3967–3973.
- 52 (a) Zemolka, S.; Schunk, S.; Englberger, W.; Kogel, B.-Y.; Linz, K.; Schick, H.; Sonnenschein, H.; Graubaum, H.; Hinze, C. (Gruenthal GmbH, Aachen, Germany) Substituted heteroaryl derivatives. U.S. Patent 8,138,187, March 20, 2012. (b) Penoni, A.; Palmisano, G.; Zhao, Y.-L.; Houk, K. N.; Volkman, J.; Nicholas, K. M. *J. Am. Chem. Soc.* **2008**, *131*, 653–661

APPENDIX 1

Spectra Relevant to Chapter 2:

*A Combined Experimental and Computational Mechanistic Study of the
KOt-Bu-Catalyzed Dehydrogenative C–H Silylation of Aromatic
Heterocycles*

Figure A1.1. ^1H NMR (400 MHz, CDCl_3) of compound 201.



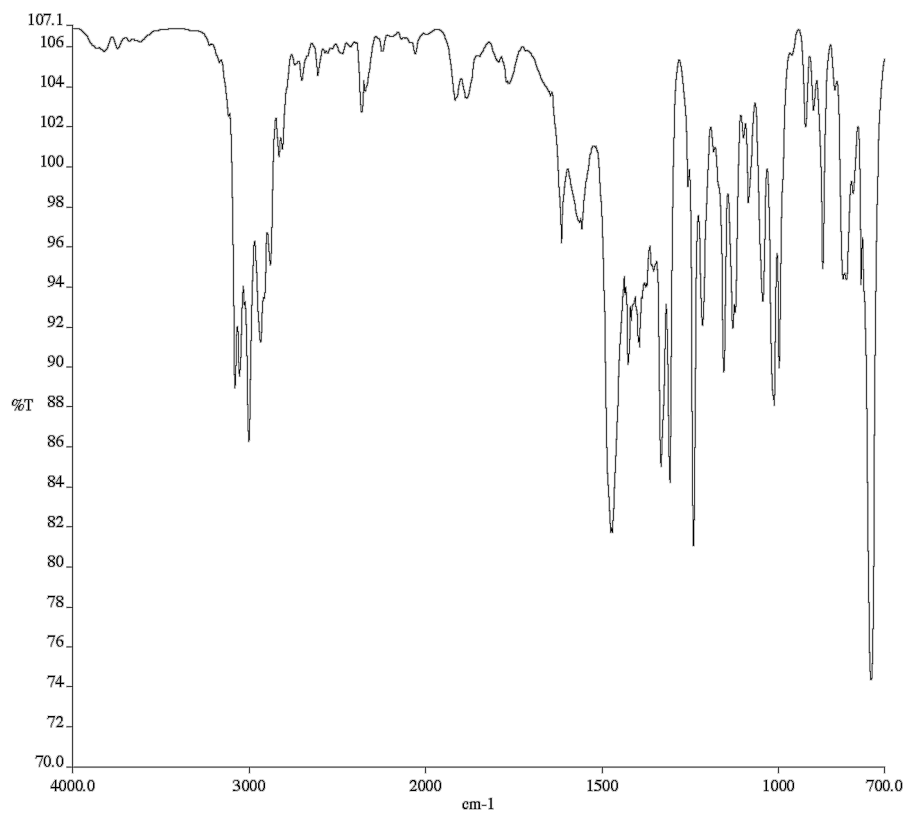


Figure A1.2. Infrared spectrum (Thin Film, NaCl) of compound **201**.

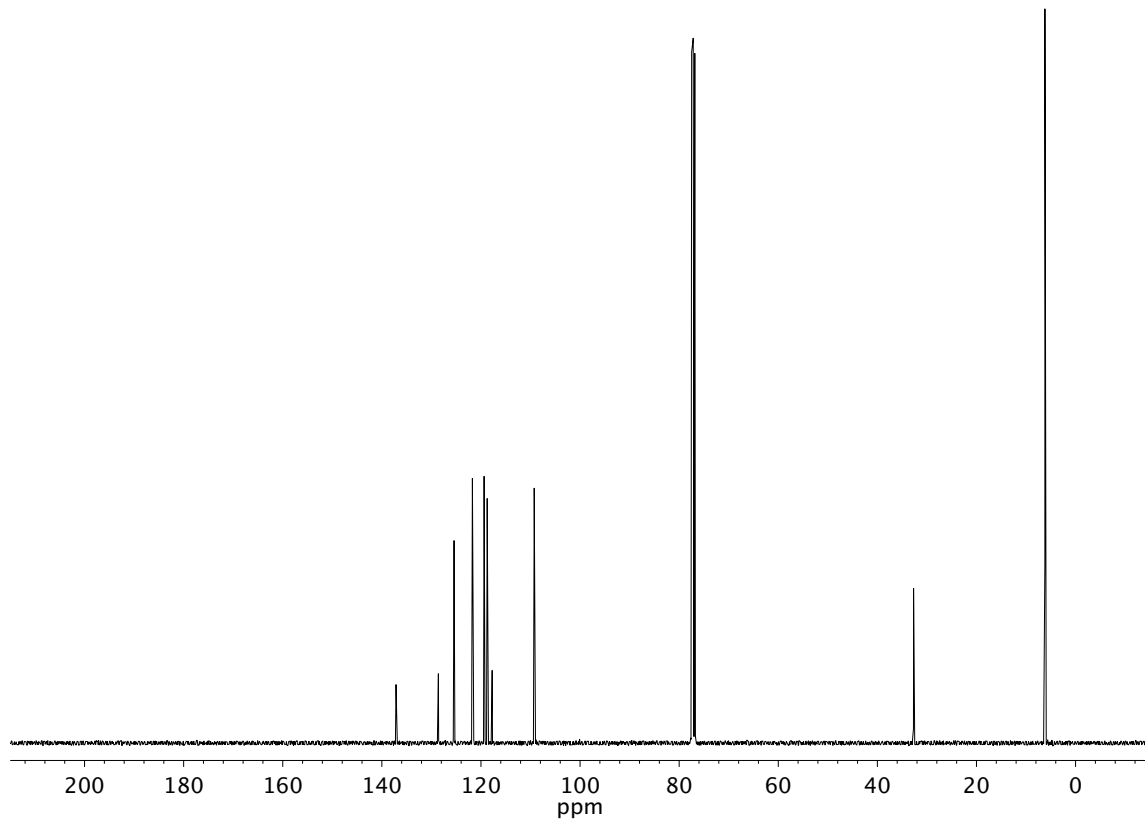
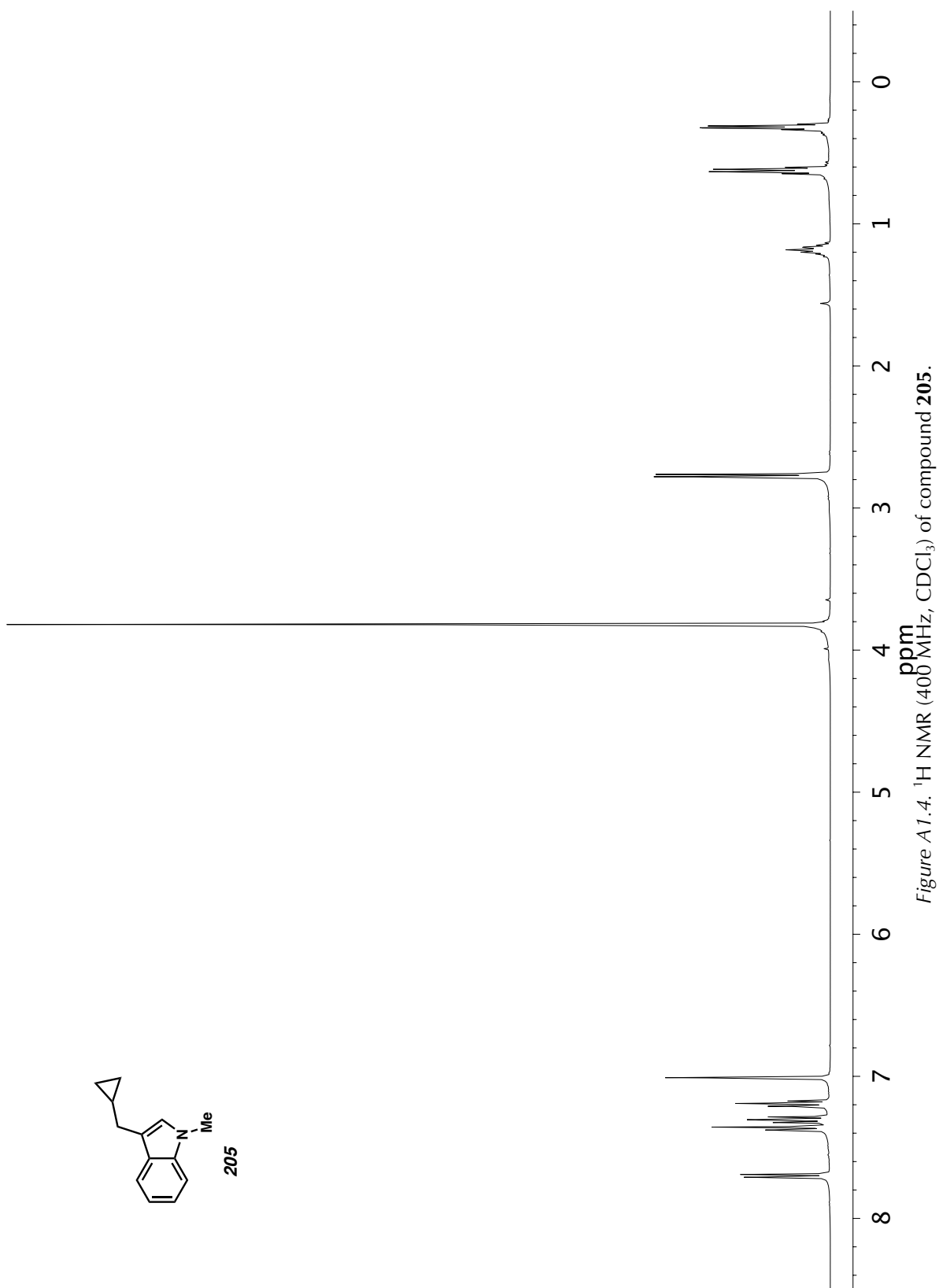


Figure A1.3. ^{13}C NMR (101 MHz, CDCl_3) of compound **201**.



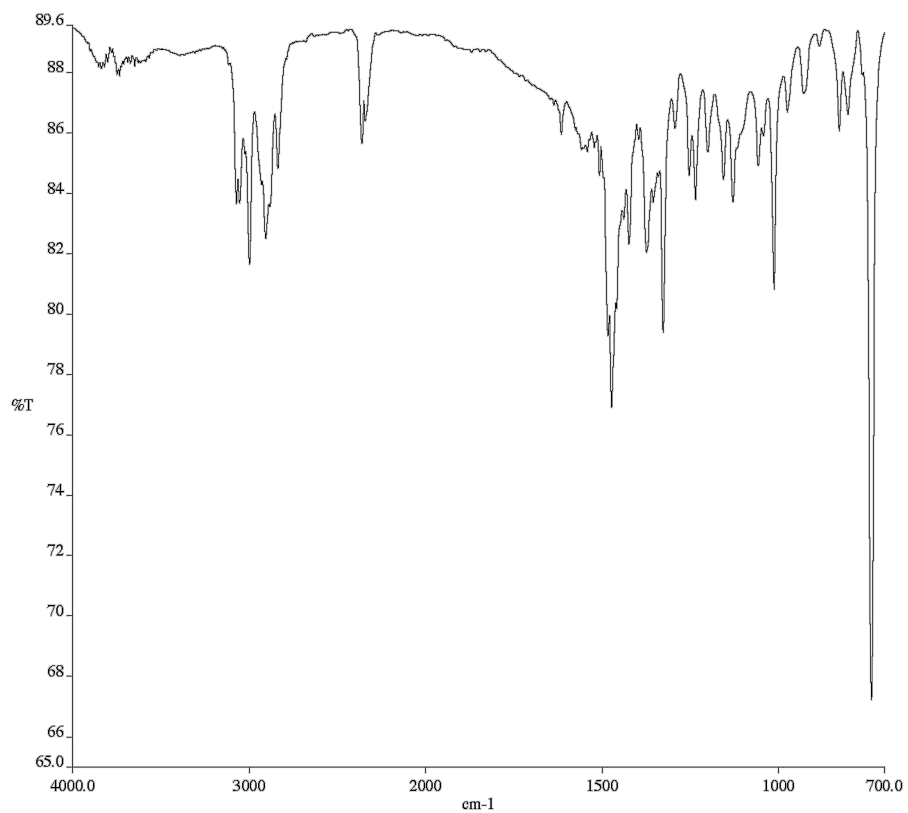


Figure A1.5. Infrared spectrum (Thin Film, NaCl) of compound **205**.

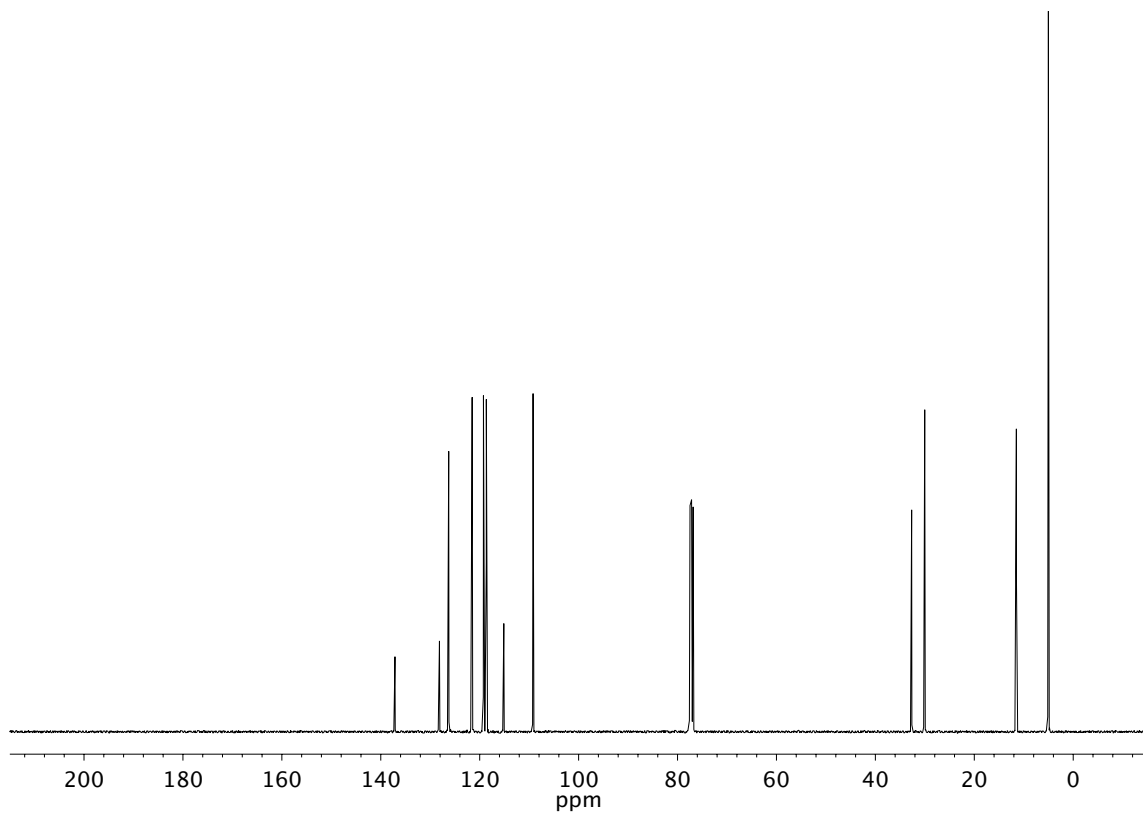
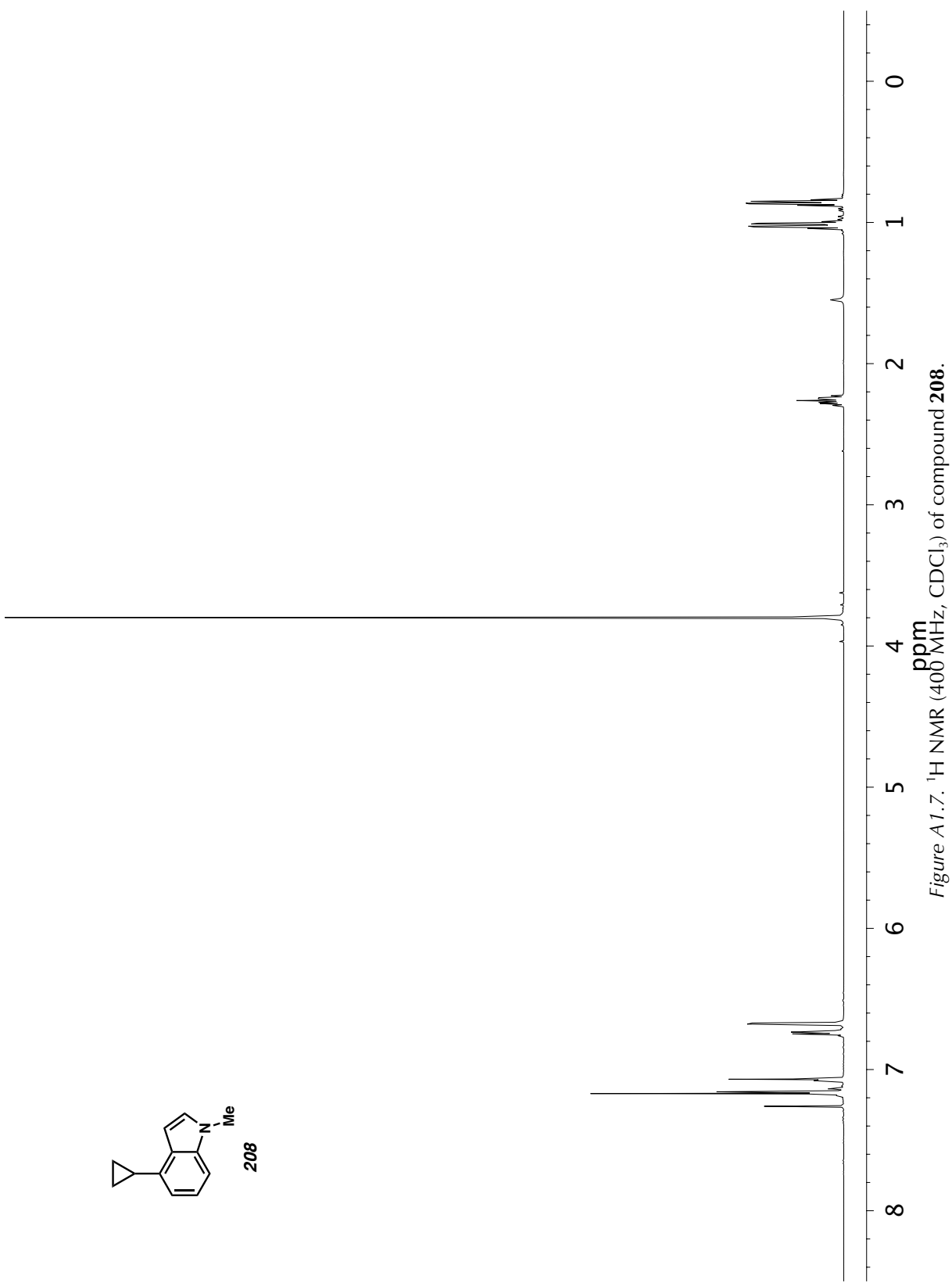


Figure A1.6. ¹³C NMR (101 MHz, CDCl₃) of compound **205**.



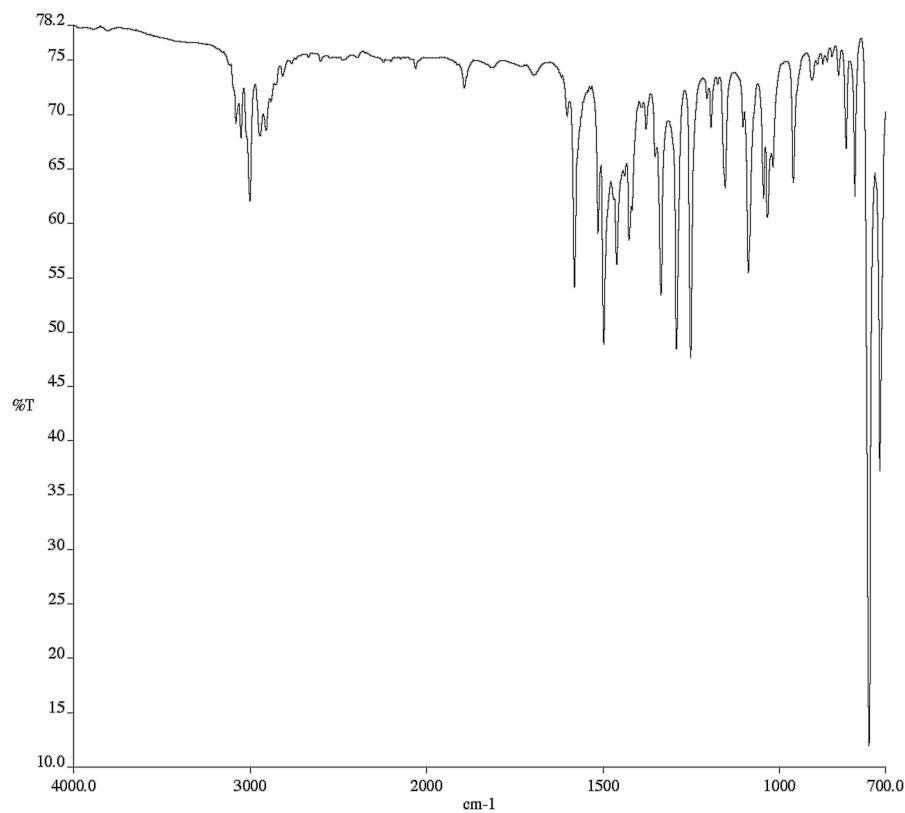


Figure A1.8. Infrared spectrum (Thin Film, NaCl) of compound **208**.

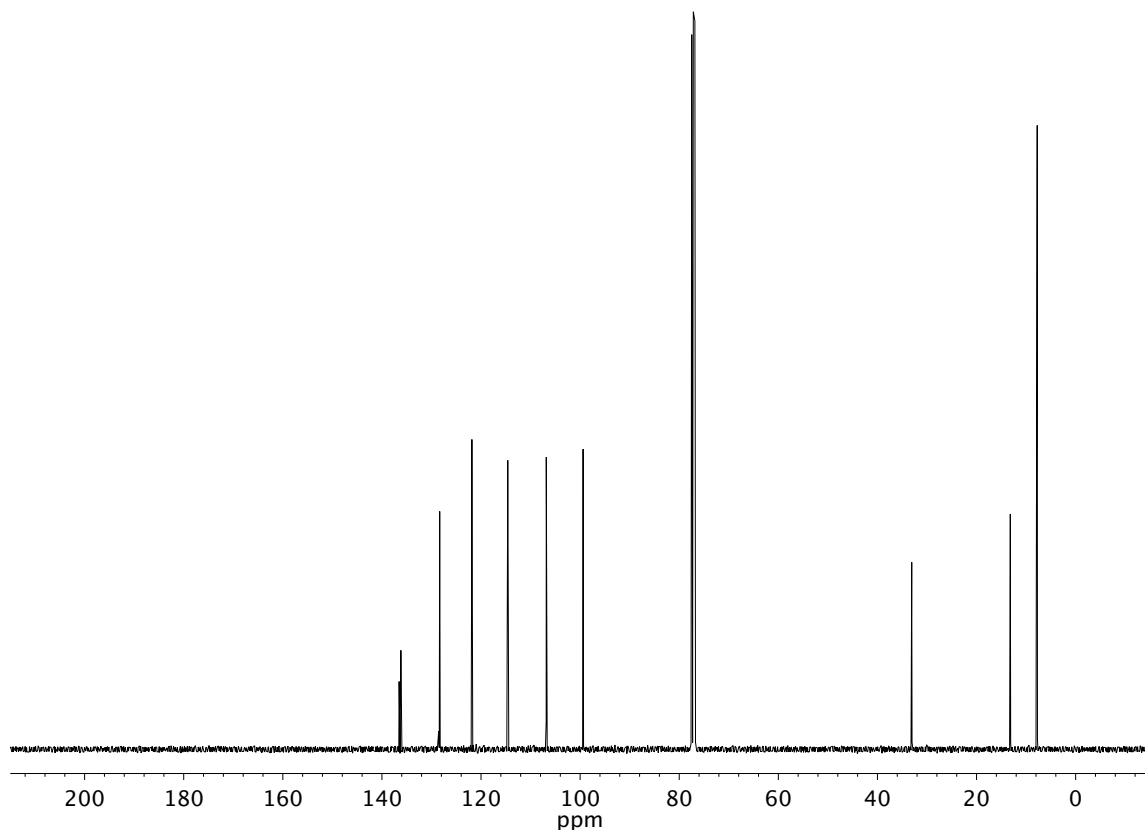


Figure A1.9. ^{13}C NMR (101 MHz, CDCl_3) of compound **208**.

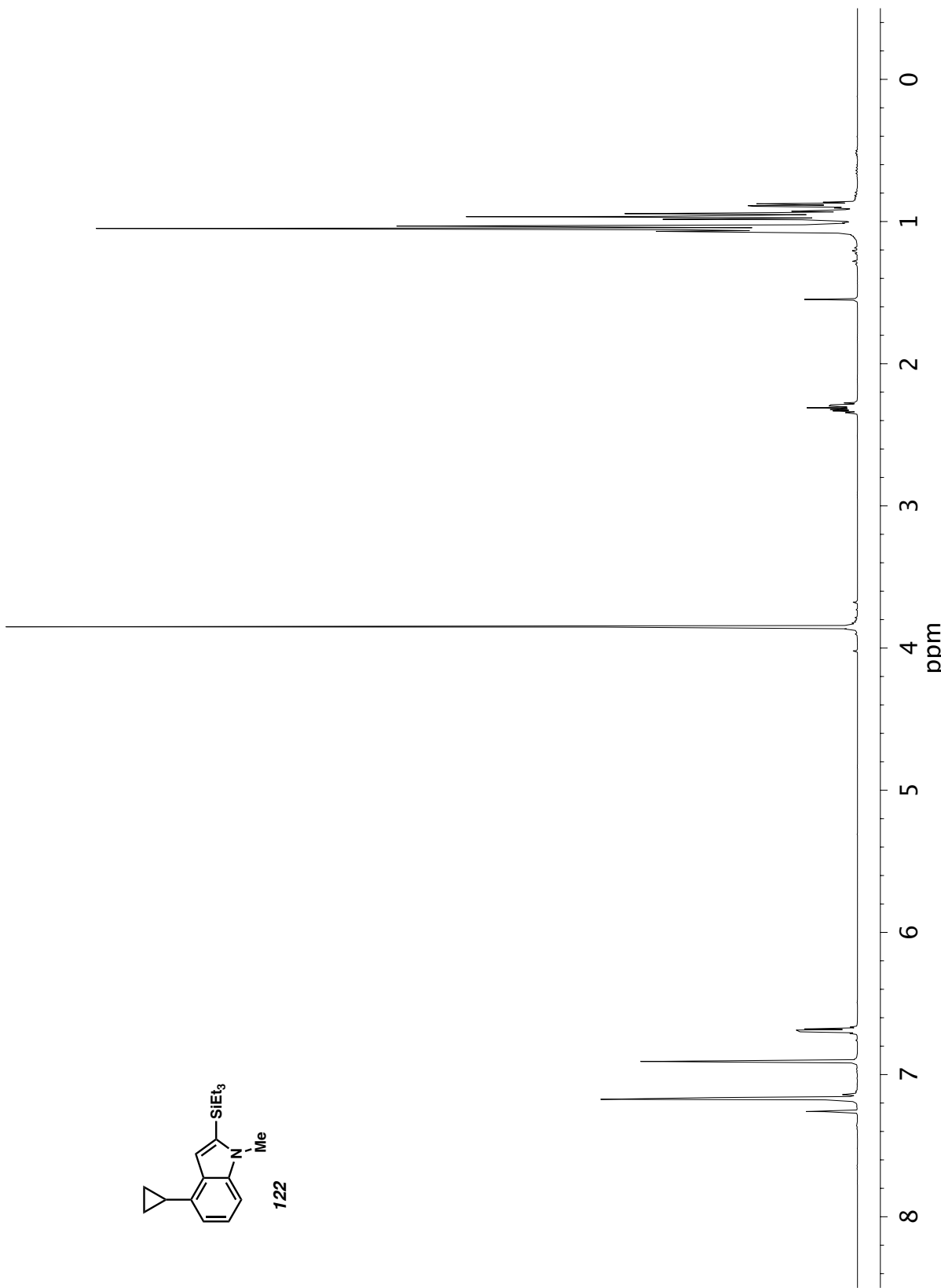


Figure A1.10. ^1H NMR (400 MHz, CDCl_3) of compound 122.

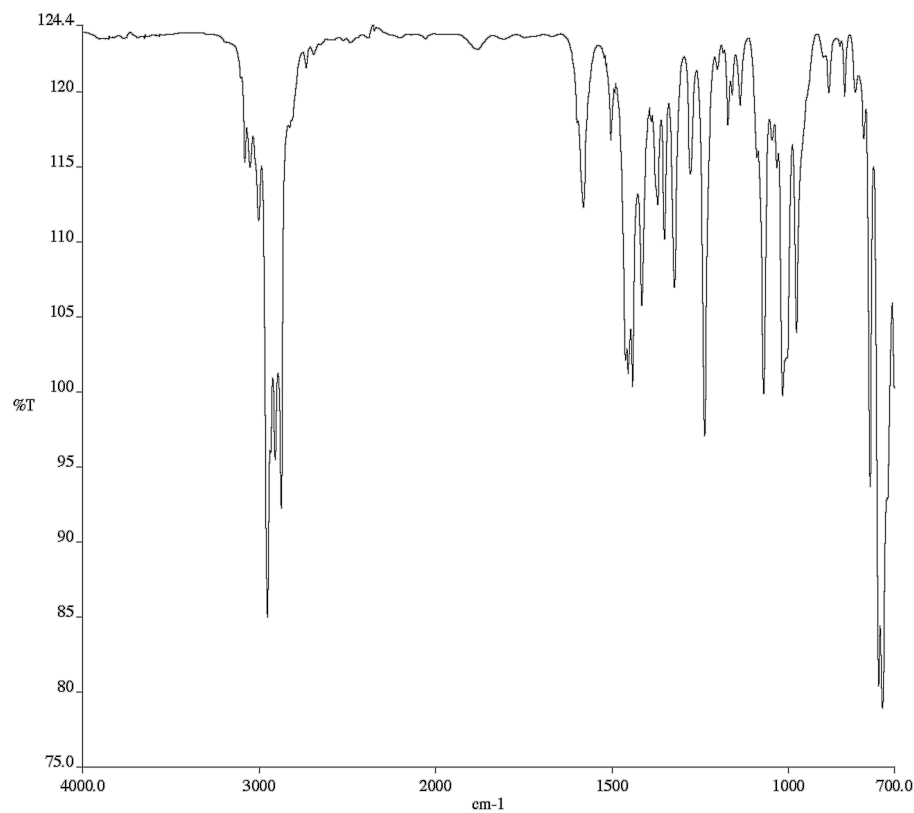


Figure A1. 11. Infrared spectrum (Thin Film, NaCl) of compound **122**.

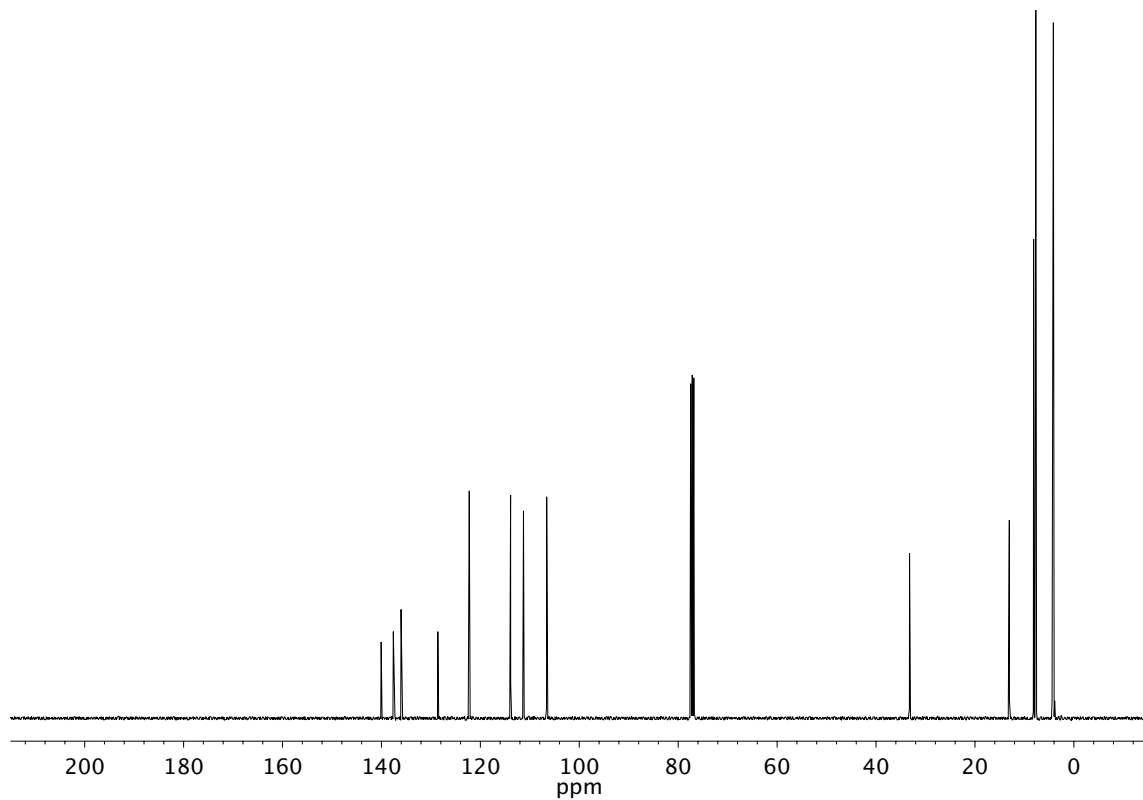
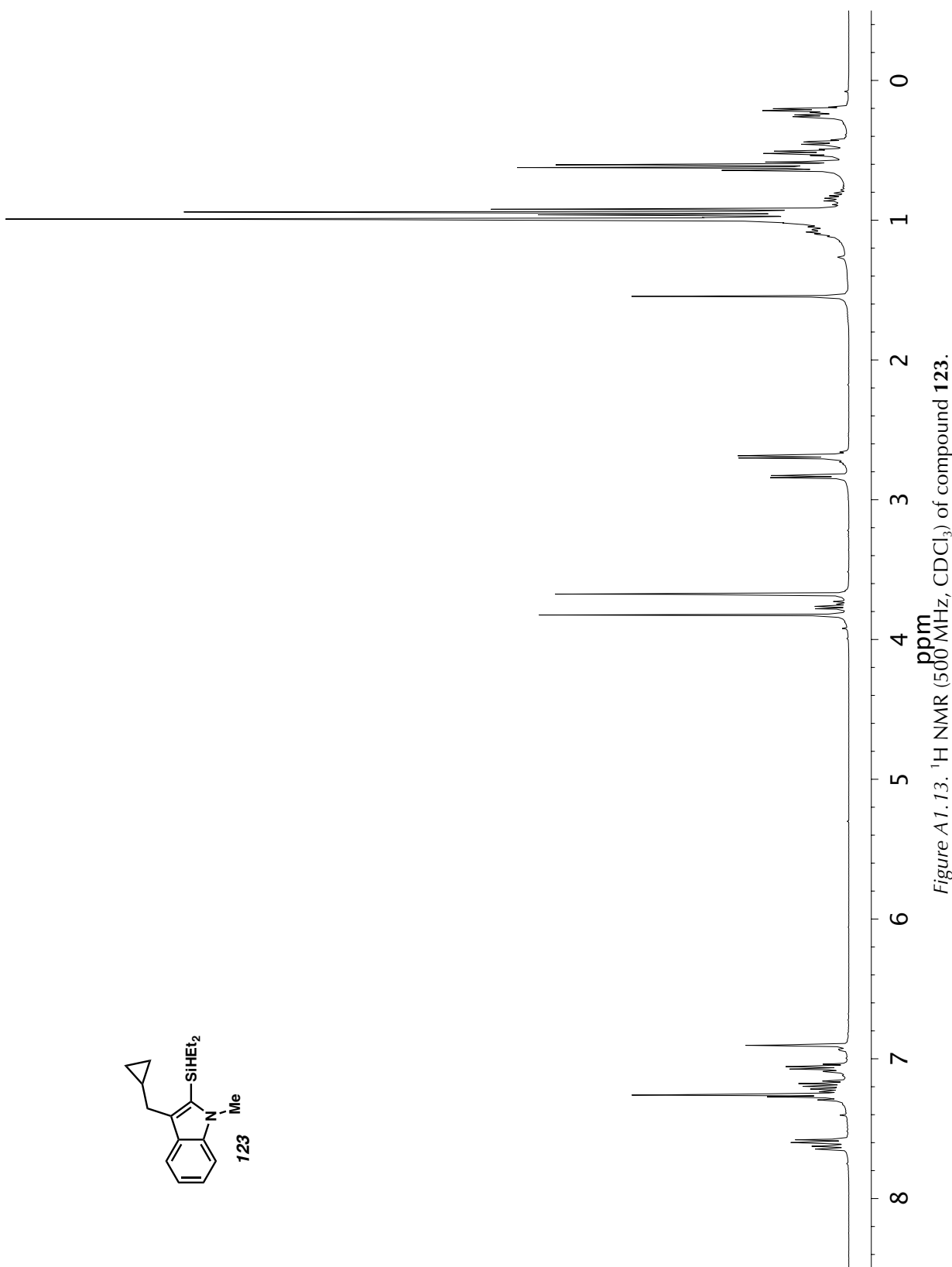


Figure A1. 12. ^{13}C NMR (101 MHz, CDCl_3) of compound **122**.



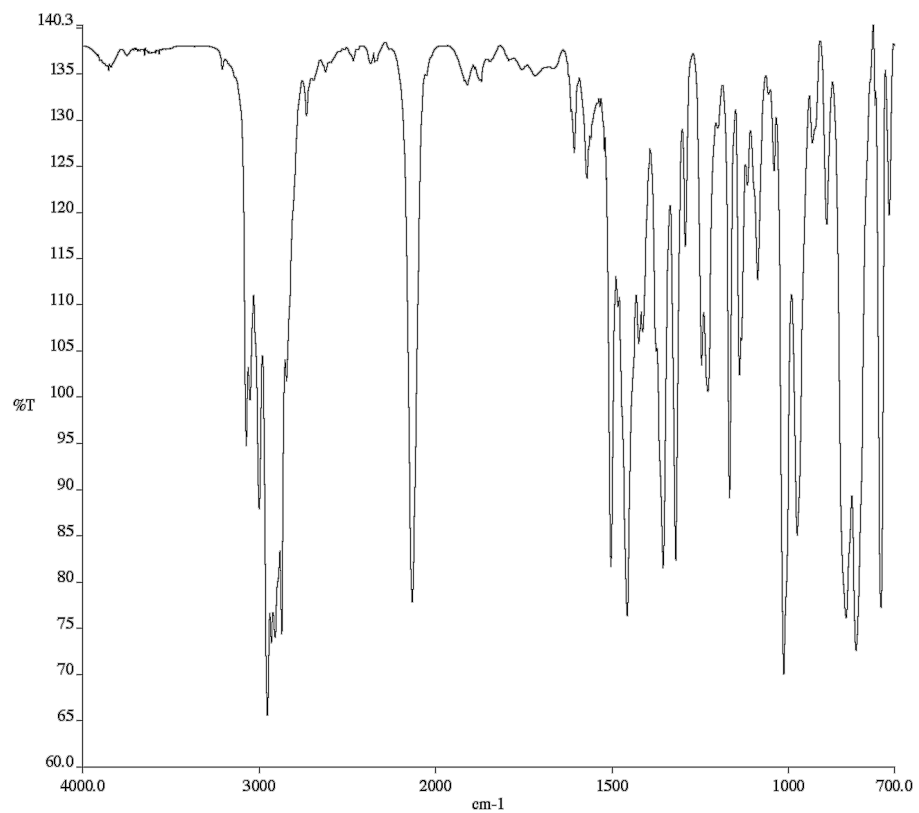


Figure A1. 14. Infrared spectrum (Thin Film, NaCl) of compound **123**.

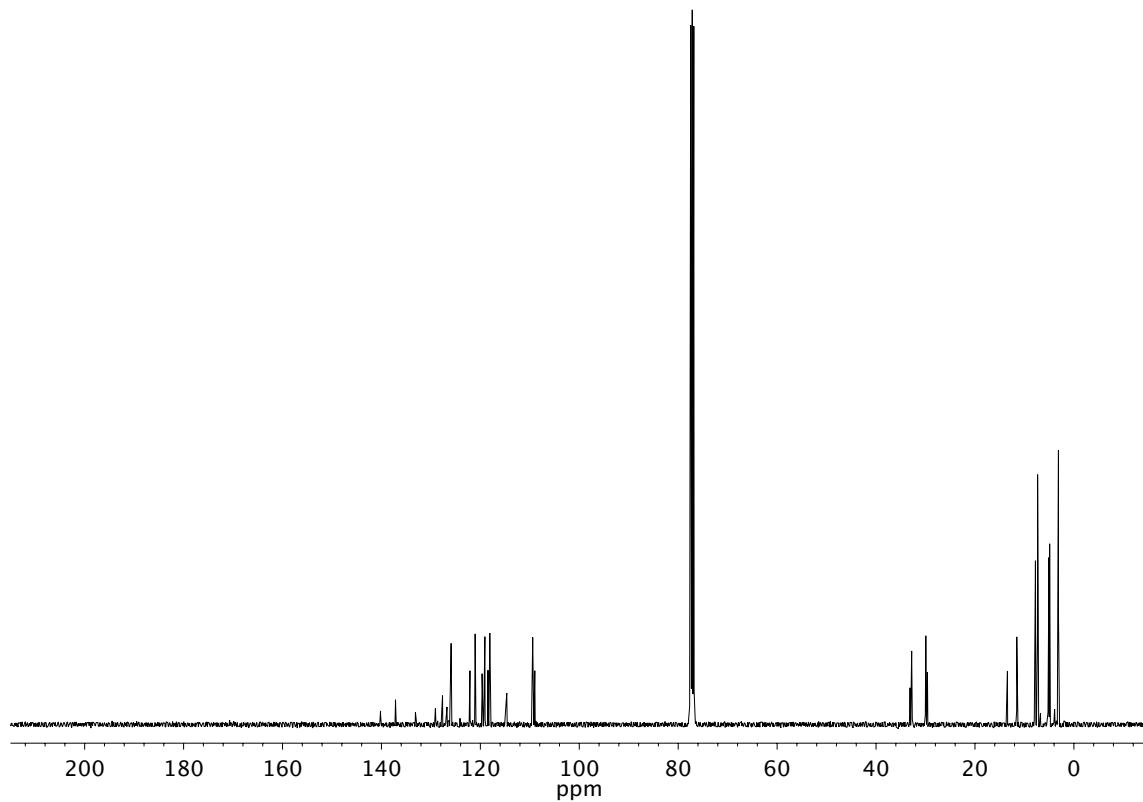


Figure A1. 15. ^{13}C NMR (125 MHz, CDCl_3) of compound **123**.

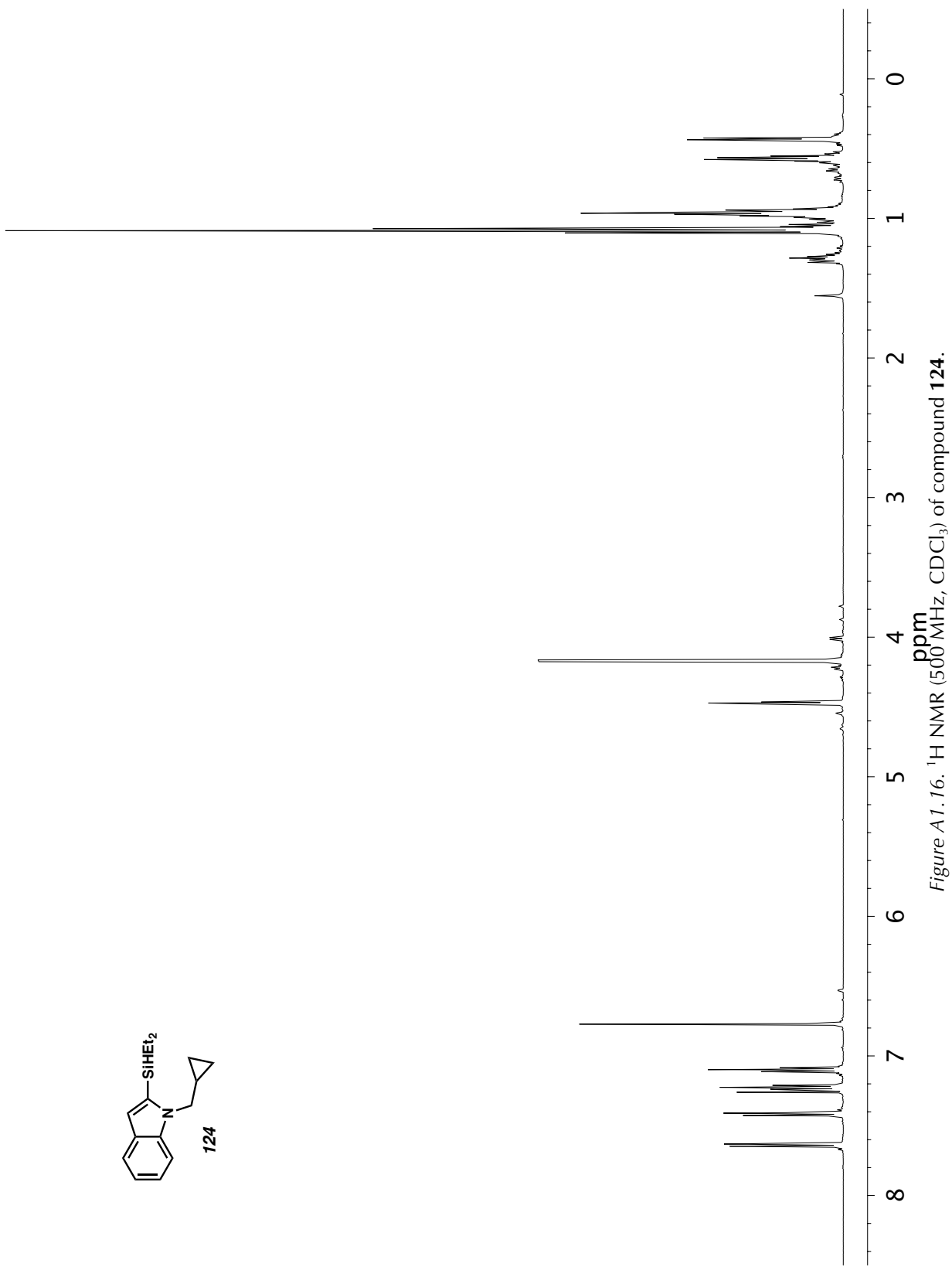


Figure A1.16. ^1H NMR (500 MHz, CDCl_3) of compound 124.

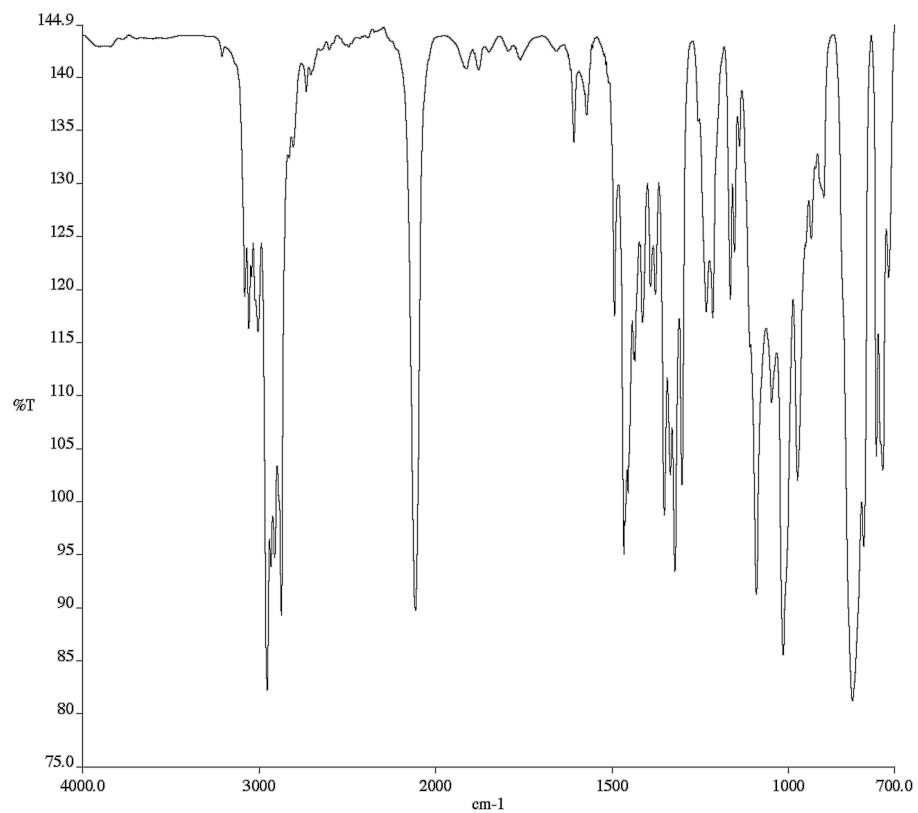


Figure A1.17. Infrared spectrum (Thin Film, NaCl) of compound **124**.

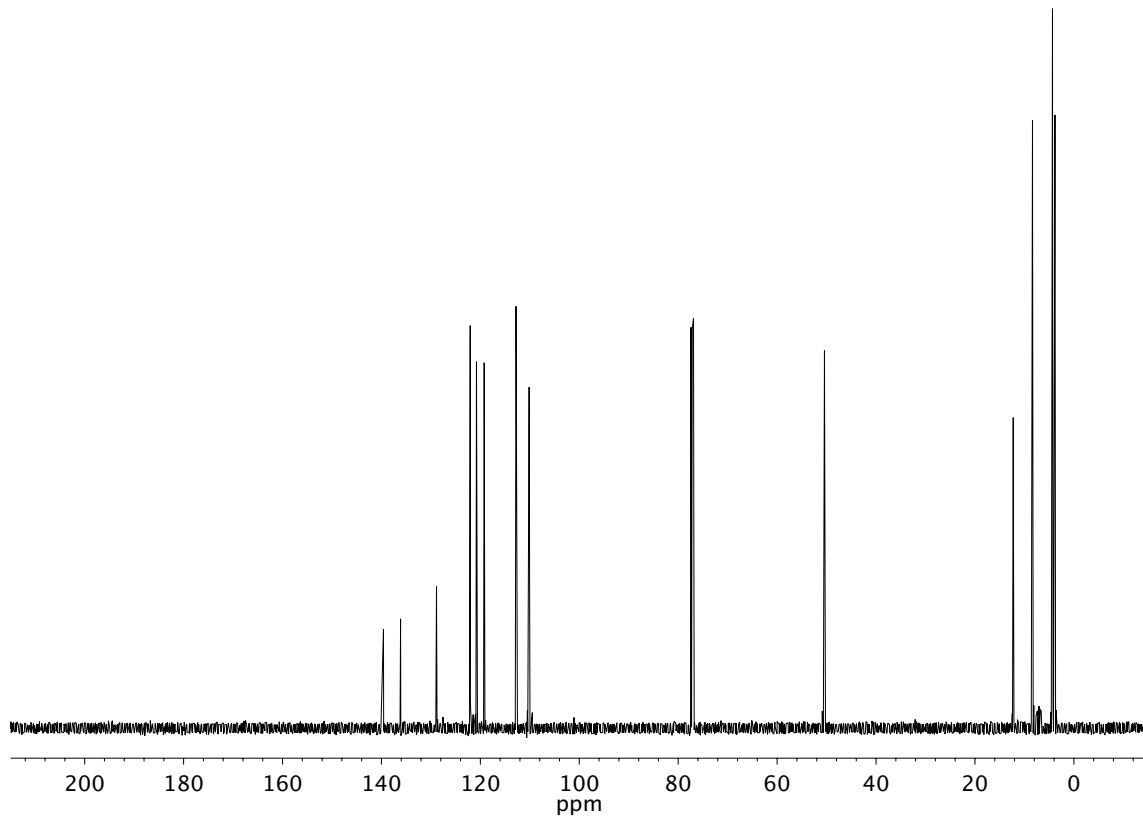


Figure A1.18. ^{13}C NMR (125 MHz, CDCl_3) of compound **124**.

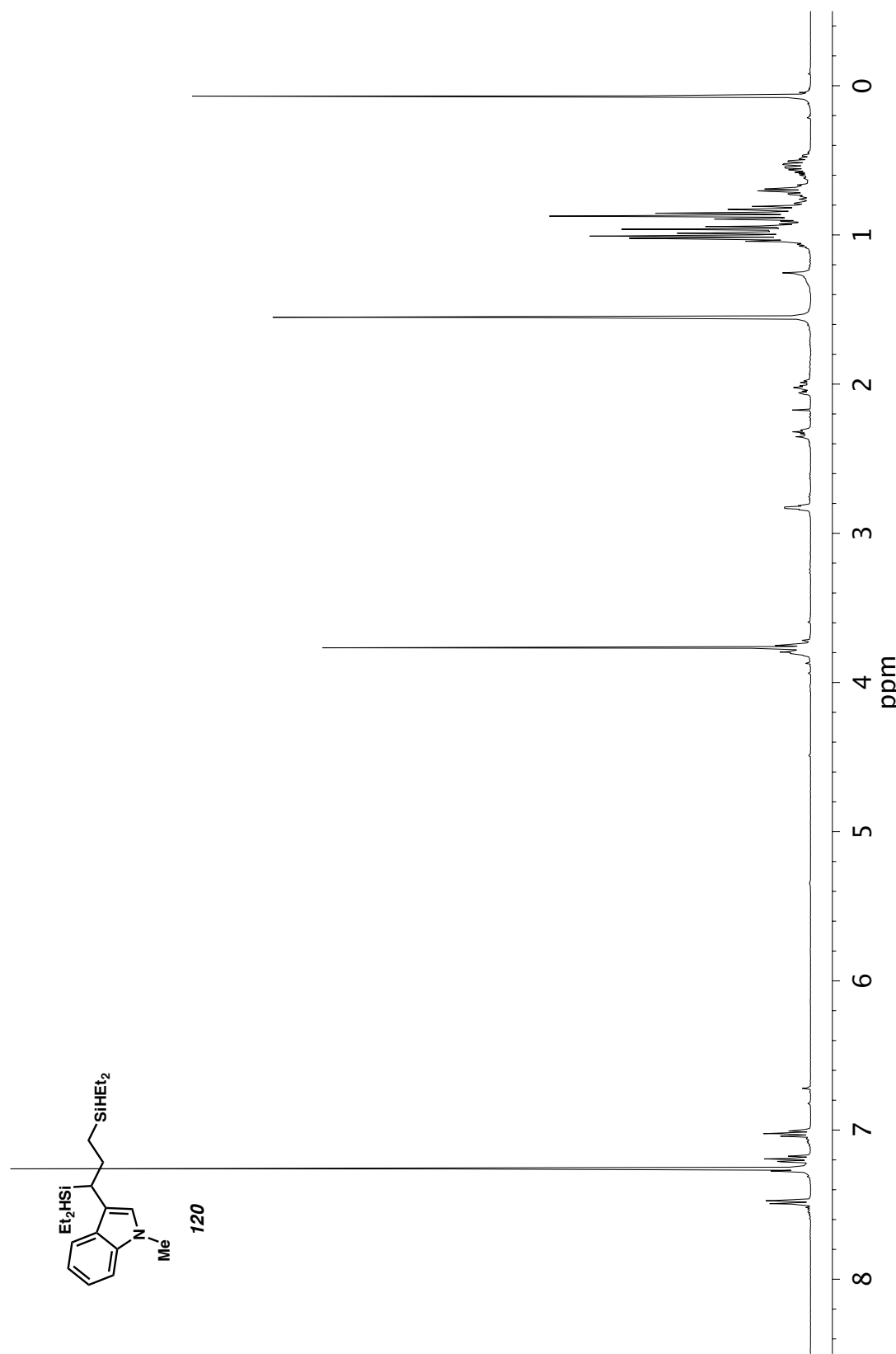


Figure A1.19. ^1H NMR (500 MHz, CDCl_3) of compound 120.

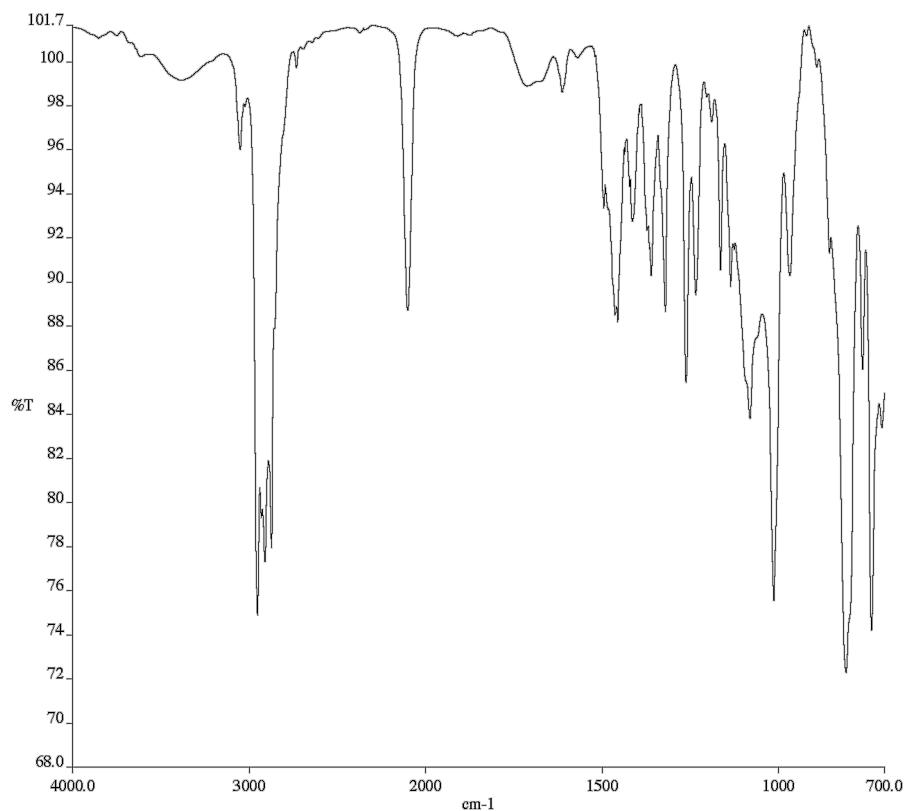


Figure A1.20. Infrared spectrum (Thin Film, NaCl) of compound **120**.

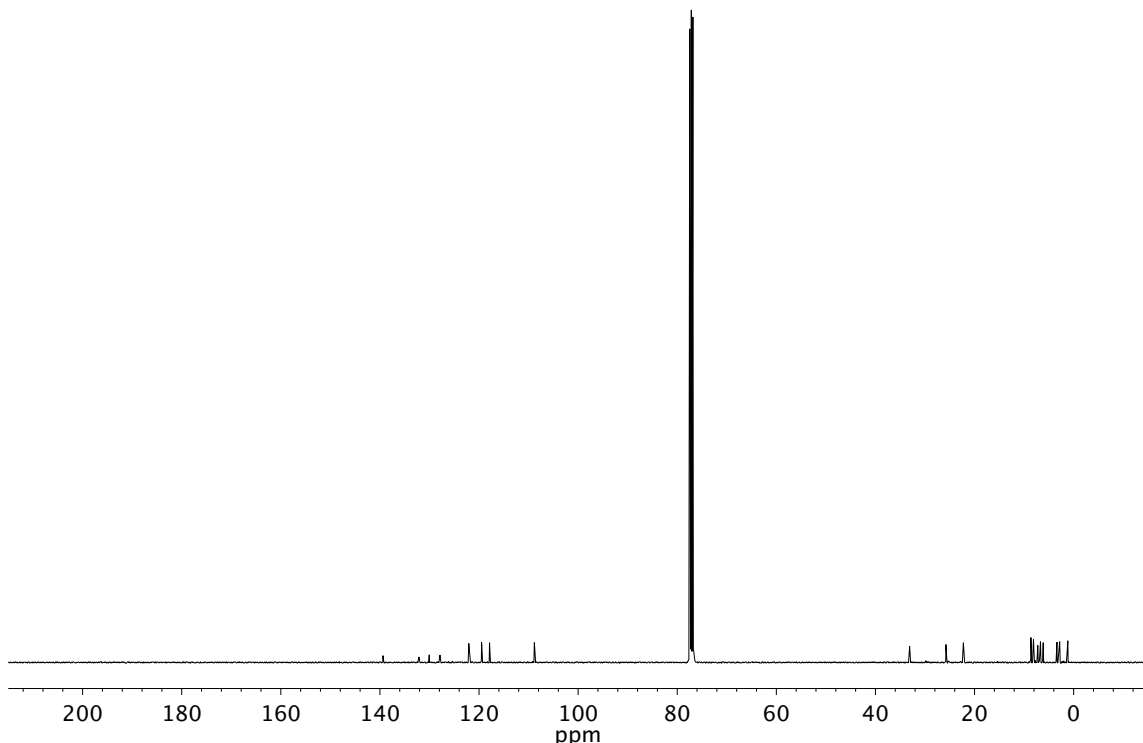


Figure A1.21. ¹³C NMR (125 MHz, CDCl₃) of compound **120**.

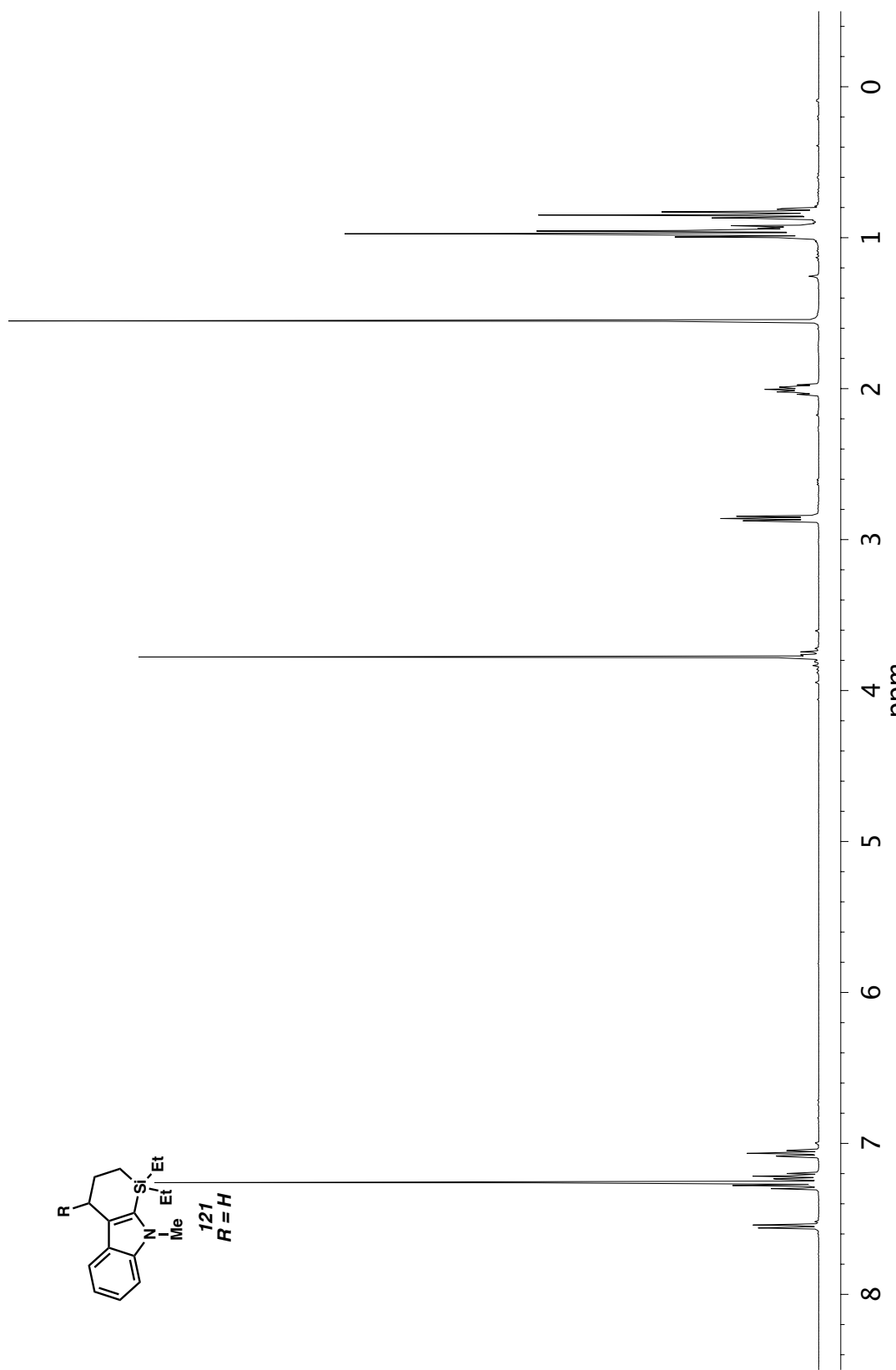


Figure A1.22. ^1H NMR (400 MHz, CDCl_3) of compound 121, $\text{R} = \text{H}$.

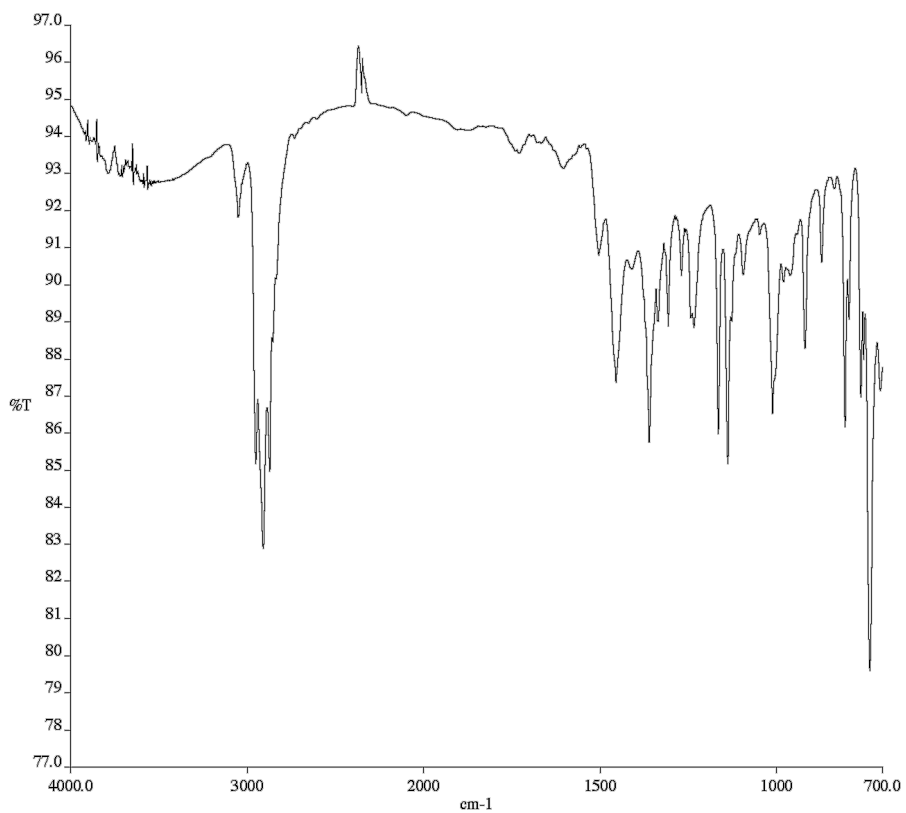


Figure A1.23. Infrared spectrum (Thin Film, NaCl) of compound **121**, $\mathbf{R} = \mathbf{H}$.

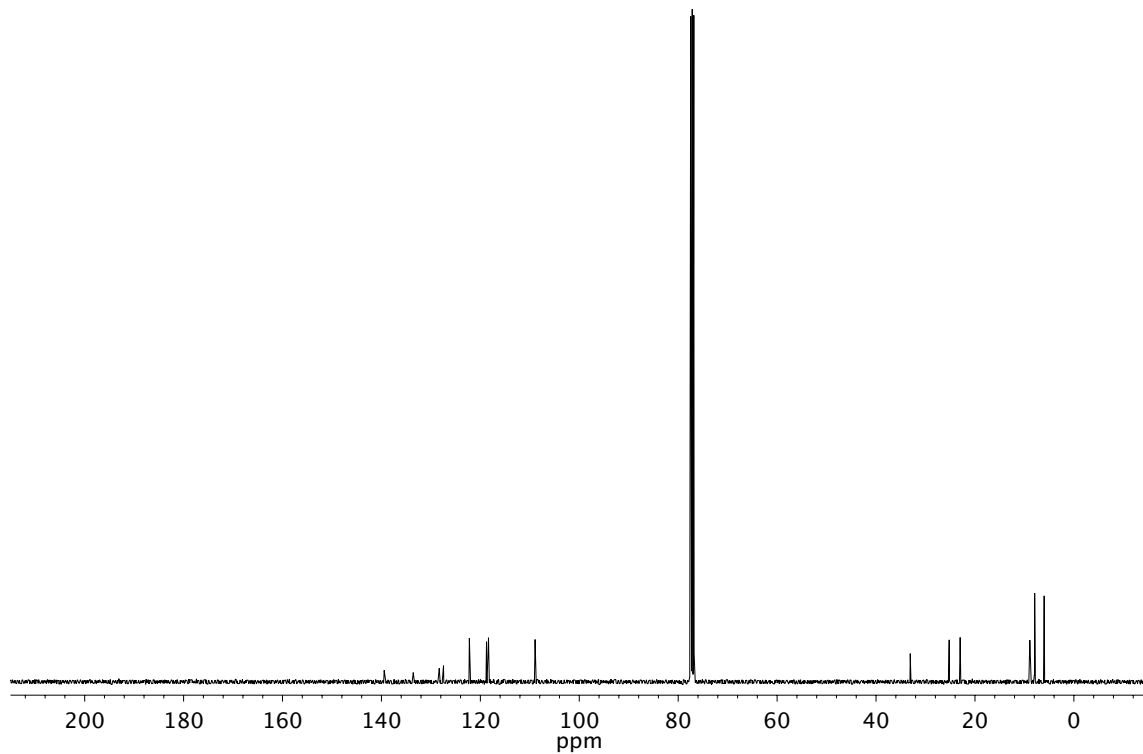


Figure A1.24. ^{13}C NMR (101 MHz, CDCl_3) of compound **121**, $\mathbf{R} = \mathbf{H}$.

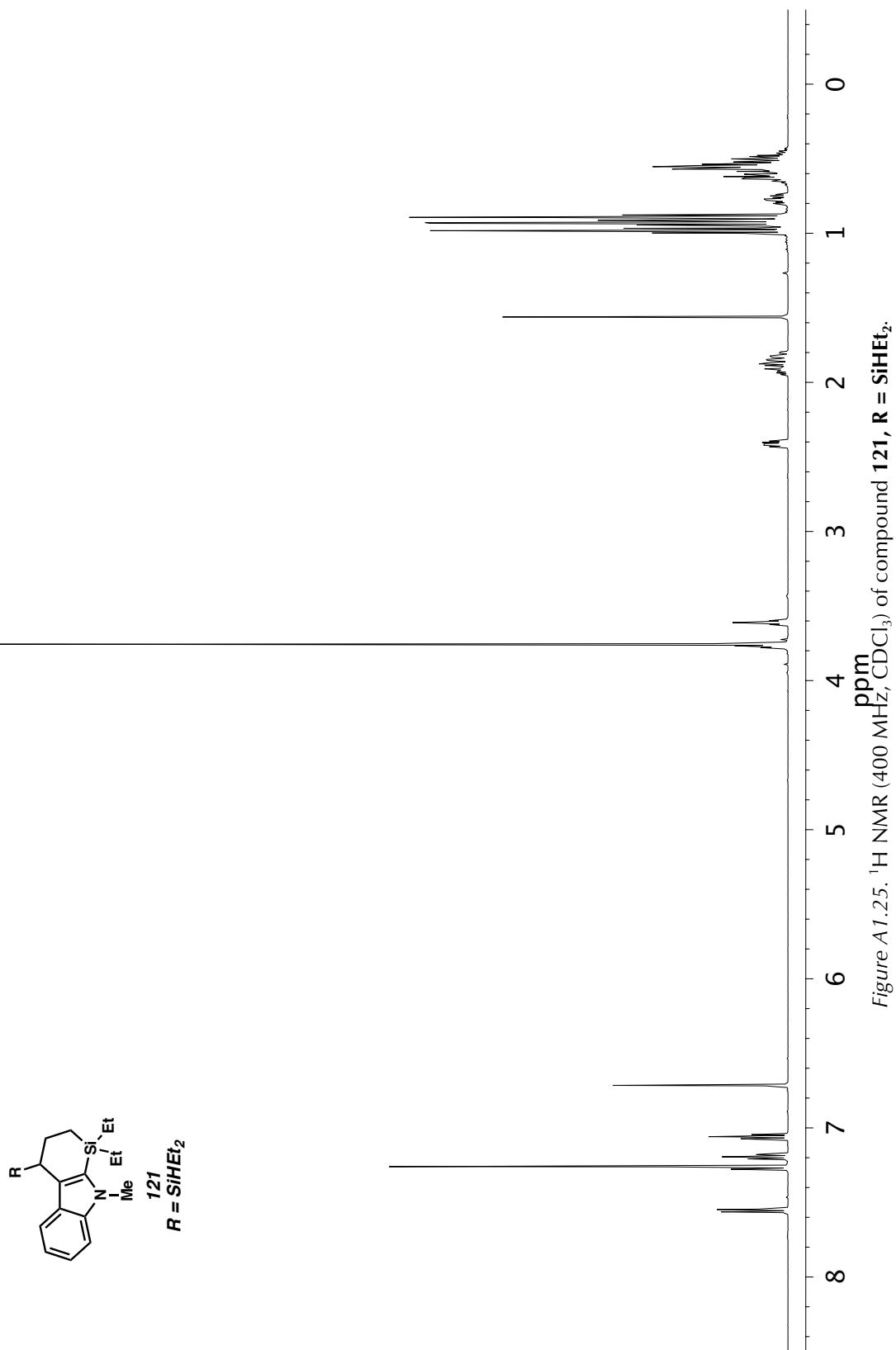


Figure A1.25. ^1H NMR (400 MHz, CDCl_3) of compound 121, $\text{R} = \text{SiHEt}_2$.

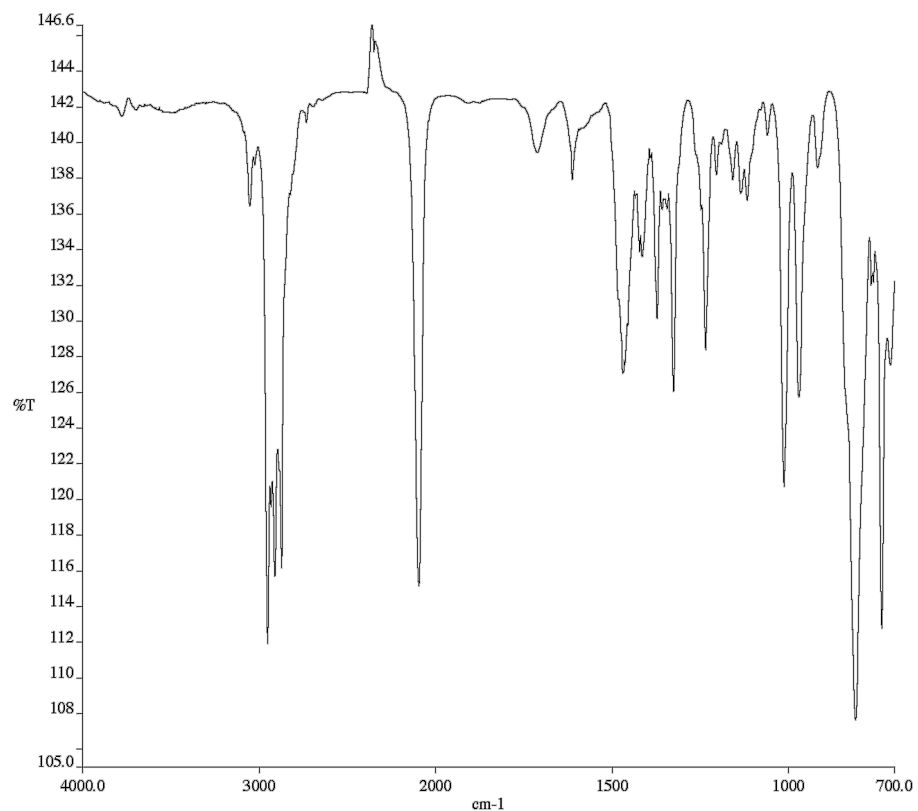


Figure A1.26. Infrared spectrum (Thin Film, NaCl) of compound **121**, $\mathbf{R} = \mathbf{SiHEt}_2$.

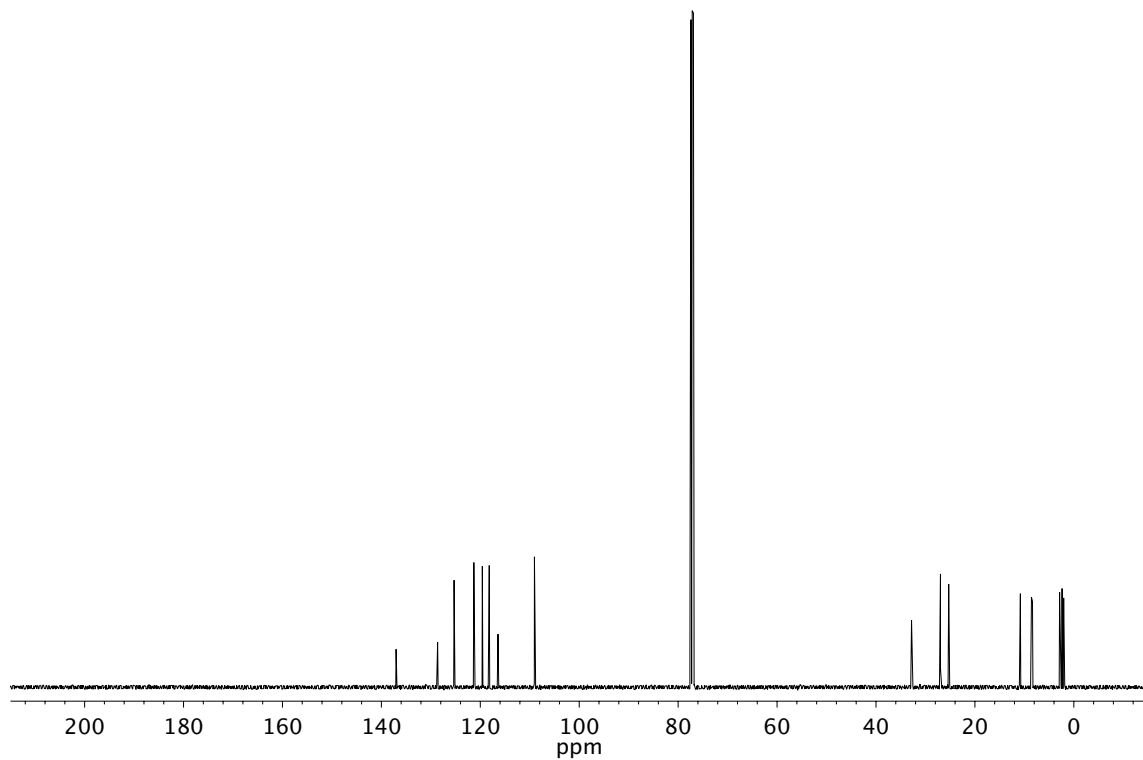


Figure A1.27. ^{13}C NMR (101 MHz, CDCl_3) of compound **121**, $\mathbf{R} = \mathbf{SiHEt}_2$.

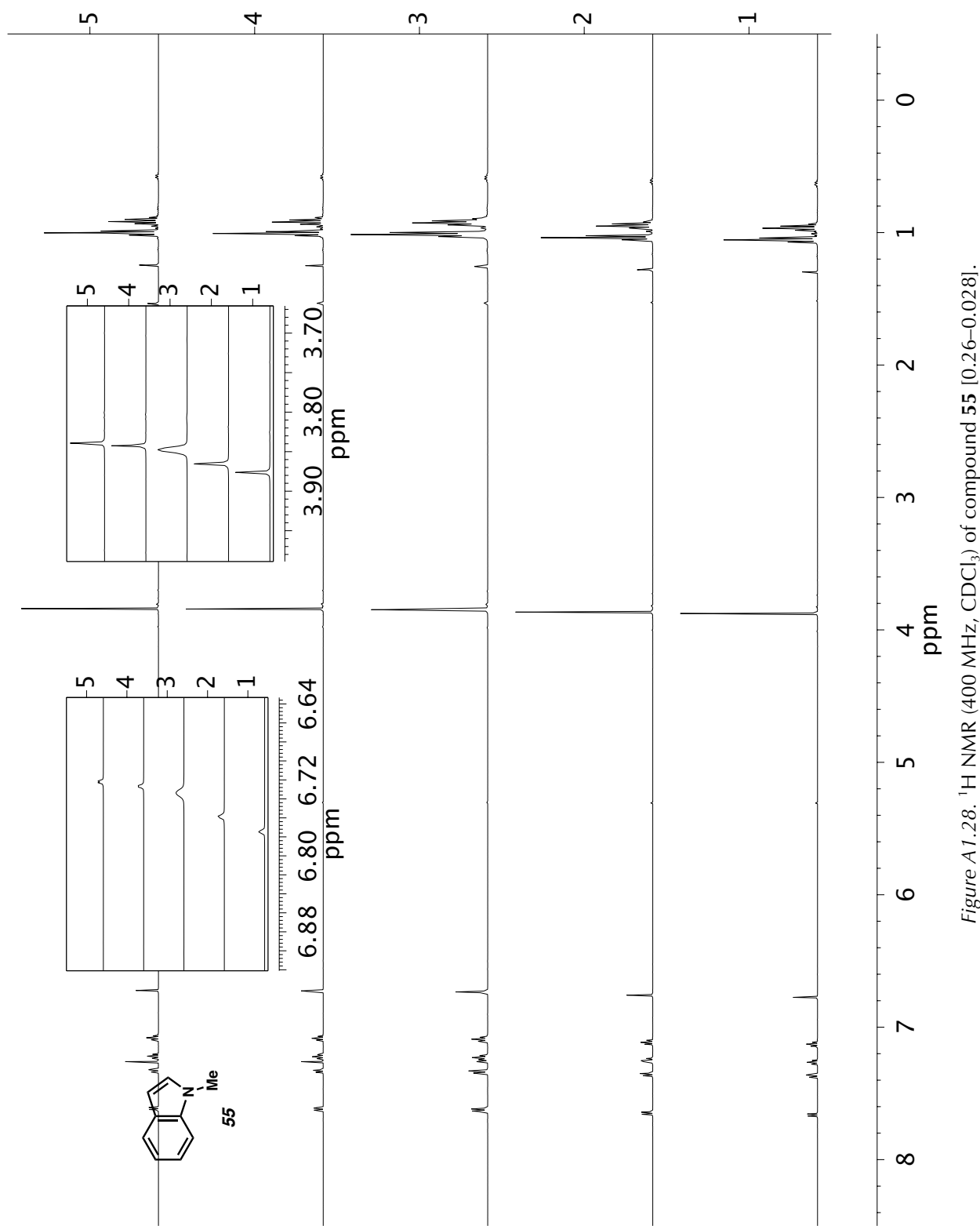


Figure A1.28. ^1H NMR (400 MHz, CDCl_3) of compound 55 [0.26–0.028].

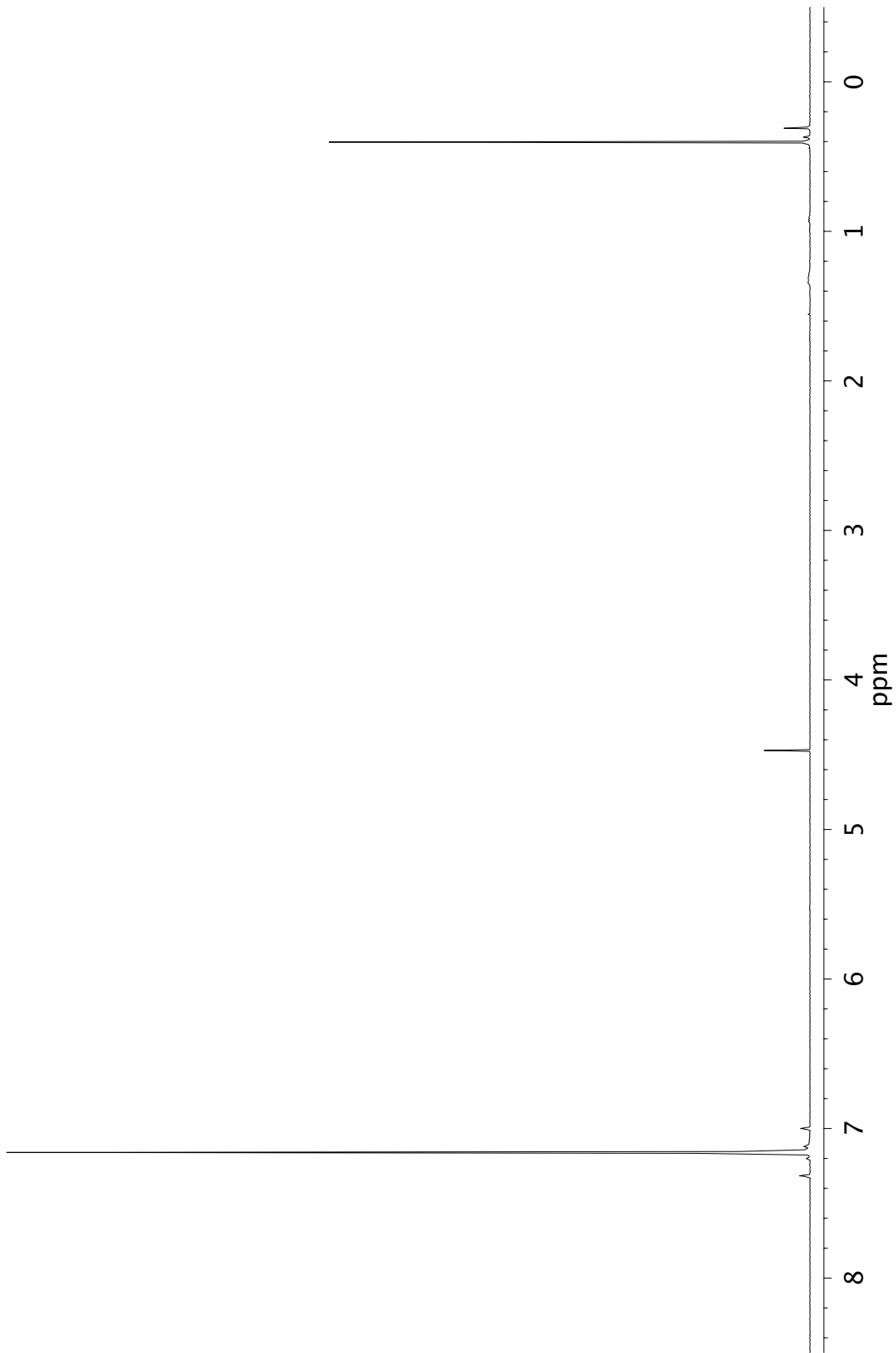


Figure A1.29 ^1H NMR (400 MHz, C_6D_6) of collected H_2 gas.

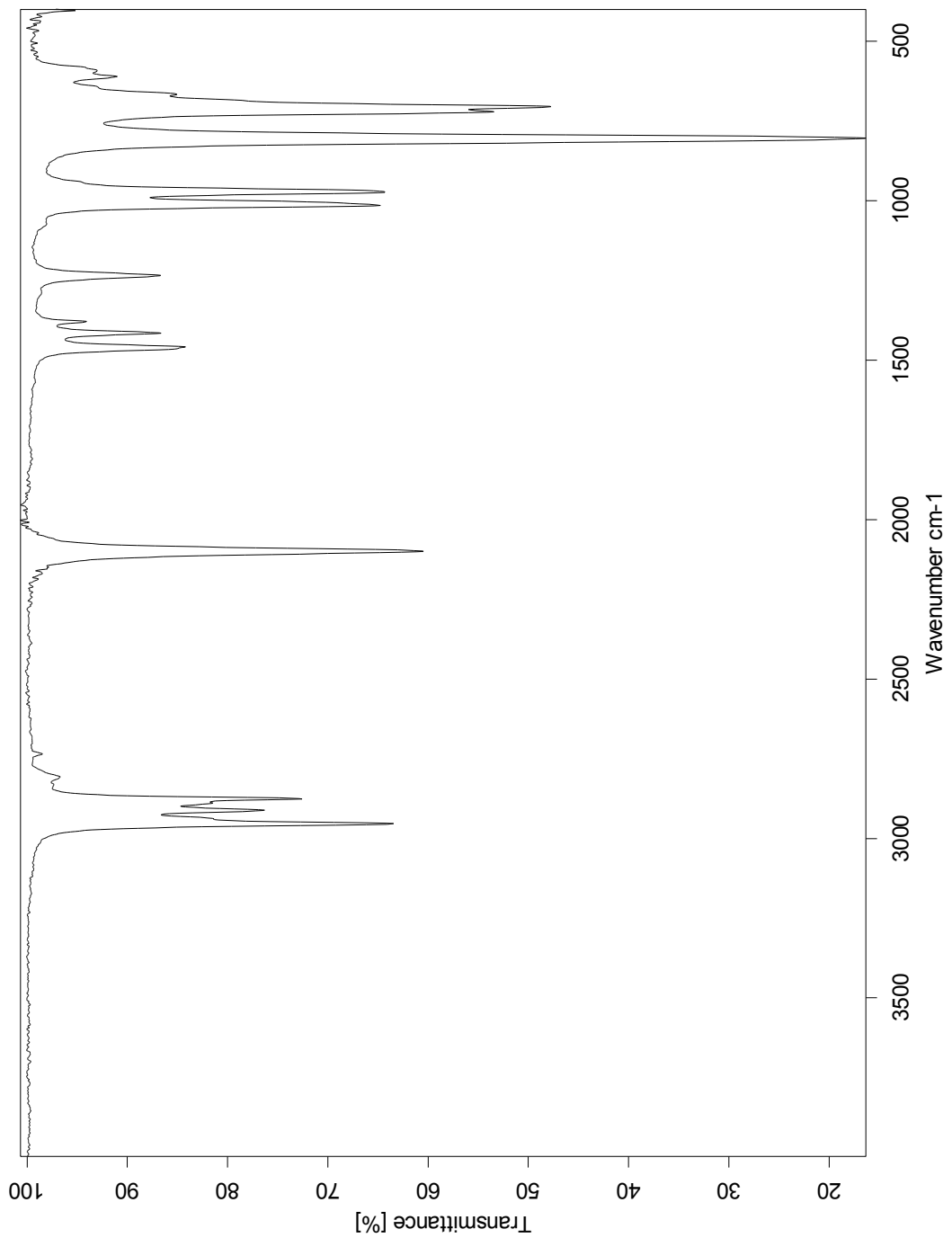


Figure A1.30. ATR-IR of Et_3SiH .

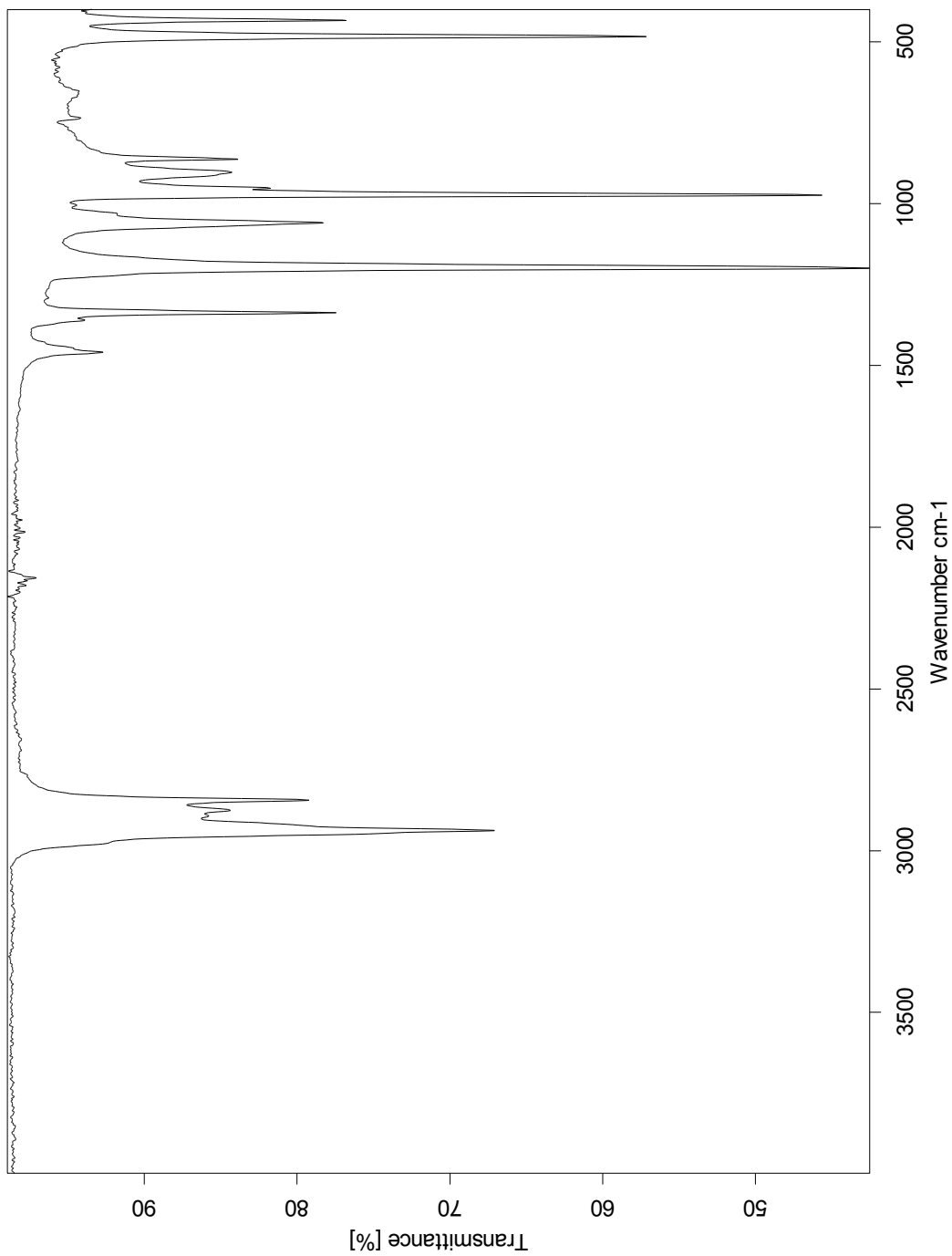


Figure A1.31. ATR-IR of $\text{KO}t\text{-Bu}$.

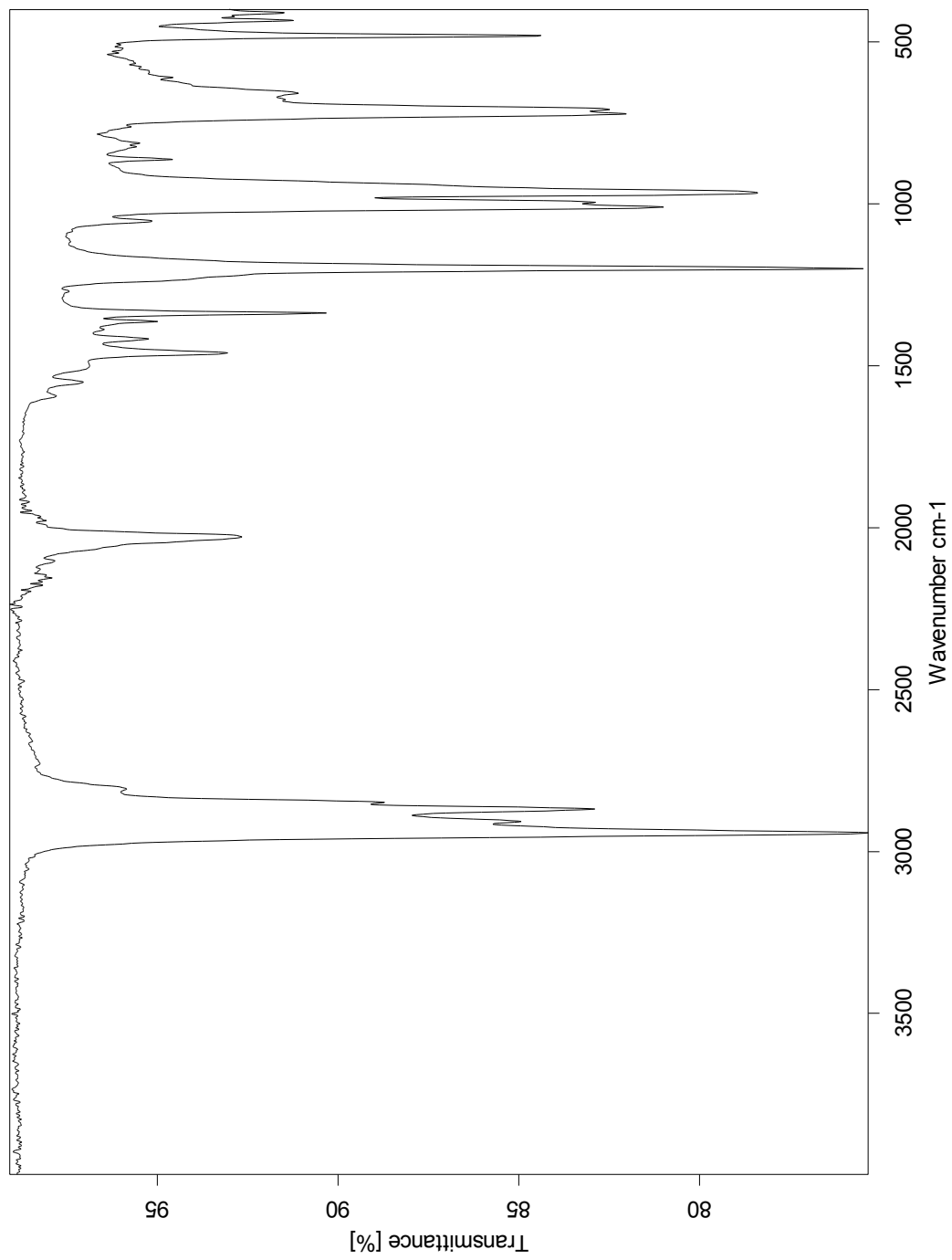


Figure A1.32. ATR-IR of KOt-Bu and Et_3SiH .

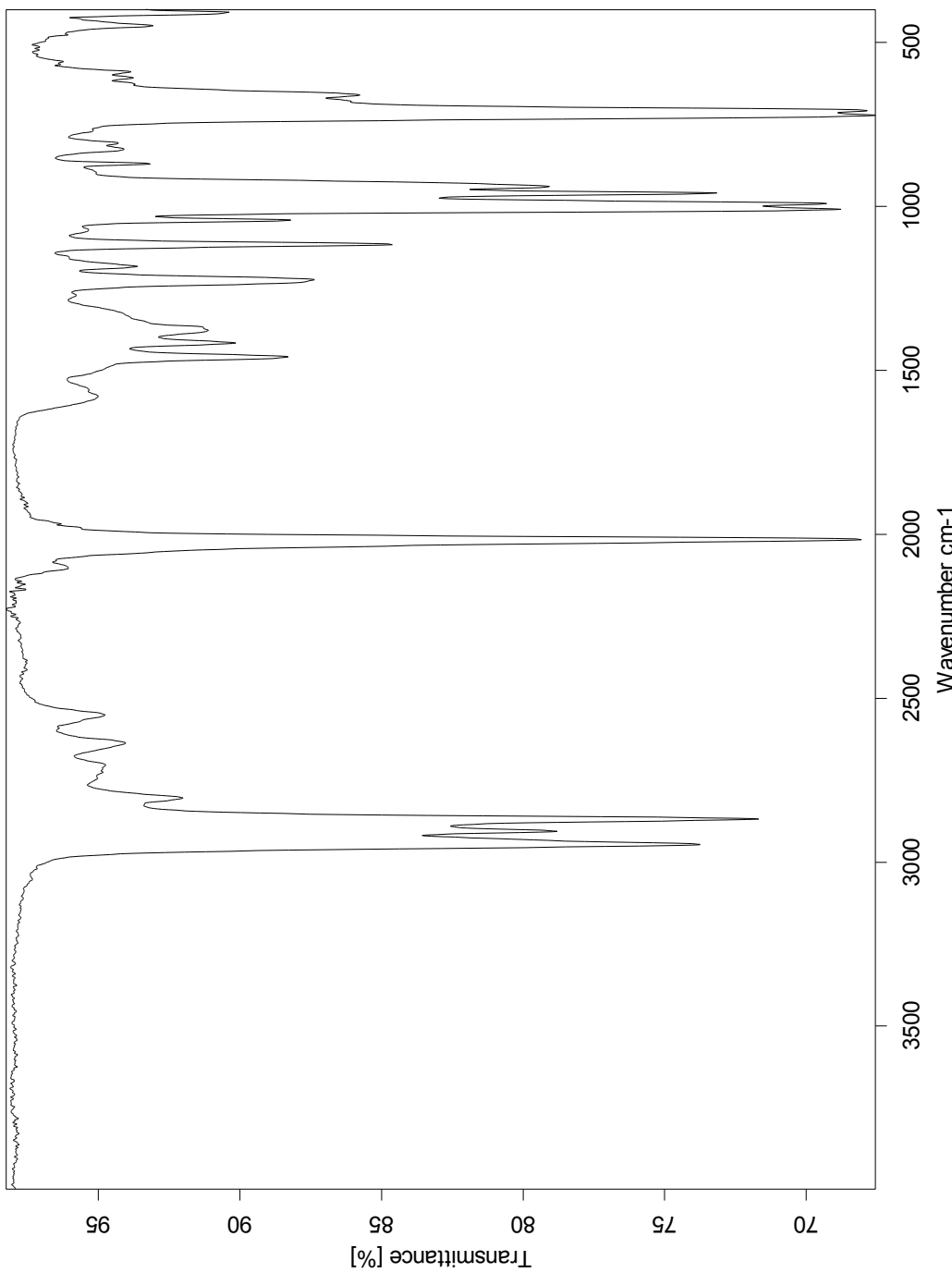


Figure A1.33. ATR-IR of KOEt and Et_3SiH .

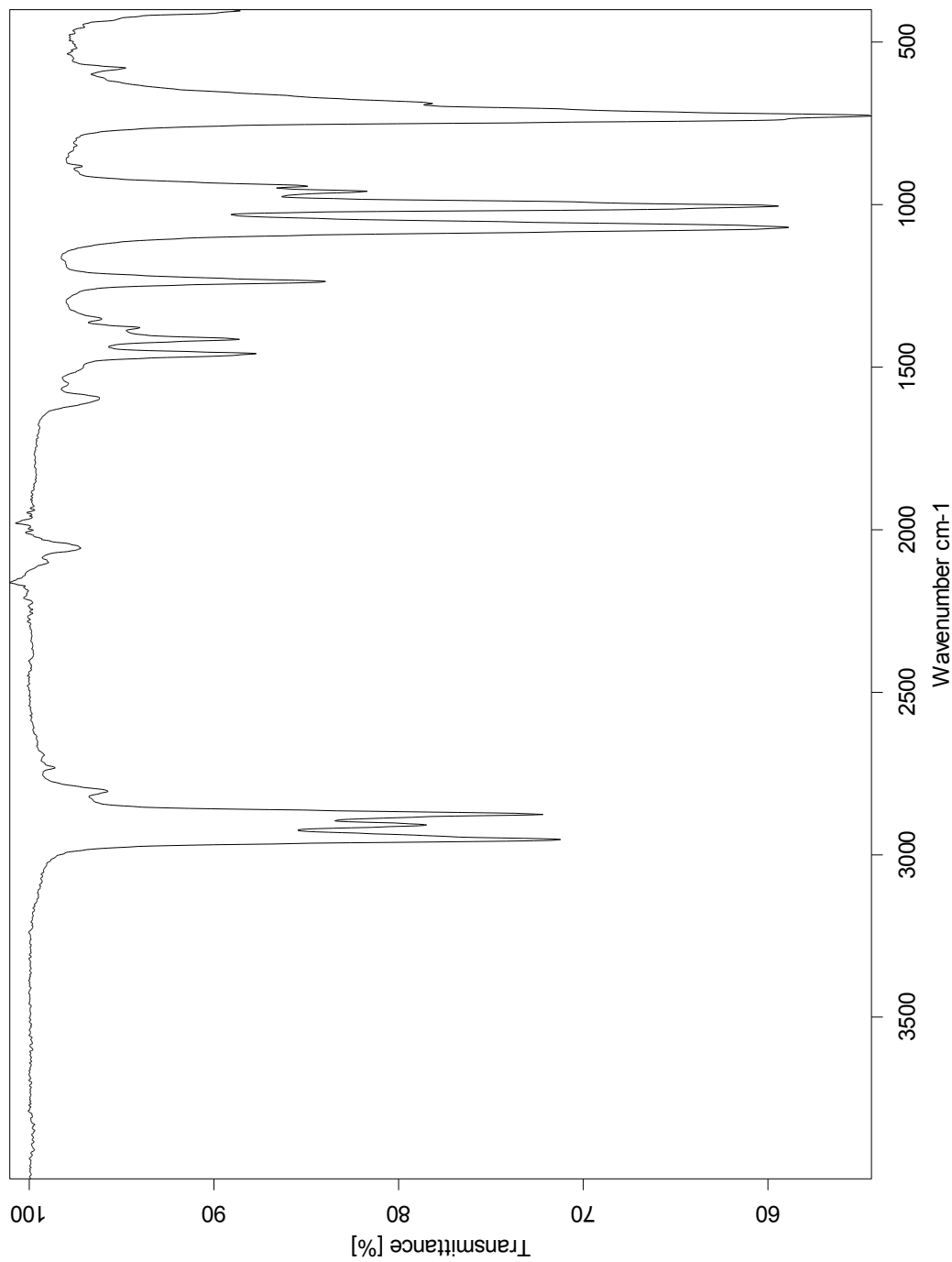


Figure A1.34. ATR-IR of KOMe and Et_3SiH .

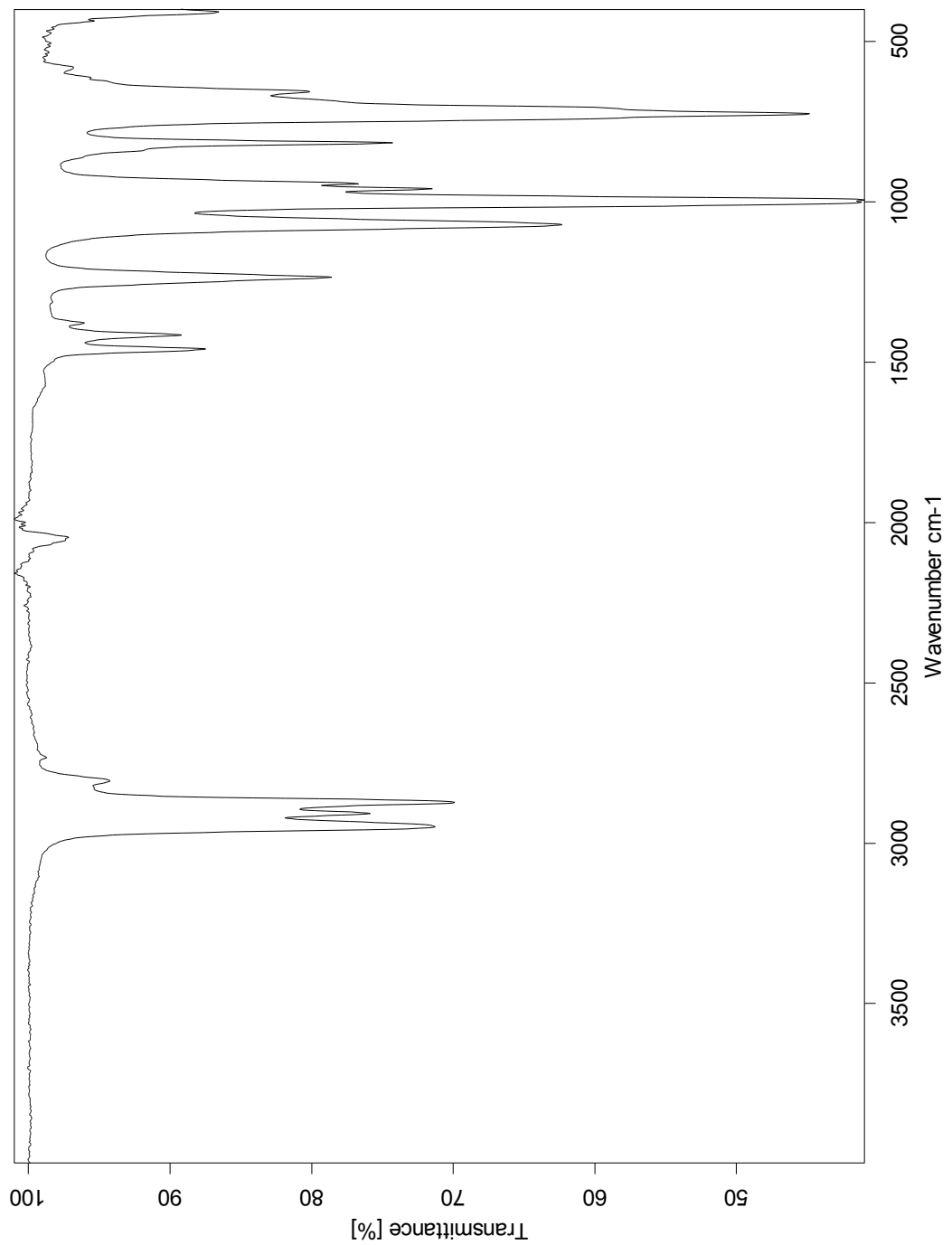


Figure A1.35. ATR-IR of KOTMS and Et_3SiH .

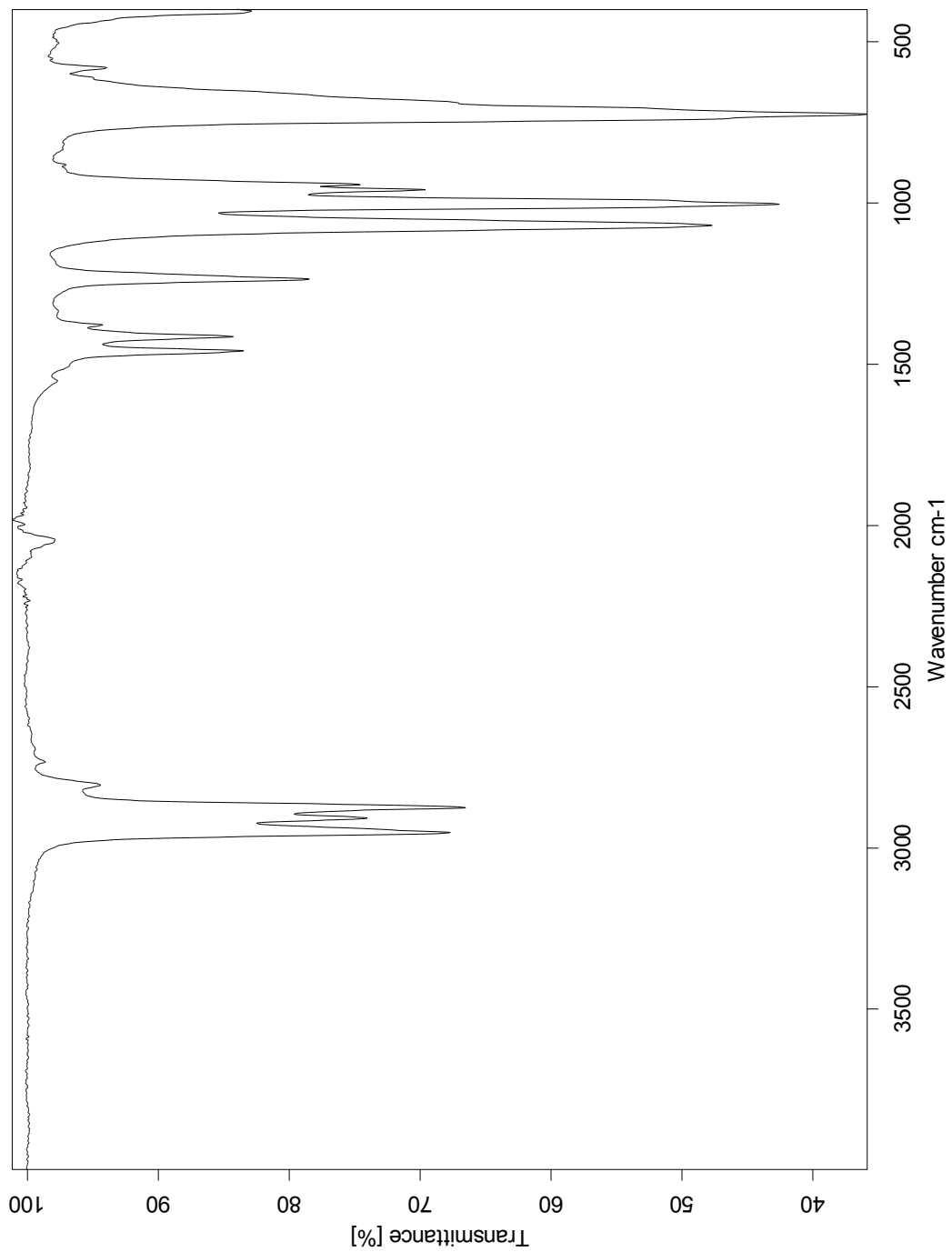


Figure A1.36. ATR-IR of KOH and Et_3SiH .

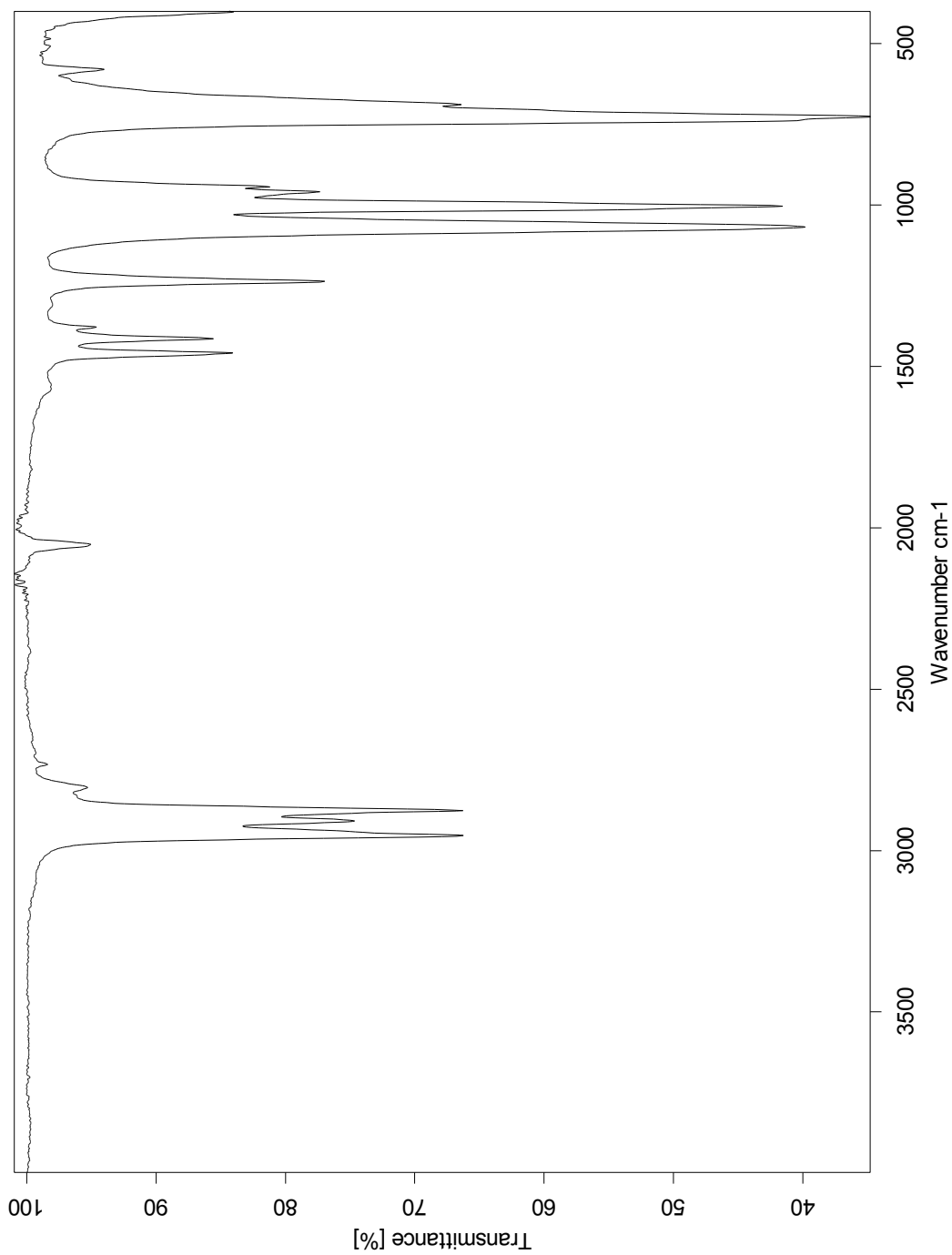


Figure A1.37. ATR-IR of RbOH•xH₂O and Et₃SiH.

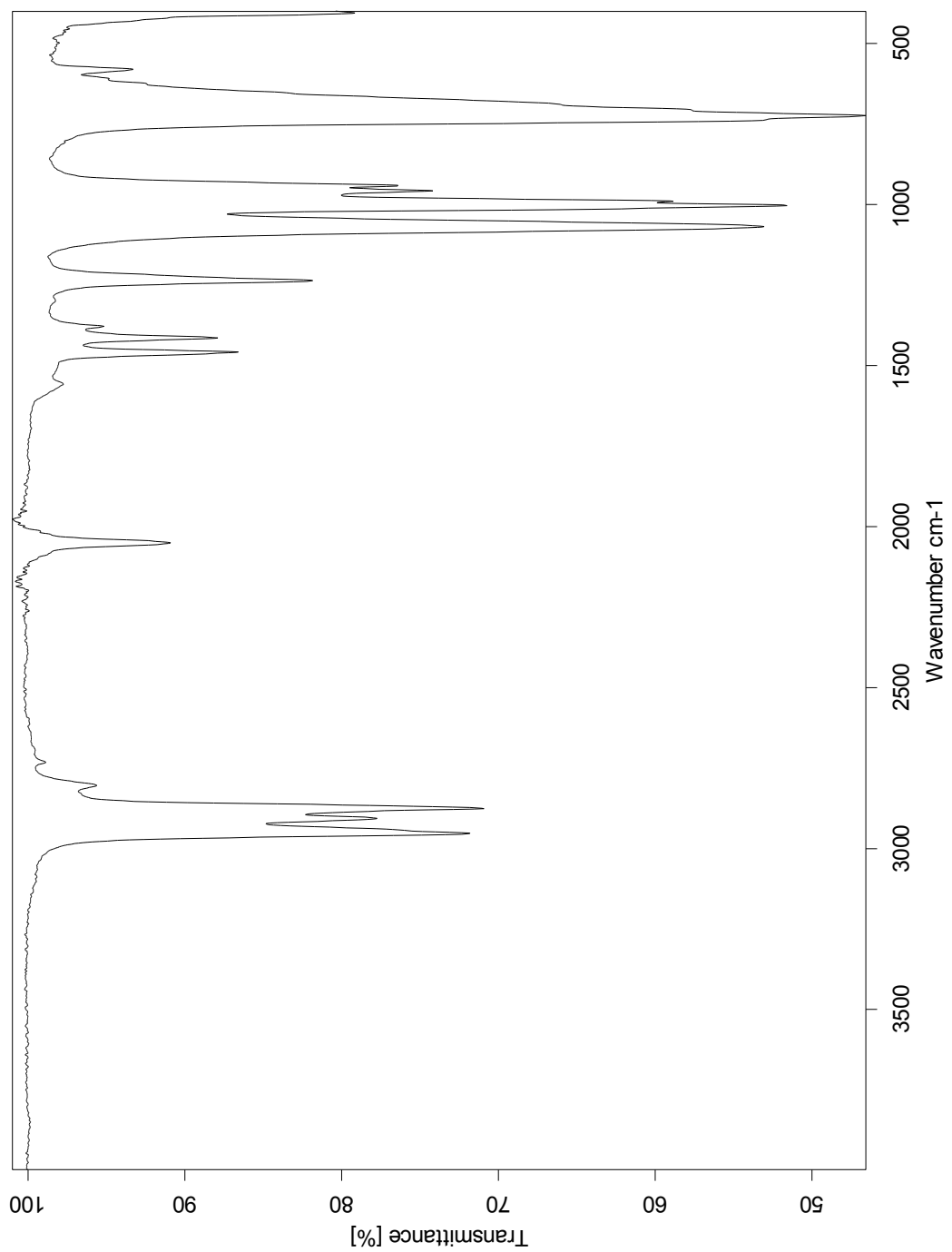


Figure A1.38. ATR-IR of $\text{CsOH}\bullet\text{xH}_2\text{O}$ and Et_3SiH .

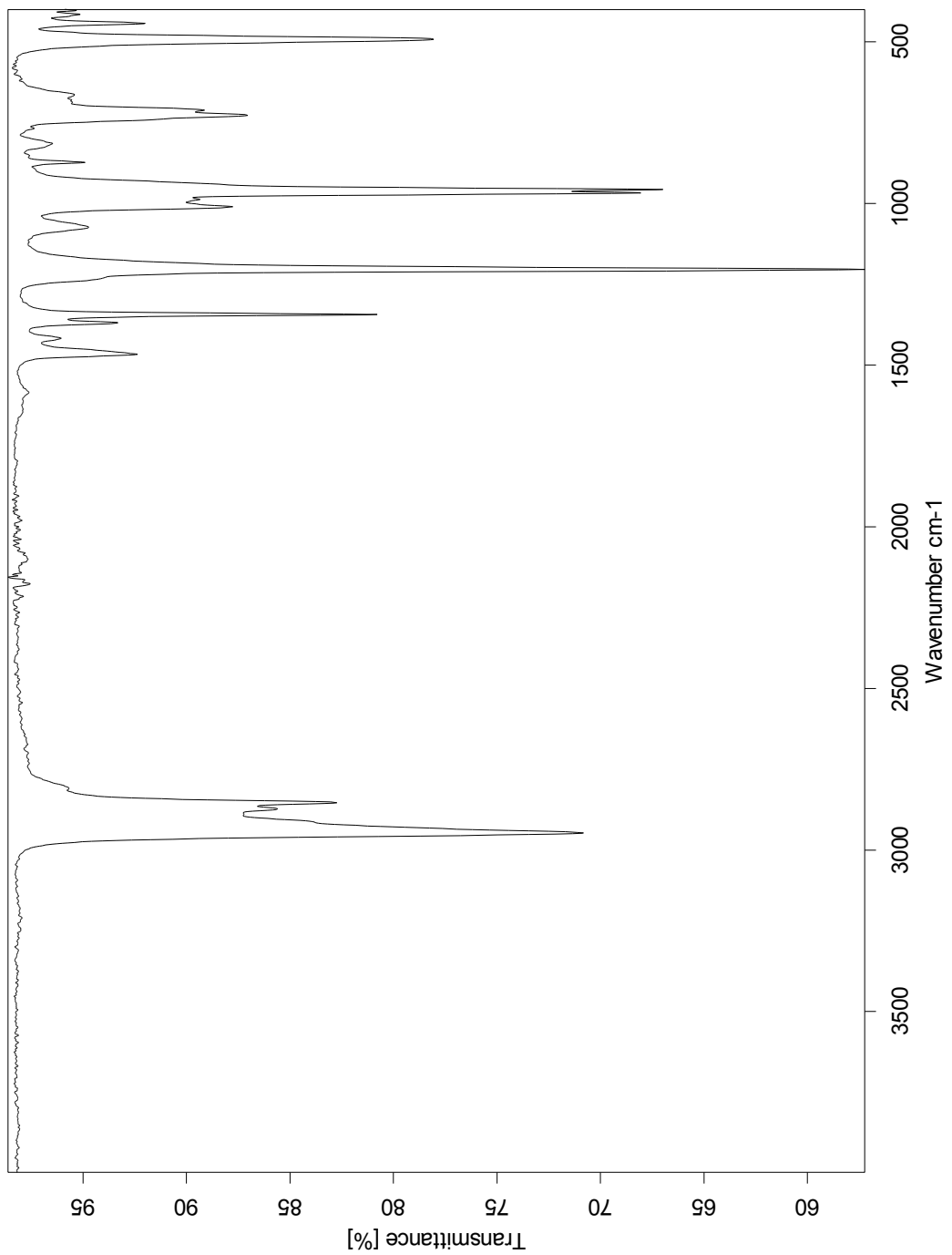


Figure A1.39. ATR-IR of NaOt-Bu and Et_3SiH .

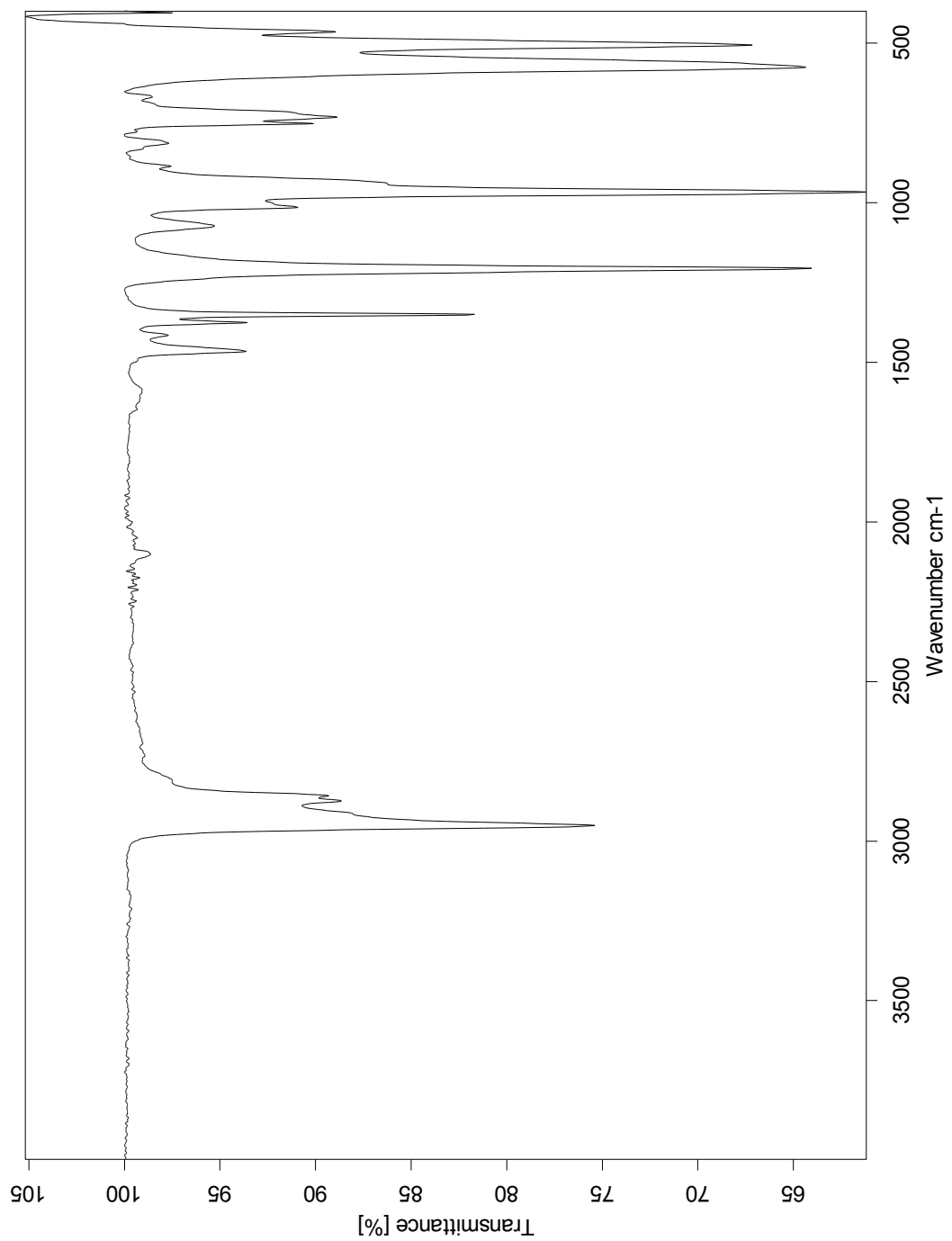


Figure A1.40. ATR-IR of LiOt-Bu and Et_3SiH .

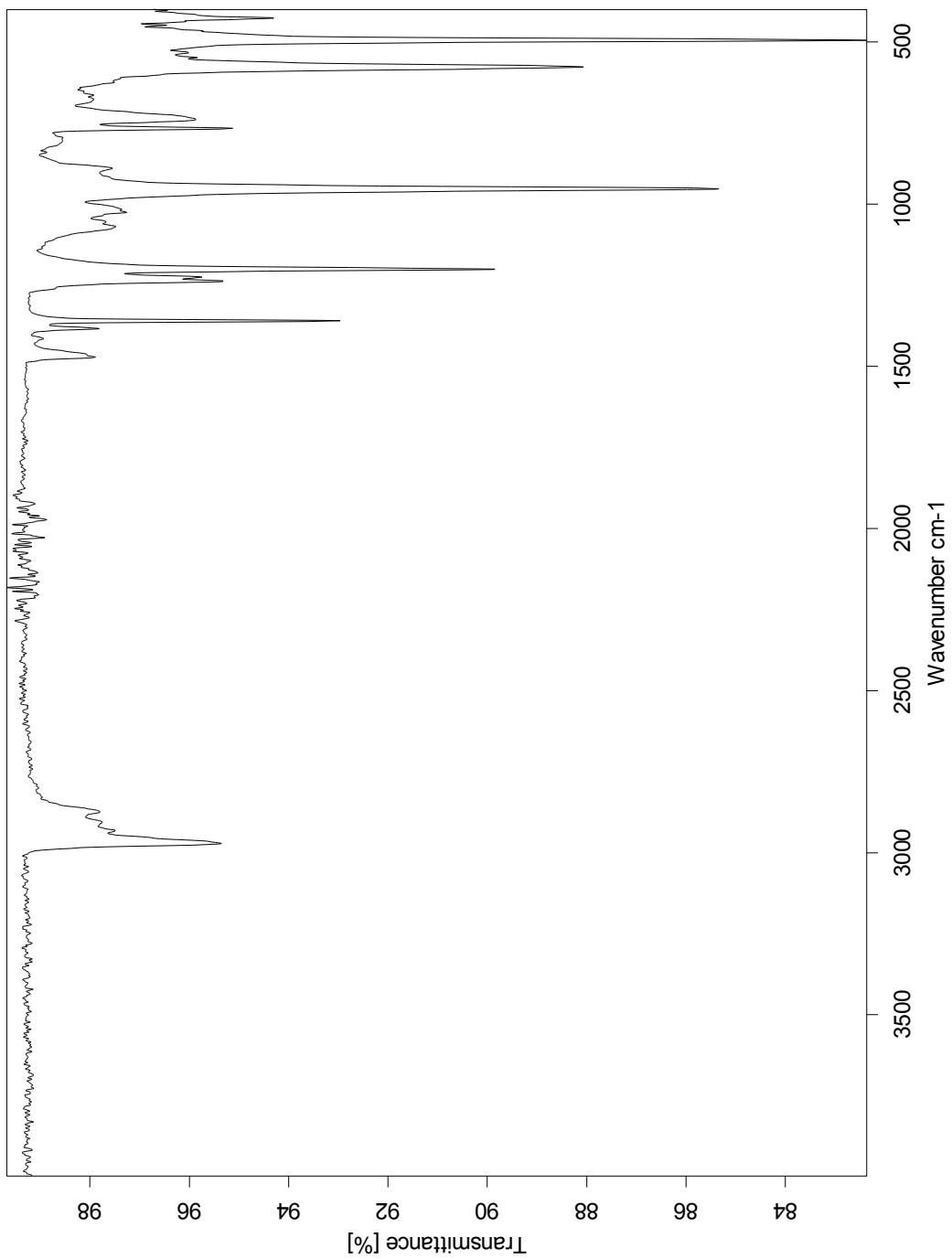


Figure A1.41. ATR-IR of $\text{Mg}(\text{Ot-Bu})_2$ and Et_3SiH .

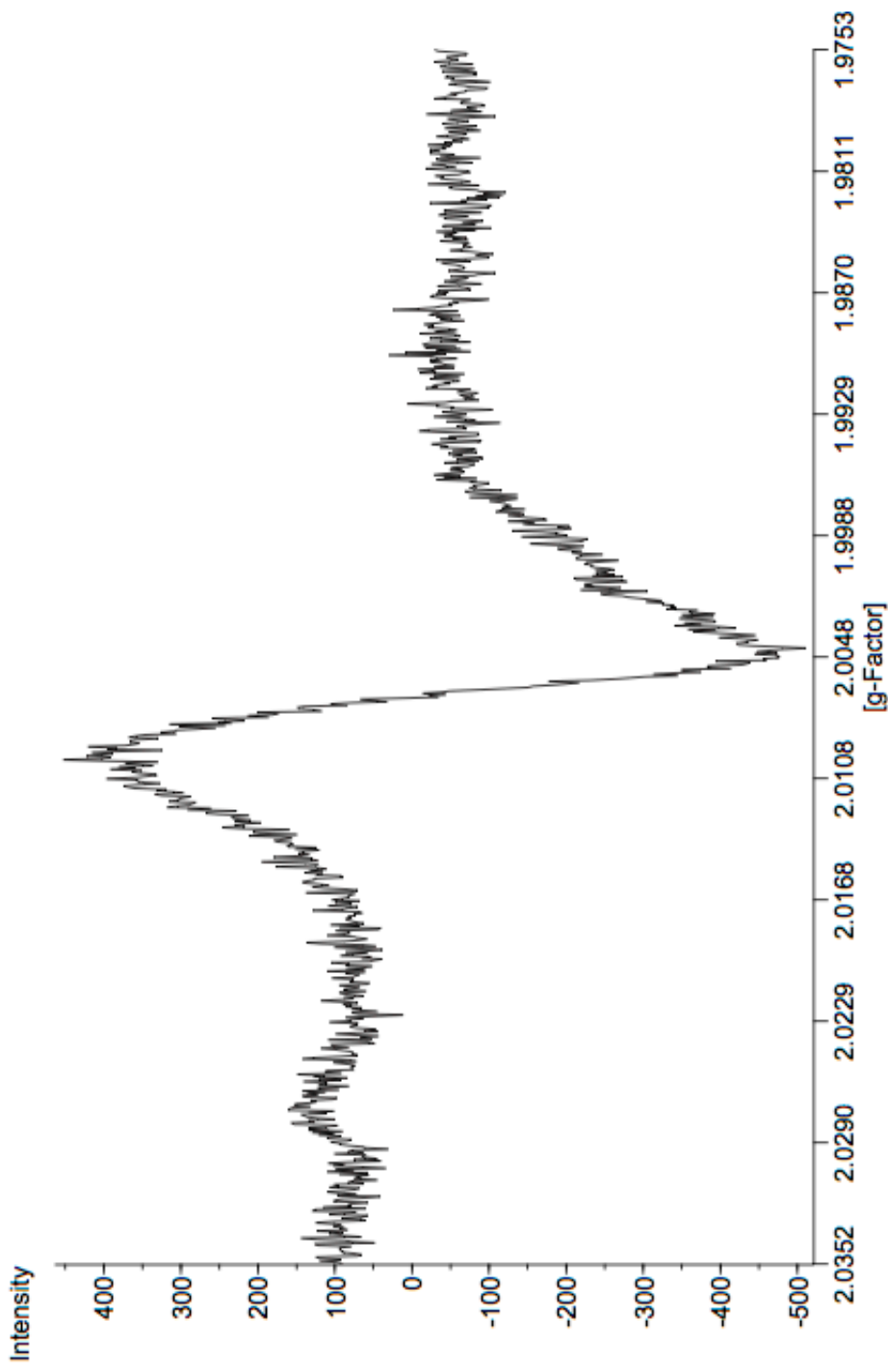


Figure A1.42. EPR of $\text{KOt}\text{-Bu}$ and Et_3SiH .

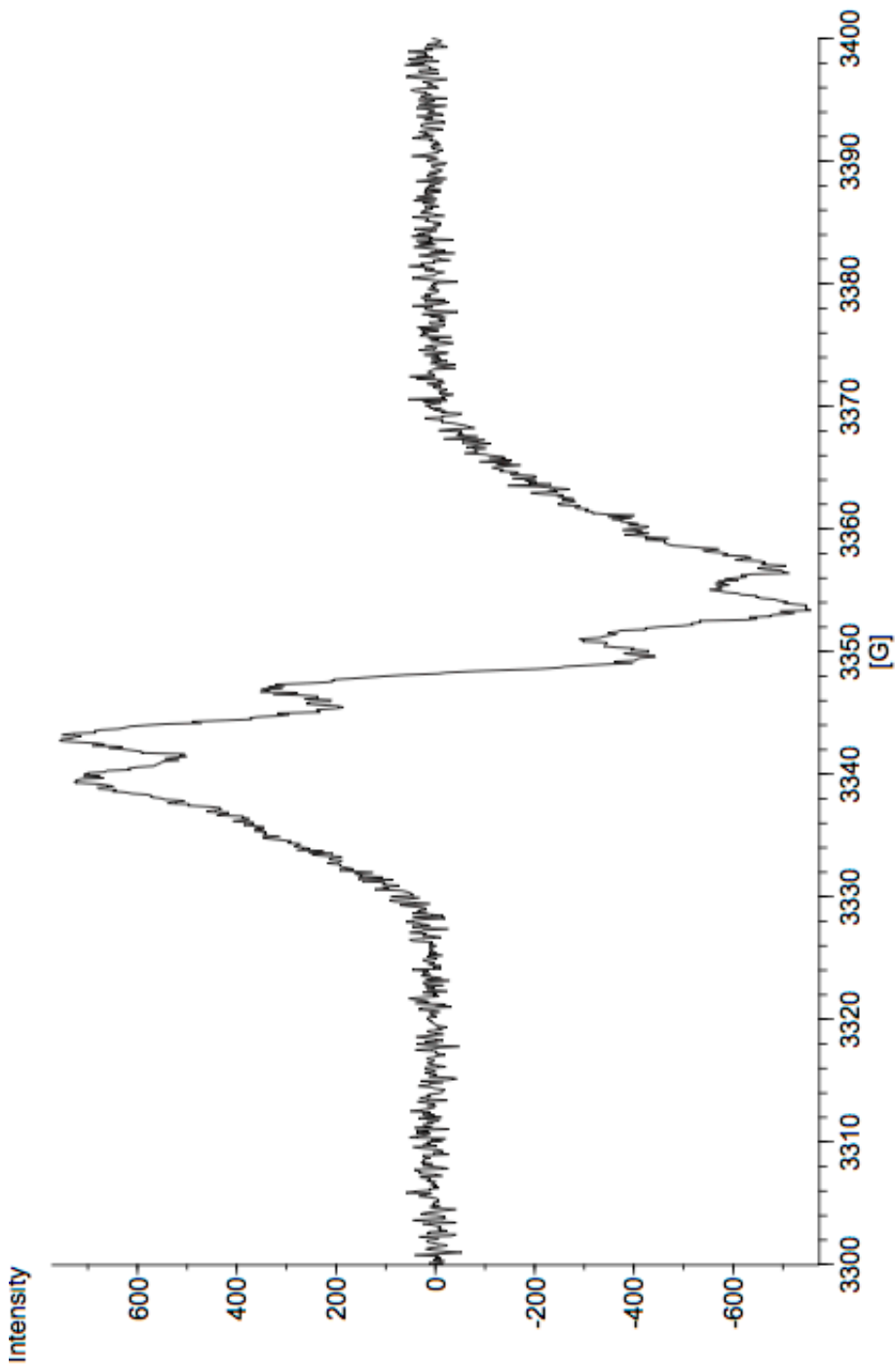


Figure A1.43. EPR of compound 55, KOt-Bu , and Et_3SiH .

APPENDIX 2

*Computational Details Relevant to Chapter 2:
A Combined Experimental and Computational Mechanistic Study of
the KOt-Bu-Catalyzed Dehydrogenative C–H Silylation of Aromatic
Heterocycles*

A2.1 GENERAL PARAMETERS

All the calculations were carried out with Gaussian 09.¹ Geometry optimization and energy calculations were performed with the B3LYP method² using the 6-31G(d) basis set³ for all atom. Frequency analysis verified that the stationary points were minima or first-order saddle points. Single point energies were calculated at the M06-2X⁴/6-311+G(d,p) level with solvent effects (solvent = THF) modeled using the CPCM⁵ solvation model. Gibbs free energies in THF at 298.15 K were calculated by adding the thermochemical quantities derived from the B3LYP frequency calculation to the M06-2X solution-phase electronic potential energy. Computed structures are illustrated using CYLVIEW.⁶

A2.1.1 Computational Values to Chapter 2

Zero-point correction (ZPE), thermal correction to energy (ΔE), thermal correction to enthalpy (ΔH), thermal correction to Gibbs free energy (ΔG), energies (E), enthalpies (H), and Gibbs free energies (G) (in Hartree) of the structures calculated at the M06-2X/6-311+G(d,p)-CPCM(THF)//B3LYP/6-31G(d) level of theory.

Structures	ZPE	ΔE	ΔH	ΔG	E	H	G	Imaginary Frequency
KOt-Bu	0.123876	0.13225	0.133194	0.089516	-833.005741	-832.872547	-832.916225	—
[KOt-Bu] ₂	0.248731	0.267161	0.268105	0.197204	-1666.044513	-1665.776408	-1665.847309	—
[KOt-Bu] ₃	0.373819	0.402210	0.403154	0.308232	-2499.076483	-2498.673329	-2498.768251	—
[KOt-Bu] ₄	0.498948	0.537092	0.538036	0.423883	-3332.132729	-3331.594693	-3331.708846	—
NaOt-Bu	0.124504	0.132747	0.133691	0.091144	-395.346359	-395.212668	-395.255215	—
[NaOt-Bu] ₂	0.250728	0.268441	0.269385	0.201573	-790.735054	-790.465669	-790.533481	—
[NaOt-Bu] ₃	0.376694	0.404037	0.404981	0.314435	-1186.1147	-1185.709722	-1185.800268	—
[NaOt-Bu] ₄	0.503381	0.539676	0.540621	0.432343	-1581.528698	-1580.988077	-1581.096355	—
[KOt-Bu] ₃ K ⁺	0.376381	0.405929	0.406873	0.313063	-3098.96526	-3098.558385	-3098.652195	—
t-BuO ⁻	0.120285	0.126780	0.127724	0.091493	-233.106915	-232.979191	-233.015422	—
K ⁺	0.000000	0.001416	0.00236	-0.015176	-599.852623	-599.850263	-599.867799	—
O ₂	0.003779	0.006142	0.007086	-0.016200	-150.307709	-150.300623	-150.323909	—
HSiMe ₃	0.119775	0.127259	0.128203	0.089443	-409.808109	-409.679906	-409.718666	—

Me₃Si'	0.110424	0.117885	0.118829	0.079221	-409.158688	-409.039859	-409.079467	—
H'	0.000000	0.001416	0.002360	-0.010654	-0.498155	-0.495795	-0.508809	—
H₂	0.010145	0.012505	0.013450	-0.001342	-1.168439	-1.154989	-1.169781	—
Me'	0.029833	0.032939	0.033883	0.011043	-39.821500	-39.787617	-39.810457	—
t-BuO'	0.123045	0.129569	0.130513	0.093490	-232.959433	-232.828920	-232.865943	—
t-BuOH	0.136186	0.142910	0.143854	0.107187	-233.635990	-233.492136	-233.528803	—
t-BuOSiMe₃	0.239087	0.253167	0.254111	0.199885	-642.300631	-642.046520	-642.100746	—
TS-172	0.240733	0.255166	0.256110	0.199354	-642.763935	-642.507825	-642.564581	-1030.485
KOO'	0.004256	0.007861	0.008805	-0.022582	-750.315795	-750.306990	-750.338377	—
[KOt-Bu]KOO'	0.129373	0.142803	0.143747	0.086220	-1583.351420	-1583.207673	-1583.265200	—
[KOt-Bu]₃KOO'(170)	0.379600	0.412799	0.413743	0.311278	-3249.440807	-3249.027064	-3249.129529	—
NaOO'	0.004544	0.007996	0.008940	-0.021306	-312.653761	-312.644821	-312.675067	—
[NaOtBu]NaOO'	0.130868	0.143717	0.144661	0.089114	-708.032569	-707.887908	-707.943455	—
[NaOtBu]₃NaOO'(171)	0.383031	0.414968	0.415912	0.314971	-1498.821038	-1498.405126	-1498.506067	—
[KOtBu]HSiMe₃	0.245120	0.262483	0.263428	0.197306	-1242.817802	-1242.554374	-1242.620496	—
TS, O₂ + HSiMe₃	0.121915	0.132160	0.133104	0.086788	-560.046427	-559.913323	-559.959639	-943.169
HOO'	0.014028	0.016885	0.017829	-0.008164	-150.895667	-150.877838	-150.903831	—
[t-BuOSiHMe₃]'	0.243120	0.257862	0.258806	0.203152	-642.926999	-642.668193	-642.723847	—
[t-BuOSiMe₃]''	0.233611	0.248473	0.249417	0.192055	-642.295269	-642.045852	-642.103214	—
[t-BuOSiMe₃]K'	0.239438	0.255819	0.256763	0.193442	-1242.210702	-1241.953939	-1242.017260	—
N-Me-Indole (55)	0.157986	0.166006	0.166950	0.124908	-403.061521	-402.894571	-402.936613	—
TS-178	0.268329	0.284870	0.285814	0.222742	-812.217393	-811.931579	-811.994651	-253.094
TS-179	0.267908	0.284619	0.285563	0.221708	-812.212867	-811.927304	-811.991159	-300.146
181	0.268657	0.285198	0.286142	0.223901	-812.246530	-811.960388	-812.022629	—
180	0.268799	0.285357	0.286301	0.224289	-812.241640	-811.955339	-812.017351	—
TS-186	0.764863	0.820531	0.821475	0.668871	-4144.369894	-4143.548419	-4143.701023	-1121.184
TS-187	0.765361	0.820865	0.821809	0.669650	-4144.362660	-4143.540851	-4143.693010	-1225.729
109	0.260259	0.276207	0.277151	0.217055	-811.697822	-811.420671	-811.480767	—
110	0.260073	0.276139	0.277083	0.216367	-811.700813	-811.423730	-811.484446	—
188	0.512625	0.550863	0.551807	0.436236	-3332.668520	-3332.116713	-3332.232284	—
195	0.110675	0.116254	0.117198	0.081661	-249.437401	-249.320203	-249.355740	—
TS-189 (195)	0.221151	0.235065	0.236009	0.179441	-658.591231	-658.355222	-658.411790	-264.932
TS-191 (195)	0.220598	0.234647	0.235591	0.178681	-658.583048	-658.347457	-658.404367	-331.395
189 (195)	0.221494	0.235260	0.236205	0.181283	-658.615251	-658.379046	-658.433968	—
191 (195)	0.221193	0.235214	0.236158	0.180305	-658.604356	-658.368198	-658.424051	—
TS-190 (195)	0.718142	0.770826	0.771770	0.627353	-3990.732654	-3989.960884	-3990.105301	-1438.218
TS-192(195)	0.718109	0.770941	0.771886	0.625561	-3990.722198	-3989.950312	-3990.096637	-1361.123
190 (195)	0.213232	0.226551	0.227495	0.173700	-658.074752	-657.847257	-657.901052	—
192(195)	0.212867	0.226375	0.227319	0.172588	-658.074938	-657.847619	-657.902350	—
194	0.070198	0.073914	0.074858	0.043925	-229.992411	-229.917553	-229.948486	—
TS-189 (194)	0.180415	0.192718	0.193662	0.139781	-639.146017	-638.952355	-639.006236	-272.557
TS-191 (194)	0.180140	0.192390	0.193334	0.140308	-639.140180	-638.946846	-638.999872	-336.416
189 (194)	0.180629	0.192870	0.193814	0.142004	-639.181256	-638.987442	-639.039252	—
191 (194)	0.181005	0.193196	0.194140	0.142344	-639.166998	-638.972858	-639.024654	—
TS-190 (194)	0.678186	0.729187	0.730131	0.587893	-3971.302116	-3970.571985	-3970.714223	-309.649

TS-192 (194)	0.677737	0.729040	0.729984	0.586542	-3971.286984	-3970.557000	-3970.700442	-1165.662
190 (194)	0.172284	0.183880	0.184824	0.134582	-638.630092	-638.445268	-638.495510	—
192 (194)	0.172511	0.184049	0.184993	0.134807	-638.630715	-638.445722	-638.495908	—
193	0.066891	0.070965	0.071909	0.039651	-552.971110	-552.899201	-552.931459	—
TS-189 (193)	0.177137	0.189897	0.190841	0.135876	-962.125143	-961.934302	-961.989267	-274.439
TS-191 (193)	0.177017	0.189742	0.190686	0.135822	-962.122093	-961.931407	-961.986271	-293.261
189 (193)	0.178025	0.190635	0.191579	0.138778	-962.167273	-961.975694	-962.028495	—
191 (193)	0.177542	0.190377	0.191322	0.137913	-962.149559	-961.958237	-962.011646	—
TS-190 (193)	0.675217	0.726765	0.727710	0.584657	-4294.296401	-4293.568691	-4293.711744	-768.651
TS-192 (193)	0.674758	0.726363	0.727307	0.584144	-4294.275331	-4293.548024	-4293.691187	-1235.687
190 (193)	0.169277	0.181245	0.182189	0.130654	-961.611436	-961.429247	-961.480782	—
192 (193)	0.169085	0.181057	0.182001	0.130709	-961.608367	-961.426366	-961.477658	—
TS-182	0.507360	0.540242	0.541186	0.439261	-1455.162461	-1454.621275	-1454.723200	-963.547
TS-183	0.507779	0.540433	0.541377	0.440999	-1455.153606	-1454.612229	-1454.712607	-1056.197
TS-190 (193), penta	0.459612	0.489892	0.490836	0.396170	-1301.521651	-1301.030815	-1301.125481	-720.947
TS-192 (193), penta	0.459901	0.490029	0.490973	0.396665	-1301.510882	-1301.019909	-1301.114217	-976.234
TS-190 (194), penta	0.418983	0.447738	0.448682	0.356704	-1282.089431	-1281.640749	-1281.732727	-699.318
TS-192 (194), penta	0.420032	0.448384	0.449328	0.358172	-1282.078620	-1281.629292	-1281.720448	-933.954
TS-190 (195), penta	0.417154	0.446125	0.447069	0.354791	-1605.083443	-1604.636374	-1604.728652	-876.649
TS-192 (195), penta	0.417118	0.446017	0.446961	0.354836	-1605.066298	-1604.619337	-1604.711462	-995.807
TS-171	0.769959	0.823590	0.824535	0.681725	-2393.761697	-2392.937162	-2393.079972	-823.408

A2.2

Cartesian Coordinates of the Structures

KOt-Bu

C	1.61010700	1.01764800	-1.04001700
C	1.07202700	0.00006500	-0.000009800
H	1.23720600	0.75376100	-2.03823200
H	1.23781900	2.02141000	-0.79701900
H	2.70796700	1.05905000	-1.08255000
C	1.61109200	0.39186400	1.40093900
C	1.60994700	-1.40984100	-0.36130400
H	1.23813600	-0.31922100	2.14954100
H	2.70904000	0.40639600	1.45700600
H	1.23997100	1.38906000	1.67139700
H	2.70776000	-1.46832900	-0.37355000
H	1.23451300	-2.14187700	0.36546100
H	1.23915100	-1.70074000	-1.35273600
O	-0.30080900	0.00007000	0.000000900
K	-2.55600700	0.00008000	0.00018400

[KOtBu]₂

K	-0.00039500	1.78010700	0.14098800
O	1.73934700	0.00038000	0.13409200
O	-1.73938200	-0.00052500	0.13447900
K	0.00035300	-1.78023100	0.14097600
C	3.10725800	0.00015200	-0.04675400

C	-3.10724800	-0.00012100	-0.04673500
C	3.83865800	0.00136600	1.31965000
H	4.93356700	0.00107400	1.22635600
H	3.54384000	0.88718500	1.89731500
H	3.54348200	-0.88322500	1.89899900
C	3.55269600	-1.25651500	-0.84377300
H	3.03047500	-1.28460600	-1.80937300
H	4.63329800	-1.29148500	-1.03821900
H	3.28812700	-2.16578600	-0.28377400
C	3.55277400	1.25527100	-0.84613700
H	4.63339100	1.28983800	-1.04057600
H	3.03057200	1.28157600	-1.81179300
H	3.28816100	2.16560700	-0.28789800
C	-3.83900700	-0.00354200	1.31946200
H	-3.54397800	0.88010200	1.90032200
H	-4.93389100	-0.00310800	1.22587600
H	-3.54434700	-0.89029800	1.89577000
C	-3.55258400	1.25777800	-0.84188300
H	-4.63314300	1.29298200	-1.03651800
H	-3.28821500	2.16617200	-0.28036500
H	-3.03016400	1.28742800	-1.80733200
C	-3.55242700	-1.25400100	-0.84824200
H	-3.28793100	-2.16521200	-0.29137100
H	-4.63298500	-1.28833400	-1.04305600
H	-3.02990900	-1.27873300	-1.81376300

[KOt-Bu]₃

O	0.00015600	1.99898400	-0.24404000
O	2.30339200	-0.91026700	-0.11571700
O	-2.30411900	-0.90944400	-0.11548200
K	-2.26639700	1.24327100	-1.24738100
K	2.26606000	1.24224500	-1.24814300
K	-0.00020800	-0.56204900	0.94732200
C	0.00059000	3.14890900	0.53473600
C	3.16018400	-1.98185400	0.04070200
C	-3.16059500	-1.98133200	0.04061100
C	-1.25165200	4.02460900	0.24927900
H	-2.16932900	3.48261300	0.52301200
H	-1.25793200	4.96449300	0.81609000
H	-1.29717900	4.27731700	-0.81940200
C	1.25368300	4.02348900	0.24957000
H	1.26073900	4.96329100	0.81650600
H	2.17081200	3.48060700	0.52337600
H	1.29960200	4.27631400	-0.81906900
C	0.00027300	2.79074600	2.04497300
H	0.89026300	2.19420700	2.28829200
H	0.00058600	3.67297100	2.69869900
H	-0.89027300	2.19496300	2.28810400
C	-4.63064600	-1.49411200	0.15035400
H	-4.91351900	-0.95694000	-0.76707100

H	-5.35112900	-2.31138700	0.29272500
H	-4.72764300	-0.79908600	0.99443600
C	-3.04955500	-2.94819200	-1.16615400
H	-2.01491100	-3.30061700	-1.26250500
H	-3.70717800	-3.82429700	-1.08088200
H	-3.30798200	-2.41724400	-2.09267400
C	-2.82034400	-2.77429200	1.33264900
H	-1.79361600	-3.16344500	1.27430400
H	-2.88873800	-2.10955600	2.20464100
H	-3.48765000	-3.62977200	1.50422400
C	3.04905500	-2.94938900	-1.16551200
H	3.70702300	-3.82521100	-1.08001000
H	2.01450200	-3.30223300	-1.26130200
H	3.30695200	-2.41884200	-2.09240900
C	4.63014600	-1.49420200	0.14976400
H	4.72717900	-0.79863700	0.99340000
H	5.35087800	-2.31120000	0.29245800
H	4.91266400	-0.95753000	-0.76806700
C	2.82050900	-2.77419000	1.33327200
H	2.88885700	-2.10893200	2.20486900
H	1.79390000	-3.16371700	1.27536900
H	3.48814700	-3.62934300	1.50519000

[KOt-Bu]₄

O	-1.35223000	-1.22398900	-1.39308300
O	1.33776900	-1.41923500	1.20966400
O	-1.29895000	1.23549700	1.43282500
O	1.31340800	1.40712700	-1.24975800
K	1.27675600	-1.21412600	-1.41362300
K	-1.29083300	-1.38866300	1.22775500
K	-1.31490700	1.39972200	-1.18877700
K	1.32898100	1.20247200	1.37432100
C	-2.17096600	-1.94544200	-2.24970100
C	2.14883000	-2.29018100	1.92258000
C	-2.08721500	1.96281600	2.31274900
C	2.10935200	2.27300200	-1.98552700
C	-1.89258000	-1.56766700	-3.72898400
H	-0.84297100	-1.77204500	-3.98192500
H	-2.52292000	-2.11815700	-4.44009400
H	-2.06704600	-0.49417300	-3.88575100
C	-3.66747600	-1.66064500	-1.95382900
H	-4.35011800	-2.21715100	-2.60988100
H	-3.90587600	-1.92758500	-0.91510700
H	-3.88178300	-0.58988600	-2.07707600
C	-1.92997000	-3.47011900	-2.08922200
H	-0.88052600	-3.71272900	-2.30610600
H	-2.13329200	-3.77922000	-1.05460000
H	-2.55996000	-4.07853500	-2.75185300
C	1.83813600	-3.76443600	1.55039700
H	1.99675500	-3.92581800	0.47513500

H	2.46150200	-4.48660800	2.09439300
H	0.78646900	-3.99726900	1.76767500
C	1.92916900	-2.12320100	3.44978300
H	2.55359700	-2.79699300	4.05164200
H	2.15595900	-1.09227600	3.75493600
H	0.87873600	-2.31959800	3.70516600
C	3.64714000	-2.02295400	1.61951400
H	3.90825500	-0.98855300	1.88195200
H	4.32386700	-2.69102000	2.16890000
H	3.84633300	-2.15169300	0.54648000
C	1.83962800	2.11308400	-3.50544100
H	0.78355000	2.32039100	-3.72671300
H	2.45104900	2.78284100	-4.12490100
H	2.04657300	1.08102000	-3.82059900
C	1.82430000	3.74880800	-1.59920300
H	2.01885500	3.90533800	-0.52912000
H	2.43652100	4.46703100	-2.16079400
H	0.76838600	3.99187500	-1.78187900
C	3.61401200	1.99110000	-1.73114300
H	3.84836800	2.11430600	-0.66458900
H	3.85711100	0.95527600	-2.00502600
H	4.27906900	2.65484500	-2.29968500
C	-1.83877100	3.48563800	2.14612900
H	-2.44463500	4.09861700	2.82681300
H	-0.78163800	3.71971100	2.33291200
H	-2.06920200	3.79703800	1.11789400
C	-3.59377600	1.69013700	2.05955700
H	-3.81305500	0.62103900	2.18837700
H	-4.25291300	2.25161800	2.73510900
H	-3.85963200	1.95971200	1.02820200
C	-1.76980400	1.58183100	3.78332400
H	-1.94855300	0.50970400	3.94460500
H	-0.71175700	1.77741800	4.00622400
H	-2.37504500	2.13699300	4.51238200

NaOt-Bu

C	1.14721600	1.45528400	-0.01297000
C	0.61947700	-0.00001700	-0.000006800
H	0.77577000	1.97449500	-0.90533400
H	0.77319000	1.99106000	0.86845300
H	2.24439000	1.51313900	-0.01193300
C	1.14518000	-0.71563600	1.26792800
C	1.14957800	-0.73951700	-1.25250600
H	0.77266300	-1.74741100	1.28993500
H	2.24227800	-0.74372100	1.32061800
H	0.77029800	-0.20292800	2.16258500
H	2.24687000	-0.76732400	-1.30104300
H	0.77827400	-1.77197300	-1.25577900
H	0.77708800	-0.24467100	-2.15813500
O	-0.75940500	-0.00017100	-0.00229800

Na	-2.69766200	0.00000100	-0.00048000
----	-------------	------------	-------------

[NaOt-Bu]₂

O	1.59627900	0.00013400	0.08503200
O	-1.59628600	-0.00034600	0.08495900
C	2.98355300	0.00005400	-0.01459600
C	-2.98355100	-0.00003900	-0.01477900
C	3.61681700	0.00079700	1.39514900
H	4.71446500	0.00070700	1.36790200
H	3.28736500	0.88677800	1.95262300
H	3.28723300	-0.88451200	1.95360800
C	3.45898900	-1.25666500	-0.78252900
H	2.99659300	-1.27947000	-1.77750500
H	4.54867600	-1.29587800	-0.90919400
H	3.15304900	-2.16311700	-0.24069700
C	3.45902700	1.25591000	-0.78390500
H	4.54871200	1.29493100	-0.91063900
H	2.99658300	1.27766000	-1.77887900
H	3.15313100	2.16296000	-0.24305700
C	-3.61693000	-0.00294700	1.39491300
H	-3.28720200	0.88138500	1.95482700
H	-4.71457400	-0.00259900	1.36757600
H	-3.28771200	-0.88990200	1.95098100
C	-3.45886800	1.25792900	-0.78075300
H	-4.54854400	1.29741900	-0.90740900
H	-3.15289600	2.16349800	-0.23746200
H	-2.99644100	1.28227300	-1.77568200
C	-3.45902500	-1.25464100	-0.78611700
H	-3.15324000	-2.16257000	-0.24668200
H	-4.54870000	-1.29338800	-0.91302400
H	-2.99645900	-1.27485100	-1.78106400
Na	-0.00018500	1.41459500	0.09327900
Na	0.00017900	-1.41477800	0.09304300

[NaOt-Bu]₃

O	0.02156900	1.86375700	-0.39069100
O	2.05954600	-0.76137900	-0.03349500
O	-2.09149100	-0.71144400	-0.08200900
C	0.03590500	3.11875700	0.23915600
C	2.97151500	-1.80996700	0.04157400
C	-3.01974500	-1.74054600	0.04611900
C	-1.04531000	4.04107400	-0.37573100
H	-2.05156300	3.63181000	-0.19217500
H	-1.03737000	5.05202200	0.05015200
H	-0.89563300	4.12639500	-1.45988000
C	1.41471500	3.80110000	0.05158500
H	1.46289400	4.79884600	0.50409400
H	2.20606600	3.20065700	0.52598000
H	1.64065600	3.91346400	-1.01910500
C	-0.23659300	2.96186000	1.75184000

H	0.53415300	2.32851400	2.20936100
H	-0.24355800	3.92266400	2.28217300
H	-1.20873600	2.47811200	1.91185400
C	-4.45745700	-1.17432300	-0.04443800
H	-4.60420900	-0.68302300	-1.01764000
H	-5.23041600	-1.94725300	0.05793500
H	-4.61354700	-0.42661500	0.74372800
C	-2.81748400	-2.78204500	-1.07824200
H	-1.80155200	-3.19279800	-1.02906100
H	-3.52943300	-3.61591300	-1.01795600
H	-2.93584700	-2.30130500	-2.05818900
C	-2.85094100	-2.43918700	1.41680700
H	-1.84353300	-2.87034500	1.49584100
H	-2.97326400	-1.70674600	2.22462900
H	-3.57493000	-3.24949400	1.57350700
C	2.42951400	-3.04220500	-0.71887700
H	3.12049200	-3.89532100	-0.69424700
H	1.47584000	-3.36334300	-0.28078800
H	2.24278600	-2.77983300	-1.76773400
C	4.32071700	-1.38890000	-0.59162100
H	4.72336500	-0.51347700	-0.06350700
H	5.07883500	-2.18210700	-0.55626600
H	4.16883900	-1.11918900	-1.64689800
C	3.21852100	-2.19140400	1.52010600
H	3.58933600	-1.31926100	2.07249200
H	2.27662000	-2.51010100	1.98603300
H	3.94468700	-3.00726000	1.63312100
Na	-1.94968600	1.14968300	-1.02837200
Na	-0.01849800	-0.45107900	0.53813600
Na	2.00290100	1.11759100	-0.96136000

[NaOt-Bu]₄

O	1.11330300	-1.15663000	-1.26273000
O	-1.73097700	-0.98967600	0.47161100
O	-0.46237700	1.76602200	-0.91121300
O	1.05880200	0.36050300	1.70742100
C	1.87642300	-1.94427100	-2.12795000
C	-2.90698700	-1.65775500	0.82109000
C	-0.78216600	2.97013400	-1.54306300
C	1.81569300	0.63437400	2.84914300
C	2.14289800	-3.32995400	-1.49377000
H	1.18966800	-3.83418700	-1.28443500
H	2.73773900	-3.98893600	-2.13939800
H	2.68696400	-3.20967700	-0.54656000
C	3.23398100	-1.25930300	-2.41484200
H	3.87453700	-1.84283800	-3.08843500
H	3.06722300	-0.27723400	-2.87909800
H	3.78232900	-1.10926700	-1.47477800
C	1.12718600	-2.14510900	-3.46656200
H	0.16755800	-2.64936500	-3.28615100

H	0.92445300	-1.17011600	-3.93046900
H	1.69234100	-2.74953200	-4.18775400
C	-2.57226800	-3.02471200	1.46395800
H	-1.96364200	-2.87389400	2.36647000
H	-3.46561500	-3.59280200	1.75381300
H	-1.99796600	-3.63922200	0.75718100
C	-3.77782400	-1.89724500	-0.43493400
H	-4.71732200	-2.41897100	-0.21156700
H	-4.02977200	-0.93598500	-0.90338200
H	-3.22284400	-2.50282200	-1.16477100
C	-3.71740600	-0.81611300	1.83550500
H	-3.97596400	0.15594000	1.39292300
H	-4.65179000	-1.30160300	2.14531500
H	-3.11620000	-0.63801600	2.73771600
C	3.08752700	1.42943900	2.46759400
H	2.80627200	2.37405000	1.98185400
H	3.71672100	1.67233000	3.33340600
H	3.69701700	0.84474200	1.76440100
C	0.98680700	1.47307800	3.85050400
H	0.08068000	0.92285000	4.13848400
H	1.53980900	1.71435600	4.76737700
H	0.68297800	2.41990800	3.38282600
C	2.24193600	-0.68466100	3.53605600
H	1.35188000	-1.26017600	3.82549200
H	2.83610900	-1.29299700	2.84036500
H	2.84465100	-0.52181800	4.43879600
C	0.50507800	3.77713600	-1.83560600
H	0.30563200	4.73944300	-2.32429300
H	1.03930300	3.98025200	-0.89738200
H	1.16825400	3.19835700	-2.49355700
C	-1.51156000	2.69479000	-2.87943200
H	-2.43733600	2.13325700	-2.69153700
H	-1.78063200	3.61319300	-3.41691900
H	-0.86942800	2.09474300	-3.53858100
C	-1.70679600	3.81845900	-0.63775400
H	-2.62885100	3.26213700	-0.42029500
H	-1.20161800	4.03705700	0.31335100
H	-1.99107600	4.77570700	-1.09321100
Na	0.40921400	-1.60661800	0.82665400
Na	-1.01458200	1.03498300	1.14947700
Na	1.55338600	0.89104100	-0.42966100
Na	-0.96867300	-0.33761800	-1.54170100

[KOt-Bu]₃K⁺

O	2.05158400	-0.56506200	-0.19895100
O	-1.51439300	-1.49425000	-0.19894200
O	-0.53689700	2.05807700	-0.19801700
K	1.82502400	1.80047300	-1.23403600
K	0.64746800	-2.48255100	-1.23409100
K	-2.47290800	0.68077600	-1.23475200

K	-0.00029000	-0.00121300	1.42548400
C	3.31049500	-0.90980400	0.30659200
C	-2.44401100	-2.41046400	0.30675100
C	-0.86609400	3.32143500	0.30684000
C	4.39740100	0.09028000	-0.16636300
H	4.18706000	1.10046100	0.21701700
H	5.40184400	-0.17440900	0.18385800
H	4.43097800	0.12543700	-1.26464500
C	3.73646100	-2.32410200	-0.16650100
H	4.73563700	-2.60775900	0.18399700
H	3.04082300	-3.08647700	0.21623900
H	3.74798200	-2.37117800	-1.26480600
C	3.29413000	-0.90589600	1.85616000
H	2.55432200	-1.62839300	2.22994500
H	4.26225400	-1.17189900	2.29733900
H	3.02680400	0.09259700	2.23107100
C	0.14785800	4.39542900	-0.16606000
H	0.18351100	4.42866100	-1.26433600
H	-0.10399100	5.40313200	0.18409600
H	1.15510600	4.17177200	0.21738600
C	-2.27489600	3.76434600	-0.16704700
H	-3.04560800	3.07819700	0.21610700
H	-2.54712700	4.76720400	0.18207600
H	-2.32149100	3.77542400	-1.26539800
C	-0.86279900	3.30573800	1.85637900
H	-1.59539300	2.57605700	2.23037700
H	0.13180800	3.02463800	2.23161900
H	-1.11550300	4.27777400	2.29679500
C	-3.88253600	-2.06284600	-0.15696700
H	-4.63010100	-2.78354000	0.19437100
H	-4.18753000	-1.07916600	0.23152200
H	-3.93502200	-2.04479100	-1.25499900
C	-2.13038100	-3.85076700	-0.17514900
H	-1.14997500	-4.17998000	0.20172900
H	-2.86334300	-4.58679000	0.17506500
H	-2.12215900	-3.89193600	-1.27366500
C	-2.42421700	-2.40660000	1.85635800
H	-1.42458400	-2.67910600	2.22453600
H	-2.67538100	-1.40621200	2.23735800
H	-3.13832400	-3.11254500	2.29715900

t-BuO⁻

C	0.76990700	-1.24423200	-0.43646700
C	-0.00013200	0.00003900	0.15967000
H	1.80129600	-1.23055200	-0.05612200
H	0.29633500	-2.16128700	-0.05785000
H	0.80755900	-1.30304500	-1.54066300
C	-1.46233400	-0.04419800	-0.43746700
C	0.69327500	1.28854000	-0.43640400
H	-2.02015500	0.82358000	-0.05747100

H -1.53137600 -0.04520400 -1.54167000
H -1.96645600 -0.94501600 -0.05922000
H 0.72747800 1.34879700 -1.54055500
H 0.16518700 2.17550300 -0.05815900
H 1.72349000 1.33736900 -0.05572100
O -0.00095700 -0.00012900 1.48392900

O₂

O 0.00000000 0.00000000 0.60729600
O 0.00000000 0.00000000 -0.60729600

HSiMe₃

C -1.65115200 -0.70715200 -0.22213800
H -1.70164300 -0.72877000 -1.31767000
H -1.79886000 -1.73251900 0.13686300
H -2.49495200 -0.10599200 0.13664300
C 0.21304900 1.78332800 -0.22197400
H -0.60064800 2.42400000 0.13790700
H 1.15591300 2.21328500 0.13607500
H 0.21849900 1.83815500 -1.31758600
C 1.43828700 -1.07596800 -0.22208500
H 2.40001400 -0.68949200 0.13542000
H 1.34133200 -2.10693900 0.13817300
H 1.48118200 -1.11009300 -1.31764100
Si -0.00013800 -0.00018300 0.37553700
H -0.00001200 -0.00031900 1.87147700

Me₃Si•

C -1.49707800 -1.00822500 0.17717800
H -1.53730000 -1.03547100 1.27530500
H -2.43733300 -0.57387800 -0.18009200
H -1.44975600 -2.04264900 -0.18063800
C 1.62207500 -0.79159600 0.17728500
H 1.71822300 -1.82261600 -0.18070000
H 2.49329800 -0.23134900 -0.17964300
H 1.66499200 -0.81318200 1.27540400
C -0.12521400 1.80036000 0.17698200
H 0.72164900 2.39781100 -0.17838200
H -1.04408300 2.27602000 -0.18319200
H -0.13146500 1.84922500 1.27520600
Si 0.00022000 -0.00051000 -0.42371000

H₂

H 0.00000000 0.00000000 0.37139400
H 0.00000000 0.00000000 -0.37139400

Me•

C 0.00000000 0.00000000 0.00015500
H 0.00000000 1.08279800 -0.00031000
H -0.93773100 -0.54139900 -0.00031000

H	0.93773100	-0.54139900	-0.00031000
---	------------	-------------	-------------

t-BuO•

C	1.28444000	-0.78208500	-0.31507600
C	0.00040800	-0.02651100	0.08147400
H	2.16791400	-0.20844400	-0.01830000
H	1.32075100	-1.75298600	0.19083000
H	1.32290000	-0.95893000	-1.39608100
C	-1.27108600	-0.80336200	-0.31547500
C	-0.01160200	1.38844700	-0.57944400
H	-2.16376300	-0.24501700	-0.01726300
H	-1.30694300	-0.97930400	-1.39670400
H	-1.29060700	-1.77542800	0.18915300
H	-0.00952400	1.26142700	-1.66749800
H	-0.90726600	1.94171900	-0.28474700
H	0.87381300	1.95737200	-0.28347000
O	-0.00253000	0.26258200	1.43190100

t-BuOH

C	1.49029100	-0.03159600	-0.35612300
C	0.00542200	-0.00042200	0.01380400
H	2.00202100	0.84324500	0.05811700
H	1.96432400	-0.92932300	0.05413200
H	1.62279900	-0.03227900	-1.44334000
C	-0.71772600	-1.24971300	-0.51177000
C	-0.66220400	1.28083700	-0.50917000
H	-1.77526300	-1.24080000	-0.21558600
H	-0.68154600	-1.30568500	-1.60601700
H	-0.25727900	-2.15453300	-0.10156900
H	-0.62395000	1.33693200	-1.60339300
H	-1.71884100	1.31844800	-0.21227200
H	-0.16130100	2.16324100	-0.09761100
O	-0.01498900	-0.00165100	1.45245600
H	-0.94575600	0.01932100	1.72744200

t-BuOSiMe₃

C	-1.53411400	-1.23720200	-1.35238600
H	-2.59102300	-1.23736700	-1.64901100
H	-0.94667900	-0.99675900	-2.24657300
H	-1.27718400	-2.25866200	-1.04848800
C	-2.31725500	-0.48686300	1.53679500
H	-2.06466900	-1.49251500	1.89193600
H	-2.16594600	0.20684700	2.37180400
H	-3.38473400	-0.47823700	1.28369500
C	-1.75796900	1.72368900	-0.53265700
H	-1.58137700	2.47348600	0.24773200
H	-1.20820700	2.03791000	-1.42690700
H	-2.82757300	1.74880900	-0.77830300
Si	-1.25814100	-0.00315800	0.05651400
C	1.99831700	-1.41884400	-0.37810500

C	1.61900600	0.00048500	0.07176700
H	1.90998800	-2.11544200	0.46213300
H	1.34135400	-1.76589300	-1.18235000
H	3.03071900	-1.45003700	-0.74568900
C	1.68847800	0.98094200	-1.10862100
C	2.54983700	0.46578500	1.19983800
H	1.38888700	1.98590600	-0.79350800
H	2.70933600	1.03649600	-1.50346100
H	1.03245900	0.66474500	-1.92773700
H	3.59362700	0.48878300	0.86633100
H	2.26852800	1.46969900	1.53483400
H	2.47200200	-0.21288500	2.05537100
O	0.30458100	-0.02857800	0.64715000

TS-172

C	-2.14636800	-1.41577200	-1.15357100
H	-3.22466700	-1.47711600	-1.35135600
H	-1.64000700	-1.28333700	-2.11644200
H	-1.82917400	-2.37852800	-0.73730500
C	-2.61552300	-0.26914600	1.70646900
H	-2.31800600	-1.22614900	2.14927300
H	-2.35401000	0.52230100	2.41755100
H	-3.70772500	-0.27475200	1.59554300
C	-2.23281000	1.67780700	-0.70170800
H	-1.97024200	2.49659800	-0.02251200
H	-1.72152400	1.85604400	-1.65455300
H	-3.31339200	1.73222300	-0.88855300
Si	-1.76254300	0.00178500	0.04194100
H	-0.17719900	0.00403800	0.37408200
C	3.37885900	-0.00601000	0.88779900
C	2.08839900	0.00073400	0.03482300
H	3.41089900	0.87516300	1.53591300
H	3.41488200	-0.90044100	1.51728300
H	4.26064400	0.00283300	0.23639000
C	2.03621200	-1.25987200	-0.84640900
C	2.03476000	1.27819100	-0.82186600
H	1.12007400	-1.27049600	-1.44851900
H	2.89099100	-1.30702200	-1.53199300
H	2.04129800	-2.15765300	-0.21954600
H	2.89098200	1.34069900	-1.50436700
H	1.12002600	1.29785700	-1.42603600
H	2.03580300	2.16356900	-0.17772100
O	1.06059600	-0.00955200	1.00405800

KOO•

O	0.67492300	-1.27141100	0.00000000
O	-0.67492300	-1.27056800	0.00000000
K	0.00000000	1.07030700	0.00000000

[KOt-Bu]KOO•

K	1.08630200	-1.84918300	0.03516300
O	-0.59874800	0.00015900	0.11880200
O	2.81050400	-0.00008000	0.62476000
K	1.08652900	1.84918400	0.03514300
C	-1.97321600	0.00003900	0.00097300
C	-2.64260900	-0.00003800	1.39900000
H	-3.74058000	0.00012500	1.35488900
H	-2.32145100	-0.88506900	1.96359500
H	-2.32119800	0.88473900	1.96385100
C	-2.45598300	1.25567700	-0.77661700
H	-1.97798900	1.28339000	-1.76482400
H	-3.54427200	1.29024000	-0.92209100
H	-2.16818300	2.16592100	-0.22929800
C	-2.45581400	-1.25561100	-0.77671900
H	-3.54405500	-1.29010000	-0.92256200
H	-1.97748300	-1.28346600	-1.76476100
H	-2.16829600	-2.16584400	-0.22922800
O	2.74392500	-0.00012100	-0.72671000

[KOt-Bu]₃KOO•(170)

O	0.02988400	-0.11123300	2.75134900
O	2.02055500	-0.82028400	-0.18396600
O	-0.33038300	2.05201500	-0.32802400
O	-1.66346100	-1.40888300	-0.17022400
K	0.35285300	-2.18278800	1.28871600
K	1.70099800	1.40359700	1.24764900
K	-2.04373800	0.80469500	1.26266700
K	0.01440400	-0.10984400	-1.73244700
C	3.26257100	-1.27660700	-0.59079000
C	-0.53791300	3.32923700	-0.81978300
C	-2.70717800	-2.21869700	-0.58387700
C	3.54262300	-2.69690100	-0.02734900
H	2.77701100	-3.39930400	-0.38739700
H	4.52250200	-3.09623800	-0.32113600
H	3.50738800	-2.67623700	1.07134000
C	4.38985400	-0.33235700	-0.09094200
H	5.39471700	-0.65811500	-0.39074400
H	4.23487500	0.67912700	-0.49279800
H	4.37162500	-0.27792800	1.00698100
C	3.34478200	-1.34798900	-2.13946700
H	3.17315100	-0.35048900	-2.56793900
H	4.31496600	-1.70741600	-2.50780300
H	2.56942900	-2.02665200	-2.52221900
C	-2.52766900	-3.66728600	-0.05327800
H	-2.49258000	-3.66090900	1.04561700
H	-3.33695400	-4.34492000	-0.35621300
H	-1.58382600	-4.08802800	-0.42901800
C	-4.06642200	-1.68063700	-0.05897500
H	-4.23828800	-0.66443800	-0.44187300

H	-4.92385400	-2.29714500	-0.36002700
H	-4.05299300	-1.64226300	1.03961900
C	-2.78007900	-2.27862100	-2.13364400
H	-2.92771100	-1.26746900	-2.53850000
H	-1.83870700	-2.67887400	-2.53615800
H	-3.59759200	-2.91005300	-2.50663800
C	-0.54944900	3.32789400	-2.37275600
H	-0.71465600	4.32284600	-2.80762400
H	0.41174800	2.95293400	-2.75247300
H	-1.34822900	2.66712800	-2.73872700
C	-1.89743700	3.89900200	-0.32986600
H	-1.91417900	3.93445800	0.76842500
H	-2.10017900	4.91324200	-0.69898200
H	-2.71804900	3.25148300	-0.67109800
C	0.58382200	4.29439400	-0.34777900
H	0.60444900	4.33474000	0.75033300
H	1.56004000	3.93338100	-0.70240000
H	0.45609400	5.32103600	-0.71618400
O	-0.17172700	1.15463300	3.15455800

NaOO•

O	1.04416800	0.20075100	0.00000000
O	0.00000000	1.06326600	0.00000000
Na	-0.75939500	-0.91928500	0.00000000

[NaOt-Bu]NaOO•

O	0.34168700	-0.04804000	0.00146000
O	-2.97506000	0.01925700	-0.68027200
C	1.73345000	-0.00684500	0.00004400
C	2.28180200	-0.72616400	-1.25311000
H	3.37765500	-0.70028700	-1.31324800
H	1.96881600	-1.77905300	-1.24711600
H	1.87429000	-0.25987500	-2.15819400
C	2.21730100	1.46341600	-0.01808500
H	1.83841300	1.99163300	0.86793000
H	3.31101000	1.55473900	-0.02037100
H	1.83614100	1.97030300	-0.91542400
C	2.28354200	-0.69594400	1.26924300
H	3.37948100	-0.66845800	1.32723600
H	1.87722400	-0.20818600	2.16348900
H	1.97054800	-1.74860700	1.28908800
O	-2.97643700	0.01926900	0.67886000
Na	-1.23087400	1.37739400	0.00077600
Na	-1.28291400	-1.40311000	0.00083100

[NaOt-Bu]3NaOO•(C-3)

O	0.09058800	0.67535300	2.92791900
O	-0.91597200	1.66045600	-0.12729800
O	-0.91801000	-1.65959800	-0.12683000
O	1.92934200	-0.00128300	-0.13775700

C	-1.69194100	2.75776900	-0.51473100
C	-1.69519100	-2.75595900	-0.51453200
C	3.26107500	-0.00190900	-0.56984500
C	-1.00053400	4.07525000	-0.09153500
H	-0.00947000	4.14498100	-0.56122200
H	-1.57002500	4.96841300	-0.37854400
H	-0.87158100	4.09757800	0.99945400
C	-3.08415100	2.68890500	0.15665500
H	-3.73180400	3.53199900	-0.11557000
H	-3.59814100	1.76408500	-0.14021600
H	-2.97355100	2.69211400	1.24985900
C	-1.87756400	2.76111100	-2.04985000
H	-2.37500100	1.83477800	-2.36797400
H	-2.48070900	3.60604300	-2.40599500
H	-0.89794900	2.81520100	-2.54455600
C	3.99290000	1.25494900	-0.04219500
H	3.96540600	1.27219600	1.05621300
H	5.04531800	1.29829700	-0.34967100
H	3.50078600	2.16254800	-0.42040800
C	3.99175700	-1.25937400	-0.04207700
H	3.49877300	-2.16655300	-0.42015200
H	5.04412000	-1.30373100	-0.34959500
H	3.96428800	-1.27646600	1.05633300
C	3.31732400	-0.00200400	-2.11478100
H	2.80734900	-0.89251700	-2.50685400
H	2.80812600	0.88891500	-2.50693900
H	4.34297700	-0.00247100	-2.50508000
C	-1.88340200	-2.75699600	-2.04934200
H	-2.48782800	-3.60093300	-2.40566600
H	-2.38058500	-1.82979800	-2.36532500
H	-0.90466600	-2.81122100	-2.54579000
C	-1.00373100	-4.07439000	-0.09440600
H	-0.87317900	-4.09847700	0.99636000
H	-1.57403700	-4.96686400	-0.38193600
H	-0.01339100	-4.14377300	-0.56564500
C	-3.08623400	-2.68734900	0.15929400
H	-2.97378100	-2.69182700	1.25229300
H	-3.60040600	-1.76200000	-0.13563700
H	-3.73466400	-3.52987600	-0.11283500
O	0.08952300	-0.67460900	2.92798300
Na	-1.55514400	0.00099900	1.27724300
Na	0.98195300	-1.65375800	1.03775600
Na	0.98399000	1.65275000	1.03726900
Na	-0.00825300	-0.00028300	-1.31890000

[KOt-Bu]HSiMe₃

C	-1.90583800	0.41794000	1.54268800
H	-0.81654300	0.27981200	1.46868100
H	-2.15111600	1.48750700	1.63399500
H	-2.25265500	-0.06226900	2.46484900

C	-2.39966200	-2.22698700	-0.00172200
H	-2.83964800	-2.70198800	0.88296500
H	-2.83945200	-2.69965500	-0.88775400
H	-1.32477200	-2.44172100	-0.00205100
C	-1.90882300	0.42192800	-1.54112600
H	-2.25881400	-0.05478400	-2.46389300
H	-2.15341600	1.49203800	-1.62811500
H	-0.81943600	0.28259100	-1.47086600
Si	-2.68538600	-0.36189000	0.00058400
H	-4.15836700	-0.08549000	0.00213300
O	1.13393500	0.30748900	-0.00293900
C	2.15257400	-0.62244700	-0.00023700
C	3.53301800	0.08313100	-0.08140100
H	4.38128600	-0.61581100	-0.08703500
H	3.58417600	0.68720000	-0.99750900
H	3.65415500	0.75690300	0.77795900
C	2.11156400	-1.46610300	1.29958200
H	2.20276000	-0.80540300	2.17149000
H	1.14853800	-1.98622500	1.37419100
H	2.91242100	-2.21701400	1.35154000
C	2.01995900	-1.57452500	-1.21627000
H	1.05565700	-2.09615700	-1.17553300
H	2.04535500	-0.99204100	-2.14622900
H	2.81725300	-2.32963200	-1.26065600
K	0.24841000	2.44795100	-0.00010000

TS, O₂ + HSiMe₃

C	1.92503200	-0.92101300	-0.97696900
H	2.81852600	-1.08402200	-0.35805200
H	1.57499300	-1.89906500	-1.32297800
H	2.22623500	-0.33400400	-1.85089100
C	1.09478000	1.72088700	0.50075100
H	1.27789300	2.32851400	-0.39229200
H	0.30662400	2.20460600	1.08521800
H	2.01709800	1.72052500	1.09647200
C	-0.20157500	-1.06261300	1.37280800
H	-0.04091700	-0.64359500	2.37220300
H	-1.29130300	-1.03637600	1.17619600
H	0.13555600	-2.10359100	1.36242300
Si	0.60092900	-0.03309900	0.04461900
H	-0.66502200	0.02705000	-1.14457700
O	-1.65236000	0.58648200	-0.74741000
O	-2.55790400	-0.22900900	-0.25608000

HOO•

O	0.05589000	-0.61174300	0.00000000
O	0.05589000	0.72018700	0.00000000
H	-0.89424400	-0.86754600	0.00000000

[t-BuOSiHMe₃]⁻

C	-1.29845800	1.70118700	-0.98968200
H	-2.12059400	2.36318200	-0.68128800
H	-0.35128400	2.22230400	-0.80311300
H	-1.41034200	1.56868100	-2.07673500
C	-1.29880500	-1.70152100	-0.98909400
H	-1.40858400	-1.56882600	-2.07635100
H	-0.35243000	-2.22353100	-0.80093200
H	-2.12215200	-2.36271100	-0.68224700
C	-2.16147300	0.00037100	1.73191600
H	-2.80117500	-0.87967200	1.89304900
H	-1.36320100	0.00137400	2.48065000
H	-2.80286100	0.87930600	1.89231500
Si	-1.52596800	0.00002200	-0.08760900
C	1.63870500	-0.00111900	-1.43250000
C	1.53036100	-0.00001300	0.11613800
H	1.15631400	-0.88697800	-1.85710800
H	1.15517300	0.88347000	-1.85845200
H	2.69110300	-0.00069100	-1.75349500
C	2.26446600	1.25806400	0.65161500
C	2.26521000	-1.25687800	0.65340600
H	2.20482200	1.27247500	1.74650500
H	3.32508100	1.29415600	0.35751900
H	1.77134300	2.16382700	0.27966300
H	3.32578000	-1.29294300	0.35914700
H	2.20579300	-1.26966100	1.74833000
H	1.77236300	-2.16339100	0.28292700
O	0.23727500	-0.00017100	0.61796400
H	-3.04983800	0.00014800	-0.61836500

[t-BuOSiMe₃]^{-•}

C	2.81747600	0.08020000	1.33350000
H	3.78867100	0.09828200	0.79919400
H	2.77108000	0.98435600	1.95984800
H	2.83677300	-0.78096600	2.01908400
C	1.82129900	-1.55331400	-0.92294300
H	1.73260000	-2.48303900	-0.34176700
H	1.22232600	-1.68062600	-1.83291200
H	2.87894000	-1.45692000	-1.21440900
C	1.67813700	1.51550200	-0.99944600
H	1.10680100	1.50832500	-1.93615400
H	1.44905300	2.46190800	-0.48749500
H	2.75062900	1.53782000	-1.24963600
Si	1.21951700	-0.01896900	0.09667100
C	-1.92333100	-1.10233900	1.16259500
C	-1.74114200	-0.01080600	0.07912600
H	-1.83966000	-2.09535500	0.70397400
H	-1.12619300	-1.00937700	1.90855600
H	-2.90052700	-1.02951600	1.66570100
C	-1.86593400	1.38404900	0.73995400

C	-2.85934000	-0.16379900	-0.97636900
H	-1.73740400	2.16682200	-0.01761400
H	-2.84376000	1.52568700	1.22689600
H	-1.07448300	1.50573700	1.48803200
H	-3.86449300	-0.07039200	-0.53679100
H	-2.74359800	0.60239300	-1.75248100
H	-2.77806800	-1.14461400	-1.46011700
O	-0.53311500	-0.15898900	-0.59922700

[t-BuOSiMe₃]K•

C	2.38384600	-0.65420300	1.36085800
H	3.08984700	-1.49460900	1.38370300
H	2.97385500	0.25827200	1.21953000
H	1.90861100	-0.59892800	2.34700500
C	0.20774900	-2.56153100	0.34965600
H	-0.35185500	-2.52437800	1.29289800
H	-0.49039100	-2.83794400	-0.45136700
H	0.93025200	-3.38377500	0.43546700
C	1.98115200	-1.09868900	-1.67618400
H	1.25498500	-1.20645300	-2.49082600
H	2.62134600	-0.24138500	-1.90899900
H	2.61560200	-1.99447700	-1.68242300
Si	1.11189300	-0.94523700	-0.00638900
C	0.11901100	2.13185300	1.45743300
C	-0.01485000	1.67837700	-0.00318700
H	-0.70659300	1.73093200	2.05541900
H	1.06018500	1.78716700	1.89641500
H	0.09273800	3.22549300	1.52674700
C	1.16729300	2.18153400	-0.84433200
C	-1.32449300	2.20670300	-0.60129700
H	1.08022400	1.84041100	-1.88090400
H	1.18675700	3.27690500	-0.84696100
H	2.12659700	1.83802400	-0.44276900
H	-1.31461400	3.30138600	-0.64960000
H	-1.47264000	1.81875800	-1.61528500
H	-2.18500100	1.91542600	0.01372100
O	-0.10826200	0.22828800	-0.03611700
K	-2.95992400	-0.97937200	-0.00426700

N-Me-Indole (I)

C	-0.65997000	-1.47306500	0.00003600
C	0.15148500	-0.33261200	-0.00000400
C	-0.38888200	0.98515800	-0.00002600
C	-1.78526900	1.14347500	-0.00002200
C	-2.59400200	0.01418700	-0.00001000
C	-2.03700600	-1.28114200	0.00002000
H	-0.23536700	-2.47317700	0.00006200
H	-2.22476500	2.13780600	-0.00000900
H	-3.67479400	0.12696900	-0.00000200
H	-2.69562200	-2.14541600	0.00003700

C	0.72629300	1.88868700	0.00005800
C	1.86038200	1.12059200	-0.00006600
H	2.90090000	1.41719200	-0.00009100
N	1.52953700	-0.22374500	-0.00005000
H	0.69119300	2.96943400	0.00003900
C	2.45994500	-1.33308700	0.00004000
H	2.32730100	-1.95880400	0.89078500
H	2.32691100	-1.95921700	-0.89035100
H	3.47962300	-0.94173300	-0.00028000

TS-178

C	-2.59032400	1.09620600	0.58236100
C	-1.56148600	0.61479800	-0.23249000
C	-1.50372500	-0.75092100	-0.65013000
C	-2.53482200	-1.62607700	-0.25564800
C	-3.56644400	-1.14226600	0.53909900
C	-3.59232800	0.20283800	0.95752900
H	-2.61673500	2.13059200	0.91310800
H	-2.51825900	-2.66710600	-0.56827300
H	-4.36495500	-1.81086200	0.84938500
H	-4.40725500	0.55140700	1.58608200
C	-0.32371400	-0.89434200	-1.43349000
C	0.34856000	0.33519100	-1.40958900
H	1.07105800	0.69185200	-2.13267200
N	-0.47525700	1.27554400	-0.77581600
H	0.01733100	-1.78538800	-1.94275300
Si	2.33151200	-0.22844300	0.27902400
C	1.46235600	-1.02968200	1.76605300
H	0.67442400	-1.71554900	1.43870400
H	2.17668200	-1.59867900	2.37728900
H	0.99697100	-0.27627000	2.41171700
C	3.62509400	1.03434800	0.90259000
H	4.40133200	0.53507500	1.50072000
H	4.12622200	1.54318400	0.07087400
H	3.16375600	1.80194700	1.53448500
C	3.23580400	-1.55825700	-0.74111300
H	3.74581400	-1.12380700	-1.60931400
H	3.99693000	-2.06540400	-0.13236700
H	2.54223900	-2.32306800	-1.10771800
C	-0.07021500	2.62364900	-0.44907500
H	0.43863400	2.67716300	0.52433800
H	0.61420700	2.99184900	-1.21807200
H	-0.94530700	3.27956000	-0.42773700

TS-179

C	-2.81248500	-0.08347300	0.64832900
C	-1.70313500	0.37539800	-0.06930500
C	-0.87271800	-0.50187100	-0.81466500
C	-1.18858500	-1.86328200	-0.85880400
C	-2.30439000	-2.32640300	-0.16263700

C	-3.10238100	-1.44503200	0.58682200
H	-3.43213300	0.59211200	1.23110500
H	-0.56616900	-2.55264100	-1.42393800
H	-2.55876500	-3.38222200	-0.19426400
H	-3.96159100	-1.83033700	1.12930500
C	0.22111900	0.29978100	-1.36513800
C	-0.10740900	1.62840000	-1.05182000
H	0.39660300	2.54635600	-1.31917300
N	-1.21716500	1.66502300	-0.21928800
C	-1.73728900	2.83687600	0.44914600
H	-2.82606400	2.88791000	0.33733500
H	-1.49575800	2.83725600	1.52070600
H	-1.30325200	3.73001100	-0.00663100
H	0.77378300	0.03195000	-2.25682400
Si	2.21919100	-0.26340900	0.13903600
C	3.06964100	-1.96925700	0.29736300
H	3.87428100	-1.94785000	1.04697500
H	2.35324500	-2.74066400	0.60277000
H	3.51242000	-2.28503400	-0.65460800
C	3.52120300	1.01849800	-0.40963500
H	4.31779100	1.12299300	0.33971000
H	3.99434300	0.72864500	-1.35557500
H	3.07292100	2.00912200	-0.55193400
C	1.53596100	0.23874500	1.84244300
H	1.04801700	1.21929000	1.79781500
H	0.79623300	-0.48472200	2.20316000
H	2.33837400	0.30011500	2.58998200

181

C	-2.60040100	1.18675900	0.33951600
C	-1.46942300	0.54444100	-0.15833800
C	-1.46732800	-0.86768900	-0.44067600
C	-2.64903000	-1.61053400	-0.20761700
C	-3.77605400	-0.96052800	0.28703400
C	-3.75531400	0.41785500	0.55698700
H	-2.59404600	2.24987300	0.56160300
H	-2.66936200	-2.67673300	-0.41757500
H	-4.68575000	-1.52653700	0.46923100
H	-4.64742000	0.90127000	0.94592800
C	-0.20300000	-1.20129100	-0.93782100
C	0.67715500	0.01137900	-0.93812200
H	1.05009300	0.26323600	-1.95135000
N	-0.23553900	1.06630800	-0.46554900
H	0.12509100	-2.17898000	-1.26718700
Si	2.22663300	-0.25261000	0.21061400
C	1.63791900	-0.58572800	1.97362100
H	0.99268900	-1.46992600	2.01178500
H	2.48585400	-0.75559500	2.64815700
H	1.06176300	0.25931600	2.36736300
C	3.34849200	1.27776500	0.16942400

H	4.27698900	1.08485300	0.72148000
H	3.62963100	1.54587300	-0.85654600
H	2.87363300	2.15311200	0.62648200
C	3.19479900	-1.73099700	-0.47300900
H	3.49555400	-1.57050700	-1.51571500
H	4.10925300	-1.89888500	0.10902900
H	2.60495200	-2.65372400	-0.43396400
C	0.05601100	2.47889600	-0.51723300
H	0.26600400	2.90984200	0.47333100
H	0.92930700	2.64816300	-1.15325500
H	-0.79127900	3.02575500	-0.95113400

180

C	-2.94993700	-0.05238500	0.33372100
C	-1.70061400	0.38392400	-0.11407400
C	-0.69747000	-0.52654200	-0.51651700
C	-0.97197100	-1.88734800	-0.51168200
C	-2.23107500	-2.34083300	-0.08499700
C	-3.19975500	-1.42930500	0.33843700
H	-3.71024900	0.64905600	0.66404700
H	-0.22148600	-2.60184100	-0.84020100
H	-2.44791000	-3.40519100	-0.08017500
H	-4.16747000	-1.78994500	0.67769800
C	0.54803700	0.25353700	-0.89767700
C	0.12072800	1.67542200	-0.62610000
H	0.50957000	2.54398700	-1.14800600
N	-1.23180100	1.68341900	-0.26022900
C	-1.93278800	2.85708900	0.20493400
H	-2.98430600	2.81488900	-0.09850200
H	-1.88832000	2.96412300	1.29945500
H	-1.48084300	3.74437700	-0.24675600
H	0.81137900	0.08925500	-1.95933200
Si	2.12555300	-0.16622000	0.13485900
C	2.74940100	-1.91003300	-0.28081800
H	3.69682300	-2.11335800	0.23406400
H	2.03701300	-2.68308600	0.02859500
H	2.92854000	-2.03051900	-1.35636600
C	3.46907900	1.08675300	-0.33192600
H	4.39471300	0.89687600	0.22530200
H	3.71321200	1.03730200	-1.40041000
H	3.15112500	2.11144100	-0.10820200
C	1.72775000	-0.04724700	1.97888600
H	1.35545200	0.95153600	2.23282200
H	0.96018800	-0.77407100	2.26813200
H	2.61911900	-0.23987400	2.58829500

TS-186

H	2.06761600	-0.97560200	-0.78352300
Si	4.31137300	-2.00057400	0.50095100
C	5.14948900	-3.04714800	-0.85040700

H	5.54813100	-3.96726300	-0.40335700
H	5.99740700	-2.52301600	-1.30746400
H	4.46318300	-3.34203100	-1.65131000
C	3.04035500	-3.12060800	1.37597700
H	3.52766500	-3.98447300	1.84489200
H	2.30417700	-3.50055600	0.65559300
H	2.50436500	-2.57799200	2.16540200
C	5.66557200	-1.52411100	1.74580500
H	5.24256500	-0.97813100	2.59674600
H	6.40843300	-0.86719200	1.27666400
H	6.19606400	-2.40310600	2.13410700
O	0.94564100	-1.21732500	-1.11045200
C	0.77620800	-1.59224900	-2.47085500
C	-0.45457200	-2.51817800	-2.56716800
H	-1.32359800	-2.10836500	-2.03875300
H	-0.23362400	-3.48715900	-2.10056100
H	-0.73465900	-2.71693200	-3.61080700
C	0.56707000	-0.32653400	-3.33041400
H	1.44772500	0.32206900	-3.26858200
H	-0.28276400	0.26291500	-2.95908200
H	0.39079300	-0.56271800	-4.38831600
C	1.98915300	-2.37387400	-3.01004500
H	2.89102900	-1.75879600	-3.01276900
H	1.80930800	-2.71583600	-4.03710600
H	2.17692600	-3.25435500	-2.38614300
K	0.07288900	1.50333200	0.19465800
C	3.73699700	1.77908100	-0.53585500
C	3.04622200	1.69371700	0.72530200
C	2.83227200	0.32930500	0.98148700
C	3.34016000	-0.49370300	-0.12301900
H	2.35654700	-0.07694400	1.86746800
O	-1.06016000	0.17284100	2.22463300
K	-0.74705800	-2.00909800	0.82667900
C	-0.92169500	0.17322700	3.60716100
C	0.09121100	1.24928900	4.06920000
H	0.20351100	1.28836800	5.16109900
H	1.07777400	1.05029500	3.63523500
H	-0.23555200	2.23972300	3.72609500
C	-2.27873900	0.46896700	4.30793000
H	-3.02773500	-0.28881200	4.03228400
H	-2.20318500	0.46809000	5.40306100
H	-2.65084900	1.46006500	4.00879800
C	-0.42599400	-1.20913400	4.11332100
H	0.53967400	-1.45281700	3.64974000
H	-0.28933400	-1.24651800	5.20206800
H	-1.15061800	-1.99339800	3.84637600
O	-2.42925500	1.96079300	-0.83149100
O	-3.21993800	-1.54870200	-0.27586700
K	-3.40223100	0.64793500	1.24117000
K	-2.99084500	-0.01527700	-2.33575800

C	-4.16792700	-2.56287000	-0.21810700
C	-3.53049500	-3.89985600	0.24672300
H	-3.11305600	-3.78687300	1.25782000
H	-4.24943600	-4.72861600	0.28351200
H	-2.72120900	-4.18964900	-0.43681200
C	-4.81274900	-2.80266200	-1.61102900
H	-5.55659500	-3.60990400	-1.60962800
H	-5.32698200	-1.89098700	-1.95229400
H	-4.03832000	-3.06401100	-2.34511000
C	-5.30357400	-2.20454700	0.77779200
H	-4.88784900	-2.05223500	1.78360300
H	-5.80189200	-1.27596100	0.46310100
H	-6.07381400	-2.98334400	0.85221100
C	-2.79111800	3.26207900	-1.16344200
C	-3.30108200	3.33836000	-2.62878500
H	-4.19298000	2.70468600	-2.75492500
H	-3.58142100	4.35396500	-2.93650800
H	-2.51937600	2.98683800	-3.31695600
C	-3.92808400	3.76828800	-0.23536500
H	-3.59011700	3.76107400	0.81040300
H	-4.25351700	4.79029300	-0.46969600
H	-4.80604700	3.11137300	-0.32190900
C	-1.58920600	4.23009000	-1.02480600
H	-1.84095300	5.26505600	-1.29043300
H	-1.22573300	4.23687900	0.01194500
H	-0.76576700	3.91012300	-1.67733900
N	4.01226100	0.50195800	-0.96710000
C	4.57599000	0.25512200	-2.27037600
H	5.47408600	0.86848200	-2.41488000
H	4.86538300	-0.79237500	-2.35842800
H	3.87612900	0.49357500	-3.09036900
C	2.68709200	2.90503400	1.38043600
C	4.01482400	3.00311400	-1.14404100
C	3.64353300	4.18657700	-0.46706500
H	3.86825300	5.15004200	-0.91707400
C	2.99951600	4.13054500	0.77358100
H	2.73885700	5.05609500	1.28294800
H	4.52688100	3.05491600	-2.10081900
H	2.21421900	2.87962700	2.35975100

TS-187

H	2.01042500	-0.68328700	-0.78720500
Si	4.03929400	-2.20834300	0.08301900
C	4.92618100	-2.67837200	-1.52945800
H	5.31733000	-3.70115400	-1.45173000
H	5.78055000	-2.01848200	-1.72065600
H	4.27076400	-2.64066500	-2.40541900
C	2.68768800	-3.51443100	0.41521500
H	3.11463100	-4.51225100	0.57705100
H	2.00031700	-3.57687200	-0.43886100

H	2.10340600	-3.25598300	1.30864400
C	5.33134100	-2.35619800	1.47366500
H	4.89037700	-2.16199100	2.45867000
H	6.14059200	-1.62964900	1.32895400
H	5.78308700	-3.35618400	1.50196000
O	0.90053200	-0.76319400	-1.27169100
C	0.82073700	-0.49544600	-2.66556400
C	-0.41570300	-1.23184000	-3.22430400
H	-1.31340400	-1.05758200	-2.61868700
H	-0.24168400	-2.31597400	-3.21770700
H	-0.62533000	-0.94546000	-4.26444500
C	0.69974300	1.02794000	-2.89537100
H	1.60596500	1.53166900	-2.54085000
H	-0.14414000	1.44766000	-2.32953200
H	0.56769300	1.28081100	-3.95611500
C	2.05596600	-1.01326500	-3.42272600
H	2.95936900	-0.49416300	-3.09613000
H	1.94710700	-0.85818900	-4.50376400
H	2.18482800	-2.08626400	-3.24424100
K	0.07791000	1.12966800	0.76855400
C	3.70555500	1.77338500	0.44954800
C	2.70163800	-0.07979200	1.38008000
C	3.22431600	-0.51473900	0.05828700
H	2.73217600	-0.67524000	2.29298400
O	-1.34954300	-0.68180800	2.14109300
K	-0.97144100	-2.18792000	0.04587500
C	-1.26547400	-1.14840800	3.44495800
C	-0.24713300	-0.31771800	4.26565200
H	-0.15798700	-0.65323400	5.30780500
H	0.74188800	-0.38476300	3.79762700
H	-0.55153400	0.73793700	4.27400200
C	-2.64320400	-1.05986200	4.16028700
H	-3.39434400	-1.64766700	3.61230000
H	-2.61737500	-1.43710000	5.19105200
H	-2.97987600	-0.01330000	4.20551500
C	-0.81381400	-2.63353100	3.47117300
H	0.16444500	-2.73366200	2.98228700
H	-0.72261000	-3.04024400	4.48715800
H	-1.54037500	-3.25807400	2.93017900
O	-2.28792800	2.24313300	-0.08923200
O	-3.33390000	-1.12429900	-0.95524700
K	-3.53524800	0.33919800	1.26607300
K	-2.88244600	1.05931000	-2.26200700
C	-4.32351000	-2.01621800	-1.34777700
C	-3.78417400	-3.47142700	-1.38543900
H	-3.45441400	-3.77735100	-0.38194600
H	-4.53548600	-4.20029100	-1.71614400
H	-2.92924200	-3.53825900	-2.07162200
C	-4.85458100	-1.67012000	-2.76628300
H	-5.62575200	-2.36585200	-3.12148900

H	-5.30241900	-0.66424700	-2.76796600
H	-4.02952400	-1.68767600	-3.49144700
C	-5.52554500	-1.97815400	-0.36562000
H	-5.19199800	-2.24443800	0.64702400
H	-5.95492800	-0.96602500	-0.33527700
H	-6.33187600	-2.67048000	-0.64154300
C	-2.49596900	3.59962400	0.12791500
C	-2.93016600	4.31146400	-1.18274600
H	-3.87196900	3.87899000	-1.55437900
H	-3.09700800	5.38892100	-1.05501600
H	-2.15710500	4.18478600	-1.95357800
C	-3.61102200	3.82328400	1.18507800
H	-3.32380600	3.35700800	2.13799700
H	-3.81174400	4.88436600	1.38335800
H	-4.55095700	3.36545300	0.84368700
C	-1.20482000	4.28964300	0.64019000
H	-1.33118700	5.36793000	0.80302700
H	-0.89648700	3.84849000	1.59877100
H	-0.39051800	4.15414000	-0.08419700
C	3.91525700	0.69361000	-0.45286800
C	4.65595600	0.95271900	-1.61464700
C	4.19144000	3.05752400	0.20806600
C	4.91637700	3.28570600	-0.97177100
C	5.14840100	2.24237600	-1.86802900
H	4.87872300	0.15103900	-2.31276300
H	5.72878600	2.42405800	-2.76949500
H	5.31081800	4.27810500	-1.17452200
H	4.03019700	3.86434100	0.91880300
N	2.94529400	1.32233800	1.54028000
C	3.09352900	1.90879800	2.85974800
H	4.07922500	1.68845300	3.30343500
H	2.97136900	2.99571500	2.81441800
H	2.31973800	1.50777900	3.52144900

109

C	-2.82273700	1.23418200	0.00976200
C	-1.63506300	0.48908600	0.01279800
C	-1.63870700	-0.93288900	-0.00152300
C	-2.86940700	-1.61371600	-0.00662500
C	-4.04690500	-0.87869600	-0.00384300
C	-4.02229900	0.53220100	0.00336000
H	-2.81419400	2.32048200	0.00854400
H	-2.89529300	-2.70063600	-0.01484200
H	-5.00410600	-1.39315000	-0.00914100
H	-4.96011300	1.08141800	0.00134300
C	-0.26641300	-1.33605200	-0.00689900
C	0.52772400	-0.20361500	0.00597000
N	-0.32094700	0.91168700	0.02837100
H	0.09957700	-2.35419000	-0.01289000
C	0.06904200	2.30607600	-0.02114600

H	-0.52580900	2.88784100	0.69116500
H	1.11866300	2.40710200	0.25663500
H	-0.07130900	2.73328700	-1.02298500
Si	2.41292200	-0.19564600	0.00091100
C	3.08569000	0.71763200	-1.51892700
H	2.80762400	1.77773100	-1.53539700
H	4.18158100	0.66688300	-1.54298600
H	2.71200400	0.26383600	-2.44424200
C	2.97746600	-1.99929200	-0.06594400
H	4.07288700	-2.05309700	-0.07503400
H	2.62637700	-2.56823100	0.80238300
H	2.61450500	-2.50467900	-0.96798000
C	3.09981200	0.60248700	1.57891100
H	2.72299500	0.08904600	2.47110000
H	4.19509600	0.53688900	1.59430800
H	2.83602200	1.66228600	1.67329700

110

C	-3.16143900	-0.16430600	-0.00035300
C	-1.85789700	0.34417000	0.00152100
C	-0.70717800	-0.49234700	0.00238600
C	-0.89640300	-1.88517900	0.00244800
C	-2.18822100	-2.39886800	0.00045200
C	-3.31039800	-1.54714100	-0.00110400
H	-4.02757300	0.49193300	-0.00161700
H	-0.04250500	-2.55811400	0.00342400
H	-2.33818500	-3.47520900	-0.00033700
H	-4.30853100	-1.97675600	-0.00320900
C	0.46433900	0.36553400	0.00156900
C	-0.03964300	1.64888000	0.00066500
H	0.49048700	2.59313000	-0.00117000
N	-1.42019700	1.65655300	0.00120000
C	-2.27216400	2.82695300	0.00080800
H	-2.91106600	2.84901200	-0.89029000
H	-2.91313200	2.84762400	0.89044500
H	-1.64660700	3.72230000	0.00230900
Si	2.27593500	-0.09709100	0.00046200
C	2.67291600	-1.18726400	-1.49934700
H	3.72752800	-1.49012200	-1.50243100
H	2.06603700	-2.10039600	-1.50832700
H	2.47501000	-0.65426600	-2.43685100
C	2.72192400	-1.03683100	1.58554100
H	3.77708800	-1.33776000	1.58529000
H	2.55109900	-0.41584200	2.47284600
H	2.11799100	-1.94464800	1.70062900
C	3.31410100	1.48702800	-0.09269500
H	3.13415700	2.14480000	0.76628800
H	4.38391200	1.24490500	-0.09905300
H	3.10296300	2.05903000	-1.00416000

188

O	-1.72862800	1.86541700	-0.20460500
O	1.39375500	-0.03456600	1.19272200
O	2.62894700	-0.07035200	-1.10788600
O	-1.75413400	-1.81702100	-0.32105800
K	-1.42164200	-0.02917500	1.52773000
K	0.83640100	2.02648900	-0.59193800
K	-2.34181700	0.09170700	-2.10200600
K	0.80406000	-2.04871700	-0.72157500
C	-2.49771800	3.00269600	0.01696300
C	2.00649600	-0.16441600	2.44790100
C	-2.55192600	-2.94505100	-0.16365200
C	-3.70083000	3.06028300	-0.95991200
H	-4.33265200	2.16968500	-0.83033500
H	-4.33586300	3.94244600	-0.80439900
H	-3.34321200	3.08516700	-1.99820400
C	-1.65626200	4.29103200	-0.18649200
H	-2.23723000	5.21154800	-0.04207600
H	-0.82009100	4.31697300	0.52899400
H	-1.24587200	4.31127700	-1.20567500
C	-3.05518300	3.01644500	1.46602600
H	-3.69100300	2.13484700	1.63310200
H	-2.22703900	2.99103800	2.18911600
H	-3.66079700	3.90569700	1.68569900
C	3.09787800	0.91655300	2.63894700
H	2.65423800	1.91780200	2.55593300
H	3.59417600	0.84721700	3.61550700
H	3.86970400	0.82416600	1.86612300
C	2.65235400	-1.56458100	2.59427400
H	3.15055200	-1.70321500	3.56273700
H	1.88285600	-2.34350100	2.50028600
H	3.39808400	-1.72686200	1.80706400
C	0.98085000	0.00292900	3.59890500
H	0.23634200	-0.80633600	3.58140300
H	1.45839000	-0.03094100	4.58585100
H	0.46615600	0.97060900	3.51670200
C	-3.72559300	-2.94124800	-1.17691200
H	-3.33543500	-2.92356400	-2.20354900
H	-4.37773200	-3.81959600	-1.08153100
H	-4.34920300	-2.04817700	-1.02602500
C	-1.73191700	-4.24390100	-0.38960900
H	-0.91093000	-4.30767900	0.34079300
H	-2.33380100	-5.15611900	-0.28368800
H	-1.30268800	-4.24455900	-1.40141300
C	-3.15217400	-3.00080700	1.26739500
H	-2.34566600	-3.02533800	2.01475000
H	-3.77078200	-2.11035800	1.45070200
H	-3.78539400	-3.88218300	1.43473400
C	3.99651900	0.09333800	-1.53082800
C	4.00201700	-0.19621100	-3.03531300

H	3.67723000	-1.22499700	-3.23007700
H	3.31482400	0.47727200	-3.55905600
H	5.00622700	-0.06555800	-3.45438700
C	4.45316400	1.53895300	-1.26663700
H	3.82860600	2.24583400	-1.82817700
H	4.38829700	1.78514100	-0.19992900
H	5.49185400	1.69194700	-1.58262800
C	4.90343800	-0.90199300	-0.79126100
H	4.91735300	-0.70398600	0.28636400
H	4.55058800	-1.92847500	-0.94837500
H	5.93505100	-0.83886000	-1.15663000
H	2.47564000	-0.03610500	-0.10388600

195

C	0.17519000	1.11963000	-0.01485600
C	1.49171700	0.71186000	0.01656000
C	1.49173400	-0.71185300	0.01655100
C	0.17519800	-1.11962700	-0.01486200
N	-0.62562000	-0.00000800	-0.04101500
H	2.35599000	-1.36255500	0.02288100
C	-2.07410700	-0.00000300	0.02737100
H	-2.46519000	0.88644200	-0.47969900
H	-2.46519100	-0.88640900	-0.47976900
H	-2.43439200	-0.00004100	1.06388200
H	2.35596300	1.36257800	0.02294300
H	-0.26313000	2.10801400	-0.02389800
H	-0.26310400	-2.10801700	-0.02381900

TS-189 (195)

C	-0.92038000	-0.13975800	-0.97230800
C	-1.29152400	-1.46617800	-0.64010700
C	-2.24015700	-1.39697800	0.39975100
C	-2.51401000	-0.05744100	0.62498600
N	-1.78769100	0.70021000	-0.26437200
H	-2.69644400	-2.22775100	0.92173500
C	-1.66534400	2.13986800	-0.23539500
H	-1.63704500	2.53872400	-1.25485200
H	-2.52919300	2.56793100	0.27913100
H	-0.74577600	2.44880000	0.28301600
H	-0.88425200	-2.35972300	-1.09343200
H	-0.55905300	0.19568300	-1.93779300
H	-3.17379000	0.41604800	1.33903100
Si	1.42961200	0.03307300	0.05649700
C	2.28491700	-1.14050900	-1.17881300
H	3.29724700	-1.39797000	-0.83889600
H	1.72871500	-2.07737000	-1.29742700
H	2.37980800	-0.68191400	-2.17092800
C	2.52291900	1.60066700	0.20426500
H	3.54710500	1.34075300	0.51065000
H	2.59169600	2.13457000	-0.75101300

H	2.12345200	2.30060500	0.94766700
C	1.33888500	-0.80848700	1.76078400
H	0.98341300	-0.11471900	2.53127800
H	0.65366200	-1.66204800	1.74109100
H	2.32789600	-1.17322200	2.07140900

TS-191 (195)

C	1.32882700	-0.47665600	-1.01496500
C	0.43058400	0.60843600	-1.17976200
C	1.01755100	1.69891400	-0.40763400
C	2.08670100	1.19826300	0.27823000
N	2.28377500	-0.12327300	-0.08100100
H	0.64082800	2.71098800	-0.34630600
C	3.21686000	-1.03371500	0.54683100
H	3.60661400	-1.73593500	-0.19739700
H	4.05704000	-0.46743300	0.95792500
H	2.74929100	-1.60853800	1.35821800
H	-0.10580300	0.76733700	-2.10898700
H	1.31682500	-1.46899600	-1.44187600
H	2.74400000	1.66764000	0.99820900
Si	-1.61108900	-0.05338400	0.03940300
C	-2.19728400	-1.63621500	-0.85019200
H	-2.91097900	-2.20308300	-0.23688500
H	-2.69228200	-1.40095700	-1.80015400
H	-1.35376300	-2.30144300	-1.07099300
C	-0.91378700	-0.53267800	1.74317400
H	-1.66572400	-1.05414500	2.35016000
H	-0.05045200	-1.20028600	1.63899000
H	-0.58550600	0.35040500	2.30280300
C	-3.11746600	1.09699700	0.30530700
H	-2.82143000	2.02320000	0.81208600
H	-3.58120400	1.37582200	-0.64830400
H	-3.89055900	0.61564700	0.92193600

189 (195)

C	-0.46405100	-0.13238300	-0.69391800
C	-1.00830200	-1.53540700	-0.62642400
C	-2.21136200	-1.51811600	0.06553200
C	-2.50355300	-0.21270800	0.44611400
N	-1.46548800	0.64665800	0.08139200
H	-2.83001700	-2.37841500	0.29373700
C	-1.75783400	2.00723100	-0.32802700
H	-2.17791800	2.05965700	-1.34811500
H	-2.48333500	2.44671800	0.36412000
H	-0.84996800	2.61702000	-0.29986700
H	-0.51654000	-2.39630600	-1.06050400
H	-0.42961600	0.24823500	-1.73749900
H	-3.34871500	0.16971200	1.00386500
Si	1.31164200	0.00030100	0.06087100
C	2.46415100	-1.08023400	-0.98843900

H	3.49569700	-1.02626500	-0.61915800
H	2.16187100	-2.13368400	-0.96647000
H	2.47413800	-0.75845300	-2.03718800
C	1.93271400	1.79270700	-0.00102900
H	2.97583700	1.85107400	0.33435400
H	1.89177700	2.20263400	-1.01764400
H	1.34409000	2.44875100	0.65068400
C	1.27857700	-0.60383300	1.85057500
H	0.58811900	-0.00123100	2.45124200
H	0.94578000	-1.64582700	1.90999700
H	2.27217700	-0.53798300	2.31021600

191 (195)

C	1.17431500	-0.73147200	-0.64577200
C	0.11670500	0.32239300	-0.84870400
C	0.80956100	1.55673700	-0.30576100
C	2.06301000	1.23231400	0.07083600
N	2.34143400	-0.10569500	-0.19401500
H	0.37200200	2.54540700	-0.25524300
C	3.47197500	-0.82520300	0.34702300
H	3.75188200	-1.63678200	-0.33407300
H	4.32701500	-0.14912300	0.44156500
H	3.25679200	-1.26539300	1.33319700
H	-0.15971300	0.45032700	-1.91693600
H	1.27085300	-1.64175400	-1.22881500
H	2.83093900	1.85636500	0.51329700
Si	-1.52180300	-0.11397600	0.07148000
C	-2.18797300	-1.74514000	-0.62792100
H	-3.12135300	-2.04177600	-0.13372300
H	-2.39480800	-1.66580200	-1.70238900
H	-1.46507000	-2.55705500	-0.48630900
C	-1.19224400	-0.28435700	1.92593900
H	-2.10787000	-0.53843300	2.47371200
H	-0.45367600	-1.07106800	2.11708300
H	-0.79756900	0.64915700	2.34317400
C	-2.79104900	1.26459100	-0.23445100
H	-2.44533900	2.22589000	0.16446400
H	-2.98474000	1.40060900	-1.30566800
H	-3.74993700	1.03577700	0.24691200

TS-190 (195)

H	2.33008500	0.09525700	-0.79600000
Si	4.83774000	-1.00449100	-0.24871300
C	5.80867300	-0.74709600	-1.86488300
H	6.46697500	-1.60873300	-2.03646300
H	6.45291800	0.13877800	-1.80631300
H	5.16941000	-0.64091700	-2.74707900
C	3.89258100	-2.65480200	-0.37113000
H	4.57249900	-3.49379400	-0.56468400
H	3.15404600	-2.62207900	-1.18162400

H	3.36159500	-2.87389900	0.56503500
C	6.13573200	-1.16002800	1.13084700
H	5.66369000	-1.39487300	2.09165700
H	6.67796900	-0.21495800	1.25820400
H	6.87413700	-1.94247800	0.91354200
O	1.27504200	-0.16452100	-1.24464100
C	1.09285400	0.11077000	-2.63163400
C	0.11001800	-0.93448300	-3.20070100
H	-0.80854900	-1.00962700	-2.60577100
H	0.57455200	-1.92936000	-3.19648800
H	-0.16419200	-0.70665700	-4.24074500
C	0.52355700	1.53653200	-2.80642200
H	1.27287300	2.28392200	-2.51873500
H	-0.34274300	1.70169000	-2.15341000
H	0.23273500	1.74269000	-3.84684000
C	2.41095800	-0.00380800	-3.41702100
H	3.14362400	0.72576800	-3.06450100
H	2.24342600	0.17258900	-4.48719900
H	2.83953900	-1.00476400	-3.29976700
K	0.20263500	1.46011400	0.87189800
C	3.55137600	2.39117800	1.26494000
C	3.01501900	1.44356700	2.14017500
C	3.01518200	0.20334900	1.50029900
C	3.55311400	0.34090200	0.13580300
H	2.68069600	-0.73093000	1.93658800
O	-0.86243800	-0.63881800	2.17266600
K	-0.26758200	-2.00338900	0.03184000
C	-0.70947800	-1.13702700	3.45926500
C	0.08822400	-0.14853000	4.34519200
H	0.22113000	-0.50571500	5.37530200
H	1.08025000	0.02030400	3.91206000
H	-0.43411500	0.81697700	4.38498300
C	-2.08982300	-1.37695200	4.13415400
H	-2.68806500	-2.08255300	3.53894400
H	-2.00579400	-1.79002800	5.14791700
H	-2.64163600	-0.42844900	4.21573100
C	0.04512000	-2.49468600	3.44028100
H	1.03056200	-2.36875700	2.97204800
H	0.20435200	-2.91465200	4.44220500
H	-0.52519900	-3.23605000	2.86038500
O	-2.35044600	2.02837700	-0.08033500
O	-2.79572800	-1.49174700	-0.90121900
K	-3.21213700	-0.05020500	1.31125400
K	-2.85565500	0.72477000	-2.22970900
C	-3.58994300	-2.57753800	-1.24830800
C	-2.77069600	-3.89619100	-1.23892900
H	-2.37787900	-4.08933000	-0.23010800
H	-3.36337600	-4.77310100	-1.52996700
H	-1.92628000	-3.81810600	-1.93728300
C	-4.18563500	-2.39983100	-2.67174400

H	-4.79776300	-3.25230000	-2.99380100
H	-4.83129300	-1.50868600	-2.70549800
H	-3.37667200	-2.27251700	-3.40376700
C	-4.76933800	-2.74077800	-0.25209700
H	-4.38413100	-2.90091500	0.76468700
H	-5.38771300	-1.83129600	-0.24942700
H	-5.42590900	-3.58665800	-0.49482900
C	-2.80738600	3.32632700	0.11527300
C	-3.36464700	3.92482900	-1.20561400
H	-4.21295500	3.32257600	-1.56705700
H	-3.72595500	4.95543000	-1.09441200
H	-2.58239100	3.92704100	-1.97706300
C	-3.94598900	3.35765700	1.17063200
H	-3.58039000	2.96457600	2.12971600
H	-4.33722400	4.36703900	1.35449100
H	-4.78702500	2.73224500	0.83671800
C	-1.66747600	4.25363500	0.61240200
H	-1.98858600	5.29527500	0.74338400
H	-1.28989100	3.90525200	1.58456100
H	-0.83588400	4.24708500	-0.10500600
N	4.02505500	1.73545100	0.13036500
C	4.25649700	2.47466300	-1.08690600
H	4.81654800	3.38893700	-0.86049400
H	4.84618600	1.87985500	-1.78778500
H	3.31464000	2.77330400	-1.58991100
H	2.67885400	1.65417300	3.15028900
H	3.81422600	3.42533400	1.44760800

TS-192(195)

H	2.25007300	-0.31785000	-0.87102600
Si	4.53129900	-1.40151500	0.02357900
C	5.45218900	-1.88293000	-1.56686300
H	6.08171600	-2.76416400	-1.38883300
H	6.11245800	-1.07113000	-1.89606800
H	4.77849700	-2.11761500	-2.39697500
C	3.38480400	-2.84908900	0.51868300
H	3.95187800	-3.76255300	0.73819900
H	2.68133700	-3.07424400	-0.29341600
H	2.80818100	-2.59920000	1.42084800
C	5.84951900	-1.23655300	1.38808900
H	5.39195700	-1.05540800	2.36814300
H	6.51596200	-0.39069300	1.17967000
H	6.46943500	-2.13925000	1.46908000
O	1.17369900	-0.61670200	-1.27500800
C	1.01983200	-0.54999200	-2.69001800
C	-0.02521800	-1.61003900	-3.09391600
H	-0.92726800	-1.54680400	-2.47220600
H	0.38524600	-2.61678300	-2.94411100
H	-0.31133200	-1.52590000	-4.15106900
C	0.55706700	0.86607500	-3.09366000

H	1.33013100	1.59421700	-2.81539600
H	-0.36394600	1.15597600	-2.56829800
H	0.38138600	0.95567600	-4.17381500
C	2.33600400	-0.86136800	-3.42293200
H	3.10429200	-0.12877100	-3.16120700
H	2.19205600	-0.83687800	-4.51049300
H	2.69514500	-1.85930300	-3.15074800
K	0.23887200	1.56702200	0.32019800
C	3.48966800	2.13159800	1.06761500
C	3.13057000	0.81782500	1.08289100
C	3.50456900	0.16717200	-0.19219200
H	2.69380000	0.31529000	1.94017200
O	-0.65620400	-0.12302000	2.20550900
K	-0.27570700	-2.03872900	0.46615800
C	-0.38989200	-0.16799100	3.56780400
C	0.29473500	1.13942000	4.04428300
H	0.49775200	1.14835600	5.12362300
H	1.24852400	1.28121300	3.52185300
H	-0.34899400	1.99932200	3.81388800
C	-1.69921000	-0.34132600	4.38944900
H	-2.23397600	-1.24484700	4.06296000
H	-1.51851400	-0.43303900	5.46840600
H	-2.35938500	0.52816300	4.24819900
C	0.53913600	-1.36280400	3.90975800
H	1.47745500	-1.28217500	3.34644400
H	0.79128400	-1.42150600	4.97691200
H	0.05255100	-2.30987800	3.63286900
O	-2.37769900	1.96760000	-0.44372700
O	-2.83967600	-1.65353400	-0.42283200
K	-3.09152600	0.24901400	1.43501000
K	-2.91695200	0.21023200	-2.21048300
C	-3.68084300	-2.75696300	-0.48629600
C	-2.89863000	-4.07312800	-0.23063400
H	-2.45377200	-4.05801500	0.77498000
H	-3.53030500	-4.96869200	-0.29277700
H	-2.09343700	-4.18120900	-0.97016400
C	-4.35106300	-2.86714700	-1.88348900
H	-5.00251400	-3.74504100	-1.98308300
H	-4.97449500	-1.98038200	-2.07641200
H	-3.58133000	-2.93124200	-2.66455900
C	-4.80684100	-2.65482500	0.57759200
H	-4.36978300	-2.60925600	1.58500700
H	-5.39599000	-1.74080900	0.41351200
H	-5.50162300	-3.50482100	0.55669400
C	-2.85459200	3.27170000	-0.50598400
C	-3.48633000	3.56491700	-1.89437100
H	-4.33803000	2.89008300	-2.07321100
H	-3.86237100	4.59176300	-1.99050600
H	-2.74112200	3.40742200	-2.68625200
C	-3.94272100	3.51246600	0.57508700

H	-3.52135500	3.34449400	1.57630100
H	-4.35209000	4.53104700	0.55647200
H	-4.78045300	2.81487300	0.42878200
C	-1.71437000	4.29704000	-0.27432100
H	-2.05674900	5.33873600	-0.32947900
H	-1.27104400	4.15075500	0.72104000
H	-0.92629500	4.16519900	-1.02803100
H	3.38868900	2.88891400	1.83737200
N	4.16856900	2.42848700	-0.11843600
C	4.22348000	3.77342400	-0.64425100
H	5.00653300	3.84013200	-1.40566100
H	3.26386900	4.07545200	-1.11400600
H	4.46239600	4.47969700	0.15771400
C	4.04727500	1.29984800	-0.96821900
H	4.77055800	1.22050300	-1.77535200

190 (195)

C	2.76920200	-0.03748400	0.01656200
C	2.59736300	1.33036400	-0.00508000
C	1.19935600	1.56227900	-0.01550400
C	0.53719200	0.33584900	0.00015800
N	1.53459400	-0.63672800	0.02456600
H	0.71253700	2.52888300	-0.02626400
C	1.33335500	-2.07396200	-0.01761500
H	2.28230200	-2.57179400	0.19551800
H	0.60681100	-2.38620700	0.73863300
H	0.98140700	-2.40318700	-1.00232300
Si	-1.31928000	0.06950000	0.00151200
C	-1.88075600	-0.96583500	-1.48687500
H	-1.47502700	-1.98407100	-1.46859800
H	-2.97468400	-1.05232200	-1.50425600
H	-1.56899900	-0.50149800	-2.42977700
C	-2.12763800	1.77728600	-0.10624900
H	-3.22031900	1.68190600	-0.10667500
H	-1.85211700	2.41192500	0.74375100
H	-1.84029800	2.30290900	-1.02393400
C	-1.90621100	-0.78052000	1.59420400
H	-1.60031500	-0.20997800	2.47879100
H	-3.00093100	-0.85739600	1.60858900
H	-1.50925300	-1.79684100	1.70263900
H	3.38590600	2.07105500	-0.00530700
H	3.66956100	-0.63715700	0.02846800

192(195)

Si	1.61223500	0.09240300	0.00204100
C	2.40598100	-0.67347600	1.54497300
H	3.49264300	-0.52116600	1.55202400
H	1.99929500	-0.22876400	2.46092000
H	2.22334600	-1.75375200	1.59544500
C	2.41146900	-0.67456800	-1.53761000

H 3.49787200 -0.52008000 -1.54221600
 H 2.23095900 -1.75525900 -1.58664200
 H 2.00621400 -0.23224000 -2.45534900
 C 1.93424400 1.96149300 0.00128300
 H 1.51213500 2.44573700 -0.88757500
 H 1.50277500 2.44797500 0.88437800
 H 3.01152600 2.16802700 0.00652300
 C -2.27128400 -1.23540500 -0.00974300
 C -0.91856400 -1.48082400 0.01005700
 C -0.22963500 -0.21921400 0.00168700
 H -3.11871600 -1.90751000 -0.01154800
 H -0.46269800 -2.46304100 0.01612300
 C -3.74295300 0.80441200 0.02836600
 H -4.47751700 0.26407600 -0.57601500
 H -4.11594800 0.87310900 1.05784900
 H -3.64115000 1.81486300 -0.37574800
 N -2.46001800 0.13008300 -0.03463900
 C -1.23054100 0.74133600 -0.02109700
 H -1.16419700 1.82126600 -0.03177000

194

C 1.09505600 -0.34701200 0.00013900
 C 0.71743600 0.96026000 0.00021000
 C -0.71827600 0.95974100 -0.00004800
 C -1.09464700 -0.34795700 -0.00019000
 H -1.37495200 1.81859400 -0.00009300
 H 1.37344000 1.81964700 0.00039800
 H 2.05048400 -0.84907400 0.00024400
 O 0.00042800 -1.16109700 -0.00010500
 H -2.04980900 -0.85058400 -0.00037400

TS-189 (194)

C 2.53815600 -0.82127300 0.28585000
 C 2.59945200 0.50728700 0.59970200
 C 1.73544900 1.17783000 -0.31070700
 C 1.12797600 0.18819300 -1.07754400
 H 1.54378800 2.23989500 -0.37481900
 H 3.19869500 0.95110900 1.38311400
 H 3.01185700 -1.70309900 0.68986400
 O 1.69841300 -1.03150100 -0.76971500
 H 0.69533100 0.24590500 -2.06531600
 Si -1.32380600 -0.04012700 0.01138400
 C -2.04297300 1.69414700 -0.31108200
 H -2.97321000 1.84719700 0.25325000
 H -1.34009800 2.47834900 -0.00667700
 H -2.27270900 1.84476300 -1.37259100
 C -2.56298900 -1.36202200 -0.58534500
 H -3.51842600 -1.28382200 -0.04657700
 H -2.77673900 -1.25779800 -1.65537800
 H -2.17075700 -2.37216900 -0.42169500

C	-1.00201700	-0.26045500	1.87194800
H	-0.67055900	-1.27967900	2.09987100
H	-0.22605700	0.42785600	2.22350700
H	-1.91346600	-0.06696400	2.45485600

TS-191 (194)

C	-2.52511800	-0.79798700	0.23107900
C	-1.65488000	-1.08140300	-0.76219800
C	-0.97714000	0.16930200	-1.10141500
C	-1.65185300	1.13425100	-0.34708500
H	-0.53362900	0.37941200	-2.06696500
H	-1.45317200	-2.05788700	-1.18048400
H	-3.19585700	-1.40415000	0.82189600
O	-2.52983700	0.54070400	0.52784000
H	-1.54852000	2.20365400	-0.25167100
Si	1.29292300	-0.04291400	-0.00596500
C	1.97677100	1.72701900	-0.16250000
H	2.84538500	1.87784000	0.49267100
H	2.29560400	1.94557200	-1.18868900
H	1.22106000	2.46989800	0.11811300
C	0.80499300	-0.38652800	1.79657800
H	1.64238800	-0.18934300	2.47913300
H	-0.03466400	0.24626200	2.10519500
H	0.50117900	-1.43031900	1.93392600
C	2.63530100	-1.28623100	-0.55464600
H	2.26936100	-2.31790300	-0.49694900
H	2.95227500	-1.10290100	-1.58789300
H	3.52791700	-1.21550300	0.08364100

189 (194)

C	2.50125300	-0.71926400	0.16369400
C	2.61622000	0.65784800	0.20646500
C	1.48406900	1.20959100	-0.38332600
C	0.59097400	0.08424400	-0.80689400
H	1.26564600	2.25756900	-0.53914500
H	3.45708800	1.19649900	0.62593200
H	3.14795500	-1.51140300	0.51306400
O	1.33874900	-1.12298600	-0.43537900
H	0.44280800	0.04194500	-1.90182700
Si	-1.13924800	0.00406500	0.05700700
C	-2.08691500	1.57679700	-0.41119100
H	-3.09274400	1.57214900	0.02637700
H	-1.57586300	2.47728100	-0.05068400
H	-2.20293200	1.67035800	-1.49788800
C	-2.05185500	-1.52617600	-0.57817800
H	-3.02854500	-1.63848600	-0.09171200
H	-2.22504500	-1.47107900	-1.65976100
H	-1.47171200	-2.43448300	-0.38024500
C	-0.88471000	-0.09598500	1.92529800
H	-0.32122600	-0.99609200	2.19488300

H	-0.32566900	0.77045100	2.29584200
H	-1.84448800	-0.13006400	2.45488400

191 (194)

C	2.53696700	0.67415000	0.18742900
C	1.45858300	1.17234000	-0.42624500
C	0.57107000	0.02412300	-0.85447300
C	1.45602400	-1.13606900	-0.50322300
H	0.33908800	0.06066400	-1.93555100
H	1.24279100	2.22245300	-0.57326800
H	3.38923300	1.15347900	0.65029900
O	2.55861500	-0.70143700	0.22647100
H	1.16156900	-2.15298700	-0.27270700
Si	-1.14429500	0.00480700	0.04990800
C	-2.09545400	-1.53257300	-0.51792600
H	-3.08292700	-1.58230600	-0.04289200
H	-2.25169100	-1.53002700	-1.60355600
H	-1.56210600	-2.45578900	-0.26182100
C	-0.87011600	-0.04441500	1.91946400
H	-1.82402100	-0.08500800	2.45907500
H	-0.28368700	-0.92316200	2.21154500
H	-0.32748100	0.84331200	2.26328500
C	-2.10837400	1.56286700	-0.43677200
H	-1.58893900	2.47409000	-0.11720500
H	-2.24970000	1.62375200	-1.52277200
H	-3.10312200	1.57318900	0.02556900

TS-190 (194)

H	2.25130800	-0.33869600	-0.81422700
Si	5.01258000	-0.80985000	0.03253100
C	5.45900700	-1.76399600	-1.54674800
H	6.37530800	-2.34700800	-1.38844000
H	5.63993800	-1.08683500	-2.38944500
H	4.66923200	-2.46293600	-1.84332400
C	4.47525800	-2.07340100	1.35277000
H	5.27451200	-2.79740500	1.55525700
H	3.59408000	-2.63822000	1.02016100
H	4.22309600	-1.58804600	2.30379500
C	6.59525100	0.05990100	0.62957500
H	6.41536700	0.59643800	1.56856500
H	6.92973400	0.79858300	-0.10917000
H	7.42016300	-0.64542600	0.79358800
O	1.26973900	-0.69757900	-1.18147200
C	1.12901300	-0.62089100	-2.60640400
C	0.09373300	-1.68707100	-3.01012800
H	-0.80587500	-1.63569800	-2.38404100
H	0.51247000	-2.69203900	-2.87510800
H	-0.19752600	-1.58968500	-4.06524200
C	0.65128300	0.79228100	-2.99971300
H	1.41506900	1.52765500	-2.72252200

H	-0.27487700	1.06916600	-2.47765500
H	0.47657400	0.87799300	-4.08061400
C	2.45439400	-0.91430400	-3.32415500
H	3.21016000	-0.17343800	-3.05272900
H	2.31502100	-0.88906900	-4.41248600
H	2.82383000	-1.90752400	-3.05136900
K	0.29557200	1.58627200	0.34307600
C	3.48376400	2.63710100	-0.75115900
C	3.21950000	2.56601300	0.60880600
C	3.27290400	1.21875500	0.99117800
C	3.57793900	0.39915200	-0.18217400
H	3.16866700	0.83655900	1.99989700
O	-0.63358100	-0.06736300	2.22940900
K	-0.23554500	-2.03809400	0.58179000
C	-0.30585400	-0.06782100	3.57925200
C	0.38023900	1.26274200	3.98190900
H	0.63829400	1.30739600	5.04846100
H	1.30371700	1.39944000	3.40585100
H	-0.28811200	2.10638400	3.76059300
C	-1.57657900	-0.23624100	4.45783200
H	-2.104449000	-1.16116100	4.18494500
H	-1.35365100	-0.28301300	5.53189000
H	-2.26021700	0.61303700	4.30632400
C	0.66010900	-1.23629200	3.90937900
H	1.56422800	-1.15910300	3.29219200
H	0.97038500	-1.25599000	4.96253000
H	0.17421700	-2.19994500	3.69328100
O	-2.31715600	1.91058100	-0.51299100
O	-2.77148000	-1.70325900	-0.35954100
K	-3.05314300	0.26961300	1.43185600
K	-2.84851200	0.09010000	-2.21727400
C	-3.60317600	-2.81491600	-0.40186200
C	-2.80451100	-4.12203600	-0.14928400
H	-2.35566600	-4.10306900	0.85466700
H	-3.42643200	-5.02461600	-0.20819200
H	-2.00099600	-4.22055900	-0.89186300
C	-4.29345700	-2.94220500	-1.78783900
H	-4.94374500	-3.82278300	-1.86843100
H	-4.92179600	-2.05893400	-1.98069200
H	-3.53550800	-3.01370600	-2.58011900
C	-4.71335900	-2.71603900	0.67832700
H	-4.26017200	-2.65053600	1.67729300
H	-5.31923800	-1.81342900	0.51250100
H	-5.39504700	-3.57673800	0.67872500
C	-2.78891600	3.21107200	-0.64589000
C	-3.44523400	3.42481100	-2.03785100
H	-4.30321000	2.74564500	-2.16134100
H	-3.81854700	4.44611000	-2.18766000
H	-2.71559500	3.21823900	-2.83333300
C	-3.85575300	3.52210100	0.43788200

H	-3.41771300	3.40540000	1.43902700
H	-4.25809100	4.54129600	0.36905800
H	-4.70087300	2.82433600	0.34488700
C	-1.63939100	4.24198900	-0.49930500
H	-1.97480100	5.27897400	-0.63107300
H	-1.19035300	4.16965700	0.50149700
H	-0.85799300	4.04512400	-1.24547500
H	3.01972600	3.42038100	1.24893600
H	3.67417300	3.47739000	-1.40467300
O	3.81236400	1.39189100	-1.25116200

TS-192 (194)

H	2.46727900	0.76767500	-0.11636900
Si	5.29359600	0.43394700	-0.00112800
C	5.67823900	1.42585800	1.57791100
H	6.72475300	1.75643800	1.57319400
H	5.54228100	0.79662700	2.46679300
H	5.05436000	2.31669100	1.70861600
C	5.58916500	1.51040500	-1.54184000
H	6.62680600	1.86601000	-1.57607300
H	4.93422000	2.38685500	-1.57552600
H	5.41504800	0.93082400	-2.45748100
C	6.56863800	-0.97804200	-0.05508800
H	6.45924200	-1.57753800	-0.96649400
H	6.43844700	-1.65512600	0.79783400
H	7.59747600	-0.59677700	-0.02530400
O	1.43502200	1.37511300	-0.29228700
C	1.42664200	2.65294800	0.32622100
C	0.20142200	3.43877300	-0.18452300
H	-0.72802300	2.86094600	-0.11694200
H	0.33378900	3.70045800	-1.24321600
H	0.06885900	4.38113800	0.36399700
C	1.35850500	2.49150100	1.86076000
H	2.23093700	1.93825700	2.22247100
H	0.47567500	1.90451900	2.15148800
H	1.32155600	3.45783400	2.38083200
C	2.68051800	3.46862300	-0.04353200
H	3.58666800	2.99476500	0.33619400
H	2.63062000	4.48461400	0.36876600
H	2.76716700	3.54457700	-1.13327200
K	0.32231100	-1.33385900	0.77907700
C	2.94643100	-2.43119000	-0.57008900
C	3.27297600	-1.22201100	-1.06645900
C	3.53414800	-0.26596900	0.03975100
H	3.35326600	-0.99696200	-2.12484800
O	-1.09612900	-1.71414000	-1.47813900
K	-0.52909700	0.75329400	-2.03633800
C	-1.03651800	-2.76367800	-2.38596400
C	-0.59937400	-4.07520400	-1.68453700
H	-0.56404500	-4.93627500	-2.36546500

H	0.39761700	-3.95232300	-1.24458400
H	-1.29886400	-4.31334100	-0.87176600
C	-2.42425600	-3.00898500	-3.04020100
H	-2.78758700	-2.08370600	-3.50805900
H	-2.40448800	-3.79285600	-3.80897900
H	-3.15821100	-3.32138800	-2.28139000
C	-0.02283400	-2.45338500	-3.51949900
H	0.95855400	-2.22941600	-3.08444400
H	0.09586400	-3.28183300	-4.23055200
H	-0.35393700	-1.57540200	-4.09552900
O	-2.03206100	-0.75537000	2.05446400
O	-2.83757300	1.45153100	-0.71458900
K	-3.27613500	-1.14356200	-0.24247900
K	-2.29368500	1.75799200	1.78690400
C	-3.77132900	2.23710700	-1.37796600
C	-3.20310400	2.76944500	-2.72107100
H	-2.94724900	1.92803400	-3.38135100
H	-3.91279100	3.40573100	-3.26557900
H	-2.29607700	3.36139300	-2.53898100
C	-4.18085200	3.46302900	-0.51597400
H	-4.90583800	4.11917300	-1.01480900
H	-4.64323400	3.12649300	0.42466200
H	-3.29519900	4.06619300	-0.27459900
C	-5.05674800	1.42499800	-1.69275200
H	-4.81285200	0.56431800	-2.33124300
H	-5.50352700	1.05102500	-0.76002100
H	-5.82299700	2.01499800	-2.21263500
C	-2.34849700	-1.41861100	3.23407800
C	-2.70756200	-0.40805400	4.35838000
H	-3.57877900	0.19627700	4.06154000
H	-2.95856300	-0.89149100	5.31140700
H	-1.85862300	0.26558700	4.54365500
C	-3.56881500	-2.35462400	3.02480000
H	-3.33909000	-3.09956800	2.25027400
H	-3.85713600	-2.89923200	3.93349800
H	-4.44060300	-1.76962700	2.69683300
C	-1.15844600	-2.28015000	3.72876100
H	-1.37201200	-2.80508400	4.66904900
H	-0.90491300	-3.04161700	2.97820300
H	-0.27521400	-1.64798800	3.89133600
H	2.69821000	-3.37179500	-1.04313400
C	3.22669900	-1.09962700	1.22295300
H	3.76522400	-1.08825700	2.16861000
O	2.94209200	-2.44682000	0.81359300

190 (194)

C	2.71776200	-0.72639700	0.00013600
C	2.88334200	0.62484900	0.00019900
C	1.56289400	1.17828200	-0.00004200
C	0.67363500	0.13386100	-0.00022500

H	1.30381300	2.22883700	-0.00012400
Si	-1.20128900	0.00625800	-0.00000200
C	-1.76539700	-0.92939200	-1.54413000
H	-1.31276000	-1.92679000	-1.58701400
H	-2.85501700	-1.05661800	-1.55534900
H	-1.48028000	-0.39608500	-2.45836300
C	-1.88689900	1.76901900	-0.00555800
H	-2.98351600	1.75382300	-0.00396800
H	-1.56409400	2.33190600	0.87799400
H	-1.56647400	2.32513500	-0.89423700
C	-1.76614000	-0.91974000	1.54970200
H	-1.48031700	-0.38133500	2.46071900
H	-2.85590300	-1.04570100	1.56182500
H	-1.31460000	-1.91737200	1.59840600
H	3.82308500	1.15977100	0.00034700
H	3.40536800	-1.55944500	0.00021500
O	1.39794300	-1.04833000	-0.00011500

192 (194)

Si	-1.21701500	-0.00489100	-0.00004600
C	-1.82519700	1.78835800	-0.00083300
H	-2.92140200	1.82290500	-0.00109600
H	-1.48064800	2.33472400	0.88523600
H	-1.48022800	2.33423200	-0.88703700
C	-1.85438900	-0.89569300	-1.54507900
H	-2.95100700	-0.92503700	-1.56081300
H	-1.51987400	-0.39168200	-2.45933500
H	-1.49603000	-1.93120600	-1.58964400
C	-1.85448500	-0.89398700	1.54594000
H	-1.49698100	-1.92975800	1.59129200
H	-1.51927900	-0.38944700	2.45965100
H	-2.95112600	-0.92240300	1.56204800
C	2.82709500	-0.65352500	0.00013400
C	1.56222200	-1.14784800	0.00012300
C	0.65871300	-0.01437000	-0.00006400
H	3.80837200	-1.10375800	0.00023900
H	1.29026000	-2.19525100	0.00023800
O	2.80369500	0.71188300	-0.00003600
C	1.48904500	1.07250700	-0.00014000
H	1.30856200	2.13744900	-0.00032800

193

C	-0.01190200	-1.24340800	-0.00000100
C	-1.27302600	-0.71463500	-0.00000900
C	-1.27239500	0.71534800	0.00000700
C	-0.01079000	1.24310900	0.00003100
H	-2.17179700	1.32175600	0.00001300
H	-2.17315100	-1.31999100	-0.00001800
H	0.28061500	-2.28473500	-0.00000500
S	1.19948300	-0.00026300	-0.00001400

H	0.28128500	2.28469900	0.00005500
---	------------	------------	------------

TS-189 (193)

C	0.90627600	0.07786600	-1.11060000
C	1.36511100	1.31445100	-0.65314200
C	2.31204500	1.20428200	0.39695600
C	2.65653900	-0.09365100	0.68310500
H	2.73034500	2.05643400	0.92294800
H	0.99949900	2.25739700	-1.04442500
H	0.45591700	-0.11437300	-2.07416300
S	1.82782500	-1.22109700	-0.35405100
H	3.33159000	-0.45530000	1.44688900
Si	-1.59798800	-0.03424200	0.01287300
C	-2.90837200	-1.31992600	-0.50571500
H	-3.81278000	-1.23459200	0.11395800
H	-3.20877800	-1.18638700	-1.55129300
H	-2.52729400	-2.34159000	-0.39567400
C	-1.13321500	-0.27990800	1.83648000
H	-1.99036300	-0.07902100	2.49383200
H	-0.79930600	-1.30620400	2.02452400
H	-0.31908300	0.39246200	2.12776100
C	-2.27725700	1.72316500	-0.25612900
H	-1.52300400	2.47840100	-0.00823900
H	-2.58297300	1.88241900	-1.29677400
H	-3.15390000	1.90961800	0.37951600

TS-191 (193)

C	-1.41695200	1.02744600	-0.71180500
C	-0.67150600	-0.03863900	-1.22670100
C	-1.21899300	-1.31084700	-0.78483900
C	-2.21864600	-1.18180700	0.12311700
H	-0.83744800	-2.26977800	-1.12015000
H	-0.12147700	0.05880000	-2.15701300
H	-1.30224100	2.08117900	-0.92436100
S	-2.60251100	0.49539700	0.45021700
H	-2.75748200	-1.96609200	0.63841600
Si	1.59247900	-0.00658700	0.04411400
C	2.23832700	1.73670000	-0.36025300
H	3.08669300	2.00408800	0.28436300
H	2.57773600	1.80956000	-1.40030900
H	1.45842200	2.49168100	-0.20856000
C	1.09296000	-0.10581700	1.87191200
H	1.94575700	0.12386100	2.52541600
H	0.29232100	0.60550600	2.10076700
H	0.73177400	-1.10670800	2.13245000
C	2.95357000	-1.29188500	-0.32642800
H	2.60764700	-2.31075300	-0.11753800
H	3.26629400	-1.25441300	-1.37636600
H	3.84490100	-1.11196800	0.29181300

189 (193)

C	0.37579600	0.12393000	-0.80768300
C	1.12115500	1.39460800	-0.52260000
C	2.33078300	1.23343400	0.12555300
C	2.69737400	-0.08918800	0.36713100
H	2.96265100	2.06660500	0.42095700
H	0.70658600	2.35532900	-0.80995800
H	0.20705500	-0.01715000	-1.88691900
S	1.51527000	-1.24008900	-0.23491900
H	3.59341900	-0.44504000	0.85794300
Si	-1.34299600	0.01548700	0.07059800
C	-2.12584100	-1.65885900	-0.33597800
H	-3.11823300	-1.74690600	0.12301400
H	-2.24948800	-1.79450700	-1.41730200
H	-1.51363500	-2.48755200	0.03789200
C	-1.12063100	0.21955700	1.93330700
H	-2.08667400	0.17491200	2.45067200
H	-0.48263700	-0.57165600	2.34167300
H	-0.65422600	1.18143000	2.17348300
C	-2.42038500	1.41027000	-0.62749800
H	-1.99981100	2.39779700	-0.40425100
H	-2.52927000	1.33146900	-1.71606400
H	-3.42761900	1.37735700	-0.19419600

191 (193)

C	1.15196400	-1.03119400	-0.53579900
C	0.25221800	0.12163000	-0.86114900
C	1.00704100	1.36037200	-0.46181100
C	2.21187200	1.15507600	0.08878800
H	0.59089400	2.35439400	-0.60017700
H	-0.00972000	0.15314100	-1.93778000
H	1.02867200	-2.04347000	-0.89640200
S	2.67660500	-0.55283300	0.18080800
H	2.89829400	1.90549100	0.46264100
Si	-1.44633700	-0.03925500	0.06731100
C	-2.27416200	-1.64681500	-0.49632000
H	-3.25433600	-1.76928000	-0.01940800
H	-2.43274000	-1.65976700	-1.58165700
H	-1.66862900	-2.52252300	-0.23610600
C	-1.15362000	-0.06240700	1.93291500
H	-2.09811400	-0.17620600	2.47876900
H	-0.49844200	-0.89364900	2.21545200
H	-0.67911000	0.86446000	2.27459700
C	-2.54627200	1.43104600	-0.41093300
H	-2.11424100	2.38554100	-0.08750800
H	-2.69750900	1.48439200	-1.49607700
H	-3.53622000	1.34612200	0.05423800

TS-190 (193)

H	2.27395300	-0.33777200	-0.74214500
---	------------	-------------	-------------

Si	4.88125300	-1.03816400	0.02548700
C	5.70771600	-1.37107300	-1.65037400
H	6.57087900	-2.03546900	-1.51654000
H	6.07739400	-0.43894400	-2.09454600
H	5.03541700	-1.84244300	-2.37378000
C	4.08482300	-2.65055000	0.65961100
H	4.83061200	-3.44414500	0.79470800
H	3.32914300	-3.01544300	-0.04778100
H	3.59372300	-2.49456800	1.62963200
C	6.25858700	-0.54303300	1.23703000
H	5.86090600	-0.37394400	2.24445700
H	6.73569000	0.39038000	0.91454200
H	7.03815600	-1.31271000	1.30484600
O	1.23479800	-0.69837800	-1.10911900
C	1.08006200	-0.76630100	-2.52624500
C	0.05260000	-1.87645700	-2.82733600
H	-0.85629600	-1.76909600	-2.22208300
H	0.47749900	-2.85854300	-2.58360800
H	-0.22680600	-1.89661000	-3.88965800
C	0.59026700	0.59778200	-3.05906100
H	1.35828200	1.35924000	-2.88000600
H	-0.31960000	0.92869000	-2.54016300
H	0.38816000	0.57083000	-4.13834700
C	2.39941300	-1.12777300	-3.22756200
H	3.15553300	-0.35602000	-3.06206900
H	2.24956300	-1.23045800	-4.30971400
H	2.78384100	-2.07937500	-2.84552400
K	0.23625800	1.60979900	0.31125900
C	3.34750500	2.88511600	0.14648800
C	3.05417900	2.20277300	1.33252700
C	3.13649100	0.81612400	1.24089900
C	3.51896800	0.26912100	-0.06766100
H	2.95050200	0.16306100	2.09048600
O	-0.79499000	0.04991800	2.24230300
K	-0.31408000	-1.97228000	0.67246200
C	-0.57077300	0.02853500	3.61251600
C	0.18810000	1.29921800	4.06991100
H	0.37155700	1.32373100	5.15251900
H	1.15584300	1.35951400	3.55922600
H	-0.39294500	2.19296000	3.80442500
C	-1.91201500	-0.03495900	4.39645200
H	-2.48822600	-0.92160600	4.09396200
H	-1.77182900	-0.08618400	5.48424200
H	-2.51473300	0.86261200	4.19076700
C	0.26980900	-1.21376100	4.01338000
H	1.22355600	-1.20844800	3.46951100
H	0.49533700	-1.25498100	5.08717900
H	-0.27256500	-2.13667800	3.75713600
O	-2.35261200	1.89475800	-0.67222800
O	-2.84294300	-1.70184800	-0.34279300

K	-3.17330800	0.36505500	1.32632900
K	-2.87263300	-0.00783300	-2.29056100
C	-3.66927700	-2.81823800	-0.33838300
C	-2.87954000	-4.09721400	0.04876400
H	-2.46811100	-3.99328500	1.06326700
H	-3.49757900	-5.00426500	0.04059300
H	-2.04928600	-4.25257800	-0.65365900
C	-4.29551900	-3.05298200	-1.74057500
H	-4.93619100	-3.94313200	-1.78524200
H	-4.92016600	-2.19224200	-2.02550400
H	-3.50209100	-3.17384900	-2.49066400
C	-4.82792900	-2.64433000	0.67992200
H	-4.42175400	-2.50505000	1.69146000
H	-5.42536600	-1.75799800	0.42117700
H	-5.50904300	-3.50491300	0.71165100
C	-2.81092800	3.18990500	-0.88315200
C	-3.41540100	3.34104800	-2.30655300
H	-4.27302300	2.66111200	-2.42917000
H	-3.77687400	4.35588200	-2.51720400
H	-2.65930700	3.09397700	-3.06478200
C	-3.91449300	3.55736100	0.14505500
H	-3.51372100	3.48863800	1.16604100
H	-4.30891100	4.57339300	0.01228300
H	-4.75978800	2.85918200	0.05573200
C	-1.66116100	4.22110400	-0.74318300
H	-1.98546600	5.25248100	-0.93348400
H	-1.24793300	4.19224800	0.27501000
H	-0.85553700	3.98732300	-1.45182800
H	2.77759100	2.72651600	2.24614800
H	3.46692300	3.95244800	0.01043000
S	3.90150700	1.75854100	-1.10132300

TS-192 (193)

H	2.32456100	-0.41412500	-0.74440500
Si	4.77188800	-1.16803600	0.03975700
C	5.67742100	-1.65962000	-1.55468800
H	6.42760800	-2.43061800	-1.33779800
H	6.20817500	-0.80016300	-1.98176800
H	5.00783300	-2.05406800	-2.32481200
C	3.83001200	-2.68304600	0.71550100
H	4.50537200	-3.51648200	0.94649500
H	3.09204600	-3.03352600	-0.01649800
H	3.29503500	-2.42937800	1.64138800
C	6.11346000	-0.70667900	1.30775000
H	5.68147300	-0.47766200	2.28924000
H	6.66583500	0.18259000	0.98063400
H	6.83850500	-1.51990600	1.44274400
O	1.22175100	-0.82783700	-1.08749300
C	1.05067300	-0.99978800	-2.48873200
C	-0.01132700	-2.09864500	-2.70839700

H	-0.91223400	-1.92307900	-2.10700000
H	0.38649700	-3.07345800	-2.39784500
H	-0.29951000	-2.18627900	-3.76527000
C	0.60026000	0.33337500	-3.12772200
H	1.38602600	1.08522300	-2.98763800
H	-0.31108300	0.72153100	-2.65122300
H	0.41171900	0.23593300	-4.20542100
C	2.35297100	-1.45098200	-3.17328600
H	3.12700800	-0.68648700	-3.07019000
H	2.19197700	-1.63379100	-4.24338000
H	2.71636300	-2.37982100	-2.72047400
K	0.25443300	1.60001000	0.11020300
C	3.16877400	2.25570700	1.04437300
C	3.16669400	0.89888600	1.02822900
C	3.53336200	0.24133800	-0.23492100
H	2.90167000	0.33263700	1.92027500
O	-0.68253300	0.19079300	2.20173700
K	-0.30495600	-1.96393300	0.77510400
C	-0.42512700	0.26475500	3.56412900
C	0.35231500	1.55846400	3.91481000
H	0.55903100	1.65619400	4.98902900
H	1.30963800	1.57767100	3.38159300
H	-0.22825900	2.43634400	3.60031900
C	-1.74680100	0.26909600	4.38409600
H	-2.33834600	-0.62993900	4.15706600
H	-1.57929700	0.28922300	5.46900500
H	-2.34655200	1.15735600	4.13421500
C	0.41501500	-0.95390200	4.03338000
H	1.35135200	-1.00351700	3.46213400
H	0.67374900	-0.91620000	5.09979000
H	-0.14351900	-1.88723700	3.86514900
O	-2.35222200	1.86694700	-0.75069200
O	-2.85728200	-1.70237800	-0.19257300
K	-3.10421800	0.45748900	1.35742700
K	-2.89368500	-0.13137700	-2.24221900
C	-3.70142600	-2.80211500	-0.10910500
C	-2.92107600	-4.07511000	0.31479100
H	-2.47461000	-3.92918300	1.30915000
H	-3.55439900	-4.96980000	0.37171900
H	-2.11703700	-4.27971700	-0.40508900
C	-4.37571300	-3.09248100	-1.47836800
H	-5.03526300	-3.96966200	-1.45826300
H	-4.99155600	-2.23367800	-1.78722400
H	-3.60915200	-3.26853700	-2.24545200
C	-4.82496700	-2.55988500	0.93452800
H	-4.38523200	-2.37849000	1.92519400
H	-5.41758100	-1.67775300	0.65165900
H	-5.51683500	-3.40713900	1.02882500
C	-2.82650200	3.14635300	-1.01657600
C	-3.44215000	3.22485200	-2.44064800

H	-4.29575200	2.53405400	-2.52431500
H	-3.81205300	4.22593200	-2.69742400
H	-2.68953000	2.94565500	-3.19099400
C	-3.92719900	3.54782900	0.00214500
H	-3.51726300	3.53682500	1.02186200
H	-4.33767900	4.55021100	-0.17726300
H	-4.76243800	2.83369300	-0.04493700
C	-1.68768500	4.19494200	-0.93032200
H	-2.02735600	5.21543100	-1.14993300
H	-1.25910600	4.20420100	0.08186100
H	-0.88999100	3.94849500	-1.64375900
H	2.94219600	2.90972400	1.87918300
S	3.66317500	2.94932500	-0.51590800
C	3.82868500	1.30961100	-1.21431700
H	4.51512000	1.21456400	-2.04975900

190 (193)

C	2.95137300	-0.16752000	0.00002100
C	2.61567500	1.15837000	0.00001900
C	1.20321000	1.36342200	0.00000000
C	0.45554700	0.20485500	-0.00001400
H	0.75066400	2.35024700	-0.00001600
Si	-1.41944000	0.02732200	0.00000500
C	-1.97082000	-0.91596800	-1.54526200
H	-1.52495800	-1.91690400	-1.58590100
H	-3.06101100	-1.03793100	-1.56429800
H	-1.67638500	-0.38637900	-2.45865200
C	-2.16568000	1.76586000	-0.00086000
H	-3.26109000	1.71010900	-0.00025200
H	-1.86448500	2.33720300	0.88479500
H	-1.86537300	2.33589100	-0.88766000
C	-1.97097900	-0.91450400	1.54610900
H	-1.67673000	-0.38399100	2.45902300
H	-3.06116200	-1.03654500	1.56509900
H	-1.52502300	-1.91535400	1.58778900
H	3.34509800	1.96164600	0.00002700
H	3.93902200	-0.60987700	0.00002400
S	1.54022800	-1.17235600	-0.00000800

192 (193)

Si	1.53858000	0.03017500	0.00001500
C	2.22009500	-0.82777100	1.54542600
H	3.31685700	-0.80342500	1.55949700
H	1.86276900	-0.34030000	2.46000100
H	1.91289700	-1.87955000	1.59096800
C	2.21965700	-0.82825100	-1.54533400
H	3.31641700	-0.80411500	-1.55975000
H	1.91225200	-1.87998800	-1.59050700
H	1.86213800	-0.34096700	-2.45993300
C	2.05343400	1.85161900	-0.00032300

H	1.68128600	2.37940100	-0.88647000
H	1.68179900	2.37965700	0.88588200
H	3.14646900	1.94220200	-0.00065700
C	-2.45693100	-1.12559100	0.00004100
C	-1.10375300	-1.31008000	0.00008800
C	-0.34360700	-0.08461400	0.00010800
H	-3.23730700	-1.87515600	0.00001300
H	-0.65214300	-2.29774800	0.00010600
C	-1.18496100	1.00253400	0.00006000
H	-0.91819400	2.05150300	0.00007200
S	-2.86556000	0.56118500	0.00001000

TS-182

C	2.33045100	-0.49880100	1.76744400
H	1.80032700	-1.41849000	2.04164200
H	3.31693600	-0.51976900	2.25066500
H	1.75619900	0.33392300	2.19219000
C	1.80997600	1.23968000	-0.98868800
H	1.43405400	1.95462800	-0.24575000
H	2.59349700	1.73814200	-1.57564100
H	0.96788300	1.01814200	-1.65269100
C	2.21777100	-1.98245100	-1.12607800
H	1.49972200	-1.84294000	-1.94305400
H	3.17043800	-2.32194500	-1.54920000
H	1.81923800	-2.77471500	-0.48067700
Si	2.42437200	-0.36148600	-0.14347600
C	4.69481300	1.85482600	0.77932400
C	5.18562200	0.63004600	-0.02246400
H	3.97611300	2.44249500	0.20044300
H	4.21209000	1.54906300	1.71269500
H	5.53882700	2.50900600	1.03534800
C	6.20633100	-0.15683700	0.82708000
C	5.86869900	1.11618600	-1.31797800
H	6.55030800	-1.03466200	0.26864900
H	7.08010700	0.45405000	1.09269300
H	5.73727500	-0.50973800	1.75245600
H	6.73228100	1.76333500	-1.11152600
H	6.20999200	0.25322300	-1.90068200
H	5.15513200	1.67616300	-1.93279500
O	4.16222100	-0.26408500	-0.39559900
H	0.45801200	-0.58119200	0.10154000
C	-3.37401700	2.58568400	1.23694300
C	-2.95307200	1.46581000	0.52650900
C	-2.98851700	1.41654700	-0.91094200
C	-3.51834800	2.53321300	-1.60622400
C	-3.96341200	3.64513200	-0.88386500
C	-3.89268600	3.68370300	0.51332700
H	-3.31414900	2.61920900	2.32215100
H	-3.55990200	2.52818600	-2.69372500
H	-4.36473800	4.50331000	-1.42190600

H	-4.23444500	4.56559000	1.05128900
C	-2.42989500	0.18817200	-1.29695300
C	-1.97802500	-0.55779000	-0.12463500
H	-0.57702700	-0.59575700	-0.03274400
N	-2.44303500	0.26836500	0.99548200
H	-2.29825800	-0.15336400	-2.31733500
C	-1.87520700	0.17063300	2.32065000
H	-1.02545200	0.85763700	2.46304600
H	-2.63212100	0.40292200	3.08243500
H	-1.51819500	-0.84593000	2.49243800
Si	-2.45179700	-2.39129200	-0.11018900
C	-4.32892200	-2.66885900	0.06390800
H	-4.70062100	-2.23233100	0.99893600
H	-4.86731900	-2.18299100	-0.75821400
H	-4.59120000	-3.73556300	0.06158100
C	-1.58975700	-3.35422200	1.29133900
H	-1.69709600	-4.43748800	1.14555100
H	-0.51827900	-3.12254600	1.31505000
H	-2.00671600	-3.11625400	2.27782200
C	-1.86863900	-3.15106300	-1.75181400
H	-0.78821200	-3.01581300	-1.87876800
H	-2.07897600	-4.22810100	-1.78823700
H	-2.36729600	-2.68407600	-2.60924200

TS-183

H	0.64634900	0.64751600	-0.01343900
Si	2.68970900	2.10709700	-0.12052400
C	2.04439900	3.36862100	1.14817000
H	2.40743500	4.38116700	0.92706400
H	2.36874900	3.11562400	2.16531000
H	0.94858100	3.39248300	1.14617500
C	2.14175100	2.68347100	-1.84798500
H	2.40526300	3.73488600	-2.02429100
H	1.05527500	2.58141700	-1.95258400
H	2.61069700	2.08782400	-2.64037800
C	4.59710100	2.14532900	-0.05898900
H	5.02429300	1.45026700	-0.79211000
H	4.95802800	1.83937800	0.93080900
H	4.99842800	3.14635400	-0.26890700
C	2.72068800	-1.82914900	0.36491600
C	2.37305500	-0.76603000	-0.51693700
C	1.98023500	0.41878300	0.28544500
C	2.61912800	-2.23056900	2.81683900
H	3.40037700	-2.99683400	2.74650500
H	1.64456500	-2.73513300	2.93379800
H	2.80506400	-1.63890600	3.71997900
N	2.66300900	-1.36287200	1.66827900
C	2.11171700	-0.05188800	1.68203700
H	2.38250500	0.57000700	2.53537300
C	2.37160300	-1.01727500	-1.89091100

C	3.03924200	-3.10613700	-0.10352700
C	3.04345700	-3.32213000	-1.49242600
C	2.71642700	-2.29327000	-2.37400500
H	2.70924300	-2.48058800	-3.44603400
H	3.29258700	-4.30961100	-1.87678800
H	2.08280100	-0.23522600	-2.58833100
H	3.27754800	-3.91636700	0.58142000
C	-1.68018900	-0.95967400	1.00115700
H	-0.82052100	-0.70183100	1.63086000
H	-2.46601100	-1.39107000	1.63631300
H	-1.33291300	-1.73959000	0.31080300
C	-2.21678500	0.56974100	-1.88953700
H	-1.64203900	-0.28978600	-2.25583400
H	-3.20928400	0.55189400	-2.36062700
H	-1.69258700	1.46707500	-2.24001400
C	-2.08251100	2.27363100	0.89390200
H	-1.71052900	3.02247900	0.18319800
H	-3.03259200	2.62787500	1.31046700
H	-1.34453800	2.20480900	1.70212400
Si	-2.26971500	0.58113500	0.03033000
C	-4.56538000	-1.69624300	-0.70064300
C	-5.04545200	-0.40629700	0.00104800
H	-4.07865600	-1.47011900	-1.65429900
H	-3.85125800	-2.24101100	-0.07590100
H	-5.41463400	-2.36216700	-0.90479600
C	-5.736444800	-0.78535500	1.32887900
C	-6.06246900	0.31629400	-0.90960800
H	-6.07374300	0.12334000	1.84033300
H	-6.60368800	-1.44191900	1.17146900
H	-5.02773300	-1.29859400	1.98850300
H	-6.93818600	-0.30972900	-1.13125900
H	-6.40457800	1.23545600	-0.42055300
H	-5.58887100	0.59654900	-1.85716100
O	-4.01837700	0.50492300	0.30495500
H	-0.37681000	0.77643000	-0.23903100

TS-190 (193), penta

C	1.70979000	-0.87048100	1.66101000
H	1.01961600	-1.71768700	1.74932700
H	2.66731500	-1.16616800	2.11382300
H	1.28407900	-0.05496000	2.25869200
C	1.56021600	1.46490100	-0.65006700
H	1.28301500	2.05633800	0.23201400
H	2.43853700	1.93457500	-1.11464600
H	0.71583700	1.54160900	-1.34308400
C	1.30032200	-1.66210200	-1.46165000
H	0.57012800	-1.22735800	-2.15326500
H	2.14861100	-2.05244000	-2.03731100
H	0.80461000	-2.50234200	-0.95974800
Si	1.85224900	-0.36372600	-0.18228400

C	4.52435800	1.10207500	1.09078800
C	4.75491000	0.00007300	0.03380000
H	3.94900600	1.93421800	0.67390800
H	3.98149300	0.71168400	1.95709500
H	5.48523900	1.49832400	1.44539500
C	5.58171800	-1.14096800	0.66383700
C	5.53548200	0.59856800	-1.15527200
H	5.74162600	-1.93205500	-0.07738100
H	6.56055200	-0.79216300	1.02102800
H	5.04010100	-1.57790900	1.51033000
H	6.51287200	0.99623400	-0.84881100
H	5.69503900	-0.17270900	-1.91712800
H	4.95892100	1.40983400	-1.61371600
O	3.57132700	-0.56471900	-0.48214500
H	-0.16826100	-0.22658900	0.10475600
C	-2.72036200	2.82465400	0.00406500
C	-2.66811600	2.54475900	-1.35222500
C	-2.60367700	1.15800200	-1.52901800
C	-2.53838100	0.50631400	-0.21668900
H	-1.10252800	0.02216100	-0.00395800
N	-2.77623400	1.61482200	0.72968500
H	-2.50796800	0.63723100	-2.47524400
C	-2.13177000	1.57318400	2.02823400
H	-1.03062000	1.62079300	1.96451500
H	-2.47766100	2.42183300	2.63402300
H	-2.39813200	0.65179600	2.55576400
Si	-3.52965300	-1.06728200	0.01584200
C	-5.42525600	-0.82207100	-0.02659800
H	-5.73709100	-0.12124600	0.75790100
H	-5.73271100	-0.39055100	-0.98706400
H	-5.97871000	-1.76055400	0.11855600
C	-3.12603400	-1.94845900	1.66046600
H	-3.56617200	-2.95462000	1.68978800
H	-2.04173300	-2.04955600	1.78783800
H	-3.51349300	-1.39829200	2.52724800
C	-3.06167200	-2.26514400	-1.38839000
H	-1.98036900	-2.44666800	-1.39714400
H	-3.56774400	-3.23391800	-1.28125800
H	-3.33500200	-1.85301800	-2.36745800
H	-2.68529600	3.29238900	-2.14046500
H	-2.83560300	3.77006700	0.52149100

TS-192 (193), penta

H	-1.12538800	-0.40814700	-0.24628300
Si	-3.47389800	-1.15775100	0.16015100
C	-2.95323600	-1.96631000	1.80264300
H	-3.54058000	-2.86766400	2.02306700
H	-3.07917900	-1.27266200	2.64377800
H	-1.89445100	-2.24802500	1.76443000
C	-3.26607300	-2.44842900	-1.22550400

H -3.83846400 -3.36366900 -1.02386400
H -2.20926500 -2.72232600 -1.32680900
H -3.60114900 -2.05528000 -2.19408200
C -5.33819800 -0.74733700 0.29807600
H -5.71839800 -0.33369300 -0.64448600
H -5.50818800 0.00747700 1.07600900
H -5.94380900 -1.63021700 0.54713000
C -2.48895500 2.38090300 -1.22512500
C -2.49529700 1.04727900 -1.45335100
C -2.37157300 0.31129600 -0.17302500
C -1.81038400 3.83839900 0.65216000
H -2.12070800 4.71462700 0.06778800
H -0.70747700 3.76088400 0.62081100
H -2.10208500 4.00928300 1.69617500
N -2.47163200 2.65211800 0.15280500
C -2.27134100 1.40123000 0.81711600
H -2.60197100 1.34551200 1.85435400
C 1.29873000 -0.04116800 1.52479500
H 0.81404900 -0.83195100 2.11286300
H 2.15610500 0.32285600 2.10785600
H 0.55904100 0.76310200 1.42885500
C 1.47492600 0.30419700 -1.75493400
H 0.88332400 1.19721000 -1.52175200
H 2.40978100 0.61388200 -2.24170300
H 0.88938400 -0.27049300 -2.48262600
C 1.60046000 -2.65581500 -0.41609600
H 1.04270600 -2.88687300 -1.33163900
H 2.58262000 -3.14166800 -0.46686400
H 1.03568800 -3.09259600 0.41689700
Si 1.75210200 -0.76315400 -0.18934700
C 4.07964100 1.60631200 0.10282700
C 4.54214000 0.13234500 0.13397900
H 3.67697200 1.87182900 -0.87951500
H 3.30229100 1.79472000 0.84911200
H 4.92300600 2.27721700 0.31547300
C 5.16280600 -0.17743100 1.51453900
C 5.61346500 -0.07602200 -0.95818200
H 5.48879600 -1.22341400 1.54303800
H 6.02771000 0.46504000 1.73180200
H 4.42009400 -0.03558600 2.30699000
H 6.48828400 0.57226800 -0.80929100
H 5.94645000 -1.12012100 -0.95354500
H 5.18702600 0.13621800 -1.94525200
O 3.52022700 -0.80262000 -0.11077400
H -0.20061400 -0.84846800 -0.28783100
H -2.55828900 0.58708400 -2.43448000
H -2.50123100 3.20576200 -1.93061800

TS-190 (194), penta

C -1.53510000 -1.17321500 -1.43348800

H	-0.80840600	-1.98883700	-1.34247100
H	-2.47298900	-1.59687900	-1.82058100
H	-1.13401100	-0.47879100	-2.18162300
C	-1.46454600	1.58231200	0.37501700
H	-1.15124200	1.98982700	-0.59422800
H	-2.36231300	2.12435000	0.70427300
H	-0.64947300	1.80202700	1.07239100
C	-1.23710300	-1.32823800	1.79405400
H	-0.55910200	-0.75305400	2.43488900
H	-2.11329500	-1.62690300	2.38237900
H	-0.69684400	-2.23269900	1.48821700
Si	-1.73296800	-0.30626400	0.26402500
C	-4.34502000	0.84938500	-1.38406600
C	-4.62379600	0.00777100	-0.11946900
H	-3.75701500	1.74034100	-1.14416900
H	-3.79477400	0.26931200	-2.13127100
H	-5.28797500	1.17881600	-1.84040900
C	-5.45819800	-1.23036900	-0.51046900
C	-5.42025600	0.86188500	0.88956000
H	-5.65521400	-1.83765000	0.38016200
H	-6.41907800	-0.95348800	-0.96602600
H	-4.90227200	-1.84965300	-1.22342000
H	-6.38047800	1.20098800	0.47668000
H	-5.61606700	0.27582900	1.79457200
H	-4.83690100	1.74290700	1.17972700
O	-3.46504600	-0.45169600	0.53746200
H	0.27739600	-0.20873600	0.03039700
C	2.71768000	2.75130100	-0.75037800
C	2.75663300	2.86646500	0.62201400
C	2.74946100	1.57436100	1.16900000
C	2.61288100	0.61953500	0.07537900
H	1.21185300	0.06929100	0.06330600
H	2.71284800	1.31708100	2.22087800
Si	3.63686900	-0.94025500	-0.06655800
C	5.51714700	-0.65320900	-0.25755500
H	5.72191000	-0.05255800	-1.15237400
H	5.91298000	-0.10079400	0.60366800
H	6.08129800	-1.59246400	-0.34652600
C	3.05366700	-1.94404400	-1.57110200
H	3.59668400	-2.89279800	-1.67594600
H	1.98349600	-2.16615900	-1.48808700
H	3.19643900	-1.36813600	-2.49342800
C	3.35532300	-1.96753900	1.51145300
H	2.28648900	-2.16360100	1.65742700
H	3.87452400	-2.93411200	1.46749500
H	3.71849100	-1.43572500	2.40007400
H	2.77661500	3.80397800	1.16875000
H	2.70842500	3.47791700	-1.55107000
O	2.69138900	1.42585200	-1.13720100

TS-192 (194), penta

H	1.22062800	0.04442700	0.19179000
Si	3.53981700	-0.95918600	0.02487500
C	3.12352000	-1.94787500	-1.54608100
H	3.67512100	-2.89641900	-1.59185800
H	3.37203300	-1.37597100	-2.44935200
H	2.05186100	-2.17415200	-1.58541100
C	3.10826500	-2.03109000	1.53859700
H	3.61231500	-3.00634500	1.51109800
H	2.02658200	-2.20594000	1.57621900
H	3.39507200	-1.53687000	2.47579300
C	5.43066400	-0.67141200	0.02838100
H	5.74389000	-0.14204100	0.93697900
H	5.72674200	-0.05105600	-0.82688800
H	5.99728500	-1.61154900	-0.02633700
C	2.80009500	2.81069800	0.70233000
C	2.68064700	1.55994000	1.18364300
C	2.52801000	0.61390800	0.05112100
C	2.56277000	1.52558900	-1.10449800
H	3.02130800	1.33130200	-2.07288700
C	-1.33985000	1.47262800	-0.50538100
H	-0.41437600	1.57549800	-1.08298400
H	-2.16486100	1.92693500	-1.07163900
H	-1.19460900	2.05882200	0.41165300
C	-1.66029200	-0.91973300	1.75497700
H	-1.26666800	-0.12416600	2.39992400
H	-2.65170700	-1.21074900	2.12983500
H	-0.98878200	-1.77860200	1.87310700
C	-1.11089100	-1.65763800	-1.37668600
H	-0.64529900	-2.51760000	-0.87880000
H	-1.95385200	-2.01663400	-1.97891700
H	-0.35548700	-1.22556200	-2.04327400
Si	-1.65789100	-0.36521500	-0.08415200
C	-4.37523600	1.15551200	1.05919800
C	-4.57203100	0.05592400	-0.00792200
H	-3.86816000	0.76059500	1.94502600
H	-3.77740800	1.98252400	0.66473300
H	-5.34575400	1.55930000	1.37778300
C	-5.29751100	0.66546800	-1.22686800
C	-5.44100700	-1.07473900	0.58569900
H	-5.43474100	-0.10339800	-1.99560500
H	-6.28195100	1.07550500	-0.96114200
H	-4.69148900	1.46911400	-1.65993600
H	-6.43033900	-0.71411700	0.90053100
H	-5.57846300	-1.86366800	-0.16248000
H	-4.94270300	-1.51953900	1.45447000
O	-3.37681900	-0.51909400	-0.47592000
H	0.25843100	-0.30034700	0.28509300
H	2.63903100	1.29858100	2.23571700
H	2.87342100	3.77193500	1.19719300

O	2.80219900	2.85893600	-0.67015600
---	------------	------------	-------------

TS-190 (195), penta

C	-1.70850400	-1.17337600	-1.48000700
H	-0.99828900	-2.00572100	-1.41000800
H	-2.66455100	-1.57386500	-1.84503900
H	-1.31005500	-0.48394600	-2.23425500
C	-1.55821500	1.57470100	0.35346300
H	-1.27769600	1.99142400	-0.62194000
H	-2.44078400	2.11675200	0.72054500
H	-0.71841100	1.78100600	1.02530500
C	-1.35139400	-1.35525600	1.74641900
H	-0.62784900	-0.81402800	2.36663700
H	-2.22334100	-1.61265400	2.35914200
H	-0.86516100	-2.28506500	1.42503300
Si	-1.84343900	-0.31159900	0.22846400
C	-4.47528000	0.90492700	-1.35307600
C	-4.74051300	0.04790400	-0.09575200
H	-3.87645500	1.78773700	-1.11015400
H	-3.94086100	0.33116900	-2.11642300
H	-5.42239700	1.24798300	-1.79041800
C	-5.59657500	-1.17488000	-0.48940700
C	-5.51035400	0.89624700	0.93898400
H	-5.78340300	-1.79321700	0.39580700
H	-6.56278300	-0.88072900	-0.92235400
H	-5.06157500	-1.78968200	-1.22193900
H	-6.47410500	1.25112500	0.54807300
H	-5.69634400	0.29955000	1.83912700
H	-4.91282000	1.76706700	1.23117300
O	-3.57618100	-0.43256200	0.53379600
H	0.11495300	-0.25545900	-0.03986700
C	2.88184600	2.98567400	-0.14879600
C	2.78982300	2.58011800	1.17779500
C	2.61494700	1.21127700	1.36272200
C	2.45628700	0.41991900	0.13971200
H	1.09533900	0.00401200	0.03269600
H	2.51516600	0.75027800	2.34216400
Si	3.37927300	-1.20274200	-0.03166800
C	5.27628400	-1.01660200	-0.04286900
H	5.58803200	-0.36087500	-0.86451200
H	5.62706400	-0.55997300	0.89070900
H	5.78828700	-1.98133600	-0.16300300
C	2.86275300	-2.06321300	-1.64593600
H	3.31497800	-3.05939400	-1.74038300
H	1.77303600	-2.17596700	-1.68516800
H	3.16508200	-1.47485300	-2.52117500
C	2.89942700	-2.32233400	1.43059000
H	1.81135600	-2.44570400	1.48069400
H	3.35157100	-3.31915700	1.34234600
H	3.22772400	-1.89275600	2.38526900

H	2.84313600	3.28867100	2.00316300
H	2.96609100	3.99170500	-0.53844700
S	2.73372900	1.60790900	-1.24696100

TS-192 (195), penta

H	-1.13480600	-0.06543900	-0.16551300
Si	-3.32031200	-1.29020500	0.08483600
C	-2.70370100	-2.14693700	1.66517600
H	-3.14216800	-3.14634900	1.78532700
H	-2.95780700	-1.55988800	2.55601400
H	-1.61298100	-2.25526000	1.63850600
C	-2.89853200	-2.40885900	-1.39785100
H	-3.34211600	-3.40769500	-1.28994600
H	-1.81255800	-2.52918900	-1.48760700
H	-3.26563100	-1.98564100	-2.34159800
C	-5.21728600	-1.13641400	0.19624700
H	-5.63448300	-0.72396400	-0.73095200
H	-5.48858700	-0.45255600	1.00897100
H	-5.70429500	-2.10323400	0.38373100
C	-2.80176600	2.49150600	-1.15435100
C	-2.69035500	1.15436300	-1.31338100
C	-2.45465200	0.37014300	-0.09086800
C	-2.62104500	1.27902200	1.06132100
H	-2.14407200	1.10017500	2.02146100
C	1.48320900	-0.04654500	1.67285700
H	0.80392100	-0.78807800	2.11126500
H	2.39667500	-0.02515200	2.28249400
H	0.98125200	0.92469000	1.76134100
C	1.58631900	0.86538400	-1.51222800
H	1.14359200	1.77349200	-1.08455200
H	2.52825500	1.13701400	-2.00737100
H	0.88685400	0.51485200	-2.28031300
C	1.45625600	-2.29540800	-0.69707700
H	0.89595000	-2.31901700	-1.64017800
H	2.38625900	-2.86122700	-0.82655200
H	0.83693200	-2.80303200	0.05282300
Si	1.78661500	-0.48827500	-0.16921100
C	4.30611100	1.57520700	0.48236400
C	4.65824200	0.12025800	0.09867800
H	3.75912700	2.07583300	-0.32217200
H	3.68853500	1.60873800	1.38490800
H	5.22059400	2.15134900	0.67805200
C	5.44568300	-0.52870700	1.25786100
C	5.54191500	0.13616900	-1.16789700
H	5.69569300	-1.56357900	0.99783900
H	6.37640400	0.01158500	1.48098600
H	4.83142400	-0.54989500	2.16511200
H	6.47435500	0.69749500	-1.01566700
H	5.79457400	-0.89144700	-1.45280800
H	4.99560800	0.59111300	-2.00183400

O	3.54667600	-0.69882600	-0.17045900
H	-0.11668500	-0.37150000	-0.19286100
H	-2.71484600	0.69462700	-2.30025300
H	-2.92058700	3.24284500	-1.92649700
S	-2.69677700	2.98703600	0.54360400

TS-171

H	-1.68210500	1.28504000	-0.15474000
Si	-4.59015300	0.92715700	0.41520400
C	-5.42457100	1.76541800	-1.07767300
H	-6.38524500	2.19213900	-0.76095300
H	-5.64574400	1.03536700	-1.86563700
H	-4.83939500	2.57447700	-1.52559100
C	-4.51466600	2.15952900	1.86151800
H	-5.52745700	2.45222700	2.16566000
H	-3.97035000	3.07796000	1.61390600
H	-4.02955900	1.71168500	2.73764000
C	-5.74648300	-0.49434100	0.91790300
H	-5.43440900	-0.95007900	1.86393100
H	-5.74487800	-1.28633800	0.15927100
H	-6.78093400	-0.14632700	1.03370100
O	-0.67806600	1.83246900	-0.34261100
C	-0.83178100	3.26606500	-0.43286700
C	-0.75448200	3.87396200	0.98034400
H	0.23413500	3.70151400	1.42573500
H	-1.51634500	3.42711300	1.62873500
H	-0.91742700	4.95836900	0.96272200
C	0.31366300	3.80945700	-1.29901900
H	0.22386900	3.43700600	-2.33056400
H	1.28045300	3.50657800	-0.88769400
H	0.28838900	4.90452700	-1.34992100
C	-2.16907300	3.63723200	-1.08959700
H	-2.27480300	3.13159200	-2.05590000
H	-2.22118400	4.71863000	-1.26267800
H	-3.01569600	3.35701400	-0.46129600
C	-2.28025800	-1.89375600	-0.68457500
C	-2.10503900	-1.88789400	0.74916500
C	-2.40528500	-0.59030800	1.19073500
C	-2.82978300	0.25765200	0.07516100
H	-2.43071100	-0.27563900	2.22881500
O	1.62647000	-1.10551000	1.68534300
C	1.86779200	-1.57479200	2.98723500
C	1.88039000	-3.12025300	3.00584800
H	2.09942200	-3.52786900	4.00109900
H	0.90844600	-3.51320000	2.68519700
H	2.64613500	-3.49403600	2.31245400
C	3.23743100	-1.06690900	3.49615400
H	3.26976900	0.03031100	3.47585200
H	3.45209000	-1.39318600	4.52184500
H	4.04789800	-1.44209600	2.85461600

C	0.76866500	-1.06817900	3.95001000
H	-0.21906700	-1.36664900	3.58304200
H	0.89094100	-1.45197100	4.97085700
H	0.79207200	0.03109200	4.01188600
O	1.78291700	-1.17024200	-1.55501200
O	2.66795200	1.61061300	0.04622800
C	3.80780000	2.40649500	0.22868300
C	3.55442500	3.47067500	1.32151500
H	3.30483600	2.98046300	2.27243000
H	4.42630900	4.11451900	1.49451900
H	2.71194100	4.11221300	1.03765300
C	4.19958500	3.11506800	-1.08964100
H	5.11635700	3.70998600	-0.98806600
H	4.36540900	2.36959700	-1.87855000
H	3.40035100	3.78759600	-1.42179900
C	5.01382600	1.53728900	0.67458100
H	4.77787300	0.99927600	1.60242400
H	5.27266100	0.80739800	-0.10896100
H	5.91675300	2.13238200	0.85950500
C	2.20833300	-1.76386300	-2.75539700
C	1.44163500	-1.15713200	-3.95394000
H	1.66177800	-0.08187800	-4.04859400
H	1.71088000	-1.62433400	-4.90967800
H	0.36184100	-1.27701600	-3.80556900
C	3.72234500	-1.51901700	-2.96126200
H	4.29662200	-1.98638900	-2.14765800
H	4.09531800	-1.93623900	-3.90533400
H	3.93876200	-0.44229000	-2.95811800
C	1.95344900	-3.28737100	-2.72290000
H	2.29296700	-3.79047700	-3.63736500
H	2.48910500	-3.73771700	-1.87563500
H	0.88324800	-3.49262900	-2.59964900
Na	0.53373300	-2.23123900	0.02454500
Na	0.86015900	1.00183800	1.33499200
Na	1.18780300	1.00514300	-1.54734700
Na	3.13776600	-0.59179800	0.14057800
N	-2.76368300	-0.66852800	-1.06373800
C	-2.81470800	-0.25521800	-2.44637300
H	-3.41102300	-0.95775100	-3.04187600
H	-3.27673100	0.72998600	-2.51303700
H	-1.80916600	-0.20048900	-2.89723700
C	-1.94638600	-3.00412000	-1.46500200
C	-1.49873600	-4.17826100	-0.80553800
C	-1.38910000	-4.21713300	0.59181300
C	-1.68099400	-3.09237000	1.38107800
H	-1.59085800	-3.13961600	2.46235900
H	-1.07502900	-5.13923800	1.07612500
H	-1.26716900	-5.06332200	-1.39150400
H	-2.05963400	-2.98932400	-2.54485500

A2.3 REFERENCES

-
- (1) Frisch, M. J.; Trucks, G. W.; Schlegel, H. B.; Scuseria, G. E.; Robb, M. A.; Cheeseman, J. R.; Scalmani, G.; Barone, V.; Mennucci, B.; Petersson, G. A.; Nakatsuji, H.; Caricato, M.; Li, X.; Hratchian, H. P.; Izmaylov, A. F.; Bloino, J.; Zheng, G.; Sonnenberg, J. L.; Hada, M.; Ehara, M.; Toyota, K.; Fukuda, R.; Hasegawa, J.; Ishida, M.; Nakajima, T.; Honda, Y.; Kitao, O.; Nakai, H.; Vreven, T.; Montgomery, Jr., J. A.; Peralta, J. E.; Ogliaro, F.; Bearpark, M.; Heyd, J. J.; Brothers, E.; Kudin, K. N.; Staroverov, V. N.; Keith, T.; Kobayashi, R.; Normand, J.; Raghavachari, K.; Rendell, A.; Burant, J. C.; Iyengar, S. S.; Tomasi, J.; Cossi, M.; Rega, N.; Millam, J. M.; Klene, M.; Knox, J. E.; Cross, J. B.; Bakken, V.; Adamo, C.; Jaramillo, J.; Gomperts, R.; Stratmann, R. E.; Yazyev, O.; Austin, A. J.; Cammi, R.; Pomelli, C.; Ochterski, J. W.; Martin, R. L.; Morokuma, K.; Zakrzewski, V. G.; Voth, G. A.; Salvador, P.; Dannenberg, J. J.; Dapprich, S.; Daniels, A. D.; Farkas, O.; Foresman, J. B.; Ortiz, J. V.; Cioslowski, J.; Fox, D. J. *Gaussian 09, Rev. D.01*; Gaussian, Inc., Wallingford, CT, 2010.
- (2) (a) Lee, C.; Yang W.; Parr, R. G. *Phys. Rev. B* **1988**, *37*, 785. (b) Becke, A. D. *J. Chem. Phys.* **1993**, *98*, 1372. (c) Becke, A. D. *J. Chem. Phys.* **1993**, *98*, 5648. (d) Stephens, P. J.; Devlin, F. J.; Chabalowski, C. F.; Frisch, M. J. *J. Phys. Chem.* **1994**, *98*, 1623.
- (3) (a) Ditchfield, R.; Hehre, W. J.; Pople, J. A. *J. Chem. Phys.* **1971**, *54*, 724. (b) Hehre, W. J.; Ditchfield, R.; Pople, J. A. *J. Chem. Phys.* **1972**, *56*, 2257. (c) Hariharan, P. C.; Pople, J. A. *Theor. Chim. Acta* **1973**, *28*, 213.

- (4) Zhao, Y.; Truhlar, D. *Theor. Chem. Acc.* **2008**, *120*, 215.
- (5) (a) Barone, V.; Cossi, M. *J. Phys. Chem. A* **1998**, *102*, 1995. (b) Cossi, M.; Rega, N.; Scalmani, G.; Barone, V. *J. Comput. Chem.* **2003**, *24*, 669. (c) Takano, Y.; Houk, K. N. *J. Chem. Theory Comput.* **2005**, *1*, 70.
- (6) Legault, C. Y. CYLView, 1.0b; Universite' de Sherbrooke, Canada, **2009**; <http://www.cylview.org>.

APPENDIX 3

Alternative Reaction Mechanisms of KOt-Bu-Catalyzed Dehydrogenative C–H Silylation of Aromatic Heterocycles[†]

A3.1 INTRODUCTION AND BACKGROUND

The unusual reactivity observed in the KOt-Bu-catalyzed C–H silylation method reported by Stoltz and Grubbs¹ has been a source of mechanistic interest for a number of research groups.^{2,3} During the course of the collaborative mechanistic investigation detailed in Chapter 2, it became apparent multiple mechanisms may account for product formation in addition to the radical mechanism presented. The possible alternative mechanisms including ionic and neutral reaction mechanism were explored.

[†]This work was performed in collaboration with Dr. Shibdas Banerjee, Dr. Yun-Fang Yang, Prof. Ian Jenkins, Dr. Yong Liang, Dr. Anton Toutov, Dr. Wen-Bo Liu, David Schuman, Prof. Robert Grubbs, Prof. Brian Stoltz, Prof. Elizabeth Krenske, Prof. Kendall Houk, and Prof. Richard Zare. Portions of this chapter have been reproduced with permission from Banerjee, S.; Yang, Y.-F.; Jenkins, I. D.; Liang, Y.; Toutov, A. A.; Liu, W.-B.; Schuman, D. P.; Grubbs, R. H.; Stoltz, B. M.; Krenske, E. H.; Houk, K. N.; Zare, R. N. *J. Am. Chem. Soc.* **2017**, *139*, 6880–6887. © 2017 American Chemical Society.

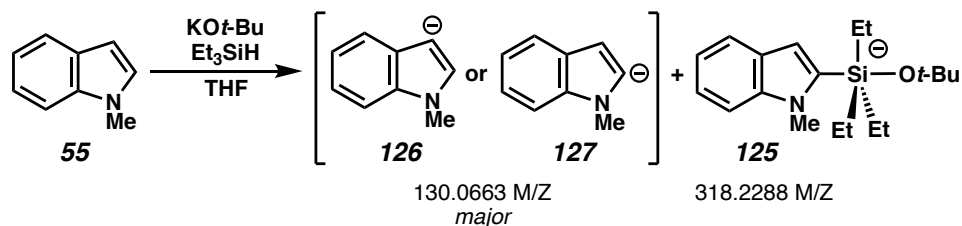
A3.2 IONIC REACTION MECHANISM

A3.2.1 Detection of Ionic Intermediates by DESI-MS

Desorption electrospray ionization mass spectrometry (DESI-MS) is an ambient ionization technique involving an electrospray solution stream impacting a stage and the resulting microdroplets fed into mass analyzers.⁴ Solution-phase, transient ionic intermediates have been detected utilizing DESI-MS in a number of reported catalytic systems.⁵

Utilizing the described DESI-MS approach with a reaction mixture containing KOt-Bu, *N*-methylindole (**55**), and Et₃SiH in THF (Scheme A3.1), the mass-to-charge ratio (m/z) corresponding to deprotonated *N*-methylindole (**126** or **127**, m/z 130.0663) and pentacoordinate **125** (or the corresponding C3 complex, not shown) was detected by DESI-MS. The same ion was not detected in control experiments with only **55** or **55** and Et₃SiH.

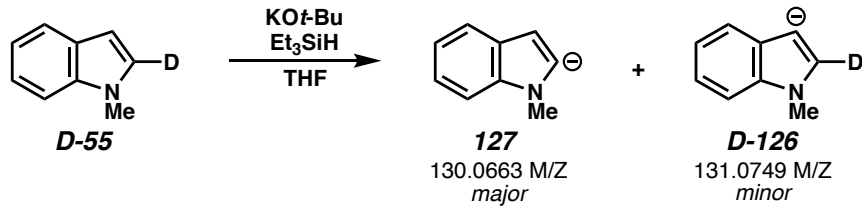
Scheme A3.1. Negative Mode DESI-MS of Silylation Reaction Mixture



The regioselectivity of deprotonation could not be determined from this experiment, as the m/z of both C2- and C3-deprotonation is identical. Using C2-deuterated **D-55** would result in different m/z for C2- and C3-deprotonation as shown in Scheme A3.2. Deprotonation was observed to occur preferentially at the C2-position (**127**) as compared to the C3-position (**D-126**), despite requiring cleavage of the stronger

C–D bond leading to **127** (Scheme A3.2). This observation is in agreement with the expected ratio of C2:C3 silylation products (i.e., ~20:1, as presented in Chapter 2).

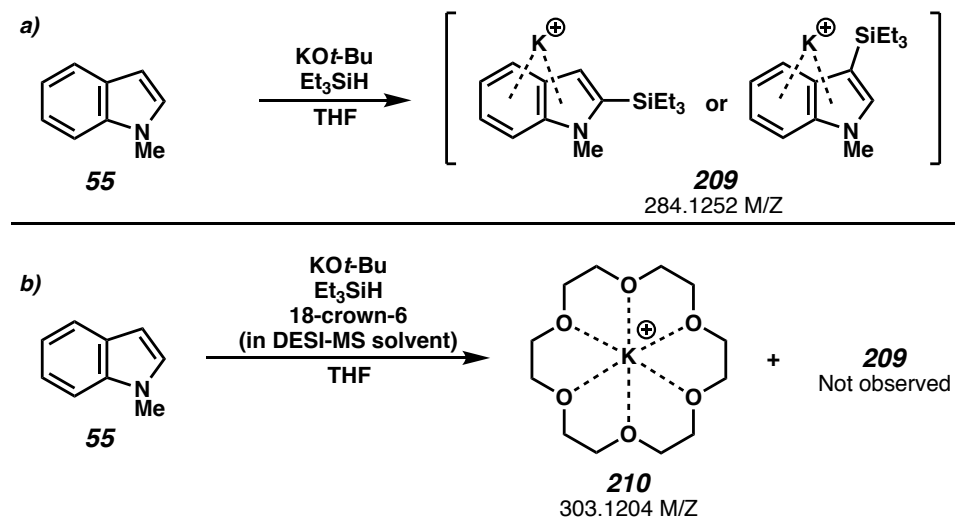
Scheme A3.2. Negative Mode DESI-MS of Silylation Reaction Mixture



Similar m/z values were also observed by DESI-MS using other substrates known to undergo silylation (e.g., dibenzofuran). In a time-course experiment the ionic intermediates are observed by DESI-MS after allowing the reaction to occur for approximately one hour, similar to the induction period observed in the bulk reaction.

The m/z corresponding to the K⁺ complex of silylation product (**209**) was observed by DESI-MS under positive ion mode (Scheme A3.3a), indicating a cation-π interaction involving K⁺ and the ‘π-excessive’ indole moiety may occur. Upon the addition of 18-crown-6 to the electrospray solvent, m/z corresponding to **209** disappeared and instead the m/z of K⁺ and 18-crown-6 complex **210** was observed (Scheme A3.3b). These results indicate the formation of a cation-π complex may be related to product formation.

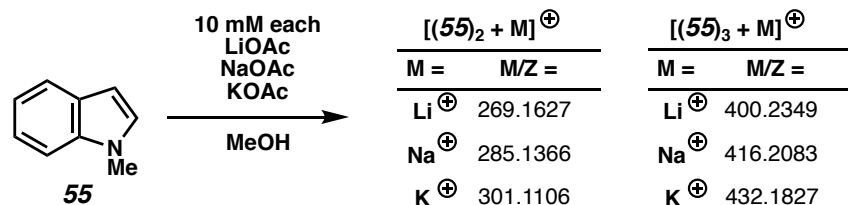
Scheme A3.3. Negative Mode DESI-MS of Silylation Reaction Mixture



A3.2.2 Cation- π Interactions

Further support for the formation of cation- π complexes comes from electrospray ionization mass spectrometry (ESI-MS) studies. Using an electrosprayed methanolic solution of **55** containing Li^+ , Na^+ , and K^+ ions in an equimolar ratio, a number of cation- π complexes were detected (Scheme A3.4). Instead of the ion signal corresponding to $[\mathbf{55}+\text{M}]^+$, the ion signal of $[(\mathbf{55})_2+\text{M}]^+$ corresponding to cation- π sandwich complexes and the ion signal of $[(\mathbf{55})_3+\text{M}]^+$ corresponding to the interaction of the central metal ion with three heteroarene molecules were observed.⁶

Scheme A3.4. ESI-MS Investigation of Cation- π Complex Formation



Interestingly, for both types of complex, the ion signal (ion current: IC) intensities followed the order: K^+ -complex > Na^+ -complex > Li^+ -complex even though the cation- π interaction strengths are expected to follow the reverse order in the gas phase.⁶ The trade-off between solvation and cation- π interaction modifies the strength of the cation- π interaction in solution (K^+ -complex > Na^+ -complex > Li^+ -complex) and hence results in the highest signal intensity for the K^+ -complex and the lowest signal intensity for the Li^+ -complex.⁷ Previous reports also support the proposal that K^+ forms stronger cation- π interactions with arenes in solution than does Na^+ or Li^+ .⁸ These studies suggest an explanation for the ineffectiveness of NaOt-Bu and LiOt-Bu as catalysts for the dehydrogenative C–H silylation.

A3.2.3 Proposed Ionic Mechanism

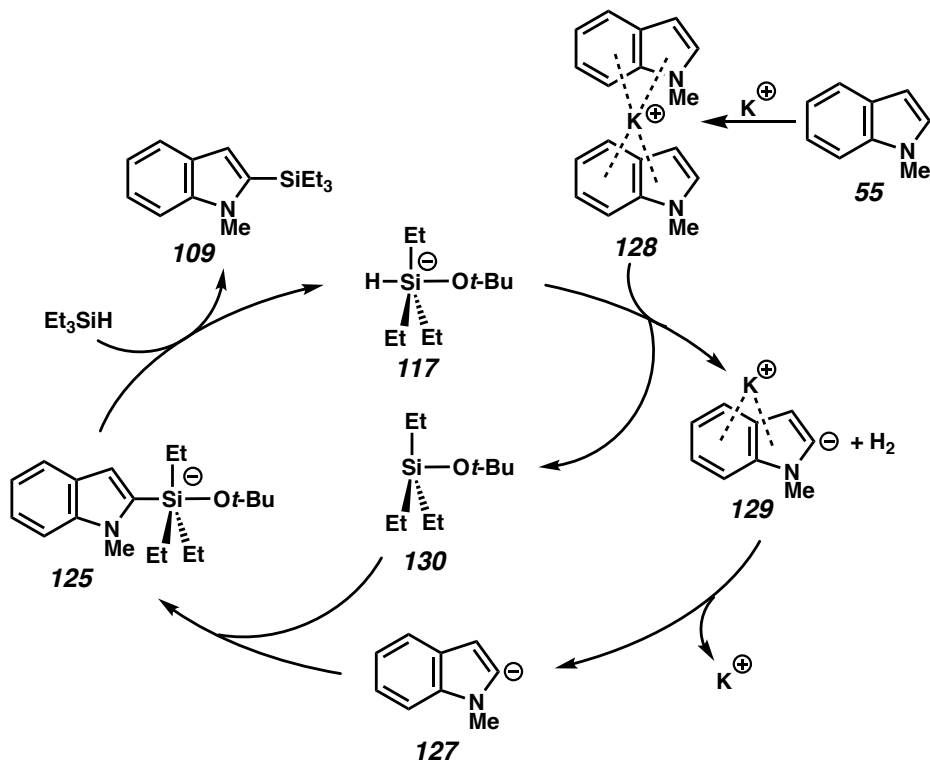
On the basis of the above observations, and considering all of the other reaction features previously presented in Chapter 2, a plausible ionic mechanism is shown in Scheme A3.5. In the first step of the mechanism, the ‘ π -rich’ heteroarene (**55**) interacts with K^+ to form the observed cation- π complex **128**. Complexation renders the heteroarene C2- and C3-protons more acidic, facilitating deprotonation by a strong base. Although the most obvious base present in the reaction mixture is $t\text{-BuO}^-$, we propose that $t\text{-BuO}^-$ does not directly deprotonate **128** but instead reacts with the hydrosilane to form a pentacoordinate silicon complex (**117**) which acts as a hydride base to deprotonate **55**. It must be noted that with the present experimental data, we cannot ascertain the precise mechanism of deprotonation or active base (i.e., whether this occurs in a concerted or a stepwise way). Deprotonation of **128** leads to the formation of ion pair

129 (major) and the corresponding C3-deprotonation (i.e., $[126\text{+}K]^+$ minor, not shown),

with hydrogen gas as a byproduct.

Ion pair **129** is proposed to dissociate to give the anion **127** (deprotonated heteroarene) that were unambiguously detected in the DESI-MS experiment (Scheme A3.1). The reactive, nucleophilic, heteroarene carbanion **127** is proposed to attack silylether **130** to form pentacoordinate silicon intermediate **125**, which was also detected by DESI-MS (Scheme A3.1). Subsequent dissociation of $t\text{-BuO}^-$ from **125** leads to the products **109**, which can form a cation- π complex with K^+ as observed by ESI-MS.

Scheme A3.5. Proposed Ionic Mechanism



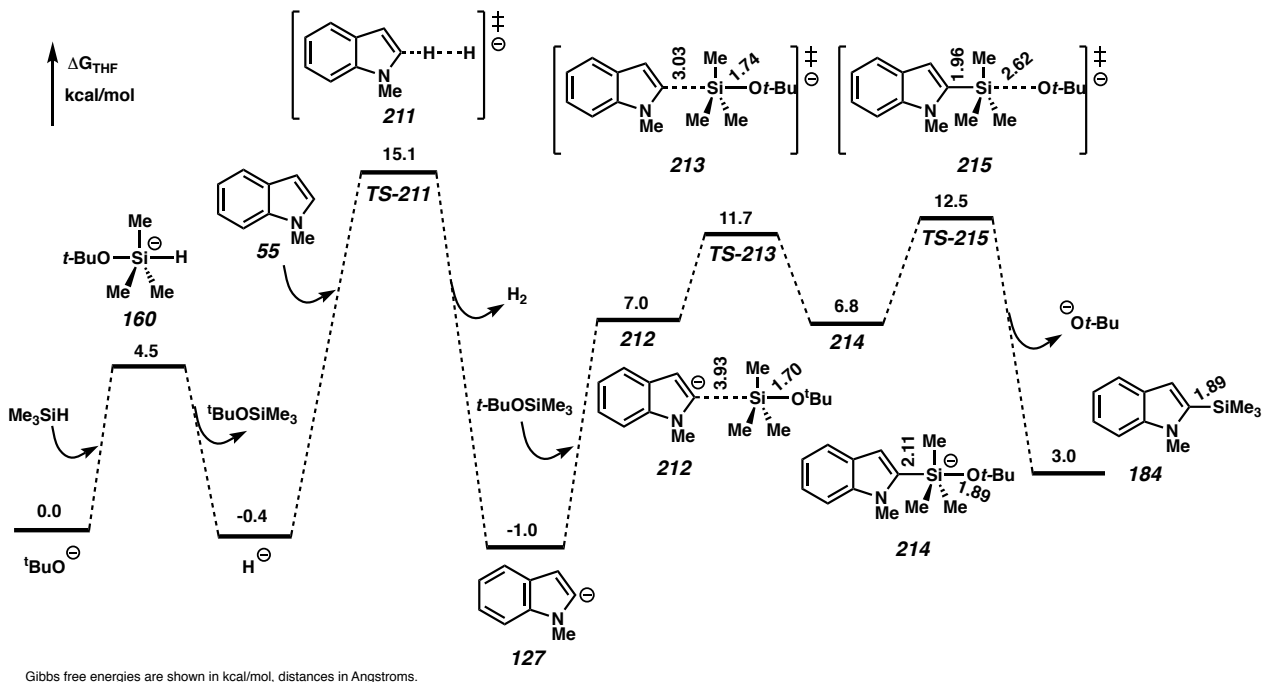
A3.2.4 Energy Profile of Proposed Ionic Mechanism

We computed the free energy profile of the ionic mechanism with DFT. Figure A3.1 summarizes the results from calculations with M06-2X/6-311+G(d,p)-

CPCM(THF)//B3LYP/6-31G(d) of the reaction of *t*-BuO[−] with **55** and a model hydrosilane, Me₃SiH, in THF. After formation of the pentacoordinate intermediate **160** (analogous to **117**), dissociation of the Si–H bond gives H[−] and *t*-BuOSiMe₃. The hydride ion then deprotonates **55**, via transition state **TS-211**, generating 2-indolyl anion **127** plus H₂. The deprotonation is regioselective: C2 deprotonation is favored by 3.8 kcal/mol relative to C3 deprotonation. Next, nucleophilic addition of 2-indolyl anion **127** to *t*-BuOSiMe₃ via **TS-213** leads to pentacoordinate intermediate **214** (analogous to **125**). Finally, dissociation of *t*-BuO[−] via **TS-215** gives the silylated heteroarene product.

The calculations predict that the deprotonation of the heteroarene is the rate-limiting step of the ionic mechanism, consistent with the experimental results discussed above. The computed barrier (ΔG^\ddagger) is 15.1 kcal/mol. This barrier would be easily surmountable at the temperatures typically used for the silylation reaction (25–65 °C), which suggests that the formation of the cation-π complex between **55** and K⁺ is not strictly essential for deprotonation to occur (although it would make the heteroarene more acidic). The major role of cation-π complex formation in this mechanism is to promote the dissociation of the KOt-Bu tetramer into K⁺ and *t*-BuO[−] ions.

Figure A3.1. Energy Profile of Ionic Mechanism

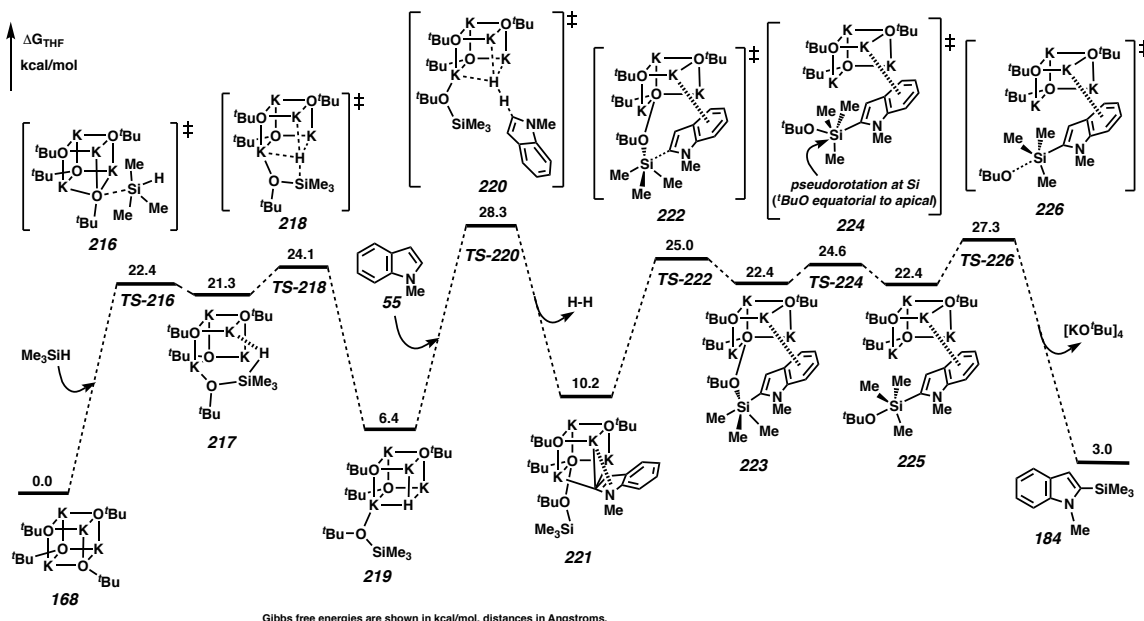


A3.2.5 Energy Profile of Proposed Neutral Mechanism

The above calculations predict that the ionic mechanism described in Figure A3.1 is facile, provided that $t\text{-BuO}^-$ can be readily generated in the reaction mixture. While mechanistic experiments indicate that KOt-Bu dissociates, at least partially, under the reaction conditions this is an energetically difficult process (ca. 36 kcal/mol). An alternative mechanism was considered which does not require dissociation of the tetramer as shown in Figure A3.2. This mechanism is broadly analogous to the ionic pathway, but the intermediates are neutral. First, a Si–O bond is formed between Me_3SiH and the KOt-Bu tetramer via transition state **TS-216**, giving pentacoordinate intermediate **217**. Next, the Si–H bond of **217** undergoes heterolysis (**TS-218**). Rather than liberating a free H^- ion, this step leads to hydride complex **219**, in which H^- occupies one corner of the K_4X_4 unit and $t\text{-BuOSiMe}_3$ is coordinated to K^+ . The coordinated hydride then

deprotonates **55**, via **TS-220**, leading to carbanion complex **221** and H_2 . Intramolecular Si–C bond formation (**TS-222**), followed by pseudorotation (**TS-224**) and finally dissociation of $^t\text{BuO}^-$ (**TS-226**), gives the silylated heteroarene product.

Figure A3.2. Energy Profile of Neutral Mechanism



Similar to the ionic mechanism, the rate-determining step of the neutral heterolytic (tetrameric) mechanism is the deprotonation of the heteroarene (**TS-220**). The overall barrier is 28.3 kcal/mol. Deprotonation of **55** is regioselective; the barrier for C2 deprotonation is 5.0 kcal/mol lower than that for C3 deprotonation (C3 deprotonation not shown). The neutral mechanism is driven by the dipolar effects mediated by the tetrameric K_4 unit, for example in the initial stage of the reaction, the pentacoordinate silicon intermediate **217** is stabilized by interaction of the silane hydrogen with the nearby potassium ion. In carbanion complex **221**, and subsequent intermediates in the catalytic cycle, the heteroarene engages in a cation- π interaction with potassium.

Although the computed barrier of the neutral mechanism (28.3 kcal/mol) is significantly higher than the barrier for the ionic mechanism shown in Figure A3.1 (15.1 kcal/mol), this does not necessarily mean that the ionic mechanism is favored over the neutral mechanism. The calculations in Figure A3.1 do not include the initial dissociation of the KOt-Bu tetramer into ions, which requires 36 kcal/mol of energy.

The tetrameric mechanism, with a rate-determining deprotonation step, provides alternative explanations for other features of the silylation chemistry discussed above. For example, the inability of NaOt-Bu to catalyze the silylation can be explained by the observation that the transition state analogous to **220** in a reaction catalyzed by NaOt-Bu has a barrier of 38.9 kcal/mol, more than 10 kcal/mol higher than the barrier for KOt-Bu-catalyzed silylation and unlikely occur under the typical experimental conditions.

A3.2.6 Ionic and Neutral Mechanism Conclusion

Two plausible mechanisms have been proposed—one ionic, the other a neutral heterolytic mechanism—for the KOt-Bu-catalyzed C–H silylation of heteroarenes, based on a combination of empirical evidence and DFT calculations. The two mechanisms are closely related, featuring cation- π interactions, preferential abstraction of the C2-proton from the indole, and formation of pentacoordinate silicon species, all of which were observed experimentally. The key steps of these mechanisms involve nucleophilic attack of KOt-Bu on the silane to form a reactive pentacoordinate silicon species, followed by rate-limiting Si–H heterolysis, deprotonation of the heteroarene substrate, addition of the heteroarene carbanion to the silylether intermediate, and eventually the release of t -BuO[−] to give the silylated heteroarene product.

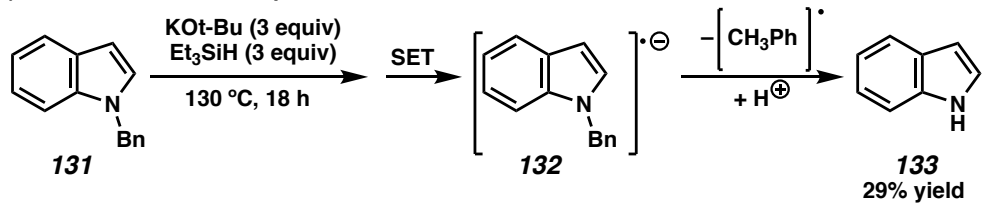
The computed activation barriers for both mechanisms are consistent with the observed reaction time for silylation of *N*-methylindole (**55**) under the reported conditions.

A3.3 ELECTRON TRANSFER REACTION MECHANISM

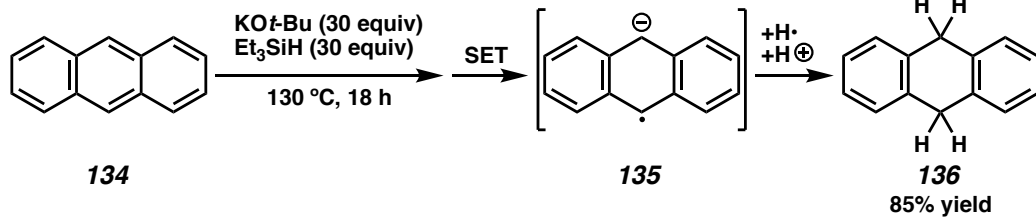
Murphy and Tuttle have reported a series of related reactions using excess base and silane along with elevated temperature as shown in Scheme A3.6.³ Based on the observed products under these more forcing conditions, the authors propose an electron transfer or hydride transfer mechanism may be operative (Scheme A3.6a and A3.6b). Similar to the previously described radical and ionic/neutral mechanism, the authors propose that a pentacoordinate silicate may be a key reaction intermediate.

Scheme A3.6. Electron Transfer and Hydrogen Atom Transfer Mechanisms

a) *Electron Transfer Example*



b) *Hydride transfer example*



It is uncertain if the mechanistic pathways proposed under these more forcing conditions are relevant to the catalytic silylation reaction, but regardless this related report describes interesting and relevant reactivity of hydrosilanes and possibly pentacoordinate silicates .

A3.4 CONCLUSION

A number of plausible mechanistic pathways have been proposed for the KOt-Bu-catalyzed C–H silylation of aromatic heterocycles. Each pathway has significant experimental, computational, and analytical support and the mechanistic evidence presented does not disprove any specific pathway. It may be possibly multiple reaction mechanisms compete under the reaction conditions or change depending on substrate and conditions. The reaction mechanism for the KOt-Bu-catalyzed C–H silylation of aromatic heterocycles has drawn considerable interest recently and a number of specific mechanistic details still remain as open questions.

A3.5 EXPERIMENTAL SECTION

A3.5.1 MATERIALS AND METHODS

All the necessary chemicals were purchased from Sigma-Aldrich (St. Louis, MO). The deuterated *N*-methylindole was prepared according to the literature procedure.²⁹ HPLC grade solvents were purchased from Fisher Scientific (Nepean, ON, Canada).

A3.5.2 Silylation Reaction for Mass Spectrometric Study

In a nitrogen-filled glove box, a 2 dram scintillation vial equipped with a magnetic stirring bar was charged with *N*-methylindole (0.1 mmol), KOt-Bu (0.05 mmol, 20 mol %), THF (100 µL) followed by the addition of Et₃SiH (0.3 mmol). The vial was then sealed and the mixture was stirred at 30 °C. After 2 h, a 20 µL reaction aliquot was removed out and dispensed immediately onto the DESI spray spot (on a glass plate, solvent: 1:1 *v/v* ACN and DMF) created ca. 2 mm away from the heated capillary inlet of the mass spectrometer.

A3.5.3 Desorption Electrospray Ionization Mass Spectrometry

The DESI-MS studies were performed on a high-resolution mass spectrometer (Thermo Scientific LTQ Orbitrap XL Hybrid Ion Trap-Orbitrap mass spectrometer) using a homebuilt DESI source. The source was constructed by using an inner fused silica capillary (100 µm i.d. and 360 µm o.d.) for solvent delivery, and an outer (coaxial) stainless steel capillary (0.5 mm i.d. and 1.6 mm o.d.) for nebulizing gas (nitrogen) delivery. A stream of charged microdroplets, produced from this DESI source at ambient temperature and atmospheric pressure, was directed to the analyte surface (on a glass plate) at an incident angle ~55° with the spray tip-to-surface distance of ~5 mm, spray tip-to-mass spectrometric inlet distance of ~10 mm, and collection angle of ~5°. The charged droplets were produced either in negative ion mode (−5 kV spray voltage) or at positive ion mode (+5 kV spray voltage), at 10 µL/min solvent (1:1 v/v ACN and DMF) flow through silica tubing with the coaxial nebulizing gas flow (N₂ at 120 psi). The splashing of these charged microdroplets on the analyte surface resulted in the formation of secondary microdroplets encapsulating the analyte molecules (ions), which were then transferred to the mass spectrometer through a heated capillary causing the complete desolvation of the analyte ions. The heated capillary (MS inlet) temperature and voltage were maintained at 275 °C and 44 V, respectively. All experiments were carried out under identical conditions, unless otherwise stated. The ion optics were tuned to get maximum ion count. Data acquisition was performed for 1 min using XCalibur software (Thermo Fisher Scientific).

A3.5.4 Electrospray Ionization Mass Spectrometry.

ESI-MS studies were performed on the same mass spectrometer as mentioned above with a homebuilt ESI source similar to the above DESI source. The analyte solution (in methanol) was injected to the ESI source (on-axis) at a flowrate 5 μ L/min in positive ion mode (+5 kV) with a coaxial sheath gas flow (N_2 at 120 psi). The mass spectrometer (MS) inlet capillary temperature was maintained at 275 °C, and capillary voltage was kept at 44 V. The spray distance (the on-axis distance from spray tip to the entrance of the heated capillary) was kept at 1.5 cm. All experiments were carried out under identical conditions. The ion optics were tuned to get maximum ion count. Data acquisition was performed for 1 min using XCalibur software (Thermo Fisher Scientific)

A3.5.5 Computational Details.

All the calculations were carried out with Gaussian 09.⁹ Geometry optimizations were performed with the B3LYP method using the 6-31G(d) basis set for all atoms.¹⁰ Frequency analyses verified that the stationary points were minima or first-order saddle points. Single point energies were calculated at the M06-2X³⁹/6-311+G(d,p) level, with solvent effects (solvent = THF) modeled using the CPCM⁴⁰⁻⁴² solvation model. Gibbs free energies in THF at 298.15 K were calculated by adding the thermochemical quantities derived from the B3LYP frequencies to the M06-2X solution-phase electronic potential energy and then correcting the energy to a standard state of 1 mol/L. Computed structures are illustrated using CYLview.⁴³

A3.6 Relevant Spectra

All relevant spectra (1H NMR, DESI-MS, ESI-MS, etc.) are available free of charge via the Internet at <http://pubs.acs.org> (DOI: 10.1021/jacs.6b13032).

A3.7 REFERENCES AND NOTES

- (1) Liu, W.-B.; Schuman, D. P.; Yang, Y.-F.; Toutov, A. A.; Liang, Y.; Klare, H. F.; Nesnas, N.; Oestreich, M.; Blackmond, D. G.; Virgil, S. C.; Banerjee, S.; Zare, R. N.; Grubbs, R. H.; Houk, K. N.; Stoltz, B. M. *J. Am. Chem. Soc.* **2017**, *139*, 6867–6879.
- (2) Banerjee, S.; Yang, Y.-F.; Jenkins, I. D.; Liang, Y.; Toutov, A. A.; Liu, W.-B.; Schuman, D. P.; Grubbs, R. H.; Stoltz, B. M.; Krenske, E. H.; Houk, K. N.; Zare, R. N. *J. Am. Chem. Soc.* **2017**, *139*, 6880–6887.
- (3) Smith, A. J.; Young, A.; Rohrbach, S.; O'Connor, E. F.; Allison, M.; Wang, H. S.; Poole, D. L.; Tuttle, T.; Murphy, J. A. *Angew. Chem. Int. Ed.* **2017**, *56*, 13747–13751.
- (4) Takáts, Z.; Wiseman, J. M.; Gologan, B.; Cooks, R. G. *Science* **2004**, *306*, 471.
- (5) (a) Perry, R. H.; Cahill, T. J.; Roizen, J. L.; Du Bois, J.; Zare, R. N. *Proc. Natl. Acad. Sci. USA* **2012**, *109*, 18295–18299; (b) Boeser, C. L.; Holder, J. C.; Taylor, B. L. H.; Houk, K. N.; Stoltz, B. M.; Zare, R. N. *Chemical Sci.* **2015**, *6*, 1917–1922; (c) Ingram, A. J.; Solis-Ibarra, D.; Zare, R. N.; Waymouth, R. M., Trinuclear Pd₃O₂ Intermediate in Aerobic Oxidation Catalysis. *Angew. Chem. Int. Ed.* **2014**, *53*, 5648–5652; (c) Perry, R. H.; Brownell, K. R.; Chingin, K.; Cahill, T. J.; Waymouth, R. M.; Zare, R. N., *Proc. Natl. Acad. Sci. USA* **2012**, *109*, 2246–2250; (d) Perry, R. H.; Splendore, M.; Chien, A.; Davis, N. K.; Zare, R. N., *Angew. Chem. Int. Ed.* **2011**, *50*, 250–254; (d) Brownell, K. R.; McCrory, C. C.

- L.; Chidsey, C. E. D.; Perry, R. H.; Zare, R. N.; Waymouth, R. M., *J. Am. Chem. Soc.* **2013**, *135* (38), 14299–14305.
- (6) Wireduaah, S.; Parker, T. M.; Lewis, M. *J. Phys. Chem. A* **2013**, *117*, 2598; b) Dougherty, D. A. *Acc. Chem. Res.* **2013**, *46*, 885.
- (7) Kumpf, R.; Dougherty, D. *Science* **1993**, *261*, 1708.
- (8) Zhu, D.; Herbert, B. E.; Schlautman, M. A.; Carraway, E. R. *J. Environ. Quality* **2004**, *33*, 276; Lu, Q.; Oh, D. X.; Lee, Y.; Jho, Y.; Hwang, D. S.; Zeng, H. *Angew. Chem. Int. Ed.* **2013**, *52*, 3944.
- (9) Frisch, M.; Trucks, G.; Schlegel, H.; Scuseria, G.; Robb, M.; Cheeseman, J.; Scalmani, G.; Barone, V.; Mennucci, B.; Petersson, G. *Inc., Wallingford, CT* **2009**
- (10) (a) Lee, C.; Yang, W.; Parr, R. G. *Phys. Rev. B* **1988**, *37*, 785; (b) Becke, A. D. *J. Chem.Phys* **1993**, *98*, 1372; (c) Becke, A. D. *J. Chem.Phys.* **1993**, *98*, 5648; (d) Stephens, P. J.; Devlin, F. J.; Cheeseman, J. R.; Frisch, M. J. *J. Chem.Phys. A* **2001**, *105*, 5356. (e) Ditchfield, R.; Hehre, W. J.; Pople, J. A. *J. Chem.Phys.* **1971**, *54*, 724. (f) Ditchfield, R.; Hehre, W. J.; Pople, J. A. *J. Chem.Phys.* **1971**, *54*, 724.; (g) Hehre, W. J.; Ditchfield, R.; Pople, J. A. *J. Chem.Phys.* **1972**, *56*, 2257; (h) Hariharan, P. C.; Pople, J. A. *Theor. Chem. Acc* **1973**, *28*, 213.

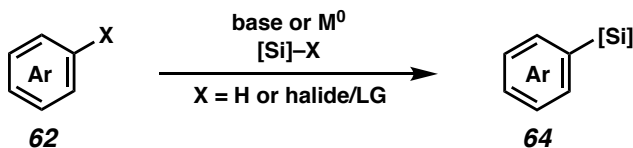
CHAPTER 3

Catalytic C–H Trimethylsilylation of Aromatic Heterocycles via Base Catalysis[†]

3.1 BACKGROUND

Organosilicon moieties have been shown to have a number of uses in the fields of synthetic chemistry,¹ polymer and organic electronics,² drug discovery,³ and nuclear medicine.⁴ Perhaps the most common method for the redox-neutral (i.e., excluding hydrosilylation) instillation of organosilicon functional groups is through the reaction of a nucleophilic substrate with an electrophilic silicon source (Scheme 3.1). Despite the widespread usage, there are a number of drawbacks associated with this approach to silylation.⁵

Scheme 3.1 Silylation via Nucleophile Trapping.



[†] This work was performed in collaboration with Dr. Wen-Bo Liu, Dr. Anton Toutov, and Kerry Betz. Portions of this chapter have been reproduced with permission from Schuman, D. P.; Liu, W.-B.; Toutov, A. A.; Betz, K. N.; Grubs, R. H.; Stoltz, B. M. *Manuscript in Preparation*

Reactions involving substrates with limited nucleophilicity or acidity often require the use of highly reactive bases and/or electrophilic silicon sources. Conversely, cryogenic reaction temperatures may be required to limit undesired reactivity, especially when using strong bases, highly reactive silicon sources, or substrates with multiple reactive sites. Limited regiochemical control is afforded by changing the reaction conditions and prefunctionalized substrates may be required to override inherent substrate control. This method may also present challenges for large scale reactions due to the formation of (super)stoichiometric salt byproducts.

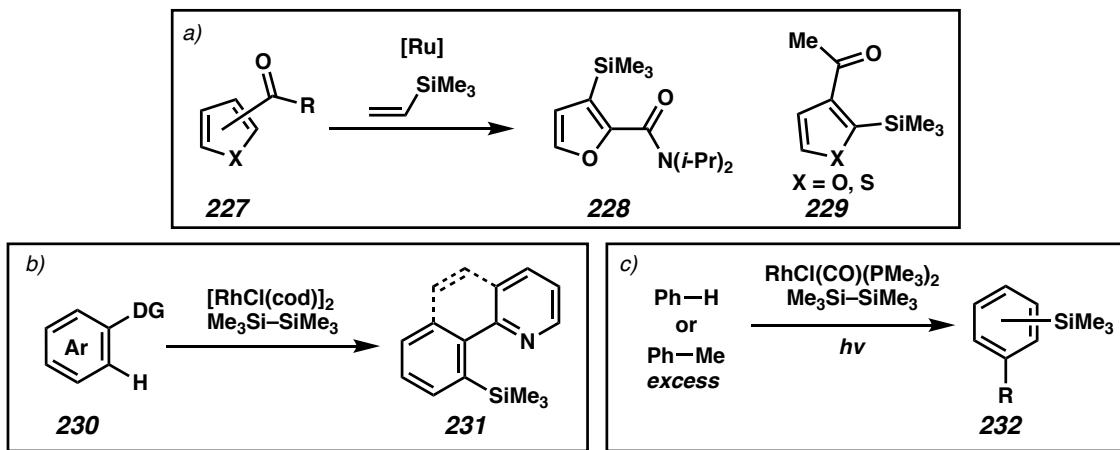
A number of research groups have sought to develop new silylation methods to address these drawbacks and catalytic C–H silylation has emerged as an especially useful manifold for the synthesis of organosilicon compounds (see Chapter 1).⁶ Many of these catalytic systems, including the C–H silylation method developed by our group (See Chapter 1 and 2),⁷ have not been reported in the context of a trimethylsilylation methodology.⁸

3.1.1 Literature Examples of Catalytic C–H Trimethylsilylation

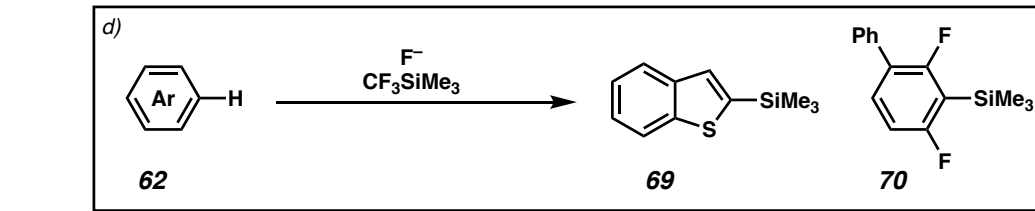
Examples of reported catalytic C–H trimethylsilylation methods are shown in Scheme 3.2. Many of these examples use transition-metal catalysts (3.2a–c),⁹ which are often expensive and may be problematic for late-state functionalization and removal.¹⁰ A transition-metal-free method was previously reported by Kondo and coworkers (Scheme 3.2d), but requires the use of catalytic fluoride anion and the expensive Ruppert–Prakash reagent ($\text{CF}_3\text{—SiMe}_3$) as the silicon source.¹¹

Scheme 3.2 Reported Examples of Catalytic, C–H Trimethylsilylation.

Transition-Metal-Catalyzed Examples



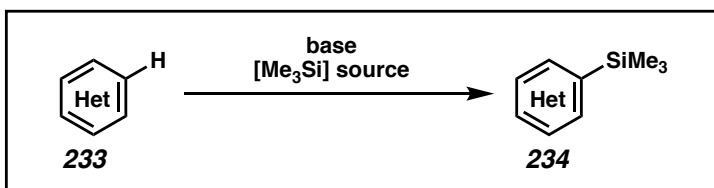
Transition-Metal-Free Example



3.2 BASE-CATALYZED C–H TRIMETHYLSILYLATION

3.2.1 Introduction

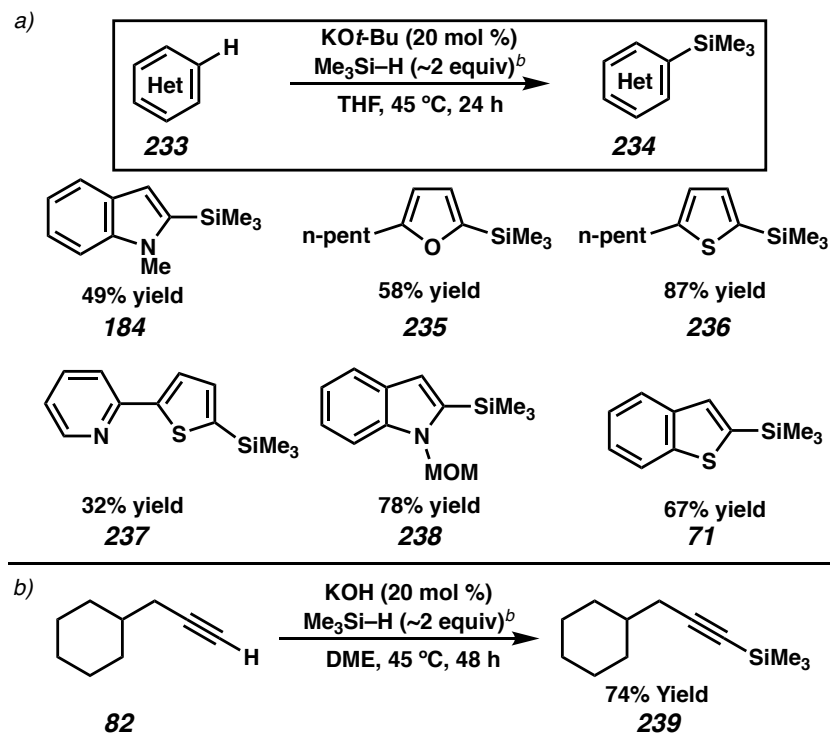
Inspired by our previous research in C–H silylation,⁷ we envisioned a method using an Earth-abundant, base metal catalyst alongside a low-cost and easily handled silicon source to access TMS-substituted products (Scheme 3.3). Such a method may be useful to the synthetic community as an alternative to traditional stoichiometric or transition-metal-catalyzed silylation processes as previously presented.

Scheme 3.3 Base-Catalyzed C–H Trimethylsilylation.

3.2.2 C–H Silylation Using Trimethylsilane Gas.

Me₃Si–H is a commercially available gas, with a boiling point of 6.7 °C, and used for a variety of industrial processes including chemical vapor deposition.¹² Therefore, we initially attempted to directly use trimethylsilane (TMS–H) under our previously reported C–H silylation conditions using hydrosilane (see Chapter 2.). After a brief optimization, we were pleased to observe moderate reactivity simply employing a sealed atmosphere of TMS–H gas (Scheme 3.4a). Inspired by these results, we found TMS–H can also be directly used in our previously reported alkyne C–H silylation chemistry (Scheme 3.4b).¹³

Scheme 3.4 KOt-Bu-Catalyzed Silylation Using $\text{Me}_3\text{Si}-\text{H}$.



[a] Reactions conducted on 0.5 mmol scale in a sealed Schlenk flask. [b] $\text{Me}_3\text{Si}-\text{H}$ gas equivalence estimated by flask volume.

Further reaction optimization (i.e., increased pressure of TMS–H) may improve product yields but these investigations surpass our equipment limitations. Catalytic C–H silylation using silane gas may find future industrial applications, but the bench-scale utility is likely limited due to operational drawbacks (i.e., using a gaseous reagent and incompatibility with many rubber products).¹⁴ Therefore, we sought to find a more easily handled source of TMS– amenable to bench-scale C–H silylation reactions.

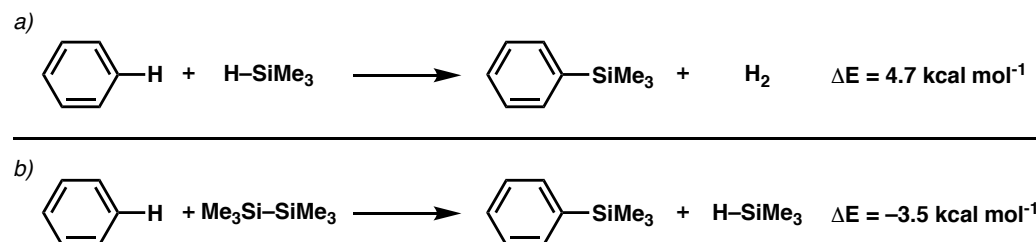
3.2.3 C-H Silylation Using Disilane.

3.2.3.1 Introduction and Background.

A number of previous literature examples detailing transition-metal-catalyzed C–H trimethylsilylation reactions utilized disilanes as a source of silicon.⁸ Of particular interest to us is hexamethyldisilane ($\text{Me}_3\text{Si}-\text{SiMe}_3$, also TMS_2 or $\text{TMS}-\text{TMS}$), a

commercially available and easily handled liquid. Additionally, the weaker Si–Si bond in hexamethyldisilane compared to the Si–H bond in trimethylsilane will result in more favorable thermodynamics for silylation (Scheme 3.5, a versus b).⁵

Scheme 3.5 KOt-Bu-Catalyzed Silylation Using $\text{Me}_3\text{Si}-\text{H}$.



3.2.3.2 Reaction Optimization.

We were pleased to find disilane bonds could be activated under similar conditions to our previously reported C–H silylation methodology using hydrosilanes (Table 3.1, entry 2, cf. Chapter 2). Potassium *tert*-butoxide and ethoxide are the most active catalysts we investigated and both were utilized in further reactions (entries 2–8). As in the previous chemistry using hydrosilanes, NaOt-Bu, LiOt-Bu, and KH are also not competent silylation catalysts using disilanes (entry 8). The strong single electron reductant potassium graphite (KC_8) was also found to be a similarly competent catalyst (entry 9).

Notable differences occurred using KOH, KOTMS, and KHMDS as catalysts. While the use of these bases result in product formation in silylation reactions using hydrosilanes, no product was observed in the case of disilanes. This difference in reactivity may be due to the additional steric congestion leading to a pentacoordinate silicate in the case of disilane compared to hydrosilane.

Using potassium ethoxide to investigate solvent effects, we found a number of polar, aprotic solvents such as DME, HMPA and THF resulted in the formation of product, with THF providing the highest yield (entries 4, 10, 11). Solvent was required for product formation and neat reaction conditions (i.e., entry 1) resulted in no observed product. This could be due to limited catalyst solubility in the disilane-substrate mixture or solvent assistance in the catalytic cycle (i.e., in the formation of pentacoordinate silicate).

Table 3.1 Optimization of C–H Silylation using $\text{Me}_3\text{Si-SiMe}_3$.

		cat. (20 mol %) $\text{Me}_3\text{Si-SiMe}_3$				
		Solvent or neat	45 °C			
entry	Cat.	$\text{Me}_3\text{Si-SiMe}_3$ (equiv.)	time (h)	solvent	yield 184	
1	KOt-Bu	2	>100	neat	0	
2	KOt-Bu	2	20	THF	72	
3	KOt-Bu	2	40	THF	85	
4	KOEt	2	20	THF	65	
5	KOEt	2	40	THF	82	
6	KOMe	2	60	THF	20	
7	KOTMS	2	60	THF	trace	
8	KOH, KHMDS, KH, NaOt-Bu or LiOt-Bu	2	60	THF	0	
9	KC ₈	2	20	THF	68	
10	KOEt	2	20	DME	11	
11	KOEt	2	20	HMPA	26	
12	KOEt	1.1	20	THF	45	
13	KOEt	1.5	20	THF	68	
14	KOEt	3	20	THF	68	

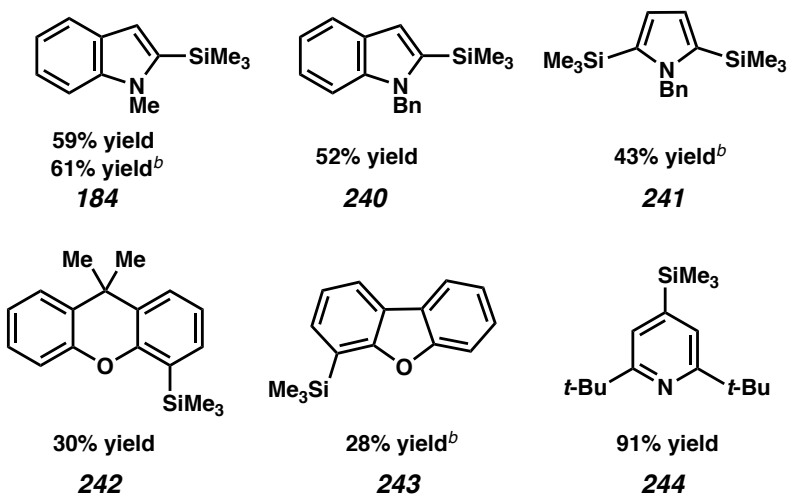
[a] Reactions conducted on 0.1–0.5 mmol scale, 1M in solvent if used, yield determined by GC.

With these optimized conditions in hand, we next turned to investigate the substrate scope of the C–H silylation using disilanes.

3.2.3.3 Substrate Scope.

A number of aromatic heterocycles undergo mono or bis C–H silylation in moderate to good yield (Scheme 3.6). Five and six membered nitrogen and oxygen containing aromatic heterocyclic substrates are amenable to silylation (**184**, **240–244**). Particularly active substrates often undergo sequential silylation resulting in the observance of bis-silylation products such as **241**. Surprisingly, pyridine **244** undergo silylation at the para position in excellent yield.

Scheme 3.6 Substrate Scope of C–H Silylation using $\text{Me}_3\text{Si}-\text{SiMe}_3$.

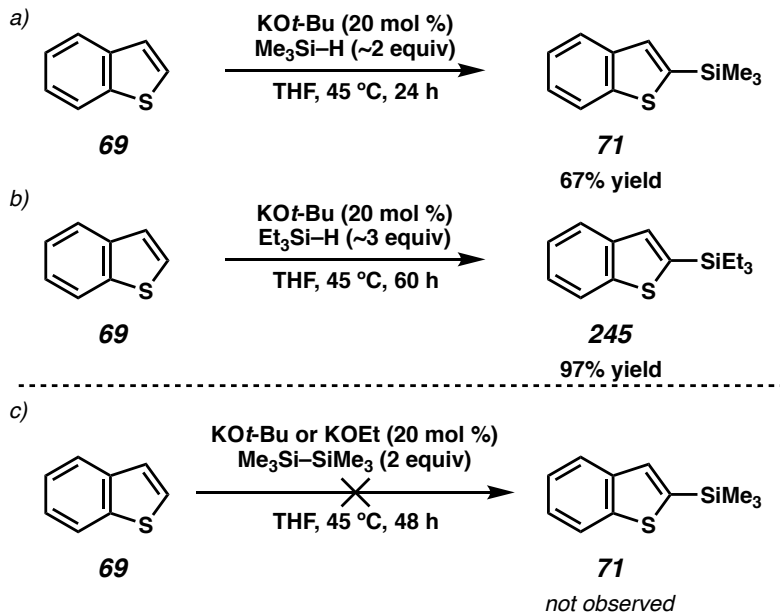


[a] Reactions conducted on 0.2–0.5 mmol scale in 1M THF using 1 equiv substrate, $\text{KO}t\text{-Bu}$ (20 mol. %) and hexamethyldisilane (2 equiv) at 45–80 °C for 24–120 h. [b] KOEt used as catalyst.

A number of significant differences were observed in the substrate scope of silylation reactions using disilanes compared to hydrosilanes. In addition to longer times and higher reaction temperatures compared to the hydrosilane methodology, reactions using disilanes demonstrated a more limited substrate scope and often lower overall yields. Sulfur containing aromatic heterocyclic substrates resulted in no product formation when subjected to the disilane reaction conditions. For example, benzothiophene (**69**), one of the most active silylation substrates in the hydrosilane

Chapter 3 – Catalytic C–H Trimethylsilylation of Aromatic Heterocycles via Base Catalysis 233
methodology, resulted in no product formation under the disilane reaction conditions (Scheme 3.7a and b versus c).

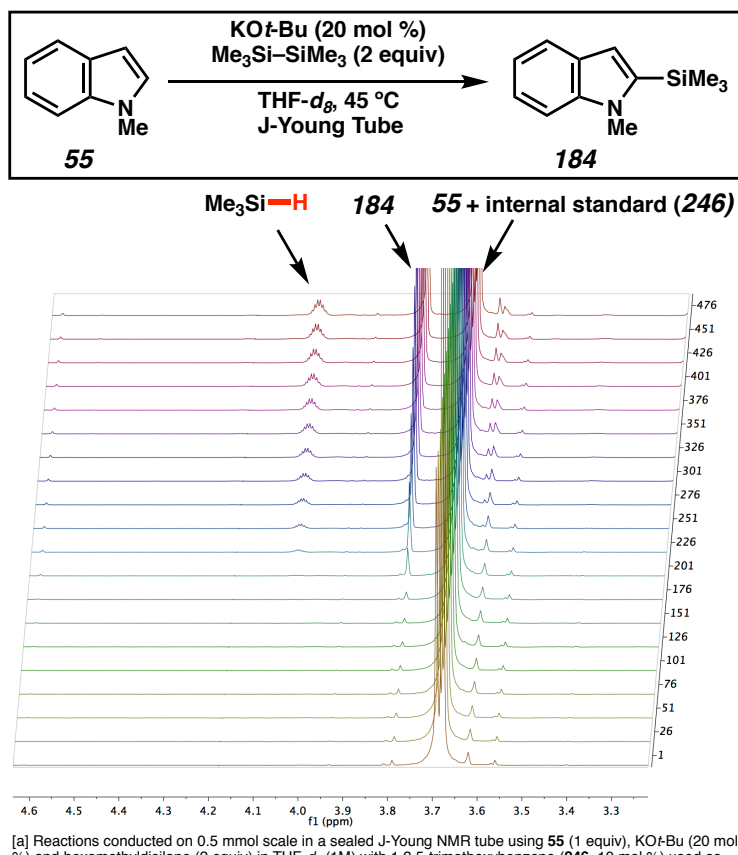
Scheme 3.7 Comparison of C–H Silylation using Hydrosilane and Disilanes.



This observation is perhaps surprising given the weaker Si–Si bond in hexamethyldisilane compared to the Si–H bond in trimethylsilane.⁵ Our previous mechanistic investigations indicated the C–H bond breaking step is rate determining and involves the hydrosilane (see Chapter 2), leading us to believe activation of a weaker bond should further favor product formation.¹⁵

3.2.3.4 Mechanistic Details.

Based on our mechanistic study detailed in Chapter 2, we conducted a limited investigation into the mechanism of the silylation reaction using disilane. Initial ^1H -NMR time–course experiments provide evidence consistent with the formation of TMS–H as shown in Figure 3.1.¹⁶ We then unambiguously confirmed the presence of TMS–H by ^1H – ^{29}Si HSQC.

Figure 3.1 Substrate Scope of C–H Silylation using $\text{Me}_3\text{Si}-\text{SiMe}_3$.

[a] Reactions conducted on 0.5 mmol scale in a sealed J-Young NMR tube using **55** (1 equiv), $\text{KO}t\text{-Bu}$ (20 mol %) and hexamethyldisilane (2 equiv) in $\text{THF}-d_8$ (1M) with 1,3,5-trimethoxybenzene (**246**, 10 mol %) used as internal standard.

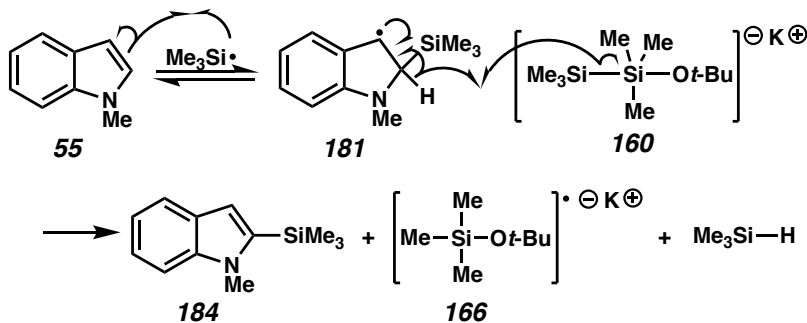
TMS–H may arise from either a radical or ionic process, similar to those presented in Chapter 2 (Scheme 3.8). In the radical mechanism, silane radical addition to **55** generates the indoline radical **181** (Scheme 3.8a). Hydrogen atom abstraction could then occur via pentacoordinate silicate **160** to generate the observed product **184**, silicate radical anion **166**, and the observed TMS–H. Both **166** and TMS–H can further participate in the catalytic cycle.

In the ionic mechanism, **55** is deprotonated by pentacoordinate silicate **160** to generate anion **166**, silyl ether **247**, and TMS–H. Reaction of anion **166** with **247** and

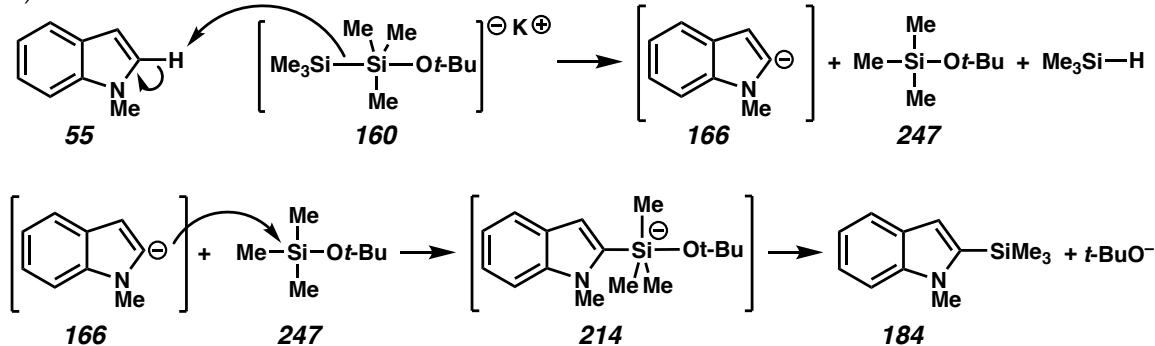
subsequent loss of $t\text{-BuO}^-$ results in formation of product **184** and closes the catalytic cycle.

Scheme 3.8 Proposed Mechanism of C–H Silylation using $\text{Me}_3\text{Si}-\text{SiMe}_3$.

a) Radical Mechanism



b) Ionic Mechanism



As we have demonstrated TMS–H to be a competent silicon source for silylation reactions (see 3.2.2), both the hydrosilane and disilane (e.g., TMS–H and TMS–TMS) may be present in the reaction mixture and contribute to product formation. Furthermore, the formation of TMS–H as an intermediate may be related to the differences observed between reactions using disilane versus hydrosilane.

3.3 CONCLUSION.

We have developed a facile method for the transition-metal-free, C–H silylation of aromatic heterocycles using an Earth-abundant base catalyst to afford trimethylsilyl substituted products. A commercially available and easily handled liquid can be used as

the source of Me₃Si– for bench-scale reactions or Me₃Si–H gas can be used directly. This methodology has a number of advantages over both traditional metalation/trapping approaches, which require the use of (super)stoichiometric base and reactive electrophile, or transition–metal catalysts.

3.4 EXPERIMENTAL SECTION

3.4.1 MATERIALS AND METHODS

Unless otherwise stated, reactions were performed in a nitrogen-filled glovebox or in flame-dried glassware under an argon or nitrogen atmosphere using dry, deoxygenated solvents. Solvents were dried by passage through an activated alumina column under argon.¹⁷ Reaction progress was monitored by thin-layer chromatography (TLC), GC or Agilent 1290 UHPLC-MS. TLC was performed using E. Merck silica gel 60 F254 precoated glass plates (0.25 mm) and visualized by UV fluorescence quenching, *p*-anisaldehyde, phosphomolybdic acid, or KMnO₄ staining. Silicycle SiliaFlash® P60 Academic Silica gel (particle size 40–63 nm) or Teledyne ISCO RediSep® Rf Gold silica prepacked column was used for flash chromatography. ¹H NMR spectra were recorded on Varian Inova 500 MHz or Bruker 400 MHz spectrometers and are reported relative to residual CHCl₃ (δ 7.26 ppm), C₆H₆ (δ 7.16 ppm), or THF (δ 3.58, 1.72 ppm). ¹³C NMR spectra were recorded on a Varian Inova 500 MHz spectrometer (125 MHz) or Bruker 400 MHz spectrometers (100 MHz) and are reported relative to CHCl₃ (δ 77.16 ppm). Data for ¹H NMR are reported as follows: chemical shift (δ ppm) (multiplicity, coupling constant (Hz), integration). Multiplicities are reported as follows: s = singlet, d = doublet, t = triplet, q = quartet, p = pentet, sept = septuplet, m = multiplet, br s = broad

singlet, br d = broad doublet, app = apparent. Data for ^{13}C NMR are reported in terms of chemical shifts (δ ppm). IR spectra were obtained by use of a Perkin Elmer Spectrum BXII spectrometer or Nicolet 6700 FTIR spectrometer using thin films deposited on NaCl plates and reported in frequency of absorption (cm^{-1}). GC-FID analyses were obtained on an Agilent 6850N gas chromatograph equipped with a HP-1 100% dimethylpolysiloxane capillary column (Agilent). GC-MS analyses were obtained on an Agilent 6850 gas chromatograph equipped with a HP-5 (5%-phenyl)-methylpolysiloxane capillary column (Agilent). High resolution mass spectra (HRMS) were obtained from Agilent 6200 Series TOF with an Agilent G1978A Multimode source in electrospray ionization (ESI+), atmospheric pressure chemical ionization (APCI+), or mixed ionization mode (MM: ESI-APCI+), or obtained from Caltech mass spectrometry laboratory.

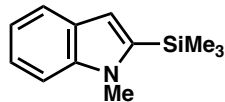
Hexamethyldisilane (98%) and KO*t*-Bu (sublimed grade, 99.99% trace metals basis) were purchased from Aldrich and used directly. Trimethylsilane was purchased from Gelest and used directly. KOH was pulverized and dried in a desiccator over P₂O₅ under vacuum for 24 h prior to use. Other reagents were purchased from Sigma-Aldrich, Acros Organics, Strem, or Alfa Aesar and used as received unless otherwise stated.

3.4.2 EXPERIMENTAL PROCEDURES AND SPECTROSCOPIC DATA

3.4.2.1 General Experimental Procedure and Spectroscopic Data for the C–H Silylation Using Trimethylsilane Gas

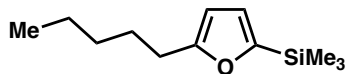
In a nitrogen-filled glove box, substrate (1 equiv), KO*t*-Bu (20 mol %), and THF (1M in substrate) were added to the reaction vessel with a magnetic stir bar. The reaction

vessel could be either a 25 mL Schlenk bomb sealed with a PTFE plug without an O-ring or a 20 mL scintillation vial sealed with PTFE-lined septum and cap. In a fume hood, the bottle of trimethylsilane (100g, Gelest) was fitted with a rubber septum and secured with a hose clamp. A gas transfer device (fabricated from a cut 10 mL syringe barrel, latex balloon, and tape) was fitted with a needle and purged with trimethylsilane. The rapidly stirring reaction mixture was momentarily placed under vacuum and immediately refilled with trimethylsilane three times. The reaction vessel was then sealed and stirred at 45 °C for 24 h, after which the reaction mixture was diluted with diethyl ether (2 mL) and concentrated under reduced pressure. The residue was purified by silica gel flash chromatography to give the desired product.

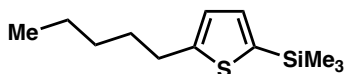


1-methyl-2-(trimethylsilyl)-1*H*-indole (184): The general procedure was followed using KO*t*-Bu (11.2 mg, 0.1 mmol, 20 mol %), **55** (66 mg, 0.5 mmol, 1 equiv), and 0.5 mL of THF at 45 °C in a sealed tube for 24 h. **184** was purified by silica gel flash chromatography (20:1 hexanes to dichloromethane) and obtained as a colorless oil (50 mg, 49% yield). R_f = 0.3 (10:1 hexanes to dichloromethane); ^1H NMR (400 MHz, CDCl₃) δ 7.61 (dt, J = 7.9, 1.0 Hz, 1H), 7.33 (dq, J = 8.4, 1.0 Hz, 1H), 7.22 (ddd, J = 8.2, 6.9, 1.2 Hz, 1H), 7.08 (ddd, J = 7.9, 7.0, 1.0 Hz, 1H), 6.70 (s, 1H), 3.86 (s, 3H), 0.40 (s, 9H); ^{13}C NMR (101 MHz, CDCl₃) δ 141.18, 140.25, 128.41, 122.12, 120.78, 119.25, 111.43, 109.13, 33.07, -0.37.; IR (Neat Film NaCl) 3046, 2955, 1492, 1466, 1407, 1357,

1326, 1300, 1250, 1233, 1072, 899, 839, 748 cm^{-1} ; HRMS (MM+) calc'd for $\text{C}_{12}\text{H}_{17}\text{NSi}$ $[\text{M}+\text{H}]^+$: 204.1203, found: 204.1196.

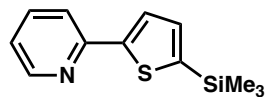


trimethyl(5-pentylfuran-2-yl)silane (235): The general procedure was followed using $\text{KO}t\text{-Bu}$ (4.5 mg, 0.04 mmol, 20 mol %), 2-pentylfuran (27.6 mg, 0.2 mmol, 1 equiv), and 0.2 mL of THF at 45 °C in a sealed tube for 24 h. **235** was purified by passage through a short pad of silica gel (100% hexanes) and obtained as a colorless oil (26.3 mg, 58% yield). ^1H NMR (500 MHz, CDCl_3) δ 6.52 (d, $J = 3.1$ Hz, 1H), 5.96 (dt, $J = 3.1, 0.9$ Hz, 1H), 3.19 – 2.17 (m, 2H), 1.70 – 1.59 (m, 2H), 1.40 – 1.25 (m, 4H), 0.99 – 0.81 (m, 3H), 0.24 (s, 9H). ^{13}C NMR (126 MHz, CDCl_3) δ 161.24, 158.25, 120.48, 104.72, 31.64, 28.33, 27.88, 22.58, 14.17, -1.37. IR (Neat Film NaCl) 2956, 2931, 1588, 1386, 1248, 1010, 834, 782, 759 cm^{-1} ; HRMS (MM+) calc'd for $\text{C}_{12}\text{H}_{22}\text{OSi}$ $[\text{M}+\text{H}]^+$: 211.1513, found: 211.1516.

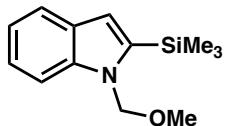


trimethyl(5-pentylthiophen-2-yl)silane (236): The general procedure was followed using $\text{KO}t\text{-Bu}$ (4.5 mg, 0.04 mmol, 20 mol %), 2-pentylthiophene (30.8 mg, 0.2 mmol, 1 equiv), and 0.2 mL of THF at 45 °C in a sealed tube for 24 h. **236** was purified by passage through a short pad of silica gel (100% hexanes) and obtained as a colorless oil (39.7 mg, 87% yield). ^1H NMR (400 MHz, CDCl_3) δ 7.06 (d, $J = 3.3$ Hz, 1H), 6.84 (dt, $J = 3.3, 0.9$ Hz, 1H), 2.88 – 2.78 (m, 2H), 1.79 – 1.60 (m, 2H), 1.43 – 1.22 (m, 4H), 1.00 –

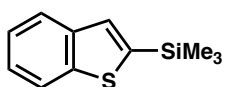
0.79 (m, 3H), 0.29 (s, 9H).; ^{13}C NMR (101 MHz, CDCl_3) δ 151.70, 137.67, 134.07, 125.56, 31.64, 31.57, 30.10, 22.58, 14.16, 0.14. IR (Neat Film NaCl) 3055, 2957, 2930, 2872, 2858, 1528, 1442, 1249, 1213, 1060, 986, 840, 800, 756 cm^{-1} ;



2-(5-(trimethylsilyl)thiophen-2-yl)pyridine (237): The general procedure was followed using KO*t*-Bu (4.5 mg, 0.04 mmol, 20 mol %), 2-(thiophen-2-yl)pyridine (32.3 mg, 0.2 mmol, 1 equiv), and 0.2 mL of THF at 45 °C for 22 h. **237** was purified by silica gel flash chromatography (10:1 hexanes to ethyl acetate) and obtained as a colorless oil (14.6 mg, 32% yield). $R_f = 0.4$ (10:1 hexanes to ethyl acetate); ^1H NMR (400 MHz, CDCl_3) δ 8.67 – 8.48 (m, 1H), 7.70 – 7.63 (m, 2H), 7.61 (d, $J = 3.5$ Hz, 1H), 7.24 (d, $J = 3.5$ Hz, 1H), 7.13 (ddd, $J = 6.3, 4.9, 2.2$ Hz, 1H), 0.35 (s, 9H).; ^{13}C NMR (101 MHz, CDCl_3) δ 152.70, 149.73, 143.24, 136.81, 134.96, 125.77, 121.99, 119.08, -0.04.; IR (Neat Film NaCl) 3056, 3002, 2955, 2896, 1588, 1563, 1523, 1466, 1424, 1316, 1290, 1250, 1208, 1168, 1152, 1078, 1066, 1066, 1048, 1006, 990, 964, 837, 774, 756, 712 cm^{-1} HRMS (MM+) calc'd for $\text{C}_{12}\text{H}_{15}\text{NSSi}$ $[\text{M}+\text{H}]^+$: 234.0767, found: 234.0778. The analytical data are in accordance with those reported.¹⁸

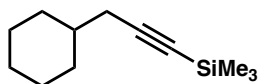


1-(methoxymethyl)-2-(trimethylsilyl)-1*H*-indole (238): The general procedure was followed using KO*t*-Bu (4.5 mg, 0.02 mmol, 20 mol %), 1-(methoxymethyl)-1*H*-indole (32.3 mg, 0.2 mmol, 1 equiv), and 0.2 mL of THF at 45 °C in a sealed tube for 24 h. **238** was purified by silica gel flash chromatography (20:1 hexanes to ethyl acetate) and obtained as a colorless oil (36.8 mg, 78% yield). $R_f = 0.25$ (20:1 hexanes to ethyl acetate); ^1H NMR (400 MHz, CDCl₃) δ 7.61 (dt, $J = 7.9, 1.0$ Hz, 1H), 7.47 (dq, $J = 8.3, 0.9$ Hz, 1H), 7.23 (ddd, $J = 8.2, 7.0, 1.2$ Hz, 1H), 7.11 (ddd, $J = 7.9, 7.0, 1.0$ Hz, 1H), 6.78 (d, $J = 0.9$ Hz, 1H), 5.52 (s, 2H), 3.25 (s, 3H), 0.39 (s, 9H); ^{13}C NMR (101 MHz, CDCl₃) δ 141.23, 140.44, 128.90, 122.71, 120.88, 120.12, 114.01, 109.72, 76.65, 55.51, -0.18.; IR (Neat Film NaCl) 2954, 2332, 1466, 1312, 1249, 1223, 1166, 1103, 1090, 1046, 897, 841, 737 cm⁻¹; HRMS (MM+) calc'd for C₁₃H₁₉NOSi [M+H]⁺: 234.1309, found: 234.1313.



benzo[*b*]thiophen-2-yltrimethylsilane (71): The general procedure was followed using KO*t*-Bu (11.2 mg, 0.1 mmol, 20 mol %), benzo[*b*]thiophene (67.1 mg, 0.5 mmol, 1 equiv), and 0.5 mL of THF at 45 °C in a sealed tube for 24 h. **71** was purified by silica gel flash chromatography (10:1 hexanes to dichloromethane) and obtained as a colorless oil (69 mg, 67% yield). $R_f = 0.4$ (10:1 hexanes to dichloromethane); ^1H NMR (400 MHz, CDCl₃) δ 7.95 – 7.85 (m, 1H), 7.85 – 7.76 (m, 1H), 7.47 (d, $J = 0.9$ Hz, 1H), 7.39 – 7.26

(m, 2H), 0.38 (s, 9H); ^{13}C NMR (101 MHz, CDCl_3) δ 143.66, 142.40, 141.21, 130.96, 124.27, 124.13, 123.54, 122.34, -0.16.; IR (Neat Film NaCl) 3054, 2954, 1492, 1454, 1290, 1249, 1017, 970, 842, 828, 800, 776, 742 cm^{-1} ; HRMS (EI $^+$) calc'd for $\text{C}_{11}\text{H}_{14}\text{SSi}$ [M] $^+$: 206.0586, found: 206.0603. The analytical data are in accordance with those reported.^{9d}



(3-cyclohexylprop-1-yn-1-yl)trimethylsilane (239): The general procedure was followed using KOH (2.8 mg, 0.05 mmol, 10 mol %), 3-cyclohexyl-1-propyne (61 mg, 0.5 mmol, 1 equiv), and 0.5 mL of DME at 45 °C in a sealed tube for 48 h. **239** purified by silica gel flash chromatography (ISCO automated, hexanes then 0 to 10% ethyl acetate in hexanes) and obtained as a colorless oil (72.3 mg, 74% yield) ^1H NMR (400 MHz, CDCl_3) δ 2.11 (d, $J = 6.7$ Hz, 2H), 1.85 – 1.75 (m, 2H), 1.75 – 1.60 (m, 3H), 1.53 – 1.38 (m, 1H), 1.32 – 1.05 (m, 3H), 1.04 – 0.88 (m, 2H), 0.15 (s, 9H); ^{13}C NMR (101 MHz, CDCl_3) δ 106.72, 85.29, 37.42, 32.79, 27.83, 26.44, 26.29, 0.37.; IR (Neat Film NaCl) 2923, 2854, 2175, 1250, 839 cm^{-1} ; HRMS (EI $^+$) calc'd for $\text{C}_{12}\text{H}_{22}\text{Si}$ [M] $^+$: 194.1491, found: 194.1505.

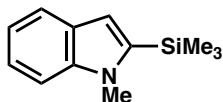
3.4.2.2 General Procedure for Optimization Using Hexamethyldisilane

Based on previously reported screening procedure.¹⁵ In a nitrogen-filled glove box, *N*-methylindole **55** (0.2–0.5 mmol, 1 equiv), hexamethyldisilane, the indicated base, and solvent were added to a 1 dram vial equipped with a magnetic stirring bar. At the

indicated time, aliquots were removed using a glass capillary tube, diluted with Et₂O, and analyzed using GC-FID to determine regioselectivity and yield.

3.4.2.3 General Experimental Procedure and Spectroscopic Data for the C–H Silylation Using Hexamethyldisilane

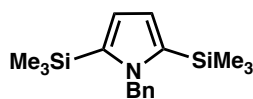
In a nitrogen-filled glove box, substrate (0.2–0.5 mmol, 1 equiv), hexamethyldisilane (2 equiv), the indicated base (20 mol %), and solvent (1M in substrate) were added to a 1 dram vial equipped with a magnetic stirring bar. Then the vial was sealed and the mixture was stirred at the indicated temperature for the indicated time. When complete, the reaction mixture was diluted with diethyl ether (2 mL) and concentrated under reduced pressure. The residue was purified by silica gel flash chromatography to give the desired product.



1-methyl-2-(trimethylsilyl)-1*H*-indole (184): The general procedure was followed using KO*t*-Bu (11.2 mg, 0.1 mmol, 20 mol %) or KOEt (8.4 mg, 0.1 mmol, 20 mol %), **55** (65.6 mg, 0.5 mmol, 1 equiv), hexamethyldisilane (146.4 mg, 1 mmol, 2 equiv), and 0.5 mL of THF at 45 °C for 48 h. **184** was purified by silica gel flash chromatography as above to obtain a colorless oil, (59% yield from KO*t*-Bu or 61% yield from KOEt). The analytical data are in accordance with those reported above.

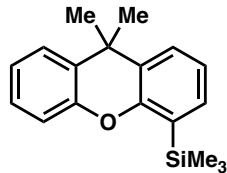


1-benzyl-2-(trimethylsilyl)-1*H*-indole (240): The general procedure was followed using KO*t*-Bu (11.2 mg, 0.1 mmol, 20 mol %), *I*-benzyl-1*H*-indole (103.63 mg, 0.5 mmol, 1 equiv), hexamethyldisilane (146.4 mg, 1 mmol, 2 equiv), and 0.5 mL of DME at 45 °C for 96 h. **240** was purified by silica gel flash chromatography (5:1 hexanes in dichloromethane) to obtain a colorless oil (73.3 mg, 52% yield). $R_f = 0.3$ (5:1 hexanes in dichloromethane); ^1H NMR (400 MHz, CDCl₃) δ 7.67 – 7.62 (m, 1H), 7.25 – 7.17 (m, 3H), 7.15 – 7.02 (m, 3H), 6.94 – 6.84 (m, 2H), 6.79 (s, 1H), 5.48 (s, 2H), 0.27 (s, 9H).; ^{13}C NMR (101 MHz, CDCl₃) δ 141.51, 139.98, 138.39, 128.81, 128.76, 127.29, 125.87, 122.37, 120.82, 119.57, 112.29, 110.05, 50.01, -0.31.; IR (Neat Film NaCl) 3060, 2955, 1606, 1495, 1466, 1450, 1353, 1333, 1301, 1250, 1197, 1164, 1115, 1096, 1014, 906, 840, 792, 748, 725 cm⁻¹; HRMS (MM+) calc'd for C₁₈H₂₁NSi [M+H]⁺: 280.1516, found: 280.1512.

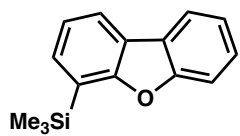


1-benzyl-2,5-bis(trimethylsilyl)-1*H*-pyrrole (241): The general procedure was followed using KOEt (8.4 mg, 0.1 mmol, 20 mol %), 1-benzyl-1*H*-pyrrole (78 mg, 0.5 mmol, 1 equiv), hexamethyldisilane (146 mg, 1 mmol, 2 equiv), and 0.5 mL of THF at 80 °C for 72 h. **241** was purified by Isco automated silica gel flash chromatography (0→10% CH₂Cl₂ in hexanes) to obtain a white, crystalline solid (64.8 mg, 43% yield, Mp.73–78 °C). $R_f = 0.2$ (9:1 hexanes to dichloromethane).; ^1H NMR (400 MHz, C₆D₆) δ 7.06 – 6.92

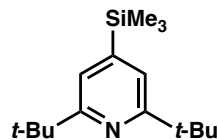
(m, 3H), 6.76 (s, 2H), 6.69 – 6.61 (m, 2H), 5.25 (s, 2H), 0.12 (s, 18H).; ^{13}C NMR (101 MHz, C_6D_6) δ 140.61, 138.39, 128.68, 127.33, 125.98, 120.90, 53.54, 0.03.; IR (Neat Film NaCl) 2958, 1348, 1248, 835, 756 cm^{-1} ; HRMS (MM+) calc'd for $\text{C}_{17}\text{H}_{27}\text{NSi}_2$ $[\text{M}+\text{H}]^+$: 302.1755, found: 302.1745.



(9,9-dimethyl-9*H*-xanthen-4-yl)trimethylsilane (242): The general procedure was followed using KO*t*-Bu (5.6 mg, 0.2 mmol, 20 mol %), 9,9-dimethyl-9*H*-xanthene (52.6 mg, 0.25 mmol, 1 equiv), hexamethyldisilane (73 mg, 0.5 mmol, 2 equiv), and 0.25 mL of THF at 80 °C for 48 h. **242** was purified by silica gel flash chromatography (hexanes → 25:1 hexanes to DCM) to obtain a colorless oil (22.1 mg, 30 % yield). $R_f = 0.7$ (20:1 hexanes to EtOAc); ^1H NMR (400 MHz, CDCl_3) δ 7.50 – 7.38 (m, 2H), 7.31 (dd, $J = 7.1, 1.6 \text{ Hz}$, 1H), 7.21 (ddd, $J = 8.0, 7.3, 1.6 \text{ Hz}$, 1H), 7.13 – 6.99 (m, 3H), 1.64 (s, 6H), 0.38 (s, 9H).; ^{13}C NMR (101 MHz, CDCl_3) δ 155.17, 150.86, 133.07, 130.49, 129.33, 127.48, 127.41, 126.98, 126.05, 123.12, 122.97, 116.18, 34.35, 32.17, -0.51.; IR (Neat Film NaCl) 3750, 2966, 2362 (minor CO_2), 1595, 1488, 1458, 1308, 1243, 1204, 1128, 1104, 858, 838, 820, 790, 752, 715 cm^{-1} ;



dibenzo[*b,d*]furan-4-yltrimethylsilane (243): The general procedure was followed using KOEt (8.4 mg, 0.1 mmol, 20 mol %), dibenzo[*b,d*]furan (84 mg, 0.5 mmol, 1 equiv), hexamethyldisilane (146 mg, 1 mmol, 2 equiv), and THF (0.5 mL, 1M) at 45 °C for 48 h. **243** was purified by silica gel flash chromatography (hexanes, $R_f = 0.5$, 34 mg, 28% yield) as a colorless oil. ^1H NMR (^1H NMR (500 MHz, Chloroform-*d*) δ 8.04 – 7.90 (m, 2H), 7.58 (dt, $J = 8.2$, 0.8 Hz, 1H), 7.52 (dt, $J = 7.1$, 1.4 Hz, 1H), 7.45 (ddd, $J = 8.3$, 7.3, 1.3 Hz, 1H), 7.38 – 7.29 (m, 2H), 0.47 (s, 9H).; ^{13}C NMR (101 MHz, CDCl₃) δ 132.52, 132.37, 126.99, 122.87, 122.78, 122.56, 122.52, 122.40, 121.74, 121.69, 120.72, 111.79, -0.85.; IR (Neat Film NaCl) 3046, 2956, 2898, 1570, 1470, 1449, 1402, 1391, 1378, 1346, 1300, 1262, 1248, 1192, 1173, 1144, 1110, 1049, 1010, 906, 840, 759, 732 cm⁻¹;



2,6-di-*tert*-butyl-4-(trimethylsilyl)pyridine (244): The general procedure was followed using KO*t*-Bu (11.2 mg, 0.1 mmol, 20 mol %), 2,6-di-*tert*-butylpyridine (51.3 mg, 0.3 mmol, 1 equiv), hexamethyldisilane (219.6 mg, 1.5 mmol, 3 equiv), and 0.5 mL of THF at 65 °C for 48 h. **244** was purified by silica gel flash chromatography (20:1 hexanes to dichloromethane) to obtain a yellow oil (119.8 mg, 91% yield). $R_f = 0.5$ (10:1 hexanes to dichloromethane); ^1H NMR (500 MHz, CDCl₃) δ 7.22 (s, 2H), 1.39 (s, 18H), 0.31 (s, 9H). ^{13}C NMR (126 MHz, CDCl₃) δ 166.30, 149.56, 119.54, 37.76, 30.41, -1.26.; IR (Neat Film NaCl) 3051, 2958, 2904, 2869, 1587, 1575, 1538, 1479, 1456, 1390, 1360, 1263,

3.4.2.4 Procedure for Time Course Reaction Monitoring by *in situ* ¹H NMR

In a nitrogen-filled glove box, a J-Young gas-tight NMR tube is charged with **55** (65.8 mg, 0.5 mmol, 1 equiv), KOt-Bu (11.2 mg, 0.1 mmol, 20 mol %), hexamethyldisilane (146.4 mg, 2 equiv), 1,2,5-trimethoxybenzene (8.4 mg as internal standard), and THF-D₈ (0.5 mL). The tube is tightly capped with the corresponding Teflon plug, removed from the glove box, placed in the bore of the NMR, and heated to 45 °C. ¹H NMR spectra were acquired in “array” mode, with a spectrum taken approximately every 3 minutes for the length of experiment. The data was processed using MestReNova and peak integrations were normalized to 1,2,5-trimethoxybenzene. Data is decimated and displayed using the MestReNova “stack” function. The presence of Me₃SiH was confirmed by a crosspeak in the ¹H-²⁹Si HSQC spectrum.

3.5 REFERENCES AND NOTES

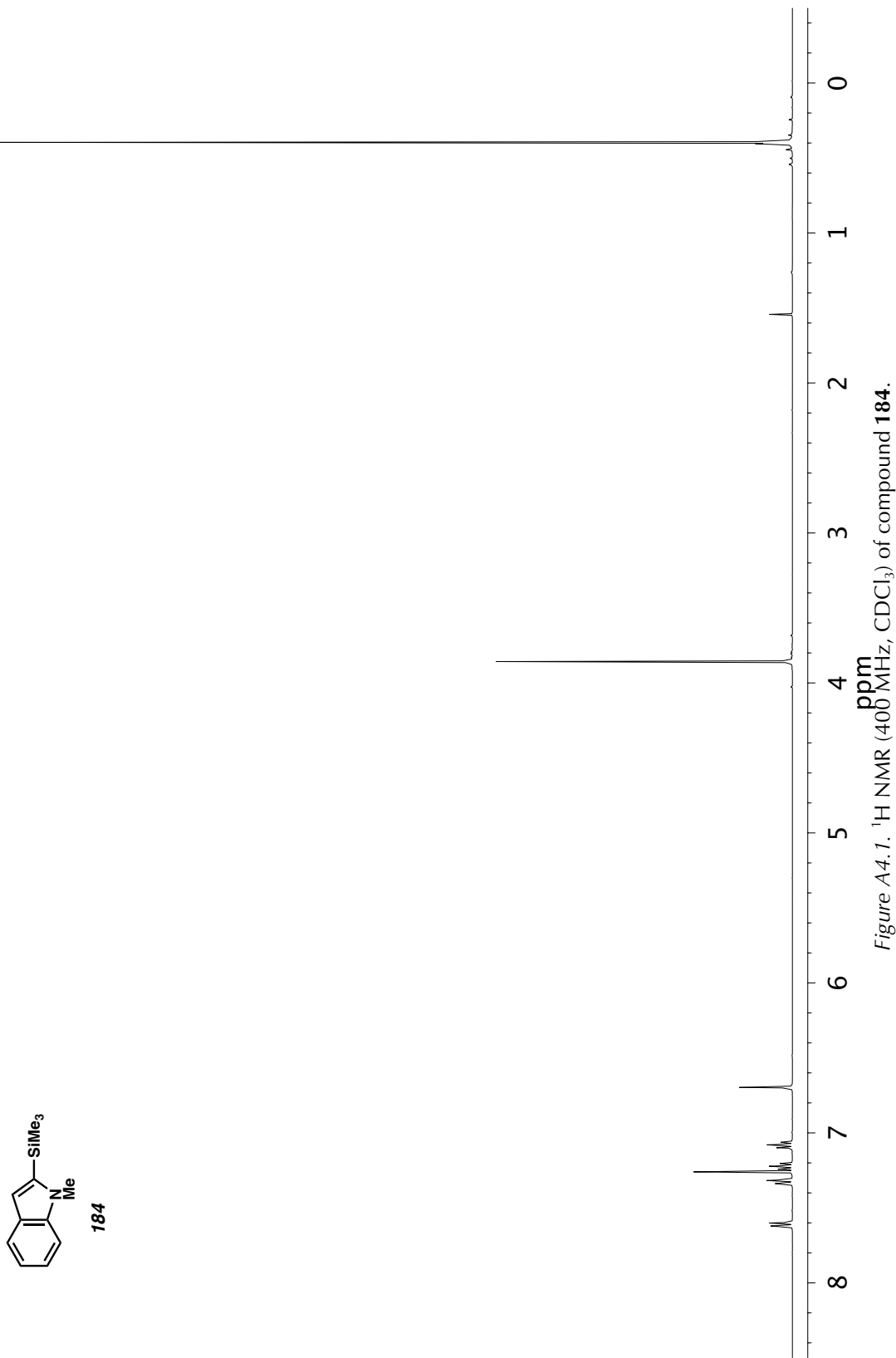
- (1) (a) Langkopf, E.; Schinzer, D. *Chem. Rev.* **1995**, *9*, 1375–1408.; (a) Tamao K. *Proc. Jpn. Acad. Ser. B. Phys. Biol. Sci.* **2008**, *84*, 123–133.
- (2) Zhang, F.; Wu, D.; Xu, Y.; Feng, X. *J. Mater. Chem.* **2011**, *21*, 17590–17600.
- (3) Showell, G. A.; Mills, J. S. *Drug Discov. Today* **2003**, *8*, 551–556.
- (4) Franz, A. K.; Wilson S. O. *J. Med. Chem.* **2013**, *56*, 388–405.

- (5) Cheng, C.; Hartwig, J. F. *Chem. Rev.* **2015**, *115*, 8946–8975.
- (6) Nakao, Y.; Hiyama, T. *Chem. Soc. Rev.* **2011**, *40*, 4893–4901.
- (7) Toutov, A. A.; Liu, W.-B.; Betz, K. N.; Fedorov, A.; Stoltz, B. M.; Grubbs, R. H. *Nature* **2015**, *518*, 80–84.
- (8) Suginome, M.; Ito, Y. *Chem. Rev.* **2000**, *100*, 3221–3256.
- (9) (a) Kakiuchi, F.; Matsumoto, M.; Sonoda, M.; Fukuyama, T.; Chatani, N.; Murai, S.; Furukawa, N.; Seki, Y. *Chem. Lett.* **2000**, *29*, 750–751.; (b) Tobisu, M.; Ano, Y.; Chatani, N. *Chem. Asian J.* **2008**, *3*, 1585–1591.; (c) Sakakura, T.; Tokunaga, Y.; Sodeyama, T.; Tanaka, M. *Chem. Lett.* **1987**, *16*, 2375–2378.; (d) Sasaki, M., Kondo, Y. *Org. Lett.* **2015**, *17*, 848–851.; (e) Nozawa-Kumada, K.; Osawa, S.; Sasaki, M.; Chataigner, I.; Shigeno, M.; Kondo, Y. *J. Org. Chem.* **2017**, *82*, 9487–9496.
- (10) Garrett, C. E.; Prasad, K. *Adv. Synth. Catal.* **2004**, *346*, 889–900.
- (11) Liu, X.; Xu, C.; Wang, M.; and Liu, Q. *Chem. Rev.* **2015**, *115*, 683–730.
- (12) Toukabri, R.; Shi, Y. *Vac. Sci. Technol. A*, **2013**, *31*, 061606-1.
- (13) Toutov, A. A.; Betz, K. N.; Schuman, D. P.; Liu, W.-B.; Fedorov, A.; Stoltz, B. M.; Grubbs, R. H. *J. Am. Chem. Soc.* **2017**, *139*, 1668–1674.
- (14) We found most rubber materials, including balloons and septa, were unable to contain TMS–H for appreciable lengths of time.
- (15) (a) Liu, W.-B.; Schuman, D. P.; Yang, Y.-F.; Toutov, A. A.; Liang, Y.; Klare, H. F. T.; Nesnas, N.; Osetreich, M.; Blackmond, D. G.; Virgil, S. C.; Banerjee, S.; Zare, R. N.; Grubbs, R. H.; Houk, K. N.; Stoltz, B. M. *J. Am. Chem. Soc.* **2017**,

- 139, 6867.; (b) Banerjee, S.; Yang, Y.-F.; Jenkins, I. D.; Liang, Y.; Toutov, A. A.; Liu, W.-B.; Schuman, D. P.; Grubbs, R. H.; Stoltz, B. M.; Krenske, E. H.; Houk, K. N.; Zare, R. N. *J. Am. Chem. Soc.* **2017**, *139*, 6880–6887.
- (16) Von Grotthuss, E.; Prey, S. E.; Bolte, M.; Lerner, H.-W.; Wagner, M. *J. Am. Chem. Soc.* **2019**, *141*, 6082–6091.
- (17) Pangborn, A. M.; Giardello, M. A.; Grubbs, R. H.; Rosen, R. K.; Timmers, F. J. *Organometallics* **1996**, *15*, 1518–1520.
- (18) Ribereau, P.; Queguiner, G. *Tetrahedron* **1983**, *39*, 3593–3602.

APPENDIX 4

Spectra Relevant to Chapter 3: Catalytic C–H Trimethylsilylation of Aromatic Heterocycles via Base Catalysis



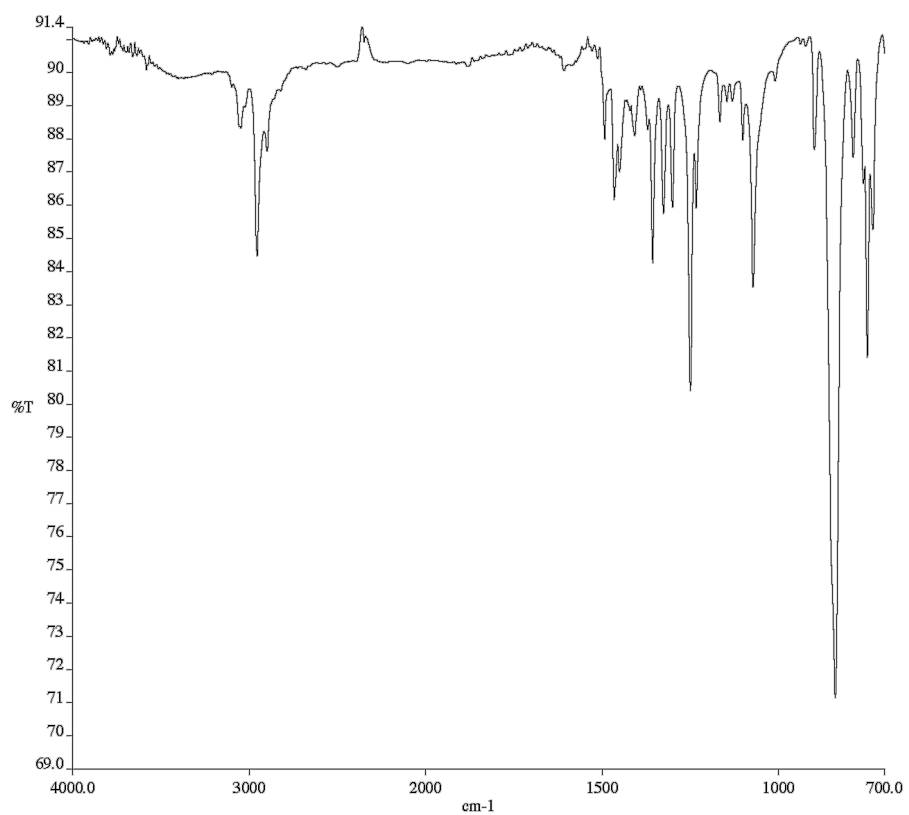


Figure A4.2. Infrared spectrum (Thin Film, NaCl) of compound **184**.

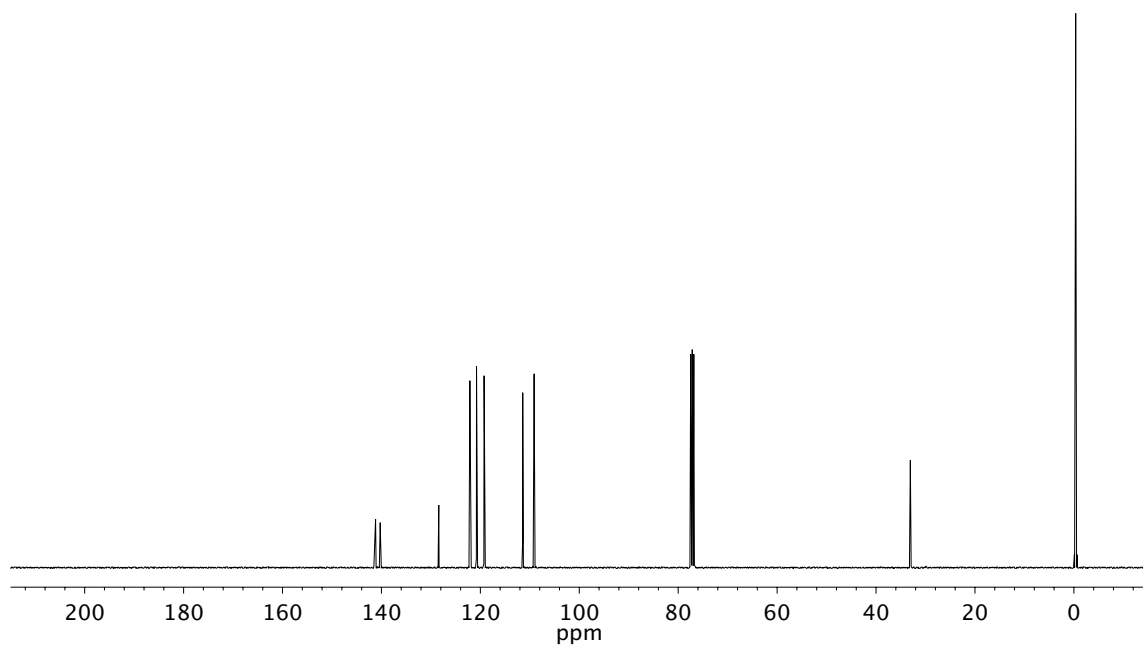
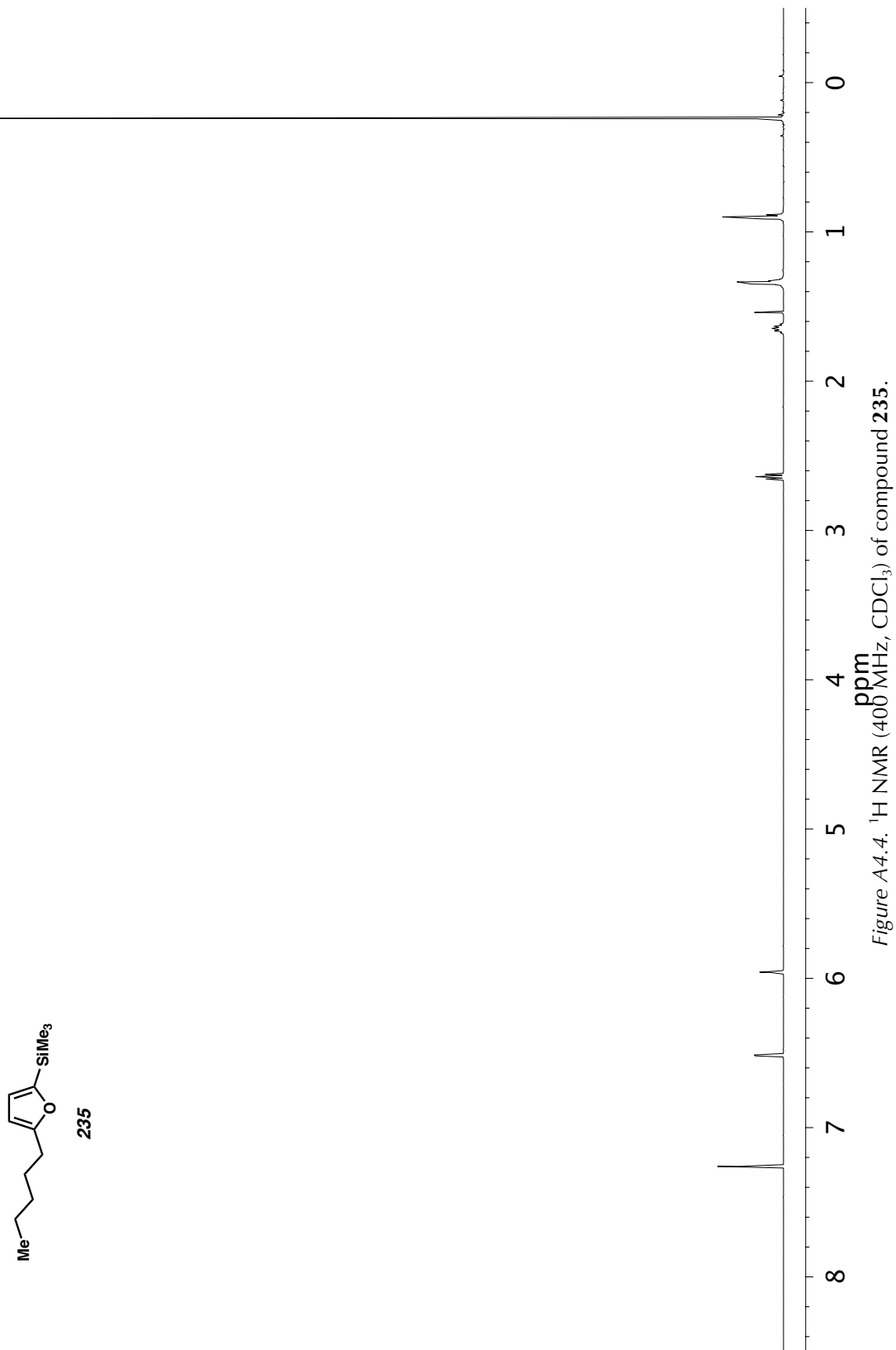


Figure A4.3. ¹³C NMR (101 MHz, CDCl₃) of compound **184**.



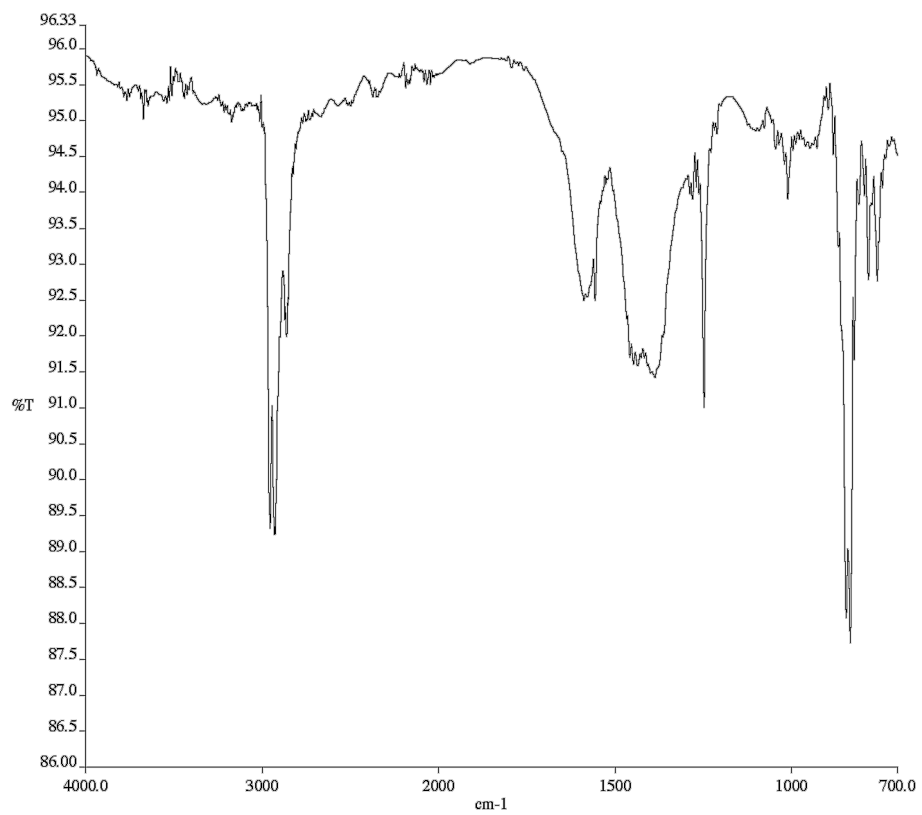


Figure A4.5. Infrared spectrum (Thin Film, NaCl) of compound 235.

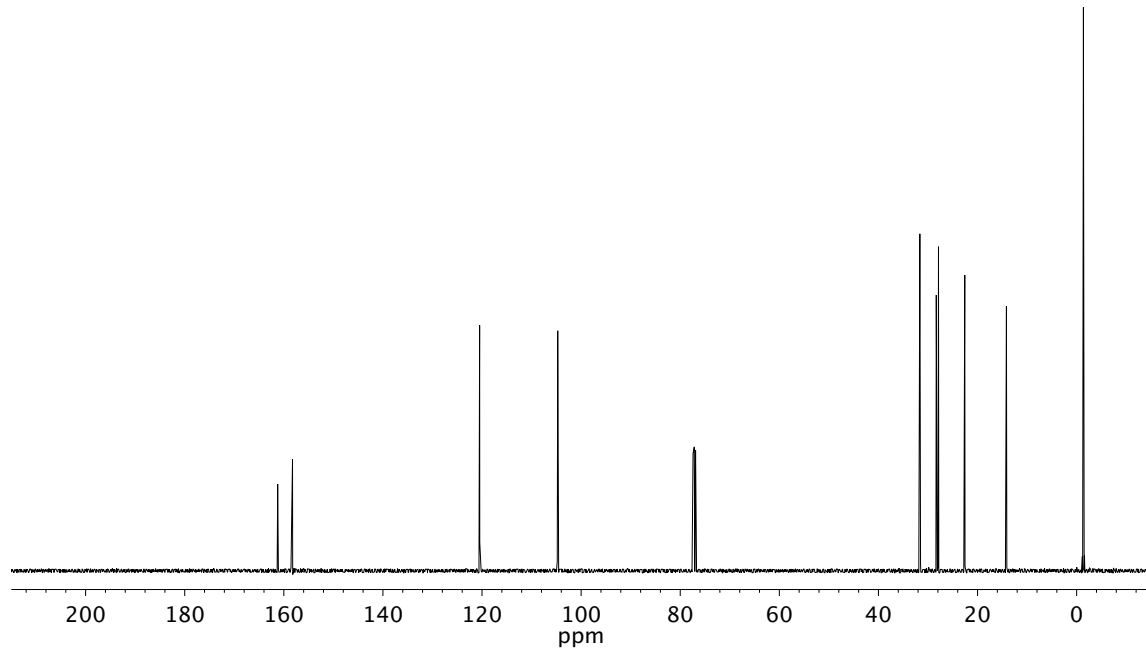


Figure A4.6. ¹³C NMR (101 MHz, CDCl₃) of compound 235.

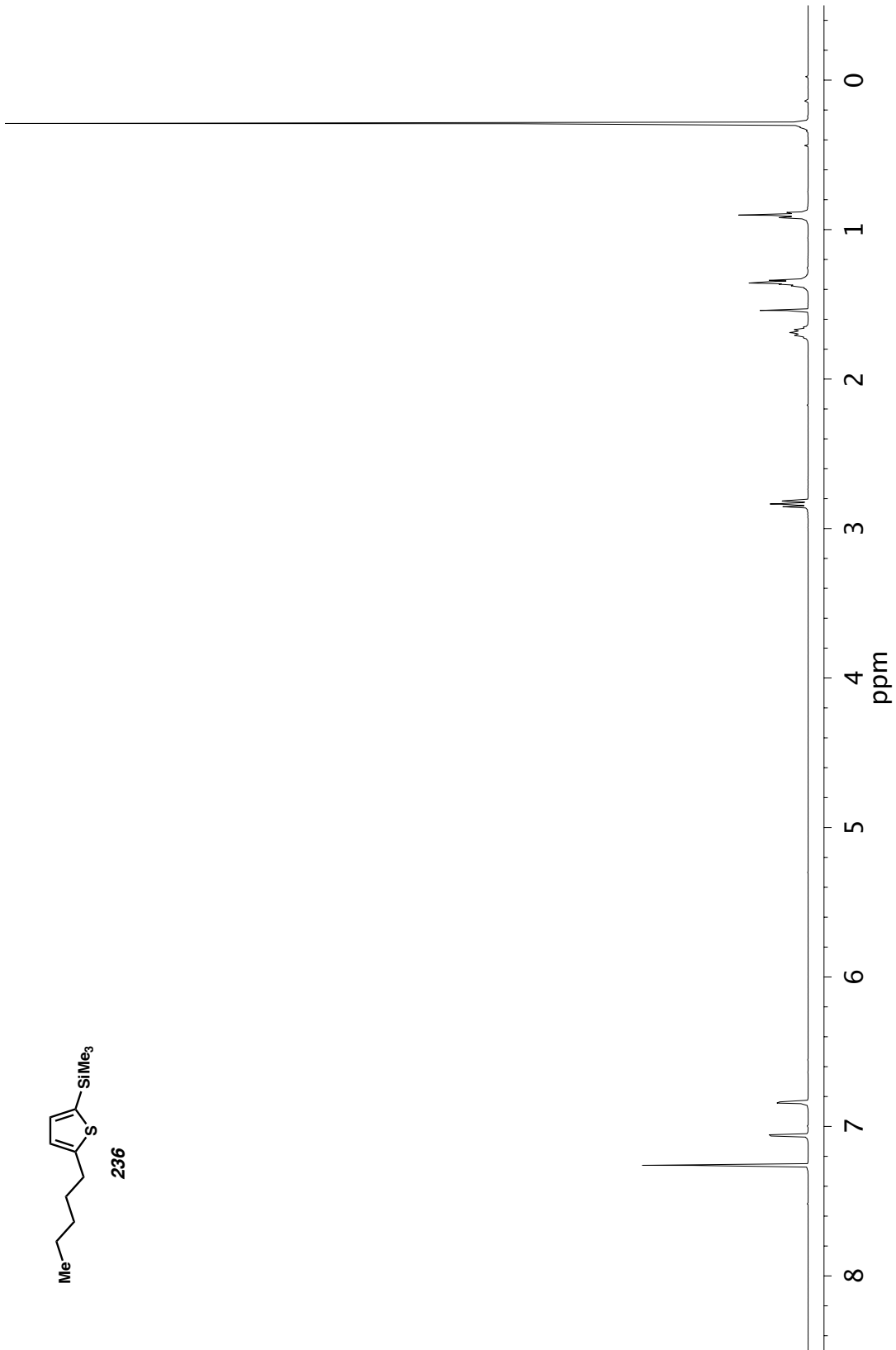
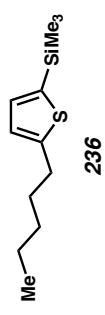


Figure A4.7. ^1H NMR (400 MHz, CDCl_3) of compound 236.

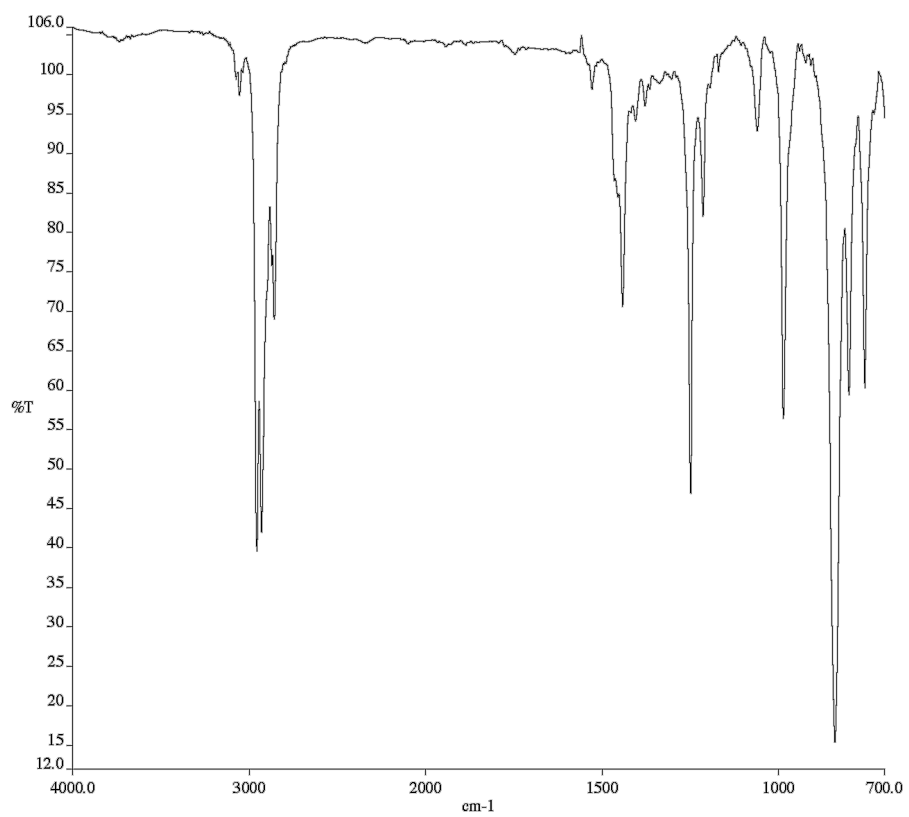


Figure A4.8. Infrared spectrum (Thin Film, NaCl) of compound 236.

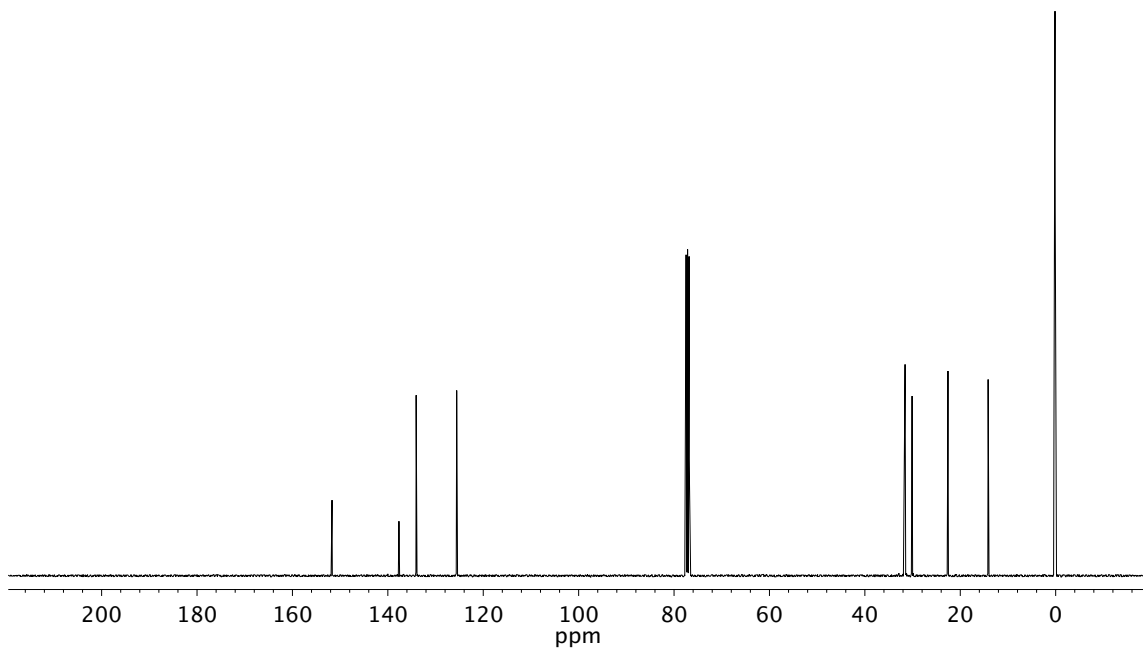


Figure A4.9. ^{13}C NMR (101 MHz, CDCl_3) of compound 236.

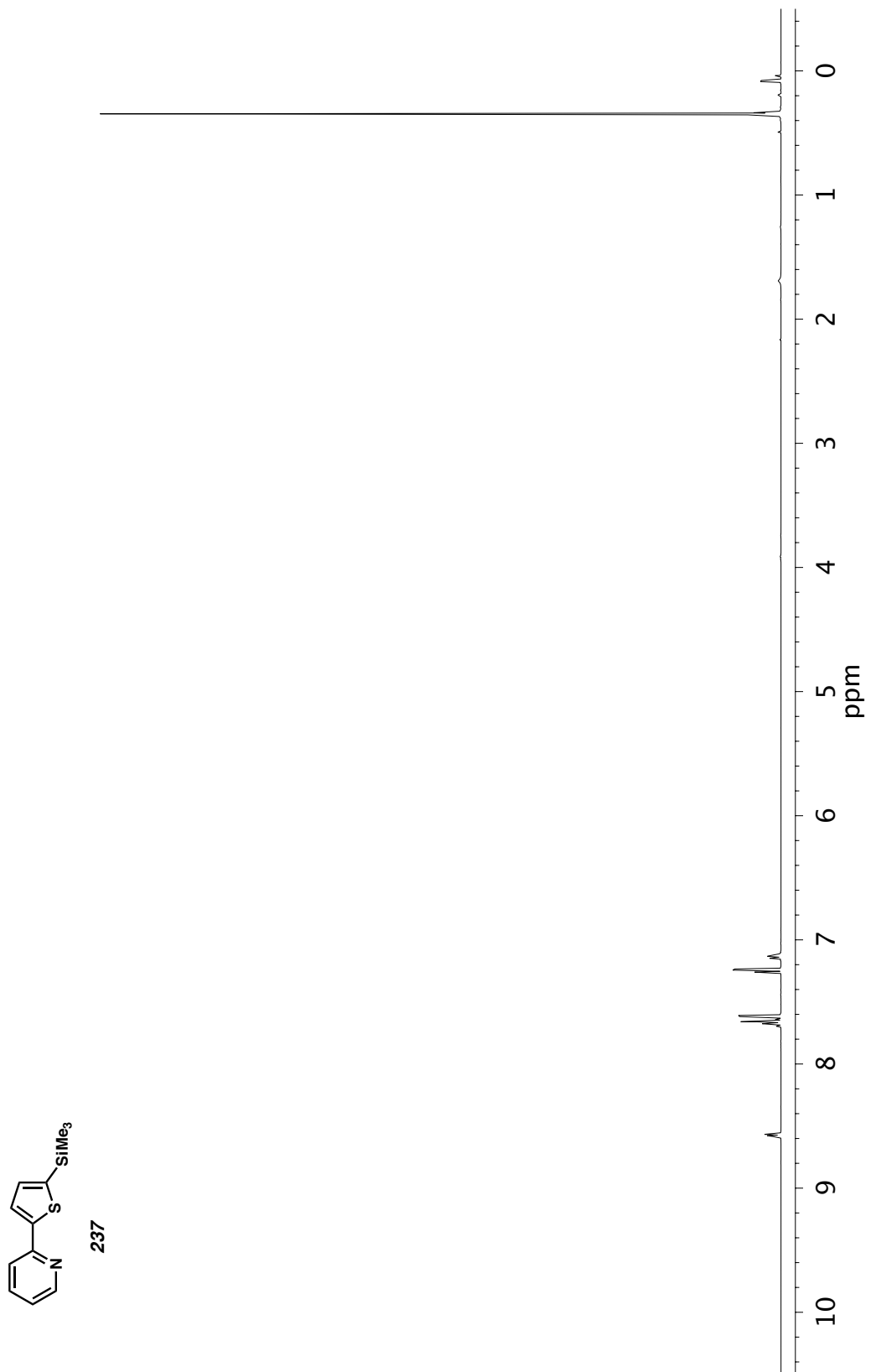


Figure A4.10. ^1H NMR (400 MHz, CDCl_3) of compound 237.

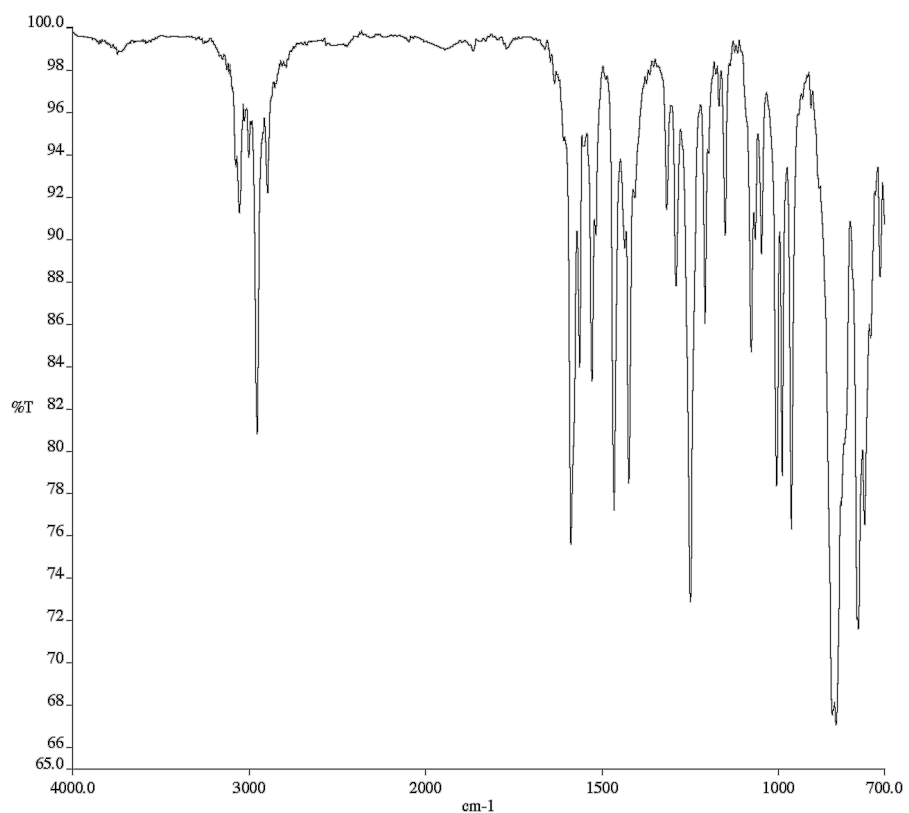


Figure A4.11. Infrared spectrum (Thin Film, NaCl) of compound 237.

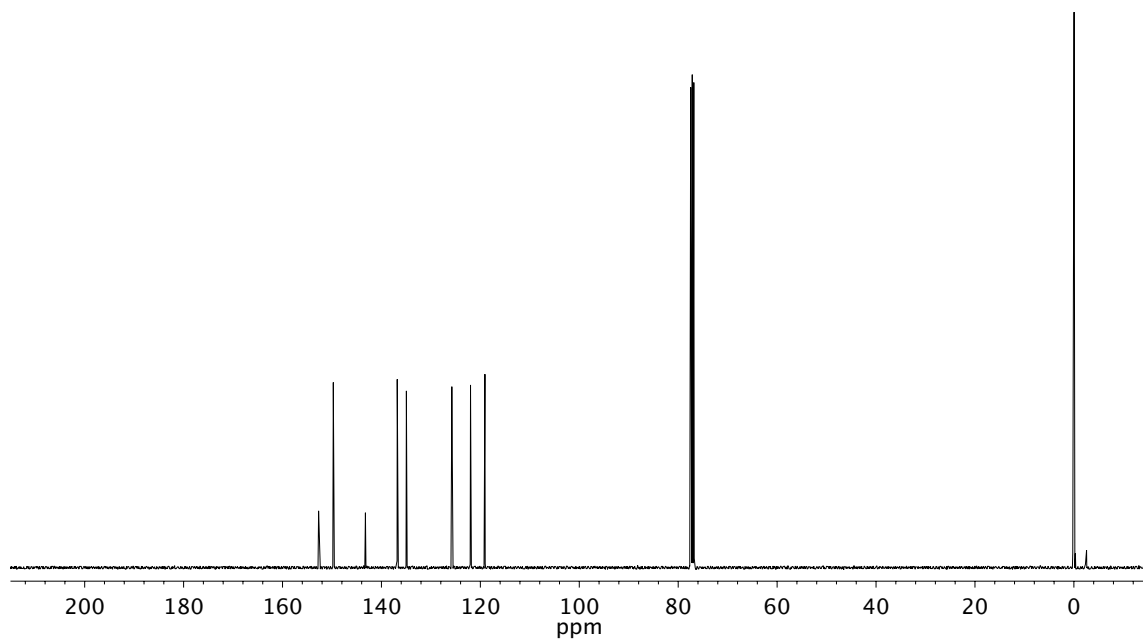


Figure A4.12. ¹³C NMR (101 MHz, CDCl₃) of compound 237.

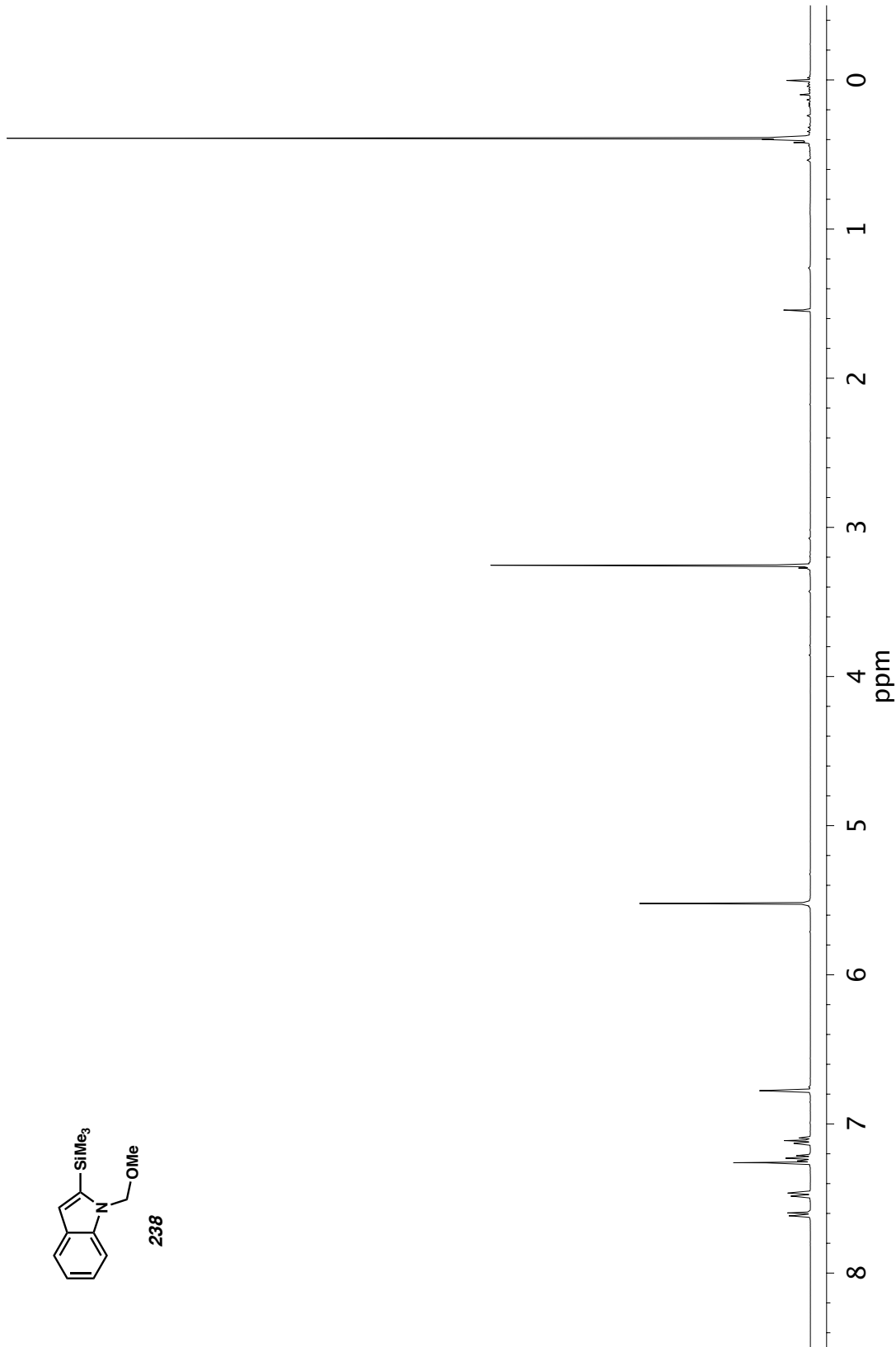
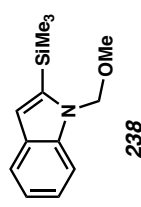


Figure A4.13. ^1H NMR (500 MHz, CDCl_3) of compound 238.

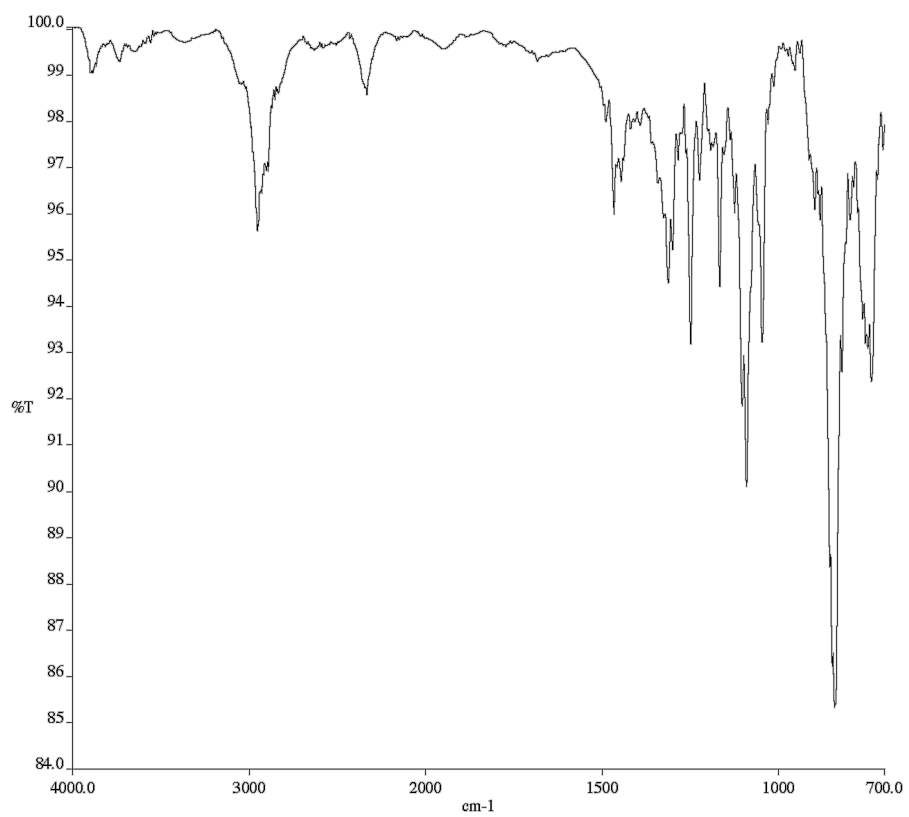


Figure A4.14. Infrared spectrum (Thin Film, NaCl) of compound 238.

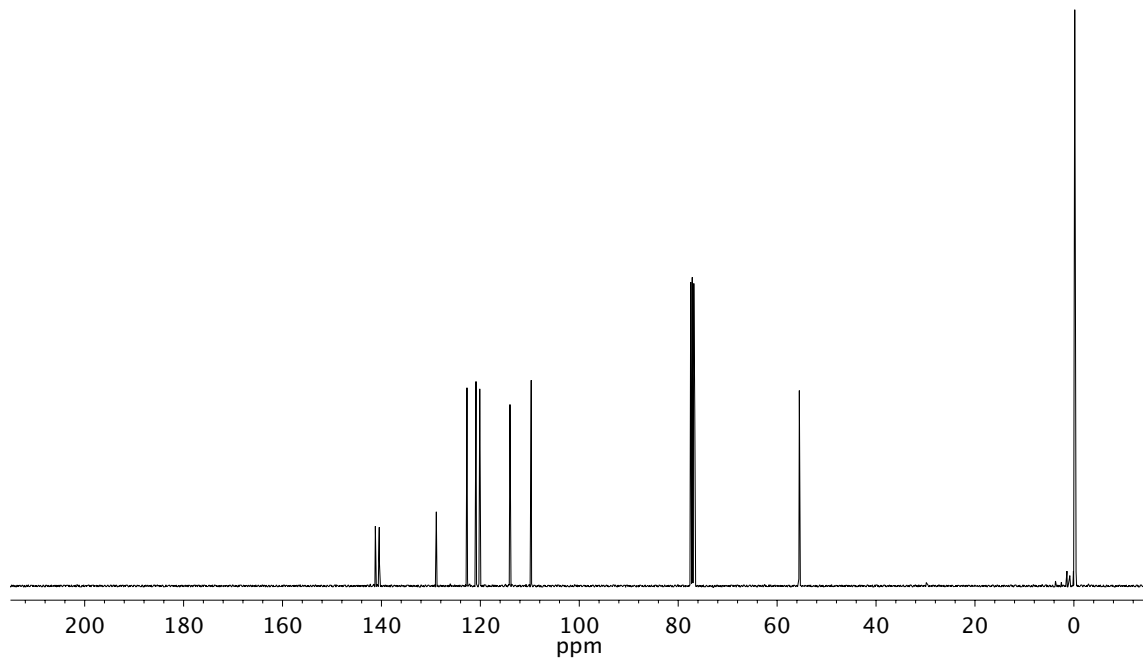


Figure A4.15. ^{13}C NMR (125 MHz, CDCl_3) of compound 238.

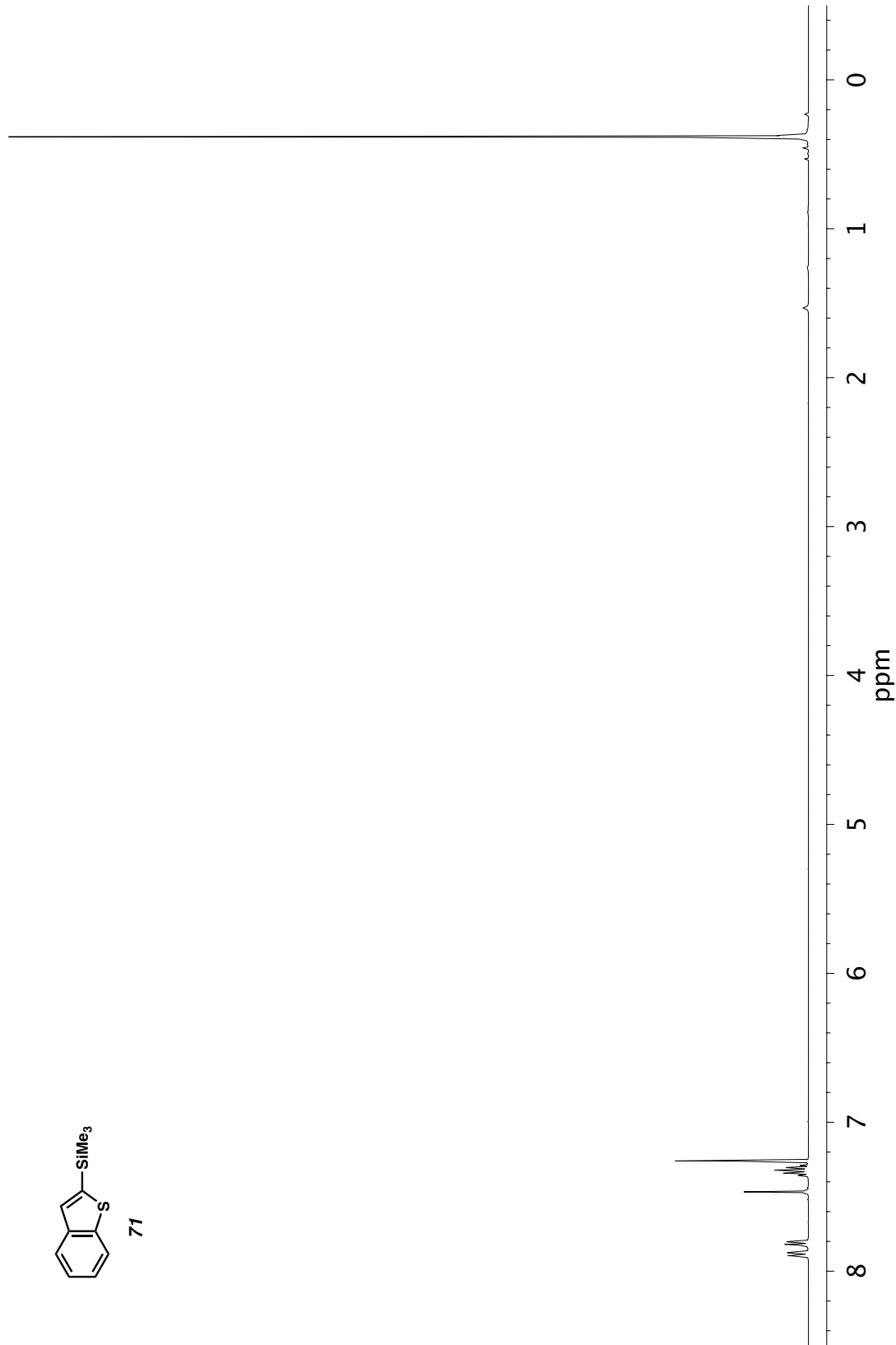
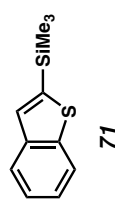


Figure A4.16. ^1H NMR (500 MHz, CDCl_3) of compound 71.

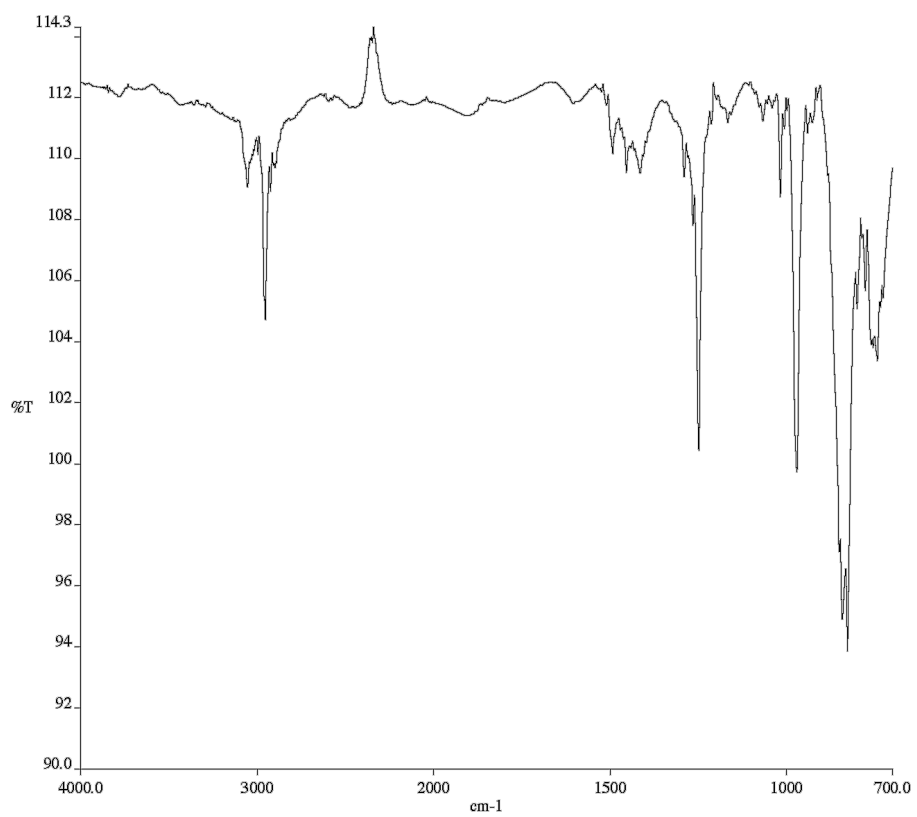


Figure A4.17. Infrared spectrum (Thin Film, NaCl) of compound 71.

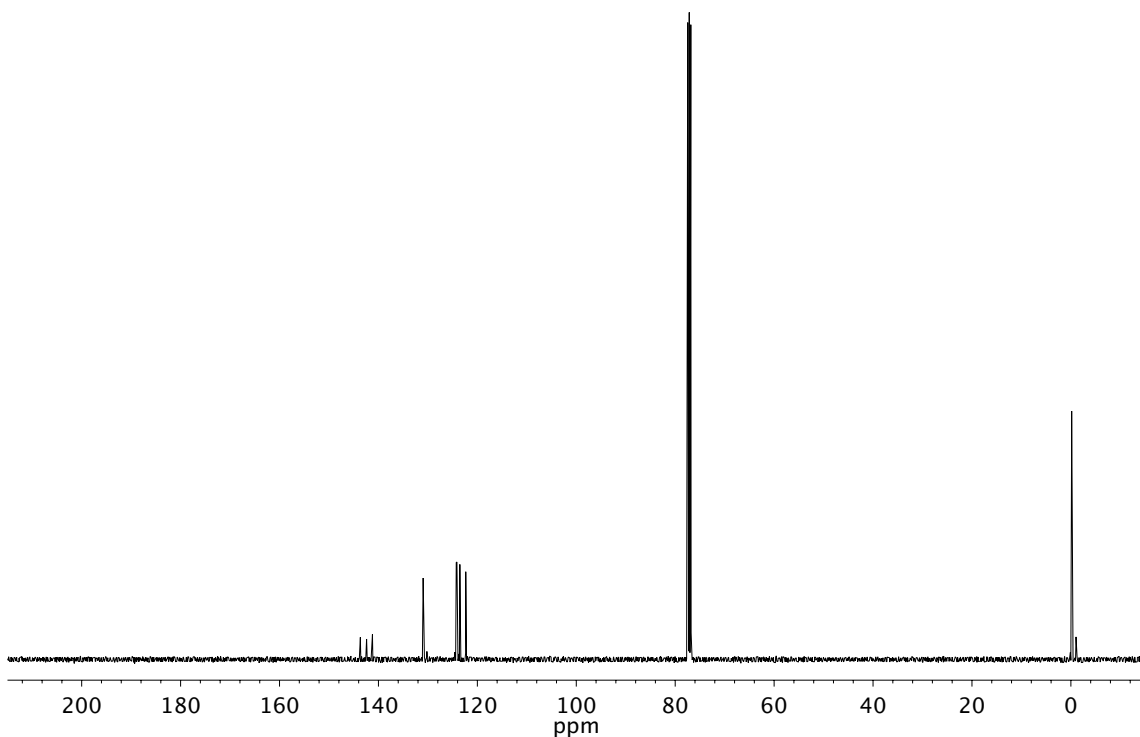


Figure A4.18. ¹³C NMR (125 MHz, CDCl₃) of compound 71.

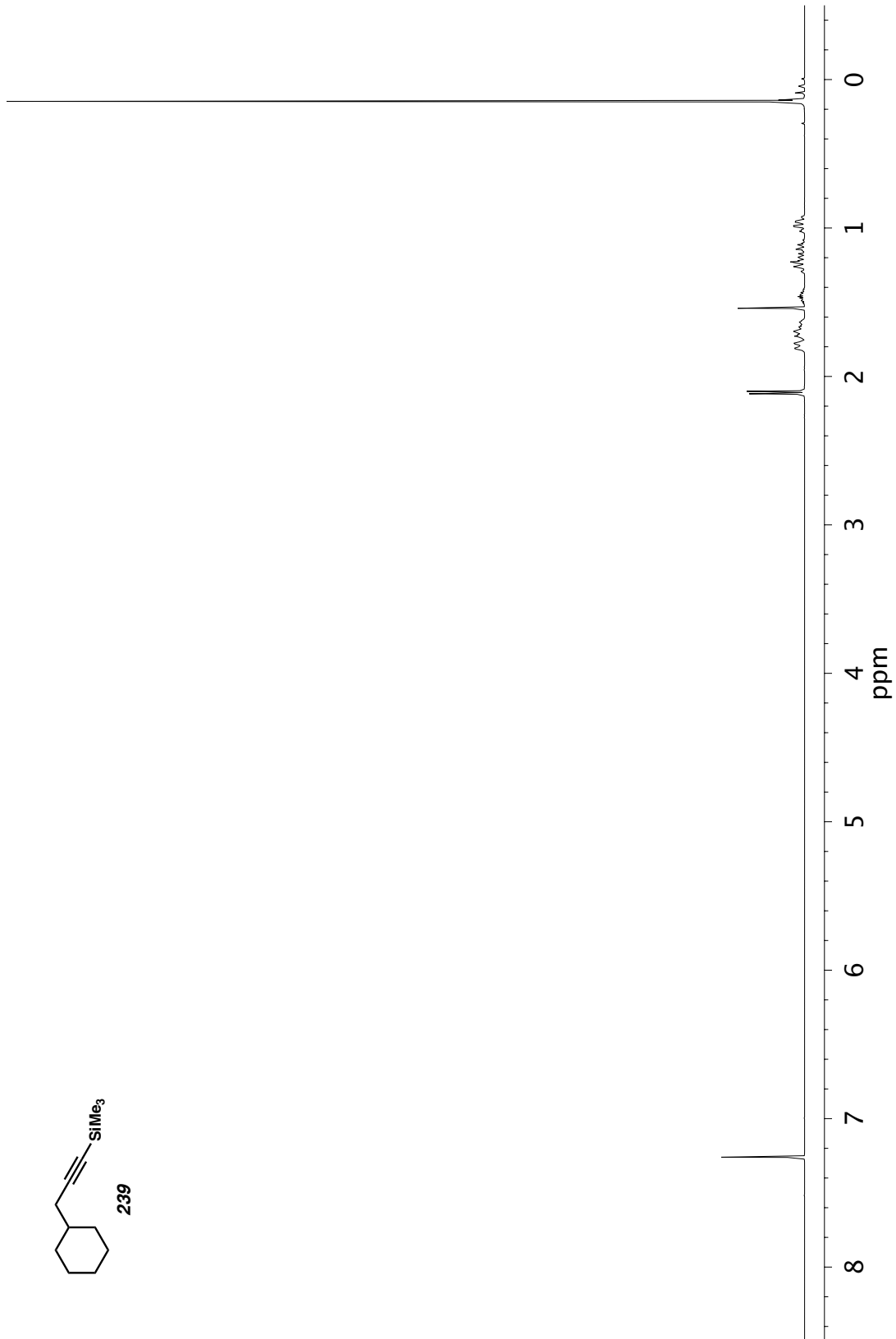


Figure A4.19. ^1H NMR (500 MHz, CDCl_3) of compound 239.

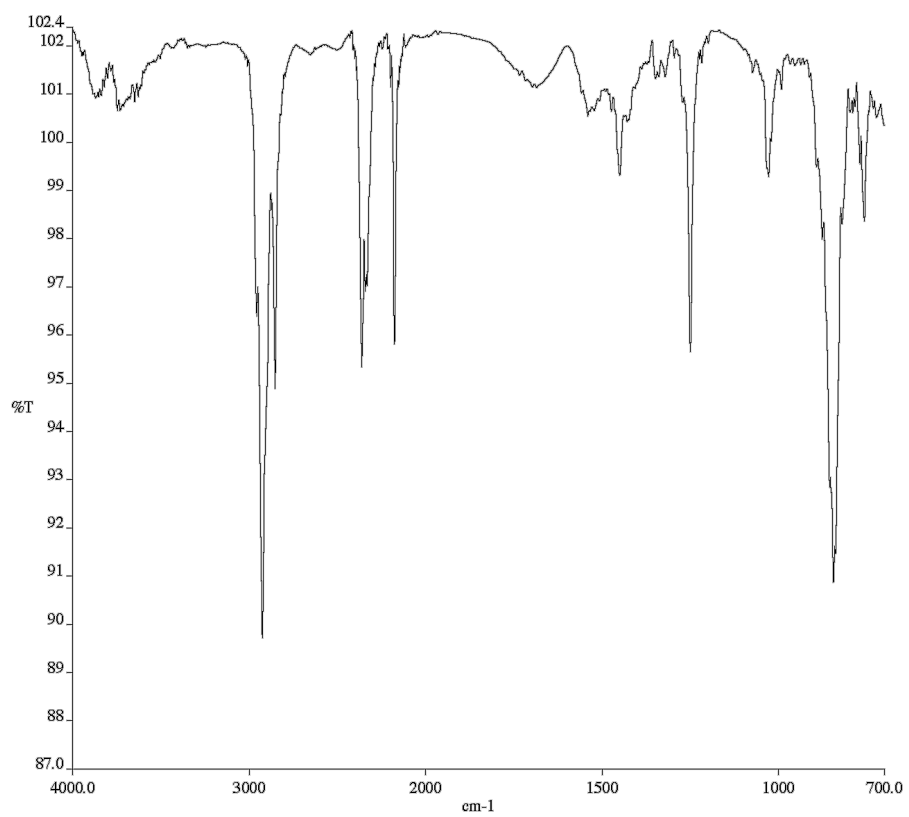


Figure A4.20. Infrared spectrum (Thin Film, NaCl) of compound 239.

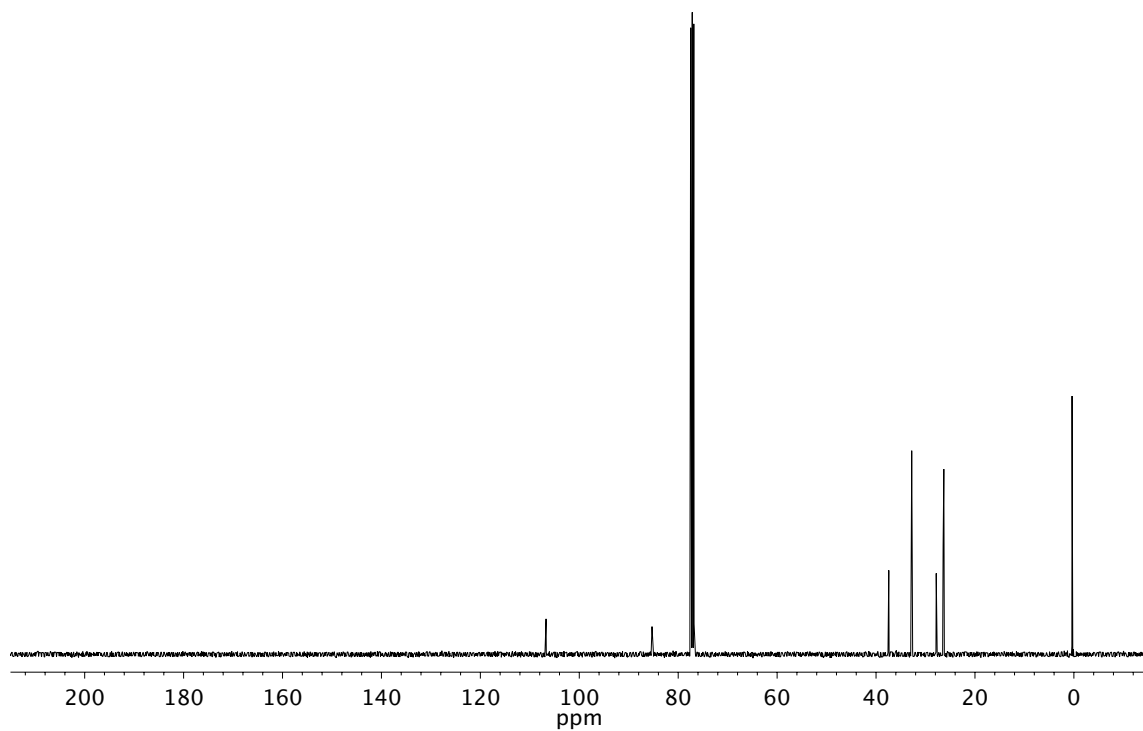


Figure A4.21. ^{13}C NMR (125 MHz, CDCl_3) of compound 239.

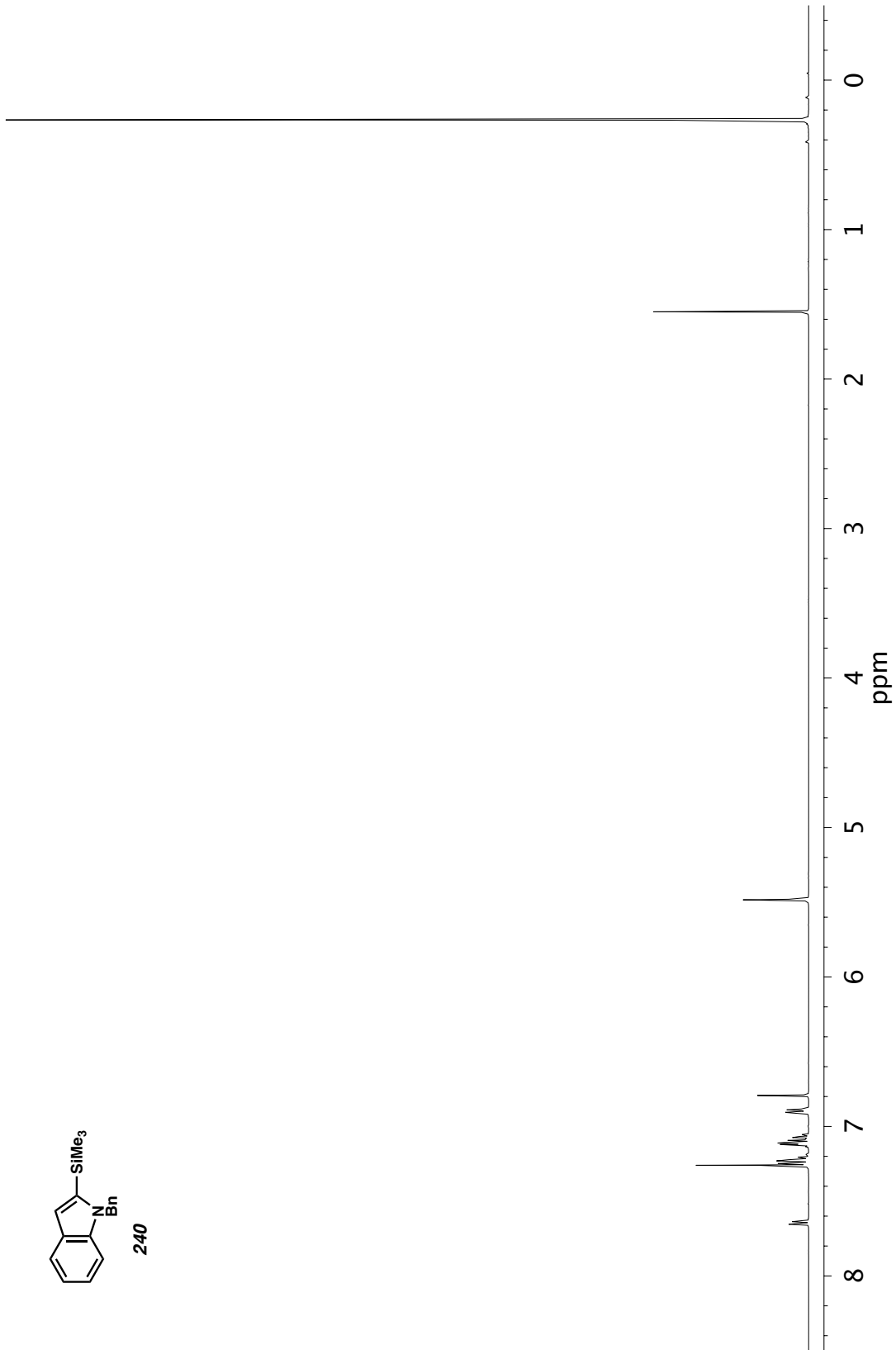
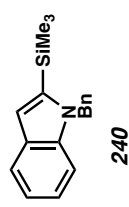


Figure A4.22. ¹H NMR (400 MHz, CDCl₃) of compound 240.

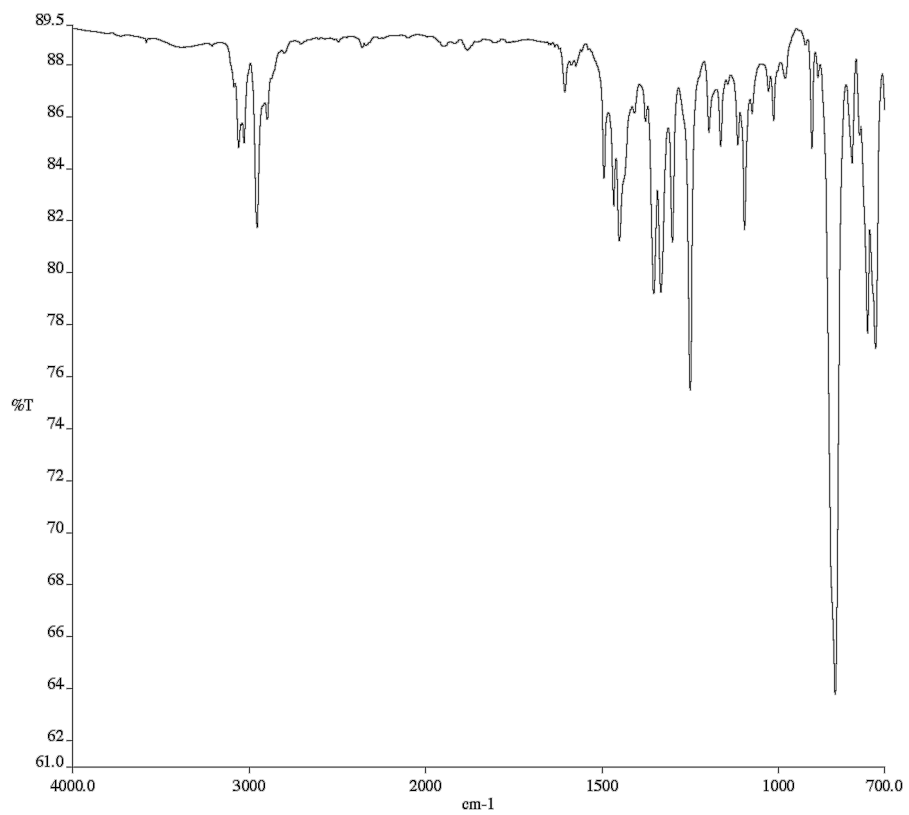


Figure A4.23. Infrared spectrum (Thin Film, NaCl) of compound **240**.

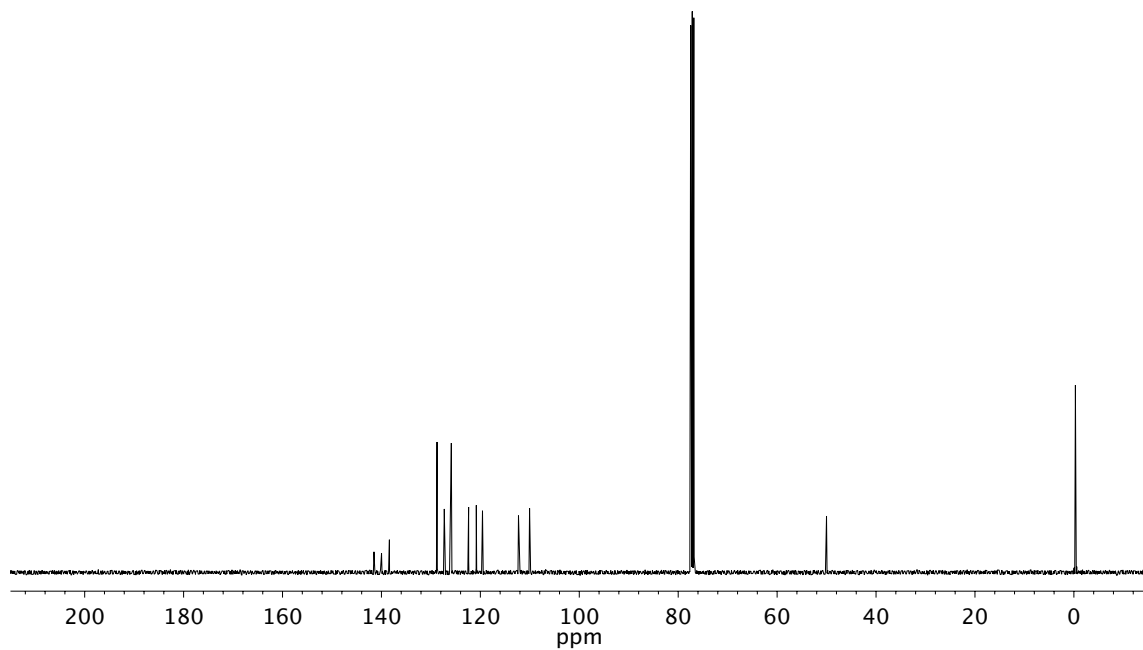


Figure A4.24. ¹³C NMR (101 MHz, CDCl₃) of compound **240**.

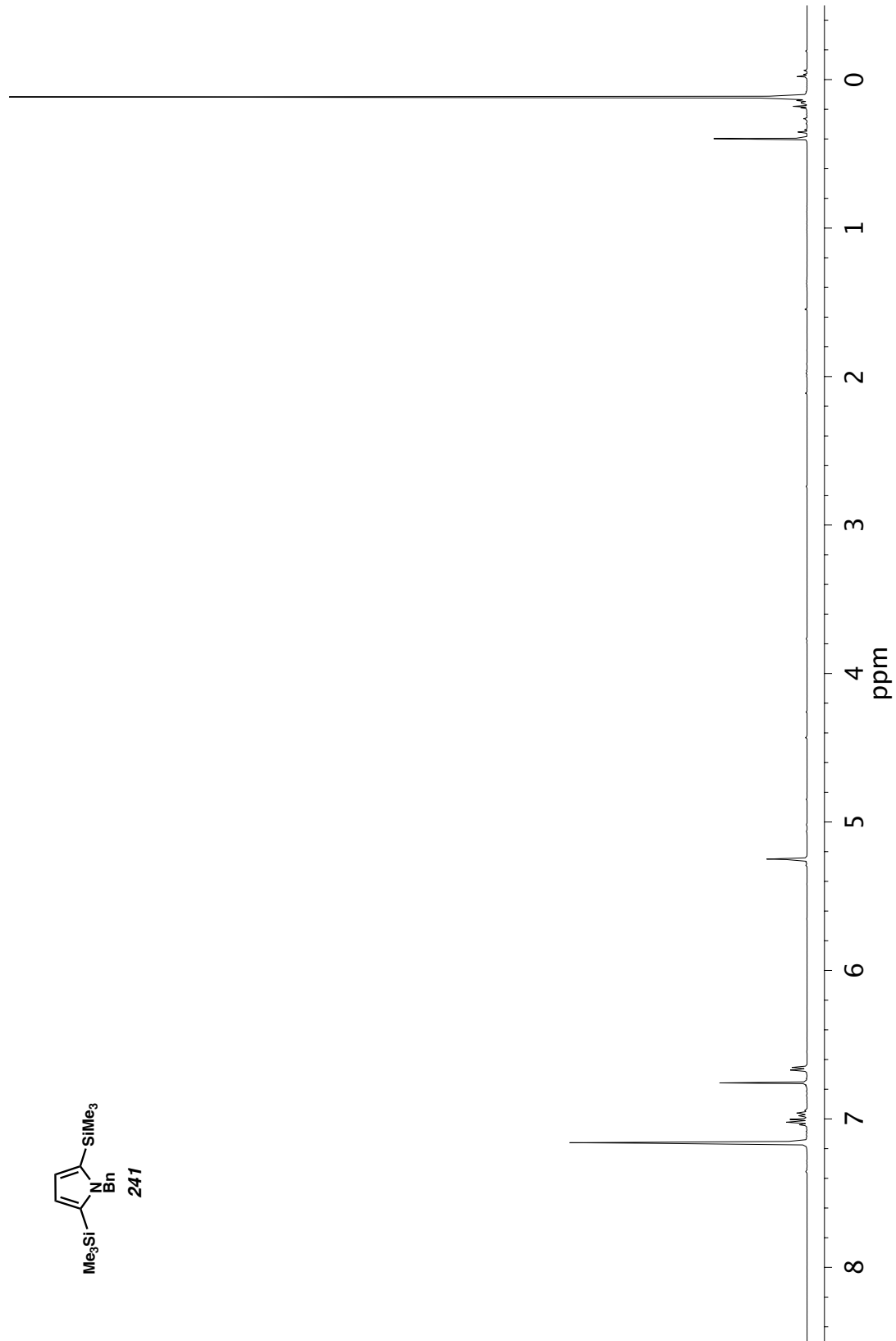
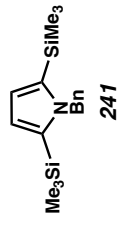


Figure A4.25. ^1H NMR (400 MHz, C_6D_6) of compound 241.

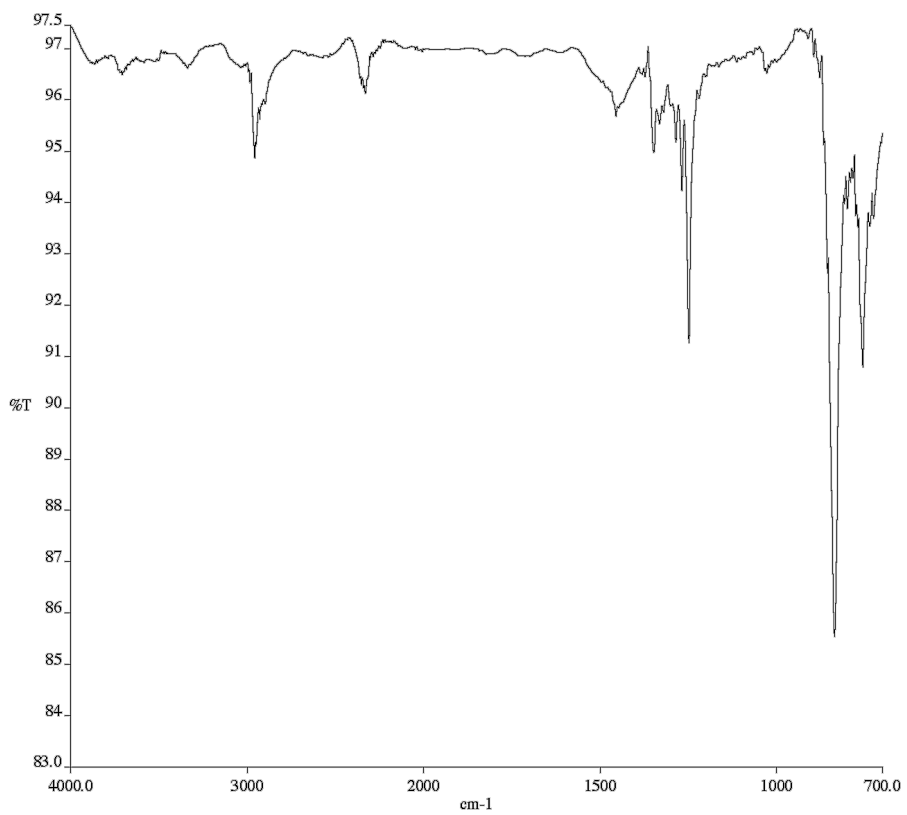


Figure A4.26. Infrared spectrum (Thin Film, NaCl) of compound **241**.

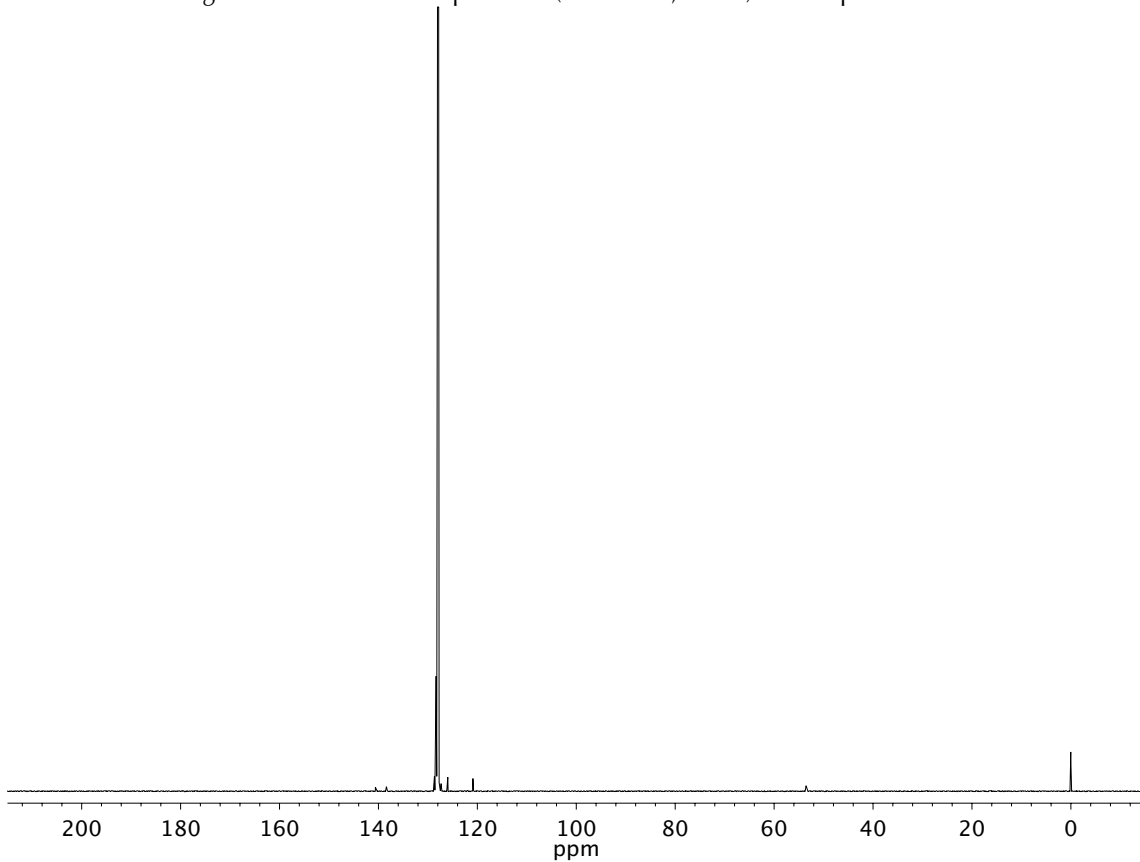


Figure A4.27. ¹³C NMR (101 MHz, C₆D₆) of compound **241**.

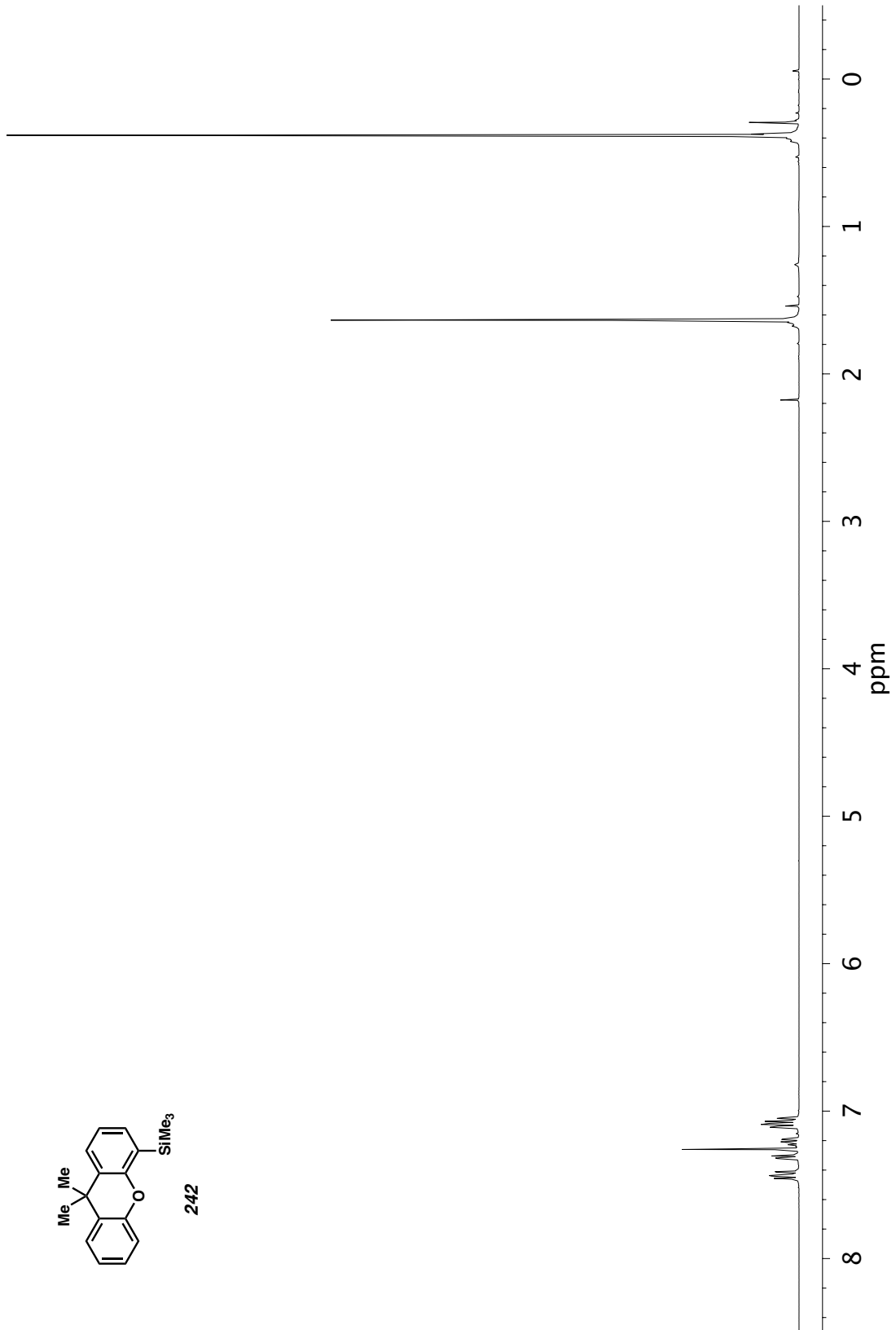
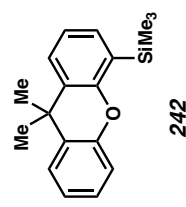


Figure A4.28. ¹H NMR (400 MHz, CDCl_3) of compound 242.

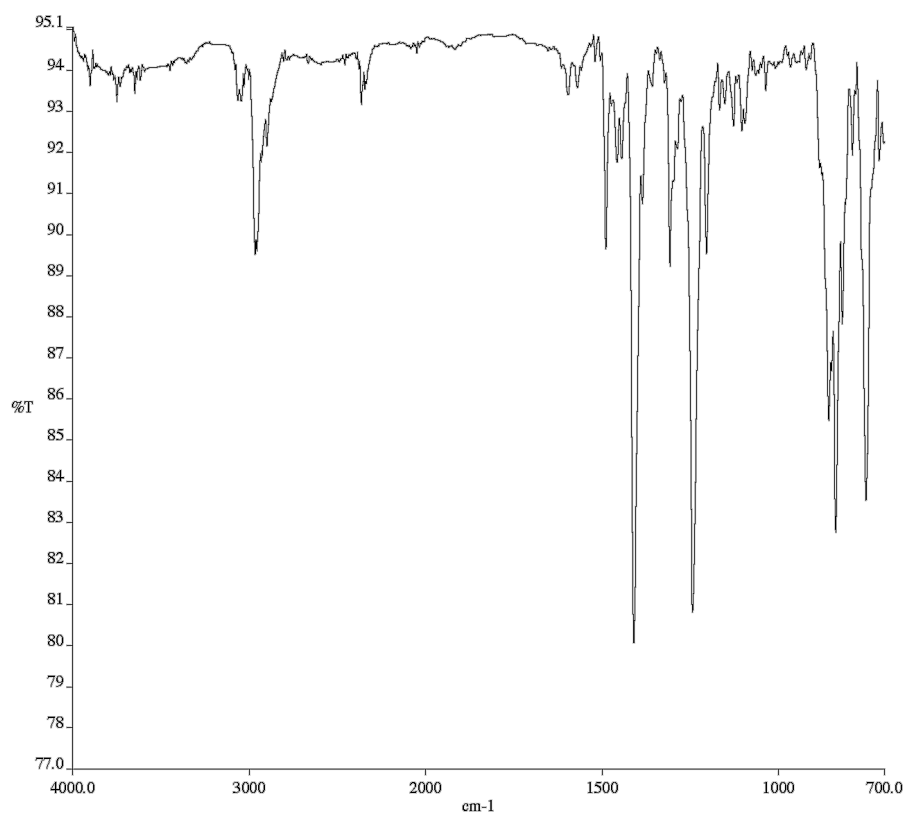


Figure A4.29. Infrared spectrum (Thin Film, NaCl) of compound **242**.

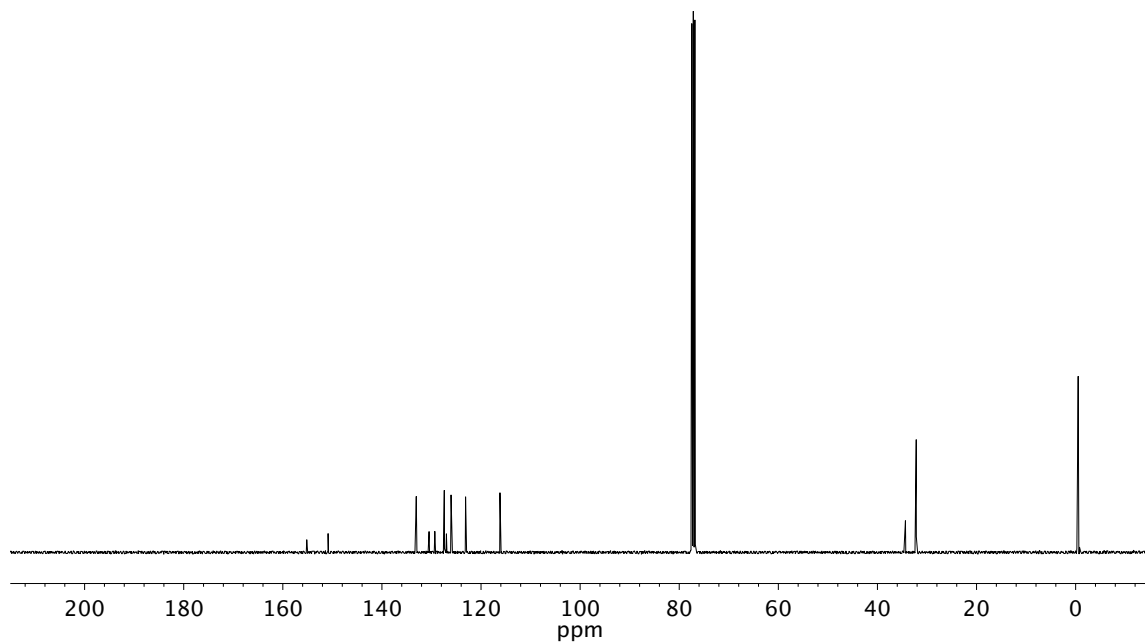


Figure A4.30. ¹³C NMR (101 MHz, C₆D₆) of compound **242**.

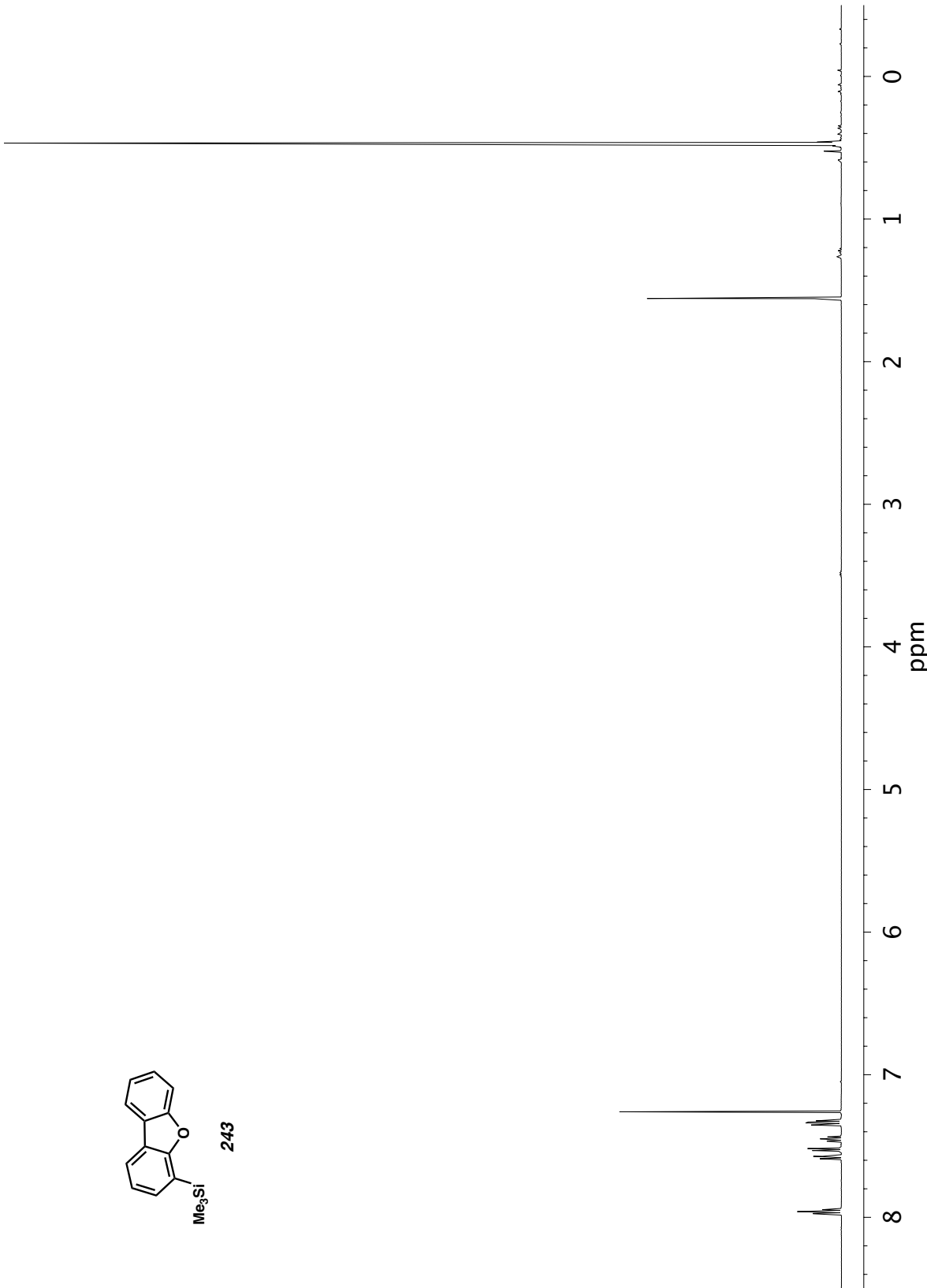
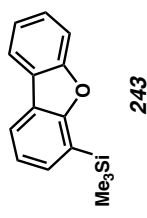


Figure A4.31. ^1H NMR (500 MHz, CDCl_3) of compound 243.

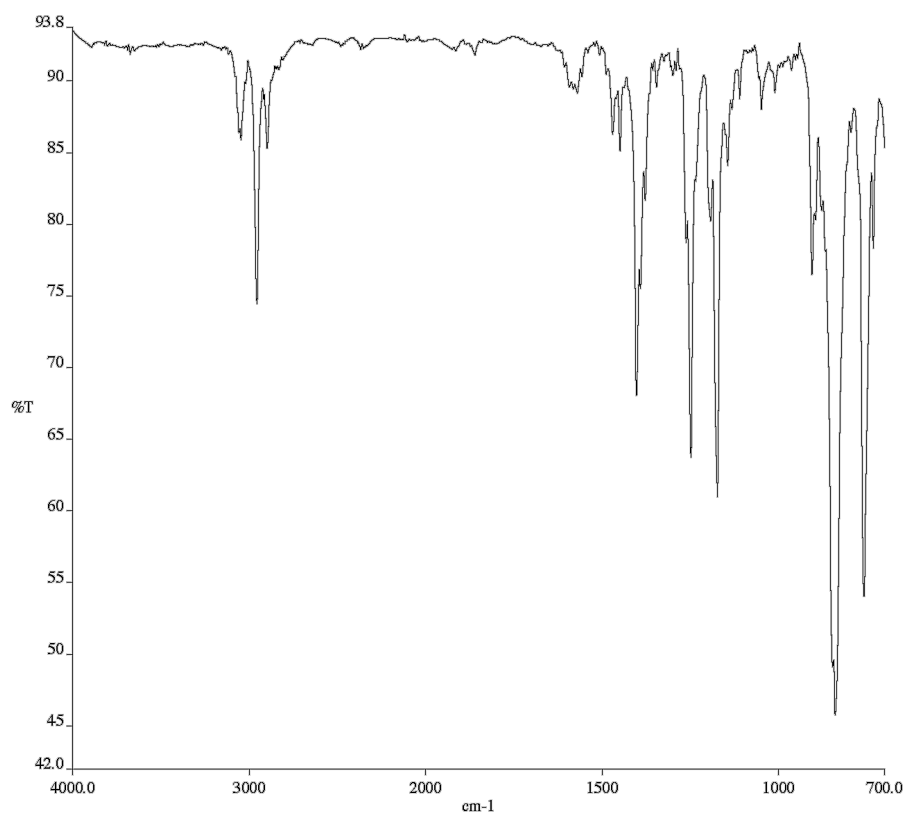


Figure A4.32. Infrared spectrum (Thin Film, NaCl) of compound 243.

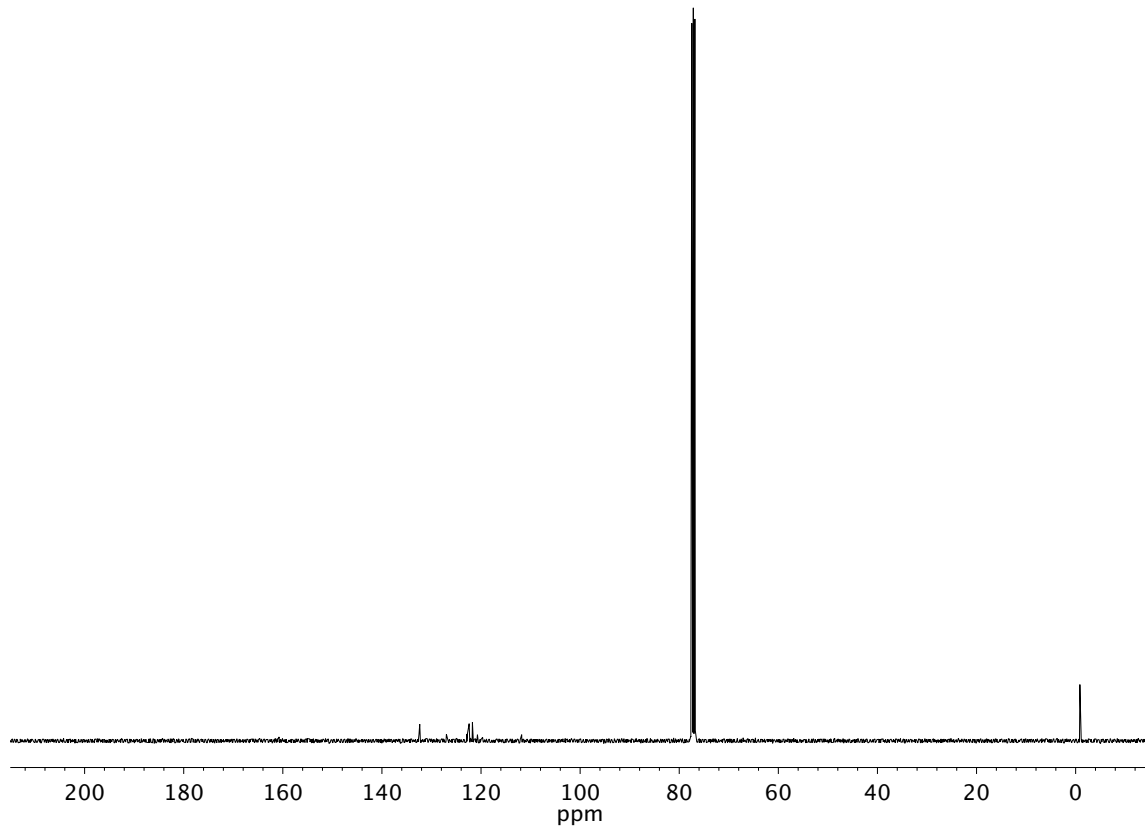
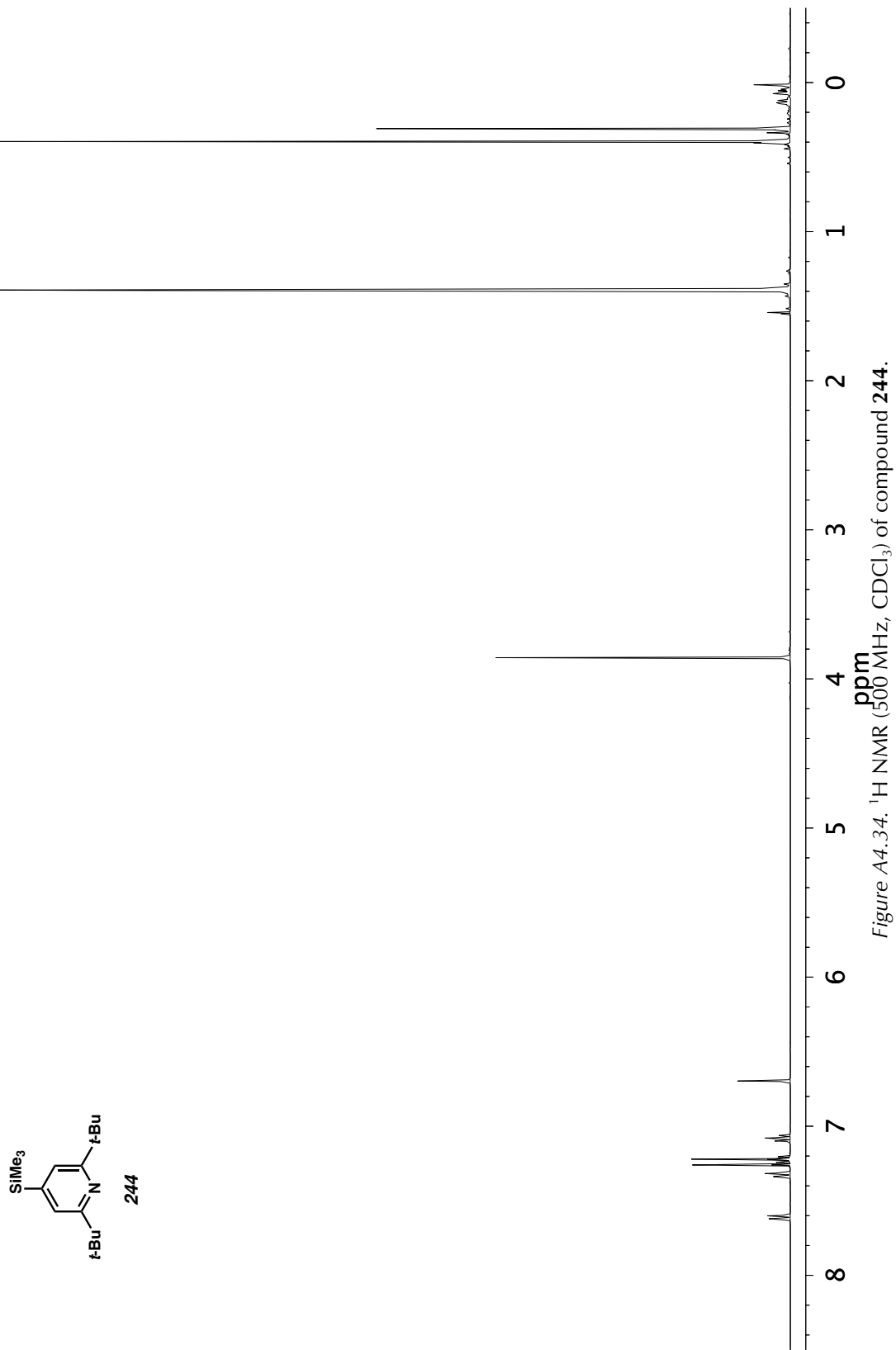


Figure A4.33. ^{13}C NMR (101 MHz, C_6D_6) of compound 243.



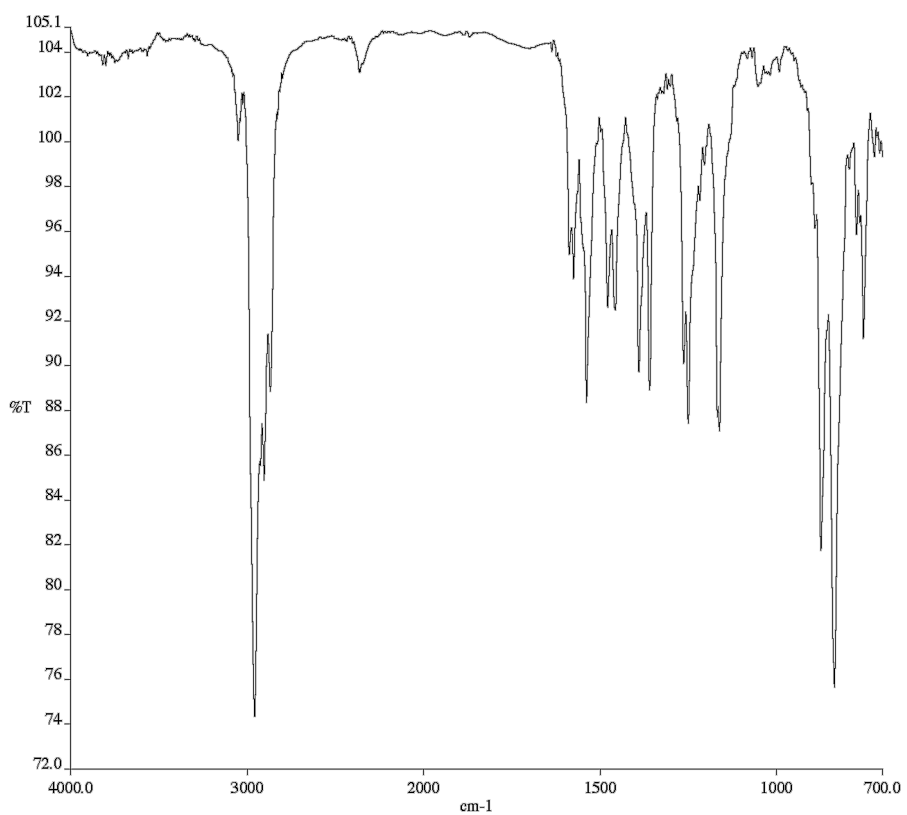


Figure A4.35. Infrared spectrum (Thin Film, NaCl) of compound 244.

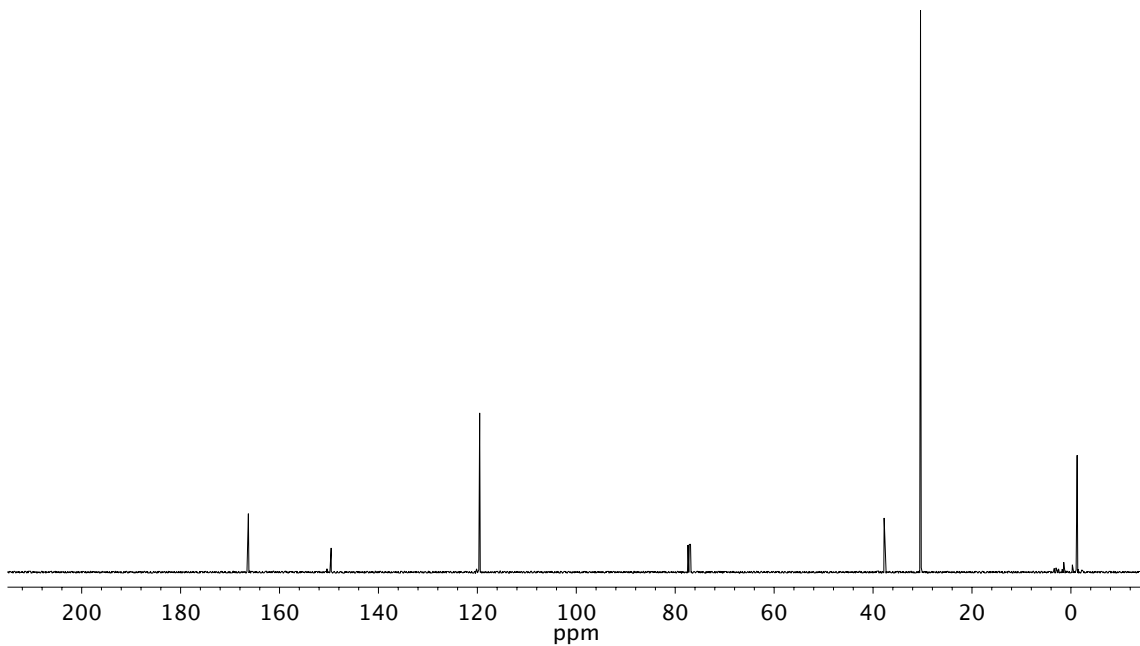


Figure A4.36. ¹³C NMR (101 MHz, CDCl₃) of compound 244.

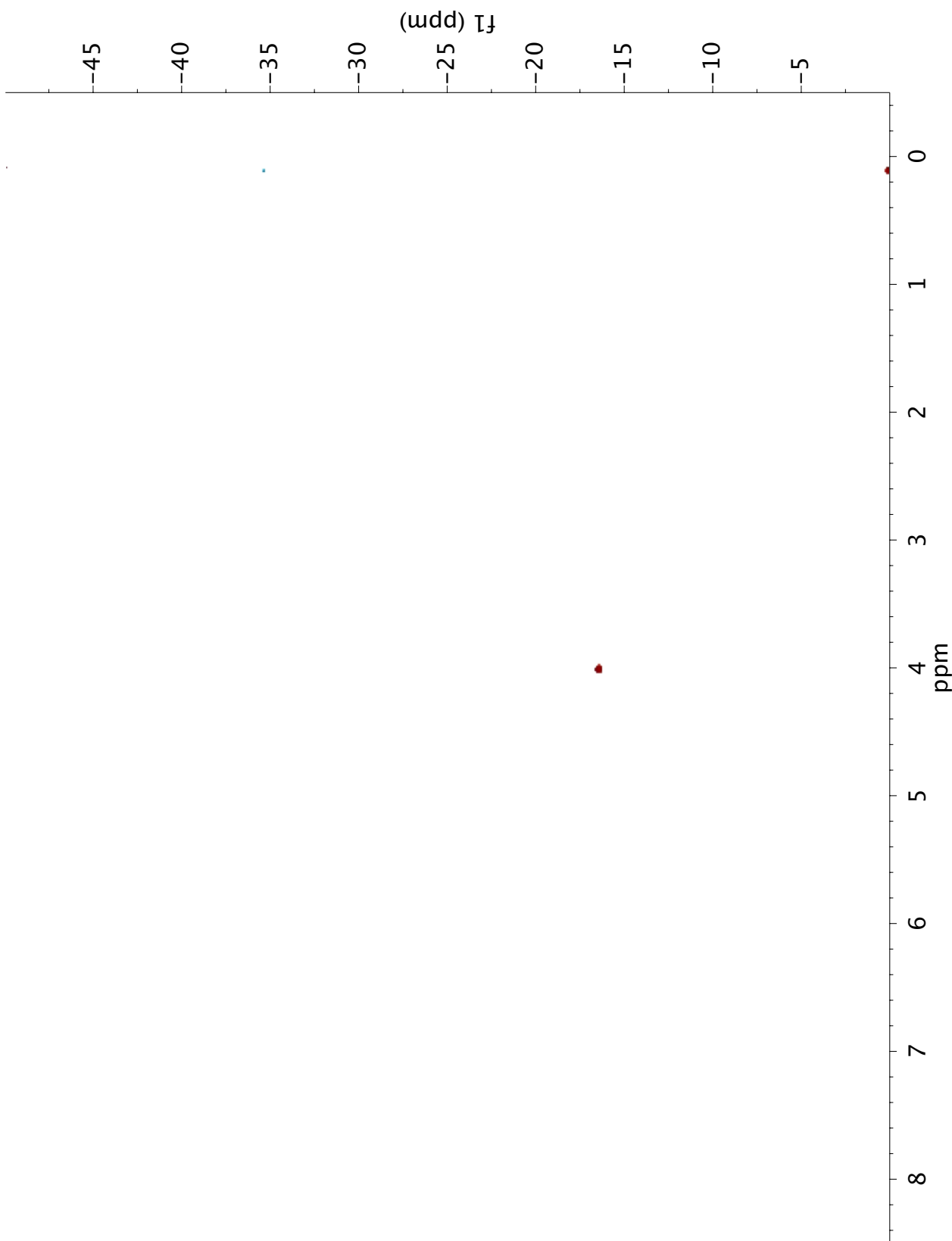


Figure A4.37. ^1H - ^{29}Si HSQC NMR (500 MHz, THF- d_8) corresponding to Figure 4.1.

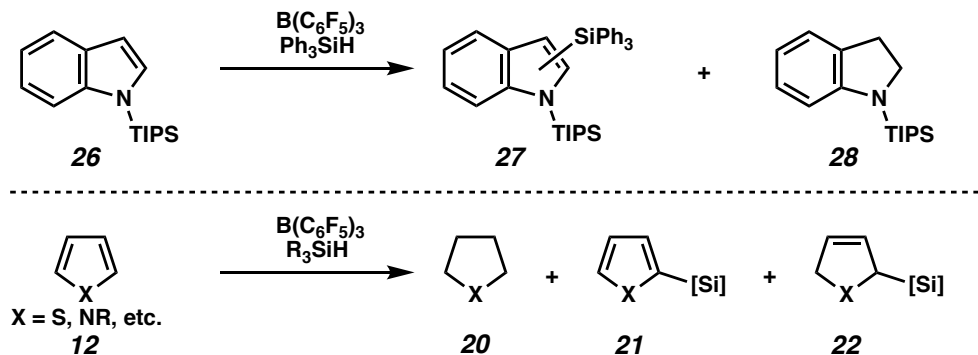
APPENDIX 5

Observation of Unusual, Double Dehydrogenative C–H Silylation Products[†]

A5.1 INTRODUCTION AND BACKGROUND

In some catalytic C–H silylation reactions, undesired substrate reduction competes with product formation (see Chapter 1). For example, undesired hydrogenation and/or hydrosilylation occur under the C–H silylation conditions shown in Scheme A5.1 employing a Lewis acid catalyst.^{1, 2} It has been proposed that this undesired reduction occurs via hydrogen or hydrosilane activation by a frustrated Lewis pair comprised of the Lewis acidic catalysts and Lewis basic heterocyclic substrate.

[†]This work was performed in collaboration with Dr. Wen-Bo Liu.

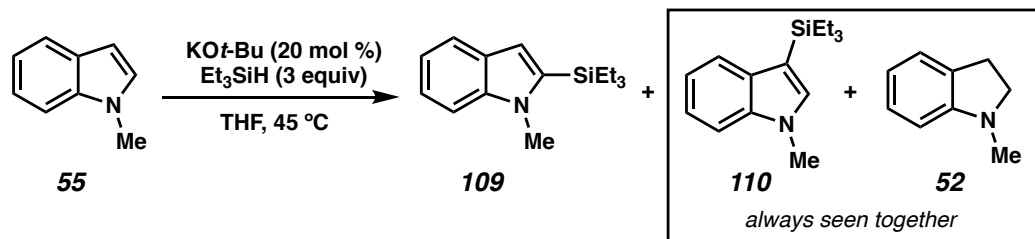
Scheme A5.1 Undesired Hydrogenation and Hydrosilylation in C–H Silylation Reactions.

Competitive substrate reduction can be a major challenge in catalytic C–H silylation reactions but is typically restricted to methods utilizing a Lewis acid catalyst.

A5.2 INDOLINE

A5.2.1 Observation of Partially Hydrogenated Substrate

Upon careful analysis of a completed reaction mixture as shown in Scheme A5.2, we observed the formation of the partially reduced indoline **52** in low yield (i.e., <5%). Furthermore, we noted that the formation of the C3 silylation product **110** was accompanied by indoline **52** in every case we investigated.

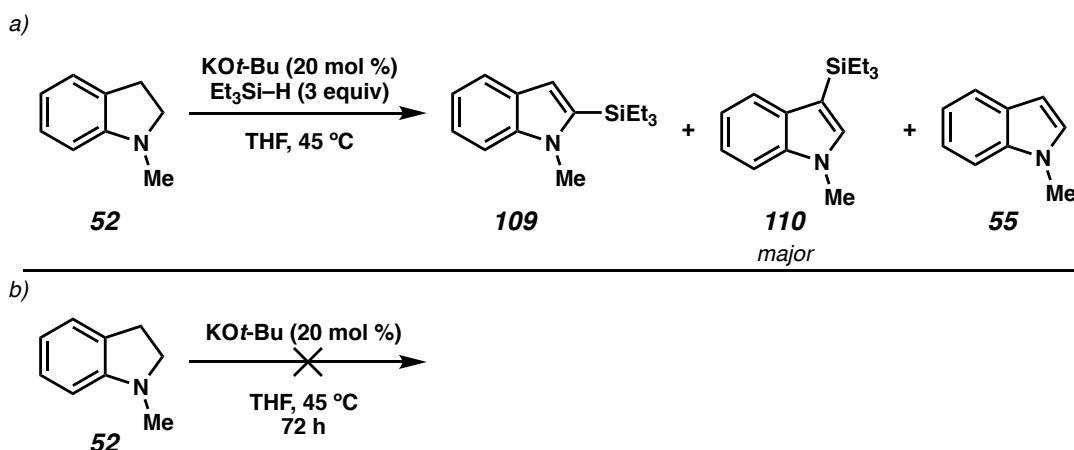
Scheme A5.2 Formation of Indoline in KOt-Bu-Catalyzed C–H Silylation of Indole.

Surprised by this unusual reactivity, we further investigated the role of indoline **52** in the KOt-Bu-catalyzed C–H silylation reaction.

A5.2.2 Unusual Reactivity of Indoline

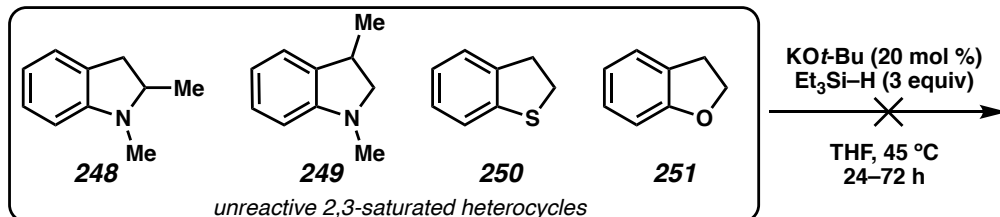
N-methylindoline **52** was separately synthesized and subjected to standard silylation conditions (Scheme A5.3a). We were surprised to observe the formation of mainly C3 silylated indole **110**, a formal double dehydrogenative C–H silylation event. A control experiment indicated no reaction occurred in the absence of silane (Scheme A5.3b).

Scheme A5.3 Unexpected Reactivity in the C–H Silylation of Indoline.



This unusual reactivity appears to be unique to substrate **52**. No products were observed when substrates having substitution at the C2 or C3 position or other heteroatoms were subjected to the same conditions (Scheme A5.4).

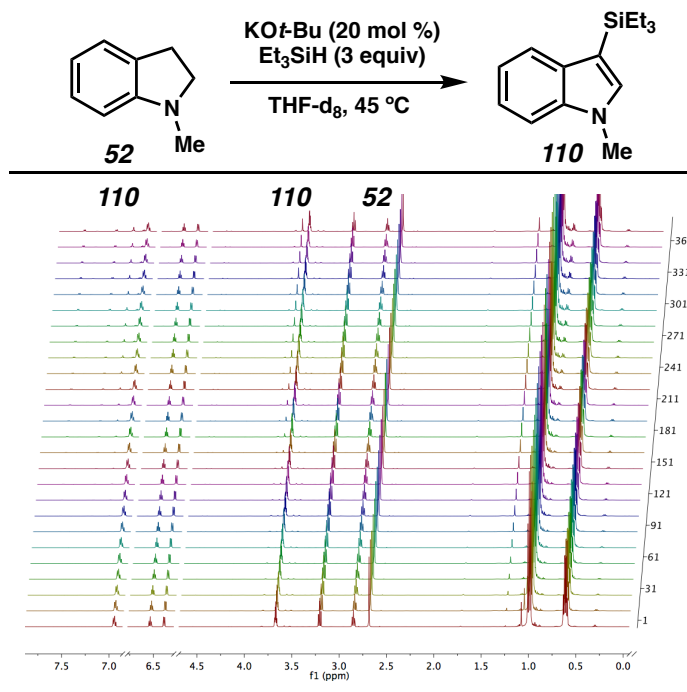
Scheme A5.4 Attempted C–H Silylation of Partially Saturated Heterocycles.



A5.2.3 Mechanistic Insights into Double Dehydrogenative C–H Silylation

A silylation reaction of indoline **52** was monitored by ^1H NMR with the overlaid time-course spectra shown in Figure A5.1. Perhaps surprisingly, no intermediate (i.e., indole **55**) is observed and instead only disappearance of indoline **52** and the growth of C3 silylated indole **110** are observed. We also observe the formation of hydrogen gas, which also accompanies product **110**.

Figure A5.1 ^1H NMR Time-Course of the C–H Silylation of *N*-methylindoline.

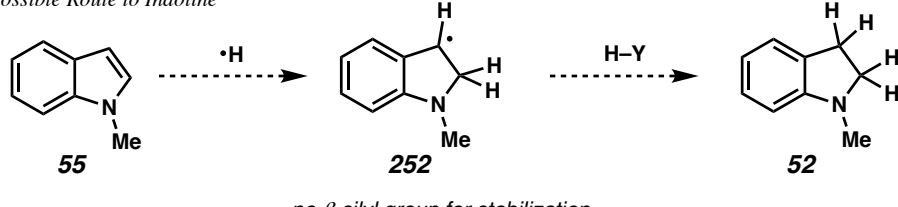


Given these results and our previous mechanistic investigation detailed in Chapter 2, we propose the following mechanisms (Scheme A5.5a).³ A net hydrogen atom addition to indole **55** would generate intermediate **252**, without a β -silicon group for stabilization, and hydrogen atom abstraction would then generate the observed product **110**. This mechanism could account for the observation of indoline **52** in silylation of indole **55**.

Indoline **52** may undergo an initial benzylic C–H silylation at the C3 position, as we have previously reported a similar benzylic C–H silylation occurs with toluene, shown in Scheme A5.5 b&c.⁴ A subsequent radical dehydrogenation, now with a β-silicon group for stabilization of the radical intermediate (i.e., **253** or **254**), could then furnish the observed product.

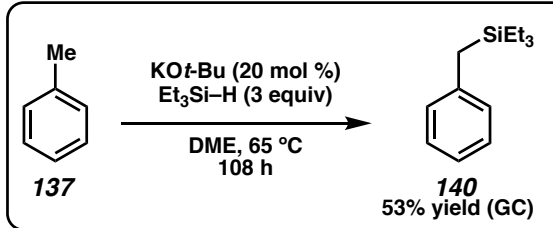
Scheme A5.5 Proposed Mechanism for the Formation and Reactivity of Indoline.

a) Possible Route to Indoline

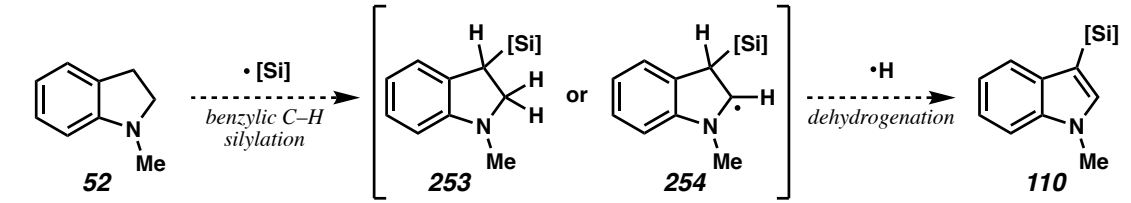


no β-silyl group for stabilization

b) Reported Benzylic C–H Silylation



c) Possible Route for Silylation and Dehydrogenation



A5.3

Conclusion

The unique reactivity detailed here describes a net double dehydrogenative reaction which occurs under what is typically considered neutral or reducing conditions. While it does not appear that this reactivity is generally applicable, indoline **52** may be a key intermediate in the formation of C3 silylated indole **110** under our previously C–H

A5.4 EXPERIMENTAL SECTION

A5.4.1 MATERIALS AND METHODS

Unless otherwise stated, reactions were performed in oven-dried brand-new Fisherbrand scintillation vials in a nitrogen filled glove box or in flame-dried Schlenk flasks under argon connected on a Schlenk line using dry, degassed solvents and brand-new stirring bars. Solvents were dried by passage through an activated alumina column under argon. Reaction progress was monitored by thin-layer chromatography (TLC) or GC-FID analyses. TLC was performed using E. Merck silica gel 60 F254 precoated glass plates (0.25 mm) and visualized by UV fluorescence quenching, phosphomolybdic acid, or KMnO₄ staining. Silicycle SiliaFlash P60 Academic Silica gel (particle size 40–63 nm) was used for flash chromatography. ¹H NMR spectra were recorded on a Varian Inova 500 MHz in CDCl₃ or THF-*d*₈ and are reported relative to residual solvent peak at 87.26 ppm or 83.58 ppm, respectively. ¹³C NMR spectra were recorded on a Varian Inova 500 MHz spectrometer (126 MHz) in CDCl₃ or THF-*d*₈ and are reported relative to residual solvent peak at 877.16 ppm or 867.21 ppm, respectively. Data for ¹H NMR are reported as follows: chemical shift (δ ppm) (multiplicity, coupling constant (Hz), integration). Multiplicities are reported as follows: s = singlet, d = doublet, t = triplet, q = quartet, p = pentet, sept = septet, m = multiplet, br s = broad singlet, br d = broad doublet, app = apparent. Data for ¹³C NMR are reported in terms of chemical shifts (δ ppm). GC-FID analyses were obtained on an Agilent 6890N gas chromatograph equipped with a

HP-5 (5%-phenyl)-methylpolysiloxane capillary column (Agilent). GC-MS analyses were obtained on an Agilent 6850 gas chromatograph equipped with a HP-5 (5%-phenyl)-methylpolysiloxane capillary column (Agilent). High resolution mass spectra (HRMS) were acquired from the California Institute of Technology Mass Spectrometry Facility. KOt-Bu (sublimed grade, 99.99% trace metals basis) and **251** were purchased from Aldrich and used directly. All other reagents were purchased from Aldrich, TCI, or Acros and used as received (unless noted). **52**⁵ and **249**⁶ were synthesized by literature procedure. **248** and **249** were synthesized by the same procedure as for **52** and the analytical data are in accordance with those reported.⁷

A5.4.2 General Procedure for Indoline Dehydrogenation and Silylation

In a nitrogen-filled glovebox, KOt-Bu (22.4 mg, 0.2 mmol, 20 mol %), *N*-methylindoline **52** (133.1 mg, 1 mmol, 1 equiv), Et₃SiH (348 mg, 3 mmol, 3 equiv) and THF (1 mL, 1 M) were added to a 2 dram scintillation vial equipped with a magnetic stirring bar. The vial was sealed and the mixture was stirred at 45 °C for 5 days. The reaction progress was monitored by removing aliquots with a dry glass capillary tube, which were diluted with Et₂O and analyzed by GC-FID. The retention times were compared to known references of compounds **52**, **55**, **109**, and **110**.³ The vial was then removed from the glovebox, diluted with diethyl ether (1mL), and concentrated under reduced pressure. The yield was determined by ¹H NMR and GC analysis of the crude mixture.

A5.4.3 General Procedure for Time-Course Reaction Monitoring by *in situ***¹H NMR**

In a nitrogen-filled glovebox, KO*t*-Bu (4.5 mg, 0.04 mmol, 20 mol %), *N*-methylindoline **52** (26.6 mg, 0.2 mmol, 1 equiv), Et₃SiH (69.8 mg, 0.6 mmol, 3 equiv) and THF-*d*₈ (0.5 mL, 0.4 M) were added to a 2 dram scintillation vial. Continuing in the glove box, a J-Young gas-tight NMR tube is then charged approximately 0.3 mL of the reaction solution. The tube is tightly capped with the corresponding Teflon plug, removed from the glove box, placed in the bore of the NMR, and heated to 45 °C. ¹H NMR spectra were acquired in “array” mode, with a spectrum taken approximately every 3 minutes for the length of experiment. The data was processed using MestReNova and data is decimated and displayed using the “stack” function.

A5.5 REFERENCES AND NOTES

- (1) Curless, L. D.; Clark, E. R.; Dunsford, J. J.; Ingleson, M. J. *Chem. Commun.* **2014**, *50*, 5270–5272
- (2) Schuman, D. P.; Liu, W.-B.; Nesnas, N.; Stoltz, B. M. Transition-Metal-Free Catalytic C–H Bond Silylation. In *Organosilicon Chemistry: Novel Approaches and Reactions*; Hiyama, T., Oestreich, M., Eds.; Wiley-VCH: Weinheim, Germany, 2019; Chapter 7, pp. 213–239. ISBN: 978-3-527-34453-6.
- (3) (a) Liu, W.-B.; Schuman, D. P.; Yang, Y.-F.; Toutov, A. A.; Liang, Y.; Klare, H. F. T.; Nesnas, N.; Oestreich, M.; Blackmond, D. G.; Virgil, S. C.; Banerjee, S.; Zare, R. N.; Grubbs, R. H.; Houk, K. N.; Stoltz, B. M. *J. Am. Chem. Soc.* **2017**,

- 139, 6867–6879.; (b) Banerjee, S.; Yang, Y.-F.; Jenkins, I. D.; Liang, Y.; Toutov, A. A.; Liu, W.-B.; Schuman, D. P.; Grubbs, R. H.; Stoltz, B. M.; Krenske, E. H.; Houk, K. N.; Zare, R. N. *J. Am. Chem. Soc.* **2017**, *139*, 6880–6887.
- (4) (a) Toutov, A. A.; Liu, W.-B.; Stoltz, B. M.; Grubbs, R. H. *Org. Synth.* **2016**, *93*, 263–271. (b) Toutov, A. A.; Liu, W.-B.; Betz, K. N.; Stoltz, B. M.; Grubbs, R. H. *Nature Protocols* **2015**, *10*, 1897–1903. (c) Toutov, A. A.; Liu, W.-B.; Betz, K. N.; Fedorov, A.; Stoltz, B. M.; Grubbs, R. H. *Nature* **2015**, *518*, 80–84. (d) Fedorov, A.; Toutov, A. A.; Swisher, N. A.; Grubbs, R. H. *Chem. Sci.* **2013**, *4*, 1640–1645.
- (5) Kumar, Y.; Florvall, L. *Syn Comm.* **1983**, *13*, 489–493.
- (6) Kursanov, D. N.; Parnes, Z. N.; Bolestova, G. I.; Belen'KII *Tetrahedron* **1975**, *31*, 311–315
- (7) Jia, W.-L.; Westerveld, N.; Wong, K. M.; Morsch, T.; Hakkenes, M.; Naksomboon, K.; Fernandez-Ibanez, M. A. *Org. Lett.* **2019**, *21*, 9339–9342.

APPENDIX 6

Hydroxide-Catalyzed Dehydrogenative C–H Silylation of Terminal Alkynes [†]

A6.1 INTRODUCTION AND BACKGROUND

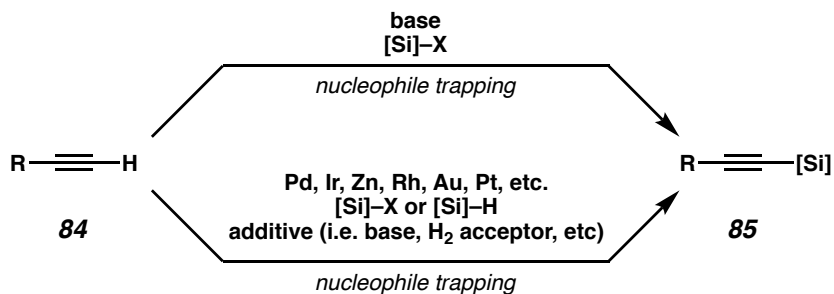
The catalytic transformation of C–H bonds into a variety of useful functional groups has revolutionized chemical synthesis.¹ However, the necessity of precious metal catalysts for these transformations remains a fundamental and longstanding limitation.² Building upon our previously reported C–H silylation of aromatic heterocycles with hydrosilanes using catalytic potassium *tert*-butoxide, we sought to evaluate alkali metal salts as catalysts for the preparation of alkynylsilanes.³ These important building blocks are used in the construction of electronically and structurally interesting materials,⁴ employed as substrates in metathesis reactions and cycloadditions,⁵ and as precursors to heterocycles and polycyclic aromatic frameworks.⁶ Moreover, alkynylsilane nucleophiles and cross-coupling partners react under mild conditions and therefore are commonly

[†]This work was performed in collaboration with Dr. Anton Toutov, Kerry Betz, Dr. Wen-Bo Liu, and Dr. Alexey Fedorov. Portions of this chapter have been reproduced with permission from Toutov, A. A.; Betz, K. N.; Schuman, D. P.; Liu, W.-B.; Fedorov, A.; Stoltz, B. M.; Grubbs, R. H. *J. Am. Chem. Soc.* **2017**, *139*, 1668–1674. © 2017 American Chemical Society.

A6.1.1 Literature Examples of Alkynylsilane Synthesis

Strategies for the synthesis of alkynylsilanes have included the use of strong bases, stoichiometric or catalytic transition-metal species and the use of activated organosilicon coupling partners (Scheme A6.1, bottom route).^{8,9} Inexpensive and convenient hydrosilanes have been investigated for C(sp)–H silylation; however, the reported methods require forcing conditions (i.e., excess base, sacrificial hydrogen acceptors, external oxidants, and elevated temperatures (i.e., 80–120 °C).

Scheme A6.1 C–H Silylation of Terminal Alkynes.



Moreover, undesired hydrosilylation of the alkyne can be competitive, further complicating catalyst and reaction design (see Chapter 1). These factors have led to, in many cases, substantial limitations in scope and practical utility.¹⁰

A6.2 DEHYDROGENATIVE C–H SILYLATION OF TERMINAL ALKYNES

A6.2.1 Initial Hit and Reaction Optimization

We initiated investigations with the silylation of alkyne **82** using Et_3SiH under our previously reported $\text{KO}t\text{-Bu}$ -catalyzed C(sp²)–H silylation conditions and gratifyingly observed alkynylsilane **83** in good yield, along with 9% of undesired alkyne migration

product **255** (Table A6.1, entry 1).¹¹ NaOt-Bu (entry 2) is unselective while LiOt-Bu along with amine bases are not catalytically active (entries 3–6). KOH is superior to KOt-Bu (entry 7 versus 1), generating desired product in 95% yield and decreased quantities (3%) of undesired migration product **255**. Moving from Et₃SiH to PhMe₂SiH permits the reaction to occur at ambient temperature while still maintaining high yield (entry 7 to 8). In sharp contrast to our previously reported heteroarene C(*sp*²)–H silylation protocol wherein the use of KOt-Bu as catalysts resulted in the highest yield of silylation product, KOH and NaOH were found to be the most active catalysts affording **83** in 89% and 93% yield, respectively (entries 8 & 9). By contrast, LiOH (entry 10) does not catalyze the reaction.

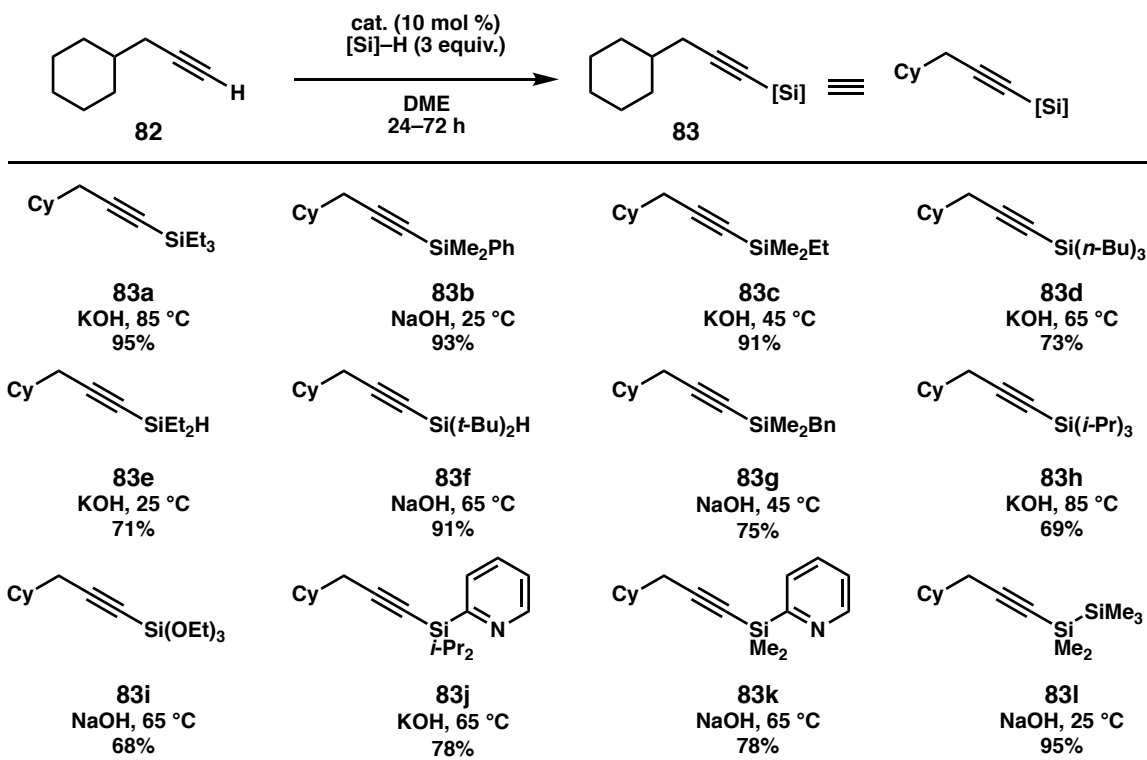
Table A6.1 Reaction Optimization.

entry	cat.	[Si]-H	T (°C)	time (h)	yield 83 (%)	yield 255 (%)
1	KOt-Bu	Et ₃ Si-H	85	24	89	9
2	NaOt-Bu	Et ₃ Si-H	85	24	46	52
3	LiOt-Bu	Et ₃ Si-H	85	24	<1	-
4	DABCO	Et ₃ Si-H	85	48	-	-
5	Pyridine	Et ₃ Si-H	85	48	1	-
6	Et ₃ N	Et ₃ Si-H	85	48	4	-
7	KOH	Et ₃ Si-H	85	24	95	3
8	KOH	PhMe ₂ Si-H	25	48	89	-
9	NaOH	PhMe ₂ Si-H	25	48	93	-
10	LiOH	PhMe ₂ Si-H	25	48	-	-

[a] Reactions conducted on 0.5 mmol scale, 1M in DME, Entries 1–5, 8: yields determined by GC-FID analysis with tridecane as an internal standard; entries 6,7: yields of analytically pure isolated materials. Reaction does not proceed without catalyst..

A6.2.2 Scope of Alkyne C–H Silylation

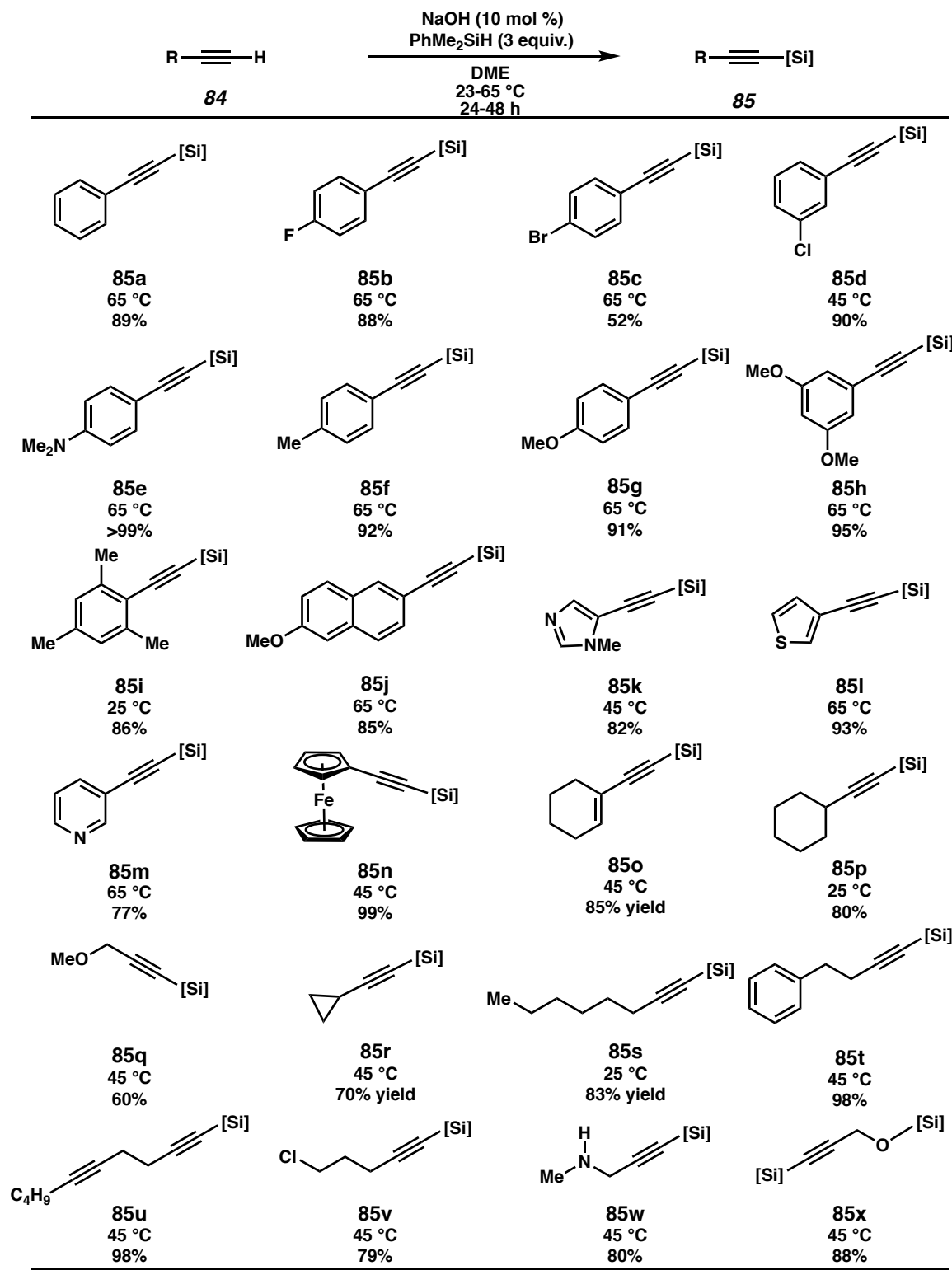
We next proceeded to evaluate the scope of the hydrosilane partner (Scheme A6.2) and found that alkyl- and phenyl-substituted hydrosilanes of varying steric demand readily undergo coupling providing alkynylsilanes **83a–d** in high yields. The mild conditions of this reaction enabled the facile preparation of alkynylsilanes containing synthetically versatile hydride- (**83e** and **83f**), benzyldimethyl- (**83g**), triisopropyl- (**83h**), and even triethoxy- (**83i**) and 2-dialkylpyridyl (**83j** and **83k**) moieties in good yield. Currently, alkynylsilylpyridines are prepared using stoichiometric organometallic methods, which intrinsically limits the substrate scope;¹² however, alkynyl dimethylsilylpyridines such as **83k** can be advanced to di-, tri-, and tetra-substituted olefins by sequential transition-metal-catalyzed protocols making them valuable C(*sp*)–Si functionalities that, given their remarkable versatility, have to this point been seemingly underused. The bulky di-*tert*-butylsilane could also be introduced for the first time by catalytic C–H silylation yielding **83f** in excellent yield, providing a point of entry into novel alkynylsilyl [¹⁸F]–PET radiochemical moieties. Using Me₃Si–SiHMe₂ as a polysilane model compound and subjecting it to our cross-dehydrogenative silylation at ambient temperature gave **83l** in 95% yield, providing a new synthetic strategy for the construction of advanced polysilane materials.¹³ To the best of our knowledge, this is the broadest scope of hydrosilanes reported to date for any single catalytic C–H silylation system.

Scheme A6.2 Hydrosilane Scope of Alkyne Silylation.

[a] Reactions were conducted on 0.5 mmol scale with 0.5 mL of solvent at the prescribed temperature.

The scope of the alkyne coupling partner was likewise substantial, affording products containing electron-rich and electron-deficient aryl (**85a–j**), heteroaryl (**85k–m**), ferrocenyl (**85n**), and alkyl (**85o–y**) groups (Scheme A6.3). Substrates containing sensitive functional groups such as aryl halides (**85b–d**), an alkyl chloride (**85v**), and a cyclopropane (**85r**) are tolerated without any undesired side reactions. Molecules bearing acidic functionalities such as propargylamines and propargyl alcohols also react well, providing **85w** and *bis*-silylated **85x**, respectively in high yields.¹⁴ Catalytic cross-dehydrogenative silylation of *N*-heterocyclic systems, such as those substrates containing an imidazole and a pyridine, are also successful affording the corresponding silylated building blocks **85k** and **85m** without any observed Minisci-type reactivity. Substrates containing C–H bonds that are susceptible to KO*t*-Bu-catalyzed silylation, or those that

could be engaged under a variety of other C–H functionalization chemistries react specifically at the terminal alkyne C–H bond, and alkynylsilane products bearing toluene (**85f**), anisole (**85g**), thiophene (**85l** and **85y**), propargyl ether (**85q**), and phenylethyl (**85t**) moieties could be readily accessed. In particular, electron-rich systems are excellent substrates and undergo the desired C(*sp*)–H silylation to furnish alkynylsilanes containing aniline (**85e**), dimethoxy benzene (**85h**), and ferrocene (**85n**) fragments without any byproducts derived from electrophilic silylation. The reaction scales well as demonstrated by the production of 19 grams of **85s** using 1.5 molar equivalents of the hydrosilane.

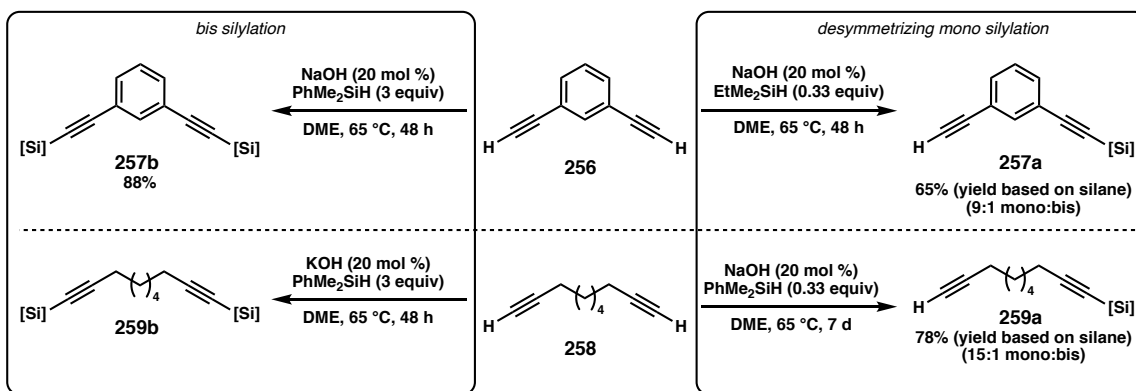
Scheme A6.3 Substrate Scope of Alkyne Silylation.

[a] Reactions were conducted on 0.5 mmol scale with 0.5 mL of solvent for 24 or 48 h (72 h for **XXI**, 96 h for **XXc**) at the prescribed temperature. Yields are of analytically pure isolated products.
 $[\text{Si}] = \text{PhMe}_2\text{Si}$

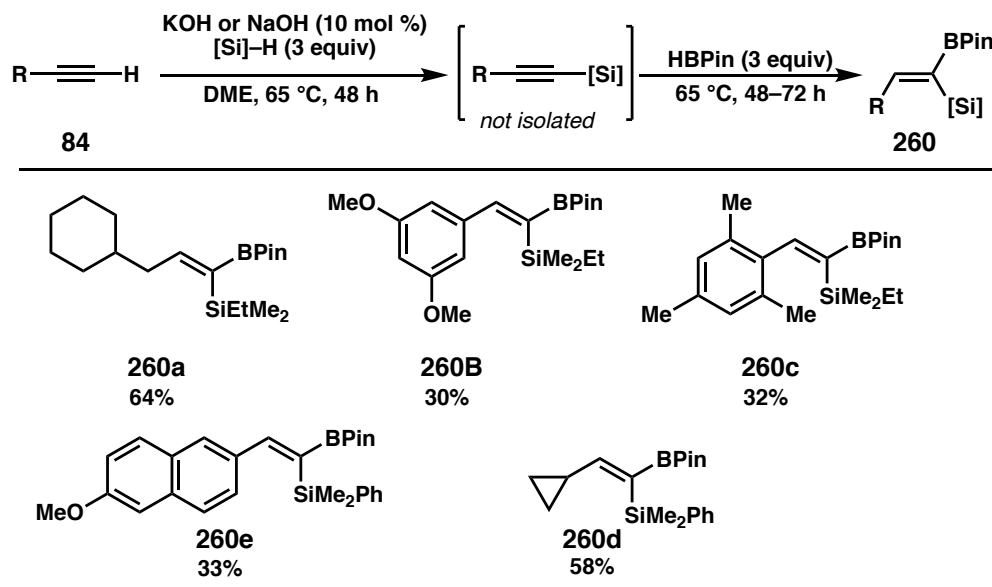
A6.2.3 Applications of Alkyne C–H Silylation

We next proceeded to investigate novel applications of our catalytic method. Symmetrical aliphatic or aromatic diynes can either undergo catalytic mono-silylation to yield valuable desymmetrized building blocks **257a** and **259a** by using an excess of substrate or *bis* functionalization to yield **257b** and **259b** (Scheme A6.4).

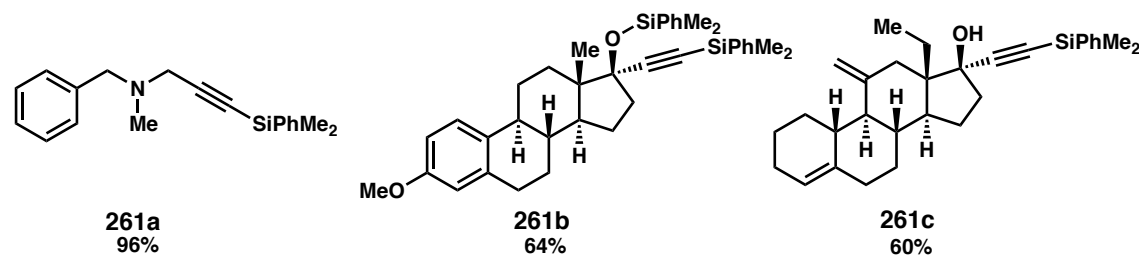
Scheme A6.4 Selective Mono and Bis Silylation of Diynes.



Hydroxide-catalyzed silylation followed by treatment with a borane (i.e., HBPin) leads to a one-pot catalytic *geminal* di-functionalization of terminal alkynes (Scheme A6.5). This method furnishes tri-substituted olefins **260a–e** containing both a vinyl C–Si and C–B bond as a single olefin isomer from inexpensive, commercially available materials. Combinations of both alkyl- and aryl-substituted silanes and alkynes are amenable to this reaction, though instability in some of the products has been observed during purification, resulting in decreased yields despite high conversions. Nevertheless, this strategy appears to be the first catalytic one-pot synthesis of *gem*-silaboryl olefins directly from terminal alkynes and constitutes a convenient and practical method toward these useful structures.¹⁵

Scheme A6.5 One-Pot Catalytic Geminal Di-Functionalization of Terminal Alkynes

Sila-drug analogues in some cases demonstrate improved pharmacokinetic properties relative to the corresponding all-carbon compounds and are garnering increased attention from medicinal chemists.¹⁶ To evaluate our method for such late-stage C–H functionalization applications, we subjected the monoamine oxidase (MAO) inhibitor pargyline, the estrogen prodrug mestranol, and third-generation oral contraceptive desogestrel to the catalytic silylation conditions, successfully providing novel sila-drug analogues **261a–c** (Figure A6.1).

Figure A6.1 One-Pot Catalytic Geminal Di-Functionalization of Terminal Alkynes

[a] Reaction conditions: PhMe₂SiH (3 equiv), DME, NaOH or KOH (10 mol %) at 45–65 °C for 24–72 h.

A6.2.4 Mechanistic Details of Alkyne C–H Silylation

A number of mechanisms for the C(*sp*)–H silylation reaction occurring under various conditions with different catalyst systems have been proposed; however, the underlying mechanistic details of the alkali metal hydroxide catalyzed silylation are not well understood at this point.⁸ Radical trapping and counter cation chelation studies were inconclusive, with no obvious trends observed based on catalyst or hydrosilane (Table A6.2). Furthermore, reactivity was highly variable between hydroxide catalysts and experimentation remains the best method to determine the optimal catalyst-substrate combination.

Table A6.2 Select Mechanistic Investigation Studies of Terminal Alkyne Silylation

entry	cat.	[Si]-H	additive	mol %	yield 83 (%)
1	NaOH	Et ₃ Si-H	—	—	99
2	NaOH	Et ₃ Si-H	galvinoxyl	10	5
3	NaOH	Et ₃ Si-H	TEMPO	10	99
4	NaOH	Et ₃ Si-H	TEMPO	300	24
5	NaOH	Et ₃ Si-H	15-crown-5	10	99
6	KOH	Et ₃ Si-H	18-crown-6	10	99
7	NaOH	(EtO) ₃ Si-H	—	—	99
8	KOH	(EtO) ₃ Si-H	—	—	0
9	NaOH	(EtO) ₃ Si-H	15-crown-5	10	0
10	KOH	(EtO) ₃ Si-H	18-crown-6	10	0

Structure 262: Galvinoxyl, a radical featuring two 2,6-di-*t*-butyl-4-oxo-4H-pyran-4-yl groups connected by a central carbon-carbon double bond. The radical center is at the 4-position of each pyran ring.

Structure 151: TEMPO, a radical featuring a 2,2,6,6-tetramethylpiperidine-1-oxyl group.

A6.3 CONCLUSION

An alkali metal-hydroxide–catalyzed cross-dehydrogenative C–H silylation of terminal alkynes has been developed by our group in collaboration with the Grubbs group. This chemistry proceeds under mild conditions and enables the direct synthesis of a wide array of useful alkynylsilanes, with high tunability in both the alkyne and hydrosilane, many of which are challenging to prepare by alternate means.

A6.4 EXPERIMENTAL SECTION

A6.4.1 MATERIALS AND METHODS

Unless otherwise stated, reactions were performed in oven-dried brand-new Fisherbrand scintillation vials in a nitrogen-filled glove box or in flame-dried Schlenk flasks under argon connected on a Schlenk line using dry, degassed solvents and brand-new stirring bars. Solvents were dried by passage through an activated alumina column

under argon. Reaction progress was monitored by thin-layer chromatography (TLC) or GC-FID analyses. TLC was performed using E. Merck silica gel 60 F254 precoated glass plates (0.25 mm) and visualized by UV fluorescence quenching, phosphomolybdic acid, or KMnO₄ staining. Silicycle SiliaFlash P60 Academic Silica gel (particle size 40–63 nm) was used for flash chromatography. ¹H NMR spectra were recorded on a Varian Inova 500 MHz in CDCl₃ or THF-*d*₈ and are reported relative to residual solvent peak at δ7.26 ppm or δ3.58 ppm, respectively. ¹³C NMR spectra were recorded on a Varian Inova 500 MHz spectrometer (126 MHz) in CDCl₃ or THF-*d*₈ and are reported relative to residual solvent peak at δ77.16 ppm or δ67.21 ppm, respectively. Data for ¹H NMR are reported as follows: chemical shift (δppm) (multiplicity, coupling constant (Hz), integration). Multiplicities are reported as follows: s = singlet, d = doublet, t = triplet, q = quartet, p = pentet, sept = septet, m = multiplet, br s = broad singlet, br d = broad doublet, app = apparent. Data for ¹³C NMR are reported in terms of chemical shifts (δppm). GC-FID analyses were obtained on an Agilent 6890N gas chromatograph equipped with a HP-5 (5%-phenyl)-methylpolysiloxane capillary column (Agilent). GC-MS analyses were obtained on an Agilent 6850 gas chromatograph equipped with a HP-5 (5%-phenyl)-methylpolysiloxane capillary column (Agilent). High resolution mass spectra (HRMS) were acquired from the California Institute of Technology Mass Spectrometry Facility. Note that the calculated mass of the quasi-molecular ion does not take into account the loss of the electron mass. ICP-MS analysis was conducted at the California Institute of Technology Mass Spectrometry Facility. Silanes were purchased from Aldrich and distilled before use. KO*t*-Bu was purchased from Aldrich (sublimed grade, 99.99% trace metals basis) and used directly. KOH was purchased from Aldrich (semiconductor grade,

pellets, 99.99% trace metals basis) and pulverized (mortar and pestle) then heated (150 °C) under vacuum for 24 h prior to use. NaOH was purchased from Aldrich (semiconductor grade, pellets, 99.99% trace metals basis) and pulverized (mortar and pestle) then heated (150 °C) under vacuum prior to use. Alkyne substrates were purchased from Aldrich, TCI, or Acros and used as received (unless noted).

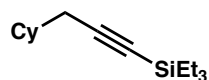
A6.4.2 General Procedure for Reaction Optimization

Procedure for reaction condition optimization: In a nitrogen-filled glovebox, catalyst and alkyne **82** (0.1 mmol, 1 equiv) were added to a 2 dram scintillation vial equipped with a magnetic stirring bar. Next, hydrosilane and solvent (0.1mL) were added. The vial was sealed and the mixture was stirred at the indicated temperature for the indicated time. The vial was then removed from the glovebox, diluted with diethyl ether (1mL), and concentrated under reduced pressure. The yield was determined by ¹H NMR or GC analysis of the crude mixture using an internal standard.

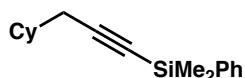
A6.4.3 General Procedure for Alkyne C–H Silylation Reactions.

In a nitrogen-filled glove box, catalyst (0.05 mmol, 10 mol %) and alkyne (0.5 mmol, 1 equiv) were added to a 2 dram scintillation vial equipped with a magnetic stirring bar, followed by solvent (0.5 mL) and silane (1.5 mmol, 3 equiv). The vial was then sealed and the mixture was stirred at the indicated temperature for the indicated time. The vial was then removed from the glovebox; the reaction mixture was diluted with diethyl ether (2 mL), filtered through a short pad of silica gel, and concentrated under reduced pressure. Volatiles were removed under high vacuum with heating as indicated and the resultant material was purified by silica gel flash chromatography if necessary to give the desired product.

A6.4.4 Spectroscopic Data for Alkyne C–H Silylation Reactions.

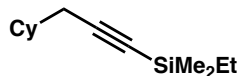


(3-Cyclohexylprop-1-yn-1-yl)triethylsilane 83a: The general procedure was followed. The reaction was performed with NaOH (2.0 mg, 0.05 mmol, 10 mol %), cyclohexylpropane (61 mg, 0.5 mmol, 1.0 equiv), Et₃SiH (174 mg, 240 μL, 1.5 mmol, 3.0 equiv), and 0.5 mL of 1,2-dimethoxyethane (DME) at 85 °C for 48 h. The desired product **83a** (111.9 mg, 95% yield) was obtained as a colorless oil in analytical purity after removal of volatiles under high vacuum (45 mtorr, 2 hours). ¹H NMR (500 MHz, CDCl₃) δ 2.13 (d, *J* = 6.6 Hz, 2H), 1.84 – 1.76 (m, 2H), 1.75 – 1.68 (m, 2H), 1.65 (dtt, *J* = 12.9, 3.4, 1.5 Hz, 1H), 1.47 (dddd, *J* = 14.8, 6.8, 4.7, 3.4 Hz, 1H), 1.24 (tdd, *J* = 15.9, 9.4, 3.4 Hz, 2H), 1.19 – 1.07 (m, 2H), 1.07 – 1.01 (m, 1H), 0.98 (t, *J* = 7.9 Hz, 9H), 0.57 (q, *J* = 7.9 Hz, 6H); ¹³C NMR (126 MHz, CDCl₃) δ 107.73, 82.39, 37.54, 32.72, 27.86, 26.47, 26.32, 7.65, 4.75. IR (Neat Film NaCl) 3422, 2925, 2172, 1645, 1449, 1018, 802, 724 cm⁻¹; HRMS (EI+) calc'd for C₁₅H₂₇Si [(M+H)–H₂]: 235.1882, found 235.1881.

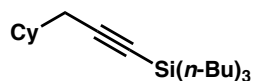


(3-Cyclohexylprop-1-yn-1-yl)dimethyl(phenyl)silane 83b: The general procedure was followed. The reaction was performed with NaOH (2.0 mg, 0.05 mmol, 10 mol %), cyclohexylpropane (61 mg, 0.5 mmol, 1.0 equiv), PhMe₂SiH (204 mg, 230 μL, 1.5 mmol, 3.0 equiv), and 0.5 mL of 1,2-dimethoxyethane (DME) at 25 °C for 48 h. The desired product **83b** (113.6 mg, 89% yield) was obtained as a colorless oil after removal of volatiles by heating to 85°C at 45 mtorr for 30 minutes and subsequent purification by

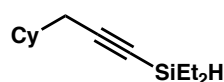
silica gel flash chromatography (100% hexanes). $R_f = 0.67$ (100% hexanes); ^1H NMR (500 MHz, CDCl_3) δ 7.67 – 7.63 (m, 2H), 7.40 – 7.34 (m, 3H), 2.19 (d, $J = 6.6$ Hz, 2H), 1.87 – 1.80 (m, 2H), 1.74 (dt, $J = 12.8, 3.3$ Hz, 2H), 1.67 (dddd, $J = 11.3, 5.2, 3.3, 1.6$ Hz, 1H), 1.52 (ddtd, $J = 14.9, 11.5, 6.7, 3.5$ Hz, 1H), 1.27 (dddd, $J = 15.9, 12.6, 9.5, 3.3$ Hz, 2H), 1.15 (qt, $J = 12.7, 3.3$ Hz, 1H), 1.08 – 0.98 (m, 2H), 0.41 (s, 6H); ^{13}C NMR (126 MHz, CDCl_3) δ 137.93, 133.81, 129.33, 127.91, 108.67, 83.19, 37.42, 32.81, 27.94, 26.42, 26.29, –0.38. IR (Neat Film NaCl) 3420, 2924, 2852, 2173, 1646, 1448, 1427, 1322, 1248, 1115, 1071, 1027, 815, 730 cm^{-1} ; HRMS (EI+) calc'd for $\text{C}_{17}\text{H}_{25}\text{Si} [\text{M}+\text{H}]$: 257.1726, found 257.1720.



(3-Cyclohexylprop-1-yn-1-yl)(ethyl)dimethylsilane 83c: The general procedure was followed. The reaction was performed with KOH (2.8 mg, 0.05 mmol, 10 mol%), cyclohexylpropane (61 mg, 0.5 mmol, 1.0 equiv), EtMe_2SiH (132 mg, 198 μL , 1.5 mmol, 3.0 equiv), and 0.5 mL of 1,2-dimethoxyethane (DME) at 45 °C for 24 h. The desired product **83c** (95.1 mg, 91% yield) was obtained as a colorless oil in analytical purity after removal of volatiles under high vacuum (45 mtorr, 2 hours). ^1H NMR (500 MHz, CDCl_3) δ 2.12 (d, $J = 6.6$ Hz, 2H), 1.86 – 1.76 (m, 2H), 1.77 – 1.69 (m, 2H), 1.66 (dtd, $J = 12.6, 3.3, 1.6$ Hz, 1H), 1.53 – 1.40 (m, 1H), 1.32 – 1.19 (m, 2H), 1.20 – 1.07 (m, 2H), 1.06 – 0.94 (m, 4H), 0.57 (q, $J = 7.9$ Hz, 2H), 0.12 (s, 6H); ^{13}C NMR (126 MHz, CDCl_3) δ 107.01, 84.30, 37.46, 32.76, 27.84, 26.45, 26.30, 8.47, 7.50, –1.85. IR (Neat Film NaCl) 3422, 2922, 2103, 1646, 1558, 1260, 1027, 720 cm^{-1} ; HRMS (EI+) calc'd for $\text{C}_{13}\text{H}_{23}\text{Si} [(\text{M}+\text{H})-\text{H}_2]$: 207.1569, found 207.1562.

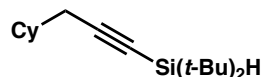


Tributyl(3-cyclohexylprop-1-yn-1-yl)silane 83d: The general procedure was followed. The reaction was performed with KOH (2.8 mg, 0.05 mmol, 10 mol%), cyclohexylpropyne (61 mg, 0.5 mmol, 1.0 equiv), *n*-Bu₃SiH (301 mg, 386 μL, 1.5 mmol, 3.0 equiv), and 0.5 mL of 1,2-dimethoxyethane (DME) at 65 °C for 48 h. The desired product **83d** (117.2 mg, 73% yield) was obtained as a colorless oil by silica gel flash chromatography (100% hexanes). $R_f = 0.78$ (100% hexanes); ¹H NMR (500 MHz, CDCl₃) δ 2.18 (d, *J* = 6.5 Hz, 2H), 1.85 (dddd, *J* = 12.3, 6.2, 3.1, 1.8 Hz, 2H), 1.77 (ddd, *J* = 14.0, 4.5, 2.3 Hz, 2H), 1.70 (dddt, *J* = 12.8, 5.1, 3.3, 1.5 Hz, 1H), 1.52 (dddt, *J* = 14.5, 7.9, 6.6, 3.2 Hz, 1H), 1.43 – 1.36 (m, 12H), 1.29 (qt, *J* = 12.6, 3.3 Hz, 2H), 1.18 (qt, *J* = 12.7, 3.3 Hz, 1H), 1.11 – 1.02 (m, 2H), 0.97 – 0.91 (m, 9H), 0.67 – 0.59 (m, 6H); ¹³C NMR (126 MHz, CDCl₃) δ 107.65, 83.25, 37.57, 32.72, 27.88, 26.64, 26.46, 26.39, 26.32, 13.98, 13.45. IR (Neat Film NaCl) 2955, 2922, 2854, 2172, 1449, 1376, 1191, 1080, 1029, 886, 758, 708 cm⁻¹; HRMS (EI+) calc'd for C₂₁H₄₀Si [M+·]: 320.2899, found 320.2905.



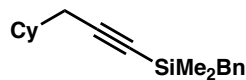
(3-Cyclohexylprop-1-yn-1-yl)diethylsilane 83e: The general procedure was followed. The reaction was performed with KOH (2.8 mg, 0.05 mmol, 10 mol%), cyclohexylpropyne (61 mg, 0.5 mmol, 1.0 equiv), Et₂SiH₂ (132 mg, 194 μL, 1.5 mmol, 3.0 equiv), and 0.5 mL of tetrahydrofuran (THF) at 25 °C for 24 h. The desired product

83e (73.6 mg, 71% yield) was obtained in as a colorless oil after removal of volatiles under high vacuum at 45 mtorr for 30 minutes and subsequent purification by silica gel flash chromatography (100% hexanes). $R_f = 0.77$ (100% hexanes); ^1H NMR (500 MHz, CDCl_3) δ 3.92 (pt, $J = 3.2, 1.2$ Hz, 1H), 2.15 (dd, $J = 6.7, 1.2$ Hz, 2H), 1.85 – 1.78 (m, 2H), 1.72 (ddd, $J = 13.9, 4.5, 2.2$ Hz, 2H), 1.66 (dddt, $J = 12.7, 5.1, 3.3, 1.5$ Hz, 1H), 1.49 (ddtd, $J = 14.9, 11.5, 6.8, 3.5$ Hz, 1H), 1.31 – 1.20 (m, 2H), 1.15 (tt, $J = 12.6, 3.2$ Hz, 1H), 1.07 – 0.95 (m, 8H), 0.70 – 0.64 (m, 4H); ^{13}C NMR (126 MHz, CDCl_3) δ 109.00, 80.24, 37.39, 32.76, 27.91, 26.41, 26.28, 8.09, 4.23. IR (Neat Film NaCl) 3422, 2957, 2174, 2120, 1646, 1558, 1457, 1260, 1055, 804 cm^{-1} ; HRMS (EI+) calc'd for $\text{C}_{13}\text{H}_{23}\text{Si}$ [(M+H)-H₂]: 207.1569, found 207.1562.

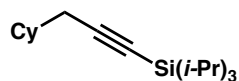


Di-tert-butyl(3-cyclohexylprop-1-yn-1-yl)silane 83f: The general procedure was followed. The reaction was performed with NaOH (2.0 mg, 0.05 mmol, 10 mol%), cyclohexylpropyne (61 mg, 0.5 mmol, 1.0 equiv), *t*-Bu₂SiH₂ (216 mg, 297 μL , 1.5 mmol, 3.0 equiv), and 0.5 mL of 1,2-dimethoxyethane (DME) at 65 °C for 48 h. The desired product **83f** (120.3 mg, 91% yield) was obtained as a colorless oil after removal of volatiles under high vacuum at 45 mtorr for 30 minutes and subsequent purification by silica gel flash chromatography (100% hexanes). $R_f = 0.88$ (100% hexanes); ^1H NMR (500 MHz, CDCl_3) δ 3.57 (t, $J = 1.2$ Hz, 1H), 2.17 (dd, $J = 6.5, 1.2$ Hz, 2H), 1.84 – 1.78 (m, 2H), 1.76 – 1.70 (m, 2H), 1.66 (dddt, $J = 12.8, 5.1, 3.3, 1.5$ Hz, 1H), 1.50 (dddt, $J = 14.5, 7.8, 6.5, 3.1$ Hz, 1H), 1.26 (qt, $J = 12.7, 3.4$ Hz, 3H), 1.19 – 1.09 (m, 2H), 1.06 (s, 18H); ^{13}C NMR (126 MHz, CDCl_3) δ 108.94, 79.54, 37.51, 32.75, 28.28, 27.88, 26.44,

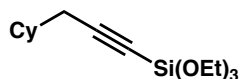
26.29, 18.63. IR (Neat Film NaCl) 2958, 2927, 2855, 2173, 2111, 1469, 1449, 1363, 1028, 1012, 810, 793, 617 cm^{-1} ; HRMS (EI+) calc'd for $\text{C}_{17}\text{H}_{31}\text{Si}$ [(M+H)-H₂]: 263.2195, found 263.2206.



Benzyl(3-cyclohexylprop-1-yn-1-yl)dimethylsilane 83g: The general procedure was followed. The reaction was performed with NaOH (2.0 mg, 0.05 mmol, 10 mol%), cyclohexylpropane (61 mg, 0.5 mmol, 1.0 equiv), BnMe_2SiH (150 mg, 238 μL , 1.5 mmol, 3.0 equiv), and 0.5 mL of 1,2-dimethoxyethane (DME) at 45 °C for 48 h. The desired product **83g** (101.9 mg, 75% yield) was obtained as a colorless oil by silica gel flash chromatography (100% hexanes). $R_f = 0.51$ (100% hexanes); ¹H NMR (500 MHz, CDCl_3) δ 7.25 – 7.21 (m, 2H), 7.12 – 7.08 (m, 3H), 2.20 (s, 2H), 2.14 (d, $J = 6.8$ Hz, 2H), 1.81 (ddd, $J = 13.3, 3.5, 1.5$ Hz, 2H), 1.75 (dt, $J = 12.7, 3.2$ Hz, 2H), 1.69 (dddd, $J = 11.3, 5.3, 3.4, 1.7$ Hz, 1H), 1.49 (tdt, $J = 11.4, 6.7, 3.3$ Hz, 1H), 1.28 (qt, $J = 12.6, 3.3$ Hz, 2H), 1.16 (qt, $J = 12.7, 3.3$ Hz, 1H), 1.06 – 0.94 (m, 2H), 0.13 (s, 6H); ¹³C NMR (126 MHz, CDCl_3) δ 139.44, 128.51, 128.19, 124.32, 108.08, 83.69, 37.38, 32.77, 27.86, 26.71, 26.41, 26.29, –1.69. IR (Neat Film NaCl) 3081, 3060, 3024, 2999, 2922, 2851, 2664, 2173, 1936, 1600, 1493, 1449, 1422, 1408, 1368, 1322, 1249, 1207, 1155, 1056, 1029, 947, 839, 761, 697 cm^{-1} ; HRMS (EI+) calc'd for $\text{C}_{18}\text{H}_{26}\text{Si}$ [M+•]: 270.1804, found 270.1810.

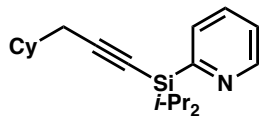


(3-Cyclohexylprop-1-yn-1-yl)triisopropylsilane 83h: The general procedure was followed. The reaction was performed with KOH (2.8 mg, 0.05 mmol, 10 mol%), cyclohexylpropane (61 mg, 0.5 mmol, 1.0 equiv), *i*-Pr₃SiH (238 mg, 307 μL, 1.5 mmol, 3.0 equiv), and 0.5 mL of 1,2-dimethoxyethane (DME) at 85 °C for 48 h. The desired product **83h** (95.6 mg, 69% yield) was obtained as a colorless oil by silica gel flash chromatography (100% hexanes). $R_f = 0.79$ (100% hexanes); ¹H NMR (500 MHz, CDCl₃) δ 2.16 (d, *J* = 6.4 Hz, 2H), 1.84 – 1.77 (m, 2H), 1.73 (dt, *J* = 12.8, 3.4 Hz, 2H), 1.66 (ddtd, *J* = 12.7, 3.3, 1.6 Hz, 1H), 1.48 (ddtd, *J* = 14.6, 11.2, 6.5, 3.4 Hz, 1H), 1.25 (qt, *J* = 12.6, 3.4 Hz, 2H), 1.15 (tt, *J* = 12.6, 3.3 Hz, 1H), 1.10 – 0.99 (m, 23H); ¹³C NMR (126 MHz, CDCl₃) δ 108.17, 80.94, 37.64, 32.71, 27.87, 26.49, 26.33, 18.80, 11.48. IR (Neat Film NaCl) 2924, 2864, 2170, 2463, 1449, 1264, 1025, 995, 883, 743, 676, 633 cm⁻¹; HRMS (EI+) calc'd for C₁₈H₃₃Si [(M+H)-H₂]: 277.2352, found 277.2349.



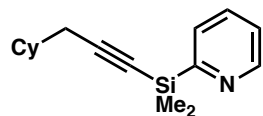
(3-Cyclohexylprop-1-yn-1-yl)triethoxysilane 83i: The general procedure was followed. The reaction was performed with NaOH (2.0 mg, 0.05 mmol, 10 mol%), cyclohexylpropane (61 mg, 0.5 mmol, 1.0 equiv), (EtO)₃SiH (246 mg, 277 μL, 1.5 mmol, 3.0 equiv), and 0.5 mL of 1,2-dimethoxyethane (DME) at 65 °C for 48 h. The desired product **83i** (97.1 mg, 68% yield) was obtained as a colorless oil by silica gel flash chromatography (5% Et₂O in hexanes). $R_f = 0.41$ (5% Et₂O in hexanes); ¹H NMR (500 MHz, CDCl₃) δ 3.87 (q, *J* = 7.0 Hz, 6H), 2.16 (d, *J* = 6.6 Hz, 2H), 1.84 – 1.78 (m, 2H),

1.72 (dp, $J = 12.6, 3.7$ Hz, 2H), 1.66 (dddt, $J = 12.8, 5.1, 3.3, 1.5$ Hz, 1H), 1.52 (ddtd, $J = 14.9, 11.5, 6.8, 3.5$ Hz, 1H), 1.26 (t, $J = 7.0$ Hz, 9H), 1.24 – 1.19 (m, 2H), 1.13 (qt, $J = 12.7, 3.3$ Hz, 1H), 1.02 (qd, $J = 12.7, 3.5$ Hz, 2H); ^{13}C NMR (126 MHz, CDCl_3) δ 106.50, 76.85, 59.02, 37.10, 32.74, 27.55, 26.33, 26.20, 18.18. IR (Neat Film NaCl) 2974, 2925, 2852, 2182, 1449, 1390, 1168, 1101, 1079, 1036, 964, 790, 721 cm^{-1} ; HRMS (EI+) calc'd for $\text{C}_{15}\text{H}_{29}\text{O}_3\text{Si}$ [M+H]: 285.1886, found 285.1889.

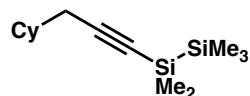


2-((3-Cyclohexylprop-1-yn-1-yl)diisopropylsilyl)pyridine 83j: The general procedure was followed. The reaction was performed with KOH (2.8 mg, 0.05 mmol, 10 mol%), cyclohexylpropyne (61 mg, 0.5 mmol, 1.0 equiv), *i*-Pr₂(Pyr)SiH (290 mg, 322 μL , 1.5 mmol, 3.0 equiv), and 0.5 mL of 1,2-dimethoxyethane (DME) at 65 °C for 48 h. The desired product **83j** (122.5 mg, 78% yield) was obtained as a colorless oil by silica gel flash chromatography (10% EtOAc in hexanes). $R_f = 0.47$ (10% EtOAc in hexanes); ^1H NMR (500 MHz, THF-*d*₈) δ 8.65 (ddd, $J = 4.8, 1.7, 1.1$ Hz, 1H), 7.76 (dt, $J = 7.5, 1.3$ Hz, 1H), 7.59 (td, $J = 7.6, 1.8$ Hz, 1H), 7.19 (ddd, $J = 7.7, 4.8, 1.4$ Hz, 1H), 2.26 (d, $J = 6.4$ Hz, 2H), 1.95 – 1.84 (m, 2H), 1.78 – 1.73 (m, 2H), 1.67 (dtt, $J = 13.0, 3.4, 1.6$ Hz, 1H), 1.55 (ddtd, $J = 14.9, 11.4, 6.6, 3.5$ Hz, 1H), 1.37 – 1.26 (m, 4H), 1.21 – 1.16 (m, 1H), 1.16 – 1.11 (m, 2H), 1.09 (d, $J = 7.4$ Hz, 6H), 0.99 (d, $J = 7.3$ Hz, 6H); ^{13}C NMR (126 MHz, THF-*d*₈) δ 164.80, 150.76, 134.42, 132.12, 123.73, 110.50, 80.33, 38.63, 33.66, 28.41, 27.38, 27.23, 18.46, 18.40, 12.71. IR (Neat Film NaCl) 2924, 2862, 2170, 1573,

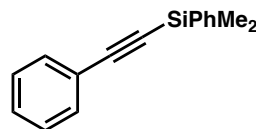
1462, 1449, 1417, 1136, 1081, 1028, 995, 882, 747, 723 cm^{-1} ; HRMS (EI $+$) calc'd for $\text{C}_{20}\text{H}_{32}\text{NSi}$ [M+H]: 314.2304, found 314.2311.



2-((3-Cyclohexylprop-1-yn-1-yl)dimethylsilyl)pyridine 83k: The general procedure was followed. The reaction was performed with NaOH (2.0 mg, 0.05 mmol, 10 mol%), cyclohexylpropane (61 mg, 0.5 mmol, 1.0 equiv), $\text{Me}_2(\text{Py})\text{SiH}$ (206 mg, 225 μL , 1.5 mmol, 3.0 equiv), and 0.5 mL of 1,2-dimethoxyethane (DME) at 65 °C for 48 h. The desired product **83k** (99.9 mg, 78% yield) was obtained as a colorless oil by silica gel flash chromatography (10% EtOAc in hexanes). $R_f = 0.42$ (10% EtOAc in hexanes); ^1H NMR (500 MHz, THF- d_8) δ 8.65 (ddd, $J = 4.8, 1.8, 1.1$ Hz, 1H), 7.74 (dt, $J = 7.5, 1.2$ Hz, 1H), 7.59 (td, $J = 7.6, 1.8$ Hz, 1H), 7.18 (ddd, $J = 7.7, 4.8, 1.4$ Hz, 1H), 2.19 (d, $J = 6.6$ Hz, 2H), 1.88 – 1.81 (m, 2H), 1.73 – 1.70 (m, 2H), 1.66 (dddd, $J = 12.7, 5.1, 3.2, 1.5$ Hz, 1H), 1.50 (dddt, $J = 14.7, 7.9, 6.7, 3.2$ Hz, 1H), 1.28 (tdd, $J = 16.0, 9.4, 3.4$ Hz, 2H), 1.17 (qt, $J = 12.7, 3.3$ Hz, 1H), 1.05 (qd, $J = 12.8, 3.4$ Hz, 2H), 0.36 (s, 6H); ^{13}C NMR (126 MHz, THF- d_8) δ 166.55, 150.96, 134.69, 130.13, 123.84, 109.23, 83.58, 38.47, 33.68, 28.42, 27.34, 27.22, –1.00. IR (Neat Film NaCl) 3423, 2924, 2852, 2175, 1646, 1449, 1255, 1044, 832, 797, 676 cm^{-1} ; HRMS (EI $+$) calc'd for $\text{C}_{16}\text{H}_{24}\text{NSi}$ [M+H]: 258.1678, found 258.1672.

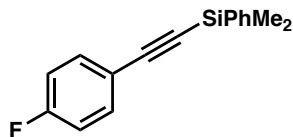


1-(3-Cyclohexylprop-1-yn-1-yl)-1,1,2,2,2-pentamethyldisilane 83l: The general procedure was followed. The reaction was performed with NaOH (2.0 mg, 0.05 mmol, 10 mol%), cyclohexylpropane (61 mg, 0.5 mmol, 1.0 equiv), Me₅Si₂H (246 mg, 277 μL, 1.5 mmol, 3.0 equiv), and 0.5 mL of 1,2-dimethoxyethane (DME) at 25 °C for 48 h. The desired product **83l** (120.0 mg, 95% yield) was obtained in analytical purity as a cloudy, colorless oil after removal of volatiles at 85°C at 45 mtorr for 30 minutes. ¹H NMR (500 MHz, THF-*d*₈) δ 2.11 (d, *J* = 6.5 Hz, 2H), 1.81 (dddd, *J* = 13.1, 6.1, 3.1, 1.9 Hz, 2H), 1.73 – 1.69 (m, 2H), 1.65 (dddt, *J* = 12.7, 5.1, 3.2, 1.5 Hz, 1H), 1.44 (dddt, *J* = 14.6, 8.0, 6.7, 3.2 Hz, 1H), 1.33 – 1.21 (m, 2H), 1.15 (qt, *J* = 12.7, 3.2 Hz, 1H), 1.03 (qd, *J* = 12.8, 3.5 Hz, 2H), 0.15 (s, 6H), 0.11 (s, 9H); ¹³C NMR (126 MHz, THF-*d*₈) δ 109.11, 84.06, 38.62, 33.61, 28.52, 27.37, 27.22, –2.25, –2.35. IR (Neat Film NaCl) 2923, 2852, 2168, 1449, 1259, 1244, 1077, 1027, 871, 833, 799, 765, 725, 691, 667 cm^{–1}; HRMS (EI+) calc'd for C₁₄H₂₈Si₂ [M+•]: 252.1730, found 252.1737.

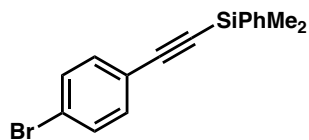


Dimethyl(phenyl)(phenylethynyl)silane 85a: The general procedure was followed. The reaction was performed with NaOH (2.0 mg, 0.05 mmol, 10 mol%), ethynylbenzene (52 mg, 0.5 mmol, 1.0 equiv), PhMe₂SiH (204 mg, 230 μL, 1.5 mmol, 3.0 equiv), and 0.5 mL of 1,2-dimethoxyethane (DME) at 65 °C for 48 h. The desired product **85a** (105.7 mg, 89% yield) was obtained as a colorless oil after removal of volatiles by heating to 85°C at

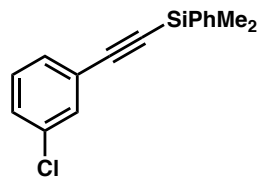
45 mtorr for 30 minutes and subsequent purification by silica gel flash chromatography (100% hexanes). $R_f = 0.38$ (100% hexanes); ^1H NMR (500 MHz, THF- d_8) δ 7.71 – 7.65 (m, 2H), 7.49 – 7.44 (m, 2H), 7.38 – 7.28 (m, 6H), 0.46 (s, 6H). ^{13}C NMR (126 MHz, THF- d_8) δ 137.86, 134.66, 132.88, 130.35, 129.75, 129.28, 128.79, 124.15, 107.86, 92.55, –0.50. IR (Neat Film NaCl) 3068, 3051, 2959, 2899, 2158, 1592, 1488, 1442, 1428, 1278, 1250, 1219, 1118, 1068, 1026, 846, 807, 780, 731, 690 cm^{-1} ; HRMS (EI+) calc'd for $\text{C}_{16}\text{H}_{17}\text{Si}$ [M+H]: 237.1100, found 237.1101.



((4-Fluorophenyl)ethynyl)dimethyl(phenyl)silane 85b: The general procedure was followed. The reaction was performed with NaOH (2.0 mg, 0.05 mmol, 10 mol%), 1-ethynyl-4-fluorobenzene (60 mg, 0.5 mmol, 1.0 equiv), PhMe₂SiH (204 mg, 230 μL , 1.5 mmol, 3.0 equiv), and 0.5 mL of 1,2-dimethoxyethane (DME) at 65 °C for 48 h. The desired product **85b** (111.9 mg, 88% yield) was obtained as a colorless oil after solvent removal at 85°C at 45 mtorr for 30 minutes and subsequent purification by silica gel flash chromatography (100% hexanes). $R_f = 0.49$ (100% hexanes); ^1H NMR (500 MHz, THF- d_8) δ 7.68 – 7.65 (m, 2H), 7.53 – 7.48 (m, 2H), 7.34 (dd, $J = 4.9, 1.9$ Hz, 3H), 7.08 (t, $J = 8.8$ Hz, 2H), 0.46 (s, 6H); ^{13}C NMR (126 MHz, THF- d_8) δ 163.94 (d, $J = 249.1$ Hz), 137.74, 135.10 (d, $J = 8.5$ Hz), 134.65, 130.38, 128.80, 120.42 (d, $J = 3.8$ Hz), 116.50 (d, $J = 21.7$ Hz), 106.67, 92.42, –0.57. IR (Neat Film NaCl) 3420, 3069, 2961, 2160, 1653, 1600, 1505, 1428, 1251, 1233, 1155, 1117, 1092, 857, 835, 816, 781, 731, 698 cm^{-1} ; HRMS (EI+) calc'd for $\text{C}_{16}\text{H}_{16}\text{FSi}$ [M+H]: 255.1005, found 255.1000.

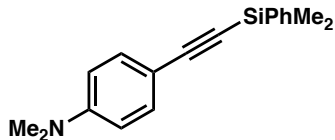


((4-Bromophenyl)ethynyl)dimethyl(phenyl)silane 85c: The general procedure was followed. The reaction was performed with NaOH (2.0 mg, 0.05 mmol, 10 mol%), 1-bromo-4-ethynylbenzene (90 mg, 0.5 mmol, 1.0 equiv), PhMe₂SiH (204 mg, 230 µL, 1.5 mmol, 3.0 equiv), and 0.5 mL of 1,2-dimethoxyethane (DME) at 65 °C for 48 h. The desired product **85c** (81.3 mg, 52% yield) was obtained as colorless crystals after solvent removal at 85°C at 45 mtorr for 30 minutes and subsequent purification by silica gel flash chromatography (100% hexanes). $R_f = 0.54$ (100% hexanes); ¹H NMR (500 MHz, THF-*d*₈) δ 7.69 – 7.63 (m, 2H), 7.51 (d, *J* = 8.5 Hz, 2H), 7.39 (d, *J* = 8.5 Hz, 2H), 7.36 – 7.30 (m, 3H), 0.46 (s, 6H); ¹³C NMR (126 MHz, THF-*d*₈) δ 137.55, 134.65, 134.53, 132.66, 130.44, 128.83, 123.94, 123.19, 106.51, 94.19, –0.66. IR (Neat Film NaCl) 3068, 2958, 2159, 1653, 1540, 1484, 1473, 1457, 1427, 1249, 1214, 1114, 1071, 1010, 846, 830, 780, 730, 698 cm⁻¹; HRMS (EI+) calc'd for C₁₆H₁₆Si¹⁸Br [M+H]: 317.0184, found 317.0180.

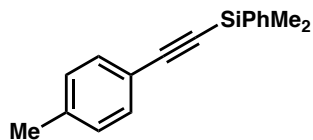


((3-Chlorophenyl)ethynyl)dimethyl(phenyl)silane 85d: The general procedure was followed. The reaction was performed with NaOH (2.0 mg, 0.05 mmol, 10 mol%), 1-chloro-3-ethynylbenzene (68 mg, 0.5 mmol, 1.0 equiv), PhMe₂SiH (204 mg, 230 µL, 1.5 mmol, 3.0 equiv), and 0.5 mL of 1,2-dimethoxyethane (DME) at 45 °C for 24 h. The

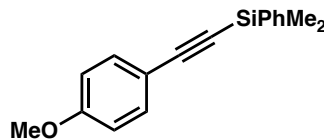
desired product **85d** (121.6 mg, 90% yield) was obtained as a colorless oil after solvent removal at 85°C at 45 mtorr for 30 minutes and subsequent purification by silica gel flash chromatography (100% hexanes). $R_f = 0.42$ (100% hexanes); ^1H NMR (500 MHz, CDCl_3) δ 7.70 – 7.66 (m, 2H), 7.49 (ddd, $J = 2.1, 1.5, 0.5$ Hz, 1H), 7.40 (dd, $J = 5.0, 1.9$ Hz, 3H), 7.38 (dt, $J = 7.6, 1.4$ Hz, 1H), 7.31 (ddd, $J = 8.1, 2.1, 1.2$ Hz, 1H), 7.24 (ddd, $J = 8.0, 7.6, 0.5$ Hz, 1H), 0.51 (s, 6H); ^{13}C NMR (126 MHz, CDCl_3) δ 136.75, 134.21, 133.86, 132.05, 130.29, 129.70, 129.61, 129.12, 128.10, 124.77, 105.13, 93.82, -0.79. IR (Neat Film NaCl) 3420, 2163, 1684, 1647, 1559, 1521, 1507, 1457, 1249, 1117, 1091, 884, 781, 681 cm^{-1} ; HRMS (EI $^+$) calc'd for $\text{C}_{16}\text{H}_{16}\text{ClSi}$ [M+H]: 271.0710, found 271.0710.



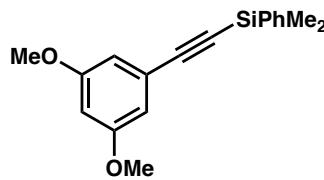
4-((Dimethyl(phenyl)silyl)ethynyl)-N,N-dimethylaniline 85e: The general procedure was followed. The reaction was performed with NaOH (2.0 mg, 0.05 mmol, 10 mol%), 4-ethynyl-N,N-dimethylaniline (73 mg, 0.5 mmol, 1.0 equiv), PhMe_2SiH (204 mg, 230 μL , 1.5 mmol, 3.0 equiv), and 0.5 mL of 1,2-dimethoxyethane (DME) at 65 °C for 48 h. The desired product **85e** (139.4 mg, 100% yield) was obtained in analytical purity as colourless crystals after removal of volatiles at 85°C at 45 mtorr for 30 minutes. ^1H NMR (500 MHz, CDCl_3) δ 7.73 – 7.68 (m, 2H), 7.41 – 7.36 (m, 5H), 6.61 (d, $J = 8.9$ Hz, 2H), 2.98 (s, 6H), 0.48 (s, 6H); ^{13}C NMR (126 MHz, CDCl_3) δ 150.46, 137.88, 133.93, 133.38, 129.36, 127.94, 111.69, 109.78, 108.49, 89.19, 40.32, -0.39. IR (Neat Film NaCl) 3067, 2957, 2147, 1682, 1607, 1519, 1487, 1427, 1360, 1248, 1186, 1115, 945, 850, 817,



Dimethyl(phenyl)(p-tolylethynyl)silane 85f: The general procedure was followed. The reaction was performed with NaOH (2.0 mg, 0.05 mmol, 10 mol %), 1-ethynyl-4-methylbenzene (58 mg, 0.5 mmol, 1.0 equiv), PhMe₂SiH (204 mg, 230 µL, 1.5 mmol, 3.0 equiv), and 0.5 mL of 1,2-dimethoxyethane (DME) at 65 °C for 48 h. The desired product **85f** (115.5 mg, 92% yield) was obtained in analytical purity as a pale yellow oil after removal of volatiles at 85°C at 45 mtorr for 30 minutes and subsequent purification by silica gel flash chromatography (100% hexanes). R_f = 0.46 (100% hexanes); ¹H NMR (500 MHz, CDCl₃) δ 7.71 (ddt, J = 6.0, 2.4, 1.1 Hz, 2H), 7.41 (ddq, J = 5.8, 3.0, 0.9 Hz, 5H), 7.16 – 7.10 (m, 2H), 2.37 (s, 3H), 0.51 (d, J = 1.1 Hz, 6H); ¹³C NMR (126 MHz, CDCl₃) δ 139.02, 137.33, 133.90, 132.10, 129.52, 129.12, 128.02, 120.00, 107.18, 91.28, 21.69, -0.59. IR (Neat Film NaCl) 3420, 3068, 3049, 2959, 2920, 2156, 1507, 1428, 1408, 1249, 1223, 1117, 1020, 851, 816, 780, 731, 700, 656 cm⁻¹; HRMS (EI+) calc'd for C₁₇H₁₉Si [M+H]: 251.1256, found 251.1257.

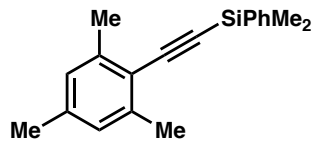


((4-Methoxyphenyl)ethynyl)dimethyl(phenyl)silane 85g: The general procedure was followed. The reaction was performed with NaOH (2.0 mg, 0.05 mmol, 10 mol%), 1-ethynyl-4-methoxybenzene (66 mg, 0.5 mmol, 1.0 equiv), PhMe₂SiH (204 mg, 230 μL, 1.5 mmol, 3.0 equiv), and 0.5 mL of 1,2-dimethoxyethane (DME) at 65 °C for 48 h. The desired product **85g** (121.6 mg, 91% yield) was obtained as a yellow oil after removal of volatiles at 85°C at 45 mtorr for 30 minutes and subsequent purification by silica gel flash chromatography (100% hexanes → 5% EtOAc in hexanes). $R_f = 0.27$ (100% hexanes); ¹H NMR (500 MHz, CDCl₃) δ 7.71 (dd, $J = 6.5, 3.0$ Hz, 2H), 7.46 (d, $J = 8.9$ Hz, 2H), 7.43 – 7.38 (m, 3H), 6.84 (d, $J = 8.9$ Hz, 2H), 3.82 (s, 3H), 0.51 (s, 6H); ¹³C NMR (126 MHz, CDCl₃) δ 160.02, 137.42, 133.89, 133.73, 129.50, 128.01, 115.20, 113.96, 107.03, 90.47, 55.42, -0.56. IR (Neat Film NaCl) 3068, 2959, 2154, 1605, 1507, 1441, 1293, 1249, 1171, 1116, 1032, 853, 832, 812, 779, 755, 731, 699 cm⁻¹; HRMS (EI+) calc'd for C₁₇H₁₈OSi [M+•]: 266.1127, found 266.1135.

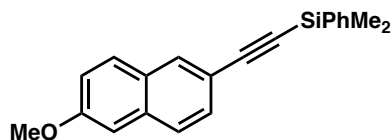


((3,5-Dimethoxyphenyl)ethynyl)dimethyl(phenyl)silane 85h: The general procedure was followed. The reaction was performed with NaOH (2.0 mg, 0.05 mmol, 10 mol%), 1-ethynyl-3,5-dimethoxybenzene (81 mg, 0.5 mmol, 1.0 equiv), PhMe₂SiH (204 mg, 230 μL, 1.5 mmol, 3.0 equiv), and 0.5 mL of 1,2-dimethoxyethane (DME) at 65 °C for 48 h.

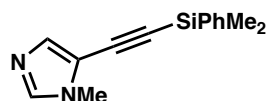
The desired product **85h** (140.6 mg, 95% yield) was obtained in analytical purity as a light yellow oil after removal of volatiles at 85°C at 45 mtorr for 30 minutes. ¹H NMR (500 MHz, CDCl₃) δ 7.70 (ddd, *J* = 5.5, 2.7, 1.2 Hz, 2H), 7.41 (dd, *J* = 4.6, 2.1 Hz, 3H), 6.67 (d, *J* = 2.3 Hz, 2H), 6.47 (t, *J* = 2.3 Hz, 1H), 3.79 (s, 6H), 0.52 (d, *J* = 1.5 Hz, 6H); ¹³C NMR (126 MHz, CDCl₃) δ 160.56, 137.05, 133.90, 129.61, 128.05, 124.29, 109.87, 106.78, 102.53, 91.75, 55.57, –0.68. IR (Neat Film NaCl) 3421, 3069, 3001, 2959, 2837, 2160, 1596, 1456, 1419, 1348, 1298, 1250, 1205, 1155, 1116, 1064, 979, 964, 817, 753, 732, 681 cm^{–1}; HRMS (EI+) calc'd for C₁₈H₂₁O₂Si [M+H]: 297.1311, found 297.1309.



(Mesitylethynyl)dimethyl(phenyl)silane 85i: The general procedure was followed. The reaction was performed with NaOH (2.0 mg, 0.05 mmol, 10 mol%), 2-ethynyl-1,3,5-trimethylbenzene (72 mg, 0.5 mmol, 1.0 equiv), PhMe₂SiH (204 mg, 230 μL, 1.5 mmol, 3.0 equiv), and 0.5 mL of 1,2-dimethoxyethane (DME) at 25 °C for 24 h. The desired product **85i** (119.1 mg, 86% yield) was obtained in analytical purity as a colorless oil after removal of volatiles at 85 °C at 45 mtorr for 30 minutes. ¹H NMR (500 MHz, CDCl₃) δ 7.73 (ddt, *J* = 4.5, 3.2, 0.8 Hz, 3H), 7.40 (dd, *J* = 2.5, 0.8 Hz, 2H), 6.88 – 6.86 (m, 2H), 2.42 (s, 6H), 2.29 (s, 3H), 0.52 (t, *J* = 0.7 Hz, 6H); ¹³C NMR (126 MHz, CDCl₃) δ 140.86, 138.23, 137.66, 133.89, 129.45, 127.99, 127.67, 119.94, 104.95, 99.66, 21.51, 21.15, –0.34. IR (Neat Film NaCl) 3440, 3068, 2959, 2146, 1646, 1610, 1474, 1428, 1224, 1117, 841, 825, 779, 753, 698 cm^{–1}; HRMS (EI+) calc'd for C₁₉H₂₃Si [M+H]: 279.1569, found 279.1561.



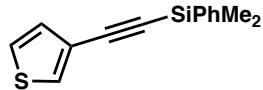
((6-Methoxynaphthalen-2-yl)ethynyl)dimethyl(phenyl)silane 85j: The general procedure was followed. The reaction was performed with NaOH (2.0 mg, 0.05 mmol, 10 mol%), 2-ethynyl-6-methoxynaphthalene (91 mg, 0.5 mmol, 1.0 equiv), PhMe₂SiH (204 mg, 230 μL, 1.5 mmol, 3.0 equiv), and 0.5 mL of 1,2-dimethoxyethane (DME) at 65 °C for 48 h. The desired product **85j** (134.8 mg, 85% yield) was obtained in as a colorless oil after removal of volatiles at 85°C at 45 mtorr for 30 minutes and subsequent purification by alumina flash chromatography (gradient 2.5% Et₂O in hexanes → 10% Et₂O in hexanes). R_f = 0.36 (5% Et₂O in hexanes); ¹H NMR (500 MHz, CDCl₃) δ 7.99 (dd, J = 1.5, 0.7 Hz, 1H), 7.78 – 7.72 (m, 2H), 7.70 (d, J = 9.0 Hz, 1H), 7.68 (d, J = 8.2 Hz, 1H), 7.53 (dd, J = 8.4, 1.6 Hz, 1H), 7.46 – 7.40 (m, 3H), 7.17 (dd, J = 8.9, 2.5 Hz, 1H), 7.11 (d, J = 2.6 Hz, 1H), 3.93 (s, 3H), 0.56 (s, 6H); ¹³C NMR (126 MHz, CDCl₃) δ 158.57, 137.30, 134.48, 133.93, 132.17, 129.56, 129.34, 128.44, 128.05, 126.85, 122.76, 119.59, 117.93, 107.50, 105.91, 91.68, 55.50, –0.57. IR (Neat Film NaCl) 3422, 2959, 2152, 1631, 1601, 1499, 1481, 1461, 1390, 1267, 1232, 1161, 1117, 1031, 937, 890, 814, 780, 731, 703, 656 cm⁻¹; HRMS (EI+) calc'd for C₂₁H₂₀OSi [M+•]: 316.1284, found 316.1296.



5-((Dimethyl(phenyl)silyl)ethynyl)-1-methyl-1H-imidazole 85k: The general procedure was followed. The reaction was performed with NaOH (2.0 mg, 0.05 mmol, 10

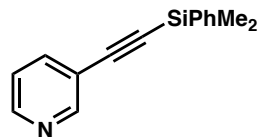
Appendix 6 Hydroxide-Catalyzed Dehydrogenative C–H Silylation of Terminal Alkynes 314

mol%), 5-ethynyl-1-methyl-1*H*-imidazole (53 mg, 0.5 mmol, 1.0 equiv), PhMe₂SiH (204 mg, 230 μL, 1.5 mmol, 3.0 equiv), and 0.5 mL of 1,2-dimethoxyethane (DME) at 45 °C for 48 h. The desired product **85k** (98.7 mg, 82% yield) was obtained as a colorless oil after removal of volatiles at 85°C at 45 mtorr for 30 minutes and subsequent purification by silica gel flash chromatography (100% EtOAc). R_f = 0.45 (100% EtOAc); ¹H NMR (500 MHz, CDCl₃) δ 7.68 – 7.65 (m, 2H), 7.40 (m, 4H), 7.31 (d, *J* = 1.0 Hz, 1H), 3.68 – 3.65 (m, 3H), 0.52 (s, 6H); ¹³C NMR (126 MHz, CDCl₃) δ 138.37, 136.49, 135.29, 133.74, 129.73, 128.09, 116.28, 100.60, 94.11, 32.11, –0.85. IR (Neat Film NaCl) 3417, 2960, 2157, 1646, 1533, 1489, 1428, 1274, 1250, 1227, 1116, 924, 823, 782, 732, 702, 661 cm^{–1}; HRMS (EI+) calc'd for C₁₄H₁₇N₂Si [M+H]: 241.1161, found 241.1169.

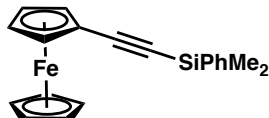


Dimethyl(phenyl)(thiophen-3-ylethynyl)silane 85l: The general procedure was followed. The reaction was performed with NaOH (2.0 mg, 0.05 mmol, 10 mol%), 3-ethynylthiophene (54 mg, 0.5 mmol, 1.0 equiv), PhMe₂SiH (204 mg, 230 μL, 1.5 mmol, 3.0 equiv), and 0.5 mL of 1,2-dimethoxyethane (DME) at 65 °C for 60 h. The desired product **85l** (113.2 mg, 93% yield) was obtained as a colorless oil after removal of volatiles at 85°C at 45 mtorr for 30 minutes and subsequent purification by silica gel flash chromatography (100% hexanes). R_f = 0.39 (100% hexanes); ¹H NMR (500 MHz, CDCl₃) δ 7.72 – 7.68 (m, 2H), 7.53 (dd, *J* = 3.0, 1.2 Hz, 1H), 7.43 – 7.39 (m, 3H), 7.27 – 7.24 (m, 1H), 7.17 (dd, *J* = 5.0, 1.2 Hz, 1H), 0.51 (s, 6H); ¹³C NMR (126 MHz, CDCl₃) δ 137.08, 133.88, 130.26, 130.11, 129.59, 128.04, 125.36, 122.32, 101.67, 91.93, –0.68. IR

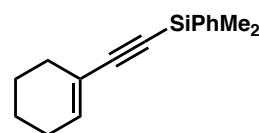
(Neat Film NaCl) 3107, 3068, 2959, 2152, 1427, 1356, 1249, 1163, 1116, 944, 870, 781, 753, 698 cm⁻¹; HRMS (EI+) calc'd for C₁₄H₁₄SSi [M+•]: 242.0586, found 242.0576.



3-((Dimethyl(phenyl)silyl)ethynyl)pyridine 85m: The general procedure was followed. The reaction was performed with NaOH (2.0 mg, 0.05 mmol, 10 mol%), 3-ethynylpyridine (52 mg, 0.5 mmol, 1.0 equiv), PhMe₂SiH (204 mg, 230 µL, 1.5 mmol, 3.0 equiv), and 0.5 mL of 1,2-dimethoxyethane (DME) at 65 °C for 48 h. The desired product **85m** (91.8 mg, 77% yield) was obtained as a colorless oil after removal of volatiles at 85°C at 45 mtorr for 30 minutes and subsequent purification by silica gel flash chromatography (100% hexanes). R_f = 0.31 (100% hexanes); ¹H NMR (500 MHz, CDCl₃) δ 8.74 (dd, J = 2.1, 0.9 Hz, 1H), 8.54 (dd, J = 4.9, 1.7 Hz, 1H), 7.77 (ddd, J = 7.9, 2.1, 1.7 Hz, 1H), 7.71 – 7.67 (m, 2H), 7.42 (dd, J = 4.9, 1.9 Hz, 3H), 7.24 (ddd, J = 7.9, 4.9, 0.9 Hz, 1H), 0.54 (s, 6H); ¹³C NMR (126 MHz, CDCl₃) δ 152.82, 149.02, 139.01, 136.49, 133.81, 129.74, 128.11, 123.00, 120.21, 103.14, 96.34, -0.88. IR (Neat Film NaCl) 3420, 3069, 3048, 3025, 2960, 2161, 1559, 1474, 1406, 1250, 1184, 1119, 1022, 847, 781, 754, 703, 670 cm⁻¹; HRMS (EI+) calc'd for C₁₅H₁₆NSi [M+H]: 238.1052, found 238.1049.

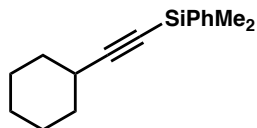


((Dimethyl(phenyl)silyl)ethynyl)ferrocene 85n: The general procedure was followed. The reaction was performed with NaOH (2.0 mg, 0.05 mmol, 10 mol %), ethynylferrocene (105 mg, 0.5 mmol, 1.0 equiv), PhMe₂SiH (204 mg, 230 μL, 1.5 mmol, 3.0 equiv), and 0.5 mL of 1,2-dimethoxyethane (DME) at 45 °C for 48 h. The desired product **85n** (170.1 mg, 99% yield) was obtained in analytical purity as an orange crystalline solid after removal of volatiles at 85°C at 45 mtorr for 30 minutes and subsequent purification by silica gel flash chromatography (gradient 100% hexanes → 5% EtOAc in hexanes). $R_f = 0.45$ (5% EtOAc in hexanes); ¹H NMR (500 MHz, CDCl₃) δ 7.70 (dd, J = 6.1, 3.1 Hz, 2H), 7.43 – 7.37 (m, 3H), 4.49 (t, J = 1.7 Hz, 2H), 4.22 (s, 5H), 4.22 – 4.20 (m, 2H), 0.47 (s, 6H); ¹³C NMR (126 MHz, CDCl₃) δ 137.71, 133.89, 129.44, 127.98, 106.30, 88.52, 72.02, 70.26, 69.00, 64.64, –0.40. IR (Neat Film NaCl) 2958, 2147, 1428, 1248, 1106, 1024, 1001, 925, 819, 779, 753, 730, 699 cm^{–1}; HRMS (EI+) calc'd for C₂₀H₂₀FeSi [M+•]: 344.0684, found 344.0696.

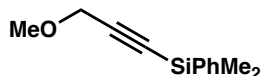


(Cyclohex-1-en-1-ylethynyl)dimethyl(phenyl)silane 85o: The general procedure was followed. The reaction was performed with NaOH (2.0 mg, 0.05 mmol, 10 mol %), 1-ethynylcyclohex-1-ene (53 mg, 0.5 mmol, 1.0 equiv), PhMe₂SiH (204 mg, 230 μL, 1.5 mmol, 3.0 equiv), and 0.5 mL of 1,2-dimethoxyethane (DME) at 45 °C for 48 h. The desired product **85o** (102.7 mg, 85% yield) was obtained as a colorless oil after removal

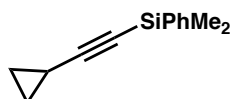
of volatiles at 85°C at 45 mtorr for 15 minutes and subsequent purification by silica gel flash chromatography (100% hexanes). $R_f = 0.50$ (100% hexanes); ^1H NMR (500 MHz, CDCl_3) δ 7.67 – 7.63 (m, 2H), 7.39 – 7.36 (m, 3H), 6.24 (tt, $J = 3.9, 1.8$ Hz, 1H), 2.17 (tdd, $J = 6.0, 2.7, 1.8$ Hz, 2H), 2.11 (tdd, $J = 6.4, 4.6, 2.5$ Hz, 2H), 1.68 – 1.55 (m, 4H), 0.43 (s, 6H); ^{13}C NMR (126 MHz, CDCl_3) δ 137.59, 136.90, 133.84, 129.40, 127.94, 120.82, 109.17, 88.79, 29.14, 25.81, 22.33, 21.54, –0.51. IR (Neat Film NaCl) 3422, 2937, 2145, 1647, 1428, 1249, 1116, 863, 819, 779, 730, 698 cm^{-1} ; HRMS (EI+) calc'd for $\text{C}_{16}\text{H}_{21}\text{Si}$ [M+H]: 241.1413, found 241.1402.



(Cyclohexylethynyl)dimethyl(phenyl)silane 85p: The general procedure was followed. The reaction was performed with NaOH (2.0 mg, 0.05 mmol, 10 mol%), ethynylcyclohexane (54 mg, 0.5 mmol, 1.0 equiv), PhMe_2SiH (204 mg, 230 μL , 1.5 mmol, 3.0 equiv), and 0.5 mL of 1,2-dimethoxyethane (DME) at 25 °C for 48 h. The desired product **85p** (97.4 mg, 80% yield) was obtained as a colorless oil after removal of volatiles at 85°C at 45 mtorr for 15 minutes and subsequent purification by silica gel flash chromatography (100% hexanes). $R_f = 0.53$ (100% hexanes); ^1H NMR (500 MHz, CDCl_3) δ 7.65 (ddd, $J = 5.4, 2.4, 1.7$ Hz, 2H), 7.37 (ddq, $J = 4.0, 1.9, 0.8$ Hz, 3H), 2.47 (tt, $J = 9.0, 3.8$ Hz, 1H), 1.89 – 1.79 (m, 2H), 1.73 (ddd, $J = 9.8, 6.2, 3.1$ Hz, 2H), 1.52 (td, $J = 9.7, 9.2, 3.8$ Hz, 3H), 1.38 – 1.26 (m, 3H), 0.40 (d, $J = 1.0$ Hz, 6H); ^{13}C NMR (126 MHz, CDCl_3) δ 133.82, 133.13, 129.29, 127.89, 113.93, 81.74, 32.70, 30.23, 26.00, 24.93, –0.30. IR (Neat Film NaCl) 2931, 2854, 2173, 1448, 1427, 1248, 1116, 1076, 843,

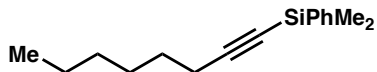


(3-Methoxyprop-1-yn-1-yl)dimethyl(phenyl)silane 85q: The general procedure was followed. The reaction was performed with NaOH (2.0 mg, 0.05 mmol, 10 mol%), 3-methoxyprop-1-yne (35 mg, 0.5 mmol, 1.0 equiv), PhMe₂SiH (204 mg, 230 μL, 1.5 mmol, 3.0 equiv), and 0.5 mL of 1,2-dimethoxyethane (DME) at 45 °C for 48 h. The desired product **85q** (61.0 mg, 60% yield) was obtained as a colorless oil after removal of volatiles at 85°C at 45 mtorr for 15 minutes (careful heating is necessary, as the product is volatile under these conditions) and subsequent purification by silica gel flash chromatography (1:1 DCM:hexanes). R_f = 0.38 (1:1 DCM:hexanes); ¹H NMR (500 MHz, CDCl₃) δ 7.65 – 7.62 (m, 2H), 7.41 – 7.36 (m, 3H), 4.16 (s, 2H), 3.41 (s, 3H), 0.45 (s, 6H); ¹³C NMR (126 MHz, CDCl₃) δ 136.63, 133.66, 129.49, 127.90, 103.05, 89.53, 60.48, 57.67, -0.97. IR (Neat Film NaCl) 3423, 2925, 2173, 1640, 1428, 1353, 1250, 1186, 1103, 1007, 990, 903, 838, 817, 781, 731, 698 cm⁻¹; HRMS (EI+) calc'd for C₁₂H₁₆OSi [M+•]: 204.0971, found 204.0977.

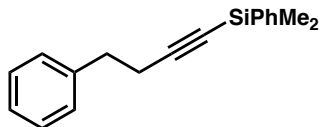


(Cyclopropylethynyl)dimethyl(phenyl)silane 85r: The general procedure was followed. The reaction was performed with NaOH (2.0 mg, 0.05 mmol, 10 mol%), ethynylcyclopropane (33 mg, 0.5 mmol, 1.0 equiv), PhMe₂SiH (204 mg, 230 μL, 1.5

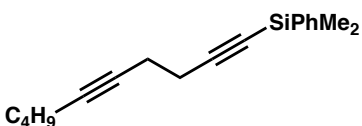
mmol, 3.0 equiv), and 0.5 mL of 1,2-dimethoxyethane (DME) at 45 °C for 48 h. The desired product **85r** (70.1 mg, 70% yield) was obtained as a colorless oil after removal of volatiles at 85°C at 45 mtorr for 30 minutes (careful heating is necessary, as this product is volatile under these conditions) and subsequent purification by silica gel flash chromatography (100% hexanes). R_f = 0.38 (100% hexanes); ^1H NMR (500 MHz, CDCl_3) δ 7.64 – 7.61 (m, 2H), 7.39 – 7.36 (m, 3H), 1.40 – 1.30 (m, 1H), 0.87 – 0.75 (m, 4H), 0.40 (s, 6H); ^{13}C NMR (126 MHz, CDCl_3) δ 137.77, 133.79, 129.36, 127.92, 112.40, 77.65, 8.97, 0.70, –0.45. IR (Neat Film NaCl) 3423, 3068, 2960, 2172, 2158, 1646, 1428, 1348, 1249, 1114, 1028, 839, 779, 730, 659 cm^{-1} ; HRMS (EI+) calc'd for $\text{C}_{13}\text{H}_{16}\text{Si} [\text{M}+\bullet]$: 200.1021, found 200.1031.



Dimethyl(oct-1-yn-1-yl)(phenyl)silane 85s: The general procedure was followed. The reaction was performed with NaOH (2.0 mg, 0.05 mmol, 10 mol%), oct-1-yne (55 mg, 0.5 mmol, 1.0 equiv), PhMe₂SiH (204 mg, 230 μL , 1.5 mmol, 3.0 equiv), and 0.5 mL of 1,2-dimethoxyethane (DME) at 25 °C for 48 h. The desired product **85s** (101.0 mg, 83% yield) was as a colorless oil after removal of volatiles at 85°C at 45 mtorr for 15 minutes and subsequent purification by silica gel flash chromatography (100% hexanes). R_f = 0.53 (100% hexanes); ^1H NMR (500 MHz, CDCl_3) δ 7.67 – 7.62 (m, 2H), 7.40 – 7.35 (m, 3H), 2.28 (t, J = 7.1 Hz, 2H), 1.59 – 1.53 (m, 2H), 1.47 – 1.39 (m, 2H), 1.35 – 1.27 (m, 4H), 0.91 (t, J = 6.9 Hz, 3H), 0.40 (s, 6H); ^{13}C NMR (126 MHz, CDCl_3) δ 137.86, 133.80, 129.35, 127.92, 109.85, 82.31, 31.43, 28.68, 28.64, 22.69, 20.12, 14.19, –0.44. IR (Neat Film NaCl) 3422, 3069, 2957, 2931, 2858, 2174, 1647, 1428, 1248, 1115, 836,

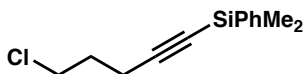


Dimethyl(phenyl)(4-phenylbut-1-yn-1-yl)silane 85t: The general procedure was followed. The reaction was performed with NaOH (2.0 mg, 0.05 mmol, 10 mol%), but-3-yn-1-ylbenzene (65 mg, 0.5 mmol, 1.0 equiv), PhMe₂SiH (204 mg, 230 μL , 1.5 mmol, 3.0 equiv), and 0.5 mL of 1,2-dimethoxyethane (DME) at 45 °C for 48 h. The desired product **85t** (130.0 mg, 98% yield) was obtained in analytical purity as a pale yellow oil after removal of volatiles at 85°C at 45 mtorr for 30 minutes. ¹H NMR (500 MHz, CDCl₃) δ 7.64 – 7.59 (m, 2H), 7.42 – 7.37 (m, 3H), 7.31 (dd, *J* = 8.0, 6.8 Hz, 2H), 7.28 – 7.23 (m, 3H), 2.90 (t, *J* = 7.5 Hz, 2H), 2.60 (t, *J* = 7.5 Hz, 2H), 0.42 (d, *J* = 0.6 Hz, 6H); ¹³C NMR (126 MHz, CDCl₃) δ 140.63, 137.56, 133.80, 129.39, 128.68, 128.47, 127.93, 126.43, 108.62, 83.39, 35.10, 22.38, –0.56. IR (Neat Film NaCl) 3423, 3086, 3067, 3027, 2959, 2174, 1647, 1602, 1495, 1453, 1427, 1248, 1114, 1077, 1042, 869, 811, 779, 729, 696, 661 cm^{-1} ; HRMS (EI+) calc'd for $\text{C}_{18}\text{H}_{19}\text{Si}$ [(M+H)-H₂]: 263.1256, found 263.1258.



Deca-1,5-diyn-1-yldimethyl(phenyl)silane 85u: The general procedure was followed. The reaction was performed with NaOH (2.0 mg, 0.05 mmol, 10 mol%), deca-1,5-diyne (67 mg, 0.5 mmol, 1.0 equiv), PhMe₂SiH (204 mg, 230 μL , 1.5 mmol, 3.0 equiv), and 0.5

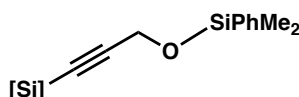
mL of 1,2-dimethoxyethane (DME) at 45 °C for 48 h. The desired product **4u** (131.3 mg, 98% yield) was obtained in analytical purity as a colorless oil after removal of volatiles at 85°C at 45 mtorr for 30 minutes. ¹H NMR (500 MHz, CDCl₃) δ 7.68 – 7.64 (m, 2H), 7.38 (dd, *J* = 5.0, 1.9 Hz, 3H), 2.49 (ddd, *J* = 7.7, 6.1, 1.7 Hz, 2H), 2.46 – 2.39 (m, 2H), 2.18 (tt, *J* = 7.0, 2.3 Hz, 2H), 1.52 – 1.39 (m, 4H), 0.92 (t, *J* = 7.2 Hz, 3H), 0.42 (s, 6H); ¹³C NMR (126 MHz, CDCl₃) δ 137.56, 133.81, 129.40, 127.92, 107.79, 83.33, 81.59, 78.33, 31.20, 22.05, 20.79, 19.16, 18.54, 13.77, –0.54. IR (Neat Film NaCl) 2958, 2932, 2872, 2177, 1465, 1428, 1336, 1249, 1115, 1042, 870, 837, 816, 780, 754, 731, 700, 662 cm^{–1}; HRMS (EI+) calc'd for C₁₈H₂₃Si [(M+H)-H₂]: 267.1569, found 267.1565.



(5-Chloropent-1-yn-1-yl)dimethyl(phenyl)silane 85v: The general procedure was followed. The reaction was performed with NaOH (2.0 mg, 0.05 mmol, 10 mol%), 5-chloropent-1-yne (51 mg, 0.5 mmol, 1.0 equiv), PhMe₂SiH (204 mg, 230 µL, 1.5 mmol, 3.0 equiv), and 0.5 mL of 1,2-dimethoxyethane (DME) at 45 °C for 48 h. The desired product **85v** (93.3 mg, 79% yield) was obtained as a colorless oil after removal of volatiles at 85°C at 45 mtorr for 15 minutes (careful heating is necessary, as this product is volatile under these conditions) and subsequent purification by silica gel flash chromatography (100% hexanes). R_f = 0.31 (100% hexanes); ¹H NMR (500 MHz, CDCl₃) δ 7.65 – 7.60 (m, 2H), 7.38 (dd, *J* = 4.9, 1.9 Hz, 3H), 3.67 (t, *J* = 6.4 Hz, 2H), 2.49 (t, *J* = 6.8 Hz, 2H), 2.01 (p, *J* = 6.6 Hz, 2H), 0.41 (s, 6H); ¹³C NMR (126 MHz, CDCl₃) δ 137.46, 133.75, 129.48, 127.99, 107.20, 83.81, 43.77, 31.40, 17.57, –0.56. IR (Neat Film NaCl) 3420, 3069, 2960, 2928, 2174, 1646, 1428, 1249, 1114, 1041, 837,



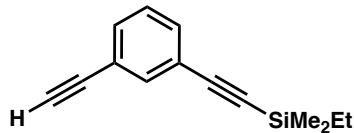
3-(Dimethyl(phenyl)silyl)-N-methylprop-2-yn-1-amine 85w: The general procedure was followed. The reaction was performed with NaOH (2.0 mg, 0.05 mmol, 10 mol%), N-methylprop-2-yn-1-amine (69 mg, 0.5 mmol, 1.0 equiv), PhMe₂SiH (204 mg, 230 µL, 1.5 mmol, 3.0 equiv), and 0.5 mL of 1,2-dimethoxyethane (DME) at 45 °C for 48 h. The desired product **85w** (81.8 mg, 80% yield) was obtained as a colorless oil after removal of volatiles at 85°C at 45 mtorr for 15 minutes (careful heating is necessary, as the product is volatile under these conditions) and subsequent purification by silica gel flash chromatography (100% EtOAc). R_f = 0.32 (100% EtOAc); ¹H NMR (500 MHz, THF-*d*₈) δ 7.63 – 7.59 (m, 2H), 7.33 – 7.29 (m, 3H), 3.36 (s, 2H), 2.39 (s, 3H), 0.36 (s, 6H); ¹³C NMR (126 MHz, THF-*d*₈) δ 138.26, 134.58, 130.18, 128.67, 108.45, 85.45, 41.75, 35.64, -0.33. IR (Neat Film NaCl) 3416, 3068, 2957, 2165, 1725, 1651, 1427, 1250, 1116, 1044, 836, 817, 730, 699 cm⁻¹; HRMS (EI+) calc'd for C₁₂H₁₈NSi [M+H]: 204.1208, found 204.1214.



(3-((Dimethyl(phenyl)silyl)oxy)prop-1-yn-1-yl)dimethyl(phenyl)silane 85x: The general procedure was followed. The reaction was performed with NaOH (2.0 mg, 0.05 mmol, 10 mol%), prop-2-yn-1-ol (28 mg, 0.5 mmol, 1.0 equiv), PhMe₂SiH (204 mg, 230

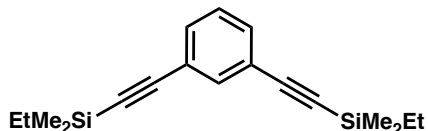
μL , 1.5 mmol, 3.0 equiv), and 0.5 mL of 1,2-dimethoxyethane (DME) at 45 °C for 24 h.

The desired product **85x** (142.9 mg, 88% yield) was obtained in analytical purity as a colorless oil after removal of volatiles at 85°C at 45 mtorr for 30 minutes (careful heating is necessary, as the product is volatile under these conditions). ^1H NMR (500 MHz, CDCl_3) δ 7.62 (ddt, J = 6.4, 1.8, 0.9 Hz, 4H), 7.44 – 7.36 (m, 6H), 4.35 (s, 2H), 0.48 (s, 6H), 0.43 (s, 6H); ^{13}C NMR (126 MHz, CDCl_3) δ 137.08, 136.80, 133.82, 133.73, 129.93, 129.57, 128.01, 127.98, 105.77, 88.23, 52.27, -0.93, -1.36. IR (Neat Film NaCl) 3069, 3049, 2959, 2177, 1428, 1363, 1250, 1117, 1085, 1043, 1004, 817, 782, 731, 698 cm^{-1} ; HRMS (EI+) calc'd for $\text{C}_{19}\text{H}_{23}\text{OSi}_2$ [(M+H)–H₂]: 323.1288, found 323.1297.

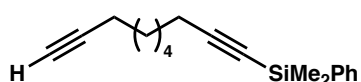


Ethyl((3-ethynylphenyl)ethynyl)dimethylsilane 257a: The general procedure was followed. The reaction was performed with NaOH (4.0 mg, 0.1 mmol, 20 mol%), 1,3-diethynylbenzene **256** (189 mg, 1.5 mmol, 3.0 equiv), EtMe₂SiH (44 mg, 66 μL , 0.5 mmol, 1.0 equiv), and 0.5 mL of 1,2-dimethoxyethane (DME) at 65 °C for 48 h. The desired product **257a** (68.9 mg, 65% yield) was obtained as a colorless oil after purification by silica gel flash chromatography (100% hexanes). The bis-silylated product **257b** was also obtained in 4% yield. R_f = 0.33 (100% hexanes); ^1H NMR (500 MHz, CDCl_3) δ 7.60 (t, J = 1.7 Hz, 1H), 7.43 (ddd, J = 7.8, 6.2, 1.4 Hz, 2H), 7.26 (t, J = 7.8 Hz, 1H), 3.07 (s, 1H), 1.04 (t, J = 7.9 Hz, 3H), 0.67 (q, J = 7.9 Hz, 2H), 0.21 (s, 6H); ^{13}C NMR (126 MHz, CDCl_3) δ 135.66, 132.32, 132.11, 128.43, 123.66, 122.44, 104.41, 94.44, 82.85, 77.87, 8.16, 7.49, -2.15. IR (Neat Film NaCl) 3300, 3063, 2956, 2914,

2874, 2152, 2111, 1593, 1569, 1474, 1407, 1249, 1152, 1014, 960, 943, 925, 839, 821, 794, 780, 701, 685 cm^{-1} ; HRMS (EI+) calc'd for $\text{C}_{14}\text{H}_{17}\text{Si}$ [M+H]: 213.1100, found 213.1089.

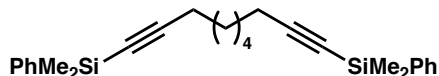


1,3-bis((dimethyl(phenyl)silyl)ethynyl)benzene 257b: The general procedure was followed. The reaction was performed with NaOH (4.0 mg, 0.1 mmol, 20 mol%), 1,3-diethynylbenzene **256** (63 mg, 0.5 mmol, 1.0 equiv), PhMe₂SiH (204 mg, 230 μL , 1.5 mmol, 3.0 equiv), and 0.5 mL of 1,2-dimethoxyethane (DME) at 65 °C for 48 h. The desired product **257b** (173.5 mg, 88% yield) was obtained as a light yellow oil after removal of volatiles at 85 °C at 45 mtorr for 30 minutes and subsequent purification by silica gel flash chromatography (100% hexanes \rightarrow 3% EtOAc in hexanes). $R_f = 0.26$ (100% hexanes); ¹H NMR (500 MHz, CDCl₃) δ 7.73 – 7.70 (m, 4H), 7.69 (t, $J = 1.7$ Hz, 1H), 7.47 (dd, $J = 7.8, 1.7$ Hz, 2H), 7.44 – 7.41 (m, 6H), 7.28 (ddd, $J = 8.0, 7.4, 0.5$ Hz, 1H), 0.53 (s, 12H); ¹³C NMR (126 MHz, CDCl₃) δ 136.88, 135.69, 133.86, 132.23, 129.64, 128.40, 128.08, 123.33, 105.73, 93.08, –0.74. IR (Neat Film NaCl) 3068, 2959, 2153, 1589, 1474, 1428, 1405, 1249, 1164, 1118, 944, 838, 816, 780, 753, 730, 702, 685 cm^{-1} ; HRMS (EI+) calc'd for $\text{C}_{26}\text{H}_{27}\text{Si}_2$ [M+H]: 395.1651, found 395.1659.



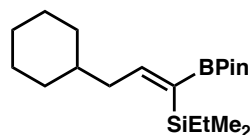
Deca-1,9-diyn-1-yl dimethyl(phenyl)silane 259a: The general procedure was followed. The reaction was performed with either KOH or NaOH (10–20 mol%), deca-1,9-diyne

258 (201 mg, 1.5 mmol, 3.0 equiv), PhMe₂SiH (68 mg, 77 μL, 0.5 mmol, 1.0 equiv), and 0.5 mL of 1,2-dimethoxyethane (DME) at either 45 °C or 65 °C for the specified amount of time. The desired product **259a** (see yield in Table 4) was obtained as a colorless oil after purification by silica gel flash chromatography (gradient 1:30 dichloromethane : hexanes → 1:10 dichloromethane : hexanes). $R_f = 0.31$ (10% dichloromethane in hexanes); ¹H NMR (500 MHz, CDCl₃) δ 7.66 – 7.61 (m, 2H), 7.40 – 7.35 (m, 3H), 2.29 (t, $J = 7.1$ Hz, 2H), 2.20 (td, $J = 7.1, 2.6$ Hz, 2H), 1.96 (t, $J = 2.6$ Hz, 1H), 1.57 (dtd, $J = 9.6, 7.1, 4.5$ Hz, 4H), 1.47 – 1.42 (m, 4H), 0.40 (s, 6H); ¹³C NMR (126 MHz, CDCl₃) δ 137.79, 133.78, 129.37, 127.93, 109.55, 84.74, 82.51, 68.34, 28.51, 28.45, 28.39, 28.31, 20.04, 18.48, –0.46. IR (Neat Film NaCl) 3420, 3306, 3068, 2936, 2859, 2173, 2117, 1646, 1457, 1428, 1325, 1248, 1114, 1026, 836, 816, 754, 731, 700, 661 cm^{–1}; HRMS (EI+) calc'd for C₁₈H₂₃Si [(M+H)-H₂]: 267.1569, found 267.1556.



1,10-Bis(dimethyl(phenyl)silyl)deca-1,9-diyne **259b:** The general procedure was followed. The reaction was performed with KOH (5.6 mg, 0.1 mmol, 20 mol%), deca-1,9-diyne **258** (67 mg, 0.5 mmol, 1.0 equiv), PhMe₂SiH (204 mg, 230 μL, 1.5 mmol, 3.0 equiv), and 0.5 mL of 1,2-dimethoxyethane (DME) at 65 °C for 48 h. The desired product **259b** (189.3 mg, 93% yield) was obtained as a colorless oil after removal of volatiles at 85 °C at 45 mtorr for 30 minutes and subsequent purification by silica gel flash chromatography (gradient 1:30 dichloromethane : hexanes → 1:10 dichloromethane : hexanes). $R_f = 0.28$ (10% dichloromethane in hexanes); ¹H NMR (500 MHz, CDCl₃) δ 7.65 (ddt, $J = 5.4, 3.0, 1.4$ Hz, 4H), 7.38 (ddt, $J = 4.4, 2.2, 1.1$ Hz, 6H), 2.30 (td, $J = 7.2,$

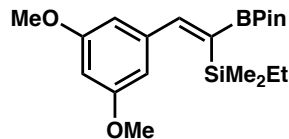
1.1 Hz, 4H), 1.59 (t, J = 6.8 Hz, 4H), 1.49 – 1.42 (m, 4H), 0.43 – 0.40 (s, 12H); ^{13}C NMR (126 MHz, CDCl_3) δ 137.79, 133.78, 129.37, 127.93, 109.58, 82.49, 28.53, 28.38, 20.04, –0.45. IR (Neat Film NaCl) 3423, 3068, 2937, 2858, 2173, 1647, 1428, 1248, 1114, 836, 815, 753, 730, 699, 661 cm^{-1} ; HRMS (EI+) calc'd for $\text{C}_{26}\text{H}_{33}\text{Si}_2$ [(M+H)-H₂]: 401.2121, found 401.2120.



(Z)-(3-cyclohexyl-1-(4,4,5,5-tetramethyl-1,3,2-dioxaborolan-2-yl)prop-1-en-1-yl)(ethyl)dimethylsilane 260a:

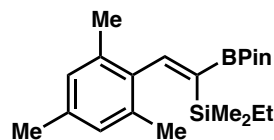
The general procedure was followed for the silylation portion of the reaction. The reaction was performed with KOH (2.8 mg, 0.05 mmol, 10 mol%), cyclohexylpropane (61 mg, 0.5 mmol, 1.0 equiv), EtMe_2SiH (132 mg, 198 μL , 1.5 mmol, 3.0 equiv), and 0.5 mL of 1,2-dimethoxyethane (DME) at 45 °C for 48 h then HBPin (192 mg, 218 μL , 1.5 mmol, 3.0 equiv) was then added and the reaction mixture was stirred for a further 48 h at 65 °C. The desired product **260a** (107.6 mg, 64% yield) was obtained as a colorless oil by silica gel flash chromatography (2.5% EtOAc in hexanes). Note: product is somewhat unstable on silica gel, possibly contributing to the lower isolated yield. R_f = 0.24 (2.5% EtOAc in hexanes); ^1H NMR (500 MHz, Benzene- d_6) δ 7.57 (t, J = 7.2 Hz, 1H), 2.23 (t, J = 7.0 Hz, 2H), 1.72 (ddd, J = 14.7, 5.0, 2.6 Hz, 2H), 1.67 – 1.51 (m, 4H), 1.34 (ddq, J = 14.6, 11.0, 7.0, 3.5 Hz, 1H), 1.14 (td, J = 7.9, 0.7 Hz, 3H), 1.09 (d, J = 0.6 Hz, 12H), 1.08 – 1.04 (m, 2H), 0.93 (q, J = 8.0 Hz, 2H), 0.89 – 0.84 (m, 2H), 0.42 (d, J = 0.6 Hz, 6H); ^{13}C NMR (126 MHz, Benzene- d_6) δ 163.13, 82.76, 43.20, 38.62, 33.68, 26.94, 26.79, 26.72, 24.93, 9.42, 8.15, -0.51. IR (Neat Film

NaCl) 2976, 2923, 2852, 1581, 1448, 1370, 1326, 1292, 1270, 1245, 1213, 1146, 1109, 1006, 981, 962, 856, 835, 817, 777, 696 cm⁻¹; HRMS (EI+) calc'd for C₁₉H₃₆BSiO₂ [(M+H)-H₂]: 335.2578, found 335.2577. Olefin geometry was confirmed by 2D-NOESY.



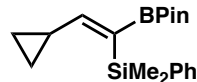
(Z)-(2-(3,5-dimethoxyphenyl)-1-(4,4,5,5-tetramethyl-1,3,2-dioxaborolan-2-yl)vinyl)(ethyl)dimethylsilane 260b:

The general procedure was followed for the silylation portion of the reaction. The reaction was performed with KOH (2.8 mg, 0.05 mmol, 10 mol%), 1-ethynyl-3,5-dimethoxybenzene (81 mg, 0.5 mmol, 1.0 equiv), EtMe₂SiH (132 mg, 198 μL, 1.5 mmol, 3.0 equiv), and 0.5 mL of 1,2-dimethoxyethane (DME) at 65 °C for 72 h to yield the silylated alkyne intermediate. HBPin (192 mg, 218 μL, 1.5 mmol, 3.0 equiv) was then added and the reaction mixture was stirred for a further 72 h at 85 °C. The desired product **260b** (56.5 mg, 30% yield) was obtained as a colorless oil by silica gel flash chromatography (10% EtOAc in hexanes). Note: product is somewhat unstable on silica gel, possibly contributing to the lower isolated yield. R_f = 0.49 (10% EtOAc in hexanes); ¹H NMR (500 MHz, Benzene-*d*₆) δ 8.59 (s, 1H), 6.60 (dt, J = 2.3, 0.6 Hz, 2H), 6.52 (t, J = 2.3 Hz, 1H), 3.30 (s, 6H), 1.12 (s, 12H), 1.06 (t, J = 7.6 Hz, 3H), 0.89 (q, J = 7.8 Hz, 2H), 0.30 (s, 6H); ¹³C NMR (126 MHz, Benzene-*d*₆) δ 161.03, 159.67, 144.06, 106.46, 100.75, 83.21, 54.86, 24.94, 9.40, 8.11, -0.93. IR (Neat Film NaCl) 2976, 2953, 2873, 1592, 1569, 1458, 1422, 1370, 1316, 1270, 1246, 1204, 1154, 1066, 1009, 960, 855, 832, 780, 691, 673 cm⁻¹; HRMS (EI+) calc'd for C₂₀H₃₄BSiO₄ [M+H]: 377.2320, found 377.2318. Olefin geometry was confirmed by 2D-NOESY.



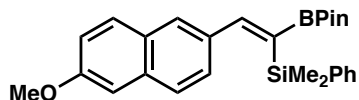
(Z)-ethyl(2-mesityl-1-(4,4,5,5-tetramethyl-1,3,2-dioxaborolan-2-yl)vinyl)dimethylsilane 260c:

The general procedure was followed for the silylation portion of the reaction. The reaction was performed with KOH (2.8 mg, 0.05 mmol, 10 mol%), 2-ethynyl-1,3,5-trimethylbenzene (72 mg, 0.5 mmol, 1.0 equiv), EtMe₂SiH (132 mg, 198 μL, 1.5 mmol, 3.0 equiv), and 0.5 mL of 1,2-dimethoxyethane (DME) at 45 °C for 48 h then HBPin (192 mg, 218 μL, 1.5 mmol, 3.0 equiv) was then added and the reaction mixture was stirred for a further 72 h at 85 °C. The desired product **260c** (57.3 mg, 32% yield) was obtained as a yellow gel by silica gel flash chromatography (2.5% EtOAc in hexanes). Note: product is somewhat unstable on silica gel, possibly contributing to the lower isolated yield. $R_f = 0.25$ (2.5% EtOAc in hexanes); ¹H NMR (500 MHz, Benzene-*d*₆) δ 8.36 (s, 1H), 6.73 (d, *J* = 1.3 Hz, 2H), 2.21 (s, 6H), 2.13 (s, 3H), 1.11 (s, 12H), 1.03 (t, *J* = 7.9 Hz, 3H), 0.77 (q, *J* = 7.9 Hz, 2H), 0.07 (s, 6H); ¹³C NMR (126 MHz, Benzene-*d*₆) δ 159.59, 138.85, 136.10, 134.38, 128.16, 83.07, 24.91, 21.16, 20.71, 8.44, 8.10, -2.33. IR (Neat Film NaCl) 2976, 2950, 2872, 1612, 1579, 1478, 1461, 1370, 1317, 1270, 1244, 1145, 1008, 960, 860, 849, 837, 822, 811, 777, 690 cm⁻¹; HRMS (EI+) calc'd for C₂₁H₃₅BSiO₂ [M+•]: 358.2499, found 358.2495. Olefin geometry was confirmed by 2D-NOESY.



(Z)-(2-cyclopropyl-1-(4,4,5,5-tetramethyl-1,3,2-dioxaborolan-2-yl)vinyl)dimethyl(phenyl)silane 260d:

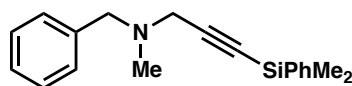
The general procedure was followed for the silylation portion of the reaction. The reaction was performed with NaOH (2.0 mg, 0.05 mmol, 10 mol%), cyclopropylacetylene (33 mg, 0.5 mmol, 1.0 equiv), PhMe₂SiH (204 mg, 230 µL, 1.5 mmol, 3.0 equiv), and 0.5 mL of 1,2-dimethoxyethane (DME) at 45 °C for 48 h then HBPin (192 mg, 218 µL, 1.5 mmol, 3.0 equiv) was then added and the reaction mixture was stirred for a further 72 h at 65 °C. The desired product **260d** (94.6 mg, 58% yield) was obtained as a colorless oil by silica gel flash chromatography (2.5% EtOAc in hexanes). Note: product is somewhat unstable on silica gel, possibly contributing to the lower isolated yield. $R_f = 0.38$ (2.5% EtOAc in hexanes); ¹H NMR (500 MHz, Benzene-*d*₆) δ 7.77 – 7.72 (m, 2H), 7.29 – 7.22 (m, 3H), 6.83 (d, *J* = 10.5 Hz, 1H), 1.58 – 1.48 (m, 1H), 1.07 (s, 12H), 0.69 (s, 6H), 0.41 – 0.36 (m, 2H), 0.27 (dt, *J* = 6.9, 4.2 Hz, 2H); ¹³C NMR (126 MHz, Benzene-*d*₆) δ 169.81, 141.35, 134.42, 128.81, 128.02, 82.75, 24.91, 17.52, 8.87, 0.56, -1.52. IR (Neat Film NaCl) 3068, 2977, 1580, 1443, 1427, 1370, 1333, 1309, 1293, 1270, 1246, 1145, 1110, 1048, 944, 849, 836, 816, 775, 730, 700, 671 cm⁻¹; HRMS (EI+) calc'd for C₁₉H₂₉BSiO₂ [M+•]: 328.2030, found 328.2037. Olefin geometry was confirmed by 2D-NOESY.



(Z)-(2-(6-methoxynaphthalen-2-yl)-1-(4,4,5,5-tetramethyl-1,3,2-dioxaborolan-2-yl)vinyl)dimethyl(phenyl)silane 260e:

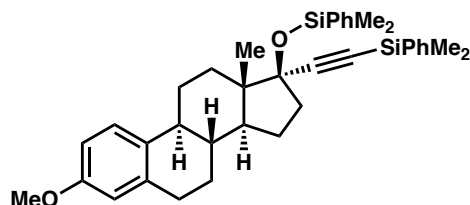
The general procedure was followed for the

silylation portion of the reaction. The reaction was performed with NaOH (2.0 mg, 0.05 mmol, 10 mol%), 2-ethynyl-6-methoxynaphthalene (91 mg, 0.5 mmol, 1.0 equiv), PhMe₂SiH (204 mg, 230 μL, 1.5 mmol, 3.0 equiv), and 0.5 mL of 1,2-dimethoxyethane (DME) at 65 °C for 48 h then HBPin (192 mg, 218 μL, 1.5 mmol, 3.0 equiv) was then added and the reaction mixture was stirred for a further 72 h at 65 °C. The desired product **260e** (73.4 mg, 33% yield) was obtained as a colorless gel by silica gel flash chromatography (gradient 2.5% EtOAc in hexanes → 10% EtOAc in hexanes). Note: product is somewhat unstable on silica gel, possibly contributing to the lower isolated yield. ¹H NMR (500 MHz, Benzene-*d*₆) δ 8.76 (d, *J* = 1.0 Hz, 1H), 7.81 (dd, *J* = 8.0, 1.4 Hz, 2H), 7.63 (d, *J* = 1.4 Hz, 1H), 7.41 – 7.33 (m, 3H), 7.26 (tt, *J* = 7.8, 1.3 Hz, 2H), 7.19 (tt, *J* = 7.5, 1.5 Hz, 1H), 7.09 (dd, *J* = 8.9, 2.5 Hz, 1H), 6.80 (d, *J* = 2.5 Hz, 1H), 3.33 (s, 3H), 1.12 (s, 12H), 0.47 (s, 6H); ¹³C NMR (126 MHz, Benzene-*d*₆) δ 160.46, 158.55, 141.64, 136.58, 134.79, 134.45, 130.16, 128.84, 128.82, 128.54, 127.44, 126.53, 119.45, 106.01, 83.31, 54.76, 24.93, 0.18. IR (Neat Film NaCl) 3049, 2976, 1630, 1604, 1563, 1499, 1481, 1462, 1427, 1410, 1370, 1392, 1315, 1265, 1220, 1166, 1110, 1032, 987, 851, 816, 733, 702 cm⁻¹; HRMS (EI+) calc'd for C₂₇H₃₃BSiO₃ [M+•]: 444.2292, found 444.2304. Olefin geometry was confirmed by 2D-NOESY.



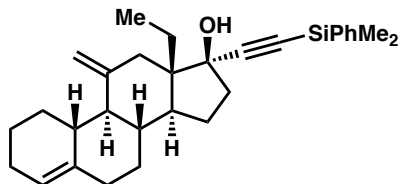
N-benzyl-3-(dimethylphenylsilyl)-N-methylprop-2-yn-1-amine 261a: The general procedure was followed. The reaction was performed with NaOH (2.0 mg, 0.05 mmol, 10 mol %), Pargyline (N-benzyl-N-methylprop-2-yn-1-amine) (80 mg, 0.5 mmol, 1.0 equiv), PhMe₂SiH (204 mg, 230 μL, 1.5 mmol, 3.0 equiv), and 0.5 mL of 1,2-dimethoxyethane

(DME) at 45 °C for 24 h. The desired product **261a** (140.4 mg, 96% yield) was obtained in analytical purity as a pale yellow oil after removal of volatiles at 85 °C at 45 mtorr for 30 minutes. ¹H NMR (500 MHz, CDCl₃) δ 7.69 (dq, *J* = 6.8, 3.4, 2.7 Hz, 2H), 7.40 (dt, *J* = 4.3, 2.1 Hz, 3H), 7.35 – 7.31 (m, 4H), 7.30 – 7.26 (m, 1H), 3.60 (d, *J* = 3.0 Hz, 2H), 3.38 (d, *J* = 3.1 Hz, 2H), 2.38 (d, *J* = 3.2 Hz, 3H), 0.47 (d, *J* = 3.4 Hz, 6H); ¹³C NMR (126 MHz, CDCl₃) δ 138.47, 137.34, 133.82, 129.54, 129.39, 128.45, 128.01, 127.35, 102.95, 88.41, 60.17, 46.08, 42.09, –0.49. IR (Neat Film NaCl) 3067, 3026, 2958, 2793, 2162, 1494, 1453, 1428, 1366, 1249, 1115, 1026, 980, 837, 817, 780, 732, 698 cm^{–1}; HRMS (EI+) calc'd for C₁₉H₂₄NSi [M+H]: 294.1678, found 294.1689.



((8R,9S,13S,14S,17S)-17-((dimethyl(phenyl)silyl)ethynyl)-3-methoxy-13-methyl-7,8,9,11,12,13,14,15,16,17-decahydro-6H-cyclopenta[a]phenanthren-17-yl)oxy)dimethyl(phenyl)silane 261b: The general procedure was followed. The reaction was performed with KOH (2.8 mg, 0.05 mmol, 10 mol%), mestranol ((8R,9S,13S,14S,17R)-17-ethynyl-3-methoxy-13-methyl- 7,8,9,11,12,13,14,15,16,17- decahydro -6H-cyclopenta[a]phenan-thren-17-ol) (155 mg, 0.5 mmol, 1.0 equiv), PhMe₂SiH (204 mg, 230 μL, 1.5 mmol, 3.0 equiv), and 0.5 mL of 1,2-dimethoxyethane (DME) at 45 °C for 24 h then 65 °C for 48 h. The product **261b** (185.5 mg, 64% yield) was obtained as a colorless oil by silica gel flash chromatography (1% → 5% EtOAc in hexanes). R_f = 0.50 (5% EtOAc in hexanes); ¹H NMR (500 MHz, THF-*d*₈) δ 7.59 (ddd, *J* = 7.6, 3.6, 2.1 Hz, 4H), 7.34 – 7.26 (m, 6H),

7.16 (d, $J = 8.6$ Hz, 1H), 6.63 (dd, $J = 8.6, 2.8$ Hz, 1H), 6.57 (d, $J = 2.7$ Hz, 1H), 3.70 (s, 3H), 2.87 – 2.79 (m, 2H), 2.36 (dq, $J = 13.4, 3.9$ Hz, 1H), 2.30 (ddd, $J = 13.3, 9.2, 5.3$ Hz, 1H), 2.16 (ddd, $J = 14.6, 7.7, 2.8$ Hz, 1H), 2.02 (dt, $J = 26.4, 12.8, 4.1$ Hz, 2H), 1.88 (ddt, $J = 12.7, 5.6, 2.5$ Hz, 1H), 1.83 – 1.74 (m, 3H), 1.51 – 1.37 (m, 3H), 1.35 – 1.26 (m, 1H), 0.93 (s, 3H), 0.44 (d, $J = 8.0$ Hz, 6H), 0.34 (s, 6H); ^{13}C NMR (126 MHz, THF- d_8) δ 158.89, 140.79, 138.43, 137.86, 134.65, 134.38, 133.10, 130.31, 129.97, 128.73, 128.44, 127.12, 114.47, 112.89, 112.38, 90.45, 82.69, 68.10, 55.34, 49.87, 49.47, 45.17, 41.66, 40.97, 34.18, 30.86, 28.64, 27.69, 24.00, 1.41, 1.36, -0.63, -0.65. IR (Neat Film NaCl) 3417, 3068, 3048, 2946, 2869, 2234, 2160, 2081, 1610, 1575, 1500, 1465, 1427, 1279, 1252, 1136, 1117, 1088, 1045, 929, 886, 818, 783, 730, 699, 642 cm^{-1} ; HRMS (EI+) calc'd for $\text{C}_{37}\text{H}_{47}\text{O}_2\text{Si}_2$ [M+H]: 579.3115, found 579.3109.



(8S,9S,10R,13S,14S,17S)-17-((dimethyl(phenyl)silyl)ethynyl)-13-ethyl-11-methylene-2,3,6,7,8,9,10,11,12,13,14,15,16,17-tetradecahydro-1H-cyclopenta[a]phenanthren-17-ol 261c:

The general procedure was followed. The reaction was performed with KOH (1.1 mg, 0.02 mmol, 10 mol %), desogestrel ((8S,9S,10R,13S,14S,17R)-13-ethyl-17-ethynyl-11-methylene-2,3,6,7,8,9,10,11,12,13,14,15,16,17-tetradecahydro-1H-cyclopenta[a]phen-anthren-17-ol) (62 mg, 0.2 mmol, 1.0 equiv), PhMe₂SiH (82 mg, 92 μL , 0.6 mmol, 3.0 equiv), and 0.2 mL of 1,2-dimethoxyethane (DME) at 45 °C for 48 h. The product **261c** (53.4 mg, 60% yield) was obtained as a colorless solid by silica gel

flash chromatography (2.5% Et₂O in hexanes). Also observed were what appear to be <5% of the *bis*-silylated product and <5% of the *mono*-O-silylated desogestrel. R_f = 0.28 (2.5% Et₂O in hexanes); ¹H NMR (500 MHz, THF-*d*₈) δ 7.63 – 7.54 (m, 2H), 7.33 – 7.28 (m, 3H), 5.44 (dt, J = 4.2, 2.4 Hz, 1H), 4.99 (s, 1H), 4.76 (s, 1H), 2.67 (d, J = 12.4 Hz, 1H), 2.24 (q, J = 7.7, 7.1 Hz, 2H), 2.17 (ddt, J = 13.8, 7.0, 3.8 Hz, 2H), 2.13 – 2.01 (m, 2H), 1.96 – 1.90 (m, 3H), 1.88 – 1.77 (m, 1H), 1.67 – 1.54 (m, 2H), 1.49 – 1.37 (m, 4H), 1.35 – 1.28 (m, 4H), 1.01 (t, J = 7.3 Hz, 3H), 0.93–0.86 (m, 1H), 0.38 (d, J = 6.0 Hz, 6H); ¹³C NMR (126 MHz, THF-*d*₈) δ 149.06, 140.69, 134.18, 130.11, 128.67, 122.17, 109.00, 91.27, 83.94, 56.19, 52.97, 52.25, 43.92, 41.63, 41.58, 37.63, 36.62, 32.98, 30.34, 26.70, 25.99, 23.13, 22.98, 21.40, 9.99, 1.60, 1.16. IR (Neat Film NaCl) 3543, 3164, 3000, 2926, 2854, 2293, 2253, 1636, 1506, 1455, 1374, 1249, 1118, 1038, 917, 829, 784, 741, 700 cm^{−1}; HRMS (EI+) calc'd for C₃₀H₄₁OSi [M+H]: 445.2927, found 445.2931.

A6.5 Relevant Spectra.

All relevant spectra (¹H NMR, ¹³C NMR, etc.) are available free of charge via the Internet at <http://pubs.acs.org> (DOI: 10.1021/jacs.6b12114).

A6.6 REFERENCES AND NOTES

- (1) (a) Bergman, R. G. *Nature* **2007**, *446*, 391–393. (b) Godula, K.; Sames, D. *Science* **2006**, *312*, 67–72.
- (2) (a) Li, C.-J.; Trost, B. M. *Proc. Natl. Acad. Sci. USA* **2008**, *105*, 13197–13202.
(b) Clark, J. H. *Green Chem.* **1999**, *1*, 1–8.

- (3) (a) Toutov, A. A.; Liu, W.-B.; Betz, K. N.; Fedorov, A.; Stoltz, B. M.; Grubbs, R. H. *Nature* **2015**, *518*, 80–84. (b) Toutov, A. A.; Liu, W.-B.; Betz, K. N.; Stoltz, B. M.; Grubbs, R. H. *Nat. Protoc.* **2015**, *10*, 1897–1903. (c) Toutov, A. A.; Liu, W.-B.; Stoltz, B. M.; Grubbs, R. H. *Org. Synth.* **2016**, *93*, 263–271. (d) Fedorov, A.; Toutov, A. A.; Swisher, N. A.; Grubbs, R. H. *Chem. Sci.* **2013**, *4*, 1640–1645.
- (4) Gleiter, R.; Werz, D. B. *Chem. Rev.* **2010**, *110*, 4447–4488.
- (5) a) Wang, J.; Gurevich, Y.; Botoshansky, M.; Eisen, M. S. *J. Am. Chem. Soc.* **2006**, *128*, 9350–9351. b) Möckel, R.; Hilt, G. *Org. Lett.* **2015**, *17*, 1644–1647.
- (6) (a) Valero, R.; Cuadrado, P.; Calle, M.; González-Nogal, A. M. *Tetrahedron* **2007**, *63*, 224–231. (b) Sun, X.; Wang, C.; Li, Z.; Zhang, S.; Xi, Z. *J. Am. Chem. Soc.* **2004**, *126*, 7172–7173. (c) Dichtel, W. R.; Keresztes, I.; Arslan, H.; Hein, S. *J. Org. Lett.* **2014**, *16*, 4416–4419.
- (7) (a) Chinchilla, R. & Nájera, C. *Chem. Soc. Rev.* **2011**, *40*, 5084–5121. (b) Shinzer, D.; Langkopf, E. *Chem. Rev.* **1995**, *95*, 1375–1406. (c) Dialer, L. O.; Selivanova, S. V.; Müller, C. J.; Müller, A.; Stellfeld, T.; Graham, K.; Dinkelborg, L. M.; Krämer, S. D.; (d) Schibli, R.; Reiher, M.; Ametamey, S. M. *J. Med. Chem.* **2013**, *56*, 7552–7563
- (8) (a) Colvin, E. *Silicon in Organic Synthesis*; Butterworth: New York, 1981. (b) Fleming, I.; Dunoguès, J.; Smithers, R. *Org. React.* **1989**, *37*, 57. (c) Ishikawa, J.-I.; Itoh, M. *J. Catal.* **1999**, *185*, 454–461. (d) Calas, R.; Bourgeois, P. *C. R. Acad. Sc. Paris* **1969**, *268*, 72–74. (e) Ishikawa, J.-i.; Inoue, K.; Itoh, M. *J. Organomet. Chem.* **1998**, *552*, 303–311.

- (9) (a) Eaborn, C. *J. Organomet. Chem.* **1975**, *100*, 43–57. (b) Voronkov, M. G.; Ushakova, N. I.; Tsikhanskaya, I. I.; Pukhnarevich, V. B. *J. Organomet. Chem.* **1984**, *264*, 39–48.
- (10) Arde, P.; Reddy, V.; Anand, R. V. *RSC Adv.* **2014**, *4*, 49775–49779.
- (11) Rochat, R.; Yamamoto, K.; Lopez, M. J.; Nagae, H.; Tsuru-gi, H.; Mashima, K. *Chem. Eur. J.* **2015**, *21*, 8112–8120 and references therein.
- (12) Itami, K.; Yoshida, J.-i. *Synlett* **2006**, *2*, 157–180.
- (13) (a) Fujiki, M. *Polymer Journal* **2003**, *35*, 297–344. (b) Feigl, A.; Bockholt, A.; Weis, J.; Rieger, B. Springer: Berlin, 2011.
- (14) (a) Weickgenannt, A.; Oestreich, M. *Chem. Asian J.* **2009**, *4*, 406–410. (b) Toutov, A. A.; Betz, K. N.; Haibach, M. C.; Romine, A. M.; Grubbs, R. H. *Org. Lett.* **2016**, *18*, 5776–5779.
- (15) (a) Kurahashi, T.; Hata, T.; Masai, H.; Kitagawa, H.; Shimizu, M.; Hiyama, T. *Tetrahedron* **2002**, *58*, 6381–6395. (b) Hata, T.; Kitagawa, H.; Masai, H.; Kurahashi, T.; Shimizu, M.; Hiyama, T. *Angew. Chem. Int. Ed.* **2001**, *40*, 790–792. (c) Zweifel, G.; Backlund, S. J. *J. Am. Chem. Soc.* **1977**, *99*, 3184–3185. (d) Tucker, C. E.; Davidson, J.; Knochel, P. *J. Org. Chem.* **1992**, *57*, 3482–3485.
- (16) (a) Franz, A. K.; Wilson, S. O. *J. Med. Chem.* **2013**, *56*, 388–405. (b) Showell, G. A.; Mills, J. S. *Drug Discov. Today* **2003**, *8*, 551–556.

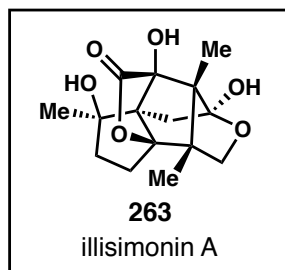
APPENDIX 7

Progress Toward the Synthesis of Illisimonin A

A7.1 INTRODUCTION AND BACKGROUND

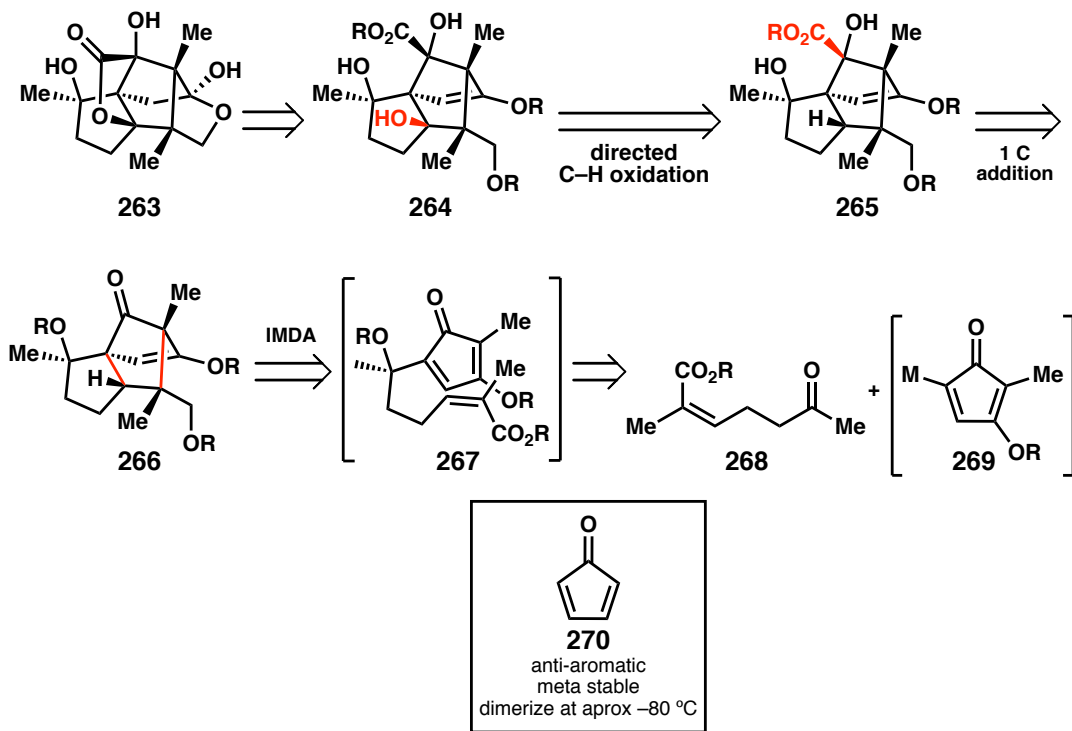
Illisimonin A (**263**) was isolated from the fruits of *Illicium simonsii* by Yu and coworkers in 2017 (Figure A7.1).¹ Portions of the *Illicium simonsii* plant have been used for a number of ailments in traditional Chinese medicine including cystic hernia, scabies, and digestive diseases. The isolation of **263** was especially low, only 4 mg of **263** was isolated from 96 kg of fruit.

263 was found to possess an unprecedented tricyclo[5.2.1.0^{1,6}]decane skeleton, unique from the other eight reported sesquiterpenoid carbon skeletons. Further structural features to note include a fully substituted 5-membered ring and 7 stereogenic centers, 3 of which are all-carbon quaternary centers. **263** was investigated for biological activity and found to provide neuroprotective effects against oxygen-glucose deprivation (OGD)-induced cell injury in SH-SY5Y cells with EC₅₀=27.7 μM.

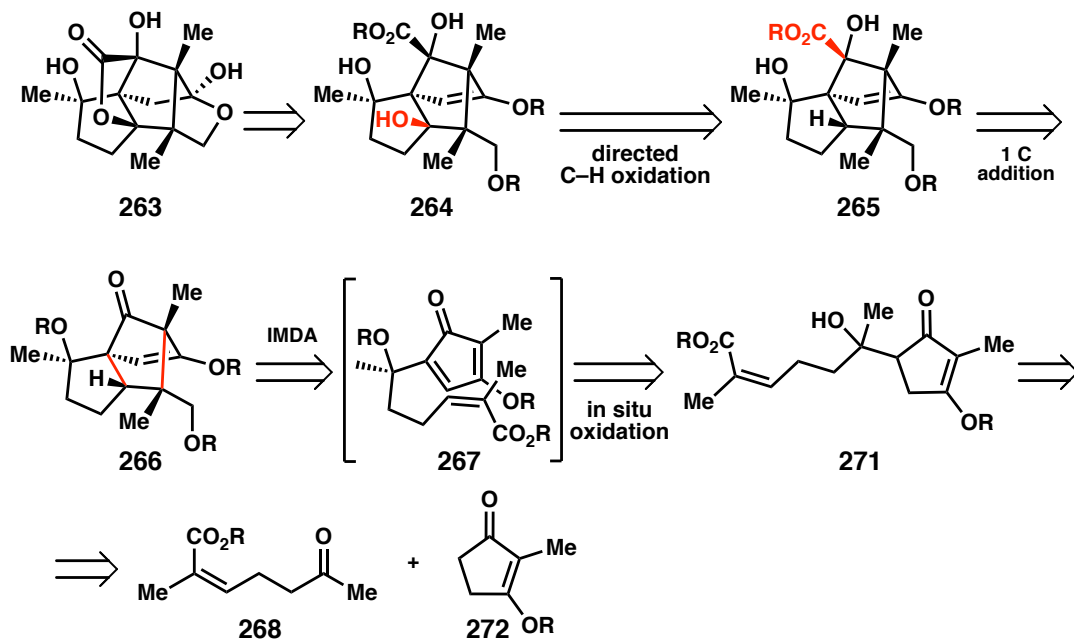
Figure A7.1 Illisimonin A and *Illicium simonsii*.

A7.2 RETROSYNTHETIC ANALYSIS OF ILLISIMONIN A

Our initial analysis of the challenging natural product illisimonin A focused on a number of key disconnects to forge the unprecedented carbon scaffold. As shown in Scheme A7.1, we believe a series of late-stage functional group manipulations would trace back to tertiary alcohol **264**. This alcohol could be installed by a directed C–H oxidation reaction utilizing the pendant carbonyl group, leading back to compound **265**. **265** could arise from a single carbon addition into the bridging ketone, leading to compound **266**. Here, we recognized **266** could be generated by a Diels–Alder reaction to forge all 3 of the all-carbon quaternary stereogenic centers in a single step (**267** to **266**). Unfortunately, it would be unlikely to synthesize such an intermediate by direct nucleophilic addition due to the unstable nature of cyclopentadienones (i.e., **268** and **269**).²

Scheme A7.1 Retrosynthetic Analysis of Illisimonin A.

Instead, we believed it may be possible to generate the cyclopentadienone by in situ oxidation of a suitable precursor **271**, which could be generated by a crossed Aldol reaction (Scheme A7.2).

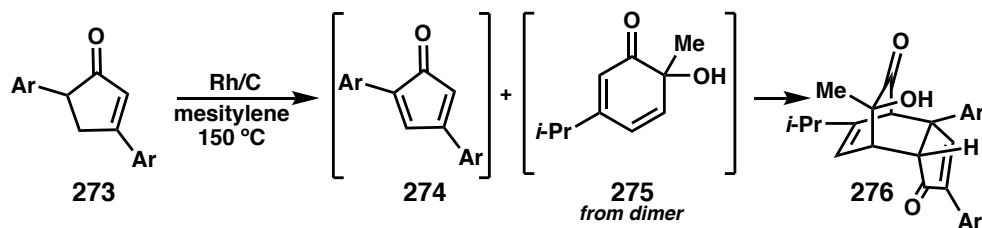
Scheme A7.2 Revised Retrosynthetic Analysis of Illisimonin A.

A7.2.1 Literature Examples of Cyclopentadienone Reactivity.

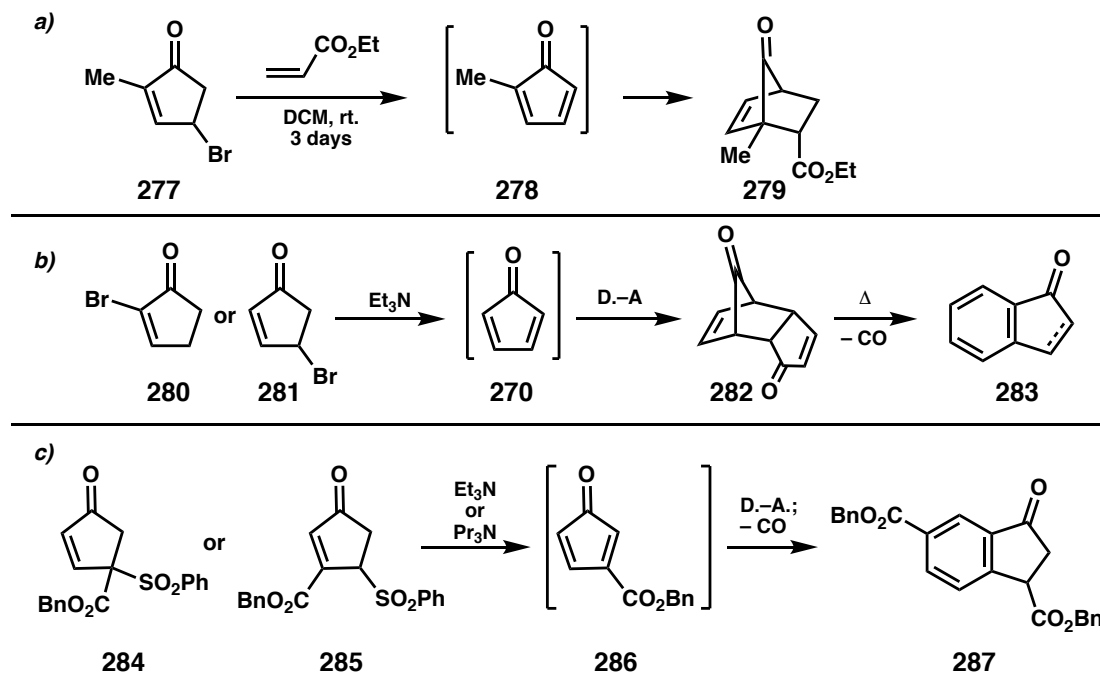
Given the highly reactive nature of cyclopentadienones, only a limited number of reports have detailed their use in synthetic reactions.

Porco and coworkers have reported the direct dehydrogenation of a cyclopentenone to generate a cyclopentadienone (**274**) which goes on to react with a diene in solution (Scheme A7.3).³

Scheme A7.3 Dehydrogenative Generation of Cyclopentadienone.



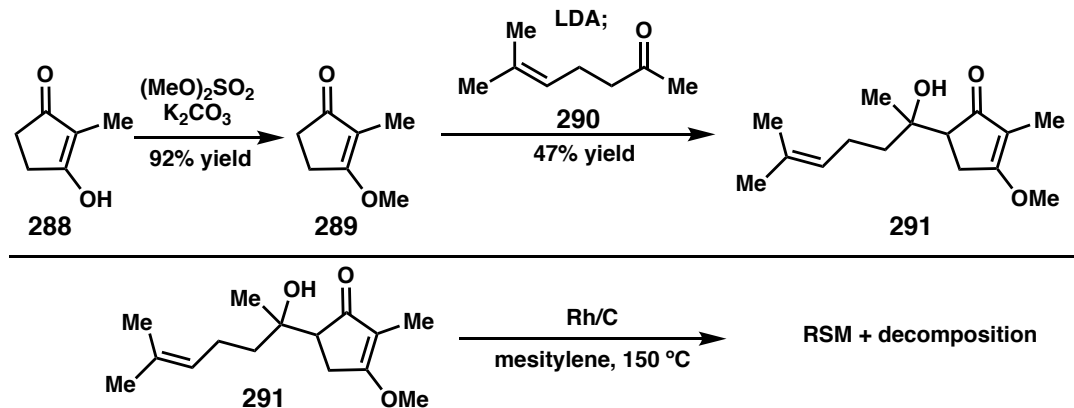
Cyclopentadienones have also been generated by elimination from a suitable cyclopentenone as shown in Scheme A7.4.^{4,5,67} The leaving group must be located at the 2- or 4-position of the cyclopentenone (i.e., **280** or **281**) or decomposition of the starting material is observed. Cyclopentadienones can react as either a dienophile or a diene in a Diels–Alder reaction (Scheme A7.3 versus A7.4a) or dimerize (Scheme A7.4 b&c).

Scheme A7.4 Generation of Cyclopentadienone via Elimination.

A7.3 FORWARD SYNTHESIS

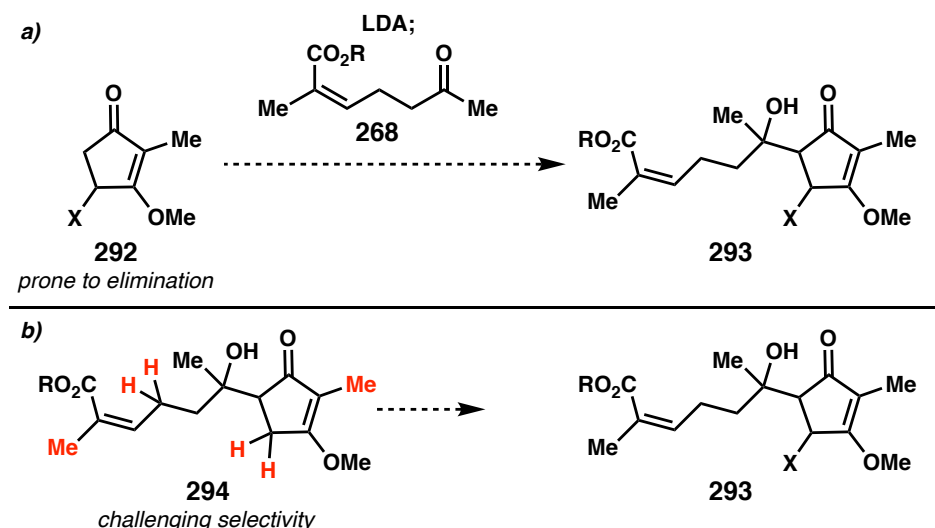
A7.3.1 Cyclopentadienone Route.

We were able to synthesize the known cyclopentenone **289** and the cross Aldol reaction with **290** resulted in the model compound **291** (Scheme A7.5). Unfortunately, the conditions previously reported to generate cyclopentadienone via direct hydrogenation did not result in the desired product.³

Scheme A7.5 Forward Synthesis of a Model System via Cyclopentadienone Route.

A considerable amount of time was spent investigating reactions conditions to generate cyclopentadienone via elimination, but this approach has two serious flaws (Scheme A7.6). The leaving group must be at the 2- or 4-position but substitution is required at the 2-position in the natural product so the leaving group must be at the 4-position (i.e., **292**). This is problematic as **292** would be prone to elimination under the cross Aldol conditions (Scheme 7.6a). Installation of the leaving groups after the Aldol reaction by allylic functionalization is similarly problematic as **294** possess a number of allylic positions (Scheme 7.6b).

Scheme A7.6 Challenges in the Cyclopentadienone Route.



Given these challenges with the cyclopentadienone route, we chose to reevaluate our retrosynthetic analysis.

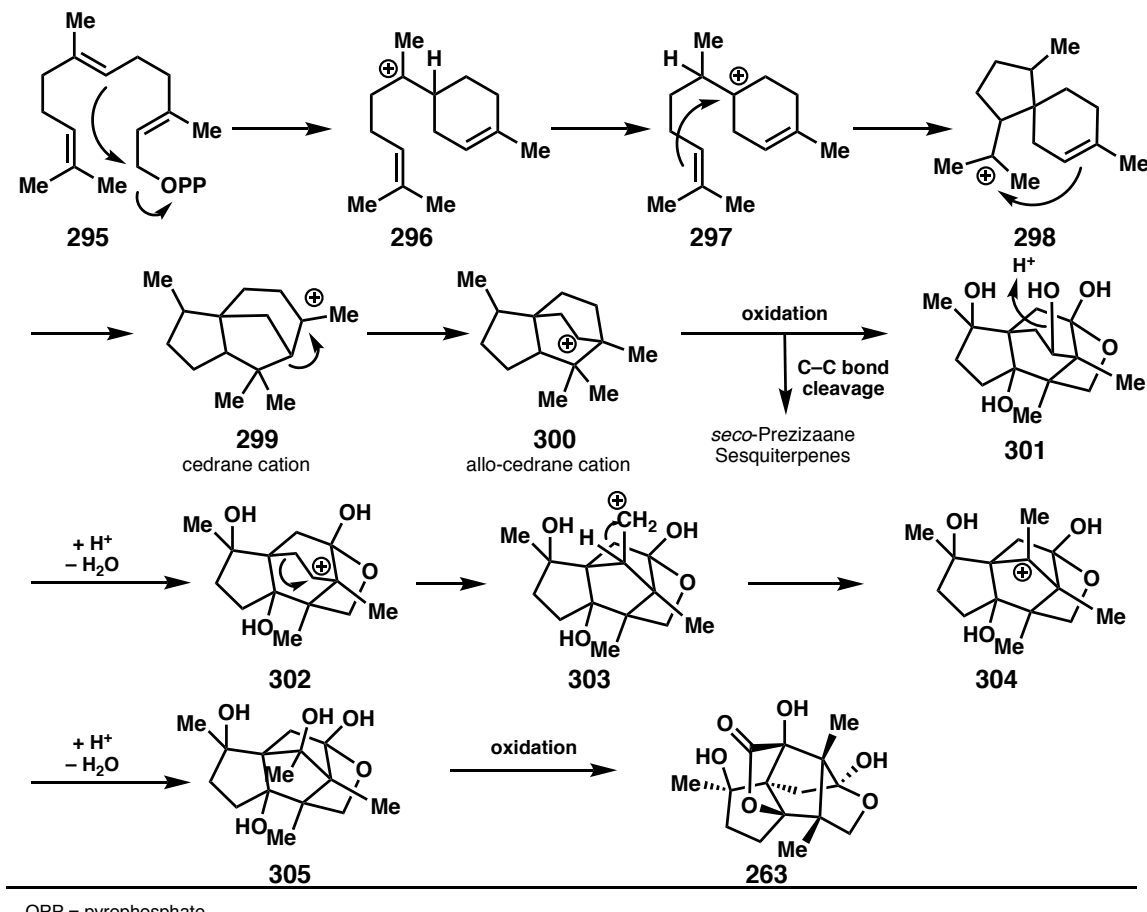
A7.4 REVISED RETROSYNTHESIS

A7.4.1 Biosynthetic Inspiration.

The isolation chemists proposed the biosynthesis of illisimonin A (**263**) shown in Scheme A7.7.¹ The biosynthetic route is based on the previously proposed biosynthesis of *sec*-prezizaane-type sesquiterpenoids from *allo*-cedrane cation (**300**). In the

biosynthesis of illisimonin A (**263**), it is proposed *allo*-cedrane cation (**300**) undergoes oxidation followed by a Wagner-Meerwein rearrangement to set the [2.2.1] bicyclic core present in the natural product (**300** to **301** to **303**).

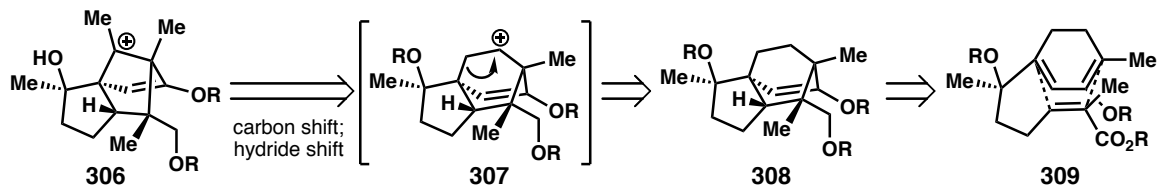
Scheme A7.7 Proposed Biosynthesis of Illisimonin A.



A7.4.2 Benzilic Acid Disconnection.

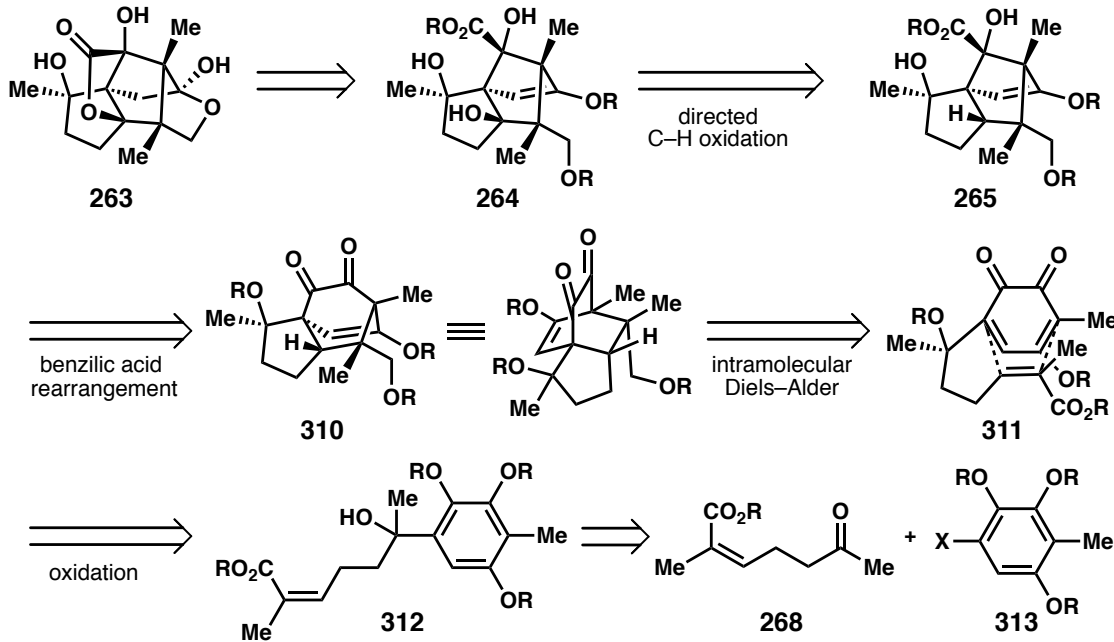
Taking inspiration from the proposed biosynthesis, we envisioned the challenging [2.2.1] bicyclic core of **263** could arise from rearrangement of a suitable [2.2.2] bicyclic system (**306** to **308**) (Scheme A7.8). This route may avoid the difficulties encountered with the challenging cyclopentadienone intermediate as a [2.2.2] bicyclic scaffold could arise from a more precedented Diels–Alder reaction (**308** to **309**).

Scheme A7.8 Wagner-Meerwein Retrosynthetic Disconnect.

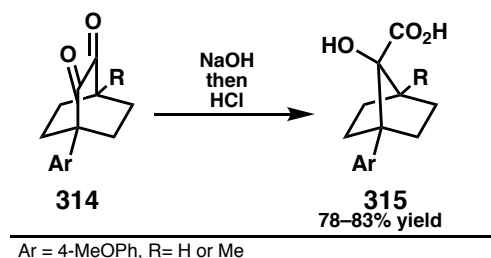


We recognized the approach shown in Scheme A7.8 would require a series of challenging oxidations at the bridging position of the [2.2.1] bicyclic core (i.e., **306** to **265**). A more reasonable approach could involve incorporation of the desired oxygenation prior to the carbon skeleton rearrangement using a benzilic acid rearrangement (Scheme A7.9).

Scheme A7.9 Retrosynthesis via Benzoic Acid Rearrangement Disconnect.

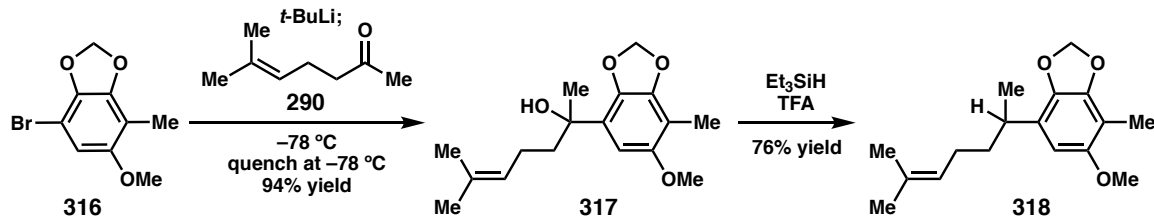


We were pleased to find a benzilic acid rearrangement has been reported to occur in a similar [2.2.2] bicyclic scaffold (**314**) as shown in Scheme A7.10.⁸

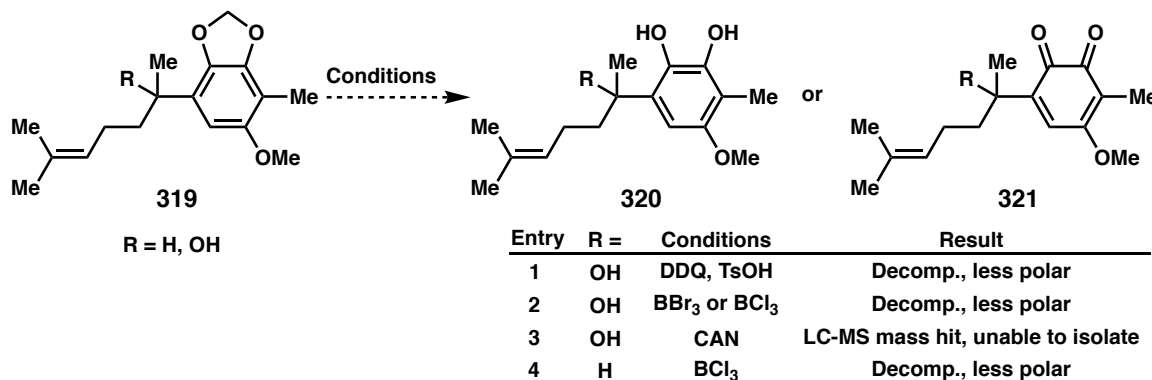
Scheme A7.10 Reported Benzilic Acid Rearrangement in a [2.2.2.] Bicyclic Scaffold.

A7.5 REVISED FORWARD SYNTHESIS

Working with a model system, we were able to synthesize the known aryl bromide **316** which undergoes lithium-halogen exchange and addition into ketone **290** to yield the tertiary alcohol **317** (Scheme A7.11).⁹ The benzylic tertiary alcohol is present in the natural product **263** but we anticipated it could be problematic under the subsequent oxidation conditions. We found **317** can be deoxygenated with Et₃SiH/TFA to **318**.

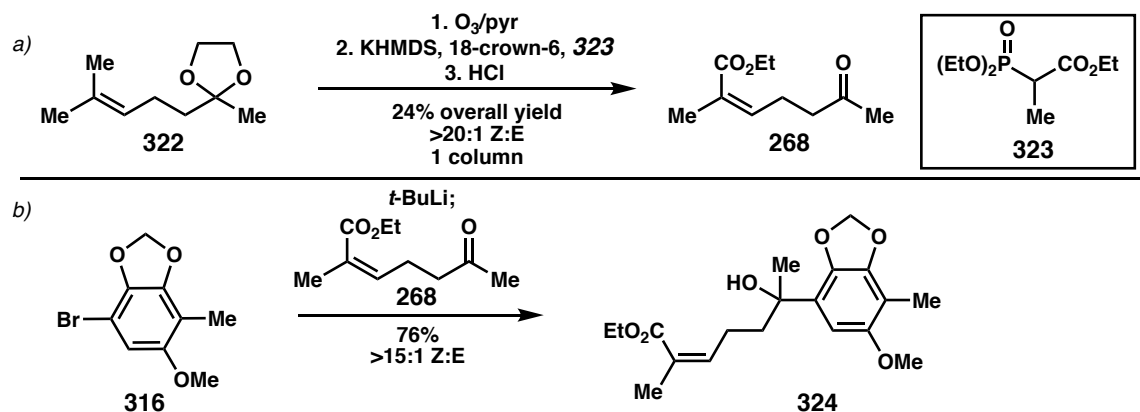
Scheme A7.11 Synthesis of Diels–Alder and Benzilic Acid Model System.

Unfortunately, the reported conditions we investigated to deprotect and/or oxidize the catechol acetal (**319**) to the diol **320** or *o*-quinone **321** resulted in decomposition of the starting material (Scheme A7.12).¹⁰

Scheme A7.12 Deprotection/Oxidation of Diels–Alder and Benzilic Acid Model System.

We recognized that deprotected catechol **320** and *o*-quinone **321** would likely be challenging to isolate and may provide only limited insight into the Diels–Alder step due to the electronics of the dienophile olefin in the model system (**319** vs **311**). Therefore, we focused on moving forward in the fully elaborated system.

The required Z-enone **268** could be synthesized in moderate yield over 3 steps which can be conducted on large scale (Scheme A7.13a).¹¹ As in the model system, lithium-halogen exchange of **316** and addition into ketone **268** generated **324** in good yield (Scheme A7.13b).

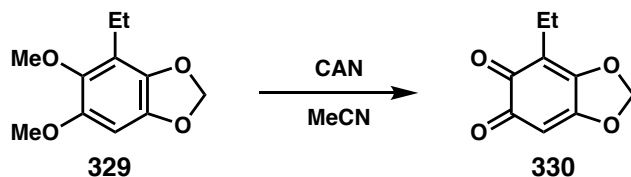
Scheme A7.13 Forward Synthesis of Diels–Alder and Benzilic Acid Route.

With the protected catechol **324** in hand, we investigated a number of reported conditions to deprotect or deprotect and oxidize the catechol acetal (Scheme A7.14).¹² We were unable to isolate the desired product using these reported reaction conditions, observing starting material decomposition or limited overall conversion.

Scheme A7.14 Deprotection and/or Oxidation of Catechol Acetal.

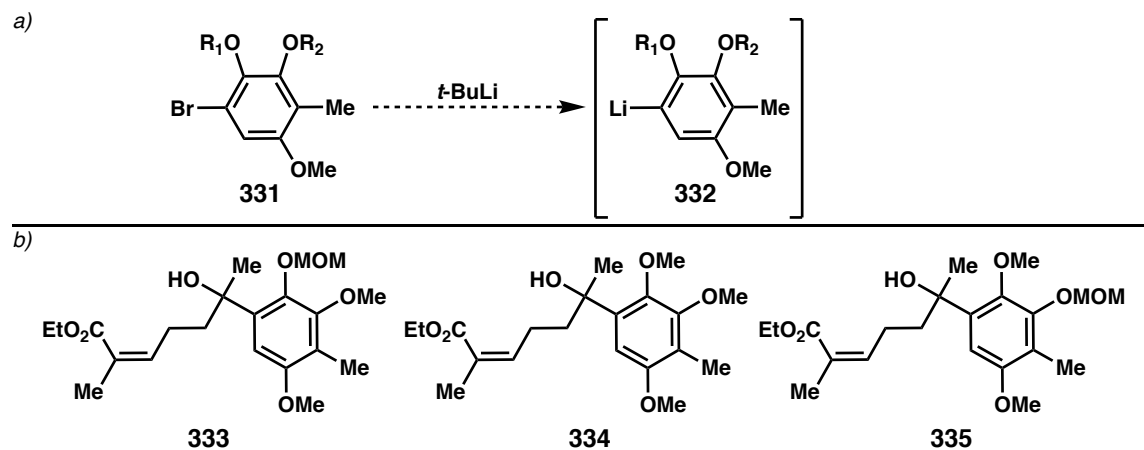
entry	conditions	desired product	result	
1	$\text{B}(\text{C}_6\text{F}_5)_3$ Et_3SiH	 325	RSM and decomp. more polar	
2	CAN	 326	full consumption of SM decomp. unable to isolated	
3	$\text{Pb}(\text{OAc})_4$	 327	 328	full consumption of SM decomp.

Prior literature reports have documented similar challenges in the selective deprotection of a catechol acetal system, such as the system shown in Scheme A7.15.¹³

Scheme A7.15 Competitive Deprotection of Catechol Acetal and Methyl Ether.

Given these results, we chose to reevaluate our protecting group strategy on the aryl fragment. We were aware the ortho lithium-halogen exchange relative to R₁ in **331** would limit possible protecting group strategies (Scheme A7.16a). We envisioned the protecting group strategies shown in Scheme A7.16b may be amenable to more facile deprotection and/or oxidation as compared to acetal **316**.

A methoxymethyl protecting group would be expected to stabilize ortho lithiation (i.e., **332** in A7.16a, R₁ = MOM) but deprotection of 1,3-diones (i.e., **333**) can be challenging.¹⁴ Trimethoxy protected **334** would simplify synthesis but there is limited direction for the subsequent oxidation. **335** would be expected to facilitate oxidation to the *p*-quinone and avoids the deprotection challenges foreseen in **333** but significantly complicates synthesis of the aryl fragment.

Scheme A7.16 Protecting Group Strategy for Arene Fragment.

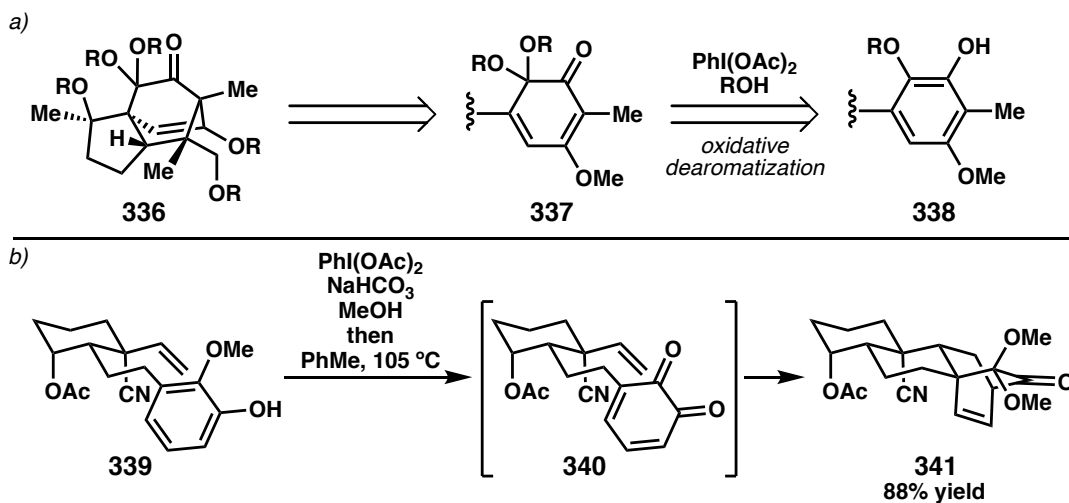
Currently, we are investigating the combination of various aryl protecting groups and oxidation conditions in order to probe the desired *o*-quinone Diels–Alder reaction.

A7.6 FUTURE DIRECTIONS

A7.6.1 Oxidative Dearomatization.

In addition to the oxidation conditions reported to generate *o*-quinones described above, we plan to investigate an oxidative dearomatization approach (Scheme A7.17a). This approach has been demonstrated in a similar bicyclic scaffold (**339**, Scheme A7.17b).¹⁵ Furthermore, differentiation of the two bridging carbons at the ketone oxidation state (i.e., monoketal **336** versus dicarbonyl **301**) could be beneficial for the benzilic acid rearrangement

Scheme A7.17 Diels–Alder via Oxidative Dearomatization Disconnect

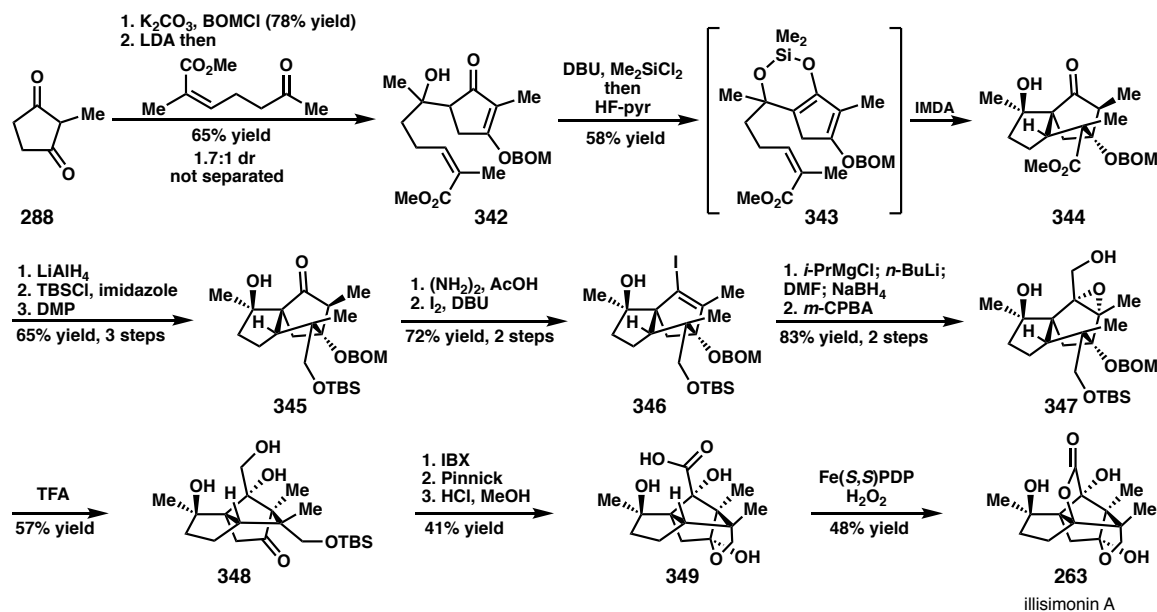


A7.7 Rychnovsky Synthesis of Illisimonin A

In the midst of the research described above, the first reported total synthesis of illisimonin A was disclosed by Rychnovsky and coworker, with the final synthetic sequence is shown in Scheme A7.18.¹⁶ The authors utilized a similar Diels–Alder

disconnect (**342** to **344**) but chose to use a sila template Diels–Alder reaction (**343**). This approach avoided the challenges we experienced with a cyclopentadienone intermediate but provides the wrong C–C bond connectivity, which later undergoes a semipinacol rearrangement to provide the desired bicyclic core (**347** to **348**). The authors note the single carbon addition to the bridging ketone (**345** to **347**) was challenging but Bouveault aldehyde synthesis with in situ reduction provided the alcohol **347** which was later reoxidized back up to the acid **349**. We were pleased to see **349** undergoes acid directed C–H oxidation using White’s FePDP catalyst.

Scheme A7.18 Rychnovsky Synthesis of Illisimonin A



A7.8 Conclusion

We continue to investigate our proposed route toward the synthesis of illisimonin A. In comparison to the Rychnovsky route, our proposed route may avoid some of the challenges by utilizing a Diels–Alder substrate with all the requisite carbons and limiting

redox manipulations. Furthermore, we are interested to demonstrate the Diels–Alder, benzilic acid rearrangement sequence in the context of a complex synthetic target.

A7.9 EXPERIMENTAL SECTION

A7.9.1 MATERIALS AND METHODS

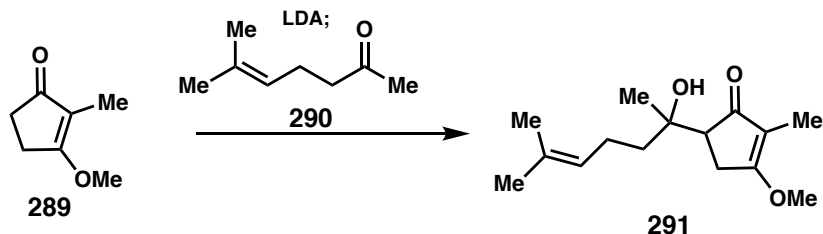
Unless otherwise stated, reactions were performed in oven-dried brand-new Fisherbrand scintillation vials in a nitrogen-filled glove box or in flame-dried Schlenk flasks under inert gas (nitrogen or argon) connected on a Schlenk line using dry, degassed solvents and stirring bars. Solvents were dried by passage through an activated alumina column under argon. Reaction progress was monitored by thin-layer chromatography (TLC) or GC-FID analyses. TLC was performed using E. Merck silica gel 60 F254 precoated glass plates (0.25 mm) and visualized by UV fluorescence quenching, phosphomolybdic acid, or KMnO₄ staining. Silicycle SiliaFlash P60 Academic Silica gel (particle size 40–63 nm) was used for flash chromatography. ¹H NMR spectra were recorded on a Varian Inova 500 MHz or Bruker 400 MHz spectrometers in CDCl₃ or C₆D₆ and are reported relative to residual solvent peak. ¹³C NMR spectra were recorded on a Varian Inova 600MHz (150 MHz), 500 MHz spectrometer (125 MHz), or Bruker 400 MHz spectrometers (100 MHz) in CDCl₃ or C₆D₆ and are reported relative to residual solvent peak. Data for ¹H NMR are reported as follows: chemical shift (δppm) (multiplicity, coupling constant (Hz), integration). Multiplicities are reported as follows: s = singlet, d = doublet, t = triplet, q = quartet, p = pentet, sept = septet, m = multiplet, br s = broad singlet, br d = broad doublet, app = apparent. Data for ¹³C NMR are reported in terms of chemical shifts (δppm). High resolution mass spectra (HRMS) were obtained

from Agilent 6200 Series TOF with an Agilent G1978A Multimode source in mixed ionization mode (MM: ESI-APCI+) or obtained from Caltech mass spectrometry laboratory. All reagents were purchased from Aldrich, TCI, or Acros and used as received (unless noted). **289**,¹⁷ **316**,⁹ and **322**¹⁸ were synthesized accord to previously reported methods.

A7.9.2 EXPERIMENTAL PROCEDURES AND SPECTROSCOPIC DATA

A7.9.2.1 Synthesis of Model Cyclopentenone Diels–Alder Precursor.

Scheme A7.19 Synthesis of Cyclopentenone Diels–Alder Precursor

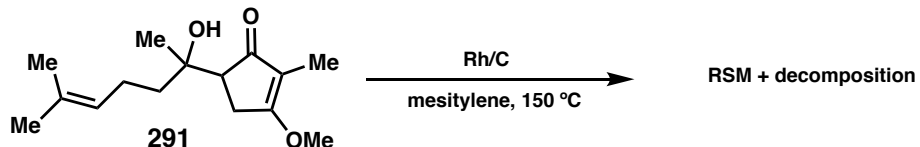


5-(2-Hydroxy-6-methylhept-5-en-2-yl)-3-methoxy-2-methylcyclopent-2-en-1-one (291). A flame-dried 2-neck flask with stir bar was placed under argon and charged with *i*Pr₂NH (1 equiv, dist. from CaH₂) and THF (1M in amine) and cooled to –78 °C. *n*-BuLi (1 equiv, 1 M in hexanes) was added dropwise and the solution was stirred for 30 minutes. To this solution of LDA was added **289** (1 equiv) in THF (1.8 M) via cannula dropwise and allowed to stir for 30 minutes. A solution of **290** (3.2 mmol, 2 equiv) in THF (3 mL) was added dropwise to the enolate. The reaction was allowed to slowly warm and monitored by TLC (2:1 hexanes to EtOAc). When judged complete by TLC, the reaction mixture was diluted with EtOAc (10 mL) then quenched with HCl (5 mL, 1 M) and H₂O (10 mL), followed by aqueous extraction (3x10mL EtOAc), brine wash, dried with MgSO₄ and concentrated in vacuo. The crude reaction mixture was purified by silica gel flash column chromatography (4:1 to 3:1 hexanes to EtOAc) to yield **291**.

(mixture of diastereomers) as a colorless oil (127.6 mg, 47% yield). ^1H NMR (600 MHz, CDCl_3) δ 5.11 (t, $J = 7.0$ Hz, 1H), 4.88 (s, 1H), 3.98 (s, 3H), 2.79 – 2.70 (m, 1H), 2.68 (dd, $J = 7.2, 2.6$ Hz, 1H), 2.27 – 2.15 (m, 2H), 2.11 (dq, $J = 13.5, 7.2, 6.6$ Hz, 1H), 1.69 (s, 3H), 1.67 – 1.60 (m, 6H), 1.54 – 1.40 (m, 2H), 1.03 (s, 3H). ^{13}C NMR (101 MHz, CDCl_3) δ 208.77, 184.86, 131.88, 124.46, 116.74, 73.70, 56.97, 51.58, 41.32, 28.74, 25.86, 22.52, 21.91, 17.83, 5.93. IR (Neat Film NaCl) 3396, 2969, 2922, 2871, 1738, 1621, 1614, 1462, 1455, 1383, 1344, 1254, 1166, 1122, 1068, 1023, 990, 951, 786, 763 cm^{-1} ; HRMS (MM:+) calc'd for $\text{C}_{15}\text{H}_{24}\text{O}_3$ [M+Na] $^+$: 275.1618, found: 275.1612.

A7.9.2.2 Attempted Oxidation of Model Cyclopentenone Diels–Alder Precursor.

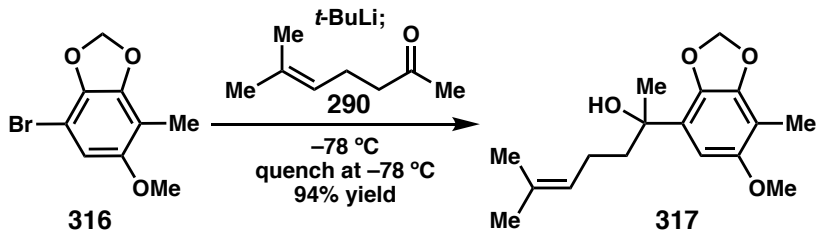
Scheme A7.20 Attempted Oxidation of Model Cyclopentenone Diels–Alder Precursor



Conducting using an adapted literature procedure.³ **291** (7.5 mg, 0.03 mmol, 1 equiv), Rh/C (5% Rh, 6.2 mg, 10 mol % Rh), and mesitylene (0.5 mL, 0.06 M in **291**) were added to a 2 dram vial with a stir bar, sealed with a PTFE-lined cap and heated to 150 °C for 24 hours. The reaction mixture was then diluted with DCM, quenched with MeOH, eluted through a short pad of silica gel, and concentrated in vacuo. The crude reaction mixture was analyzed by TLC, UHPLC-MS, and ^1H NMR.

A7.9.2.3 Synthesis of Model o-Quinone Precursor.

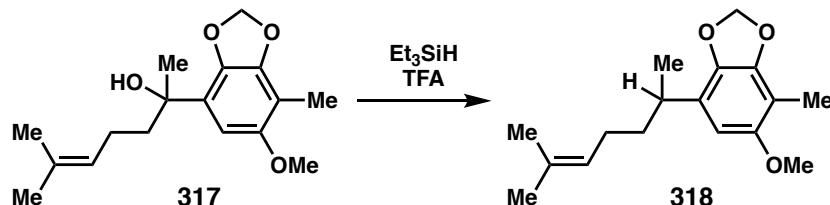
Scheme A7.21 Synthesis of Model *o*-Quinone Precursor



2-(6-Methoxy-7-methylbenzo[*d*][1,3]dioxol-4-yl)-6-methylhept-5-en-2-ol (317). A flame-dried 2-neck flask with stir bar was placed under argon, charged with **316** (20 mg, 0.082 mmol, 1 equiv), and evacuated/refilled with argon (3x). Et₂O (1 mL) was added and the stirring solution is cooled to -78 °C for 10 minutes. *t*-BuLi (0.09 mL, 2 equiv, 1.7 M in hexanes) was added dropwise and the resulting solution was stirred at -78 °C for 45 minutes. A solution of **290** (14.5 μL, 0.098 mmol, 1.2 equiv) in Et₂O (1 mL) was added via cannula dropwise. While stirring at -78 °C, the reaction progress was monitored by TLC (9:1 hexanes to EtOAc). After 3 hours, the reaction was quenched by addition of H₂O (ca. 2 mL) at -78 °C and allowed to slowly warm. The aqueous layer was extracted with Et₂O (3x5 mL), the combined organic layers were washed with brine and dried with MgSO₄. The crude product was purified by silica gel flash column chromatography (15:1 to 5:1 hexanes to EtOAc) to yield **317** as a colorless oil (22.5 mg, 94% yield, >20:1 Z:E). ¹H NMR (400 MHz, CDCl₃) δ 6.41 (s, 1H), 5.88 (q, *J* = 1.4 Hz, 2H), 5.12 (ddt, *J* = 8.5, 5.3, 1.5 Hz, 1H), 3.79 (s, 3H), 2.39 (s, 1H), 2.08 (s, 3H), 2.06 – 1.73 (m, 4H), 1.69 – 1.63 (m, 3H), 1.55 – 1.51 (m, 6H); ¹³C NMR (100 MHz, CDCl₃) δ 153.41, 146.65, 136.56, 132.28, 126.35, 124.52, 107.84, 100.62, 100.12, 74.50, 56.40, 41.87, 28.71, 25.87, 23.20, 17.84, 8.77.; IR (Neat Film NaCl) 3471, 2965, 2925, 2772,

1897, 1652, 1606, 1487, 1463, 1416, 1379, 1273, 1200, 1166, 1121, 1062, 1035, 964, 941, 886, 841, 817, 778, 748 cm⁻¹; HRMS (MM:+) calc'd for C₁₇H₂₄O₄ [M+Na]⁺: 315.1567, found: 315.1564.

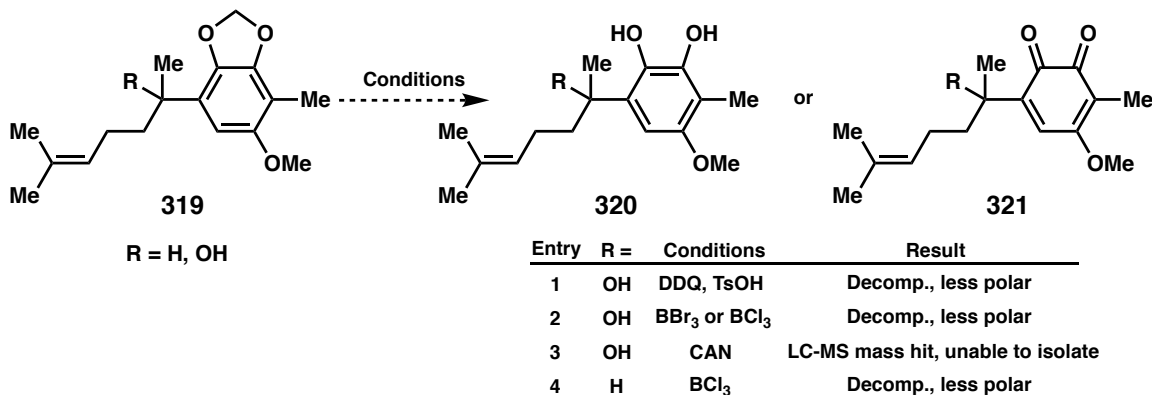
Scheme A7.22 Deoxygenation of Model o-Quinone Precursor



5-Methoxy-4-methyl-7-(6-methylhept-5-en-2-yl)benzo[d][1,3]dioxole (318) Adapted from a literature procedure.¹⁹ A solution of **317** (19 mg, 0.065 mmol, 1 equiv) in DCM (0.7 mL) was cooled to 0 °C. Et₃SiH (29 μL, 0.18 mmol, 2.8 equiv) was added followed by TFA (2.3 μL, 0.3 mmol, 4.7 equiv). The reaction progress was monitored by TLC (9:1 hexanes to EtOAc). After 3 hours the reaction was quenched with dilute NaHCO₃ and the aqueous layer was extracted with Et₂O (3x5 mL), the combined organic layers were washed with brine and dried with MgSO₄. The crude product was purified by silica gel flash column chromatography (20:1 hexanes to EtOAc) to yield **318** as a colorless oil (17.1 mg, 95% yield). ¹H NMR (500 MHz, CDCl₃) δ 6.12 (s, 1H), 5.87 (s, 2H), 5.21 – 4.93 (m, 1H), 3.77 (s, 3H), 2.80 (h, *J* = 7.0 Hz, 1H), 2.08 (s, 3H), 1.93 (hept, *J* = 7.4 Hz, 2H), 1.68 (s, 5H), 1.62 – 1.50 (m, 5H), 1.24 (d, *J* = 6.9 Hz, 3H); ¹³C NMR (101 MHz, CDCl₃) δ 153.39, 146.18, 138.49, 131.42, 125.00, 124.52, 106.60, 101.32, 100.45, 56.28, 36.69, 34.45, 26.28, 25.74, 20.79, 17.68, 8.58. IR (Neat Film NaCl) 2963, 2926, 1654, 1611, 1496, 1425, 1401, 1376, 1226, 1199, 1121, 1038, 963, 941, 819, 746.

A7.9.2.4 Attempted Oxidation of Model o-Quinone Precursor.

Scheme A7.23 Attempted Deprotection/Oxidation of Catechol Acetal



Entry 1. Conducting using **317** (**319, R=OH**) (4 mg, 0.014 mmol, 1 equiv), DDQ (6 mg, 0.027 mmol, 2 equiv), TsOH (2.7 mg, 0.014 mmol, 1 equiv), and 1,4-dioxane (0.5 mL, 0.03 M) in a sealed 1 dram vial with a stir bar. After 3 hours the reaction was quenched with water and the aqueous layer was extracted with Et₂O (3x5 mL), the combined organic layers were washed with brine, dried with MgSO₄, and concentrated in vacuo. The crude reaction mixture was analyzed by TLC, UHPLC-MS, and ¹H NMR.

Entry 2. Adapted from a literature procedure.²⁰ Conducting using **317** (**319, R=OH**) (5.6 mg, 0.019 mmol, 1 equiv), BBr₃ (29 μL, 0.029 mmol, 1 M in DCM) and DCM (1.7 mL). After 5 hours, the crude reaction mixture was filtered through a short pad of silica gel, eluting DCM/MeOH and concentrated in vacuo. The reaction mixture was analyzed by TLC, UHPLC-MS, and ¹H NMR.

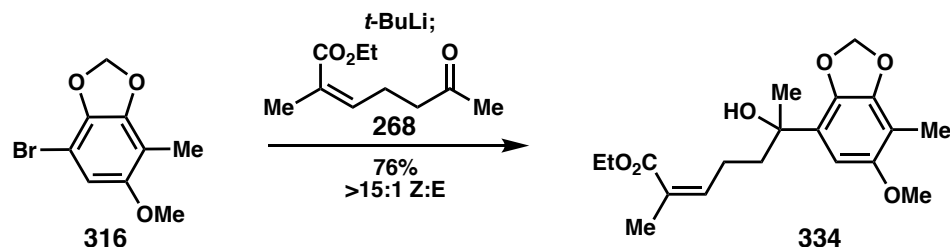
Entry 3. Adapted from a literature procedure.^{10b} Conducting using **317** (**319, R=OH**) (5.5 mg, 0.019 mmol, 1 equiv), CAN (28 mg, 0.0513 mmol, 2.7 equiv) and MeCN (1.7 mL). Immediate color change (colorless to black to orange). After 5 hours the reaction

was quenched with water and the aqueous layer was extracted with EtOAc (3x5 mL), the combined organic layers were washed with brine, dried with MgSO₄, and concentrated in vacuo. The crude reaction mixture was analyzed by TLC, UHPLC-MS, and ¹H NMR.

Entry 4. Adapted from a literature procedure.²⁰ Conducting using **318** (**319, R=H**) (4 mg, 0.014 mmol, 1 equiv), BCl₃ (0.0579 mmol, 4 equiv) and DCM (0.5 mL). Reaction was run as described for Entry 2.

A7.9.2.5 Synthesis of Fully Elaborated o-Quinone Precursor.

Scheme A7.24 Synthesis of Fully Elaborated o-Quinone Precursor.

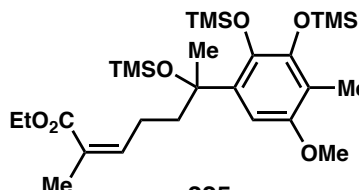
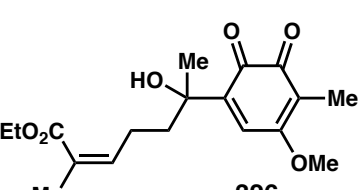
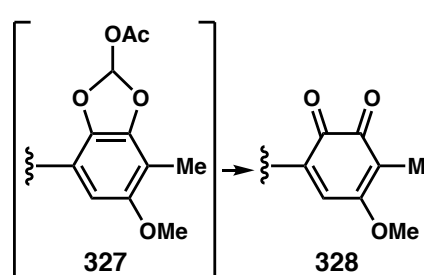


Ethyl (Z)-6-hydroxy-6-(6-methoxy-7-methylbenzo[d][1,3]dioxol-4-yl)-2-methylhept-2-enoate (334) Reaction was conducted in a similar manner to that described for the synthesis of **317**. The reaction was conducted using **316** (107.8 mg, 0.44 mmol, 1 equiv), *t*-BuLi (0.88 mmol, 2 equiv), Et₂O (4.4 mL), and **268** (97 mg, 0.528 mmol, 1.2 equiv, in 5.3 mL Et₂O). When the reaction was judged complete by TLC, the reaction was quenched by addition of 10% citric acid at -78 °C and allowed to slowly warm. The aqueous layer was extracted with Et₂O (3x), the combined organic layers were washed with brine and dried with MgSO₄. The crude product was purified by silica gel flash column chromatography (5:1 hexanes to EtOAc, R_f = 0.15) to yield **334** as a colorless oil (117.4 mg, 76% yield, >15:1 Z:E). ¹H NMR (400 MHz, C₆D₆) δ 6.80 (s, 1H), 5.74 (tq, *J* =

8.0, 1.5 Hz, 1H), 5.32 (dd, $J = 20.3, 1.4$ Hz, 2H), 3.91 (dq, $J = 8.7, 7.1$ Hz, 3H), 3.48 (s, 3H), 2.77 (s, 1H), 2.75 – 2.57 (m, 2H), 2.42 – 2.21 (m, 5H), 1.96 (ddd, $J = 13.7, 9.2, 5.7$ Hz, 1H), 1.78 (q, $J = 1.2$ Hz, 3H), 1.70 (s, 3H), 1.65 (s, 1H), 0.92 (td, $J = 7.1, 1.6$ Hz, 4H).; ^{13}C NMR (101 MHz, C_6D_6) δ 167.93, 153.89, 147.05, 143.63, 136.70, 127.37, 127.24, 107.69, 100.47, 100.37, 73.48, 60.12, 55.65, 41.44, 29.34, 25.16, 20.78, 14.15, 9.03.; IR (Neat Film NaCl) 3470, 2929, 1704, 1456, 1416, 1371, 1196, 1216, 1168, 1120, 1060, 1034, 966, 940, 901 cm^{-1} ; HRMS (MM+) for $\text{C}_{19}\text{H}_{26}\text{O}_6$ [M+Na]⁺ calc'd: 373.1622 found: 373.1602.

A7.9.2.6 Attempted Oxidation of Fully Elaborated o-Quinone Precursor.

Scheme A7.25 Attempted Oxidation of Fully Elaborated *o*-Quinone Precursor.

entry	conditions	desired product	result
1	$B(C_6F_5)_3$ Et_3SiH	 325	RSM and decomp. more polar
2	CAN	 326	full consumption of SM decomp. unable to isolated
3	$Pb(OAc)_4$	 327 → 328	full consumption of SM decomp.

Entry 1. Conducting using an adapted literature procedure.^{12a} **334** (10 mg, 0.03 mmol, 1 equiv), $B(C_6F_5)_3$ (1.5 mg, 10 mol %), Et_3SiH (13 μ L, 0.08 mmol, 3 equiv) and hexanes (2.8 mL) were added to a 2 dram vial with a stir bar, sealed with a PTFE-lined cap and stirred at room temperature for 72 h. The reaction mixture was then diluted with DCM, eluted through a short pad of silica gel, and concentrated in vacuo. The crude reaction mixture was analyzed by TLC and UHPLC-MS.

Entry 2. Adapted from a literature procedure.^{10b} Conducting using **334** (10 mg, 0.028 mmol, 1 equiv), CAN (154 mg, 0.28 mmol, 10 equiv) and MeCN:H₂O (1:1, 1.5 mL total volume). The reaction was quenched with water and the aqueous layer was extracted with CHCl₃ (3x5 mL), the combined organic layers were washed with brine, dried with MgSO₄, and concentrated in vacuo. The crude reaction mixture was analyzed by TLC, UHPLC-MS, and ¹H NMR.

Entry 3. Conducting using an adapted literature procedure.^{12c} Conducting using **334** (5 mg, 0.014 mmol, 1 equiv), Pb(OAc)₄ (18.6 mg, 0.042 mmol, 3 equiv) and benzene (0.2 mL) in a 2 dram vial with a stir bar sealed with a PTFE-lined cap heated to 80 °C. After 24 h, the reaction was diluted with EtOAc and water and the aqueous layer was extracted with EtOAc (3x5 mL), the combined organic layers were washed with brine, dried with MgSO₄, and concentrated in vacuo. The crude material was then diluted with THF:H₂O (5:1, 0.6 M) and AcOH (0.35 M) and stirred for 6 h. The reaction was quenched with sat. NaHCO₃ solution and the aqueous layer was extracted with EtOAc (3x5 mL), the combined organic layers were washed with brine, dried with MgSO₄, and concentrated in vacuo. The reaction mixture was analyzed by TLC, UHPLC-MS, and ¹H NMR.

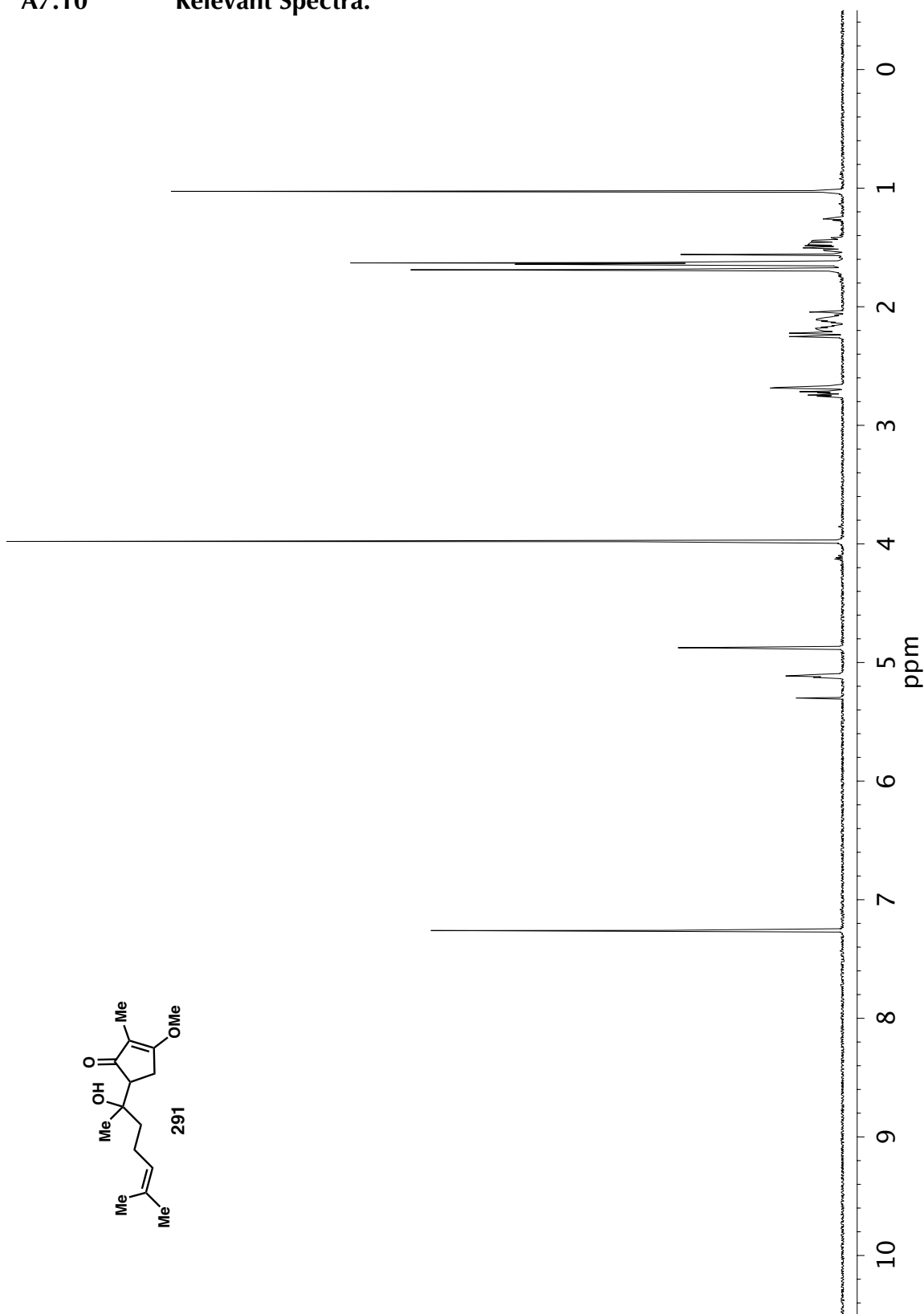
A7.10 Relevant Spectra.

Figure A7.2. ^1H NMR (600 MHz, CDCl_3) of compound 291.

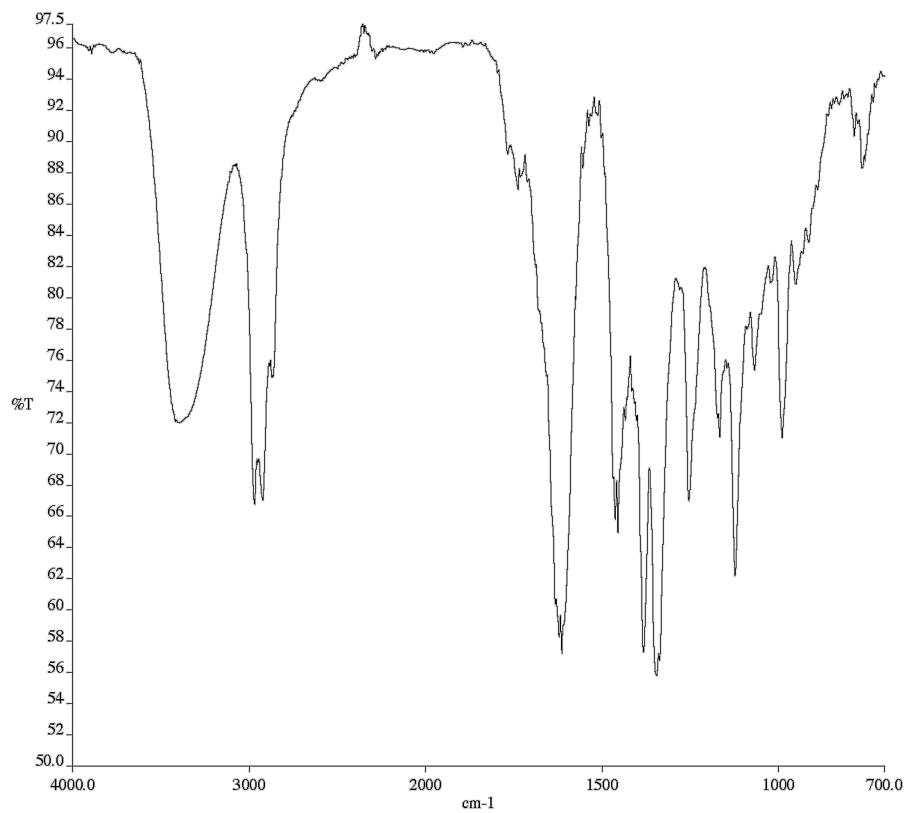


Figure A7.3. Infrared spectrum (Thin Film, NaCl) of compound **291**.

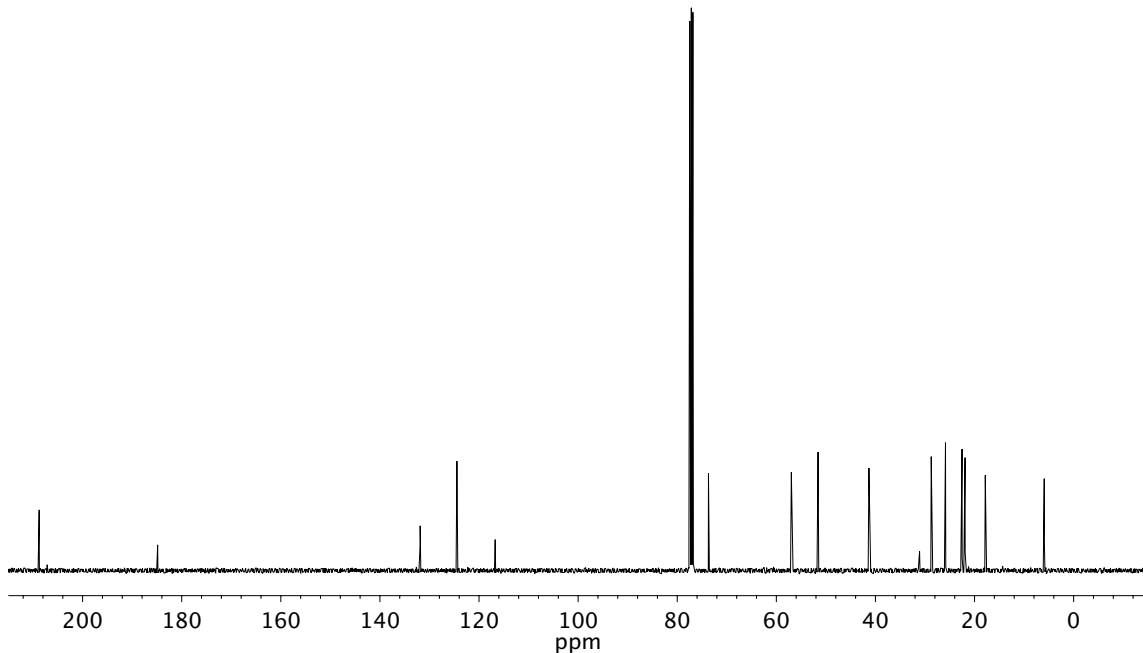


Figure A7.4. ^{13}C NMR (125 MHz, CDCl_3) of compound **291**.

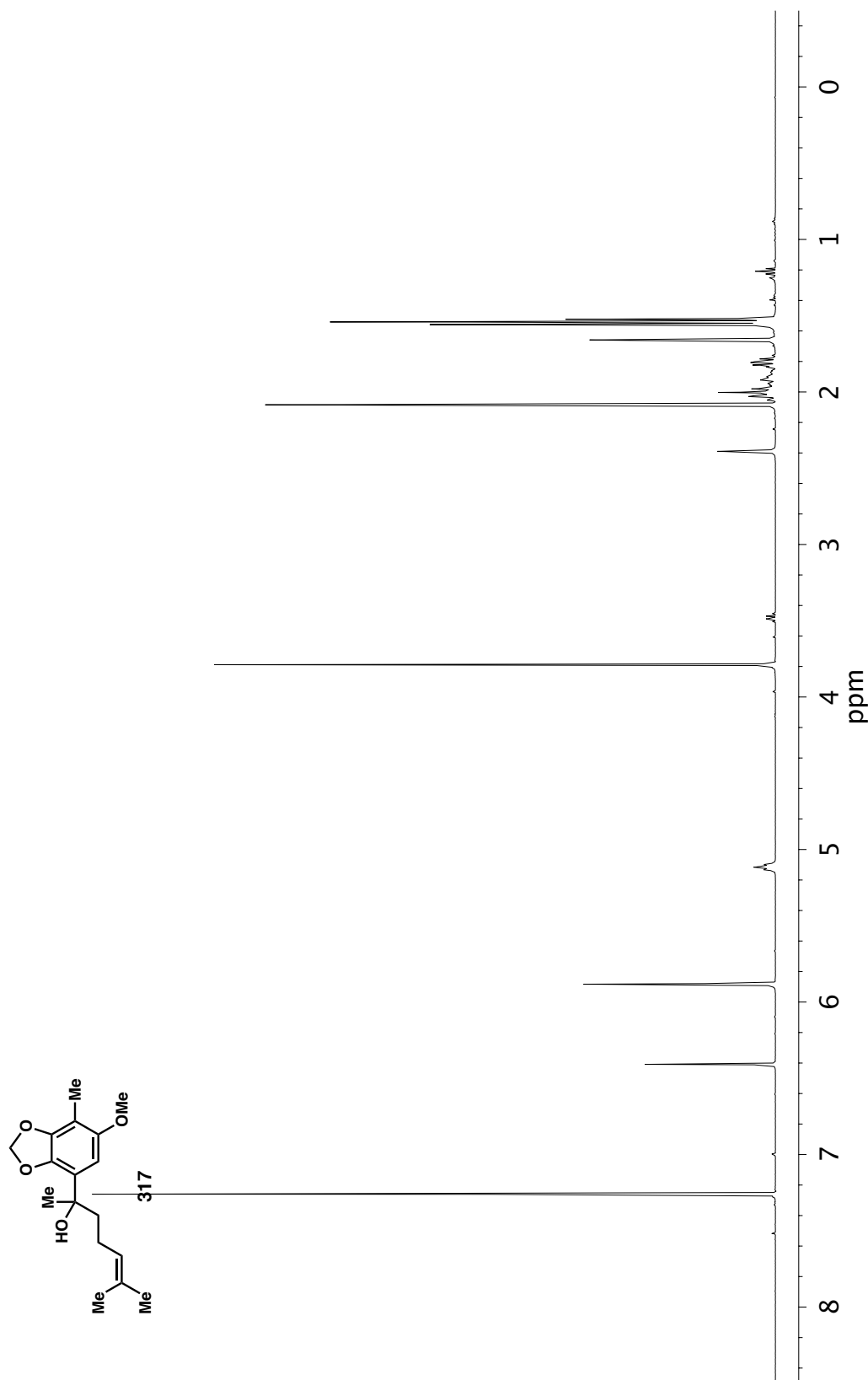


Figure A7.5. ^1H NMR (400 MHz, CDCl_3) of compound 317.

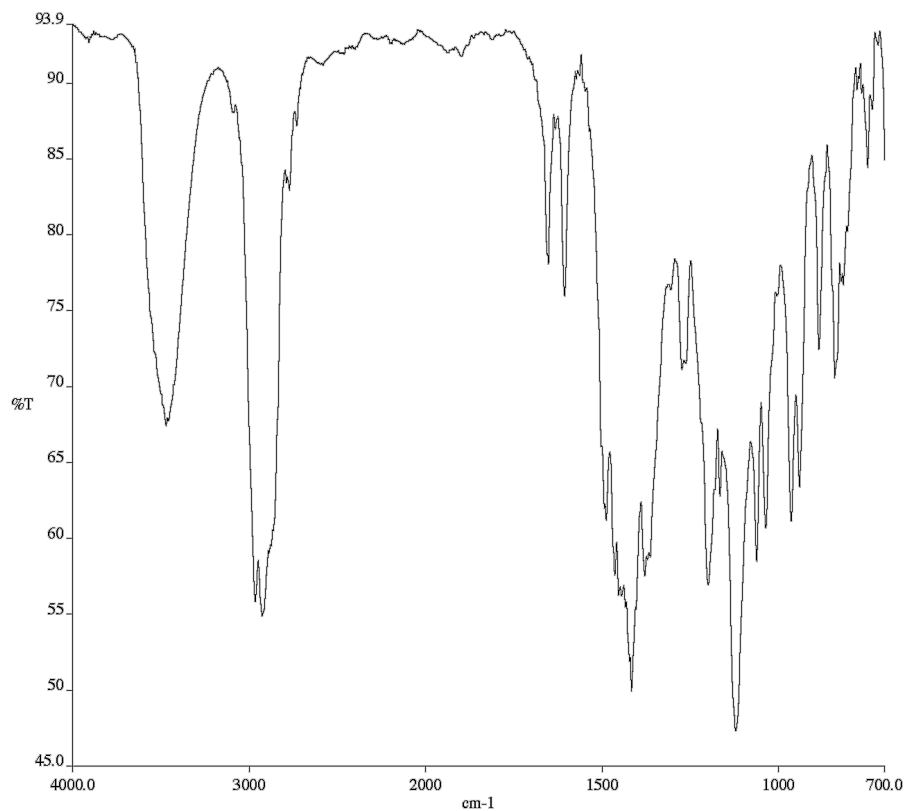


Figure A7.6. Infrared spectrum (Thin Film, NaCl) of compound 317.

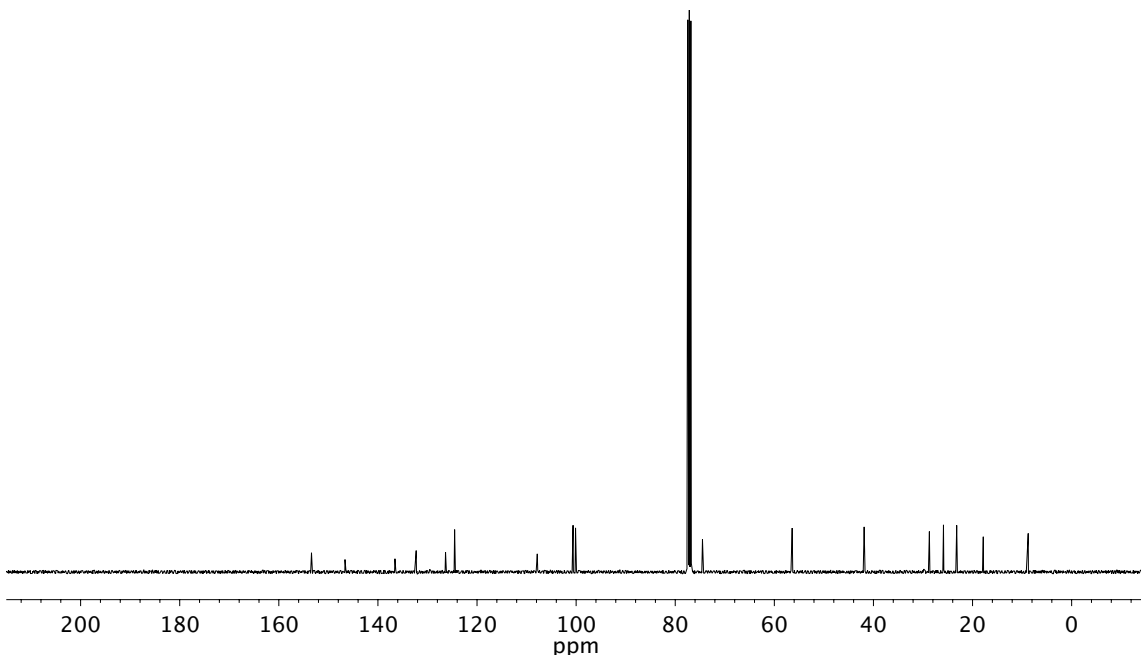


Figure A7.7. ^{13}C NMR (100 MHz, CDCl_3) of compound 317.

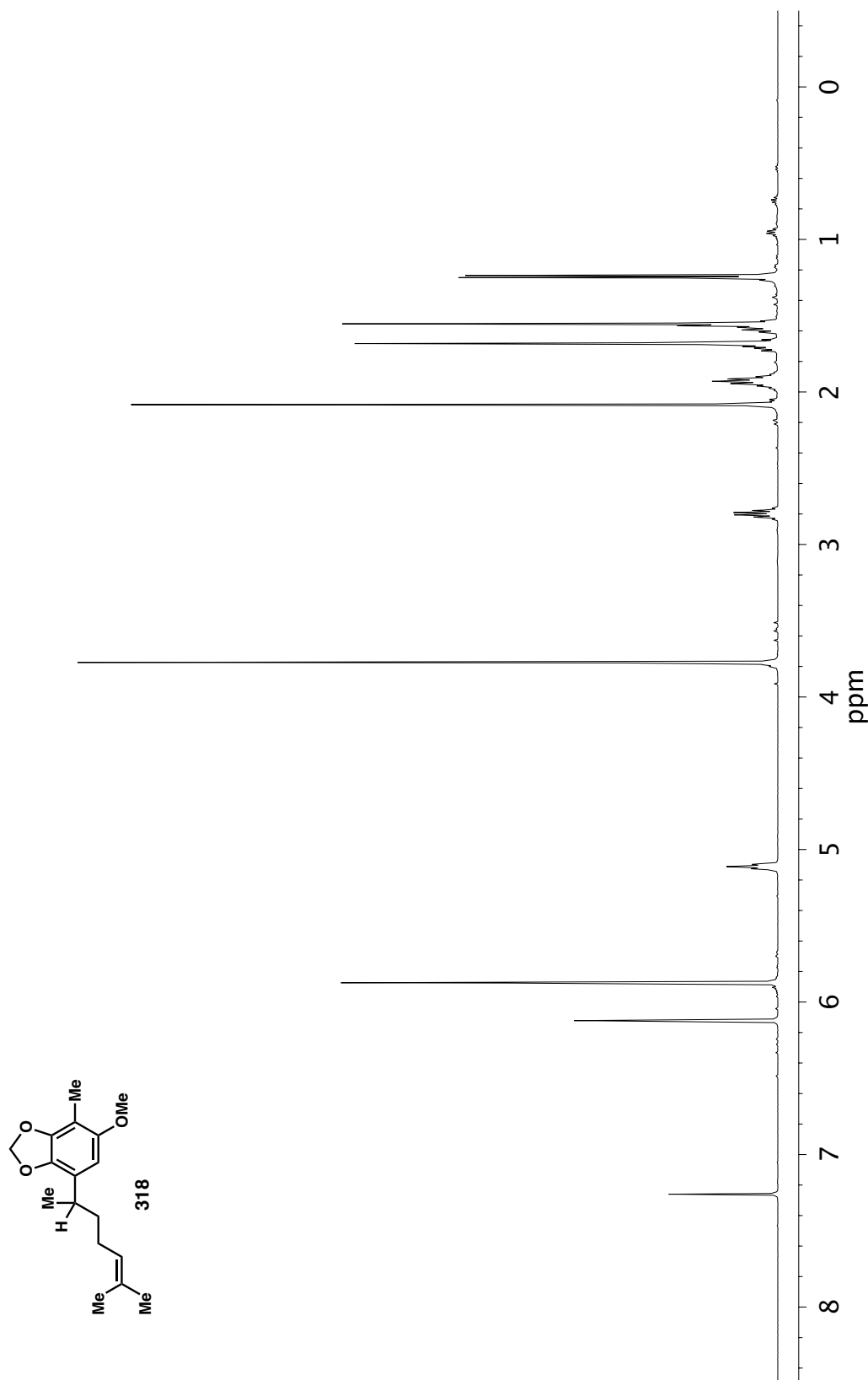


Figure A7.8. ^1H NMR (400 MHz, CDCl_3) of compound 318.

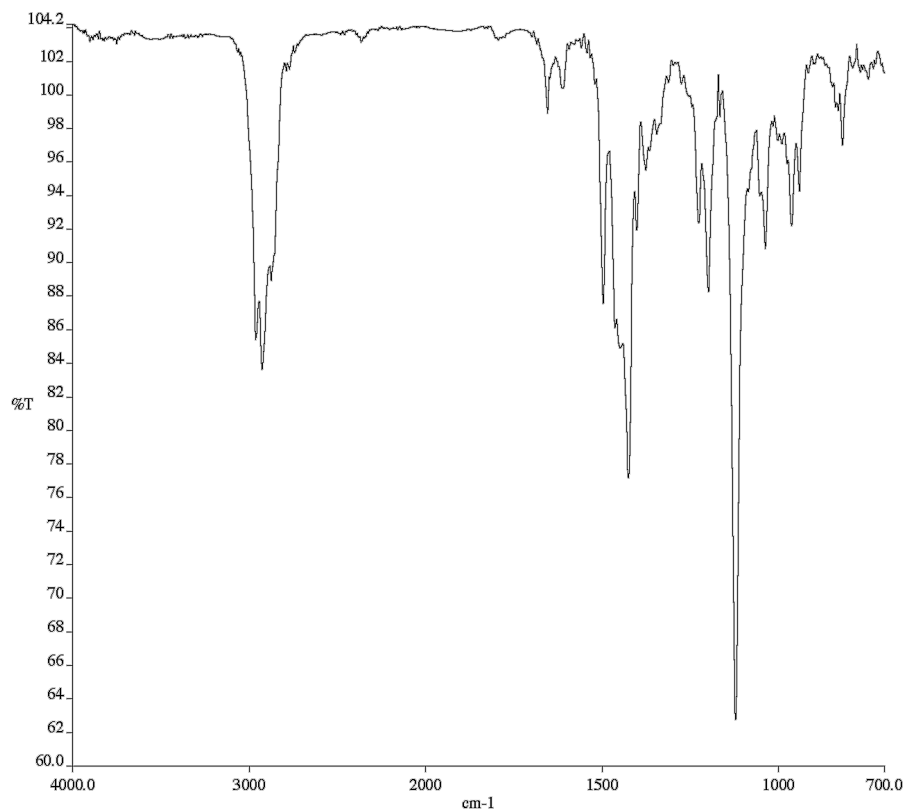


Figure A7.9. Infrared spectrum (Thin Film, NaCl) of compound 318.

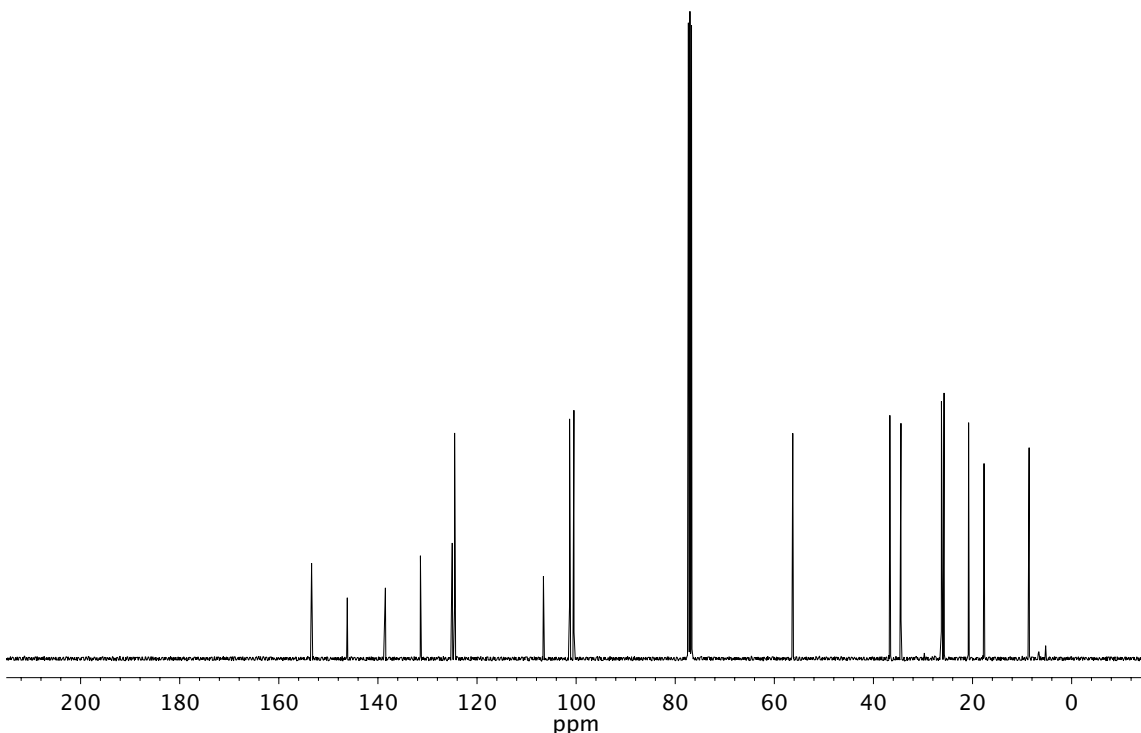


Figure A7.10. ¹³C NMR (100 MHz, CDCl₃) of compound 318.

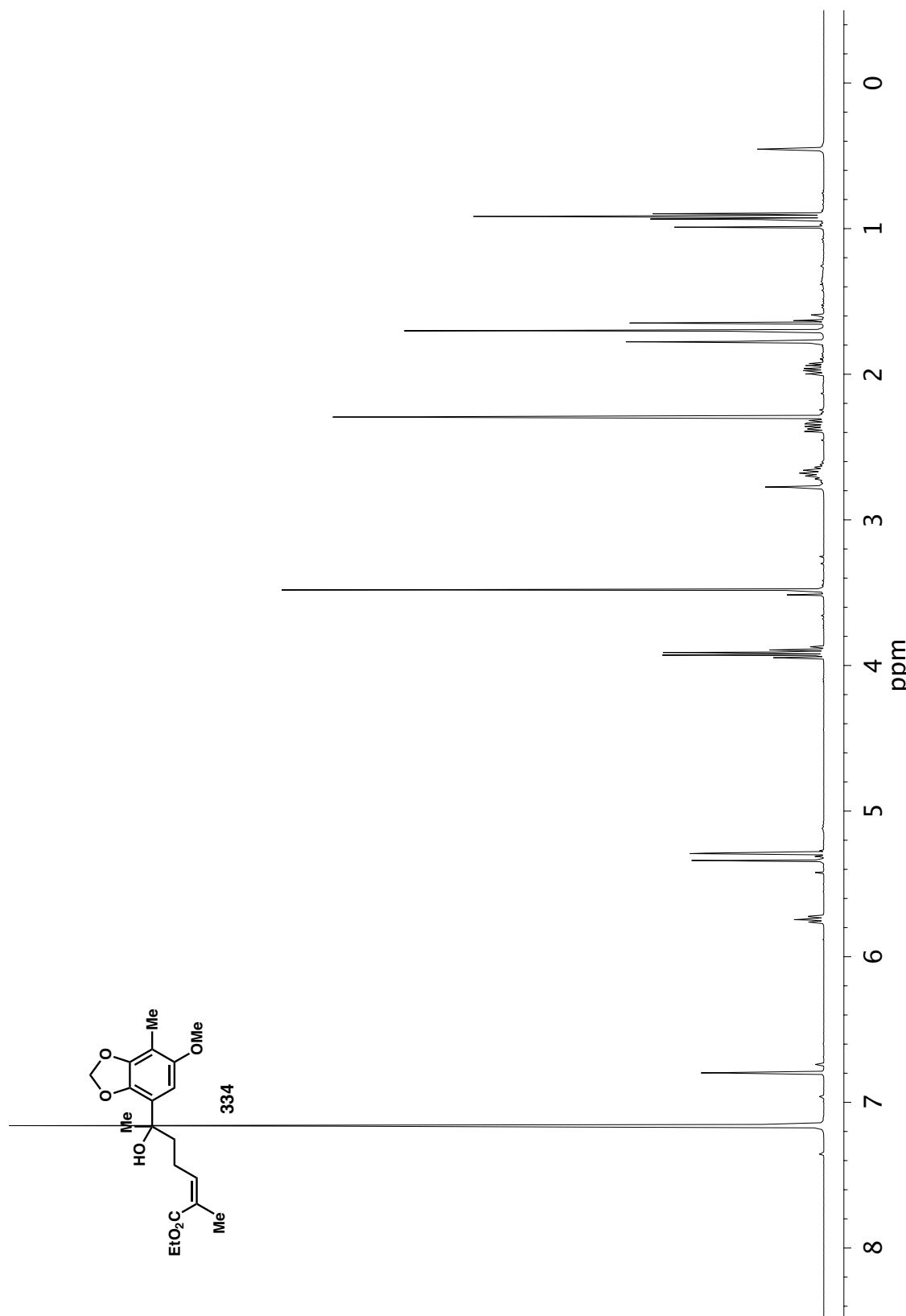


Figure A7.11. ^1H NMR (400 MHz, C_6D_6) of compound 334.

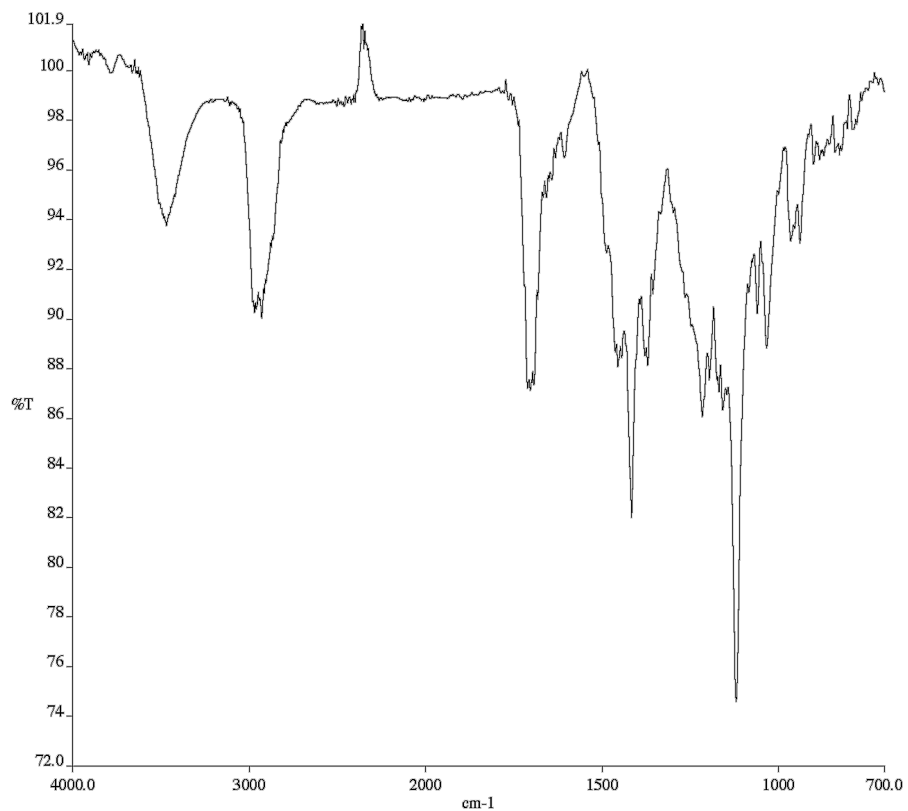


Figure A7.12. Infrared spectrum (Thin Film, NaCl) of compound **334**.

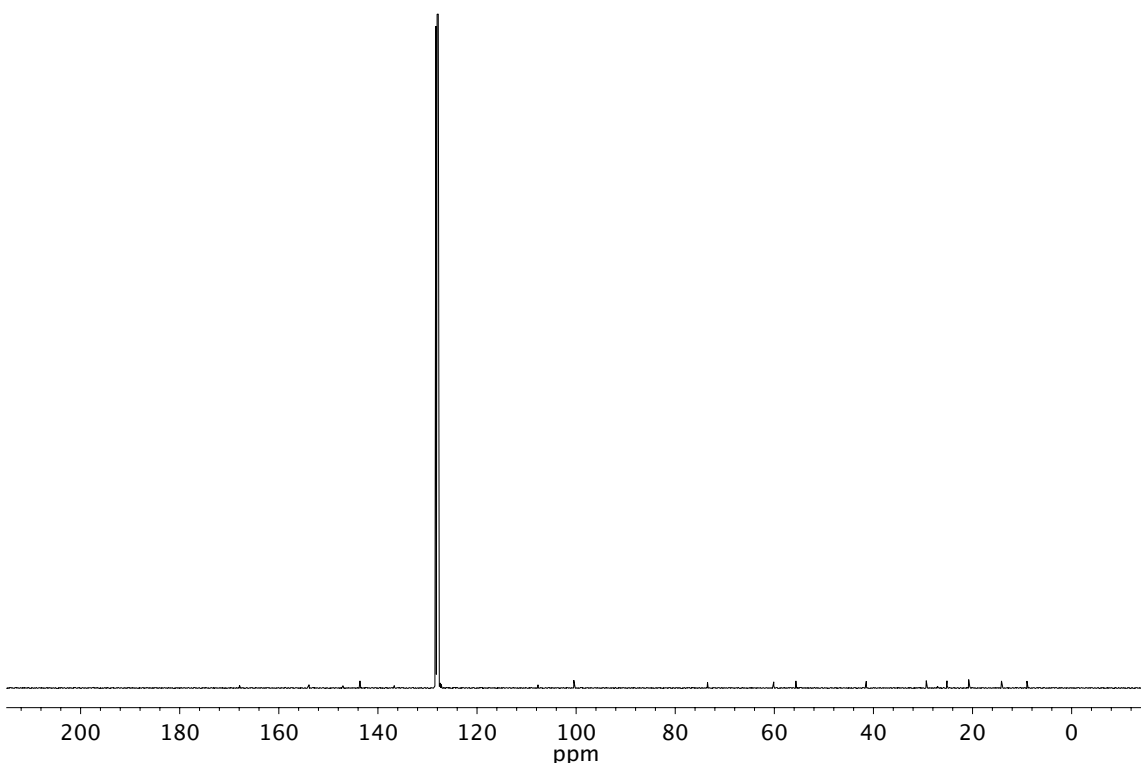


Figure A7.13. ^{13}C NMR (100 MHz, C_6D_6) of compound **334**.

A7.11 REFERENCES AND NOTES

- (1) Ma, S.-G.; Lin, M.-B.; Li, L.; Liu, Y.-B.; Qu, J.; Li, Y.; W, X.-J.; Wang, R.-B.; Xu, S.; Hou, Q.; Yu, S.-S. *Org. Lett.* **2017**, *19*, 6160–6163.
- (2) Ogliaruso, M. A.; Romanelli, M. G.; Becker, E. I. *Chem. Rev.* **1965**, *65*, 261–367.
- (3) Dong, S.; Qin, T.; Hamel, E.; Beutler, J. A.; Porco, J. A. Jr. *J. Am. Chem. Soc.* **2012**, *134*, 19782–19787.
- (4) Hafner, K.; Rieper, W. *Angew. Chemie. Int. Ed.* **1970**, *9*, 248.
- (5) Harmata, M.; Barnes, C. L.; Brackley, J.; Bohnert, G.; Kirchoefer, P.; Kurti, L.; Rashatasakhon, P. *J. Org. Chem.* **2001**, *66*, 5232–5236.
- (6) Toth, J. E.; Fuchs, P. L. *J. Org. Chem.* **1987**, *52*, 473–475.
- (7) Baraldi, P. G.; Barco, A.; Benetti, S.; Pollini, G. P.; Polo, E.; Simoni, D. *J. Soc. Chem. Commun.* **1984**, *16*, 1049–1050.
- (8) (a) Deb, S.; Chakraborti, R.; Ghatak, U. R. *Synth. Comm.* **1992**, *23*, 913–924.; (b) Selman, S.; Eastham, J. F. *Quarterly Reviews, Chem. Soc.* **1960**, *14*, 221–235.
- (9) Zhou, B.; Guo, J.; Danishefsky, S. J.; *Org. Lett.* **2002**, *4*, 43–46.
- (10) (a) Huang, Z.; Lumb, J.-P. *Angew. Chemie. Int. Ed.* **2016**, *55*, 11543–11547.; (b) Hayakawa, I.; Watanbe, H.; Kigoshi, H. *Tetrahedron* **2008**, *64*, 5873–5877.; (c) Churcher, I.; Hallett, D.; Magnus, P. *J. Am. Chem. Soc.* **1998**, *120*, 3518–3519.
- (11) Banwell, M. G.; Jury, J. C. *OPPI Briefs* **2004**, *36*, 87–91.
- (12) (a) Ishibashi, H.; Ishihara, K.; Yamamoto, H. *J. Am. Chem. Soc.* **2004**, *126*, 11122–11123.; (b) Kubo, A.; Nakahara, S.; Inaba, K.; Kitahara, Y. *Chem. Pharm.*

- Bull.* **1986**, *34*, 4056–4068. (c) Nicolaou, K. C.; Wang, J.; Tang, Y.; Botta, L. *J. Am. Chem. Soc.* **2010**, *132*, 11350–11363.
- (13) Chen, J.; Nikolovska-Coleska, Z.; Wang, G.; Qiu, S.; Wang, S. *Bioorg. Med. Chem. Lett.* **2006**, *16*, 5805–5808.
- (14) Barot, B. C.; Pinnick, H. W. *J. Org. Chem.* **1981**, *46*, 2981–2983.
- (15) Liu, J.; Ma, D. *Angew. Chem. Int. Ed.* **2008**, *57*, 6676–6680.
- (16) Burns, A. S.; Rychnovsky, S. D. *J. Am. Chem. Soc.* **2019**, *141*, 13295–13300.
- (17) Emsermann, J.; Opatz, T. *Eur. J. Org. Chem.* **2017**, *23*, 3362–3372.
- (18) Lee, H.-Y.; Kim, W.-Y.; Lee, S. *Tetrahedron Lett.* **2007**, *48*, 1407–1410.
- (19) Liao, X.; Stanley, L. M.; Hartwig, J. F. *J. Am. Chem. Soc.* **2011**, *133*, 2088–2091.
- ²⁰ Glowacka, I. E.; Balzarini, J.; Wroblewski, A. E. *Eur. J. Med. Chem.* **2013**, *70*, 703–722.

APPENDIX 8

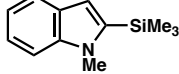
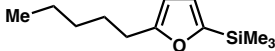
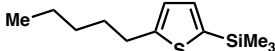
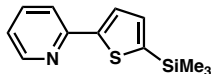
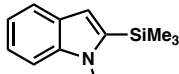
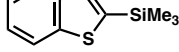
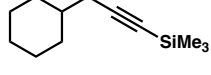
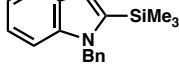
Notebook Cross-Reference for New Compounds

The following notebook cross-reference provides the file name for all original spectroscopic data obtained for new compounds presented within this thesis. The information is organized by chapter or appendix and sequentially by compound number. All ^1H NMR, ^{13}C NMR, as well as any additional data (i.e., two-dimensional NMR) are electronically stored on the Caltech NMR laboratory server (mangia.caltech.edu, most typically under the usernames ‘dschuman’ or ‘bogerliu’, or ‘nnesnas’ and on the Stoltz group server. Electronic copies of all IR spectra can also be found on the Stoltz group server. All laboratory notebooks are stored in the Stoltz group archive.

Table A8.1 Notebook cross-reference for compounds in Chapter 2

Compound	Chemical Structure	¹ H NMR	¹³ C NMR	IR
120		WLB-X-159-1-7-prepHPLC	WLB-X-159-1-7-prepHPLC	WLB-X-159-1-7-prepHPLC
121 R = H		WBL-X-159-1-5-prepHPLC	WBL-X-159-1-5-prepHPLC	WBL-X-159-1-5-prepHPLC
121 R = SiHET2		WBL-X-159-1-6-prepHPLC	WBL-X-159-1-6-prepHPLC	WBL-X-159-1-6-prepHPLC
122		WBL-X-271-C=H	WBL-X-271-C=H	WBL-X-271
123		WBL-IX-241-1-C+H	WBL-IX-241-1-C+H	WBL-IX-241-1
124		WBL-IX-245-C_H	WBL-IX-245-C_H	WBL-IX-245
201		NN-103p2	NN-103p2	NN-103-N-Me-3cyclopropylindole
205		WBL-IX-239-H	WBL-IX-239-C	DPS-WBL-ix-239
208		WBL-X-261-C+H+HSQC	WBL-X-261-C+H+HSQC	WBL-X-261

Table A8.2 Notebook cross-reference for compounds in Chapter 3

Compound	Chemical Structure	¹ H NMR	¹³ C NMR	IR
184		DPS-II-131d	DPS-II-191d	DPS-IV-203_v1
235		DPS-III-23b	DPS-III-23b	DPS-VI-241
236		DPS-III-27c	DPS-III-27c	DPS-VI-233
237		DPS-III-19_b_H	DPS-III-19_b_H	DPS-VI-235
238		DPS-III-29b	DPS-III-29b_13c	DPS-VI-213_4
71		DPS-VI-197	DPS-VI-197	DPS-VI-197
239		DPS-VI-199_f8_char	DPS-VI-199_f8_char_13c	DPS-VI-199_2
240		DPS-III-283_v60	DPS-III-283_v60	DPS-IV-207
241		DPS-IV-209_4-8_c6d6_2	DPS-IV-209_4-8_c6d6_2	DPS-IV-201_4

Compound	Chemical Structure	^1H NMR	^{13}C NMR	IR
242		DPS-II-81	DPS-VI-231	DPS-VI-231
243		DPS-I-95D	DPS-VI-239_11	DPS-VI-239_11
244		WBL-IX-55-C+H	WBL-IX-55-C+H	DPS-VI-203

Table A8.3 Notebook cross-reference for compounds in Appendix 7.

Compound	Chemical Structure	^1H NMR	^{13}C NMR	IR
291		DPS-IV-269	DPS-IV-269	DPS-VI-121_20-22
317		DPS-V-123	DPS-V-123	DPS-VI-33
318		DPS-VI-39	DPS-VI-39	DPS-VI-39
334		DPS-VI-71	DPS-VI-71	DPS-VI-71

COMPREHENSIVE BIBLIOGRAPHY

Arde, P.; Reddy, V.; Anand, R. V. *RSC Adv.* **2014**, *4*, 49775–49779.

Baba, T.; Kato, A.; Yuasa, H. Toriyama, F.; Handa, H.; Ono, Y. *Catal. Today* **1998**, *44*, 271–276.

Bähr, S.; Oestreich, M. *Angew. Chem. Int. Ed.* **2017**, *56*, 52–59.

Ball, L. T.; Lloyd-Jones, G. C.; Russell, C. A. *Science* **2012**, *337*, 1644–1648.

Bandini, M.; Eichholzer, A. *Angew. Chem., Int. Ed.* **2009**, *48*, 9608–9644.

Banerjee, S.; Yang, Y.-F.; Jenkins, I. D.; Liang, Y.; Toutov, A. A.; Liu, W.-B.; Schuman, D. P.; Grubbs, R. H.; Stoltz, B. M.; Krenske, E. H.; Houk, K. N.; Zare, R. N. *J. Am. Chem. Soc.* **2017**, *139*, 6880–6887.

Banks, J. T.; Scaiano, J. C.; Adam, W.; Oestrich, R. S. *J. Am. Chem. Soc.* **1993**, *115*, 2473.

Banwell, M. G.; Jury, J. C. *OPPI Briefs* **2004**, *36*, 87–91.

Baraldi, P. G.; Barco, A.; Benetti, S.; Pollini, G. P.; Polo, E.; Simoni, D. *J. Soc. Chem. Commun.* **1984**, *16*, 1049–1050.

Barham, J. P.; Coulthard, G.; Emery, K. J.; Doni, E.; Cumine, F.; Nocera, G.; John, M. P.; Berlouis, L. E. A.; McGuire, T.; Tuttle, T.; Murphy, J. A. *J. Am. Chem. Soc.* **2016**, *138*, 7402–7410.

Barham, J. P.; Coulthard, G.; Kane, R. G.; Delgado, N.; John, M. P.; Murphy, J. A. *Angew. Chem., Int. Ed.* **2016**, *55*, 4492–4496.

Barone, V.; Cossi, M. *J. Phys. Chem. A* **1998**, *102*, 1995–2001.

Barot, B. C.; Pinnick, H. W. *J. Org. Chem.* **1981**, *46*, 2981–2983.

Barry, A. J.; Gilkey, J. W.; Hook, D. E. in *Metal-Organic Compounds*, Vol. 23, Advances in Chemistry; American Chemical Society, Washington D.C., USA **1959**, pp 246–264.

Barry, A. J.; Gilkey, J. W.; Hook, D. E. *Ind. Eng. Chem. Res.* **1959**, *51*, 131–138.

Becke, A. D. *J. Chem. Phys.* **1993**, *98*, 1372–1377.

Becke, A. D. *J. Chem. Phys.* **1993**, *98*, 5648–5652.

Bennett, S. W.; Eaborn, C.; Hudson, A.; Jackson, R. A.; Root, K. D. *J. Chem. Soc., A* **1970**, 348–351.

Bergman, R. G. *Nature* **2007**, *446*, 391–393.

Blanksby, S. J.; Ellison, G. B. *Acc. Chem. Res.* **2003**, *36*, 255–263.

Boeser, C. L.; Holder, J. C.; Taylor, B. L. H.; Houk, K. N.; Stoltz, B. M.; Zare, R. N. *Chemical Sci.* **2015**, *6*, 1917–1922;

Bottoni, A. *J. Phys. Chem. A.* **1997**, *101*, 4402–4408.

Boyer, J.; Corriu, R. J. P.; Perz, R.; Reye, C. *Tetrahedron* **1981**, *37*, 2165–2171.

Bravo-Zhivotovskii, D.; Ruderfer, I.; Yuzefovich, M.; Kosa, M.; Botoshansky, M.; Tumanskii, B.; Apeloig, Y. *Organometallics* **2005**, *24*, 2698–2704.

Brownell, K. R.; McCrory, C. C. L.; Chidsey, C. E. D.; Perry, R. H.; Zare, R. N.; Waymouth, R. M., *J. Am. Chem. Soc.* **2013**, *135*, 14299–14305.

Burns, A. S.; Rychnovsky, S. D. *J. Am. Chem. Soc.* **2019**, *141*, 13295–13300.

Cai, Y.; Roberts, B. P. *J. Chem. Soc., Perkin Trans. I* **1998**, 467–476.

Calas, R.; Bourgeois, P. *C. R. Acad. Sc. Paris* **1969**, *268*, 72–74.

Cernak, T.; Dykstra, K. D.; Tyagarajan, S.; Vachal, P.; Krska, S. W. *Chem. Soc. Rev.* **2016**, *45*, 546–576.

Chatgilialoglu, C. *Acc. Chem. Res.* **1992**, *25*, 188–194.

Chatgilialoglu, C. *Chem. Rev.* **1995**, *95*, 1229–1251.

Chatgilialoglu, C. *J. Organomet. Chem.* **2004**, *689*, 2912–2919.

Chatgilialoglu, C.; Ingold, K. U.; Scaiano, J. C. *J. Am. Chem. Soc.* **1983**, *105*, 3292–3296.

Chatgilialoglu, C.; Scaiano, J. C.; Ingold, K. U. *Organometallics* **1982**, *1*, 466–469.

Chen, J.; Nikolovska-Coleska, Z.; Wang, G.; Qiu, S.; Wang, S. *Bioorg. Med. Chem. Lett.* **2006**, *16*, 5805–5808.

Chen, Q.-A.; Klare, H. F. T.; Oestreich, M. *J. Am. Chem. Soc.* **2016**, *138*, 7868–7871.

Cheng, C.; Hartwig, J. F. *Chem. Rev.* **2015**, *115*, 8946–8975.

Cheng, C.; Hartwig, J. F. *J. Am. Chem. Soc.* **2015**, *137*, 592–595.

Cheng, C.; Hartwig, J. F. *Science* **2014**, *343*, 853–857.

Chinchilla, R. Nájera, C. *Chem. Soc. Rev.* **2011**, *40*, 5084–5121.

Chisholm, M. H.; Drake, S. R.; Naiini, A. A.; Streib, W. E. *Polyhedron* **1991**, *10*, 337–345.

Chuit, C.; Corriu, R. J. P.; Reye, C.; Young, J. C. *Chem. Rev.* **1993**, *93*, 1371–1448.

Churcher, I.; Hallett, D.; Magnus, P. *J. Am. Chem. Soc.* **1998**, *120*, 3518–3519.

Cole, S. J.; Kirwan, J. N.; Roberts, B. P.; Willis, C. R. *J. Chem. Soc., Perkin Trans. I* **1991**, 103–112.

Colvin, E. *Silicon in Organic Synthesis*; Butterworth: New York, 1981.

Corriu, R. J. P.; Guerin, C.; Henner, B.; Wang, Q. *Organometallics* **2002**, *10*, 2297–2303.

Corriu, R. J. P.; Perz, R.; Reye, C. *Tetrahedron* **1983**, *39*, 999–1009.

Corriu, R.; Guérin, C.; Henner, B.; Wang, Q. *J. Organomet. Chem.* **1989**, *365*, C7–C10.

Cossi, M.; Rega, N.; Scalmani, G.; Barone, V. *J. Comput. Chem.* **2003**, *24*, 669–681.

Couzijn, E. P. A.; Ehlers, A. W.; Schakel, M.; Lammertsma, K. *J. Am. Chem. Soc.* **2006**, *128*, 13634–13639.

Couzijn, E. P. A.; Slootweg, J. C.; Ehlers, A. W.; Lammertsma, K. *J. Am. Chem. Soc.* **2010**, *132*, 18127–18140.

Curless, L. D.; Clark, E. R.; Dunsford, J. J.; Ingleson, M. J. *Chem. Commun.* **2014**, *50*, 5270–5272

Curless, L. D.; Ingleson, M. J. *Organometallics* **2014**, *33*, 7241–7246.

Deb, S.; Chakraborti, R.; Ghatak, U. R. *Synth. Comm.* **1992**, *23*, 913–924.;

Deiters, J. A.; Holmes, R. R. *J. Am. Chem. Soc.* **1990**, *112*, 7197–7202.

Denmark, S. E.; Baird, J. D. *Chem. Eur. J.* **2006**, *12*, 4954–4963.

Denmark, S. E.; Beutner, G. L. *Angew. Chem., Int. Ed.* **2008**, *47*, 1560–1638.

Denmark, S. E.; Ober, M. H. *Aldrichimica Acta* **2003**, *36*, 75–85.

Dialer, L. O.; Selivanova, S. V.; Müller, C. J.; Müller, A.; Stellfeld, T.; Graham, K.; Dinkelborg, L. M.; Krämer, S. D.; Dichtel, W. R.; Keresztes, I.; Arslan, H.; Hein, S. J. *Org. Lett.* **2014**, *16*, 4416–4419.

DiRocco, D. A.; Dykstra, K.; Krska, S.; Vachal, P.; Conway, D. V.; Tudge, M. *Angew. Chem., Int. Ed.* **2014**, *53*, 4802–4806.

Ditchfield, R.; Hehre, W. J.; Pople, J. A. *J. Chem. Phys.* **1971**, *54*, 724–728.

Dong, S.; Qin, T.; Hamel, E.; Beutler, J. A.; Porco, J. A. Jr. *J. Am. Chem. Soc.* **2012**, *134*, 19782–19787.

Dougherty, D. A. *Acc. Chem. Res.* **2013**, *46*, 885.

Du, W.; Kaskar, B.; Blumbergs, P.; Subramanian, P. K.; Curran, D. P. *Bioorg. Med. Chem.* **2003**, *11*, 451–458.

Eaborn, C. *J. Organomet. Chem.* **1975**, *100*, 43–57.

Emsermann, J.; Opatz, T. *Eur. J. Org. Chem.* **2017**, *23*, 3362–3372.

Fallon, T.; Oestreich, M. *Angew. Chem., Int. Ed.* **2015**, *54*, 12488–12491.

Fedorov, A.; Toutov, A. A.; Swisher, N. A.; Grubbs, R. H. *Chem. Sci.* **2013**, *4*, 1640–1645.

Feigl, A.; Bockholt, A.; Weis, J.; Rieger, B. Springer: Berlin, 2011.

Fleming, I.; Dunoguès, J.; Smithers, R. *Org. React.* **1989**, *37*, 57.

Fornarini, S. *J. Org. Chem.* **1988**, *53*, 1314–1316.

Franz, A. K.; Wilson, S. O. *J. Med. Chem.* **2013**, *56*, 388–405.

Frisch, M. J.; Trucks, G. W.; Schlegel, H. B.; Scuseria, G. E.; Robb, M. A.; Cheeseman, J. R.; Scalmani, G.; Barone, V.; Mennucci, B.; Petersson, G. A.; Nakatsuji, H.; Caricato, M.; Li, X.; Hratchian, H. P.; Izmaylov, A. F.; Bloino, J.; Zheng, G.; Sonnenberg, J. L.; Hada, M.; Ehara, M.; Toyota, K.; Fukuda, R.; Hasegawa, J.; Ishida, M.; Nakajima, T.; Honda, Y.; Kitao, O.; Nakai, H.; Vreven, T.; Montgomery, Jr., J. A.; Peralta, J. E.; Ogliaro, F.; Bearpark, M.; Heyd, J. J.; Brothers, E.; Kudin, K. N.; Staroverov, V. N.; Keith, T.; Kobayashi, R.; Normand, J.; Raghavachari, K.; Rendell, A.; Burant, J. C.; Iyengar, S. S.; Tomasi, J.; Cossi, M.; Rega, N.; Millam, J. M.; Klene, M.; Knox, J. E.; Cross, J. B.; Bakken, V.; Adamo, C.; Jaramillo, J.; Gomperts, R.; Stratmann, R. E.; Yazyev, O.; Austin, A. J.; Cammi, R.; Pomelli, C.; Ochterski, J. W.; Martin, R. L.; Morokuma, K.; Zakrzewski, V. G.; Voth, G. A.; Salvador, P.; Dannenberg, J. J.; Dapprich, S.;

Daniels, A. D.; Farkas, O.; Foresman, J. B.; Ortiz, J. V.; Cioslowski, J.; Fox, D. J. Gaussian 09, Rev. D.01; Gaussian, Inc., Wallingford, CT, 2010.

Fujiki, M. *Polymer Journal* **2003**, *35*, 297–344.

Fujiwara, Y.; Dixon, J. A.; O’Hara, F.; Funder, E. D.; Dixon, D. D.; Rodriguez, R. A.; Baxter, R. D.; Herlé, B.; Sach, N.; Collins, M. R.; Ishihara, Y.; Baran, P. S. *Nature* **2012**, *492*, 95–99.

Garrett, C. E.; Prasad, K. *Adv. Synth. Catal.* **2004**, *346*, 889–900.

Gleiter, R.; Werz, D. B. *Chem. Rev.* **2010**, *110*, 4447–4488.

Godula, K.; Sames, D. *Science* **2006**, *312*, 67–72.

Hafner, K.; Rieper, W. *Angew. Chemie. Int. Ed.* **1970**, *9*, 248.

Hagemann, M.; Berger, R. J. F.; Hayes, S. A.; Stammler, H-G.; Mitzel, N. W. *Chem. Eur. J.* **2008**, *14*, 11027–11038.

Han, Y.; Zhang, S.; He, J.; Zhang, Y. *J. Am. Chem. Soc.* **2017**, *139*, 7399–7407.

Hariharan, P. C.; Pople, J. A. *Theor. Chim. Acta* **1973**, *28*, 213–222.

Harmata, M.; Barnes, C. L.; Brackley, J.; Bohnert, G.; Kirchoefer, P.; Kurti, L.; Rashatasakhon, P. *J. Org. Chem.* **2001**, *66*, 5232–5236.

Hartwig, J. F. *Acc. Chem. Res.* **2012**, *45*, 864–873.

Hata, T.; Kitagawa, H.; Masai, H.; Kurahashi, T.; Shimizu, M.; Hiyama, T. *Angew. Chem. Int. Ed.* **2001**, *40*, 790–792.

Hayakawa, I.; Watanbe, H.; Kigoshi, H. *Tetrahedron* **2008**, *64*, 5873–5877.;

Hehre, W. J.; Ditchfield, R.; Pople, J. A. *J. Chem. Phys.* **1972**, *56*, 2257–2261.
Holmes, R. R. *Chem. Rev.* **1996**, *96*, 927–950.

Honraedt, A.; Raux, M.-A.; Le Grogne, E.; Jacquemin, D.; Felpin, F.-X. *Chem. Commun.* **2014**, *50*, 5236–5238.

Hu, S.-W.; Wang, Y.; Wang, X.-Y.; Chu, T.-W.; Liu, X.-Q. *J. Phys. Chem. A* **2004**, *108*, 1448–1459.

Huang, Z.; Lumb, J.-P. *Angew. Chemie. Int. Ed.* **2016**, *55*, 11543–11547.;

Ido, E.; Kakiage, K.; Kyomen, T.; Hanaya, M. *Chem. Lett.* **2012**, *41*, 853–854.

Ingram, A. J.; Solis-Ibarra, D.; Zare, R. N.; Waymouth, R. M. *Angew. Chem. Int. Ed.* **2014**, *53*, 5648–5652;

Ishibashi, H.; Ishihara, K.; Yamamoto, H. *J. Am. Chem. Soc.* **2004**, *126*, 11122–11123.;

Ishikawa, J.-I.; Inoue, K.; Itoh, M. *J. Organomet. Chem.* **1998**, *552*, 303–311.

Ishikawa, J.-I.; Itoh, M. *J. Catal.* **1999**, *185*, 454–461.

Itami, K.; Yoshida, J.-i. *Synlett* **2006**, *2*, 157–180.

Itoh, M.; Kobayashi, M.; Ishikawa, J. *Organometallics* **1997**, *16*, 3068–3070.

Itoh, M.; Mitsuzuka, M.; Utsumi, T.; Iwata, K.; Inoue, K. *J. Organomet. Chem.* **1994**, *476*, C30–C31.

Jia, W.-L.; Westerveld, N.; Wong, K. M.; Morsch, T.; Hakkenes, M.; Naksomboon, K.; Fernandez-Ibanez, M. A. *Org. Lett.* **2019**, *21*, 9339–9342.

Jin, J.; MacMillan, D. W. C. *Nature* **2015**, *525*, 87–90.

Kakiuchi, F.; Matsumoto, M.; Sonoda, M.; Fukuyama, T.; Chatani, N.; Murai, S.; Furukawa, N.; Seki, Y. *Chem. Lett.* **2000**, *29*, 750–751.;

Kanabus-Kaminska, J. M.; Hawari, J. A.; Griller, D.; Chatgilialoglu, C. *J. Am. Chem. Soc.* **1987**, *109*, 5267–5268.

Klare, H. F. T.; Oestreich, M.; Ito, J.-i.; Nishiyama, H.; Ohki, Y.; Tatsumi, K. *J. Am. Chem. Soc.* **2011**, *133*, 3312–3315.

Kozhushkov, S. I.; Wagner-Gillen, K.; Khlebnikov, A. F.; de Meijere, A. *Synthesis* **2010**, *2010*, 3967–3973.

Kubo, A.; Nakahara, S.; Inaba, K.; Kitahara, Y. *Chem. Pharm. Bull.* **1986**, *34*, 4056–4068.

Kumar, Y.; Florvall, L. *Syn Comm.* **1983**, *13*, 489–493.

Kumpf, R.; Dougherty, D. *Science* **1993**, *261*, 1708.

Kurahashi, T.; Hata, T.; Masai, H.; Kitagawa, H.; Shimizu, M.; Hiyama, T. *Tetrahedron* **2002**, *58*, 6381–6395.

Kursanov, D. N.; Parnes, Z. N.; Bolestova, G. I.; Belen'KII *Tetrahedron* **1975**, *31*, 311–315

Labinger, J. A.; Bercaw J. E. *Nature* **2002**, *417*, 507–514.

Langkopf, E.; Schinzer, D. *Chem. Rev.* **1995**, *95*, 1375–1408.

Lee, C.; Yang W.; Parr, R. G. *Phys. Rev. B* **1988**, *37*, 785–789.

Lee, H.-Y.; Kim, W.-Y.; Lee, S. *Tetrahedron Lett.* **2007**, *48*, 1407–1410.

Légaré, M.-A.; Courtemanche, M.-A.; Rochette, É.; Fontaine, F.-G. *Science* **2015**, *349*, 513–516.

Legault, C. Y. CYLView, 1.0b; Université de Sherbrooke, Canada, **2009**;
<http://www.cylview.org>.

Leifert, D.; Studer, A. *Org. Lett.* **2015**, *17*, 386–389.

Li, C.-J.; Trost, B. M. *Proc. Natl. Acad. Sci. USA* **2008**, *105*, 13197–13202. Clark, J. H. *Green Chem.* **1999**, *1*, 1–8.

Liao, X.; Stanley, L. M.; Hartwig, J. F. *J. Am. Chem. Soc.* **2011**, *133*, 2088–2091.

Liu, C.; Yuan, J.; Gao, M.; Tang, S.; Li, W.; Shi, R.; Lei, A. *Chem. Rev.* **2015**, *115*, 12138–12204.

Liu, J.; Ma, D. *Angew. Chem. Int. Ed.* **2008**, *57*, 6676–6680

Liu, W.-B.; Schuman, D. P.; Yang, Y.-F.; Toutov, A. A.; Liang, Y.; Klare, H. F. T.; Nesnas, N.; Oestreich, M.; Blackmond, D. G.; Virgil, S. C.; Banerjee, S.; Zare, R. N.; Grubbs, R. H.; Houk, K. N.; Stoltz, B. M. *J. Am. Chem. Soc.* **2017**, *139*, 6867–6879.

Liu, X.; Xu, C.; Wang, M.; and Liu, Q. *Chem. Rev.* **2015**, *115*, 683–730.

Lu, B.; Falck, J. R. *Angew. Chem., Int. Ed.* **2008**, *47*, 7508–7510.

Lucarini, M.; Marchesi, E.; Pedulli, G. F.; Chatgilialoglu, C. *J. Org. Chem.* **1998**, *63*, 1687–1693.

Ma, S.-G.; Lin, M.-B.; Li, L.; Liu, Y.-B.; Qu, J.; Li, Y.; W, X.-J.; Wang, R.-B.; Xu, S.; Hou, Q.; Yu, S.-S. *Org. Lett.* **2017**, *19*, 6160–6163.

Ma, Y.; Wang, B.; Zhang, L.; Hou, Z. *J. Am. Chem. Soc.* **2016**, *138*, 3663–3666.

Mendenhall, G. D. *Tetrahedron Lett.* **1983**, *24*, 451.

Möckel, R.; Hilt, G. *Org. Lett.* **2015**, *17*, 1644–1647.

Murai, M.; Takeuchi, Y.; Yamauchi, K.; Kuninobu, Y.; Takai, K. *Chem. Eur. J.* **2016**, *22*, 6048–6058.

Nakao, Y.; Hiyama, T. *Chem. Soc. Rev.* **2011**, *40*, 4893–4901.

Newcomb, M. *Tetrahedron* **1993**, *49*, 1151–1176.

Nicolaou, K. C.; Wang, J.; Tang, Y.; Botta, L. *J. Am. Chem. Soc.* **2010**, *132*, 11350–11363.

Nozawa-Kumada, K.; Osawa, S.; Sasaki, M.; Chataigner, I.; Shigeno, M.; Kondo, Y. *J. Org. Chem.* **2017**, *82*, 9487–9496.

O'Brien, A. G.; Maruyama, A.; Inokuma, Y.; Fujita, M.; Baran, P. S.; Blackmond, D. G. *Angew. Chem., Int. Ed.* **2014**, *53*, 11868–11871.

O'Hara, F.; Blackmond, D. G.; Baran, P. S. *J. Am. Chem. Soc.* **2013**, *135*, 12122–12134

Oglieruso, M. A.; Romanelli, M. G.; Becker, E. I. *Chem. Rev.* **1965**, *65*, 261–367.

Pangborn, A. M.; Giardello, M. A.; Grubbs, R. H.; Rosen, R. K.; and Timmers, F. J. *Organometallics*, **1996**, *15*, 1518.

Pangborn, A. M.; Giardello, M. A.; Grubbs, R. H.; Rosen, R. K.; Timmers, F. J. *Organometallics* **1996**, *15*, 1518–1520.

Penoni, A.; Palmisano, G.; Zhao, Y-L.; Houk, K. N.; Volkman, J.; Nicholas, K. M. *J. Am. Chem. Soc.* **2008**, *131*, 653–661

Perry, R. H.; Brownell, K. R.; Chingin, K.; Cahill, T. J.; Waymouth, R. M.; Zare, R. N., *Proc. Natl. Acad. Sci. USA* **2012**, *109*, 2246–2250;

Perry, R. H.; Cahill, T. J.; Roizen, J. L.; Du Bois, J.; Zare, R. N. *Proc. Natl. Acad. Sci. USA* **2012**, *109*, 18295–18299;

Perry, R. H.; Splendore, M.; Chien, A.; Davis, N. K.; Zare, R. N., *Angew. Chem. Int. Ed.* **2011**, *50*, 250–254;

Piers, W. E.; Marwitz, A. J. V.; Mercier, L. G. *Inorg. Chem.* **2011**, *50*, 12252–12262.
Postigo, A.; Kopsov, S.; Zlotsky, S. S.; Ferreri, C.; Chatgilialoglu, C. *Organometallics* **2009**, *28*, 3282–3287.

Rendler, S.; Oestreich, M. *Synthesis* **2005**, *11*, 1727–1747.

Ribereau, P.; Queguiner, G. *Tetrahedron* **1983**, *39*, 3593–3602.

Roberts, B. P. *Chem. Soc. Rev.* **1999**, *28*, 25–35.

Rochat, R.; Yamamoto, K.; Lopez, M. J.; Nagae, H.; Tsuru-gi, H.; Mashima, K. *Chem. Eur. J.* **2015**, *21*, 8112–8120

Rossi, R.; Bellina, F.; Lessi, M.; Manzini, C. *Adv. Synth. Catal.* **2014**, *356*, 17–117.

Sakakura, T.; Tokunaga, Y.; Sodeyama, T.; Tanaka, M. *Chem. Lett.* **1987**, *16*, 2375–2378.;

Sakurai, H.; Murakami, M. *Chem. Lett.* **1972**, *1*, 7–8.

Sakurai, H.; Murakami, M.; Kumada, M. *J. Am. Chem. Soc.* **1969**, *91*, 519–520.

Sasaki, M., Kondo, Y. *Org. Lett.* **2015**, *17*, 848–851.;

Schibli, R.; Reiher, M.; Ametamey, S. M. *J. Med. Chem.* **2013**, *56*, 7552–7563

Schley, N. D.; Fu, G. C. *J. Am. Chem. Soc.* **2014**, *136*, 16588–16593.

Schuman, D. P.; Liu, W.-B.; Nesnas, N.; Stoltz, B. M. Transition-Metal-Free Catalytic C–H Bond Silylation. In *Organosilicon Chemistry: Novel Approaches and*

Reactions; Hiyama, T., Oestreich, M., Eds.; Wiley-VCH: Weinheim, Germany, 2019; Chapter 7, pp. 213–239. ISBN: 978-3-527-34453-6.

Selman, S.; Eastham, J. F. *Quarterly Reviews, Chem. Soc.* **1960**, *14*, 221–235.

Sharma, R.; Kumar, R.; Kumar, I.; Singh, B.; Sharma, U. *Synthesis* **2015**, *47*, 2347–2366.

Shekar, S.; Brown, S. N. *J. Org. Chem.* **2014**, *79*, 12047–12055.

Shinzer, D.; Langkopf, E. *Chem. Rev.* **1995**, *95*, 1375–1406.

Showell, G. A.; Mills, J. S. *Drug Discov. Today* **2003**, *8*, 551–556.

Smith, A. J.; Young, A.; Rohrbach, S.; O'Connor, E. F.; Allison, M.; Wang, H. S.; Poole, D. L.; Tuttle, T.; Murphy, J. A. *Angew. Chem. Int. Ed.* **2017**, *56*, 13747–13751.

Sommer, L. H.; Korte, W. D.; Rodewald, P. G. *J. Am. Chem. Soc.* **1967**, *89*, 862–868.

Sommer, L. H.; Rodewald, P. G.; Parker, G. A. *Tetrahedron Lett.* **1962**, *3*, 821–824.

Sommer, L. H.; Ulland, L. A. *J. Am. Chem. Soc.* **1972**, *94*, 3803–3806.

Sommer, L. H.; Ulland, L. A. *J. Org. Chem.* **1972**, *37*, 3878–3881.

Sonnenschein, H.; Graubaum, H.; Hinze, C. (Gruenenthal GmbH, Aachen, Germany)

Substituted heteroaryl derivatives. U.S. Patent 8,138,187, March 20, 2012.

Sore, H. F.; Galloway, W. R. J. D.; Spring, D. R. *Chem. Soc. Rev.* **2012**, *41*, 1845–1866.

Stephan, D. W. *J. Am. Chem. Soc.* **2015**, *137*, 10018–10032.

Stephens, P. J.; Devlin, F. J.; Chabalowski, C. F.; Frisch, M. J. *J. Phys. Chem.* **1994**, *98*, 11623–11627.

Stephens, P. J.; Devlin, F. J.; Cheeseman, J. R.; Frisch, M. J. *J. Chem. Phys. A* **2001**, *105*, 5356.

Suginome, M.; Ito, Y. *Chem. Rev.* **2000**, *100*, 3221–3256.

Sun, X.; Wang, C.; Li, Z.; Zhang, S.; Xi, Z. *J. Am. Chem. Soc.* **2004**, *126*, 7172–7173.

Takano, Y.; Houk, K. N. *J. Chem. Theory Comput.* **2005**, *1*, 70–77.

Takáts, Z.; Wiseman, J. M.; Gologan, B.; Cooks, R. G. *Science* **2004**, *306*, 471.

Tamao K. *Proc. Jpn. Acad. Ser. B. Phys. Biol. Sci.* **2008**, *84*, 123–133.

Tauber, J.; Imbri, D.; Opatz, T. *Molecules* **2014**, *19*, 16190–16222.

Tobisu, M.; Ano, Y.; Chatani, N. *Chem. Asian J.* **2008**, *3*, 1585–1591.;

Toth, J. E.; Fuchs, P. L. *J. Org. Chem.* **1987**, *52*, 473–475.

Toukabri, R.; Shi, Y. *Vac. Sci. Technol. A*, **2013**, *31*, 061606-1.

Toutov, A. A.; Betz, K. N.; Haibach, M. C.; Romine, A. M.; Grubbs, R. H. *Org. Lett.* **2016**, *18*, 5776–5779.

Toutov, A. A.; Betz, K. N.; Schuman, D. P.; Liu, W.-B.; Fedorov, A.; Stoltz, B. M.; Grubbs, R. H. *J. Am. Chem. Soc.* **2017**, *139*, 1668–1674.

Toutov, A. A.; Liu, W.-B.; Betz, K. N.; Fedorov, A.; Stoltz, B. M.; Grubbs, R. H. *Nature* **2015**, *518*, 80–84.

Toutov, A. A.; Liu, W.-B.; Betz, K. N.; Stoltz, B. M.; Grubbs, R. H. *Nat. Protoc.* **2015**, *10*, 1897–1903.

Toutov, A. A.; Liu, W.-B.; Stoltz, B. M.; Grubbs, R. H. *Org. Synth.* **2016**, *93*, 263–271.

Toutov, A. A.; Salata, M.; Fedorov, A.; Yang, Y.-F.; Liang, Y.; Cariou, R.; Betz, K. N.; Couzijn, E. P. A.; Shabaker, J. W.; Houk, K. N.; Grubbs, R. H. *Nature Energy* **2017**, *2*, 17008.

Tucker, C. E.; Davidson, J.; Knochel, P. *J. Org. Chem.* **1992**, *57*, 3482–3485.

Valero, R.; Cuadrado, P.; Calle, M.; González-Nogal, A. M. *Tetrahedron* **2007**, *63*, 224–231.

Von Grotthuss, E.; Prey, S. E.; Bolte, M.; Lerner, H.-W.; Wagner, M. *J. Am. Chem. Soc.* **2019**, *141*, 6082–6091.

Voronkov, M. G.; Ushakova, N. I.; Tsukhanskaya, I. I.; Pukhnarevich, V. B. *J. Organomet. Chem.* **1984**, *264*, 39–48.

Wang, J.; Gurevich, Y.; Botoshansky, M.; Eisen, M. S. *J. Am. Chem. Soc.* **2006**, *128*, 9350–9351.

Wang, Y.; Watson, M. D. *J. Am. Chem. Soc.* **2006**, *128*, 2536–2537.

Weickgenannt, A.; Oestreich, M. *Chem. Asian J.* **2009**, *4*, 406–410.

Whisler, M. C.; MacNeil, S.; Snieckus, V.; Beak, P. *Angew. Chem., Int. Ed.* **2004**, *43*, 2206–2225.

Wireduaah, S.; Parker, T. M.; Lewis, M. *J. Phys. Chem. A* **2013**, *117*, 2598;

Wright, A. *J. Organomet. Chem.* **1978**, *145*, 307–314.

Xu, L.; Zhang, S.; Li, P. *Org. Chem. Front.* **2015**, *2*, 459–463.

Xu, Z.; Huang, W.-S.; Zhang, J.; Xu, L.-W. *Synthesis* **2015**, *47*, 3645–3668.

Yang, D.; Tanner, D. D. *J. Org. Chem.* **1986**, *51*, 2267–2270.

Yang, Y.; Wang, C. *Sci. China Chem.* **2015**, *58*, 1266–1279.

Yi, H.; Jutand, A.; Lei, A. *Chem. Commun.* **2015**, *51*, 545–548.

Yin, Q.; Klare, H. F. T.; Oestreich, M. *Angew. Chem., Int. Ed.* **2016**, *55*, 3204–3207.

Zaborovskiy, A. B.; Lutsyk, D. S.; Prystansky, R. E.; Kopylets, V. I.; Timokhin, V. I.
Zemolka, S.; Schunk, S.; Englberger, W.; Kogel, B.-Y.; Linz, K.; Schick, H.;
Zhang, F.; Wu, D.; Xu, Y.; Feng, X. *J. Mater. Chem.* **2011**, *21*, 17590–17600.

Zhang, L.; Yang, H.; Jiao, L. *J. Am. Chem. Soc.* **2016**, *138*, 7151–7160.

Zhao, Y.; Truhlar, D. G. *Theor. Chem. Acc.* **2008**, *120*, 215–241.

Zhou, B.; Guo, J.; Danishefsky, S. J.; *Org. Lett.* **2002**, *4*, 43–46.

Zhou, S.; Doni, E.; Anderson, G. M.; Kane, R. G.; MacDougall, S. W.; Ironmonger, V. M.; Tuttle, T.; Murphy, J. A. *J. Am. Chem. Soc.* **2014**, *136*, 17818–17826.

Zhu, D.; Herbert, B. E.; Schlautman, M. A.; Carraway, E. R. *J. Environ. Quality* **2004**, *33*, 276; Lu, Q.; Oh, D. X.; Lee, Y.; Jho, Y.; Hwang, D. S.; Zeng, H. *Angew. Chem. Int. Ed.* **2013**, *52*, 3944.

Zweifel, G.; Backlund, S. J. *J. Am. Chem. Soc.* **1977**, *99*, 3184–3185.

INDEX**A**

alkyne.....6, 8, 20, 21, 23, 29, 286–298

C

catalyst/ catalysis2–4, 6, 8, 11, 13–17, 19, 20, 22, 24, 25, 35–37, 41, 43, 45, 46, 48, 61, 66, 68, 71, 73, 76, 79, 82, 224, 277, 286, 295, 298, 350

computations/computed71, 74, 88, 215, 216, 219, 220, 223

H

heterocycle.....8, 30

I

iridicycle.....204, 205, 460, 470

L

Lewis acid.....1–12, 277

M

mechanism76, 77, 81, 213–219, 280

S

silylation1–37, 40–49, 50, 52, 53, 57, 59, 61, 62, 64–66, 73, 78, 79, 81, 83, 84, 85, 90, 93, 94, 99, 103, 209–213, 216, 219–221, 276–298, 327–331.

T

time course49, 211, 279,

ABOUT THE AUTHOR

David Phillip Schuman was born in Aurora, Illinois on October 28th, 1990 to Gayle and Phillip Schuman. David grew up in Lisle, IL where he was an active athlete throughout junior high and high school and competed in the state championships for both swimming and track.

After high school, David was awarded a Congress Bundestag Youth Exchange, Vocational Exchange Scholarship and spent a year in Germany as an exchange student. He lived near Cologne and then near Nuremberg where he worked part time in a brewery.

In the fall of 2009, David moved to Madison, Wisconsin to attend the University of Wisconsin. Early in his time at UW, David became interested in research and performed undergraduate research on the development of aza-Wacker cyclization method to synthesize vicinal aminoalcohols under the supervision of Prof. Shannon Stahl. When not working on classes or undergraduate research, David spent his time outdoors; hiking, whitewater kayaking, and camping.

David continued to follow his love of science and chose to attend the California Institute of Technology in Pasadena, California. At Caltech, he pursued doctoral studies under the supervision of Professor Brian Stoltz. David's graduate work has focused on the mechanistic investigation and further development of C-H silylation methods along with natural product total synthesis

Upon completion of his doctoral research in March 2020, David will begin his professional career as a medicinal chemist at Janssen in San Diego.